Oxidative Medicine and Cellular Longevity

Oxidative Stress-Mediated Reperfusion Injury 2014

Guest Editors: Zhengyuan Xia, Yanfang Chen, Qian Fan, Mengzhou Xue, and Ke-xuan Liu

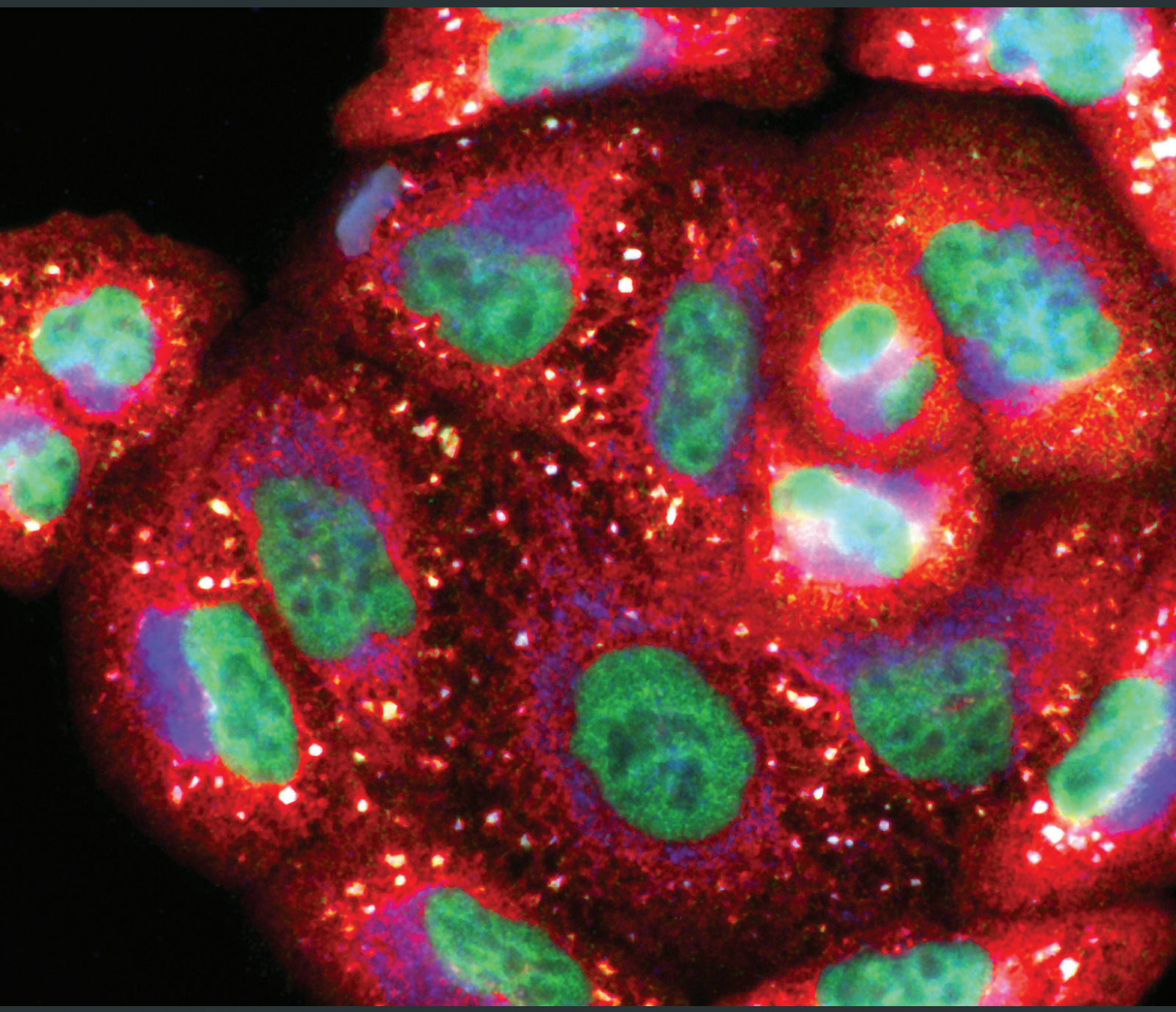

Oxidative Stress-Mediated Reperfusion Injury 2014

Oxidative Medicine and Cellular Longevity

Oxidative Stress-Mediated Reperfusion Injury 2014

Guest Editors: Zhengyuan Xia, Yanfang Chen, Qian Fan, Mengzhou Xue, and Ke-xuan Liu

Editorial Board

Contents

Hindawi Publishing Corporation
Oxidative Medicine and Cellular Longevity
Volume 2015, Article ID 689416, 2 pages
http://dx.doi.org/10.1155/2015/689416

Editorial

Oxidative Stress-Mediated Reperfusion Injury 2014

Zhengyuan Xia,[1,2] Yanfang Chen,[3,4] Qian Fan,[5] Mengzhou Xue,[6] and Ke-xuan Liu[7]

[1]*Department of Anesthesiology, The University of Hong Kong, 102 Pokfulam Road, Hong Kong*
[2]*Department of Anesthesiology, The Second Affiliated Hospital & Yuying Children's Hospital of Wenzhou Medical University, Wenzhou, Zhejiang 325027, China*
[3]*Department of Pharmacology & Toxicology, Boonshoft School of Medicine, Wright State University, 3640 Colonel Glenn Highway, Dayton, OH 45435, USA*
[4]*Cardiovascular Department, Guangzhou Institute of Cardiovascular Disease, The Second Affiliated Hospital of Guangzhou Medical University, Guangzhou 510000, China*
[5]*Department of Cardiology, Beijing Anzhen Hospital, Capital Medical University, Beijing 100029, China*
[6]*Department of Neurology, The First Affiliated Hospital, Henan University, 357 Ximen Street, Kaifeng 470010, China*
[7]*Department of Anesthesiology, The First Affiliated Hospital, Sun Yat-Sen University, Guangzhou 510080, China*

Correspondence should be addressed to Zhengyuan Xia; zyxia@hku.hk

Received 15 April 2015; Accepted 15 April 2015

Ischemia/reperfusion injury (IRI) and organ failure especially IRI-induced remote and multiple organ failure contribute significantly to postoperative mortality and morbidity, and reperfusion induced oxidative stress plays a critical role in this pathology [1, 2].

Reactive oxygen species (ROS) induced vascular endothelial dysfunction plays an important role in the development of IRI in various organs. In this special issue, Q. Yang et al. reported that the otherwise cardiac protective polymerized hemoglobin, when used at high dose, failed to alleviate cardiac IRI due to induction of oxidative damage in coronary artery. On the other hand, natural herbal extracts such as Licochalcone B as reported by J. Han et al. in this special issue conferred protection against myocardial IRI through attenuating ischemia-reperfusion induced oxidative damage.

The intravenous anesthetic propofol possesses antioxidant capacity and has been shown to attenuate IRI in patients undergoing cardiac surgery and in animal models of myocardial [3] and intestinal IRI [4]. In this special issue, X. Gan et al. further identified that propofol attenuated intestinal IRI through inhibiting the ROS generating NADPH oxidase mediated mast cell activation. Given that mast cell activation has been shown to play an important role in IRI-induced remote organ injury [5], the finding by X. Gan et al. may promote further in-depth studies, both experimental and clinical, regarding the potential protective effects of propofol in attenuating or preventing postischemic remote organ injuries.

Disturbances of *mitochondrial homeostasis* play critical roles in Acute Organ Failure [6] and in postischemic cellular injury [7], while the governing mechanism of *mitochondrial homeostasis alterations during these pathologies is largely unclear*. In this special issue, S. Cao et al. provided genome-wide expression profiling of cardiomyocytes subjected to hypoxia-reoxygenation injury in an effort to uncover the roles of mitoKATP in energy homeostasis and its regulation.

We hope that the original and review articles presented in this special issue, representing the current advances in the oxidative stress-mediated ischemia-reperfusion injury, with respect to their potential impact in cellular survival pathways and therapeutic strategies, will stimulate further exploration of this important area. Despite diversity, it is our belief that the articles comprised in this special issue could represent an important advancement and contribution to improve our knowledge of the mechanisms governing reperfusion injury.

Acknowledgments

This special issue would not be possible without the great efforts of the authors and the reviewers. In this regard, we

would like to thank all these people that took part in the achievement of this issue.

Zhengyuan Xia
Yanfang Chen
Qian Fan
Mengzhou Xue
Ke-xuan Liu

References

[1] Z. Xia, Y. Chen, Q. Fan, and M. Xue, "Oxidative stress-mediated reperfusion injury: mechanism and therapies," *Oxidative Medicine and Cellular Longevity*, vol. 2014, Article ID 373081, 2 pages, 2014.

[2] F. Chiazza, K. Chegaev, M. Rogazzo et al., "A nitric oxide-donor furoxan moiety improves the efficacy of edaravone against early renal dysfunction and injury evoked by ischemia/reperfusion," *Oxidative Medicine and Cellular Longevity*, vol. 2015, Article ID 804659, 12 pages, 2015.

[3] D. Zhao, Q. Li, Q. Huang et al., "Cardioprotective effect of propofol against oxygen glucose deprivation and reperfusion injury in H9c2 cells," *Oxidative Medicine and Cellular Longevity*, vol. 2015, Article ID 184938, 8 pages, 2015.

[4] K.-X. Liu, T. Rinne, W. He, F. Wang, and Z. Xia, "Propofol attenuates intestinal mucosa injury induced by intestinal ischemia-reperfusion in the rat," *Canadian Journal of Anesthesia*, vol. 54, no. 5, pp. 366–374, 2007.

[5] A. Zhang, X. Chi, G. Luo et al., "Mast cell stabilization alleviates acute lung injury after orthotopic autologous liver transplantation in rats by downregulating inflammation," *PLoS ONE*, vol. 8, no. 10, Article ID e75262, 2013.

[6] L. J. Stallons, J. A. Funk, and R. G. Schnellmann, "Mitochondrial Homeostasis in Acute Organ Failure," *Current Pathobiology Reports*, vol. 1, no. 3, pp. 169–177, 2013.

[7] C. H. Huang, C. Y. Chiang, R. H. Pen et al., "Hypothermia treatment preserves mitochondrial integrity and viability of cardiomyocytes after ischaemic reperfusion injury," *Injury*, vol. 46, no. 2, pp. 233–239, 2015.

Hindawi Publishing Corporation
Oxidative Medicine and Cellular Longevity
Volume 2015, Article ID 481405, 8 pages
http://dx.doi.org/10.1155/2015/481405

Research Article

Protective Effects of Kaempferol against Myocardial Ischemia/Reperfusion Injury in Isolated Rat Heart via Antioxidant Activity and Inhibition of Glycogen Synthase Kinase-3β

Mingjie Zhou,[1,2] Huanhuan Ren,[3] Jichun Han,[3] Wenjuan Wang,[3] Qiusheng Zheng,[3,4] and Dong Wang[1]

[1] *Shandong Provincial Qianfoshan Hospital, Jinan 250014, China*
[2] *Weifang Medical University, Weifang 261031, China*
[3] *Binzhou Medical University, Yantai 264003, China*
[4] *Pharmacy School, Shihezi University, Shihezi 832002, China*

Correspondence should be addressed to Qiusheng Zheng; zqsyt@sohu.com and Dong Wang; wangdong9859@sina.com

Received 23 September 2014; Revised 9 November 2014; Accepted 11 November 2014

Academic Editor: Yanfang Chen

Objective. This study aimed to evaluate the protective effect of kaempferol against myocardial ischemia/reperfusion (I/R) injury in rats. *Method*. Left ventricular developed pressure (LVDP) and its maximum up/down rate ($\pm dp/dt_{max}$) were recorded as myocardial function. Infarct size was detected with 2,3,5-triphenyltetrazolium chloride staining. Cardiomyocyte apoptosis was determined using terminal deoxynucleotidyl nick-end labeling (TUNEL). The levels of creatine kinase (CK), lactate dehydrogenase (LDH), malondialdehyde (MDA), superoxide dismutase (SOD), glutathione/glutathione disulfide (GSH/GSSG) ratio, and tumor necrosis factor-alpha (TNF-α) were determined using enzyme linked immunosorbent assay (ELISA). Moreover, total glycogen synthase kinase-3β (GSK-3β), phospho-GSK-3β (P-GSK-3β), precaspase-3, cleaved caspase-3, and cytoplasm cytochrome C were assayed using Western blot analysis. *Results*. Pretreatment with kaempferol significantly improved the recovery of LVDP and $\pm dp/dt_{max}$, as well as increased the levels of SOD and P-GSK-3β and GSH/GSSG ratio. However, the pretreatment reduced myocardial infarct size and TUNEL-positive cell rate, as well as decreased the levels of cleaved caspase-3, cytoplasm cytochrome C, CK, LDH, MDA, and TNF-α. *Conclusion*. These results suggested that kaempferol provides cardioprotection via antioxidant activity and inhibition of GSK-3β activity in rats with I/R.

1. Introduction

Nowadays, cardiovascular diseases are responsible for the majority of elderly mortality [1]; the most important presentation of cardiovascular disease is ischemia. A long period of ischemia leads to myocardial injury. Theoretically, restoring blood supply to the ischemic myocardium can reduce myocardial injury. However, reperfusion can aggravate myocardial damage through ischemia-reperfusion (I/R) injury [2]. Excessive reactive oxygen species (ROS), calcium overload, inflammatory reaction, and other factors can lead to cellular necrosis, apoptosis, and organ dysfunction in severe cases [3]. Prevention of I/R is important to alleviate ischemic heart disease [4].

Network pharmacology is a method for treating polygenic diseases based on the target and drug perspectives. Mapping the polypharmacology network onto the human disease-gene network can reveal important drug targets that could demonstrate the mechanism of botanical drugs in treating different diseases. Our previous studies identified the potential targets of kaempferol in cardiovascular diseases [5]. Thirteen potential targets were identified and annotated to have significant relationships with the pharmacologic effects of kaempferol. Among these targets, the main protein

involved in I/R injury is glycogen synthase kinase-3 beta (GSK-3β). GSK-3β is a serine/threonine kinase that participates in various cell activities through phosphorylation of the substrate protein [6]. GSK-3β is important in glycogen metabolism, as well as in cell proliferation, growth, and death [7, 8]. GSK-3β has received increasing attention because of its involvement in some common and serious diseases, such as neurological disease, cancer, and I/R injury. In the cardiovascular system, GSK-3β has major roles in glucose metabolism, cardiomyocyte hypertrophy [9], and cell death [10]. Many studies have shown that GSK-3β inhibition during I/R is an important mechanism of myocardial adaptation; cardioprotective agents use the inhibition of GSK-3β (phosphorylation) as the common downstream target [11], and protection is related to the mitochondrial permeability transition pore (mPTP) [12].

Epidemiological studies have demonstrated that some flavonoids may affect treatment for several diseases [13]. A research on the plants used in traditional medicines revealed that flavonoids are their common bioactive constituents [14]. The flavonoid kaempferol, a yellow compound with low molecular weight (MW: 286.2 g/mol), is commonly found in plant-derived foods and in plants used in traditional medicines. Numerous preclinical studies have shown that kaempferol has a wide range of pharmacological activities, including antioxidant [15], anti-inflammatory [16], and anticancer activities [17].

Therefore, we aimed to evaluate the cardioprotective effects of kaempferol and the mechanisms underlying such effects in the present study.

2. Methods

2.1. Animals and Reagents. All procedures were performed in accordance with the National Institutes of Health Guideline on the Use of Laboratory Animals and were approved by the Shihezi University Committee on Animal Care. Adult male Sprague-Dawley rats (250–280 g) were obtained from the Xinjiang Medicine University Medical Laboratory Animal Center (SDXK 2011-004) and housed in a room with temperature of 22–25°C, relative humidity of 50–60%, and a 12-h light/12-h dark cycle.

Kaempferol (purity ≥ 98%) was purchased from Shanghai Lichen Biotechnology Co., Ltd. (Shanghai, China). Antibodies against total GSK-3β, as well as P-GSK-3β (Ser9), caspase-3, and cytoplasm cytochrome C, were obtained from Cell Signaling Technology (1 : 10000, Beverly, MA, USA). Terminal deoxynucleotidyl nick-end labeling (TUNEL) assay was conducted using in situ cell death detection kit (POD, Roche, Germany). All other reagents were of standard biochemical quality and were obtained from commercial suppliers.

2.2. Establishment of Animal Model of Myocardial I/R Injury. The rats were randomly divided into four groups as follows: control group, I/R group, kaempferol group, and TDZD-8 (4-benzyl-2-methyl-1,2,4-thiadiazolidine-3,5-dione) group. Hearts from control group were perfused for 120 min stabilization. Hearts from I/R group were stabilized for 20 min and then subjected to 15 min of global ischemia and 85 min of reperfusion. Hearts in kaempferol group were treated with K-H buffer containing kaempferol (15 mmol/L) for 10 min after being stabilized and then subjected to global ischemia for 15 min and reperfusion for 85 min. Hearts in TDZD-8 group were treated with K-H buffer containing TDZD-8 (0.01 mmol/L) for 10 min after being stabilized and then subjected to global ischemia for 15 min and reperfusion for 85 min.

2.3. Heart Isolation and Perfusion. Rats were anesthetized with an intraperitoneal injection of 60 mmol/L chloral hydrate (0.35 g/kg) and provided with 250 U/kg heparin through sublingual venous injection to prevent coagulation. The hearts were quickly removed and mounted on a Langendorff apparatus via the aorta for retrograde perfusion with Krebs-Henseleit (K-H) buffer at constant pressure (10 KPa) and constant temperature (37°C). The composition of K-H buffer (in mmol/L) was as follows: NaCl, 118; KCl, 4.7; $MgSO_4$, 1.2; $CaCl_2$, 2.5; KH_2PO_4, 1.2; $NaHCO_3$, 25; glucose, 11. The buffer was saturated with 95% O_2/5% CO_2 (pH 7.4) [18]. The left atrial appendage was cut. A latex balloon filled with water was inserted into the left ventricle through the left atrial appendage. Finally, hemodynamic parameters, LVDP (LVSP is left ventricular systolic pressure; LVEDP is left ventricular end-diastolic pressure; LVDP = LVSP − LVEDP), $\pm dp/dt_{max}$ (reflecting the important indicators of left ventricular systolic function and diastolic function), CF, and HR, were displayed on the recorder screen.

2.4. Evaluation of Myocardial Infarct Size (IS). After reperfusion was concluded, the heart was frozen at −20°C and cut into five slices along the transverse direction. Each piece was 2 mm thick. The slices were incubated in 1% triphenyltetrazolium chloride (TTC) at 37°C for 20 min. The heart slices were imaged using a digital camera. Area at risk (AAR) and IS were digitally measured using Image Pro Plus software [19]. Myocardial IS was expressed as the ratio between IS and AAR.

2.5. Assay of Cellular Injury. To determine the activities of lactate dehydrogenase (LDH) and creatinine kinase (CK), the samples were collected from the coronary effluent before ischemia and after 85 min of reperfusion. The levels of LDH and CK in the effluent were detected spectrophotometrically using their corresponding cytotoxicity detection kits (Nanjing Jiancheng Biological Product, Nanjing, China).

2.6. Assay of Oxidative Stress. After perfusion, we obtained the same part of the ventricular apical. Subsequently, the tissue was homogenized in appropriate buffer and centrifuged, after which the supernatant was removed. The levels of superoxide dismutase (SOD) and malondialdehyde (MDA) and glutathione (GSH)/GSH disulfide (GSSG) ratio were analyzed spectrophotometrically using their corresponding assay kits (Nanjing Jiancheng Biological Product, Nanjing, China).

Table 1: Effect of kaempferol on cardiac function in the rats subjected to I/R ($\overline{x} \pm s$, %, $n = 8$); $^{**}P < 0.01$, compared with the control group; $^{\#\#}P < 0.01$, compared with the I/R group.

Reperfusion	Control	I/R	Kaempferol	TDZD-8
LVDP (mmHg)	87.98 ± 3.98	52.43 ± 2.62**	69.47 ± 2.26$^{\#\#}$	64.53 ± 2.47$^{\#\#}$
+LV$dp/dt_{max}$ (mmHg·s^{-1})	89.37 ± 3.73	45.86 ± 2.53**	63.27 ± 2.76$^{\#\#}$	60.58 ± 2.96$^{\#\#}$
−LV$dp/dt_{max}$ (mmHg·s^{-1})	86.76 ± 3.56	42.16 ± 2.38**	61.54 ± 3.14$^{\#\#}$	60.79 ± 3.35$^{\#\#}$
CF (mL·min^{-1})	82.19 ± 3.63	51.46 ± 2.36**	67.21 ± 4.06$^{\#\#}$	64.59 ± 3.97$^{\#\#}$
HR (beats·min^{-1})	90.51 ± 4.58	70.68 ± 4.87**	83.92 ± 3.99$^{\#\#}$	78.68 ± 4.13$^{\#\#}$

2.7. Assay of Inflammation. Tumor necrosis factor alpha (TNF-α) was analyzed spectrophotometrically according to the instructions in the TNF-α ELISA kit (Tsz Biosciences, Greater Boston, USA).

2.8. TUNEL Assay. TUNEL assay was carried out according to the manufacturer's instructions. After deparaffinization and rehydration, the sections were treated with 10 mmol/L protease K for 15 min. The slides were immersed in TUNEL reaction mixture for 60 min at 37°C in a humidified atmosphere in the dark. A converter POD was used to incubate the slides for 30 min. The slides were then analyzed using an optical microscope. To evaluate the apoptosis index of the TUNEL-stained heart tissues, we captured 10 random fields per tissue section at 400x magnification. TUNEL index (%) is calculated as the ratio of the number of TUNEL-positive cells divided by the total number of cells [20] (see Figure 4).

2.9. Western Blot Analysis. The protein levels of total GSK-3β, phospho-GSK-3β (P-GSK-3β, Ser9), precaspase-3, cleaved caspase-3, and cytoplasm cytochrome C were determined using Western blot analysis. After perfusion by Langendorff apparatus, we cut off the same part in ventricular apical of the rats, then homogenized the cut tissue in appropriate buffer, and centrifuged it. Supernatant was extracted and boiled for 15 min to make protein denaturation. Then the whole-cell protein extracts were separated using 12% SDS-polyacrylamide gel electrophoresis. Proteins were transferred to nylon membranes by electrophoretic transfer system. The membranes were blocked with 5% skimmed milk blocking buffer at room temperature for 1 h and then incubated with primary antibodies overnight (18 h) at 4°C. After being washed with TBST buffer, the corresponding secondary antibodies were used to identify primary antibody binding. In the end, the blots were visualized with ECL-plus reagent.

2.10. Statistical Analysis. Results were expressed as mean ± S.D. and analyzed using one-way analysis of variance. The values with $P < 0.05$ were considered statistically significant. All statistical tests were performed with GraphPad Prism software version 5.0 (GraphPad Software, San Diego, CA).

3. Results

3.1. Kaempferol Improved the Recovery of I/R-Induced Cardiac Function. As shown in Table 1, the hearts in the I/R group demonstrated significant decrease in the recovery of cardiac function compared with that in the control group. Moreover, the hearts in the kaempferol and TDZD-8 treatment groups showed higher recovery of cardiac function than that in the I/R group ($P < 0.05$). Hemodynamic data confirmed that kaempferol improved the recovery of the cardiac systolic and diastolic function of the rats after I/R.

Table 2: Effect of kaempferol on the levels of CK and LDH in the coronary effluent before ischemia and after 85 min of reperfusion ($\overline{x} \pm s$, $n = 8$); $^{**}P < 0.01$, compared with the control group; $^{\#\#}P < 0.01$, compared with the I/R group.

Groups	Before ischemia	Reperfusion
CK (U/L)		
Control	16.73 ± 1.46	24.81 ± 1.31
I/R	15.76 ± 1.21	56.74 ± 2.97**
Kaempferol	16.72 ± 1.23	32.30 ± 2.48$^{\#\#}$
TDZD-8	16.45 ± 1.26	36.73 ± 2.54$^{\#\#}$
LDH (U/L)		
Control	14.47 ± 1.36	19.51 ± 1.35
I/R	14.58 ± 1.38	60.54 ± 2.35**
Kaempferol	15.35 ± 0.96	36.63 ± 1.83$^{\#\#}$
TDZD-8	15.49 ± 1.12	39.67 ± 1.64$^{\#\#}$

3.2. Kaempferol Reduced Myocardial IS Post-I/R. The representative slices of the hearts are shown in Figure 1(a). The ratio of IS and AAR in the control group was 5.31% ± 1.34%, which was significantly different from that of the I/R group (46.73% ± 1.88%) ($P < 0.01$; Figure 1(b)). The ratio remarkably decreased in the kaempferol (16.49% ± 1.23%) and TDZD-8 groups (21.42% ± 1.48%) compared with that in the I/R group ($P < 0.01$; Figure 1(b)).

3.3. Kaempferol Attenuated the I/R-Induced Enzyme Release in Rat Heart. As shown in Table 2, the levels of perfusate CK and LDH in the I/R group (56.74 ± 2.97 and 60.54 ± 2.35, resp.) significantly increased compared with that in the control group ($P < 0.01$); however, the levels of CK and LDH in the kaempferol (32.30 ± 2.48 and 36.63 ± 1.83, resp.) and TDZD-8 groups (36.73 ± 2.54 and 39.67 ± 1.64, resp.) ($P < 0.01$) were significantly decreased compared with the I/R group.

3.4. Kaempferol Improved the Oxidative Stress State Induced by I/R. To identify the possible mechanisms of kaempferol involving antioxidants on cardioprotection, we evaluated

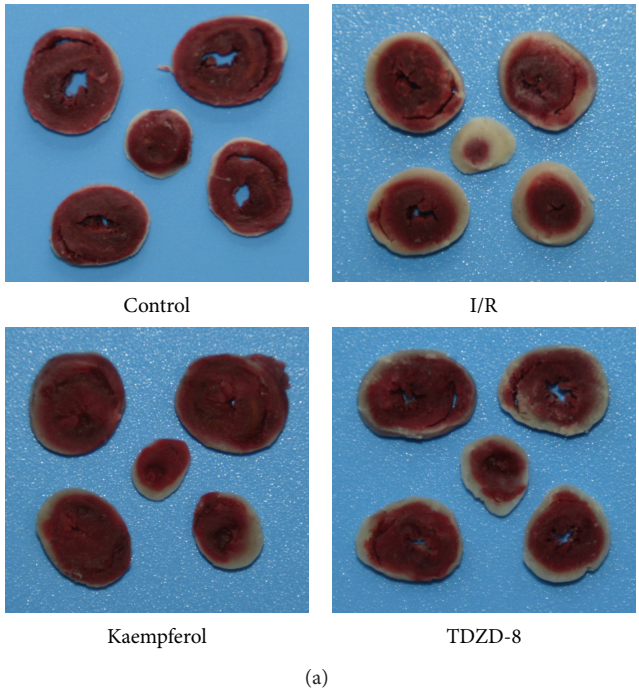

Figure 1: Kaempferol reduces the I/R-induced IS. (a) Images of myocardial tissue sections after TTC staining. (b) The ratio between IS and AAR, in which AAR is the area at risk and IS is the infarct size; values are presented as means with their standard deviations ($\overline{x} \pm s$, $n = 8$); $^{**}P < 0.01$, compared with the control group; $^{\#\#}P < 0.01$, compared with the I/R group.

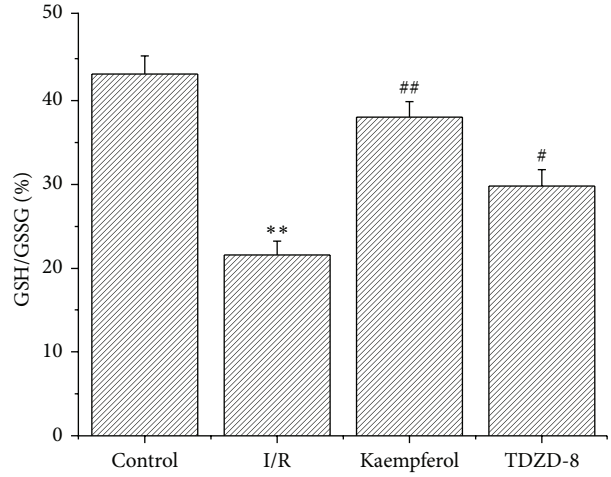

Figure 2: Kaempferol increases the ratio of GSH/GSSG. Values are presented as means with their standard deviation ($\overline{x} \pm s$, $n = 8$); $^{**}P < 0.01$, compared with control group; $^{\#\#}P < 0.01$ and $^{\#}P < 0.05$, compared with the I/R group.

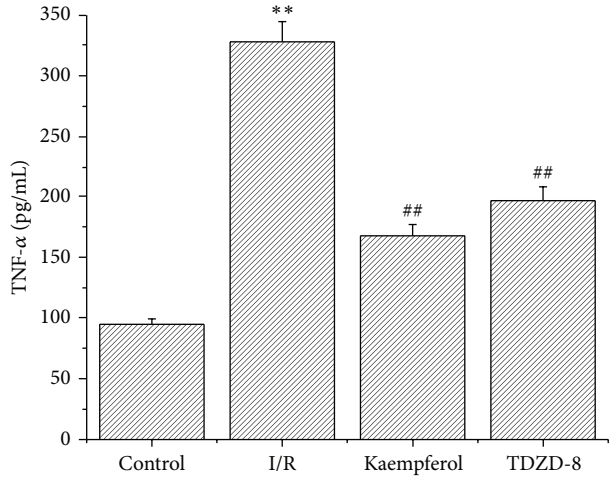

Figure 3: Kaempferol reduces inflammatory response. Values are presented as means with their standard deviations ($\overline{x} \pm s$, $n = 8$); $^{**}P < 0.01$, compared with the control group; $^{\#\#}P < 0.01$, compared with the I/R group.

SOD activity, MDA level, and GSH/GSSG ratio in the myocardial tissues. As shown in Table 3, and Figure 2, the SOD activity and the ratio of GSH/GSSG in the kaempferol or TDZD-8 groups significantly increased, compared with those of the control group, whereas the MDA level significantly decreased in the kaempferol or TDZD-8 groups.

3.5. Kaempferol Reduced the Inflammatory Response. As shown in Figure 3, the level of TNF-α increased from 95 ± 4.5 pg/mL in the control group to 328 ± 16.7 pg/mL in the I/R group. The levels of TNF-α in the kaempferol (168 ± 9.3 pg/mL) and TDZD-8 groups (197 ± 11.4 pg/mL) significantly decreased compared with that in the I/R group ($P < 0.01$).

3.6. Kaempferol Weakened the Cardiomyocyte Apoptosis Induced by I/R. TUNEL staining did not show a significant apoptotic phenomenon in the control group, whereas the number of apoptotic cells evidently increased in the I/R group (58 ± 3.21). Apoptotic cells significantly decreased in the kaempferol (35 ± 1.48) and TDZD-8 groups (47 ± 2.79) compared with those in the I/R group ($P < 0.01$).

Table 3: Effects of kaempferol on SOD activity and MDA level. Values are presented as means with their standard deviations ($\bar{x} \pm s$, $n = 8$); $^{**}P < 0.01$, compared with the control group; $^{\#\#}P < 0.01$ and $^{\#}P < 0.05$, compared with the I/R group.

Group	Dosage	Reperfusion	
		SOD (U/mgPr)	MDA (nmol/mgPr)
Control	—	10.48 ± 0.79	210.43 ± 12.56
I/R	—	3.35 ± 0.41**	489.71 ± 30.25**
Kaempferol	15 mmol/L	8.15 ± 0.57$^{\#\#}$	285.76 ± 19.04$^{\#\#}$
TDZD-8	0.01 mmol/L	5.43 ± 0.62$^{\#}$	370.24 ± 22.50$^{\#\#}$

3.7. Effects of Kaempferol on GSK-3β Phosphorylation, Cytochrome C Release, and Caspase-3 Activity. As shown in Figure 5, the level of GSK-3β phosphorylation in the kaempferol (0.65 ± 0.039) and TDZD-8 groups (0.74 ± 0.043) significantly increased compared with those in the control (0.32 ± 0.018) and I/R groups (0.35 ± 0.02) ($P < 0.01$). However, no evident difference was observed between the control and I/R groups. The release of cytochrome C and the dissociation of caspase-3 in the I/R groups (0.52 ± 0.039 and 0.37 ± 0.021, resp.) were significantly increased compared with those in the control groups ($P < 0.01$), whereas the kaempferol (0.32 ± 0.024 and 0.25 ± 0.018, resp.) and TDZD-8 groups (0.21 ± 0.013 and 0.29 ± 0.019, resp.) were significantly decreased compared with those in the I/R groups ($P < 0.01$).

4. Discussion

In this study, we investigated the effects of kaempferol on cardiac function, myocardial IS, cardiomyocyte apoptosis, inflammation factor, and myocardial enzyme in the isolated rat heart model of I/R. We provided evidence that kaempferol improves the recovery of cardiac function, reduces intracellular oxidation status and myocardial IS, and inhibits myocardial apoptosis induced by I/R. Finally, we demonstrated that the phosphorylation of GSK-3β is involved in the cardioprotection of kaempferol.

Reactive oxygen species (ROS) induced injury plays an important role in the development of I/R in various organs [21]. Few free radicals are present under physiological conditions during ischemia; thus, the absorbance of oxygen radical decreases [22]. During recovery, the blood supply of the tissues triggers the "explosion" of oxygen free radicals; hence, the accumulated ROS attack the cells and cause damage [23]. ROS causes damage to the cell membranes in rat heart, subsequently causes cell membrane lipid peroxidation and structural failure, and results in leakage of myocardial enzyme. Inhibiting the ROS generation or the antagonist of reactive oxygen toxicity is important to alleviate myocardial reperfusion injury [24]. In the present experiment, SOD activity and GSH/GSSG ratio significantly increased, whereas MDA level significantly decreased in the kaempferol group. Therefore, we speculated that kaempferol has good antioxidant effect that functions as myocardial protection.

During I/R, oxidative stress activates NF-κB because cardiac stress rapidly responds to the expressed genes. NF-κB

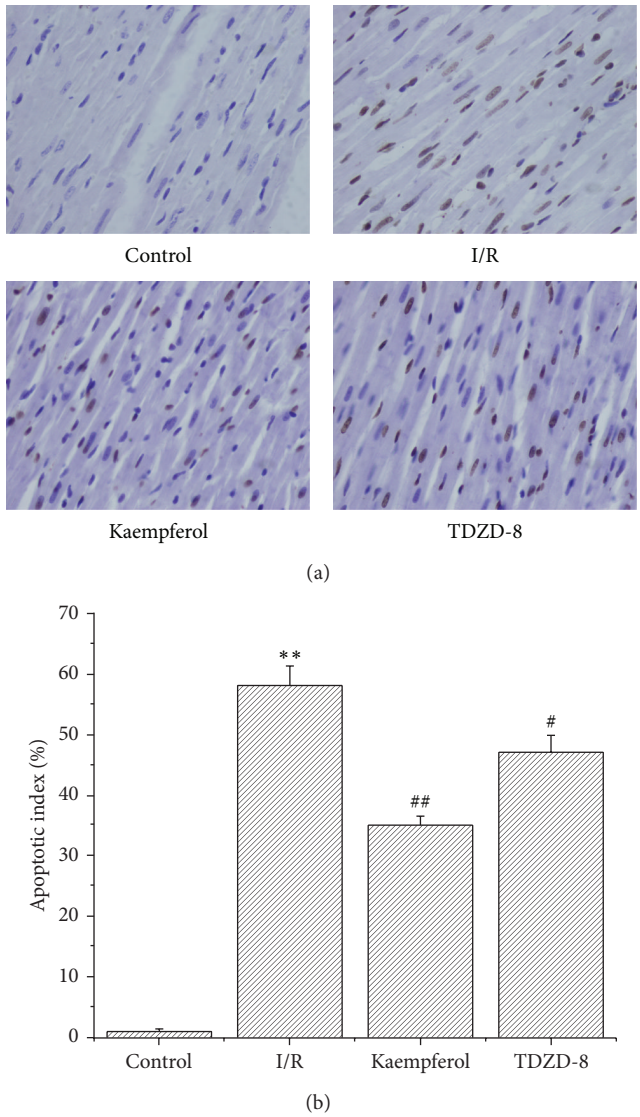

Figure 4: Kaempferol prevents myocardial cell apoptosis in I/R. (a) Cell apoptosis was analyzed using TUNEL staining. Magnification: 400x. (b) Apoptosis cells/total cells (%). Values are presented as means with their standard deviations ($\bar{x} \pm s$, $n = 8$); $^{**}P < 0.01$, compared with the control group; $^{\#\#}P < 0.01$ and $^{\#}P < 0.05$, compared with the I/R group.

stimulates the cardiac cells and macrophages and produces large amounts of TNF-α; thus, the myocardial cells after I/R are the sites for TNF-α synthesis and the target organs of TNF-α. Studies have shown that TNF-α dose dependently decreases myocardial contractility, whereas the application of anti-TNF-α reduces I/R injury and confers protection for the ischemic myocardium [25]. The TNF-α bioactivity in the heart increases from the early stage of I/R; such increase has been speculated to partially contribute to the increased area of myocardial infarction [26]. The ROS generated within cells can induce apoptosis through multiple pathways. Cardiomyocytes, which are abundant in the mitochondria, are the major endogenous source and are the susceptible target

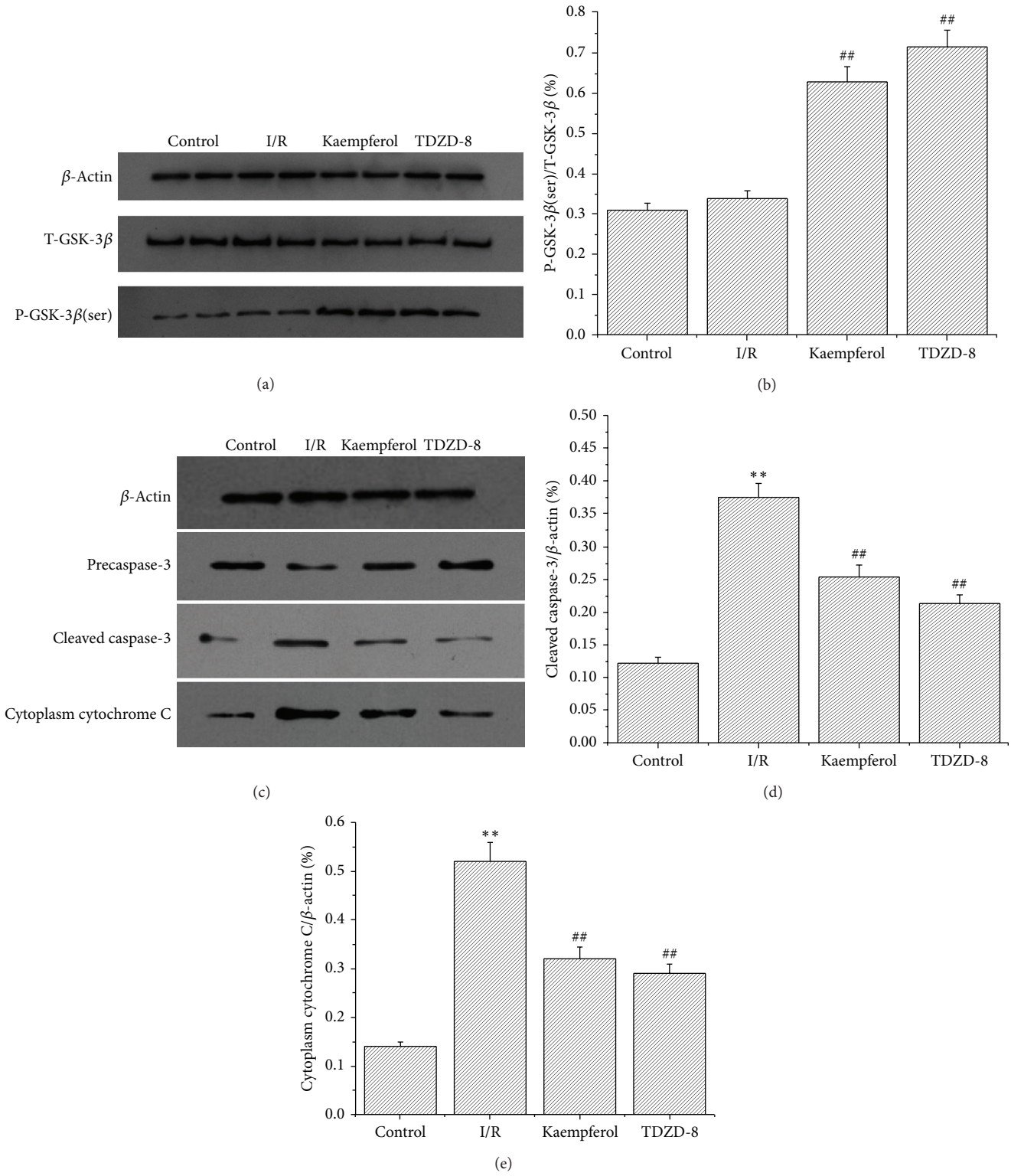

FIGURE 5: Kaempferol increases the phosphorylation of GSK-3β and reduces the release of cytochrome C and the dissociation of caspase-3. (a) Representative Western blots for T-GSK-3β and P-GSK-3β (Ser9). Lanes 1 and 2 are the control group, lanes 3 and 4 are the I/R group, lanes 5 and 6 are the kaempferol group, and lanes 7 and 8 are the TDZD-8 group. (b) Grey value analysis demonstrates that kaempferol increases the ratio of P-GSK-3β (ser)/T-GSK-3β. (c) Representative Western blot for cleaved caspase-3 and cytoplasm cytochrome C. Lane 1 is the control group, lane 2 is the I/R group, lane 3 is the kaempferol group, and lane 4 is the TDZD-8 group. (d) Grey value analysis demonstrates that kaempferol reduces the ratio of cleaved caspase-3/β-actin. (e) Grey value analysis demonstrates that kaempferol reduces the ratio of cytoplasm cytochrome C/β-actin. Values are presented as means with their standard deviations ($\overline{x} \pm s$, $n = 8$); $^{**}P < 0.01$, compared with the control group; $^{\#\#}P < 0.01$, compared with the I/R group.

of ROS damage [27]; the abundant ROS within the mitochondria can decrease its selective ion permeability or change its membrane permeability, which changes the mitochondrial membrane and thereby induces mitochondrial permeability transition pore (MPTP) opening during reperfusion [28]. The mitochondria release cytochrome C, which activates the aspartate-specific cysteine proteases (caspases) and induces apoptosis [29].

Cytochrome C is located within the intermembrane space under normal conditions; the released cytochrome C binds to the C-terminal domain of the apoptotic protease activating factor-1 (Apaf-1) and changes its conformation [30]. The activated Apaf-1/cytochrome C complex promotes caspase activation [31]. Several studies in the literature showed that GSK-3β inhibition might delay or suppress mPTP opening and inhibit the release of cytochrome C [32, 33]. TDZD-8 is a GSK-3β inhibitor with significant myocardial protection effect via inhibition of inflammation and apoptosis [34]. We used TDZD-8 as a positive control agent to demonstrate the mechanisms of the cardioprotective effects of kaempferol. Our research showed that kaempferol or TDZD-8 can increase the level of GSK-3β phosphorylation and reduce the release of cytochrome C compared with those in the control and I/R groups. We inferred that kaempferol can function similarly to that of TDZD-8 on GSK-3β phosphorylation. Thus, we speculated that kaempferol decreases the apoptosis induced by I/R injury via GSK-3β inhibition.

Conflict of Interests

No conflict of interests, financial or otherwise, is declared by the authors.

Authors' Contribution

Dong Wang and Mingjie Zhou conceived and designed the experiments. Mingjie Zhou and Qiusheng Zheng performed the experiments. Wenjuan Wang, Jichun Han, and Huanhuan Ren analyzed the data. Wenjuan Wang, Jichun Han, and Huanhuan Ren contributed reagents/materials/analysis tools. Mingjie Zhou wrote the paper.

Acknowledgments

This study was supported by the Natural Science Foundation of Shandong Province (no. ZR2011HL013) to Dong Wang and by the Science and Technology Foundation of Shihezi (2014QY16) to Qiusheng Zheng.

References

[1] Q. Fan, L. Chen, S. Cheng et al., "Aging aggravates nitrate-mediated ROS/RNS changes," *Oxidative Medicine and Cellular Longevity*, vol. 2014, Article ID 376515, 7 pages, 2014.

[2] M. Juhaszova, D. B. Zorov, Y. Yaniv, H. B. Nuss, S. Wang, and S. J. Sollott, "Role of glycogen synthase kinase-3β in cardioprotection," *Circulation Research*, vol. 104, no. 11, pp. 1240–1252, 2009.

[3] R. B. Jennings, "Historical perspective on the pathology of myocardial ischemia/reperfusion injury," *Circulation Research*, vol. 113, no. 4, pp. 428–438, 2013.

[4] K. Przyklenk, Y. Dong, V. V. Undyala, and P. Whittaker, "Autophagy as a therapeutic target for ischaemia/reperfusion injury? Concepts, controversies, and challenges," *Cardiovascular Research*, vol. 94, no. 2, pp. 197–205, 2012.

[5] H. Liu, J. Wang, W. Zhou, Y. Wang, and L. Yang, "Systems approaches and polypharmacology for drug discovery from herbal medicines: an example using licorice," *Journal of Ethnopharmacology*, vol. 146, no. 3, pp. 773–793, 2013.

[6] A. Ali, K. P. Hoeflich, and J. R. Woodgett, "Glycogen synthase kinase-3: properties, functions, and regulation," *Chemical Reviews*, vol. 101, no. 8, pp. 2527–2540, 2001.

[7] S. H. Ramirez, S. Fan, M. Zhang et al., "Inhibition of glycogen synthase kinase 3β (GSK3β) decreases inflammatory responses in brain endothelial cells," *The American Journal of Pathology*, vol. 176, no. 2, pp. 881–892, 2010.

[8] S. Cuzzocrea, C. Crisafulli, E. Mazzon et al., "Inhibition of glycogen synthase kinase-3β attenuates the development of carrageenan-induced lung injury in mice," *British Journal of Pharmacology*, vol. 149, no. 6, pp. 687–702, 2006.

[9] P. H. Sugden, S. J. Fuller, S. C. Weiss, and A. Clerk, "Glycogen synthase kinase 3 (GSK3) in the heart: a point of integration in hypertrophic signalling and a therapeutic target? A critical analysis," *British Journal of Pharmacology*, vol. 153, no. S1, pp. S137–S153, 2008.

[10] A. Mora, K. Sakamoto, E. J. McManus, and D. R. Alessi, "Role of the PDK1-PKB-GSK3 pathway in regulating glycogen synthase and glucose uptake in the heart," *FEBS Letters*, vol. 579, no. 17, pp. 3632–3638, 2005.

[11] M. Juhaszova, D. B. Zorov, S.-H. Kim et al., "Glycogen synthase kinase-3β mediates convergence of protection signalling to inhibit the mitochondrial permeability transition pore," *Journal of Clinical Investigation*, vol. 113, no. 11, pp. 1535–1549, 2004.

[12] M. Nishihara, T. Miura, T. Miki et al., "Modulation of the mitochondrial permeability transition pore complex in GSK-3β-mediated myocardial protection," *Journal of Molecular and Cellular Cardiology*, vol. 43, no. 5, pp. 564–570, 2007.

[13] W. Ren, Z. Qiao, H. Wang, L. Zhu, and L. Zhang, "Flavonoids: promising anticancer agents," *Medicinal Research Reviews*, vol. 23, no. 4, pp. 519–534, 2003.

[14] M. López-Lázaro, "Distribution and biological activities of the flavonoid luteolin," *Mini-Reviews in Medicinal Chemistry*, vol. 9, no. 1, pp. 31–59, 2009.

[15] A. R. Verma, M. Vijayakumar, C. S. Mathela, and C. V. Rao, "*In vitro* and *in vivo* antioxidant properties of different fractions of *Moringa oleifera* leaves," *Food and Chemical Toxicology*, vol. 47, no. 9, pp. 2196–2201, 2009.

[16] M. J. Park, E. K. Lee, H.-S. Heo et al., "The anti-inflammatory effect of kaempferol in aged kidney tissues: the involvement of nuclear factor-κB via nuclear factor-inducing kinase/IκB kinase and mitogen-activated protein kinase pathways," *Journal of Medicinal Food*, vol. 12, no. 2, pp. 351–358, 2009.

[17] M. A. Gates, S. S. Tworoger, J. L. Hecht, I. de Vivo, B. Rosner, and S. E. Hankinson, "A prospective study of dietary flavonoid intake and incidence of epithelial ovarian cancer," *International Journal of Cancer*, vol. 121, no. 10, pp. 2225–2232, 2007.

[18] J. L. Zweier, J. Fertmann, and G. Wei, "Nitric oxide and peroxynitrite in postischemic myocardium," *Antioxidants & Redox Signaling*, vol. 3, no. 1, pp. 11–22, 2001.

[19] Y. Wang, P. Xu, H. Liu, Y. Zhou, and X. Cao, "The protection of salidroside of the heart against acute exhaustive injury and molecular mechanism in rat," *Oxidative Medicine and Cellular Longevity*, vol. 2013, Article ID 507832, 8 pages, 2013.

[20] H. Pang, B. Han, T. Yu, and Z. Peng, "The complex regulation of tanshinone IIA in rats with hypertension-induced left ventricular hypertrophy," *PLoS ONE*, vol. 9, no. 3, Article ID e92216, 2014.

[21] Z. Xia, Y. Chen, Q. Fan, and M. Xue, "Oxidative stress-mediated reperfusion injury: mechanism and therapies," *Oxidative Medicine and Cellular Longevity*, vol. 2014, Article ID 373081, 2 pages, 2014.

[22] M. Valko, D. Leibfritz, J. Moncol, M. T. D. Cronin, M. Mazur, and J. Telser, "Free radicals and antioxidants in normal physiological functions and human disease," *International Journal of Biochemistry and Cell Biology*, vol. 39, no. 1, pp. 44–84, 2007.

[23] W. Dröge, "Free radicals in the physiological control of cell function," *Physiological Reviews*, vol. 82, no. 1, pp. 47–95, 2002.

[24] Y. Wang, X. Li, X. Wang et al., "Ginsenoside Rd attenuates myocardial ischemia/reperfusion injury via Akt/GSK-3β signaling and inhibition of the mitochondria-dependent apoptotic pathway," *PLoS ONE*, vol. 8, no. 8, Article ID e70956, 2013.

[25] B. S. Cain, D. R. Meldrum, C. A. Dinarello et al., "Tumor necrosis factor-α and interleukin-1β synergistically depress human myocardial function," *Critical Care Medicine*, vol. 27, no. 7, pp. 1309–1318, 1999.

[26] M. Sugano, T. Hata, K. Tsuchida et al., "Local delivery of soluble TNF-alpha receptor 1 gene reduces infarct size following ischemia/reperfusion injury in rats," *Molecular and Cellular Biochemistry*, vol. 266, no. 1-2, pp. 127–132, 2004.

[27] P. Korge, P. Ping, and J. N. Weiss, "Reactive oxygen species production in energized cardiac mitochondria during hypoxia/reoxygenation: modulation by nitric oxide," *Circulation Research*, vol. 103, no. 8, pp. 873–880, 2008.

[28] T. Miura and T. Miki, "GSK-3β, a therapeutic target for cardiomyocyte protection," *Circulation Journal*, vol. 73, no. 7, pp. 1184–1192, 2009.

[29] A. Wyllie, "Clues in the p53 murder mystery," *Nature*, vol. 389, no. 6648, pp. 237–238, 1997.

[30] P. Korge, H. M. Honda, and J. N. Weiss, "Protection of cardiac mitochondria by diazoxide and protein kinase C: implications for ischemic preconditioning," *Proceedings of the National Academy of Sciences of the United States of America*, vol. 99, no. 5, pp. 3312–3317, 2002.

[31] V. Borutaite, A. Jekabsone, R. Morkuniene, and G. C. Brown, "Inhibition of mitochondrial permeability transition prevents mitochondrial dysfunction, cytochrome c release and apoptosis induced by heart ischemia," *Journal of Molecular and Cellular Cardiology*, vol. 35, no. 4, pp. 357–366, 2003.

[32] S.-S. Park, H. Zhao, Y. Jang, R. A. Mueller, and Z. Xu, "N^6-(3-Iodobenzyl)-adenosine-5′-N-methylcarboxamide confers cardioprotection at reperfusion by inhibiting mitochondrial permeability transition pore opening via glycogen synthase kinase 3β," *Journal of Pharmacology and Experimental Therapeutics*, vol. 318, no. 1, pp. 124–131, 2006.

[33] J. Feng, E. Lucchinetti, P. Ahuja, T. Pasch, J.-C. Perriard, and M. Zaugg, "Isoflurane postconditioning prevents opening of the mitochondrial permeability transition pore through inhibition of glycogen synthase kinase 3β," *Anesthesiology*, vol. 103, no. 5, pp. 987–995, 2005.

[34] H. K. Gao, Z. Yin, N. Zhou, X. Y. Feng, F. Gao, and H. C. Wang, "Glycogen synthase kinase 3 inhibition protects the heart from acute ischemia-reperfusion injury via inhibition of inflammation and apoptosis," *Journal of Cardiovascular Pharmacology*, vol. 52, no. 3, pp. 286–292, 2008.

Hindawi Publishing Corporation
Oxidative Medicine and Cellular Longevity
Volume 2015, Article ID 167014, 15 pages
http://dx.doi.org/10.1155/2015/167014

Research Article

Propofol Attenuates Small Intestinal Ischemia Reperfusion Injury through Inhibiting NADPH Oxidase Mediated Mast Cell Activation

Xiaoliang Gan,[1,2] Dandan Xing,[1] Guangjie Su,[1] Shun Li,[1] Chenfang Luo,[1] Michael G. Irwin,[3] Zhengyuan Xia,[3] Haobo Li,[3] and Ziqing Hei[1]

[1] *Department of Anesthesiology, The Third Affiliated Hospital, Sun Yat-sen University, Guangzhou 510630, China*
[2] *Zhongshan Ophthalmic Center, Department of Anesthesiology, Sun Yat-sen University, Guangzhou 510060, China*
[3] *Department of Anesthesiology, University of Hong Kong, Hong Kong*

Correspondence should be addressed to Haobo Li; haoboli@hku.hk and Ziqing Hei; heiziqing@sina.com

Received 18 July 2014; Accepted 7 September 2014

Academic Editor: Mengzhou Xue

Both oxidative stress and mast cell (MC) degranulation participate in the process of small intestinal ischemia reperfusion (IIR) injury, and oxidative stress induces MC degranulation. Propofol, an anesthetic with antioxidant property, can attenuate IIR injury. We postulated that propofol can protect against IIR injury by inhibiting oxidative stress subsequent from NADPH oxidase mediated MC activation. Cultured RBL-2H3 cells were pretreated with antioxidant N-acetylcysteine (NAC) or propofol and subjected to hydrogen peroxide (H_2O_2) stimulation without or with MC degranulator compound 48/80 (CP). H_2O_2 significantly increased cells degranulation, which was abolished by NAC or propofol. MC degranulation by CP further aggravated H_2O_2 induced cell degranulation of small intestinal epithelial cell, IEC-6 cells, stimulated by tryptase. Rats subjected to IIR showed significant increases in cellular injury and elevations of NADPH oxidase subunits $p47^{phox}$ and $gp91^{phox}$ protein expression, increases of the specific lipid peroxidation product 15-F_{2t}-Isoprostane and interleukin-6, and reductions in superoxide dismutase activity with concomitant enhancements in tryptase and β-hexosaminidase. MC degranulation by CP further aggravated IIR injury. And all these changes were attenuated by NAC or propofol pretreatment, which also abrogated CP-mediated exacerbation of IIR injury. It is concluded that pretreatment of propofol confers protection against IIR injury by suppressing NADPH oxidase mediated MC activation.

1. Introduction

Small intestinal ischemia reperfusion (IIR) injury has been emerged in many pathophysiological settings, including septic and hemorrhagic shock induced hypoperfusion [1], as well as acute mesenteric ischemia [2] and small intestine transplantation or liver resection [3]. IIR remains to be a critical problem associated with high mortality [4].

During IIR, oxidative stress is increased due to burst production of reactive oxygen species (ROS), which is a major mechanism of IIR injury [5]. Numerous studies have revealed that increased ROS production resulted from overactivation of the prooxidant enzyme NADPH oxidase, which abundantly exists in intestine tissue [6] and plays critical roles in mediating tissue injury related to a range of inflammatory diseases [7], including ischemia reperfusion injury [8, 9]. Inhibition of NADPH oxidase by N-acetylcysteine (NAC), a scavenger of oxygen radicals, has been shown to greatly attenuate myocardial ischemia reperfusion injury [10, 11]. However, the mechanism governing ROS production, specifically, from overactivation of NADPH oxidase, during IIR is yet to be explored.

Activation of NADPH oxidase can lead to mast cells (MC, cells that widely present throughout small intestine) degranulation/activation [12], wherever MCs activation has been demonstrated to be a key mediator in the pathogenesis of IIR and contributing to many disorders as a result of increased release a diverse range of mediators including histamine, tryptase, and inflammatory cytokines such as interleukin-6 (IL-6) [13] and that inhibition of MCs from degranulation

can alleviate IIR injury [14, 15]. We have previously found that ROS production was significantly increased after IIR which is parallel with the enhancements in MC degranulation [16], but it is unknown whether a causal relationship exists between increased ROS production and MC degranulation in the setting of IIR *in vivo*. These findings [6, 17] together with reports showing that MC can be activated in a ROS-dependent pathway [18], both *in vitro* [18] and *in vivo* [16], prompted us to postulate that during IIR increased ROS production initiates and/or exacerbates IIR injury primarily via activating MC and that NADPH oxidase activation is increased during IIR which may be a major source of ROS overproduction during IIR.

Propofol, an intravenous anesthetic with antioxidant property that we widely used in intensive care unit and operation theatre, has been shown to dose-dependently attenuate myocardial ischemia reperfusion injury in patients [19]. Propofol has also been shown to inhibit mast cell exocytosis in a dose-dependent manner *in vitro* [20]. A most recent study shows that propofol attenuates brain trauma induced cerebral injury through inhibiting NADPH oxidase activation [21]. We, therefore, hypothesized that inhibition of ROS mediated MC activation subsequent to attenuation of intestinal NADPH oxidase activation may represent a major mechanism by which propofol attenuates IIR injury. This hypothesis was tested in a rat model of mesenteric ischemia reperfusion *in vivo* and a rat cell line of mast cell exposed to ROS *in vitro*.

2. Materials and Methods

2.1. Cell Culture. Rat mast cell line (RBL-2H3) was purchased from the cell bank of the Chinese Academy of Sciences (Shanghai, China) and was cultured in Eagle's minimum essential medium containing 10% fetal bovine serum, supplemented with 100 U/mL penicillin and 100 μg/mL streptomycin at 37°C in a humidified atmosphere of 5% CO_2 as described [22]. A rat small intestinal epithelial cell line (IEC-6) was also obtained from the cell bank of the Chinese Academy of Sciences (Shanghai, China). This cell line was cultured in 1640 RPMI medium with 10% fetal bovine serum at 37°C in a 5% CO_2 incubator.

2.2. Measurement of Cell Degranulation. Degranulation of RBL-2H3 cells was measured by determining the activity of released β-hexosaminidase in the culture supernatants and cell lysates [23]. The RBL-2H3 cells were incubated with different concentrations of NAC [24] or propofol [20] for 12 h; after the cells were washed with 1 × PBS for 3 times, RBL-2H3 cells were incubated in a 24-well plate (1×10^6 cells/well) at 37°C overnight. The above cells were washed with 1 × PBS and then incubated with different concentrations of lipopolysaccharides (LPS) [25] or H_2O_2 [26] or Compound 48/80 [27] for 1 h or 4 h. To measure the amount of β-hexosaminidase activity released from the cells, the cultured media were transferred and centrifuged at 4°C. The supernatant (25 μL) was mixed with 50 μL p-NAG (10 mM) in 0.1 M sodium citrate buffer (pH 4.5) into a 96-well plate and incubated for 1 h at 37°C. The reaction was terminated by the addition of stop buffer (0.1 M sodium carbonate buffer, pH 10.0). The β-hexosaminidase activity was determined by measuring the difference of absorbance at wavelength 405 nm.

2.3. Measurement of Cell Viability. IEC-6 cells were seeded into 96-well flat bottom culture plates at a density of 5×10^4 cells/well and incubated for 24 h. After exposure to tryptase (0–1000 ng/mL) for 12 h in RPMI 1640 culture medium, the cell viability was measured by modified MTT assay as described [28]. The assay detected the reduction of the tetrazolium to formazan product. The cell viability was evaluated using the following formula. Survival rate (%) = $(A_{\text{sample}} - A_{\text{blank}})/(A_{\text{control}} - A_{\text{blank}}) \times 100\%$.

2.4. Assessment of Cell Cytotoxicity. Cytotoxicity (cell necrosis) was assessed by measuring the release of lactate dehydrogenase (LDH). After exposure of the cells to various concentrations of tryptase (0–1000 ng/mL) for 2 h in RPMI 1640 culture medium, cell necrosis was assessed by LDH-release assay using a commercial kit (Jiancheng, China) according to the manufacturer's instruction.

2.5. Animals. Female Sprague-Dawley (SD) rats weighing 180–200 g, purchased from Animal Center of Guangdong Province (Guangzhou, China), were housed individually in wire-bottomed cages and were placed under pathogen free condition illuminated from 8:00 AM to 8:00 PM (12:12 h light-dark cycle) for one week before use. The experimental protocol and design was approved by the Sun Yat-sen University Animal Experimentation Committee and performed according to Sun Yat-sen University Guidelines for Animal Experimentation.

2.6. In Vivo Rat IIR Model and Treatments. All the ani mals were fasted for 16 h (while free access to water was allowed) before surgery. Rats were, respectively, injected with N-acetylcysteine (NAC, 0.5 g/kg, from Sigma company), propofol (50 mg/kg, commercial product Diprivan from AstraZeneca), intralipid (50 mg/kg, 20%, emulsion from Sigma), or normal saline (0.5 mL/100 g), which served as the control group, intraperitoneally at 6:00 PM for 3 successive days. The dosages of NAC were chosen based on the results showing that treatment of rats with i.p. NAC (500 mg kg^{-1} per day for 9 days) improved the renal hemodynamic changes triggered by cisplatin-mediated nephrotoxicity [29]. The dose of propofol was chosen based on the finding that propofol 50 mg/kg given intraperitoneally provided sedative effect but not anesthetic effect [30] and that propofol when used at this dosage attenuated IIR injury in rats [31]. At the 4th day, parts of the rats were sacrificed by overdose of anesthetic chloral hydrate, and the intestinal mucous was obtained and scraped for further determination and the intestinal morphological changes were assessed.

2.7. Experimental Groups. The other rats were divided into the following groups.

(1) Sham-operated group (SHAM) ($n = 6$): rats pretreated with normal saline (10 mL/kg, i.p.) were subjected to identical surgical procedures except for superior mesenteric artery (SMA) occlusion for 75 min and were kept under anesthesia during the experiment and were administrated with the same volume of normal saline (1 mL/kg, i.v.) as reagent solvent control.

(2) Sole IIR group (IIR) ($n = 6$): rats pretreated with normal saline (10 mL/kg, i.p.) were subjected to small intestinal ischemia by occluding SMA (75 min), followed by reperfusion (2 h) plus administration of normal saline (1 mL/kg, i.v.) 5 min immediately before reperfusion.

(3) IIR + Compound 48/80 group (IIR + CP) ($n = 12$): rats pretreated with normal saline (10 mL/kg, i.p.) were subjected to small intestinal ischemia by occluding SMA (75 min), followed by reperfusion (2 h) plus administration of Compound 48/80 (0.75 mg/kg, i.v.) dissolved in normal saline (1 mL/kg) 5 min immediately before reperfusion.

(4) NAC + IIR group (NAC + IIR) ($n = 6$): rats pretreated with NAC (0.5 g/kg, i.p./day) dissolved in normal saline (10 mL/kg) for 3 successive days were subjected to small intestinal ischemia by occluding SMA (75 min), followed by reperfusion (2 h) plus administration of normal saline (1 mL/kg, i.v.).

(5) NAC + IIR + Compound 48/80 group (NAC + IIR + CP) ($n = 6$): rats pretreated with NAC (0.5 g/kg, i.p.) were subjected to small intestinal ischemia by occluding SMA (75 min), followed by reperfusion (2 h) plus administration of Compound 48/80 (0.75 mg/kg, i.v.).

(6) Propofol + IIR group (Pro + IIR) ($n = 6$): rats pretreated with propofol (50 mg/kg, i.p./day) dissolved in intralipid (10 mL/kg) for 3 successive days were subjected to small intestinal ischemia by occluding SMA (75 min), followed by reperfusion (2 h) plus administration of normal saline (1 mL/kg, i.v.).

(7) Propofol + IIR + Compound 48/80 group (Pro + IIR + CP) ($n = 6$): rats pretreated with propofol (50 mg/kg, i.p.) were subjected to small intestinal ischemia by occluding SMA (75 min), followed by reperfusion (2 h) plus administration of Compound 48/80 (0.75 mg/kg, i.v.).

(8) Intralipid + IIR group (Lip + IIR) ($n = 12$): rats pretreated with intralipid (50 mg/kg, i.p.) (with a volume of 10 mL/kg) were subjected to small intestinal ischemia by occluding SMA (75 min), followed by reperfusion (2 h) plus administration of normal saline (1 mL/kg, i.v.).

(9) Intralipid + IIR + Compound 48/80 group (Lip + IIR + CP) ($n = 12$). rats pretreated with intralipid (50 mg/kg, i.p.) were subjected to small intestinal ischemia by occluding SMA (75 min), followed by reperfusion (2 h) plus administration of Compound 48/80 (0.75 mg/kg, i.v.).

It is of notice that, with respect to the low survival rate in rats that underwent IIR in the presence of CP, experiments were performed on a total of 12 animals in IIR + CP and IIR + CP + intralipid groups. In all the experimental groups, the rats were anesthetized by intraperitoneal injection of 10% chloral hydrate (3.5 mL/kg) after fasting for 16 h. The Compound 48/80 (Sigma, USA; 0.75 mg/kg) or the same volume of physiological saline was intravenously injected via the tail vein at 5 min before reperfusion. The doses of agents were adjusted in accordance with our previous study [15]. During the surgery, all the rat body temperature was maintained at 38°C using heated pad. And 10 mL/kg 37°C normal saline was injected subcutaneously to avoid dehydration after the abdomen had been closed.

2.8. Collection of Intestinal Mucosa. Upon the completion of the abovementioned treatments and experiments, the rats were anesthetized and then euthanized. The whole small intestine was removed carefully, and a segment of 1.0 cm intestine (located at 10 cm away from the terminal ileum) was cut and fixed in 10% formaldehyde and then embedded in paraffin for section. The remaining small intestine was washed thoroughly with 0°C normal saline and then opened longitudinally to expose the intestinal epithelium, after being rinsed completely with 0°C normal saline and dried with suction paper. The mucosal layer was harvested by gentle scraping of the epithelium with a glass slide with a plate on the ice and then was stored at −70°C for further measurements.

2.9. Intestinal Histology. Five μm thick sections were prepared from paraffin-embedded intestine tissue; the segment of small intestine was stained with hematoxylin-eosin. And the damage of intestinal mucosa was evaluated by two histologists blinded to the experiment according to Chiu's standard [32]: Grade 0, normal mucosa; Grade 1, development of subepithelial Gruenhagen's space at the tip of villus; Grade 2, extension of the space with moderate epithelial lifting; Grade 3, massive epithelial lifting with a few denuded villi; Grade 4, denuded villi with exposed capillaries; Grade 5, disintegration of the lamina propria, ulceration, and hemorrhage.

2.10. Detection of 15-F_{2t}-Isoprostane Content in the Small Intestinal Mucosa. Small intestinal mucosa was homogenized with normal saline. The tissue content of free 15-F_{2t}-isoprostane, an index of *in vivo* oxidative stress-induced lipid peroxidation, was measured using commercial immunoassay kits (Cayman Chemical, Ann Arbor, MI) as we described [33].

2.11. Assay of Superoxide Dismutase (SOD) Activity and Hydrogen Peroxide Content in Small Intestinal Mucosa. Small intestinal mucosa was made into a homogenate with normal saline, frozen at −20°C for 5 min, and centrifuged for 15 min at 4000 r/min. Supernatants were transferred into fresh tubes for evaluation of SOD activity and hydrogen

peroxide content. SOD activity and hydrogen peroxide content were assessed by SOD and hydrogen peroxide detection kits according to the manufacturer's instructions (Jiancheng Bioengineering Ltd, Nanjing, China). Presented data were normalized to tissue weight.

2.12. Measurement of β-Hexosaminidase Level in Serum. β-hexosaminidase level in the serum was determined using modification of a previously described method [34]. Briefly, 50 μL of serum was incubated with 50 μL of 1 mM p-nitrophenyl-N-acetyl-β-D-glucosaminide dissolved in 0.1 M citrate buffer (pH 5) in a 96-well plate at 37°C for 1 h. The reaction was terminated with 200 μL/well of 0.1 M carbonate buffer (pH 10.5). The absorbance at 405 nm was measured using a Microplate reader.

2.13. Western Blotting. Intestinal mucosa samples were homogenized with lysis buffer for 30 seconds in a mortar and pestle with liquid nitrogen. Homogenates were centrifuged at 13000 rpm for 10 min at 4°C and the supernatant was collected as the source of protein sample. The proteins were processed with standard methods for Western blot analysis as described [10]. Rat monoclonal anti-tryptase antibody, rat monoclonal anti-gp91^{phox} and anti-p47^{phox} antibodies, rat monoclonal anit-P-selectin and anti-ICAM-1 antibodies, and α-tubulin antibody were obtained from Santa Cruz (Santa Cruz, CA, USA). The secondary antibody conjugated to horseradish peroxidase was diluted at 1 : 2,000 (Santa Cruz, USA). Immunoblots were incubated with an enhanced chemiluminescence detection system (KeyGen Biotech, China) and the densitometry analysis was performed using Quantity One software.

2.14. Determination of IL-6 Production in Small Intestinal Mucosa by Enzyme Immunoassay. Intestinal mucosa tissues were made into homogenates with frozen normal saline and spun at 4000 r/min for 15 minutes. Supernatants were then transferred into fresh tubes for detection of IL-6 contents. Briefly, intestinal protein was measured by BCA Protein Assay Kit provided by KenGen Biotech Company, Nanjing, China, and the protein contents were expressed as g/L. The levels of IL-6 were measured using commercial ELISA kits following manufacturer's instructions (R&D systems Inc, USA). The absorbance was read at 450 nm by a Biokinetics microplate reader Model EL340 (Biotek Instruments, USA), and the results were expressed as ng/L; then the final levels of IL-6 in the intestine were calculated as ng/g protein.

2.15. Determination of Myeloperoxidase (MPO) Activity in Small Intestinal Mucosa. Myeloperoxidase (MPO) activity was determined with the O-dianisidine method [35], using a MPO detection kit (Nanjing Jiancheng Bioengineering Institute) as we described [36]. MPO activity was defined as the quantity of enzyme degrading 1 μmol of peroxide per minute at 37°C and was expressed in units per gram weight of wet tissue.

2.16. Statistical Analysis. The data (except for the survival rates) were expressed as Mean ± SEM. All biochemical assays were performed in duplicate. Analysis of variance was performed using Graphpad Prism software. One-way analysis of variance was used for multiple comparisons, followed by Bonferroni's Student's *t*-test for unpaired values. The survival rate was expressed as the percentage of live animals, and the Mantel Cox log rank test was used to determine differences between groups. Differences were considered significant when *P* values were less than 0.05.

3. Results

3.1. Oxidative Stress but Not LPS-Induced RBL-2H3 Cell Degranulation Can Be Reversed by NAC and Propofol Pretreatments. Bacterial translocation and oxidative stress are the two characterizations of small IIR [37], and our previous study showed that mast cell (MC) degranulation could exacerbate the injury [14]. Therefore, in the current study, we initially sought to explore whether bacteria and oxidative stress can induce MC degranulation. As shown in Figure 1, exposure of the RBL-2H3 to different concentrations of LPS for 1 or 4 h did not cause significant changes in the release of β-hexosaminidase activities as compared with the control group (Figure 1(a)) whereas MC activator Compound 48/80 significantly increased the released β-hexosaminidase activities as compared with the control group (Figure 1(b)). This result indicates that LPS *per se* has no effects on MC degranulation at least in this experimental setting. However, treatment of RBL-2H3 cell with H_2O_2 dose-dependently increased the activity of the released β-hexosaminidase (Figure 1(c)). Pretreatments with NAC, a scavenger of oxygen radicals, abolished H_2O_2 mediated elevations of the released β-hexosaminidase activities (Figure 1(d)). Similarly, pretreatment with propofol, but not intralipid (propofol solvent), abrogated the enhancements of the released β-hexosaminidase activities induced by H_2O_2 (Figure 1(e)), indicating that oxidative stress contributes to MC degranulation and propofol inhibits MC degranulation via its antioxidant property.

3.2. Tryptase Contributed to Small Intestinal Epithelium Injury. Tryptase, the unique mediator released from MC degranulation [38], plays a critical role in the IIR mediated acute lung injury *in vivo* [15]. Therefore, we sought to define the direct role of tryptase in the small intestinal epithelium injury *in vitro*. A small intestinal epithelial cell line IEC-6 was employed and exposed to different concentrations of tryptase. The results showed that tryptase could directly cause IEC-6 injury in a dose-dependent manner manifested as dramatic increases in LDH activities and concomitant reductions in cell viability as compared with the control group (Figures 1(f) and 1(g)).

3.3. NAC, Propofol, and Intralipid Pretreatments Did Not Affect Small Intestinal Structure before IIR. First, we sought to assess if pretreatment of rats with NAC, propofol, or intralipid may cause significant intestinal injury. At the dosages used, neither

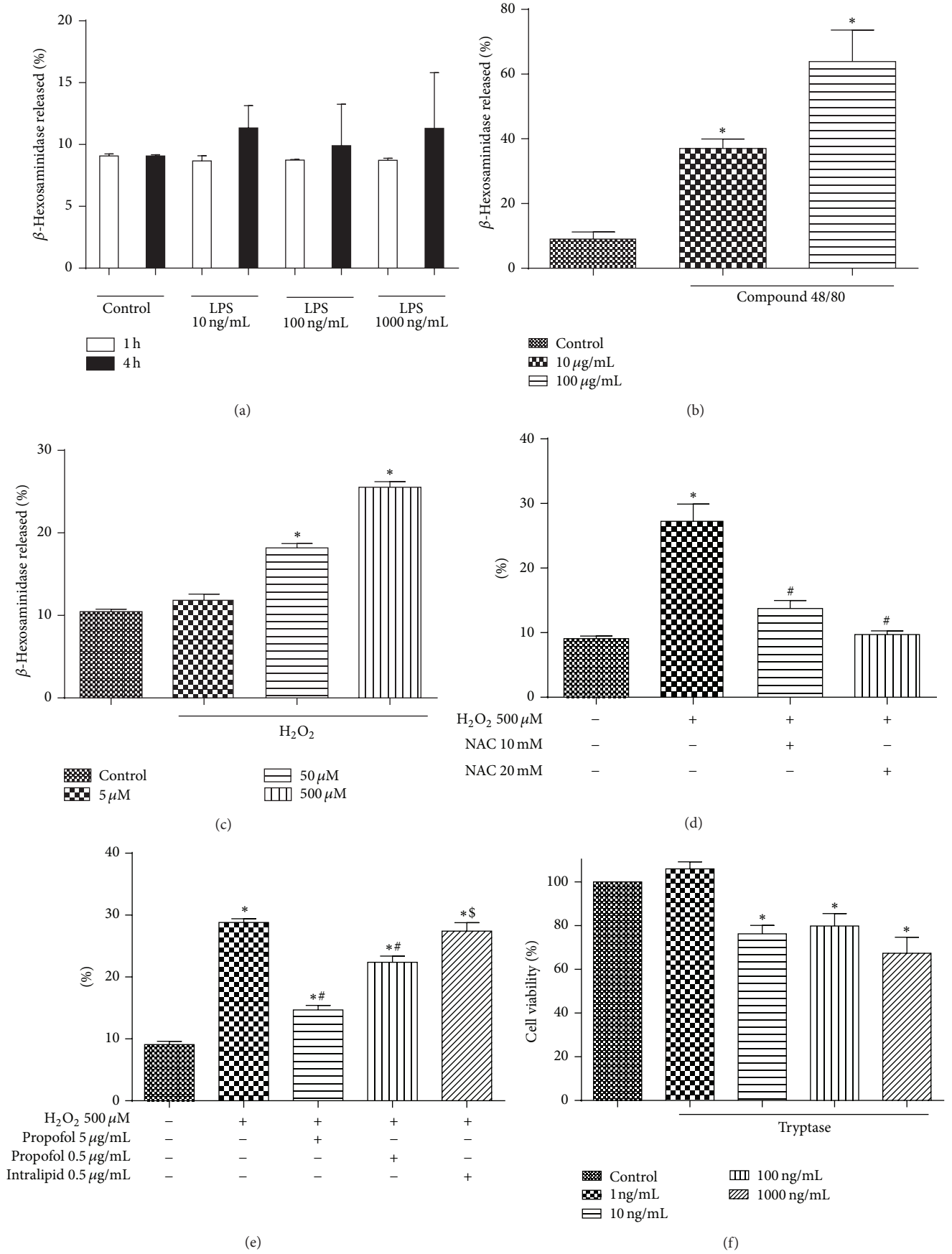

Figure 1: Continued.

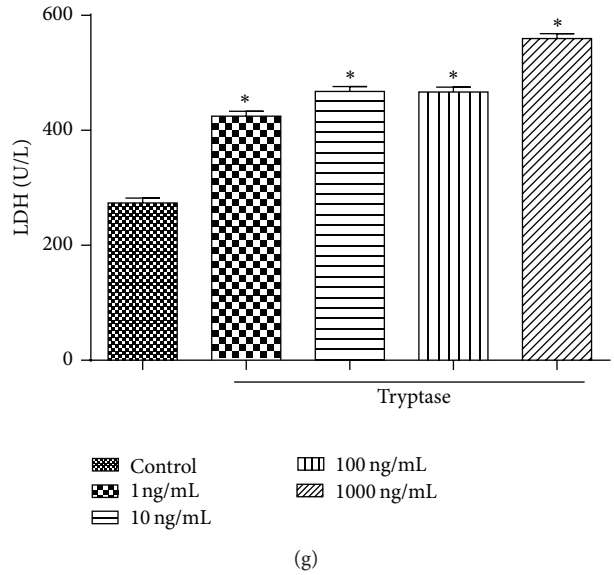

Figure 1: Effects of LPS, Compound 48/80, and hydrogen peroxide (H_2O_2) on the degranulation of RBL-2H3 cells with or without NAC or propofol treatment. (a) β-Hexosaminidase release after LPS treatment for 1 h or 4 h, (b) β-hexosaminidase release after Compound 48/80 stimulation for 1 h, and (c) β-hexosaminidase release after H_2O_2 treatment for 1 h. (d) and (e) quantified the degranulation of RBL-2H3 cells, pretreated with NAC or propofol for 12 h, induced by H_2O_2 stimulation for 1 h, respectively. (f) Cell viability of IEC-6 cells treated with tryptase for 12 h. Results were expressed as percentage of control group; error bars represented the standard error of the mean. (g) Lactate dehydrogenase (LDH) activity of IEC-6 cells treated with tryptase for 2 h. Results were expressed as Mean ± SEM. $^*P < 0.05$ versus control group, $^\#P < 0.05$ versus H_2O_2 500 μM group, $^\$P < 0.05$ versus propofol 0.5 μg/mL group.

NAC nor propofol or intralipid caused any challenges to small intestinal structure as compared to that in rats treated with normal saline (NS). As shown in Figure 2, all the layers of intestine were normal in all the groups and there was no significant difference among groups in terms of injury score (Figure 2(d)).

3.4. NAC and Propofol but Not Intralipid Pretreatment Altered Intestinal Oxidant and Antioxidant Levels before IIR. NAC and propofol are well known for their antioxidative properties [10, 39]. As shown in Figure 3, NAC and propofol similarly attenuated oxidant level as demonstrated by significant decreases in 15-F_{2t}-isoprostane (Figure 3(a)) contents and increases in SOD activities (Figure 3(b)) in small intestinal mucosa as compared with NS treated group. In addition, NAC and propofol pretreatment led to significant reductions in protein expressions of $gp91^{phox}$ and $p47^{phox}$, the important components of NADPH enzymes, in small intestinal mucosa compared with NS treated group before IIR (Figures 3(c)–3(e)). By contrast, intralipid showed comparative results to NS treated group. The data indicated that propofol, at the dose used, confers similar antioxidant effects to that of NAC.

3.5. NAC, Propofol, and Intralipid Pretreatments Did Not Activate Mast Cell before IIR. Trypatse and β-hexosaminidase are specific markers for the assessment of mast cells degranulation [40]. As shown in Figures 3(f) and 3(g), NAC, propofol, or intralipid alone had no significant effect on mast cell degranulation. There were no significant differences in tryptase protein expressions in small intestinal mucosa and β-hexosaminidase levels among all pretreated groups before IIR. The findings from the current study indicated that NAC and propofol pretreatments can substantially ameliorate superoxide productions without affecting mast cell and small intestine morphology under normal condition.

3.6. NAC and Propofol Improved Reduction of Survival Rates in Rats Challenged to IIR through Inhibiting Mast Cell Activation. We, next, sought to investigate the effects of NAC and propofol in combating IIR and inhibiting mast cell in the process of IIR injury. As illustrated in Figure 4(a), activation of mast cell by Compound 48/80 resulted in significant decreases in 2 h survival rates after the clamp releasing as compared with sole IIR group. By contrast, NAC and propofol pretreatments showed similar promising benefits in reducing mast cell degranulation mediated injury during 2 h reperfusion period evidenced as increased postischemic 2 h survival rates to 100% (Figure 4(b)). Intralipid did not attenuate Compound 48/80 mediated exacerbation of postischemic survival rate in rats subjected to IIR (Figure 4(c)). These data suggested that oxidative stress is a major mechanism whereby mast cell degranulation exacerbated IIR injury.

3.7. NAC and Propofol Attenuated Small Intestinal Injury in Rats Undergoing IIR through Inhibiting Mast Cell Activation. After 2 h reperfusion, the sections of small intestine were evaluated by HE staining; IIR induced severe damage to small intestine. As depicted in Figures 4(d) and 4(e), multiple erosions and bleeding were observed in IIR group, while Compound 48/80 further aggravated IIR injury manifested

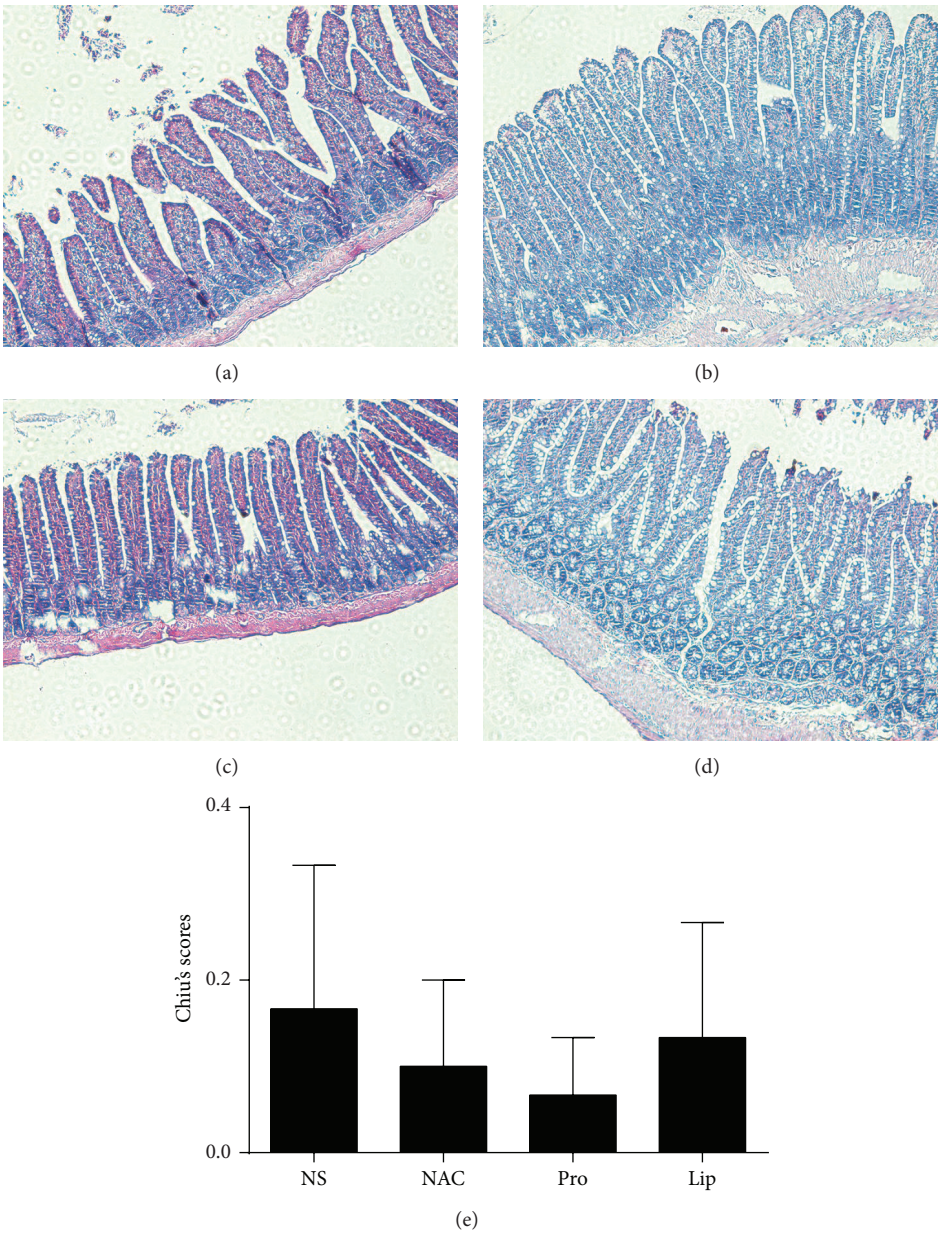

Figure 2: Morphological changes of intestine under light microscope in rats treated with NAC, propofol, or intralipid. ((a)–(d)) Representative images of rats treated with normal saline (NS), NAC (0.5 g/kg, i.p.), propofol (50 mg/kg, i.p.), and intralipid (50 mg/kg, i.p.) prior to ischemia reperfusion (HE staining, ×200). (e) quantified the intestine histological scores in normal saline pretreated group (NS), NAC pretreated group (NAC), propofol pretreated group (Pro), and intralipid pretreated group (Lip). Results are expressed as Mean ± SEM. $n = 3$ per group.

as more multiple erosions and bleedings and more inflammatory cell sequestrations seen in the IIR + CP group, whereas the villus and glands were normal and no inflammatory cell infiltration was observed in mucosal epithelial layer in Sham-operated group. NAC and propofol similarly and significantly reduced the injuries in small intestine and only slight edema of mucosa villus and infiltration of few necrotic epithelial inflammatory cells were found in mucosa epithelial layer. Moreover, NAC and propofol pretreatments blocked Compound 48/80 induced exacerbation in small intestinal morphology changes after 2 h reperfusion. In contrast, pretreatment with intralipid could not attenuate IIR and Compound 48/80 induced injury. Consistent with morphological changes, Chiu's scores markedly increased in IIR group as compared with Sham-operated group while treatment with mast cell degranulator Compound 48/80 after ischemia led to further increases in Chiu's scores. NAC and propofol similarly dramatically lowered Chiu's scores and significantly limited the changes induced by Compound 48/80 ($P < 0.05$, NAC + IIR + CP or propofol + IIR + CP versus IIR + CP group). Of

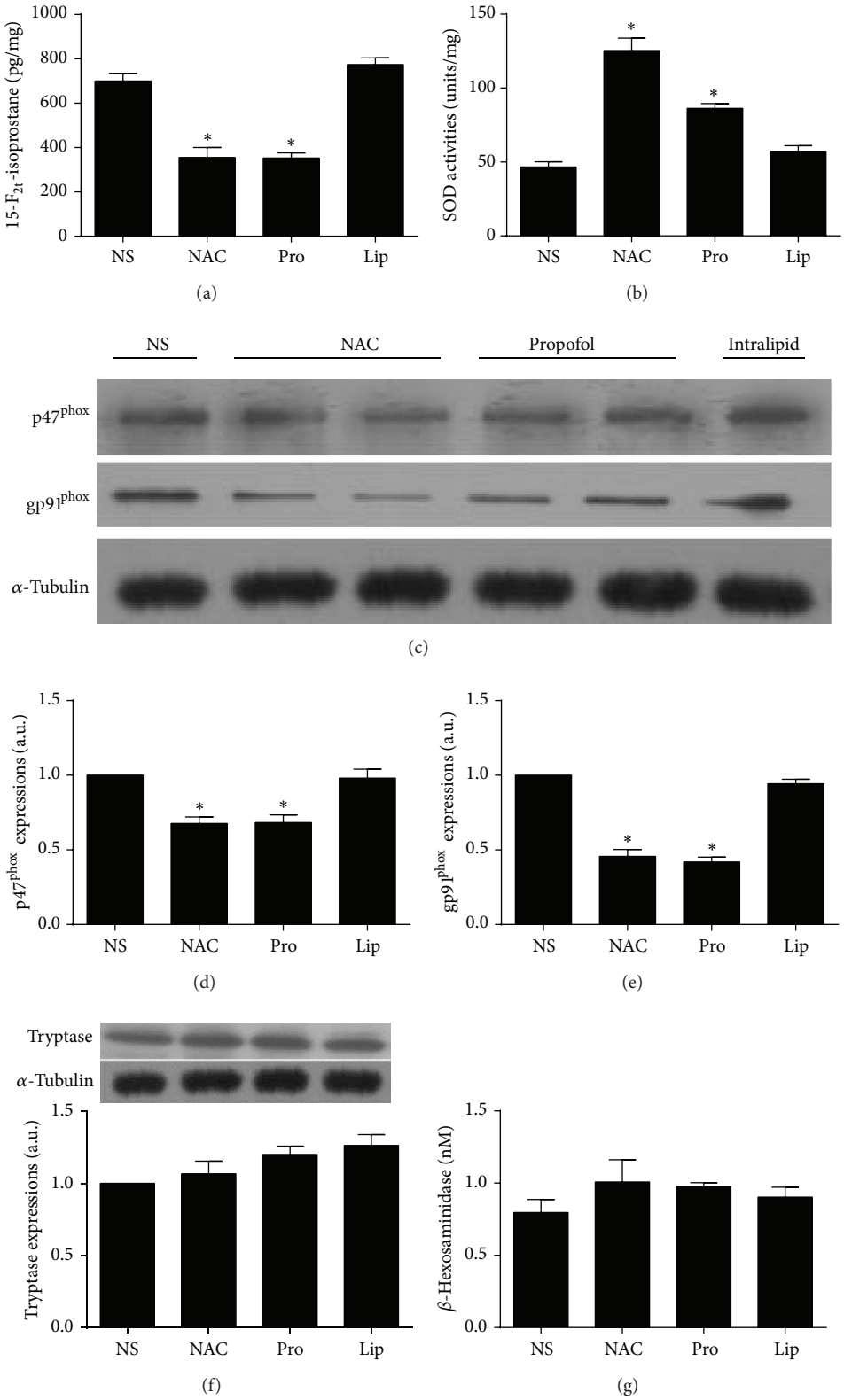

FIGURE 3: Changes of 15-F_{2t}-isoprostane contents, SOD activities, $p47^{phox}$ and $gp91^{phox}$ protein expressions in intestine mucosa, and intestinal tryptase protein expression, and serum β-hexosaminidase levels in rats treated with NAC, propofol, and intralipid. (a) 15-F_{2t}-isoprostane contents, (b) SOD activities, ((c)–(e)) intestinal $p47^{phox}$ and $gp91^{phox}$ protein expressions, (f) tryptase protein expression, and (g) β-hexosaminidase levels in normal saline pretreated group (NS), NAC pretreated group (NAC), propofol pretreated group (Pro), and intralipid pretreated group (Lip) ($n = 3$). Results are expressed as Mean ± SEM. $^*P < 0.05$ versus NS.

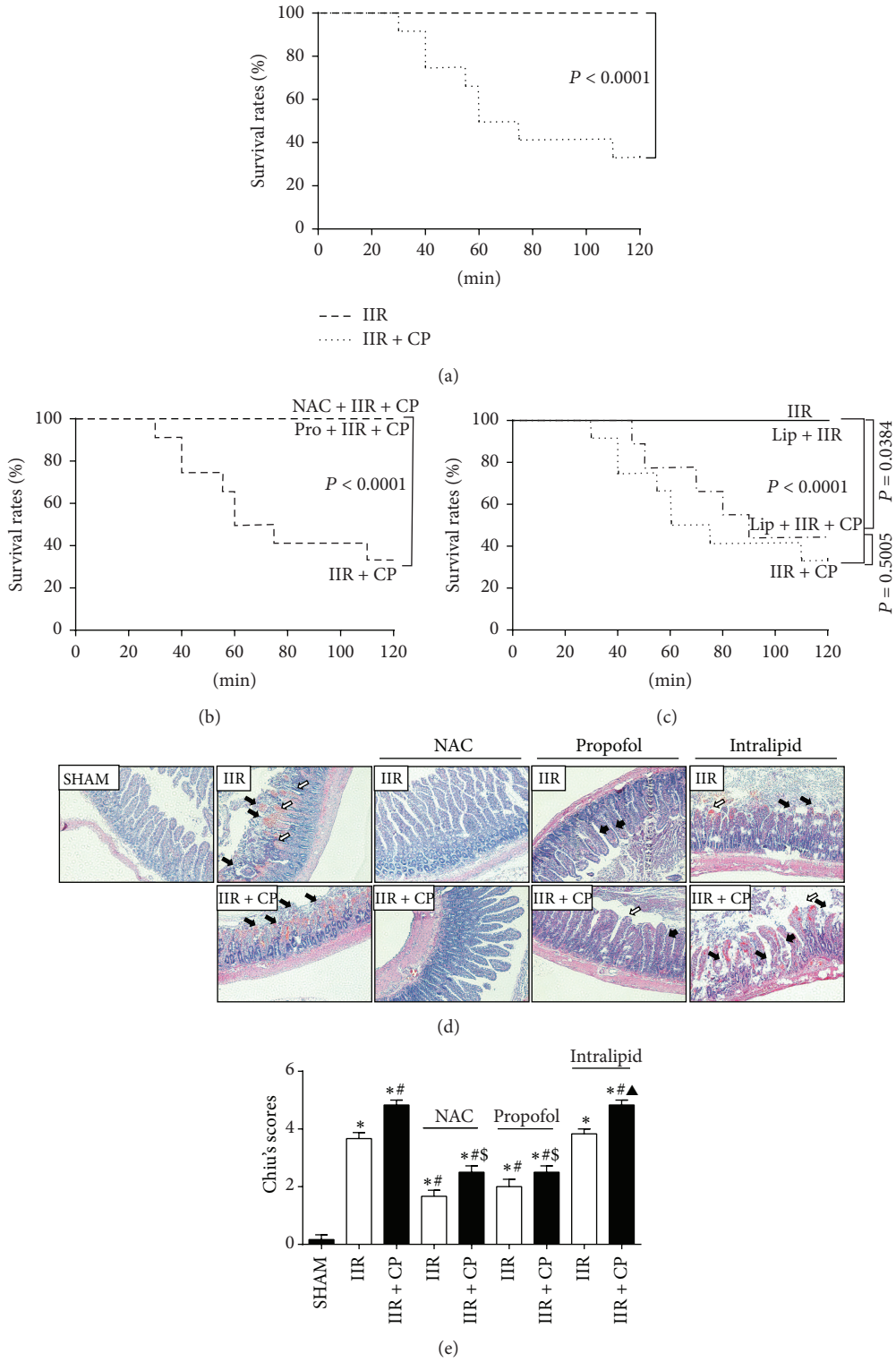

FIGURE 4: Survival rates and morphological changes of intestine and intestinal histological score under light microscope after IIR. SHAM group (Sham-operated group), IIR group (75 min intestinal ischemia and 2 h reperfusion), and IIR + CP group (IIR group + Compound 48/80 1 mg/kg) in the absence or presence of NAC (0.5 g/kg) or propofol (50 mg/kg) or intralipid (50 mg/kg). ((a)–(c)) Survival rats in rats subjected to IIR with or without NAC, propofol, or intralipid pretreatment. Results are expressed as percentage of live animals, $n = 6$ per group, whereas $n = 12$ in IIR + CP group and IIR + CP + intralipid group. (d) Representative images of HE staining (×200). Black arrow: lamina propria villus shedding. Red arrow: engorgement of capillary vessel. White arrow: top villus shedding. (e) quantified the intestine histological scores. Results are expressed as Mean ± SEM. $n = 6$ per group, whereas $n = 4$ in IIR + CP group. $^{*}P < 0.05$ versus SHAM group, $^{\#}P < 0.05$ versus IIR group, $^{\$}P < 0.05$ versus IIR + CP group, $^{\&}P < 0.05$ versus IIR with NAC pretreated group, $^{\triangle}P < 0.05$ versus IIR with propofol pretreated group, and $^{\blacktriangle}P < 0.05$ versus IIR with intralipid pretreated group.

note, there were no differences in Chiu's scores between IIR and intralipid pretreated groups.

3.8. NAC and Propofol Reduced Oxidative Stress in Small Intestine in Rats Undergoing IIR through Inhibiting Mast Cell Activation. Ischemia reperfusion injury is characterized by upregulation of ROS [10]. In line with previous results [16], we observed that 75 min ischemia followed by 2 h reperfusion led to substantial enhancements in 15-F_{2t}-isoprostane contents in small intestinal mucosa and marked reductions in SOD activities as compared with Sham-operated group (Figures 5(a) and 5(b)). Meanwhile, IIR also caused great increases in $gp91^{phox}$ and $p47^{phox}$ protein expression when compared with Sham-operated group. Moreover, Compound 48/80 further aggravated the changes of oxidative stress induced by IIR ($P < 0.05$ IIR + CP versus IIR). Not surprisingly, propofol and NAC similarly attenuated IIR mediated oxidative stress evidenced as downregulation of 15-F_{2t}-isoprostane contents and $gp91^{phox}$ and $p47^{phox}$ protein expression and upregulation of SOD activities in propofol and NAC treated groups as compared with group IIR. Furthermore, propofol and NAC pretreatments also limited the further increases of oxidative stress induced by Compound 48/80. As expected, intralipid did not show any antioxidative properties as the markers of oxidative stress measured were comparable between group IIR and group intralipid + IIR. Intralipid had no protective effect against Compound 48/80 induced upregulation of oxidative stress.

3.9. NAC and Propofol Attenuated Inflammation in Small Intestine in Rats Undergoing IIR through Inhibiting Mast Cell Activation. Interleukin 6 (IL-6) is one of the inflammatory cytokines that has been demonstrated to be implicated in the pathogenesis of IIR injury [41]. In the present study, we observed that IL-6 levels in small intestinal mucosa in group IIR were significantly increased as compared to that in the Sham-operated group (Figure 5(e)). Moreover, administration with Compound 48/80 further resulted in dramatic enhancements in IL-6 levels in group IIR + CP ($P < 0.05$ versus group IIR). Pretreatments with propofol and NAC not only similarly abrogated the increases in IL-6 levels, but also block the enhancements in IL-6 levels resulting from IIR in the presence of the MC activator Compound 48/80 (Figure 5(e)).

3.10. NAC and Propofol Inhibited Neutrophil Rolling in Small Intestine in Rats Undergoing IIR through Inhibiting Mast Cell Activation. IIR injury is also characterized by neutrophil sequestrating into the inflamed tissues [42]. Consistent with previous results [42], we also found that IIR led to substantial increases in MPO activities (Figure 5(f)) and ICAM-1 (Figure 5(g)) and P-selectin (Figure 5(h)) protein expressions as compared with Sham-operated group; moreover, Compound 48/80 resulted in further increases in MPO activities and P-selectin protein expression in group IIR + CP than that in group IIR. Administrations with propofol and NAC significantly inhibited neutrophil infiltration/activation evidenced as downregulation of MPO activities and P-selectin protein expression caused by IIR. Furthermore, propofol and NAC also blocked Compound 48/80 mediated exacerbation of IIR induced neutrophil infiltration.

3.11. NAC and Propofol Reduced Mast Cell Degranulation in Small Intestine in Rats Undergoing IIR. Mast cell releases a number of mediators that contribute to the aggravation of IIR injury, and there are many factors that can induce mast cell degranulation during IIR. Tryptase and β-hexosaminidase are the unique markers released from mast cell and their increased release can be recognized as mast cell degranulation. As shown in Figure 6, after 2 h reperfusion, we found that tryptase protein expression and β-hexosaminidase level were greatly increased in group IIR as compared with Sham-operated group, and Compound 48/80 resulted in further mast cell degranulation evidenced as dramatic increases in tryptase protein expression and β-hexosaminidase level observed in group IIR + CP relative to that in group IIR. Of note, propofol and NAC similarly inhibited mast cell degranulation by downregulating tryptase protein expression and β-hexosaminidase level triggered by IIR and Compound 48/80. Collectively, the findings from the current study indicated that oxidative stress mediated mast cell degranulation aggravated IIR injury and propofol through its antioxidative properties protects against IIR by stabilizing mast cell.

4. Discussion

We have shown in the current study that increased ROS during IIR exacerbated IIR injury primarily via activating mast cells evidenced as concomitant increases of postischemic 15-F_{2t}-isoprostane and elevations in tryptase and β-hexosaminidase and increases in intestinal injury score, leading to significantly reduced postischemic survival. Further, we showed that activation of intestinal NADPH oxidase is a major source of postischemic ROS production. Antioxidant NAC and propofol inhibited postischemic intestinal NADPH oxidase activation by reducing $gp91^{phox}$ and $p47^{phox}$ protein overexpression and reduced ROS and the subsequent mast cell activation *in vivo* and *in vitro*, which may represent the major mechanism whereby propofol attenuates IIR injury and enhances postischemic survival.

Mast cell (MC), which contains a diverse range of mediators, resides throughout gastrointestinal tract and is also known as intestinal mucosal mast cell (IMMC). Despite the fact that MC may function as host defense to prevent bacterial invasion [43], enhanced MC activation may contribute to the development of a variety of disorders including IIR injury by releasing histamine, tryptase, TNF-α, and other factors. It should be noted that MC is the main source of TNF-α in the tract [44]. Ramos et al. reported that mast cell degranulation plays a significant role in the development of sepsis by regulating cell death, which resulted in multiorgan dysfunction [45]. Consistent with the previous studies showing that stabilizing MC from degranulation would be one of the potential strategies in combating IIR injury [14], our current study further revealed that increased oxidative stress during IIR plays an important role in mast cell activation/degranulation

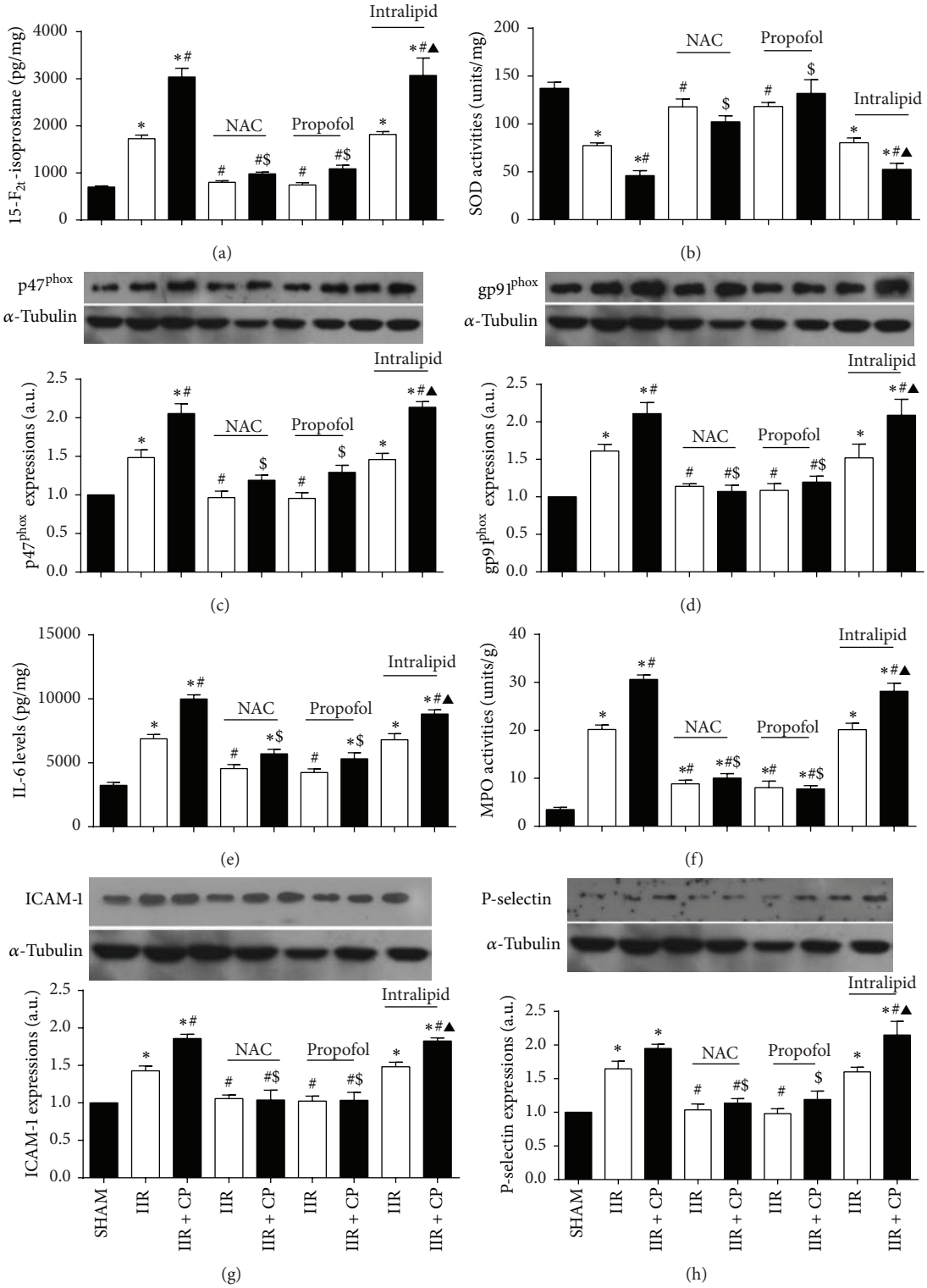

Figure 5: Changes of SOD activities, 15-F_{2t}-isoprostane contents, $p47^{phox}$ protein expression, $gp91^{phox}$, P-selectin, and ICAM-1 protein expressions, IL-6 levels, and MPO activities in intestine mucosa after IIR injury. SHAM group (Sham-operated group), IIR group (75 min intestinal ischemia and 2 h reperfusion), and IIR + CP group (IIR group + Compound 48/80 1 mg/kg) in the absence or presence of NAC (0.5 g/kg), propofol (50 mg/kg), intralipid (50 mg/kg). (a) SOD activities, (b) 15-F_{2t}-isoprostane contents in intestine ($n = 6$, except $n = 4$ in IIR + CP group). ((c) and (d)) $p47^{phox}$ and $gp91^{phox}$ protein expressions, respectively ($n = 3$), ((e) and (f)) IL-6 levels and MPO activities in intestinal mucosa ($n = 6$, except $n = 4$ in IIR + CP group). ((g) and (h)) ICAM-1 and P-selectin protein expressions, respectively ($n = 3$). Results are expressed as Mean ± SEM. $^{*}P < 0.05$ versus SHAM group, $^{\#}P < 0.05$ versus IIR group, $^{\$}P < 0.05$ versus IIR + CP group, $^{\&}P < 0.05$ versus IIR with NAC pretreated group, $^{\triangle}P < 0.05$ versus IIR with propofol pretreated group, and $^{\blacktriangle}P < 0.05$ versus IIR with intralipid pretreated group.

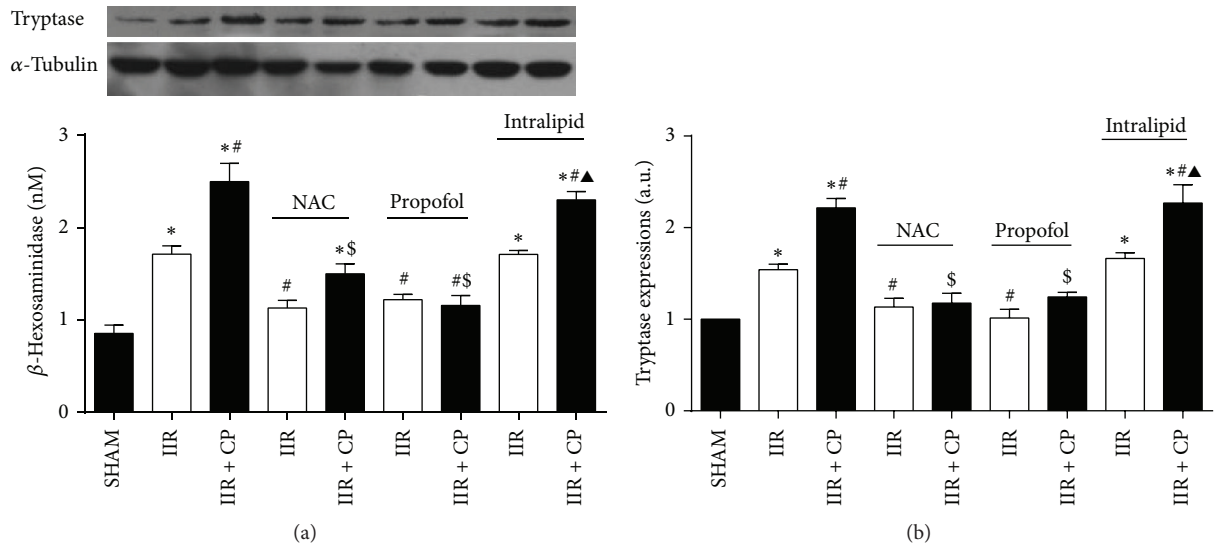

Figure 6: Changes of intestinal tryptase protein expression and serum β-hexosaminidase levels after IIR injury. SHAM group (Sham-operated group), IIR group (75 min intestinal ischemia and 2 h reperfusion), and IIR + CP group (IIR group + Compound 48/80 1 mg/kg) in the absence or presence of NAC (0.5 g/kg), propofol (50 mg/kg), intralipid (50 mg/kg). (a) Intestinal tryptase protein expression ($n = 3$). (b) β-hexosaminidase levels in serum ($n = 6$, except $n = 4$ in IIR + CP group). Results are expressed as Mean ± SEM. $^{*}P < 0.05$ versus SHAM group, $^{\#}P < 0.05$ versus IIR group, $^{\$}P < 0.05$ versus IIR + CP group, $^{\&}P < 0.05$ versus IIR with NAC pretreated group, $^{\triangle}P < 0.05$ versus IIR with propofol pretreated group, and $^{\blacktriangle}P < 0.05$ versus IIR with intralipid pretreated group.

evidenced as enhancements in tryptase protein expression and β-hexosaminidase levels, which causes or exacerbates IIR injury. This notion is further supported by the fact that activating mast cell by Compound 48/80 further aggravated IIR injury and tryptase directly damaged small intestinal epithelium evidenced by the reduced cell viability and the enhanced LDH activity *in vitro*. The data from the current study further proved that mast cell activation plays a central role in exacerbating IIR injury, although the mechanism governing mast cell activation during IIR is yet to be explored.

Mast cell can be activated by several distinct mechanisms; in addition to IgE/Fcε, the classical signal pathway of activation, there is a growing body of evidence to suggest that nonimmunological stimuli such as trauma and physical stress also contribute to mast cell activation [46]. Yoshimaru and colleagues demonstrated that silver mediated mast cell activation by upregulation of NADPH oxidase mediated ROS production [18]. Additionally, Collaco et al. found that superoxide production contributes to mast cell degranulation, and inhibiting ROS can stabilize mast cell *in vitro* [12]. Moreover, our previous study in a rat model of IIR revealed significant increase of mast cell activation with concomitant elevations in ROS [16]. These results provided us sound rationale to speculate that there exists a linkage between mast cell activation and superoxide production. Our current study extended findings of previous studies [16] by showing that NADPH oxidase is overexpressed during IIR which contributed to increased oxidative stress and MC activation, leading to exacerbation of IIR injury. Further, using antioxidant N-acetylcysteine (NAC), which has been shown to prevent myocardial NADPH oxidase overexpression in diabetes [47, 48] and attenuate myocardial ischemia reperfusion injury [10], we found that, in *in vivo* model of IIR, pretreatment of rats with NAC not only attenuated NADPH oxidase overexpression and reduced ROS production, but concomitantly reduced MC activation and consequently attenuated IIR injury and increased survival rate. We also found that NAC reversed the oxidative stress mediated mast cell degranulation *in vitro*. The results from the current study indicated that oxidative stress subsequent to NADPH oxidase overexpression during IIR plays a critical role in mast cell activation, which in turn led to a deleterious injury. Of note, in the current study, mast cell activation by CP also induced oxidative stress manifested as increased 15-F_{2t}-isoprostane and reduced SOD, associated with increased $p47^{phox}$ and $gp91^{phox}$ protein expression in IIR + CP group compared to IIR group (Figures 5(a)–5(d)). This is consistent with study from Collaco et al. showing that sodium sulfite activated mast cell degranulation and subsequently increased intercellular oxidative stress in RBL-2H3 cells [12]. These indicate that mast cell activation *per se* induces oxidative stress.

Excessive production of ROS by NADPH oxidase is generally considered to be involved in the pathogenesis of inflamed tissues [49], including ischemic tissues. There are a number of NADPH homologs presented in many diverse organs, such as Nox1, Nox2 (also named as $gp91^{phox}$), and Nox3-4 [50]. It is important to appreciate that Nox2 is predominantly expressed within epithelial cells. In addition to ROS scavenger, NAC also inhibits NADPH oxidase activities; our previous results showed that pretreatment of diabetic rats with NAC attenuated cardiac ischemia reperfusion injury by downregulating NADPH subunits $p67^{phox}$ and $p22^{phox}$ expression and reducing oxidative stress [48]. Inoue et al.

have demonstrated that blockade of ROS generation by NADPH oxidase inhibition can limit mast cell degranulation [51]. Guan et al. demonstrated that intracellular NADPH concentration in villus tip cells in intestine was significantly rapidly increased even after short-term ischemia [52]. In the current study, we also found that elevations of $gp91^{phox}$ and $p47^{phox}$ protein expression are the prominent features of IIR. Furthermore, precondition of IIR-rats with antioxidant NAC or propofol not only significantly reduced $gp91^{phox}$ and $p47^{phox}$ protein expression, but also played a significant role in stabilizing mast cell.

Propofol is a short-acting, intravenously administered hypnotic agent. In addition to its sedation/hypnotic properties, propofol displays protective effects in many organs subjected to ischemia reperfusion injury by inhibiting oxidative cellular damage [53, 54]. Hama-Tomioka et al. recently reported that propofol can block superoxide production originated from NADPH oxidase *in vitro* [55]. Although, as described previously, a single intraperitoneal injection of 50 or 100 mg/kg propofol could significantly attenuate IIR injury in acute rat models [31], propofol is the most commonly used agent overall during short-term and intermediate-length sedation in ICU [56]; thus, in the current study, we explored propofol pretreatment for three successional days and incorporated the investigation of postischemic mortality in addition to observing its effect on IIR injury. To our knowledge, our study is the first to show that propofol pretreatment given at a sedative dosage significantly inhibited the overexpression of NADPH oxidase and reduced oxidative mediated MC action during IIR or *in vitro* and reduced IIR injury and subsequently enhanced postischemic mortality in rats.

IIR injury is also characterized by uncontrollable inflammation and neutrophils sequestration in inflamed tissues. Migration of neutrophils to injurious site is mediated by selectins and intercellular adhesion molecules (ICAMs) by the activated endothelium [57]. Compton et al. reviewed that tryptase released from mast cell degranulation can attract leukocytes infiltrate and migrate to ischemic tissues [58]. And treatment of rats with mast cell stabilizer cromolyn sodium has been shown to greatly reduce the expressions of ICAM-1 in the lungs in pancreatitis-associated lung injury and decreased IL-6 release [59]. These findings point to the importance of mast cell degranulation through increased release of proinflammatory mediator in inducing neutrophil migration to inflamed tissues. In the present study, we found that, during IIR, mast cell degranulation resulted in more neutrophils infiltration into small intestine evidenced as significant increases in MPO activities and ICAM-1 and P-selectin protein expressions and that propofol and NAC similarly blocked the alterations induced by IIR and prevented MC stimulator Compound 48/80 mediated exacerbation of IIR injury. Our finding that propofol can inhibit intestinal MC activation during IIR and reduce tissue neutrophils infiltration as well as the subsequent systemic inflammation may have potential clinical importance given that IIR occurs often in patient who underwent major surgeries such as cardiac surgery with cardiopulmonary bypass [60] and is a challenging and life-threatening clinical problem. The delay in diagnosis and treatment of IIR injury contributes to the continued high in-hospital mortality rate [61]. Preventive administration of propofol may be a promising approach in attenuating postoperative intestinal ischemia and mortality.

In a summary, we have shown that mast cell activation, through increased release of mediators, contributed to deleterious injury induced by IIR and that oxidative stress plays a central role in mast cell activation. Propofol, similar to the antioxidant NAC, inhibited ROS mediated mast cell activation and attenuated IIR injury and enhanced postischemic mortality. Propofol mediated reduction of oxidative stress and MC activation during IIR is achieved at least in part through attenuating IIR induced NADPH oxidase overexpression, while the underlying mechanism merits further study. Mast cell activation contributes to and exacerbates small intestinal ischemia reperfusion injury.

Conflict of Interests

The authors declare that there is no conflict of interests.

Authors' Contribution

Xiaoliang Gan, Dandan Xing, Guangjie Su, Shun Li, Chenfang Luo, and Michael Irwin performed the experiment and analyzed the data. Xiaoliang Gan wrote the paper. Zhengyuan Xia, Haobo Li, and Ziqing Hei conceived and designed the study and revised the paper. Haobo Li and Ziqing Hei share senior authorship. Dr. Ziqing Hei takes full responsibility for the work as a whole, including the study design, access to data, and the decision to submit and publish the paper. Xiaoliang Gan and Dandan Xing contributed equally to this study.

Acknowledgments

This study was supported by National Natural Science Foundation of China (NSFC, 30901408) and was partly supported by the Fundamental Research Funds for the Central Universities of China (12ykpy37).

References

[1] Q. Lu, D. Z. Xu, S. Sharpe et al., "The anatomic sites of disruption of the mucus layer directly correlate with areas of trauma/hemorrhagic shock-induced gut injury," *Journal of Trauma*, vol. 70, no. 3, pp. 630–635, 2011.

[2] O. Corcos, Y. Castier, A. Sibert et al., "Effects of a multimodal management strategy for acute mesenteric ischemia on srvival and intestinal failure," *Clinical Gastroenterology and Hepatology*, vol. 11, no. 2, pp. 158.e2–165.e2, 2013.

[3] S. A. W. G. Dello, K. W. Reisinger, R. M. van Dam et al., "Total intermittent pringle maneuver during liver resection can induce intestinal epithelial cell damage and endotoxemia," *PLoS ONE*, vol. 7, no. 1, Article ID e30539, 2012.

[4] A. Siniscalchi, A. Cucchetti, Z. Miklosova et al., "Post-reperfusion syndrome during isolated intestinal transplantation: outcome and predictors," *Clinical Transplantation*, vol. 26, no. 3, pp. 454–460, 2012.

[5] P. R. Bertoletto, A. T. Ikejiri, F. Somaio Neto et al., "Oxidative stress gene expression profile in inbred mouse after ischemia/reperfusion small bowel injury," *Acta Cirúrgica Brasileira*, vol. 27, no. 11, pp. 773–782, 2012.

[6] T. Otamiri and R. Sjodahl, "Oxygen radicals: their role in selected gastrointestinal disorders," *Digestive Diseases*, vol. 9, no. 3, pp. 133–141, 1991.

[7] Q.-G. Zhang, M. D. Laird, D. Han et al., "Critical role of nadph oxidase in neuronal oxidative damage and microglia activation following traumatic brain injury," *PLoS ONE*, vol. 7, no. 4, Article ID e34504, 2012.

[8] J. Shen, X.-Y. Bai, Y. Qin et al., "Interrupted reperfusion reduces the activation of NADPH oxidase after cerebral I/R injury," *Free Radical Biology and Medicine*, vol. 50, no. 12, pp. 1780–1785, 2011.

[9] G. T. Gang, J. H. Hwang, Y. H. Kim et al., "Protection of NAD(P)H: quinone oxidoreductase 1 against renal ischemia/reperfusion injury in mice," *Free Radical Biology and Medicine*, vol. 67, pp. 139–149, 2014.

[10] T. Wang, S. Qiao, S. Lei et al., "N-acetylcysteine and allopurinol synergistically enhance cardiac adiponectin content and reduce myocardial reperfusion injury in diabetic rats," *PLoS ONE*, vol. 6, no. 8, Article ID e23967, 2011.

[11] T. Wang, X. Mao, H. Li et al., "N-Acetylcysteine and allopurinol up-regulated the Jak/STAT3 and PI3K/Akt pathways via adiponectin and attenuated myocardial postischemic injury in diabetes," *Free Radical Biology and Medicine*, vol. 63, pp. 291–303, 2013.

[12] C. R. Collaco, D. J. Hochman, R. M. Goldblum, and E. G. Brooks, "Effect of sodium sulfite on mast cell degranulation and oxidant stress," *Annals of Allergy, Asthma and Immunology*, vol. 96, no. 4, pp. 550–556, 2006.

[13] B. Y. de Winter, R. M. van den Wijngaard, and W. J. de Jonge, "Intestinal mast cells in gut inflammation and motility disturbances," *Biochimica et Biophysica Acta*, vol. 1822, no. 1, pp. 66–73, 2012.

[14] H. Zi-Qing, G. Xiao-Liang, H. Pin-Jie, W. Jing, S. Ning, and G. Wan-Ling, "Influence of Ketotifen, Cromolyn Sodium, and Compound 48/80 on the survival rates after intestinal ischemia reperfusion injury in rats," *BMC Gastroenterology*, vol. 8, article 42, 2008.

[15] X. Gan, D. Liu, P. Huang, W. Gao, X. Chen, and Z. Hei, "Mast-cell-releasing tryptase triggers acute lung injury induced by small intestinal ischemia-reperfusion by activating PAR-2 in rats," *Inflammation*, vol. 35, no. 3, pp. 1144–1153, 2012.

[16] Z. Q. Hei, X. L. Gan, G. J. Luo, S. R. Li, and J. Cai, "Pretreatment of cromolyn sodium prior to reperfusion attenuates early reperfusion injury after the small intestine ischemia in rats," *World Journal of Gastroenterology*, vol. 13, no. 38, pp. 5139–5146, 2007.

[17] A. T. Canada, R. F. Werkman, C. M. Mansbach II, and G. M. Rosen, "Biochemical changes in the intestine associated with anoxia and reoxygenation: in vivo and in vitro studies," *Journal of Free Radicals in Biology and Medicine*, vol. 2, no. 5-6, pp. 327–334, 1986.

[18] T. Yoshimaru, Y. Suzuki, T. Inoue, O. Niide, and C. Ra, "Silver activates mast cells through reactive oxygen species production and a thiol-sensitive store-independent $Ca2^{+}$ influx," *Free Radical Biology and Medicine*, vol. 40, no. 11, pp. 1949–1959, 2006.

[19] Z. Xia, Z. Huang, and D. M. Ansley, "Large-dose propofol during cardiopulmonary bypass decreases biochemical markers of myocardial injury in coronary surgery patients: a comparison with isoflurane," *Anesthesia and Analgesia*, vol. 103, no. 3, pp. 527–532, 2006.

[20] T. Fujimoto, T. Nishiyama, and K. Hanaoka, "Inhibitory effects of intravenous anesthetics on mast cell function," *Anesthesia and Analgesia*, vol. 101, no. 4, pp. 1054–1059, 2005.

[21] T. Luo, J. Wu, S. V. Kabadi et al., "Propofol limits microglial activation after experimental brain trauma through inhibition of nicotinamide adenine dinucleotide phosphate oxidase," *Anesthesiology*, vol. 119, no. 6, pp. 1370–1388, 2013.

[22] H. Komiyama, K. Miyake, K. Asai, K. Mizuno, and T. Shimada, "Cyclical mechanical stretch enhances degranulation and IL-4 secretion in RBL-2H3 mast cells," *Cell Biochemistry and Function*, vol. 32, no. 1, pp. 70–76, 2014.

[23] J.-I. Onose, Y. Yoshioka, Y. Q. Ye et al., "Inhibitory effects of vialinin A and its analog on tumor necrosis factor-α release and production from RBL-2H3 cells," *Cellular Immunology*, vol. 279, no. 2, pp. 140–144, 2012.

[24] N. A. Kretzmann, E. Chiela, U. Matte, N. Marroni, and C. A. Marroni, "N-acetylcysteine improves antitumoural response of Interferon alpha by NF-kB downregulation in liver cancer cells," *Comparative Hepatology*, vol. 11, no. 1, p. 4, 2012.

[25] T. Zhu, D. X. Wang, W. Zhang et al., "Andrographolide protects against LPS-Induced Acute Lung Injury by Inactivation of NF-κB," *PLoS ONE*, vol. 8, no. 2, Article ID e56407, 2013.

[26] K. Módis, A. Asimakopoulou, C. Coletta, A. Papapetropoulos, and C. Szabo, "Oxidative stress suppresses the cellular bioenergetic effect of the 3-mercaptopyruvate sulfurtransferase/hydrogen sulfide pathway," *Biochemical and Biophysical Research Communications*, vol. 433, no. 4, pp. 401–407, 2013.

[27] X.-Y. Zhu, E. Daghini, A. R. Chade et al., "Myocardial microvascular function during acute coronary artery stenosis: effect of hypertension and hypercholesterolaemia," *Cardiovascular Research*, vol. 83, no. 2, pp. 371–380, 2009.

[28] T. Wu, X. Gan, S. Zhou, M. Ge, Z. Zhang, and Z. Hei, "Histamine at low concentrations aggravates rat liver BRL-3A cell injury induced by hypoxia/reoxygenation through histamine H2 receptor in vitro," *Toxicology In Vitro*, vol. 27, no. 1, pp. 378–386, 2013.

[29] A. M. Abdelrahman, S. Al Salam, A. S. Almahruqi, I. S. Al Husseni, M. A. Mansour, and B. H. Ali, "N-acetylcysteine improves renal hemodynamics in rats with cisplatin-induced nephrotoxicity," *Journal of Applied Toxicology*, vol. 30, no. 1, pp. 15–21, 2010.

[30] G. Inagawa, K. Sato, T. Kikuchi et al., "Chronic ethanol consumption does not affect action of propofol on rat hippocampal acetylcholine release in vivo," *British Journal of Anaesthesia*, vol. 93, no. 5, pp. 737–739, 2004.

[31] K.-X. Liu, T. Rinne, W. He, F. Wang, and Z. Xia, "Propofol attenuates intestinal mucosa injury induced by intestinal ischemia-reperfusion in the rat," *Canadian Journal of Anesthesia*, vol. 54, no. 5, pp. 366–374, 2007.

[32] C. J. Chiu, H. J. Scott, and F. N. Gurd, "Intestinal mucosal lesion in low-flow states. II. The protective effect of intraluminal glucose as energy substrate.," *Archives of Surgery*, vol. 101, no. 4, pp. 484–488, 1970.

[33] Z. Xia, D. V. Godin, and D. M. Ansley, "Propofol enhances ischemic tolerance of middle-aged rat hearts: effects on 15-F2t-isoprostane formation and tissue antioxidant capacity," *Cardiovascular Research*, vol. 59, no. 1, pp. 113–121, 2003.

[34] H. Oda, M. Fujimoto, M. S. Patrick et al., "RhoH plays critical roles in FcεRI-dependent signal transduction in mast cells," *Journal of Immunology*, vol. 182, no. 2, pp. 957–962, 2009.

[35] J. E. Krawisz, P. Sharon, and W. F. Stenson, "Quantitative assay for acute intestinal inflammation based on myeloperoxidase activity: assessment of inflammation in rat and hamster models," *Gastroenterology*, vol. 87, no. 6, pp. 1344–1350, 1984.

[36] B. Xu, X. Gao, J. Xu et al., "Ischemic postconditioning attenuates lung reperfusion injury and reduces systemic proinflammatory cytokine release via heme oxygenase 1," *Journal of Surgical Research*, vol. 166, no. 2, pp. e157–e164, 2011.

[37] M. Karabeyoglu, B. Unal, B. Bozkurt et al., "The effect of ethyl pyruvate on oxidative stress in intestine and bacterial translocation after thermal injury," *Journal of Surgical Research*, vol. 144, no. 1, pp. 59–63, 2008.

[38] G. Pejler, E. Rönnberg, I. Waern, and S. Wernersson, "Mast cell proteases: multifaceted regulators of inflammatory disease," *Blood*, vol. 115, no. 24, pp. 4981–4990, 2010.

[39] S. Basu, A. Miclescu, H. Sharma, and L. Wiklund, "Propofol mitigates systemic oxidative injury during experimental cardiopulmonary cerebral resuscitation," *Prostaglandins Leukotrienes and Essential Fatty Acids*, vol. 84, no. 5-6, pp. 123–130, 2011.

[40] F. Schiemann, E. Brandt, R. Gross et al., "The cathelicidin LL-37 activates human mast cells and is degraded by mast cell tryptase: counter-regulation by CXCL4," *Journal of Immunology*, vol. 183, no. 4, pp. 2223–2231, 2009.

[41] K. Yoshiya, P. H. Lapchak, T.-H. Thai et al., "Depletion of gut commensal bacteria attenuates intestinal ischemia/reperfusion injury," *American Journal of Physiology: Gastrointestinal and Liver Physiology*, vol. 301, no. 6, pp. G1020–G1030, 2011.

[42] M. Ghyczy, C. Torday, J. Kaszaki, A. Szabó, M. Czóbel, and M. Boros, "Oral phosphatidylcholine pretreatment decreases ischemia-reperfusion induced methane generation and the inflammatory response in the small intestine," *Shock*, vol. 30, no. 5, pp. 596–602, 2008.

[43] A. B. Penissi, M. I. Rudolph, and R. S. Piezzi, "Role of mast cells in gastrointestinal mucosal defense," *Biocell*, vol. 27, no. 2, pp. 163–172, 2003.

[44] N. G. Frangogiannis, C. W. Smith, and M. L. Entman, "The inflammatory response in myocardial infarction," *Cardiovascular Research*, vol. 53, no. 1, pp. 31–47, 2002.

[45] L. Ramos, G. Peña, B. Cai, E. A. Deitch, and L. Ulloa, "Mast cell stabilization improves survival by preventing apoptosis in sepsis," *Journal of Immunology*, vol. 185, no. 1, pp. 709–716, 2010.

[46] C. Wolber, F. Baur, and J. R. Fozard, "Interaction between adenosine and allergen or compound 48/80 on lung parenchymal strips from actively sensitized Brown Norway rats," *European Journal of Pharmacology*, vol. 498, no. 1–3, pp. 227–232, 2004.

[47] Y. Liu, S. Lei, X. Gao et al., "PKCβ inhibition with ruboxistaurin reduces oxidative stress and attenuates left ventricular hypertrophy and dysfuntion in rats with streptozotocin-induced diabetes," *Clinical Science*, vol. 122, no. 4, pp. 161–173, 2012.

[48] Z. Guo, Z. Xia, J. Jiang, and J. H. McNeill, "Downregulation of NADPH oxidase, antioxidant enzymes, and inflammatory markers in the heart of streptozotocin-induced diabetic rats by N-acetyl-L-cysteine," *The American Journal of Physiology—Heart and Circulatory Physiology*, vol. 292, no. 4, pp. H1728–H1736, 2007.

[49] S. Lei, W. Su, H. Liu et al., "Nitroglycerine-induced nitrate tolerance compromises propofol protection of the endothelial cells against TNF-α: the role of PKC-β_2 and nadph oxidase," *Oxidative Medicine and Cellular Longevity*, vol. 2013, Article ID 678484, 9 pages, 2013.

[50] G. R. Drummond, S. Selemidis, K. K. Griendling, and C. G. Sobey, "Combating oxidative stress in vascular disease: NADPH oxidases as therapeutic targets," *Nature Reviews Drug Discovery*, vol. 10, no. 6, pp. 453–471, 2011.

[51] T. Inoue, Y. Suzuki, T. Yoshimaru, and C. Ra, "Reactive oxygen species produced up- or downstream of calcium influx regulate proinflammatory mediator release from mast cells: role of NADPH oxidase and mitochondria," *Biochimica et Biophysica Acta: Molecular Cell Research*, vol. 1783, no. 5, pp. 789–802, 2008.

[52] Y. Guan, R. T. Worrell, T. A. Pritts, and M. H. Montrose, "Intestinal ischemia-reperfusion injury: reversible and irreversible damage imaged in vivo," *American Journal of Physiology-Gastrointestinal and Liver Physiology*, vol. 297, no. 1, pp. G187–G196, 2009.

[53] M.-C. Lee, K. Kobayashi, F. Yoshino et al., "Direct assessments of the antioxidant effects of propofol medium chain triglyceride/long chain triglyceride on the brain of stroke-prone spontaneously hypertensive rats using electron spin resonance spectroscopy," *Anesthesiology*, vol. 109, no. 3, pp. 426–435, 2008.

[54] W. Yao, G. Luo, G. Zhu et al., "Propofol activation of the nrf2 pathway is associated with amelioration of acute lung injury in a rat liver transplantation model," *Oxidative Medicine and Cellular Longevity*, vol. 2014, Article ID 258567, 9 pages, 2014.

[55] K. Hama-Tomioka, H. Kinoshita, K. Nakahata et al., "Roles of neuronal nitric oxide synthase, oxidative stress, and propofol in N-methyl-D-aspartate-induced dilatation of cerebral arterioles," *The British Journal of Anaesthesia*, vol. 108, no. 1, pp. 21–29, 2012.

[56] K. M. Ho and J. Y. Ng, "The use of propofol for medium and long-term sedation in critically ill adult patients: a meta-analysis," *Intensive Care Medicine*, vol. 34, no. 11, pp. 1969–1979, 2008.

[57] F. Spiller, M. I. L. Orrico, D. C. Nascimento et al., "Hydrogen sulfide improves neutrophil migration and survival in sepsis via K^+ATP channel activation," *American Journal of Respiratory and Critical Care Medicine*, vol. 182, no. 3, pp. 360–368, 2010.

[58] S. J. Compton, J. A. Cairns, S. T. Holgate, and A. F. Walls, "Human mast cell tryptase stimulates the release of an IL-8-dependent neutrophil chemotactic activity from human umbilical vein endothelial cells (HUVEC)," *Clinical and Experimental Immunology*, vol. 121, no. 1, pp. 31–36, 2000.

[59] X. Zhao, M. Dib, X. Wang, B. Widegren, and R. Andersson, "Influence of mast cells on the expression of adhesion molecules on circulating and migrating leukocytes in acute pancreatitis-associated lung injury," *Lung*, vol. 183, no. 4, pp. 253–264, 2005.

[60] C. A. Efthymiou and W. I. Weir, "Salmonella sepsis simulating gastrointestinal ischaemia following cardiopulmonary bypass," *Interactive Cardiovascular and Thoracic Surgery*, vol. 12, no. 2, pp. 334–336, 2011.

[61] W. T. Kassahun, T. Schulz, O. Richter, and J. Hauss, "Unchanged high mortality rates from acute occlusive intestinal ischemia: six year review," *Langenbeck's Archives of Surgery*, vol. 393, no. 2, pp. 163–171, 2008.

Hindawi Publishing Corporation
Oxidative Medicine and Cellular Longevity
Volume 2015, Article ID 125106, 10 pages
http://dx.doi.org/10.1155/2015/125106

Research Article

High-Dose Polymerized Hemoglobin Fails to Alleviate Cardiac Ischemia/Reperfusion Injury due to Induction of Oxidative Damage in Coronary Artery

Qian Yang,[1,2] Wei Wu,[3] Qian Li,[1] Chan Chen,[1] Ronghua Zhou,[1] Yanhua Qiu,[1] Ming Luo,[1] Zhaoxia Tan,[1] Shen Li,[4] Gang Chen,[4] Wentao Zhou,[4] Jiaxin Liu,[4] Chengmin Yang,[4] Jin Liu,[1] and Tao Li[1]

[1]*Department of Anesthesiology and Translational Neuroscience Center, West China Hospital, Sichuan University, Chengdu 610041, China*
[2]*Department of Medicinal Chemistry, School of Pharmacy, Chengdu Medical College, Chengdu 610083, China*
[3]*Department of Anesthesiology, Chengdu Military General Hospital, Chengdu 610083, China*
[4]*Institute of Blood Transfusion, Chinese Academy of Medical Sciences, Chengdu 610052, China*

Correspondence should be addressed to Tao Li; scutaoli1981@scu.edu.cn

Received 6 September 2014; Revised 19 December 2014; Accepted 22 December 2014

Academic Editor: Mengzhou Xue

Objective. Ischemia/reperfusion (I/R) injury is an unavoidable event for patients in cardiac surgery under cardiopulmonary bypass (CPB). This study was designed to investigate whether glutaraldehyde-polymerized human placenta hemoglobin (PolyPHb), a hemoglobin-based oxygen carrier (HBOC), can protect heart against CPB-induced I/R injury or not and to elucidate the underlying mechanism. *Methods and Results*. A standard dog CPB model with 2-hour cardiac arrest and 2-hour reperfusion was established. The results demonstrated that a low-dose PolyPHb (0.1%, w/v) provided a significant protection on the I/R heart, whereas the high-dose PolyPHb (3%, w/v) did not exhibit cardioprotective effect, as evidenced by the impaired cardiac function, decreased myocardial oxygen utilization, and elevated enzymes release and pathological changes. Further study indicated that exposure of isolated coronary arteries or human umbilical vein endothelial cells (HUVECs) to a high-dose PolyPHb caused impaired endothelium-dependent relaxation, which was companied with increased reactive oxygen species (ROS) production, reduced superoxide dismutase (SOD) activity, and elevated malonaldehyde (MDA) formation. Consistent with the increased oxidative stress, the NAD(P)H oxidase activity and subunits expression, including $gp91^{phox}$, $p47^{phox}$, $p67^{phox}$, and Nox1, were greatly upregulated. *Conclusion*. The high-dose PolyPHb fails to protect heart from CPB-induced I/R injury, which was due to overproduction of NAD(P)H oxidase-induced ROS and resultant endothelial dysfunction.

1. Introduction

Ischemia/reperfusion (I/R) injury is harmful to cardiovascular system and responsible to cardiac infarction, which is thought to be involved in the severity and outcome of ischemic heart disease [1]. For these patients, percutaneous intervention or surgical procedure under cardiopulmonary bypass (CPB) is usually adopted to achieve coronary artery revascularization, but revascularization and cardiac arrest during CPB may induce I/R injury in myocardium [2]. Therefore, I/R injury is the major cause of death and poor prognosis of patients in cardiac surgery and transplantation.

Hemoglobin-based oxygen carriers (HBOCs) are red blood cell substitutes under development for more than three decades [3]. Our previous work and other studies indicated that HBOCs are promising candidates to prevent many organs from I/R injury [4–7]. Functionally, they allow delivery of more oxygen (O_2) to hypoxic tissues due to their

higher O_2 affinity, lower viscosity, and smaller mean diameter than human erythrocytes. Mechanistic studies suggested that this effect is related to attenuation of myocardial apoptosis, oxidative stress, and nitroso-redox imbalance [8, 9]. However, this protection was not observed in clinical settings. A meta-analysis by Natanson et al. [10] demonstrated that those patients receiving a HBOC have a statistically increased risk of death and myocardial infarction. To address this discrepancy, this study employed a more clinically relevant animal model—dog CPB model—to investigate the effect of glutaraldehyde-polymerized human placenta hemoglobin (PolyPHb) with different dosage on cardiac I/R injury.

2. Materials and Methods

All animal experimental procedures were performed in accordance with the policies of the Animal Care and Use Committee of Sichuan University and conformed to the *Guide for the Care and Use of Laboratory Animals* published by the US National Institutes of Health (NIH Publication Number 85-23, revised 1996).

2.1. Preparation of Hemoglobin-Based Oxygen Carrier. PolyPHb, a HBOC developed in China, was prepared as reported previously with some modifications [11]. Briefly, purified and viral inactivated fresh human placenta hemoglobin was modified with bis(3,5-dibromosalicyl) fumarate to achieve optimal O_2 affinity. After cross-linkage with glutaraldehyde, the mixture was subjected to ultrafiltration and molecular sieve chromatography. Before being used, the PolyPHb was mixed with St. Thomas' solution (STS) to a final concentration of 0.1 gHb/dL or 3 gHb/dL and then equilibrated with 95% O_2 and 5% CO_2 at 37°C for 15 min.

2.2. Dog Cardiopulmonary Bypass Model. A beagle dog cardiopulmonary bypass (CPB) model was established as described previously [12]. In brief, adult male beagle dogs, weighing 8–10 kg, were used. After induction (4 mg/kg propofol, 0.1 mg/kg midazolam, and 5 μg/kg fentanyl) and muscle relaxation (1 mg/kg scoline), all the dogs were intubated with an Fr. 7.5 endotracheal tube and mechanically ventilated using an air/O_2 mixture (1 : 4) with tidal volume 10 mL/kg (Datex-Ohmeda Excel 210, Soma Technology, Cheshire, Connecticut, USA). Each group received a continuous infusion of fentanyl at 0.3 μg/kg/min and vecuronium bromide at 0.2 mg/kg/hr during surgery. Anesthesia was maintained with 150 μg/kg/min propofol. After heart exposure through a mid-sternal incision and heparinization (3 mg/kg), the ascending aorta and the right atrial appendage were cannulated. The CPB circuit was composed of a rolling pump (StÖckert II, Munich, Germany), a membrane oxygenator (1500 mL/min, Kewei Medical Ltd., Guangdong, China), and an arterial filter (Kewei Medical Ltd.). The CPB was primed with Lactate Ringer's solution containing 5% sodium bicarbonate (10 mL/L), 20% mannitol (2.5 mL/L), furosemide (0.5–1.0 mg/L), dexamethasone (5 mg/L), heparin (10 mg/L), and 10% potassium chloride (5 mL/L). Also, a 10% calcium gluconate (2–4 mL) was added every 30 min for 4 times.

2.3. Experimental Protocol. The experimental protocol is schematically illustrated in Figure 1. Twenty adult male beagle dogs were divided into 4 groups ($n = 5$): Sham group, I/R group, 0.1% PolyPHb group, and 3% PolyPHb group. Except for the Sham group, hearts in other 3 groups were arrested by intra-aortic infusion of 40 mL/kg STS alone (I/R group), STS with 0.1 gHb/dL PolyPHb (0.1% PolyPHb group), or STS with 3 gHb/dL PolyPHb (3% PolyPHb group). After 2 hours of cardiac arrest, the hearts were reperfused for 2 hours by aortic declamping. The hearts without cardiac arrest and reperfusion were allocated into the Sham group. After the experiment, all the dogs were sacrificed with an intravenous bolus injection of sodium pentobarbital (120 mg/kg).

2.4. Measurement of Hemodynamic Parameters. A water-filled latex balloon attached to a pressure sensor (model SP844; MEMSCAP Inc., Durham, NC) was inserted into the left ventricle (LV) via the mitral valve. Then, the cardiac functional parameters including heart rate (HR), LV systolic pressure (LVSP), and LV end-diastolic pressure (LVEDP) were collected by a PowerLab data-acquisition system (ADInstruments Pty, Bella Vista, NSW, Australia). Also, a Swan-Ganz Float Catheter (Number 7, Edwards Laboratories, Irvine, CA, USA) was inserted via femoral vein and advanced to pulmonary artery to measure cardiac output (CO), pulmonary artery wedge pressure (PAWP), pulmonary arterial pressure (PAP), central venous pressure (CVP). Mean arterial pressure (MAP) was monitored by a polyethylene catheter placed in the left femoral artery.

2.5. Calculation of Cardiac O_2 Utilization. Blood samples from artery and coronary vein sinus were collected. To assess the level of cardiac O_2 utilization, cardiac O_2 consumption (VO_2) and O_2 extraction index (O_2EI) were calculated from the values of CO, hemoglobin concentration (Hb), arterial O_2 partial pressure (PaO_2), venous O_2 partial pressure (PvO_2), arterial O_2 saturation (SaO_2), and venous O_2 saturation (SvO_2) (ABL800 FLEX blood gas analyzer, Radiometer Medical A/S, Copenhagen, Denmark) by using following formula:

$$VO_2\,(\text{mL/min}) = CO \times \left[1.38 \times Hb \times \left(SaO_2 - SvO_2\right) + 0.0031 \times \left(PaO_2 - PvO_2\right)\right] \times 10 \quad (1)$$

$$O_2EI\,(\%) = 1 - \left[\frac{\left(1.38 \times Hb \times SvO_2 + 0.0031 \times PvO_2\right)}{\left(1.38 \times Hb \times SaO_2 + 0.0031 \times PaO_2\right)}\right] \times 100\%. \quad (2)$$

2.6. Determination of Myocardial Enzyme Release. Myocardial necrosis estimated by the releases of creatine kinase-MB (CK-MB), lactate dehydrogenase (LDH), and cardiac troponin-I (cTnI) in plasma were measured as described previously [8].

2.7. Measurement of Vascular Reactivity on Isolated Vessel Rings. Arterial rings (3-4 mm in length) from beagle dog coronary artery, free of fat and connective tissue, were mounted between two stainless steel hooks in organ bath chambers (PanLab Systems, Harvard apparatus, Barcelona,

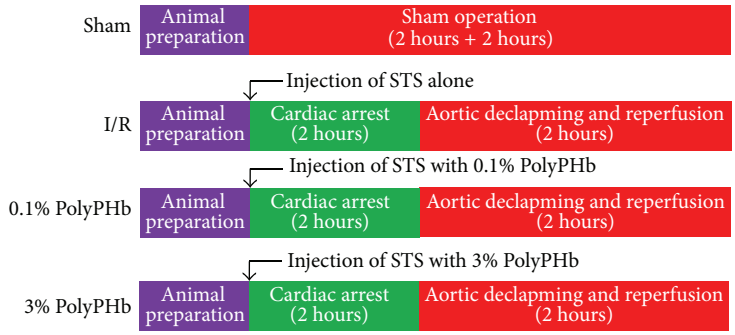

Figure 1: A schematic representation of the experimental protocol. After respective treatment, the hearts were subjected to 2-hour cardiac arrest and were reperfused for 2 hours. PolyPHb: glutaraldehyde-polymerized human placenta hemoglobin; STS: St. Thomas' solution.

Spain). Each chamber contained 10 mL of Krebs-Henseleit (KH) solution (118 mM NaCl, 4.7 mM KCl, 1.2 mM KH_2PO_4, 1.2 mM $MgSO_4$, 1.77 mM $CaCl_2$, 25 mM $NaHCO_3$, 11.4 mM glucose; pH 7.4, 37°C) and aerated continuously with 95% O_2 and 5% CO_2. Special attention was paid during the preparation to avoid damaging endothelium. During 60 minutes of equilibration period, resting tension of 3.5 g was periodically adjusted and the KH solution was changed every 30 minutes. The arterial viability was checked by stable and reproducible constriction to the addition of potassium chloride (KCl, 60 mM). Contracted arteries were then washed and subjected to 30 minutes of equilibration. After that, these arteries were incubated with KH buffer alone (Control group), KH buffer with 0.1% PolyPHb or 3% PolyPHb for 10 minutes and isometric tension of each vessel was recorded. To measure the effect of HBOC on endothelium, isolated coronary arterial rings were incubated with PolyPHb at 37°C for 2 hours. After washed and equilibrated for 60 minutes under resting tension of 3.5 g, these arteries were evoked using phenylephrine (10^{-7} M) to elicit reproducible contractile responses. Acetylcholine (ACh; 1×10^{-8} to 1×10^{-4} M) or sodium nitroprusside (SNP; 1×10^{-10} to 1×10^{-6} M) was then progressively added to induce endothelium-dependent or -independent relaxation, respectively.

2.8. Oxidative Stress and NAD(P)H Oxidase Activity Assays. Isolated dog coronary artery after treatment was embedded in aluminium cups of about 1 mL of OCT resin (Tissue Tek, Sakura, USA) and frozen in liquid nitrogen. To assess reactive oxygen species (ROS) production, cryosections (8 μm) were stained with the superoxide-sensitive dye dihydroethidine (DHE, 10 μM in PBS) and incubated for 30 minutes at 37°C. Red DHE fluorescence was detected with Olympus BX51 microscope and DP70 digital camera (Olympus corp.) at room temperature. Also, human umbilical vein endothelial cells (HUVECs) after treatment were incubated with DHE (10 μM) for 30 minutes; then ROS production was quantified by fluorescent measurement under Em/Ex = 480/580 nm (LS55 fluorescence spectrometer, Perkin-Elmer corp., Boston, MA, USA). As markers of oxidative stress, the superoxide dismutase (SOD) activity and malondialdehyde (MDA) formation in HUVECs were also measured by using commercially available kits (Nanjing Jiancheng corp., Nanjing, China). The NAD(P)H oxidase activity of HUVECs was measured as described previously [13]. Briefly, 20 μg of protein was incubated with DHE (10 μM) and DNA (1.25 μg/mL) in PBS with the addition of NAD(P)H (50 μM), in a final volume of 120 μL, for 30 minutes at 37°C in the dark. Fluorescence intensity was recorded in a microplate reader under Em/Ex = 480/580 nm (LS55 fluorescence spectrometer).

2.9. Immunohistochemistry. Paraffin sections (5 μm) or cryosections (8 μm) of dog coronary arteries were prepared and stained for $P46^{phox}$, $P67^{phox}$, $gp91^{phox}$, Nox1, Nox4, and von Willebrand factor (vWF) by using standard and widely accepted immunostaining techniques. The vWF was used to indicate endothelium. Moreover, paraffin sections of dog LV tissue were stained with hematoxylin and eosin (H&E) and assessed in a blinded fashion by a pathologist for the following histological examination: hyaline change, cloudy swelling, fatty change, inflammatory infiltration, perinuclear halo, interstitial edema, and acute myocardial necrosis. Semiquantitative analysis of histopathological changes was performed using an arbitrary grading system from score 0 to 5 (score 0: <10% positive cells; score 1: 10%–20% positive cells; score 2: 21–30% positive cells; score 3: 31–40% positive cells; score 4: 41–50% positive cells; score 5: >50% positive cells).

2.10. Statistical Analysis. All values are presented as mean ± SD. An unpaired Student's t-test was used to detect significant differences when two groups were compared. One-way or two-way ANOVA was used to compare the differences among three or more groups followed by Bonferroni's multiple comparison tests as applicable (SPSS 16.0 software). P values < 0.05 were considered statistically significant.

3. Results

3.1. High-Dose PolyPHb Failed to Improve Cardiac Function after CPB-Induced I/R Injury. All the hemodynamic parameters at baseline, as well as the HR, CVP, and MAP during reperfusion, were not different among groups (Figures 2(a)–2(c)). Treatment with the low-dose PolyPHb exhibited cardioprotective effect. Increase of the dosage of PolyPHb did not enhance this effect, as shown by the increased PAWP, PAP, and LVEDP and reduced LVSP and CO (all $P < 0.001$ versus the Sham group; Figures 2(d)–2(h)). The recovery of LVEDP and CO during the first 60 minutes of reperfusion

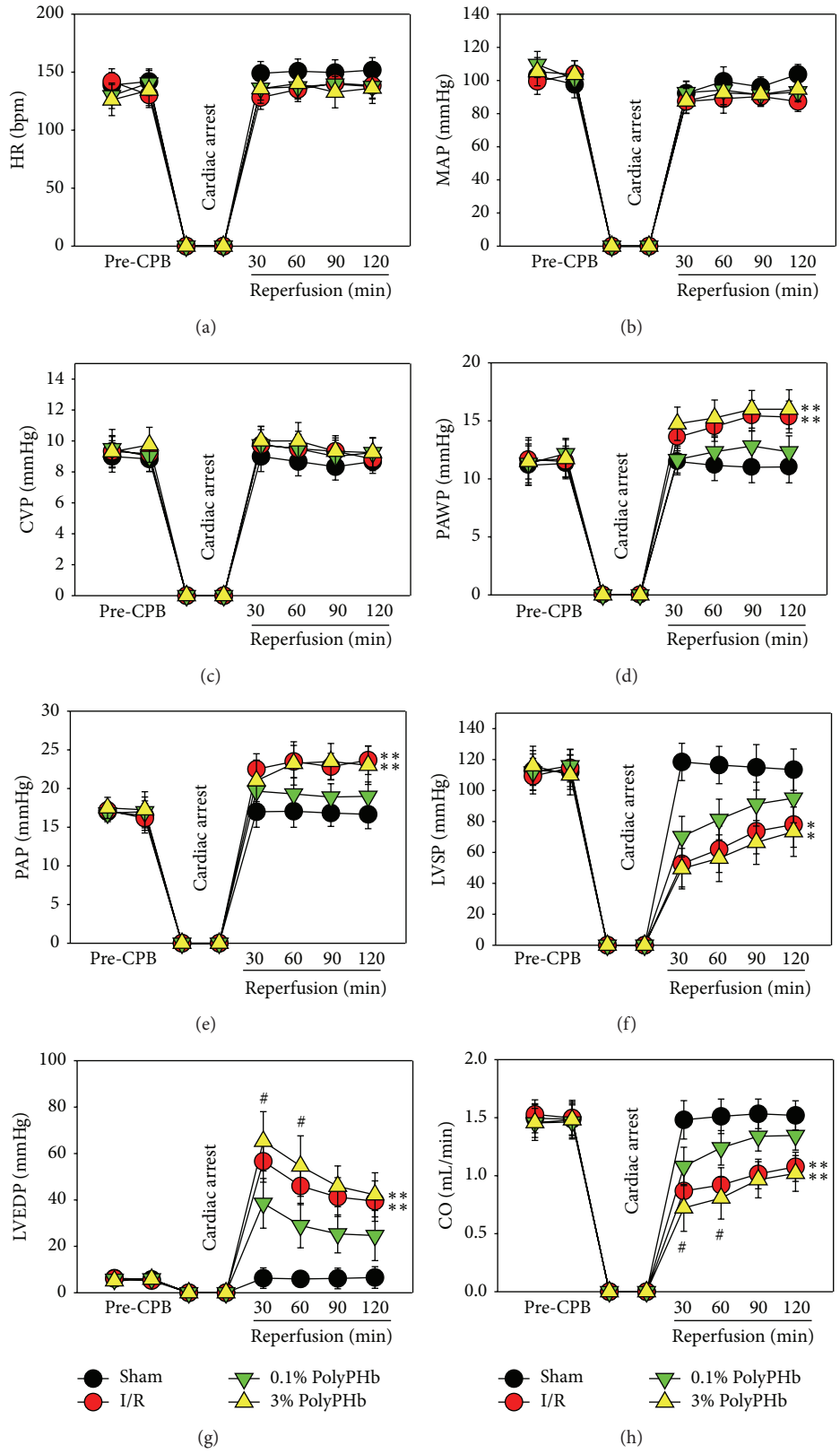

Figure 2: The HR (a), MAP (b), CVP (c), PAWP (d), PAP (e), LVSP (f), LVEDP (g), and CO (h) at baseline and during 2-hour of reperfusion ($n = 5$). Values are presented as mean ± SD. $^{*}P < 0.05$ and $^{**}P < 0.01$ versus the 0.1% group; $^{\#}P < 0.05$ versus the I/R group. HR: heart rate; MAP: mean arterial pressure; CVP: central venous pressure; PAWP: pulmonary artery wedge pressure; PAP: pulmonary arterial pressure; LVSP: left ventricular systolic pressure; LVEDP: left ventricular end-diastolic pressure; CO: cardiac output.

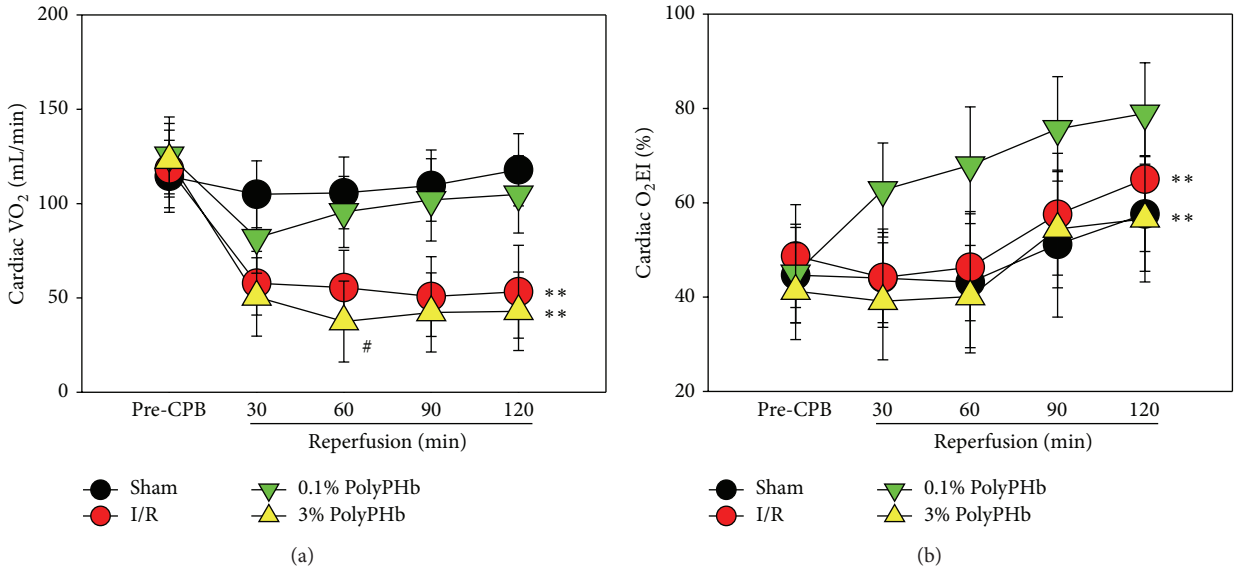

FIGURE 3: The cardiac utilization, including VO_2 (a) and O_2EI (b) at baseline and during 2 hours of reperfusion ($n = 5$). Values are presented as mean ± SD. $^{**}P < 0.01$ versus the 0.1% group; $^{\#}P < 0.05$ versus the I/R group. VO_2: cardiac oxygen consumption; O_2EI: oxygen extraction index.

were even worse as compared to the I/R group ($P < 0.05$ and $P < 0.05$, respectively; Figures 2(g) and 2(h)). In addition, the 0.1% PolyPHb alleviated the reduction of cardiac VO_2 and elevated O_2EI as compared to the I/R group, while the 3% PolyPHb failed to improve these parameters and further decreased cardiac VO_2 at 60 minutes of reperfusion ($P < 0.05$ versus the I/R group; Figure 3).

3.2. High-Dose PolyPHb Did Not Reverse Myocardial Necrosis after I/R Injury. As markers of myocardial necrosis, the levels of CK-MB, LDH, and cTnI in plasma were greatly increased in the I/R group. Less cardiac enzymes release was observed in the 0.1% PolyPHb group, whereas in the 3% PolyPHb group, the enzymes release was still in a high level and not different from the I/R group (Figures 4(a)–4(c)). Moreover, the results of H&E staining showed that the 3% PolyPHb did not limit myocardial histopathological changes after I/R injury and further increased myocardial necrosis ($P < 0.05$ versus the I/R group; Figures 4(d) and 4(e)).

3.3. High-Dose PolyPHb Impaired Endothelium-Dependent Vasorelaxation. Incubation with the 0.1% PolyPHb did not alter the net tension of coronary artery, whereas it was greatly elevated by the 3% PolyPHb (0.29 ± 0.07 g; Figure 5(a)). Further study found that the endothelium-independent vasorelaxation induced by SNP did not differ among groups (Figure 5(b)). However, treatment with the 3% PolyPHb induced a significant impairment in vasodilatory responses to ACh ($P < 0.05$ versus the Sham group and $P < 0.05$ versus the 0.1% PolyPHb group; Figure 5(c)).

3.4. High-Dose PolyPHb Induced Oxidative Stress in Coronary Artery. An increase of positive staining of DHE was observed after coronary artery exposure to the 3% PolyPHb, indicating an overproduction of ROS in the coronary artery (Figure 6(a)). Also, the cell study confirmed that 3% PolyPHb treatment resulted in increased ROS production ($P < 0.01$ versus the 0.1% PolyPHb group; Figure 6(b)), inhibited SOD activity, and elevated MDA formation in HUVECs ($P < 0.05$ and $P < 0.05$ versus the 0.1% PolyPHb group; Figures 6(c) and 6(d)).

3.5. HBOC-Induced NAD(P)H Oxidase Subunit Overexpression and Activity. Next, we measured the expression of the essential subunits of NAD(P)H oxidase using immunohistochemistry staining. Except for Nox4, vascular expression of $p47^{phox}$, $p67^{phox}$, and $gp91^{phox}$, as well as the catalytic subunit Nox1, was markedly increased by the 3% PolyPHb, compared with control and vessels treated with the 0.1% PolyPHb (Figures 7(a) and 7(b)). Consistently, the NAD(P)H oxidase activity was also greatly upregulated by the 3% PolyPHb ($P < 0.05$ versus the Control group and $P < 0.05$ versus the 0.1% PolyPHb group; Figure 7(c)).

4. Discussion

As we know, in addition to cardiac I/R injury, CPB is usually companied with a reduction in hemoglobin level because of the colloid solution primed in CPB circuit and unexpected blood loss after heparinization. A higher dose of PolyPHb—3% in this study—was expected to supplement hemoglobin in circulation, thereby providing additional benefits. However, the present study provides distinct evidence that the high-dose PolyPHb cannot protect heart against CPB-induced I/R injury. With regard to some parameters, it even causes additional damage on the heart. In contrast, a clear cardioprotection is observed in the low-dose PolyPHb group, suggesting the *in vivo* cardiac effect of HBOC is highly correlated to its dosage. Moreover, our current study confirms that the high-dose PolyPHb is vasoactive and induces coronary artery endothelial dysfunction and damage. These findings to

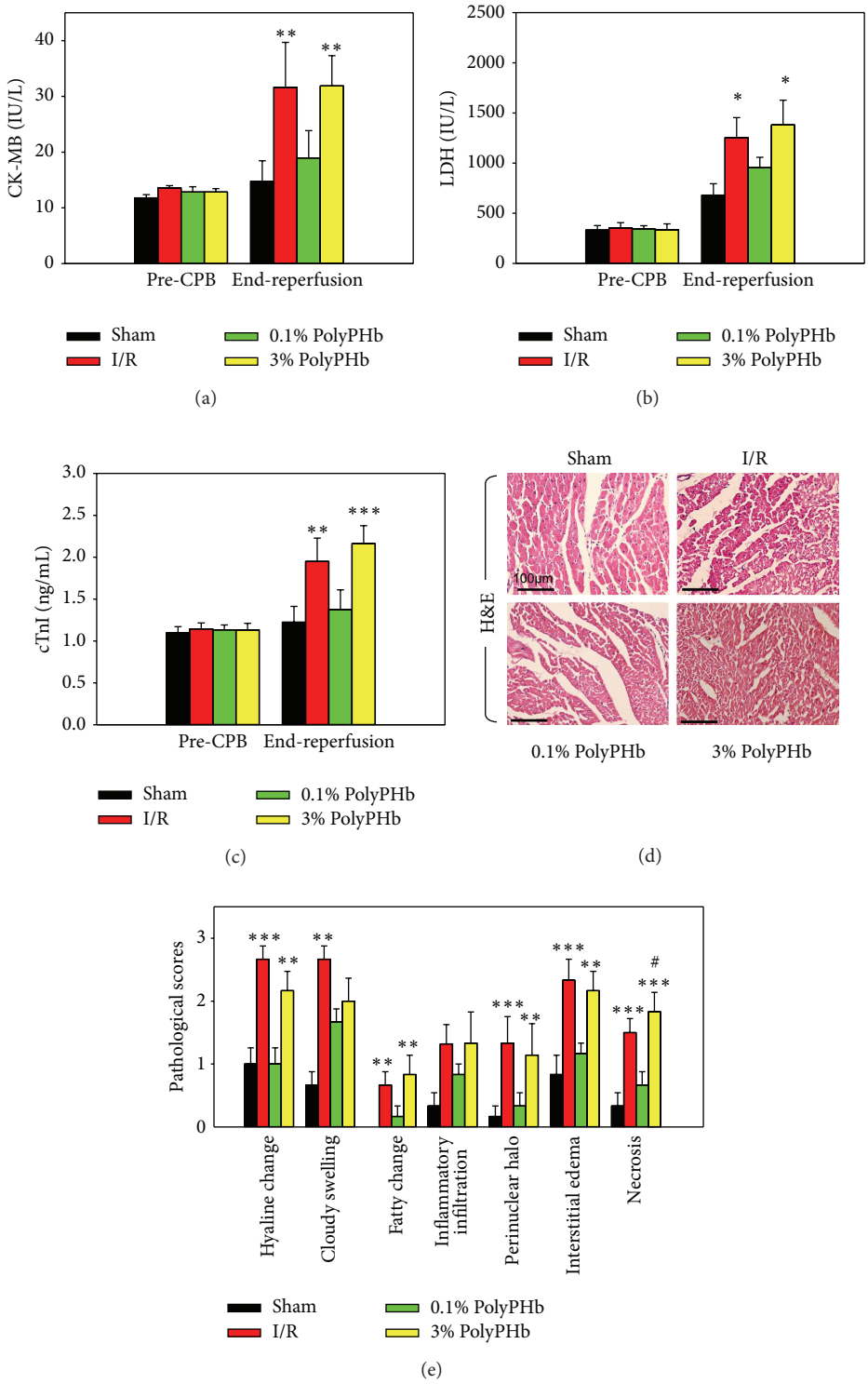

Figure 4: Total CK-MB (a), LDH (b), and cTnI (c) releases at baseline and after 2-hour reperfusion ($n = 6$). (d) Representative photomicrographs of H&E-stained left ventricular tissue section ($n = 5$). Scale bar: 100 μm. (e) Pathological scores for hyaline change, cloudy swelling, fatty change, inflammatory infiltration, perinuclear halo, interstitial edema, and acute myocardial necrosis. Values are presented as mean ± SD. $^{*}P < 0.05$, $^{**}P < 0.01$, and $^{***}P < 0.001$ versus the 0.1% PolyPHb group; $^{\#}P < 0.05$ versus the I/R group. CK-MB: creatine kinase-MB; LDH: lactate dehydrogenase; cTnI: cardiac troponin-I; H&E: hematoxylin and eosin.

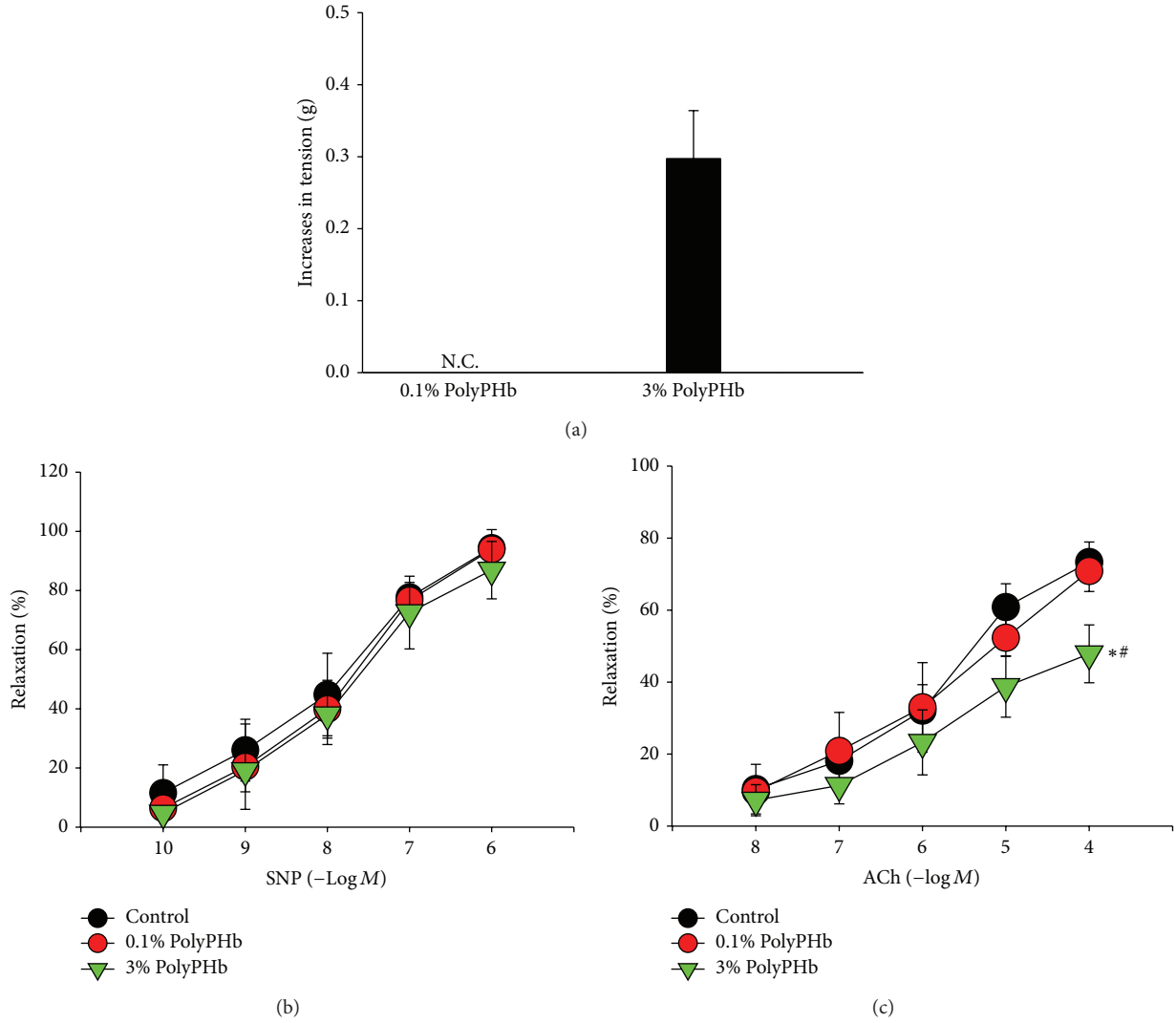

FIGURE 5: The net tension of coronary arteries (a) after incubation with 0.1% or 3% PolyPHb. SNP-induced endothelium-independent relaxation (b) and ACh-induced endothelium-dependent relaxation (c) in coronary arteries after incubation with 0.1% or 3% PolyPHb. Control vessels were treated with KH solution alone. Values are presented as mean ± SD (n = 5 to 6 per group). $^{*}P < 0.05$ versus the 0.1% PolyPHb group; $^{\#}P < 0.05$ versus the Control group. SNP: sodium nitroprusside; Ach: acetylcholine; KH: Krebs-Henseleit.

some extent may explain the paradoxical results about HBOC in animal and clinical studies. In clinical studies, a patient presenting with hypovolemic shock in hospital could receive HBOC up to 750–1000 mL, which means the estimated HBOC level in circulation is higher than 2 gHb/dL [10]. From the data of our study, this dosage is highly susceptible to induce vasoconstriction and cause damage on heart. Moreover, in the presence of physiological level of antioxidants, lower dosage of HBOC may be protective because of its peroxidase activity and excellent oxygen delivery capacity [14, 15]. However, as HBOC overwhelms the body's antioxidant defences, its own prooxidative function emerges and adverse effects become predominant.

To date, the mechanism(s) responsible for HBOC-induced vasoconstriction has not been completely understood. Scavenging of endothelium-derived nitric oxide (NO) is the most accepted theory, which proposes that the severity of vasoconstriction depends on the extent of the acellular hemoglobin extravasate through the endothelial lining of the vasculature [16]. However, there are problems with the extravasation concept. The logic of the extravasation process is not clear, because the quantities of hemoglobin molecules that can be located in the interstitium between endothelium and smooth muscle should be small compared to the blood compartment. Moreover, the amount of hemoglobin present in the interstitium would be rapidly exhausted and converted to methemoglobin (metHb), thus hindering vascular tone changes [17]. Another theory of HBOC-induced vasoconstriction is autoregulation in response to enhanced O_2 delivery, but no direct evidence was found to support this hypothesis [18]. The data of this study suggest an "endothelial damage theory" that HBOC-induced vasoconstriction is

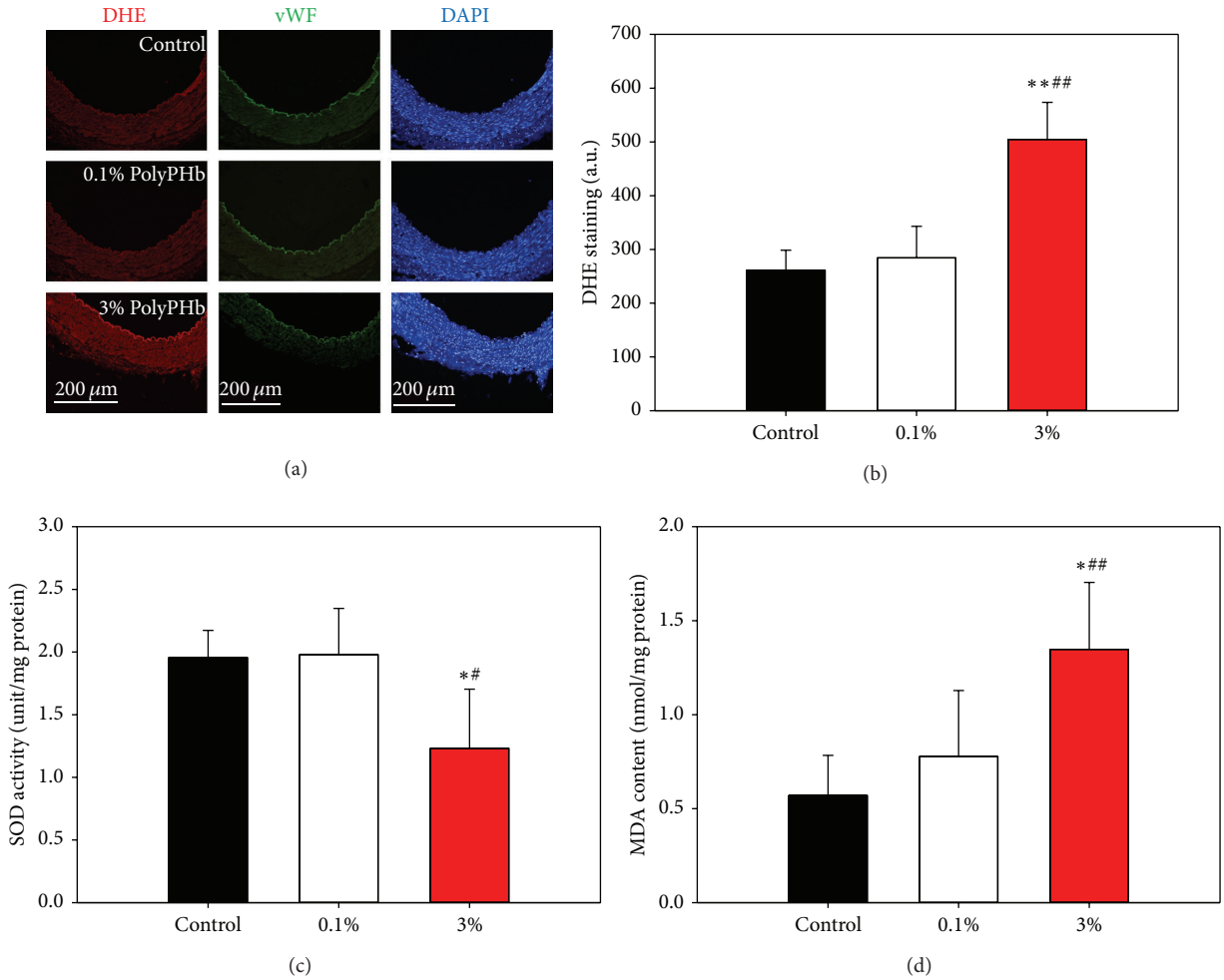

Figure 6: (a) Representative immunohistochemical staining of coronary arteries for DHE and vWF. Scale bar: 200 μm. (b–d) The ROS production, SOD activity, and MDA formation in HUVECs after incubation with 0.1% or 3% PolyPHb. One unit of SOD activity corresponded to 50% reduction of absorbance at 550 nm. Values are presented as mean ± SD ($n = 5$ to 6 per group). $^{*}P < 0.05$ and $^{**}P < 0.01$ versus the 0.1% PolyPHb group; $^{\#}P < 0.05$ and $^{\#\#}P < 0.01$ versus the Control group. DHE: dihydroethidium; ROS: reactive oxygen species; SOD: superoxide dismutase; MDA: malonaldehyde; HUVECs: human umbilical vein endothelial cells.

probably due to the increased generation of ROS in the vascular endothelium and resultant endothelial dysfunction. Furthermore, we demonstrate that the high-dose PolyPHb increases the expression of NAD(P)H oxidase subunits, including $P47^{phox}$, $P67^{phox}$, $gp91^{phox}$, and Noxl, suggesting that the NAD(P)H oxidase is probably responsible to HBOC-induced ROS burst and vascular redox imbalance. Although our data suggest that NAD(P)H oxidase is important to endothelial oxidative stress, we believe that this damage is multifactorial, for that excessive O_2 delivered by HBOC and heme-auto-oxidation are both capable of producing ROS and accelerating oxidative stress. In addition, ferryl hemoglobin can mediate lipid oxidation reactions and generate powerful vasoactive molecules isoprostanes, which may also contribute to HBOC-induced vasoactivity [19].

Although HBOCs possess inherent advantages compared to stored erythrocytes, vasoactivity is regarded to be the major obstacle hindering its clinical application [17]. Reducing NO affinity has long been regarded as a solution for limitation of vasoconstriction after HBOC administration. The strategies included genetic modification of the heme pocket in hemoglobin and attenuation of HBOC extravasation through endothelial junctions by producing larger hemoglobin molecules [20, 21]. However, our study suggests that using antioxidants to counteract the oxidative damage may be a potential alternative to solve this problem. Several years ago, D'Agnillo and Change [22] reported a HBOC with antioxidant properties by cross-linking polymerized hemoglobin with SOD and catalase, which decreased the formation of oxygen radicals in a rat intestinal I/R model. Consistently, our recent study indicated that captopril, an angiotensin-converting enzyme (ACE) inhibitor with antioxidative effect, is also capable of limiting HBOC-related vasoactivity and adverse cardiac effect [23]. Therefore, manufacture of HBOC products with enhanced antioxidative properties is a possible way to reduce its vasoactivity and limit adverse cardiovascular effects.

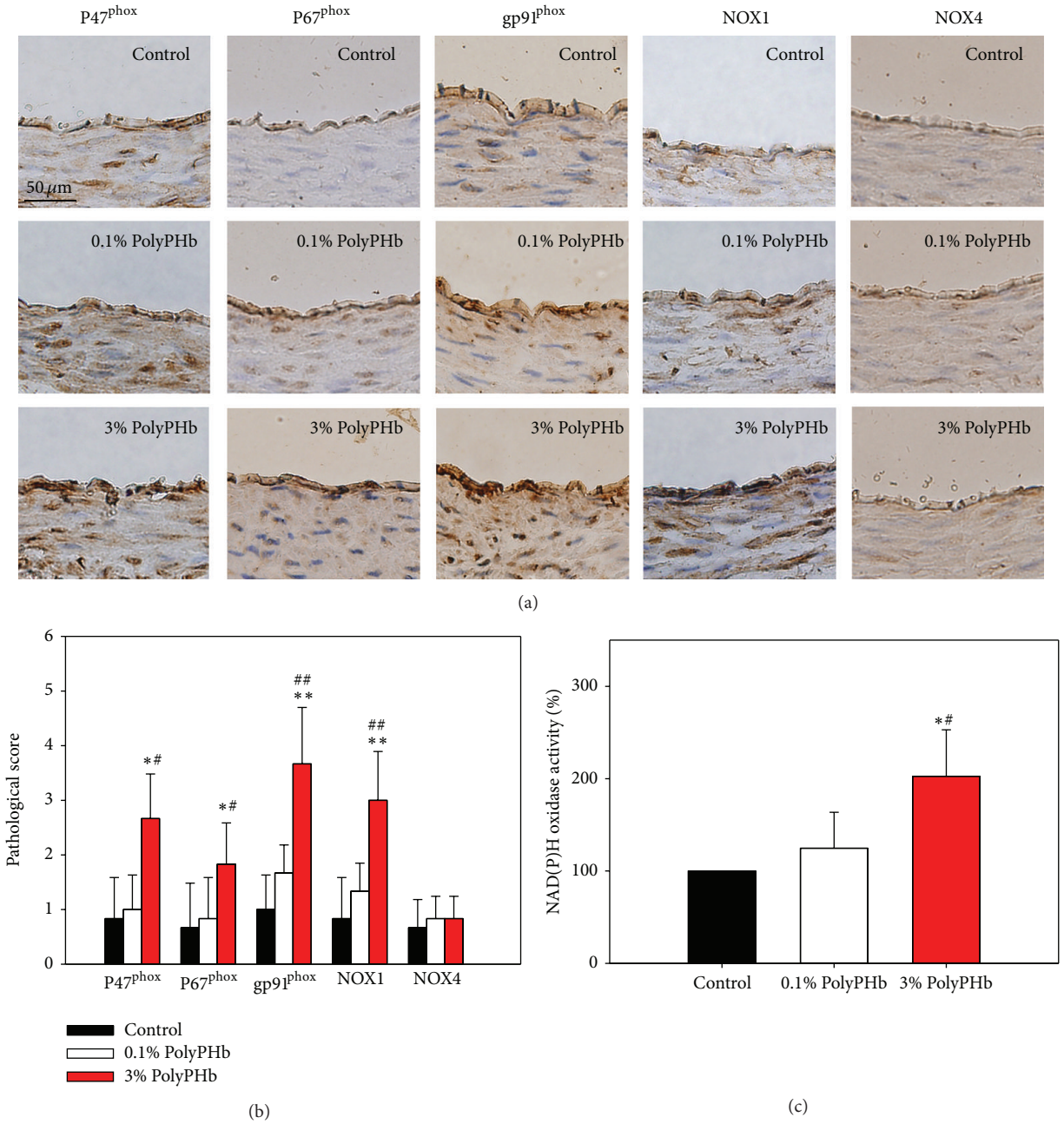

FIGURE 7: Representative of immunohistochemical staining (a) and semiquantification analysis (b) for expressions of P46^{phox}, P67^{phox}, gp91^{phox}, Nox1, and Nox4 in coronary arteries. Scale bar: 50 μm. (c) NAD(P)H oxidase activity in HUVECs. Values are presented as mean ± SD (n = 5 to 6 per group). $^{*}P < 0.05$ and $^{**}P < 0.01$ versus the 0.1% PolyPHb group; $^{\#}P < 0.05$ and $^{\#\#}P < 0.01$ versus the Control group.

In summary, we report that the high-dose PolyPHb fails to protect heart from CPB-induced I/R injury, which is due to induction of NAD(P)H oxidase-induced ROS overproduction and endothelial dysfunction.

Conflict of Interests

The authors declare that there is no conflict of interests regarding the publication of this paper.

Acknowledgments

This study was supported by grants from the National Natural Science Foundation of China (81100180 and 81471042), the 2013 Research Fund for Outstanding Young Scholars of Sichuan University, the National High Technology Research and Development Program of China (863 Program, 2012AA021903), the Science and Technology Support Program of Sichuan Province (2013SZ0059), the Special

Foundation for Technology Innovation Program of Sichuan Province (2013ZZ0006), and Research Funds in Chengdu Military Hospital (2011YG-B08 and 2013YG-B028).

References

[1] D. K. de Vries, K. A. Kortekaas, D. Tsikas et al., "Oxidative damage in clinical ischemia/reperfusion injury: a reappraisal," *Antioxidants and Redox Signaling*, vol. 19, no. 6, pp. 535–545, 2013.

[2] A. T. Turer and J. A. Hill, "Pathogenesis of myocardial ischemia-reperfusion injury and rationale for therapy," *The American Journal of Cardiology*, vol. 106, no. 3, pp. 360–368, 2010.

[3] A. I. Alayash, "Blood substitutes: why haven't we been more successful?" *Trends in Biotechnology*, vol. 32, no. 4, pp. 177–185, 2014.

[4] T. Li, D. Zhu, R. Zhou, W. Wu, Q. Li, and J. Liu, "Hboc attenuates intense exercise-induced cardiac dysfunction," *International Journal of Sports Medicine*, vol. 33, no. 5, pp. 338–345, 2012.

[5] T. Li, R. Zhou, X. Xiang et al., "Polymerized human placenta hemoglobin given before ischemia protects rat heart from ischemia reperfusion injury," *Artificial Cells, Blood Substitutes, and Biotechnology*, vol. 39, no. 6, pp. 392–397, 2011.

[6] I. George, G.-H. Yi, A. R. Schulman et al., "A polymerized bovine hemoglobin oxygen carrier preserves regional myocardial function and reduces infarct size after acute myocardial ischemia," *American Journal of Physiology—Heart and Circulatory Physiology*, vol. 291, no. 3, pp. H1126–H1137, 2006.

[7] M. T. L. Hekkert, G. P. Dubé, E. Regar et al., "Preoxygenated hemoglobin-based oxygen carrier HBOC-201 annihilates myocardial ischemia during brief coronary artery occlusion in pigs," *American Journal of Physiology: Heart and Circulatory Physiology*, vol. 298, no. 3, pp. H1103–H1113, 2010.

[8] T. Li, P. Zhang, J. Liu et al., "Protective effects of hemoglobin-based oxygen carrier given to isolated heart during ischemia via attenuation of mitochondrial oxidative damage," *Free Radical Biology & Medicine*, vol. 48, no. 8, pp. 1079–1089, 2010.

[9] T. Li, J. Li, J. Liu et al., "Polymerized placenta hemoglobin attenuates ischemia/reperfusion injury and restores the nitroso-redox balance in isolated rat heart," *Free Radical Biology and Medicine*, vol. 46, no. 3, pp. 397–405, 2009.

[10] C. Natanson, S. J. Kern, P. Lurie, S. M. Banks, and S. M. Wolfe, "Cell-free hemoglobin-based blood substitutes and risk of myocardial infarction and death: a meta-analysis," *JAMA—Journal of the American Medical Association*, vol. 299, no. 19, pp. 2304–2312, 2008.

[11] T. Li, R. Yu, H. H. Zhang et al., "A method for purification and viral inactivation of human placenta hemoglobi," *Artificial Cells, Blood Substitutes and Biotechnology*, vol. 34, no. 2, pp. 175–188, 2006.

[12] T. Li, W. Wu, Z. You et al., "Alternative use of isoflurane and propofol confers superior cardioprotection than using one of them alone in a dog model of cardiopulmonary bypass," *European Journal of Pharmacology*, vol. 677, no. 1–3, pp. 138–146, 2012.

[13] D. C. Fernandes, J. Wosniak Jr., L. A. Pescatore et al., "Analysis of DHE-derived oxidation products by HPLC in the assessment of superoxide production and NADPH oxidase activity in vascular systems," *American Journal of Physiology—Cell Physiology*, vol. 292, no. 1, pp. C413–C422, 2007.

[14] C. E. Cooper, R. Silaghi-Dumitrescu, M. Rukengwa, A. I. Alayash, and P. W. Buehler, "Peroxidase activity of hemoglobin towards ascorbate and urate: a synergistic protective strategy against toxicity of Hemoglobin-Based Oxygen Carriers (hboc)," *Biochimica et Biophysica Acta—Proteins and Proteomics*, vol. 1784, no. 10, pp. 1415–1420, 2008.

[15] C. C. Widmer, C. P. Pereira, P. Gehrig et al., "Hemoglobin can attenuate hydrogen peroxide-induced oxidative stress by acting as an antioxidative peroxidase," *Antioxidants & Redox Signaling*, vol. 12, no. 2, pp. 185–198, 2010.

[16] C.-M. Hai, "Systems biology of HBOC-induced vasoconstriction," *Current Drug Discovery Technologies*, vol. 9, no. 3, pp. 204–211, 2012.

[17] P. Cabrales and J. M. Friedman, "HBOC vasoactivity: interplay between nitric oxide scavenging and capacity to generate bioactive nitric oxide species," *Antioxidants and Redox Signaling*, vol. 18, no. 17, pp. 2284–2297, 2013.

[18] R. M. Winslow, "Current status of blood substitute research: towards a new paradigm," *Journal of Internal Medicine*, vol. 253, no. 5, pp. 508–517, 2003.

[19] B. J. Reeder, D. A. Svistunenko, C. E. Cooper, and M. T. Wilson, "The radical and redox chemistry of myoglobin and hemoglobin: from in vitro studies to human pathology," *Antioxidants and Redox Signaling*, vol. 6, no. 6, pp. 954–966, 2004.

[20] C. L. Varnado, T. L. Mollan, I. Birukou, B. J. Z. Smith, D. P. Henderson, and J. S. Olson, "Development of recombinant hemoglobin-based oxygen carriers," *Antioxidants & Redox Signaling*, vol. 18, no. 17, pp. 2314–2328, 2013.

[21] J. S. Olson, E. W. Foley, C. Rogge, A.-L. Tsai, M. P. Doyle, and D. D. Lemon, "NO scavenging and the hypertensive effect of hemoglobin-based blood substitutes," *Free Radical Biology and Medicine*, vol. 36, no. 6, pp. 685–697, 2004.

[22] F. D'Agnillo and T. M. Chang, "Polyhemoglobin-superoxide dismutase-catalase as a blood substitute with antioxidant properties," *Nature Biotechnology*, vol. 16, no. 7, pp. 667–671, 1998.

[23] T. Li, R. Zhou, Y. Yao et al., "Angiotensin-converting enzyme inhibitor captopril reverses the adverse cardiovascular effects of polymerized hemoglobin," *Antioxidants & Redox Signaling*, vol. 21, no. 15, pp. 2095–2108, 2014.

Hindawi Publishing Corporation
Oxidative Medicine and Cellular Longevity
Volume 2015, Article ID 486148, 10 pages
http://dx.doi.org/10.1155/2015/486148

Research Article

Glutathione Supplementation Attenuates Oxidative Stress and Improves Vascular Hyporesponsiveness in Experimental Obstructive Jaundice

Jiaying Chen,[1,2] Feixiang Wu,[1] Yue Long,[1] and Weifeng Yu[1]

[1]*Department of Anesthesia & Intensive Care, Eastern Hepatobiliary Surgery Hospital, the Second Military Medical University, Shanghai 200438, China*
[2]*Department of Anesthesiology, 81st Hospital of the Chinese PLA, Nanjing 210002, China*

Correspondence should be addressed to Weifeng Yu; ywf808@yeah.net

Received 24 September 2014; Revised 31 January 2015; Accepted 31 January 2015

Academic Editor: Yanfang Chen

We investigated the protective effects and mechanism of glutathione (GSH) on vascular hyporesponsiveness induced by bile duct ligation (BDL) in a rat model. Seventy-two male Sprague-Dawley rats were randomly divided into four groups: a NS group, a GSH group, a BDL + NS group, and a BDL + GSH group. GSH was administrated into rats in the GSH and BDL + GSH groups by gastric gavage. An equal volume of normal saline was, respectively, given in the NS group and BDL + NS group. Blood was gathered for serological determination and thoracic aorta rings were isolated for measurement of isometric tension. Obstructive jaundice led to a significant increase in the serum total bilirubin, AST, and ALT levels. The proinflammatory cytokines levels (TNF-α and IL-1β), concentration of NO, and oxidative stress markers (MDA and 3-NT) were increased as well. All of those were reduced by the treatment of GSH. Meanwhile, contraction of aorta rings to NA and vasorelaxation to ACh or SNP in the BDL group rats were markedly decreased, while GSH administration reversed this change. Our findings suggested that GSH supplementation attenuated overexpressed ONOO(−) from the reaction of excessive NO with $O_2^{\bullet-}$ and protected against obstructive jaundice-induced vascular hyporesponsiveness in rats.

1. Introduction

Surgeries in patients with obstructive jaundice (OJ) are associated with high prevalence of postoperative complications and mortality rates [1]. Hemodynamic instability induced by hypotension and impaired vascular reactivity in obstructive jaundice plays a central role in the pathogenesis of the complications in the perioperative period [2]. A decrease in vasoconstrictor tone as well as vascular hyporesponsiveness along with a lesser sensitivity to vasoactive agents such as catecholamine, vasopressin, angiotensin II, and serotonin can ultimately lead to death of patients [3].

Reactive oxygen species (ROS) play a major role in the pathogenesis of cholestasis [4]. ROS contribute to vascular dysfunction and remodeling, an initial episode progressing towards hypertension and atherosclerosis, through oxidative damage by reducing the bioavailability of nitric oxide (NO), impairing endothelium-dependent vasodilatation and endothelial cell growth; hence, cellular events underlying these processes involve changes in vascular smooth muscle cell growth and vasoconstriction [5]. A functional impairment of endothelial cells (ECs) and vascular smooth muscle cells (VSMCs) induced by ROS contributes to endothelial and vascular dysfunction, which probably initiate and induce vascular hyporesponsiveness and vasodilatation. The administration of antioxidants has been shown to exert beneficial effects in the prevention of cholestasis liver injury [6, 7]. However, whether antioxidant therapies maintaining the balance between oxidation and antioxidant systems improve vascular reactivity status remains controversial.

NO is known to play an important role as a key paracrine regulator of vascular tone [8]. Physiologically, NO maintains the health of the vascular endothelium [9]. The enzyme that catalyzes the formation of NO from oxygen is nitric oxide

synthase (NOS), which in fact is a whole family of enzymes, including endothelial NOS (eNOS), inducible NOS (iNOS), and neuronal NOS (nNOS). eNOS is the predominant NOS isoform in the vessel wall. Excessive production of NO (nanomolar concentrations) by iNOS hence resulted in an altered contractile response [10]. When large quantities of NO and $O_2^{\bullet-}$ collide in the same tissues, they spontaneously interact to form peroxynitrite (ONOO(−)) [11], a potent oxidant, which markedly aggravated oxidative stress (OS) [12].

During OJ, high-concentration bile salts and hyperbilirubinemia may be two major factors contributing to the production of oxygen free radicals, including superoxide anion ($O_2^{\bullet-}$), hydroxyl radical, and ONOO(−). Free radicals lead to oxidative damage in many molecules, such as lipids, proteins, and nucleic acids. OJ leads to oxidative injury and inflammation in hepatocytes [13], biliary epithelial and parenchymal cell [14], kidney, heart, intestinal, bladder [15], placenta [16], and red blood cells [17].

GSH, a main nonprotein thiol in cells, serves as a cofactor for a number of antioxidant and detoxifying enzymes [18]. Upon reaction with ROS or electrophiles, GSH becomes oxidized to glutathione disulfide (GSSG), which can be reduced by the GSSG reductase (GR). Thus, the GSH/GSSG ratio reflects the oxidative state and interacts with redox couples to maintain appropriate redox balance [19].

Reaction with GSH was proposed to be a major detoxification pathway of ONOO(−) in the biological system. The redox homeostasis between ONOO(−) and GSH is closely associated with the physiological and pathological processes, for example, vascular tissue prolonged relaxation and smooth muscle preparations, attenuation hepatic necrosis, and activation matrix metalloproteinase-2 [20]. Conversely, the increase in endogenous production of ONOO(−) by inducing a depletion of endogenous glutathione stores aggravates vascular hyporeactivity [21].

Thus, we hypothesized that the elevated concentration of ONOO(−) which is generated by overexpressed NO and $O_2^{\bullet-}$ could be critically instrumental in the vascular hyporesponsiveness by increasing oxidative stress during OJ. A supplementation of GSH on the improvement of vascular hyporesponsiveness in rats determines whether GSH administration attenuates ONOO(−) to exert protective effects induced by bile duct ligation.

2. Materials and Methods

2.1. Animals. A total of 72 pathogen-free, adult male Sprague-Dawley rats (weighing 200–250 g) were obtained from the Shanghai Slac Experimental Animal Centre (Shanghai, China). The rats were housed in individual cages in a temperature-controlled room with alternating 12 h light/dark cycles. Food was withheld 8 h before the start of experiments, but all animals had free access to water. This study was approved by the Animal Care Committee of the Second Military Medical University and performed in accordance with the Guide for the Care and Use of Laboratory Animals.

2.2. Experimental Design and Sample Collection. The experimental animals were randomly divided into four groups of 18 rats each: a SHAM-operated group (NS), a bile duct ligated group (BDL + NS), a Sham treated with GSH group (GSH), and a BDL treated with GSH group (BDL + GSH). GSH-treated rats received daily administration of GSH (FuHua Pharmaceutical Co., Ltd., Shanghai, China), 300 mg/kg dissolved in normal saline by gastric gavage for 7 days. In the NS group and BDL + NS group, rats only received an equal volume of normal saline. The dose of GSH given to rats was selected based on information from previous reports [22]. On the eighth day, laparotomy was performed under general anesthesia induced by the injection of chloral hydrate (300 mg/kg, i.p.). The NS and GSH groups were subjected to laparotomy as well as bile duct identification and manipulation without ligation or resection. In the BDL groups, the main bile duct was first ligated using two ligatures approximately 0.5 cm apart and then transected at the midpoint between the two ligatures. GSH administration was then undertaken for another 7 days. At the end of the study, the animals were sacrificed and blood samples were transferred to tubes and immediately centrifuged (3000 r/min for 10 min at 4°C). Serum samples were stored at −20°C in form of frozen for biochemical analyses.

2.3. Artery Isolation and Vascular Reactivity Protocol. Thoracic aortas were isolated and prepared for vascular function studies as described previously [23]. Rats were anesthetized using 300 mg/kg chloral hydrate, decapitated, and through opening the abdomen, thoracic aorta was carefully excised and placed in a petri dish filled with cold Krebs solution (KHS) containing (in mM) NaCl 118.5, KCl 4.7, KH_2PO_4 1.2, $MgSO_4$ 1.2, $NaHCO_3$ 25.0, $CaCl_2$ 2.5, and glucose 5.5 at 37°C continuously bubbled with a 95% O_2-5% CO_2 mixture (pH 7.4). The aorta was cleaned of excess connective tissue and cut into rings of approximately 3 mm in length. Thoracic aorta segments were mounted on two parallel stainless steel pins for arterial isometric tension recording through a MAP2000 isometric force transducer (Alcott Biotech Co., Ltd., Shanghai, China) connected to a computer. In all experiments, special care was taken to avoid damage to the luminal surface of endothelium. In a subgroup of BDL + NS + Endo(−) group or BDL + GSH + Endo(−) group, the endothelium was mechanically removed by gently rubbing the internal surface with a syringe needle. Segments were suspended in an organ bath containing 20 mL of KHS and subjected to a tension of 2 g which was readjusted every 30 min during a 120 min equilibration period before drug administration.

The vessels were then exposed to KCl (60 mmol/L) to check their functional integrity. After a washout period, isometric contractions were induced by the addition of phenylephrine (PE, 10^{-6} mol/L). A single concentration of acetylcholine (ACh, 10^{-5} mol/L) was added to the bath in order to assess the endothelial integrity of the preparations after the contraction was stabilized. Endothelium was considered to be intact when this drug elicited a vasorelaxation ≥ 75% of the maximal contraction obtained in vascular rings precontracted with PE. The absence of ACh relaxant action in the vessels indicated the total removal of endothelial cells.

At the end of the equilibration period, dose-response curves for norepinephrine (NA, 10^{-9}, 3×10^{-9}, 10^{-8}, $3 \times$

10^{-8}, 10^{-7}, 3×10^{-7}, 10^{-6}, 3×10^{-6}, and 10^{-5} mol/L) in the presence and absence of endothelium were obtained in aortic rings in a cumulative manner. To analyse the participation of NO on the response of NA, the NO synthase inhibitor L-NAME (L-NG-Nitroarginine methyl ester, 10^{-4} mol/L) [24] was added 30 min before the concentration-response curves were performed.

After this, the segments were rinsed several times with KHS over 2 h period, and then cumulative concentration-response curves to ACh (10^{-9}, 3×10^{-9}, 10^{-8}, 3×10^{-8}, 10^{-7}, 3×10^{-7}, and 10^{-6} mol/L), to the NO donor sodium nitroprusside (SNP, 3×10^{-10}, 10^{-9}, 3×10^{-9}, 10^{-8}, 3×10^{-8}, and 10^{-7} mol/L) were obtained in PE-precontracted segments (PE, 10^{-6} mol/L).

NA responses were expressed as a percentage of the maximum response to KCl. The relaxations induced by ACh or SNP were expressed as a percentage of the initial contraction elicited by PE.

2.4. Measurement of TBIL, ALT, and AST in Serum. Rat serum activity of total bilirubin (TBIL), alanine transaminase (ALT), and aspartate transaminase (AST) were measured by an automatic biochemistry analyzer (HITACHI 7110).

2.5. Measurement of 3-NT, GSH, MDA, NO, TNF-α, and IL-1β in Serum. The content of GSH, malondialdehyde (MDA), and NO in serum was detected with reagents kits purchased from Jiancheng Biologic Company (Nanjing, China).

GSH was initiated by the addition of 5,5′-di-thiobis(2-nitrobenzoic acid) and the change in absorbance at 420 nm was monitored by a spectrophotometer.

MDA, the OS product of lipid peroxidation, reacts with thiobarbituric acid under acidic conditions at 95°C to form a pink-colored complex with an absorbance at 532 nm. The results are expressed as nmol or/mL serum.

NO has a half-life of only a few seconds for it is readily oxidized to nitrite (NO_2^-) and subsequently to nitrate (NO_3^-), which serve as index parameters of NO production. The method for plasma nitrite and nitrate levels was based on the Griess reaction. Total nitrite was measured by spectrophotometry at 545 nm after conversion of nitrate to nitrite by copperized cadmium granules. The results were expressed as μmol/L.

Rat serum 3-nitrotyrosine (3-NT), the OS product of proteins and the proinflammatory cytokines levels (TNF-α and IL-1β) were measured, using a sandwich enzyme Immunoassay Kit (ELISA) protocol supplied by the manufacturer of the antibodies (Multisciences Biologic Company, Hangzhou, China) and resultant optical density determined, using a microplate reader (Thermo Multiskan MK3) at 450 nm. Results were expressed as pg or ng/mL serum.

2.6. Statistical Analysis. Statistical analysis was performed using SPSS version 18.0 software. Data are given as mean ± standard deviation (SD). Analysis of variance (ANOVA) was used to assess differences between multiple groups. A $P < 0.05$ was considered statistically significant.

Table 1: TBIL, ALT, and AST in serum (mean ± SD).

Group	n	TBIL μmol/L	ALT U/L	AST U/L
NS	6	0.53 ± 0.24	53 ± 7	95 ± 12
GSH	6	0.37 ± 0.39	49 ± 7	94 ± 9
BDL + NS	6	118.79 ± 9.67[a]	209 ± 22[a]	463.81 ± 49.96[a]
BDL + GSH	6	88.53 ± 22.02[b]	165 ± 29[b]	298.95 ± 35.62[b]

[a]$P < 0.01$ versus NS group; [b]$P < 0.01$ versus BDL + NS group.

3. Results

3.1. General Observations. No deaths were observed during the experiment. Animals that underwent sham surgery (NS group and GSH group) showed no alterations in the clinical conditions. BDL rats were clinically jaundiced within three days. In the BDL rats (BDL + NS group and BDL + GSH group), however, 24 h after surgery the clinical conditions of the animals deteriorated, as shown by decreased activity, irritability, vertical hair, body weight loss, yellowed tails, darkened urine, and pale feces. Seven days after surgery, jaundice was observed in the visceral and parietal peritoneum and varying degrees of ascites, enlarged livers and dilated bile ducts above the obstruction point were also observed in BDL rats. Compared with the rats in the BDL + NS group, rats with supplementation of GSH, demonstrated relatively lighter clinical conditions.

3.2. Serum Concentrations of TBIL, ALT, and AST. The serum concentrations of TBIL, ALT, and AST in the BDL + NS group increased visibly compared with those in the NS group ($P < 0.01$, Table 1). The serum concentrations of TBIL, ALT, and AST were significantly lower in the BDL + GSH group than in the BDL group ($P < 0.01$, Table 1).

3.3. Levels of GSH, NO, MDA, 3-NT, IL-1β, and TNF-α in Serum. The levels of GSH, NO, MDA, 3-NT, IL-1β, and TNF-α were higher in the BDL + NS group than in the NS group ($P < 0.01$, $P < 0.05$, Figure 1). However, GSH was more active in serum and the level of 3-NT, MDA, NO, TNF-α, and IL-1β was lower in the BDL + GSH group than that in the BDL + NS group ($P < 0.01$, Figure 1).

3.4. Vascular Reactivity. Cumulative addition of NA (10^{-9}–10^{-5} mol/L) resulted in concentration dependent contractions in aortas of all groups. The maximum contractile responses to NA (10^{-8}–10^{-5} mol/L) in the aortas from the NS group rats in the presence of endothelium were significantly ($P < 0.01$) greater than the BDL + NS group rats. Compared with the BDL + NS group, GSH pretreatment (BDL + GSH group) enhanced contractile response of thoracic aortic rings to NA (3×10^{-8}–10^{-5} mol/L) (Figure 2).

Although endothelium-denuded aortic rings showed a higher contractile response to NA (3×10^{-9}–10^{-5} mol/L), there were also no significant differences between BDL + GSH and BDL + GSH + Endo(−) (Figure 3), indicating the necessity of endothelium presence for beneficial vascular effect of GSH.

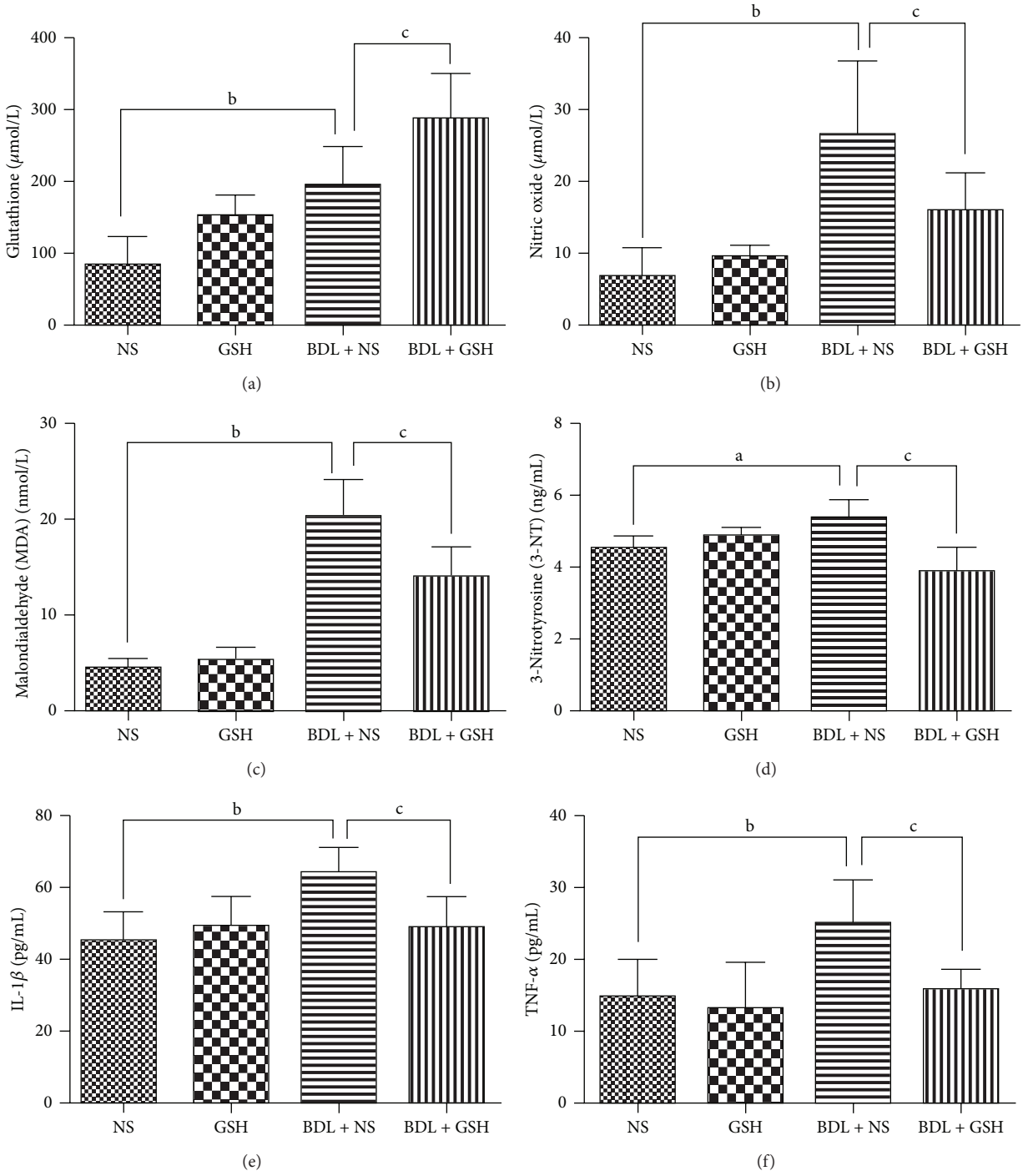

Figure 1: Levels of GSH, NO, MDA, 3-NT, IL-1β, and TNF-α in serum from the NS group, GSH group, BDL + NS group, and BDL + GSH group ($n = 6$). Data are presented as mean ± SD. $^{a}P < 0.05$, $^{b}P < 0.01$ versus NS group; $^{c}P < 0.01$ versus BDL + NS group.

Preincubation of aortic rings with L-NAME significantly increased the contractile response of aortic rings from BDL + NS + L-NAME group rats to NA (3×10^{-8}–10^{-5} mol/L). Likewise, GSH did not modify the contractile response in the BDL + NS + L-NAME and BDL + GSH + L-NAME group (Figure 4).

Aortic rings precontracted with PE from the BDL + NS group showed a significant reduction in relaxation response to ACh ($P < 0.01$, 10^{-8}–10^{-7} mol/L) (Figure 5) and SNP ($P < 0.01$, $P < 0.05$, 10^{-9}–10^{-8} mol/L) (Figure 6) as compared to the NS group. The relaxation to ACh ($P < 0.01$, 10^{-8}–10^{-7} mol/L) was significantly greater in aortic rings from

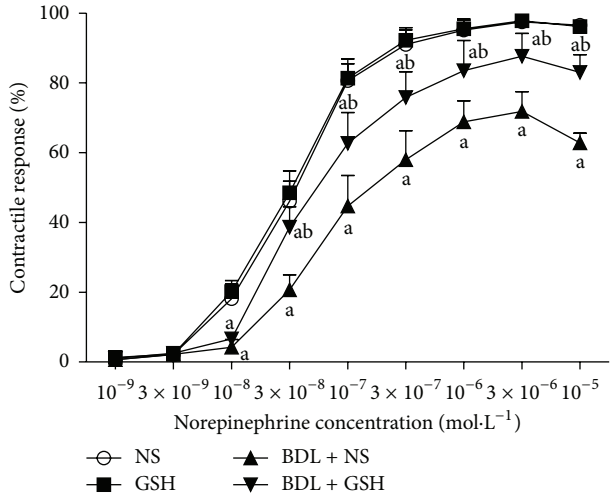

Figure 2: Response elicited by NA in rat thoracic aortic rings from NS group, GSH group, BDL + NS group, and BDL + GSH group ($n = 6$). Data are presented as mean ± SD. [a]$P < 0.01$ versus NS group for % maximum response; [b]$P < 0.01$ versus BDL + NS group.

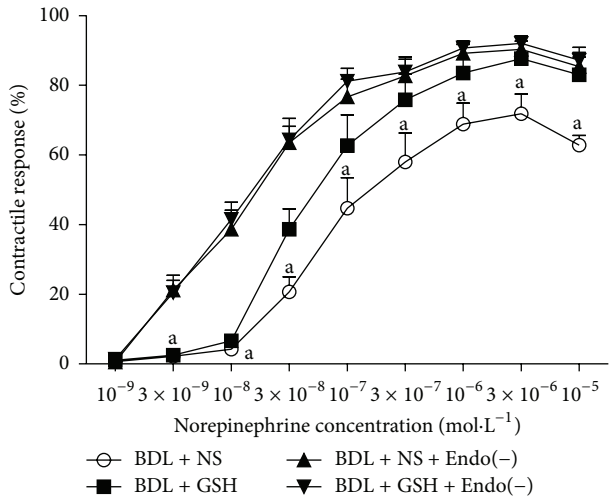

Figure 3: Response elicited by NA in rat thoracic aortic rings from the BDL + NS group, BDL + GSH group, BDL + NS + Endo(−) group, and BDL + GSH + Endo(−) group ($n = 6$). Endothelial was mechanically stripped in BDL + NS + Endo(−) group and BDL + GSH + Endo(−) group. Data are presented as mean ± SD. [a]$P < 0.01$ versus BDL + NS + Endo(−) group for % maximum response.

the BDL + GSH group than in those from the BDL + NS (Figure 5), while the SNP-induced response was similar in the BDL + NS and BDL + GSH groups (Figure 6).

These results suggest that GSH enhances the endothelium dependent vascular responses in the pathogenesis of cholestasis, without affecting the endothelium-independent mechanisms.

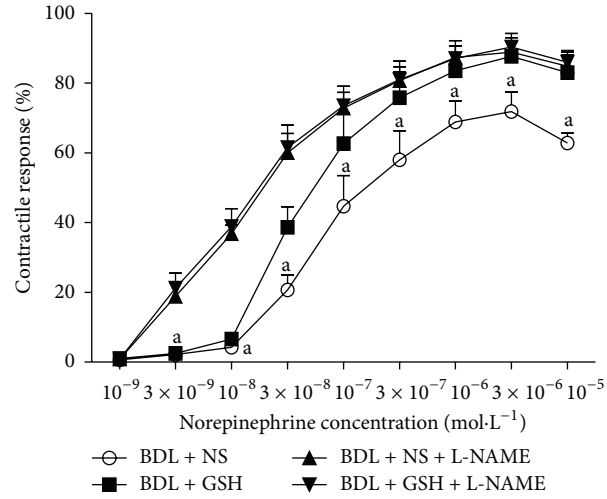

Figure 4: Response elicited by NA in rat thoracic aortic rings from the BDL + NS group, BDL + GSH group, BDL + NS + L-NAME group, and BDL + GSH + L-NAME group ($n = 6$). Incubation of L-NAME in the BDL + NS + L-NAME group and BDL + GSH + L-NAME group. Data are presented as mean ± SD. [a]$P < 0.01$ versus BDL + NS + L-NAME group for % maximum response.

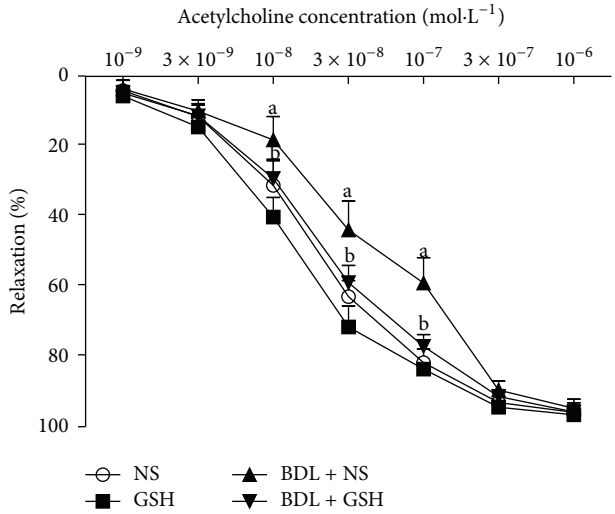

Figure 5: Response elicited by ACh in rat thoracic aortic rings from NS group, GSH group, BDL + NS group, and BDL + GSH group ($n = 6$). Data are presented as mean ± SD. [a]$P < 0.01$ versus NS group for % maximum response.

4. Discussion

The present study demonstrated that oral administration of GSH reduced total bilirubin, ALT, AST, and proinflammatory cytokines levels in the systemic circulation in an experimental OJ animal model with BDL for 7 d. Moreover, GSH supplementation to the rats in the BDL + GSH not only reduced serum 3-NT levels, a protein damage marker induced by ONOO(−), but substantially improved vascular hyporesponsiveness.

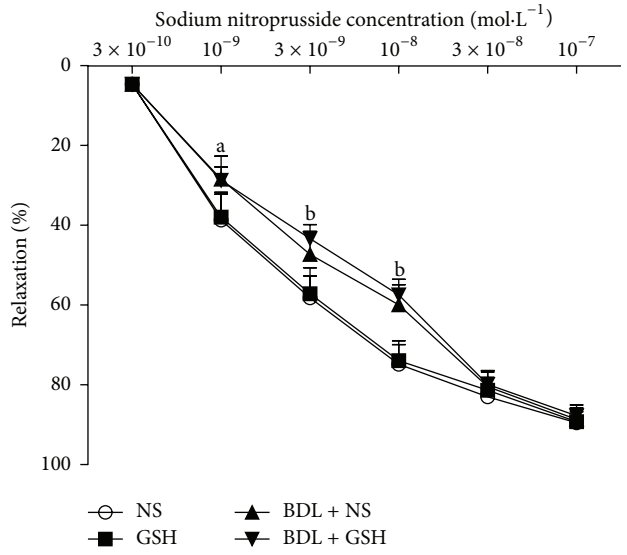

Figure 6: Response elicited by SNP in rat thoracic aortic rings from NS group, GSH group, BDL + NS group, and BDL + GSH group ($n = 6$). Data are presented as mean ± SD. $^{a}P < 0.05$, $^{b}P < 0.01$ versus NS group for % maximum response.

4.1. Oxidative Stress in Obstructive Jaundice. Biliary obstruction is associated with an intense state of OS affecting both the liver and extrahepatic organs [25]. OJ increases OS, characterized by a rise of systemic MDA and a decrease in cellular antioxidant defenses, such as GSH and antioxidant enzymes [26]. Overproduction of ROS, which take a pivotal role of OS, has been shown to induce hypotension and fluid depletion [27]. Intrahepatic and extrahepatic accumulation of ROS is thought to be an important cause for the possible mechanisms of the pathogenesis of cholestatic tissue injury from jaundice. ROS, produced in the course of several biochemical reactions, are extremely reactive intermediates. These free radicals can cause damage to various biological targets, such as proteins, DNA, and lipids [28].

OJ is greatly assumed to increase hepatic OS, as indicated by elevations in hepatic plasma enzymes and bilirubin fractions. In our study, the levels of TBIL, ALT, and AST as indicatives of hepatic functions were found to increase significantly in OJ, indicating that OJ has affected liver functions. In addition, the increased productions of proinflammatory cytokines, such as TNF-α and IL-1β are suggested to be responsible for liver damage in OJ. Proinflammatory cytokines exert a considerably amplifying effect in hepatic inflammatory response and cause severe hepatic tissue damage. In our experimental model of OJ, the increased MDA accumulation in serum was indicative of the extent of lipid peroxidation and the level of 3-NT significantly increased by the oxidation damage of ONOO(−).

4.2. Overexpressed NO and ONOO(−) in Obstructive Jaundice. ROS are involved in metabolizing NO and, among them, $O_2^{\bullet-}$ plays a crucial role since it is source of many other reactive nitrogen intermediates. ONOO(−), a powerful oxidant, is much more reactive than its parent molecules NO and $O_2^{\bullet-}$ [29]. Under physiological conditions, the production of ONOO(−) will be low and oxidative damage minimized by endogenous antioxidant defenses [30]. Even modest increases in the simultaneous production of $O_2^{\bullet-}$ and NO will greatly stimulate the formation of ONOO(−); a 10-fold increase in $O_2^{\bullet-}$ and NO production will increase ONOO(−) formation 100-fold.

Consequently, pathological conditions can greatly increase the production of ONOO(−) [31]. ONOO(−) affects the activity of functional proteins such as receptors, ion-channels, and enzymes by oxidation of cysteine residues (i.e., disulfide-bond formation) and/or nitration of susceptible residues such as tyrosine, tryptophan, and phenylalanine in these proteins [32–36], result in substantial oxidation and potential destruction of host cellular constituents, leading to the dysfunction of critical cellular processes, disruption of cell signaling pathways, and the induction of cell death through both apoptosis and necrosis [31]. It has been shown that ONOO(−) causes tissue damage including adrenergic α1-adrenoceptors, arginine vasopressin V1a receptors [37], adrenergic β-adrenoceptor [38], pulmonary artery, cardiomyocyte apoptosis, insulin sensitivity [39], and endothelial injury.

Increased level of 3-NT, a marker of oxidative protein modification [40], caused by excessive concentration of ONOO(−), significantly increased the BDL + NS group. Similar results were observed in mesenteric artery from orchidectomized rats in which products generated from NO metabolism, such as ONOO(−) and hydrogen peroxide, are able to induce relaxation [41].

4.3. GSH, an Antioxidant in Obstructive Jaundice. GSH, an antioxidant, one of the major drugs used in the treatment of hepatocellular jaundice, prevents damage to important cellular components caused by ROS such as ONOO(−) and peroxides. Panozzo et al. [42] reported that extrahepatic cholestasis reduced bioavailability of blood GSH in rats. The antioxidant defense system is impaired by the decrease in GSH reductase (GR) and in the activity of glutathione peroxidase (GPx) in OJ [43]. Lopze et al. [44] observed that biliary obstruction was accompanied by increased levels of lipid peroxidation in plasma and hepatic tissue and by the depletion of GSH in both biological tissues. Sheen et al. [45] also reported that BDL-induced liver, kidney, and brain tissue damage were associated with increased oxidative stress, represented by decreased total GSH levels in BDL rats. However, Orellana et al. [46] reported that the GSH and MDA levels of kidney and liver tissues increased in the cholestasis-induced rats.

In our study, we found an increase in GSH levels in serum in BDL rats. The content of total serum GSH was increased as a response to the increased oxidative stress in rats. Purucker et al. [47] found that liver GSH significantly increased 24 h (+37%) and 5 days (+53%) after bile-duct ligation. Thereafter, GSH continuously declined at the end of the observation period after 38 days. BDL induced a 3.7-fold increase in hepatic GSH content over 4 days. This increase was not due to the increased hepatic activity of gamma-glutamylcysteine

synthetase (GCS); on the contrary, liver GCS activity was substantially diminished to 34% and 11% of normal rats on the 4th and 7th days after ligation, respectively [48]. The level of common bile duct diameter and pressure was on the peak level at 7 days after operation and the excretion of bile to canalicular and sinusoidal was also depressed. Furthermore, the accumulation of GSH entered the systemic circulation and increased the level of GSH in serum on the 7th day in BDL model.

In the present study, we showed that GSH supplementation increased the level of GSH in the BDL + GSH group and reduced serum TBIL, ALT, and AST in OJ rats. Compared with the BDL + NS group, GSH significantly reduced TNF-α and IL-1β in the BDL + GSH group, which suggested that the protective effects of GSH on liver injury might be mediated by the suppression of the excessive inflammatory response and its cascade induced by OJ. What is more, GSH treatment 300 mg/kg for 14 days attenuated NO, 3-NT, and MDA levels of the serum on the 7 days after ligation, which indicated that GSH reduced the OS induced by OJ. Administration of GSH could exert a significantly unique anti-ONOO(−) effect in BDL + GSH rats and decrease 3-NT content.

Although the antioxidant properties of GSH are thought to play a role in the protective effects, other possible mechanisms, such as modulations of glutathione synthetase (GS), GR, GPx and GSH/GSSG ratio, may be involved. Further researches are needed.

4.4. Vasoconstriction and Vasodilator Response in Obstructive Jaundice. In our previous work, we reported that the systolic and diastolic functions of isolated thoracic aorta rings induced by high potassium, NA, PE, and SNP were changed in cholestatic rats. The weakened systolic function might be due to the vascular endothelial dysfunction, vascular smooth muscle cell damage, and decreased expression of α1D-AR albumen induced by endotoxemia and hyperbilirubinemia [49]. In this research, we supported the hypothesis that antioxidant supplementation might protect the vascular endothelial dysfunction induced by OS and then improved the vascular hyporesponsiveness to adrenergic agonists. Moreover, we found that rings with endothelium removed from BDL + NS + Endo(−) and BDL + GSH + Endo(−) animals had a greater tension. It enhanced contractility of aortic rings to NA and abolished the protective effect between the BDL + NS group and BDL + GSH group, suggesting that GSH changes at the endothelial level rather than vascular smooth muscle cell.

Endothelial-derived relaxing factors including NO, prostacyclin, and endothelium-derived hyperpolarizing factor released from endothelial cells in vascular vessel lead to relaxation of vascular smooth muscle in an endothelium-dependent manner [50, 51]. Compared with the rings in the BDL + NS group, NA contractility increased with L-NAME incubation in the BDL + NS + L-NAME group and BDL + GSH + L-NAME group, which suggested that the protective effect of GSH was partly due to involvement of NO pathway.

Furthermore, the contribution of NO and endothelium mechanisms in the vasodilator response induced by ACh or SNP were studied. The ACh-induced relaxation response is endothelium-dependent and NO-mediated [52]. The NO donor SNP induces relaxation by direct effect on the smooth muscle and via an endothelium-independent pathway.

Compared with the NS group, we observed a decrease in vascular response to ACh in the BDL + NS group in OJ. Relaxation response to SNP was also significantly attenuated. GSH treatment increased the endothelial-dependent vasodilator response induced by ACh in the BDL + GSH group. Response to SNP was not altered after GSH treatment suggesting that vascular smooth muscle cell was not well protected on the 14th day after administration or the dosage was not enough to alter the vasodilator response.

Bioavailability of endothelial NO alters vascular function, depending on a balance between NO production and degradation. Increased production of NO is beneficial after arterial injury because of its positive effects on vasorelaxation, prevention of platelet aggregation, and regulation of endothelial cell migration [53]. Constitutive NOS (eNOS and nNOS) and not the iNOS, are the isoforms involved in the relaxation.

ACh-induced vasorelaxation is mediated predominantly by eNOS [54]. Increased serum level of NO may be due to increased activity of NOS. However, an increase in iNOS may lead to over production of NO which is an important factor in BDL rats. The iNOS expression has been reported to attenuate the ACh response [55]. Increases in NO level rats may be the first stage of the toxic oxidative reaction that is harmful for the tissues [56]. Indeed, vascular contractility and relaxation may be associated with the deficient basal endothelial activity, besides, increased OS due to excessive production of oxygen-free radicals and decreased antioxidant defense systems may also involve in the process [57]. These results suggest that OJ induces NOS and increases the NO production along with inducing OS.

The effect of GSH on the improvement of endothelial dysfunction could be related to its antioxidant activity. Oxidative degradation of lipids is a well-defined mechanism of cellular damage caused by excessive production of ROS, and MDA is the most widely employed assay used to determine lipid peroxidation. GSH treatment with significantly decreased MDA content indicating that the improvement in endothelium-dependent vasoreactivity from GSH may be partly due to amelioration of lipid peroxidation and oxidative injury in vascular endothelial cells. More specifically, GSH declines ONOO(−) production and increases NO availability. In this case, endothelial dysfunction may be limited to the impairment in the homeostatic balance maintained between GSH and ONOO(−).

4.5. Deficiency of This Research. However, the mechanisms of the beneficial effects of GSH on vascular function have not been clarified. We have also questioned the potential anti-inflammatory mechanisms of OJ vasculopathy and among them are the aortic NO and TNF-α levels. GSH dose in the current study was selected from previous studies on rats [22]. It should be noted that this dose was much higher than those clinically used in the treatment of hepatocellular jaundice (1200 mg p.o. tid). Additionally, it should be reminded that this is an ex vivo, not an in vivo, study which is performed on the large, but not small, arteries of BDL rats. Therefore,

any potential antioxidant activity of GSH requires to be investigated in well-conducted clinical trials performed on humans.

5. Conclusion

In conclusion, GSH supplementation attenuates overexpressed ONOO(−) from the reaction of excessive NO with $O_2^{\bullet-}$ and protects against OJ-induced vascular hyporesponsiveness in rats. GSH supplementation may be a novel and promising therapeutic strategy for the treatment of OJ-induced vascular hyporesponsiveness during perioperative period. Further researches are necessary to ascertain the possible mechanisms.

Disclosure

All the authors have no competing interests to declare.

Conflict of Interests

The authors declare that there is no conflict of interests regarding the publication of this paper.

Authors' Contribution

Jiaying Chen and Feixiang Wu contributed equally to this study. Jiaying Chen performed the majority of experiments and wrote the paper; Weifeng Yu, Feixiang Wu, and Yue Long provided vital reagents and analytical tools, designed the study, revised the paper, and provided financial support for this work.

Acknowledgment

This study was supported by the National Natural Science Foundation of China (81170427).

References

[1] A. B. Ballinger, J. A. Woolley, M. Ahmed et al., "Persistent systemic inflammatory response after stent insertion in patients with malignant bile duct obstruction," *Gut*, vol. 42, no. 4, pp. 555–559, 1998.

[2] J. Green and O. S. Better, "Systemic hypotension and renal failure in obstructive jaundice—mechanistic and therapeutic aspects," *Journal of the American Society of Nephrology*, vol. 5, no. 11, pp. 1853–1871, 1995.

[3] A. Kimmoun, N. Ducrocq, and B. Levy, "Mechanisms of vascular hyporesponsiveness in septic shock," *Current Vascular Pharmacology*, vol. 11, no. 2, pp. 139–149, 2013.

[4] B. L. Copple, H. Jaeschke, and C. D. Klaassen, "Oxidative stress and the pathogenesis of cholestasis," *Seminars in Liver Disease*, vol. 30, no. 2, pp. 195–204, 2010.

[5] L. M. Yung, F. P. Leung, X. Yao, Z.-Y. Chen, and Y. Huang, "Reactive oxygen species in vascular wall," *Cardiovascular and Hematological Disorders-Drug Targets*, vol. 6, no. 1, pp. 1–19, 2006.

[6] V. Barón and P. Muriel, "Role of glutathione, lipid peroxidation and antioxidants on acute bile- duct obstruction in the rat," *Biochimica et Biophysica Acta—General Subjects*, vol. 1472, no. 1-2, pp. 173–180, 1999.

[7] M. Galicia-Moreno, L. Favari, and P. Muriel, "Antifibrotic and antioxidant effects of N-acetylcysteine in an experimental cholestatic model," *European Journal of Gastroenterology and Hepatology*, vol. 24, no. 2, pp. 179–185, 2012.

[8] D. D. Rees, J. E. Monkhouse, D. Cambridge, and S. Moncada, "Nitric oxide and the haemodynamic profile of endotoxin shock in the conscious mouse," *British Journal of Pharmacology*, vol. 124, no. 3, pp. 540–546, 1998.

[9] J. González, N. Valls, R. Brito, and R. Rodrigo, "Essential hypertension and oxidative stress: new insights," *World Journal of Cardiology*, vol. 6, no. 6, pp. 353–366, 2014.

[10] W. A. Boyle III, L. S. Parvathaneni, V. Bourlier, C. Sauter, V. E. Laubach, and J. P. Cobb, "iNOS gene expression modulates microvascular responsiveness in endotoxin-challenged mice," *Circulation Research*, vol. 87, no. 7, pp. E18–E24, 2000.

[11] P. Pacher, J. S. Beckman, and L. Liaudet, "Nitric oxide and peroxynitrite in health and disease," *Physiological Reviews*, vol. 87, no. 1, pp. 315–424, 2007.

[12] M. L. Pall, "The NO/ONOO-cycle as the central cause of heart failure," *International Journal of Molecular Sciences*, vol. 14, no. 11, pp. 22274–22330, 2013.

[13] F. Çelebi, I. Yilmaz, H. Aksoy, M. Gümüş, S. Taysi, and D. Oren, "Dehydroepiandrosterone prevents oxidative injury in obstructive jaundice in rats," *Journal of International Medical Research*, vol. 32, no. 4, pp. 400–405, 2004.

[14] L. Carpenter-Deyo, D. H. Marchand, P. A. Jean, R. A. Roth, and D. J. Reed, "Involvement of glutathione in 1-naphthylisothiocyanate (ANIT) metabolism and toxicity to isolated hepatocytes," *Biochemical Pharmacology*, vol. 42, no. 11, pp. 2171–2180, 1991.

[15] G. Şener, O. Şehirli, H. Toklu, F. Ercan, and I. Alican, "Montelukast reduces ischaemia/reperfusion-induced bladder dysfunction and oxidant damage in the rat," *Journal of Pharmacy and Pharmacology*, vol. 59, no. 6, pp. 837–842, 2007.

[16] M. J. Perez, R. I. R. Macias, and J. J. G. Marin, "Maternal cholestasis induces placental oxidative stress and apoptosis. Protective effect of ursodeoxycholic acid," *Placenta*, vol. 27, no. 1, pp. 34–41, 2006.

[17] A. Engin and N. Altan, "Effects of obstructive jaundice on the antioxidative capacity of human red blood cells," *Haematologia (Budap)*, vol. 30, no. 2, pp. 91–96, 2000.

[18] V. Ribas, C. García-Ruiz, and J. C. Fernández-Checa, "Glutathione and mitochondria," *Frontiers in Pharmacology*, vol. 5, article 151, 2014.

[19] A. Pompella, A. Visvikis, A. Paolicchi, V. De Tata, and A. F. Casini, "The changing faces of glutathione, a cellular protagonist," *Biochemical Pharmacology*, vol. 66, no. 8, pp. 1499–1503, 2003.

[20] F. Yu, P. Li, B. Wang, and K. Han, "Reversible near-infrared fluorescent probe introducing tellurium to mimetic glutathione peroxidase for monitoring the redox cycles between peroxynitrite and glutathione in vivo," *Journal of the American Chemical Society*, vol. 135, no. 20, pp. 7674–7680, 2013.

[21] Z. Cao and Y. Li, "Protecting against peroxynitrite-mediated cytotoxicity in vascular smooth muscle cells via upregulating endogenous glutathione biosynthesis by 3H-1,2-dithiole-3-thione," *Cardiovascular Toxicology*, vol. 4, no. 4, pp. 339–353, 2004.

[22] P. R. Ramires and L. L. Ji, "Glutathione supplementation and training increases myocardial resistance to ischemia-reperfusion in vivo," *The American Journal of Physiology—Heart and Circulatory Physiology*, vol. 281, no. 2, pp. H679–H688, 2001.

[23] F. T. Spradley, D. H. Ho, K.-T. Kang, D. M. Pollock, and J. S. Pollock, "Changing standard chow diet promotes vascular NOS dysfunction in Dahl S rats," *American Journal of Physiology—Regulatory Integrative and Comparative Physiology*, vol. 302, no. 1, pp. R150–R158, 2012.

[24] S. Omanwar, B. Saidullah, K. Ravi, and M. Fahim, "Modulation of vasodilator response via the nitric oxide pathway after acute methyl mercury chloride exposure in rats," *BioMed Research International*, vol. 2013, Article ID 530603, 8 pages, 2013.

[25] T. P. Fernández, P. L. Serrano, E. Tomás et al., "Diagnostic and therapeutic approach to cholestatic liver disease," *Revista Española de Enfermedades Digestivas*, vol. 96, no. 1, pp. 60–73, 2004.

[26] P. Montilla, A. Cruz, F. J. Padillo et al., "Melatonin versus vitamin E as protective treatment against oxidative stress after extra-hepatic bile duct ligation in rats," *Journal of Pineal Research*, vol. 31, no. 2, pp. 138–144, 2001.

[27] F. J. Padillo, M. Rodriguez, J. M. Gallardo et al., "Preoperative assessment of body fluid disturbances in patients with obstructive jaundice," *World Journal of Surgery*, vol. 23, no. 7, pp. 681–687, 1999.

[28] H. S. Basaga, "Biochemical aspects of free radicals," *Biochemistry and Cell Biology*, vol. 68, no. 7-8, pp. 989–998, 1990.

[29] J. S. Beckman and W. H. Koppenol, "Nitric oxide, superoxide, and peroxynitrite: the good, the bad, and the ugly," *The American Journal of Physiology—Cell Physiology*, vol. 271, no. 5, pp. C1424–C1437, 1996.

[30] R. Radi, A. Cassina, R. Hodara, C. Quijano, and L. Castro, "Peroxynitrite reactions and formation in mitochondria," *Free Radical Biology and Medicine*, vol. 33, no. 11, pp. 1451–1464, 2002.

[31] L. Virág, É. Szabó, P. Gergely, and C. Szabó, "Peroxynitrite-induced cytotoxicity: mechanism and opportunities for intervention," *Toxicology Letters*, vol. 140-141, pp. 113–124, 2003.

[32] R. Radi, J. S. Beckman, K. M. Bush, and B. A. Freeman, "Peroxynitrite oxidation of sulfhydryls: the cytotoxic potential of superoxide and nitric oxide," *The Journal of Biological Chemistry*, vol. 266, no. 7, pp. 4244–4250, 1991.

[33] B. Alvarez and R. Radi, "Peroxynitrite reactivity with amino acids and proteins," *Amino Acids*, vol. 25, no. 3-4, pp. 295–311, 2003.

[34] H. Li, D. D. Gutterman, N. J. Rusch, A. Bubolz, and Y. Liu, "Nitration and functional loss of voltage-gated K^+ channels in rat coronary microvessels exposed to high glucose," *Diabetes*, vol. 53, no. 9, pp. 2436–2442, 2004.

[35] T. Nomiyama, Y. Igarashi, H. Taka et al., "Reduction of insulin-stimulated glucose uptake by peroxynitrite is concurrent with tyrosine nitration of insulin receptor substrate-1," *Biochemical and Biophysical Research Communications*, vol. 320, no. 3, pp. 639–647, 2004.

[36] K. Takakura, T. Taniguchi, I. Muramatsu, K. Takeuchi, and S. Fukuda, "Modification of α1-adrenoceptors by peroxynitrite as a possible mechanism of systemic hypotension in sepsis," *Critical Care Medicine*, vol. 30, no. 4, pp. 894–899, 2002.

[37] S. J. Lewis, A. Hoque, K. Sandock, T. P. Robertson, J. N. Bates, and N. W. Kooy, "Differential effects of peroxynitrite on the function of arginine vasopressin V_{1a} receptors and alpha$_1$-adrenoceptors in vivo," *Vascular Pharmacology*, vol. 46, no. 1, pp. 24–34, 2007.

[38] S. J. Lewis, A. Hoque, T. M. Walton, and N. W. Kooy, "Potential role of nitration and oxidation reactions in the effects of peroxynitrite on the function of beta-adrenoceptor sub-types in the rat," *European Journal of Pharmacology*, vol. 518, no. 2-3, pp. 187–194, 2005.

[39] H. Duplain, C. Sartori, P. Dessen et al., "Stimulation of peroxynitrite catalysis improves insulin sensitivity in high fat diet-fed mice," *The Journal of Physiology*, vol. 586, no. 16, pp. 4011–4016, 2008.

[40] I. Dalle-Donne, R. Rossi, R. Colombo, D. Giustarini, and A. Milzani, "Biomarkers of oxidative damage in human disease," *Clinical Chemistry*, vol. 52, no. 4, pp. 601–623, 2006.

[41] M. D. C. Martín, G. Balfagón, N. Minoves, J. Blanco-Rivero, and M. Ferrer, "Androgen deprivation increases neuronal nitric oxide metabolism and its vasodilator effect in rat mesenteric arteries," *Nitric Oxide*, vol. 12, no. 3, pp. 163–176, 2005.

[42] M. P. Panozzo, D. Basso, L. Balint et al., "Altered lipid peroxidation/glutathione ratio in experimental extrahepatic cholestasis," *Clinical and Experimental Pharmacology and Physiology*, vol. 22, no. 4, pp. 266–271, 1995.

[43] M. Dirlik, H. Canbaz, D. Düşmez Apa et al., "The monitoring of progress in apoptosis of liver cells in bile duct-ligated rats," *Turkish Journal of Gastroenterology*, vol. 20, no. 4, pp. 247–256, 2009.

[44] P. M. Lopze, I. T. Fiñana, M. C. M. de Agueda et al., "Protective effect of melatonin against oxidative stress induced by ligature of extra-hepatic biliary duct in rats: comparison with the effect of S-adenosyl-L-methionine," *Journal of Pineal Research*, vol. 28, no. 3, pp. 143–149, 2000.

[45] J.-M. Sheen, L.-T. Huang, C.-S. Hsieh, C.-C. Chen, J.-Y. Wang, and Y.-L. Tain, "Bile duct ligation in developing rats: temporal progression of liver, kidney, and brain damage," *Journal of Pediatric Surgery*, vol. 45, no. 8, pp. 1650–1658, 2010.

[46] M. Orellana, R. Rodrigo, L. Thielemann, and V. Guajardo, "Bile duct ligation and oxidative stress in the rat: effects in liver and kidney," *Comparative Biochemistry and Physiology Part C: Pharmacology, Toxicology and Endocrinology*, vol. 126, no. 2, pp. 105–111, 2000.

[47] E. Purucker, R. Winograd, E. Roeb, and S. Matern, "Glutathione status in liver and plasma during development of biliary cirrhosis after bile duct ligation," *Research in Experimental Medicine*, vol. 198, no. 4, pp. 167–174, 1998.

[48] B. A. Neuschwander-Tetri, C. Nicholson, L. D. Wells, and T. F. Tracy Jr., "Cholestatic liver injury down-regulates hepatic glutathione synthesis," *Journal of Surgical Research*, vol. 63, no. 2, pp. 447–451, 1996.

[49] G. Wu, X.-W. Xu, X.-R. Miao, L.-Q. Yang, Q. Li, and W.-F. Yu, "Changes of vasoconstrictor and vasodilator functions of isolated thoracic aorta rings in rats with obstructive jaundice," *Academic Journal of Second Military Medical University*, vol. 30, no. 2, pp. 162–165, 2009.

[50] A. Takaki, K. Morikawa, Y. Murayama et al., "Roles of endothelial oxidases in endothelium-derived hyperpolarizing factor responses in mice," *Journal of Cardiovascular Pharmacology*, vol. 52, no. 6, pp. 510–517, 2008.

[51] L.-N. Zhang, J. Vincelette, D. Chen et al., "Inhibition of soluble epoxide hydrolase attenuates endothelial dysfunction in animal models of diabetes, obesity and hypertension," *European Journal of Pharmacology*, vol. 654, no. 1, pp. 68–74, 2011.

[52] M. Roghani and T. Baluchnejadmojarad, "Chronic epigallocatechingallate improves aortic reactivity of diabetic rats:

underlying mechanisms," *Vascular Pharmacology*, vol. 51, no. 2-3, pp. 84–89, 2009.

[53] V. Poppa, J. K. Miyashiro, M. A. Corson, and B. C. Berk, "Endothelial NO synthase is increased in regenerating endothelium after denuding injury of the rat aorta," *Arteriosclerosis, Thrombosis, and Vascular Biology*, vol. 18, no. 8, pp. 1312–1321, 1998.

[54] A. Gericke, E. Goloborodko, J. J. Sniatecki, A. Steege, L. Wojnowski, and N. Pfeiffer, "Contribution of nitric oxide synthase isoforms to cholinergic vasodilation in murine retinal arterioles," *Experimental Eye Research*, vol. 109, pp. 60–66, 2013.

[55] J. Tian, Z. Yan, Y. Wu et al., "Inhibition of iNOS protects endothelial-dependent vasodilation in aged rats," *Acta Pharmacologica Sinica*, vol. 31, no. 10, pp. 1324–1328, 2010.

[56] K. Takagi, Y. Kawaguchi, M. Hara, T. Sugiura, M. Harigai, and N. Kamatani, "Serum nitric oxide (NO) levels in systemic sclerosis patients: correlation between NO levels and clinical features," *Clinical and Experimental Immunology*, vol. 134, no. 3, pp. 538–544, 2003.

[57] J. B. Majithiya, A. N. Paramar, and R. Balaraman, "Pioglitazone, a PPARγ agonist, restores endothelial function in aorta of streptozotocin-induced diabetic rats," *Cardiovascular Research*, vol. 66, no. 1, pp. 150–161, 2005.

Hindawi Publishing Corporation
Oxidative Medicine and Cellular Longevity
Volume 2015, Article ID 876825, 9 pages
http://dx.doi.org/10.1155/2015/876825

Research Article

The Protective Effects of Salidroside from Exhaustive Exercise-Induced Heart Injury by Enhancing the *PGC-1α–NRF1/NRF2* Pathway and Mitochondrial Respiratory Function in Rats

Zheng Ping,[1] Long-fei Zhang,[1] Yu-juan Cui,[1] Yu-mei Chang,[1] Cai-wu Jiang,[2] Zhen-zhi Meng,[3] Peng Xu,[1] Hai-yan Liu,[1] Dong-ying Wang,[1] and Xue-bin Cao[1]

[1]*Department of Cardiology, Geriatric Cardiovascular Disease Research and Treatment Center, No. 252 Hospital of PLA, Baoding 071000, China*
[2]*Institute of Chinese Materia Medica, Guangxi University of Chinese Medicine, Nanning 530200, China*
[3]*School of Preclinical Medicine, Youjiang Medical University for Nationalities, Baise, Guangxi 533000, China*

Correspondence should be addressed to Xue-bin Cao; caoxb252@163.com

Received 20 September 2014; Revised 11 December 2014; Accepted 11 December 2014

Academic Editor: Yanfang Chen

Objective. To test the hypothesis that salidroside (SAL) can protect heart from exhaustive exercise-induced injury by enhancing mitochondrial respiratory function and mitochondrial biogenesis key signaling pathway *PGC-1α–NRF1/NRF2* in rats. *Methods*. Male Sprague-Dawley rats were divided into 4 groups: sedentary (C), exhaustive exercise (EE), low-dose SAL (LS), and high-dose SAL (HS). After one-time exhaustive swimming exercise, we measured the changes in cardiomyocyte ultrastructure and cardiac marker enzymes and mitochondrial electron transport system (ETS) complexes activities *in situ*. We also measured mitochondrial biogenesis master regulator *PGC-1α* and its downstream transcription factors, *NRF1* and *NRF2*, expression at gene and protein levels. *Results*. Compared to C group, the EE group showed marked myocardium ultrastructure injury and decrease of mitochondrial respiratory function ($P < 0.05$) and protein levels of *PGC-1α*, *NRF1*, and *NRF2* ($P < 0.05$) but a significant increase of *PGC-1α*, *NRF1*, and *NRF2* genes levels ($P < 0.05$); compared to EE group, SAL ameliorated myocardium injury, increased mitochondrial respiratory function ($P < 0.05$), and elevated both gene and protein levels of *PGC-1α*, *NRF-1*, and *NRF-2*. *Conclusion*. Salidroside can protect the heart from exhaustive exercise-induced injury. It might act by improving myocardial mitochondrial respiratory function by stimulating the expression of *PGC-1α–NRF1/NRF2* pathway.

1. Introduction

Exercise training is a double-edged sword, as proper intensity exercise is beneficial to human health, whereas excessive exercise can do harm to the body, especially the heart. Heart injury induced by excessive exercise training includes severe arrhythmia, heart failure, and even sudden cardiac death, which are common in military and athletic training. Research on heart injury induced by exhaustive exercise is quite important, yet few systematic studies of heart injury induced by exhaustive exercise have been published and the underlying signaling pathway mechanisms remain to be elucidated.

The term "heart failure energy starvation" was proposed decades ago [1]; however, very little is currently known about the origins of energetic failure. It appears that the transcriptional coactivator peroxisome proliferator-activated receptor-γ coactivator-1α (*PGC-1α*), which is a master regulator of mitochondrial biogenesis [2], plays a role in controlling the rate of the mitochondrial proliferation. Energy deficit and *PGC-1α* are markers of heart dysfunction, which can lead to impaired energy metabolism and contribute to heart failure. The term mitochondrial biogenesis refers to mitochondrial proliferation. Exercise, cold, energy restriction, oxidative stress, and other environmental stresses can all induce

mitochondrial biogenesis. The discovery that maladapitive accumulation of mitochondrial biogenesis can lead to pathological phenomena, such as myocardial hypertrophy and heart failure, highlights the importance of elucidating the molecular regulatory mechanism for mitochondrial biogenesis.

Mitochondrial biogenesis requires the coordinated expression of the nuclear and mitochondrial DNA; the signaling pathways that coordinate the transcription and replication signaling pathways between genomic and mitochondrial DNA remain to be fully elucidated. It has been reported that *PGC-1α* plays a key role in skeletal muscle mitochondrial biogenesis and its expression level is rate limiting for skeletal muscle mitochondrial gene expression. *PGC-1α* cooperates with nuclear respiratory factors (*NRFs*), including *NRF1* and *NRF2*, and promotes the expression of multiple nuclear-encoded genes and the mitochondrial transcriptional factor A (*Tfam*). Nevertheless, some points of debate remain; for example, the expression of *PGC-1α* mRNA did not change after acute or endurance exercise training and the gene and protein levels of *NRF1* and *NRF2* were not correlated with *PGC-1α* gene or protein content [3].

Enzymatic assays for individual mitochondrial respiratory chain complexes have been widely used to estimate mitochondrial function and dysfunction. However, it has been established that this approach is not sufficient for a complete analysis of a potential mitochondrial injury, as it cannot reveal interactions between enzyme complexes. Additionally, routine mitochondrial isolation procedures will result in altered mitochondrial morphology and damaged function [4]. Respirometry [5] offers a powerful and physiologically relevant method to characterize coupled respiratory function in permeabilized tissue. A specially designed substrate-inhibitor titration approach allows for the step-by-step analysis of several mitochondrial complexes. However, the specific adaptive changes of myocardial mitochondrial respiratory function after exhaustive exercise remain unclear.

The stems of *Rhodiola crenulata* have been used as a traditional Chinese medicine for more than 1000 years [6]. *R. crenulata* has the effect of supplementing qi (vital energy) and activating blood circulation and has been recognized as a plant-derived adaptogen that is capable of maintaining physiological homeostasis upon exposure to stress. Salidroside (SAL) is an effective extract component from *R. crenulata*. Many studies have found that SAL had protective effects on myocardial ischemia reperfusion [7], myocardial hypoxia [8], and myocardial injury [9]. Our previous research has suggested that SAL could improve hypoxia-induced cardiac myocyte energy metabolism by increasing the intracellular activity of the respiratory enzyme succinate dehydrogenase (SDH) [10]. However, there is no research regarding whether SAL is protective against acute myocardial injury caused by exhaustive exercise at present or not. In this study, we established the model of exhaustive swimming exercise-induced rat heart injury to investigate the effect of SAL on cardiac mitochondrial respiratory function and discuss whether the protection mechanism is through mitochondrial biogenesis *PGC-1α–NRF1/NRF2* signaling pathway or not.

2. Methods

2.1. Materials. SAL (98%) was purchased from Nanjing Zelang Medical Technology Co. (Lot: ZL201204012A) (Nanjing, Jiangsu, China). ELISA kits for heart injury markers were obtained from BD (New York City, NY, USA). Reagents for measuring mitochondrial respiratory function were purchased from Sigma-Aldrich (St. Louis, MO, USA). Antibodies to *PGC-1α*, *NRF1*, *NRF2*, and *β*-actin protein were purchased from CST (USA).

We obtained 40 male Sprague-Dawley rats (190–200 g) from Laboratory Animal Center of the Academy of Military Medical Sciences (Beijing, China), certification number SCXK: 2003-1-003. Animals were housed at 25°C-26°C under a 12 h dark, 12 h light cycle. Food and water were provided *ad libitum* both prior to and during the 1-day experimental period. All procedures were performed in accordance with the guidelines established by *the Convention for the Protection of Laboratory Animals of the PLA 252nd Hospital*.

A high-resolution respirometry (Oroboros Instruments, Austria), a microplate reader (Thermo Fisher SC, FI), a biochemical analyzer (7600-02, HITACHI, Japan), and a transmission electron microscope (TEM) (H-7500, HITACHI, Japan) were used in the experiments.

2.2. Experimental Groups and Exercise Training. Rats were trained in a water sink for 3 days prior to the formal experiment and those rats that were unable to adapt to swimming were excluded. A total of 32 rats ultimately entered the formal experiment. They were randomly divided into 4 groups: the sedentary control group (C, $n = 8$), the exhaustive exercise group (EE, $n = 8$), the pretreatment with low-dose SAL group (LS, $n = 8$), and the pretreatment with high-dose SAL group (HS, $n = 8$). The C and EE groups were administered 0.9% NaCl ($12\,mg{\cdot}kg^{-1}{\cdot}d^{-1}$) intragastrically for 14 days and the LS and HS groups were administered $100\,mg{\cdot}kg^{-1}{\cdot}d^{-1}$ or $300\,mg{\cdot}kg^{-1}{\cdot}d^{-1}$ SAL, respectively, intragastrically for 14 days [11].

Rats in the EE, HS, and LS groups were subjected to one-time exhaustive swimming tests individually in a water sink (60 cm × 90 cm × 50 cm), with a water depth of 50 cm and temperature of 35°C ± 0.5°C. Exhaustion was defined by two criteria: greater than 10 s spent below the surface and lack of a "righting reflex" when placed on a flat surface [12]. At the point of exhaustion, all rats were anesthetized by the intraperitoneal injection of pentobarbital ($50\,mg{\cdot}kg^{-1}$). Serum was collected and preserved at −80°C and the hearts were removed. The left ventricular tissue was isolated and part was immediately used for mitochondrial function measurements and part was preserved at −80°C for further analyses.

2.3. Histomorphometric Analysis. Rat hearts were fixed in 10% formaldehyde, preserved at room temperature, and observed using an Optical Microscope after H&E staining.

A small piece (2 mm × 1 mm × 1 mm) of subendocardial myocardium from the root of the left ventricular papillary muscle was harvested and fixed in 0.1 mmol/L phosphate buffer and observed by transmission electron microscopy (TEM).

Table 1: Primers used for real-time PCR analyses of mRNA expression.

	Forward	Reverse
PGC-1α	5′-ACCCACAGGATCAGAACAAACC-3′	5′-GACAAATGCTCTTTGCTTTATTGC-3′
NRF1	5′-GGCACAGGCTGAGCTGATG-3′	5′-CTAGTTCCAGGTCAGCCACCTTT-3′
NRF2	5′-CCTAAAGCACAGCCAACACA-3′	5′-ACAGTTCTGAGCGGCAACTT-3′
β-actin	5′-GGCTGTATTCCCTCCATCG-3′	5′-CCAGTTGGTAACAATGCCATGT-3′

2.4. Assay for Measuring Cardiac Marker Enzyme Activities. Enzyme linked immunosorbent assay (ELISA) kits were used to determine the levels of mitogen-activated protein kinases (CK), creatine kinase isoenzyme (CK-MB), lactate dehydrogenase (LDH), myoglobin (MB), and troponin (cTn-I) in serum. All assays were performed according to the manufacturer's instructions.

2.5. In Situ Studies of Mitochondrial Respiratory Function. We used permeabilized myocardial fibers, which provide an excellent way to study the mitochondria *in situ* without isolating them from tissue. Myocardial fibers were isolated by dissecting muscle tissue (left ventricle) in BIOPS solution on ice followed by saponin permeabilization. Cell membrane permeabilization with saponin enables the study of organelle function while maintaining cellular architecture and controlling the intracellular milieu. Mitochondrial function was measured by high-resolution respirometry at 37°C using dual-chamber titration injection respirometers. The respiration medium (MiR05) included 110 mM sucrose, 60 mM K-lactobionate, 0.5 mM EGTA, 1 g/L bovine serum albumin (essentially fatty acid-free), 3 mM $MgCl_2$, 20 mM taurine, 10 mM KH_2PO_4, and 20 mM HEPES (pH 7.1). DatLab software (Oroboros Instruments) was used for data acquisition and analysis. A series of respiratory titration protocols were designed to test for multiple mitochondrial defects, including cytochrome c depletion. We used 1 mM adenosine diphosphate (ADP) to stimulate respiration (state 3) and measured it sequentially through complex I (10 mM glutamate and 2 mM malate), complex II (10 mM succinate and 0.5 μM rotenone), and complex IV (0.5 mM TMPD, 5 mM ascorbate, and 2.5 μM antimycin A). Chemical background controls were used to correct for TMPD autoxidation and ascorbate. Respiration was measured before and after stimulation by adding cytochrome c (10 μM). Respiratory rates were expressed per mg dry weight and measured on samples collected from the oxygraph chamber at the end of the experiment.

2.6. Real-Time Polymerase Chain Reaction. RNA was isolated from frozen rat myocardia using an ultrapure RNA kit according to manufacturer's protocol. Real-time PCR was performed and analyzed using a fluorescent PCR instrument (IQ-5) using cDNA and SYBR Green PCR Master Mix. Primers sequences are listed in Table 1. The relative amounts of mRNA were determined based on $2^{-\Delta\Delta Ct}$ calculations.

2.7. Western Blotting. Tissue protein reagent was used to extract protein. The protein concentration was determined using the bicinchoninic acid assay (BCA). Then, the protein was added to SDS-PAGE sample loading buffer after dilution in a similar volume and it was placed in a 100°C water bath for 5 min. Protein samples were separated by SDS-PAGE at 100 V for 15 min and 150 V for 45 min and were then transferred to polyvinylidene fluoride (PVDF) membranes. Membranes were blocked in 5% skim milk blocking buffer at room temperature for 1.5 h and then were incubated overnight at 4°C with primary antibodies. After washing the samples with Tris-buffered saline (TBS) Tween, the membranes were incubated with secondary antibody for 2 h at room temperature. ECL was used for colorimetric detection for 5 min after washing with TBS Tween three times. Values were normalized to those of the internal control (*β*-actin).

2.8. Statistical Analyses. SPSS version 16.0 (SPSS Inc., Chicago, IL, USA) was used for statistical analyses. Results were expressed as means ± SD. *t*-test was used to compare data between two groups. One-way analysis of variance (ANOVA) was used to compare data among multiple groups. Statistical significance was considered when $P < 0.05$.

3. Results

3.1. The Effect of Exhaustive Exercise and Salidroside Interference on Histomorphometric Analyses

3.1.1. Light Microscopy. Figure 1 showed an optical microscopy analysis of the rat myocardial structure. Figure 1(a) shows that, in the C group, muscle fibers were arranged neatly as an interstitial substance without edema, the muscle membranes showed no damage, and the muscle fibers had no fractures, degeneration, or necrosis. Figure 1(b) showed that the EE group myocardial fibers were arranged irregularly as interstitial substance with edema, there was muscle membrane damage, and the muscle fibers showed evidence of fracture, degeneration, and necrosis. Figures 1(c) and 1(d) showed that, in the LS and HS groups, the muscle fiber direction changed, the interstitial areas showed slight edema, and the muscle membrane had no damage.

3.1.2. Electron Microscopy. Figure 2 showed the cardiomyocyte ultrastructure. Figure 2(a) showed a TEM structure representative of C group rats: sarcomeres were arranged neatly, the density was uniform, the organelles had no edema, and the membrane and crest of the mitochondria were normal. Figure 2(b) showed the myocardial structures of the EE group rats: the myocardial nuclear matrix had edema, the nuclear gap widened, the number of mitochondria and glycogen content decreased significantly, the membrane and

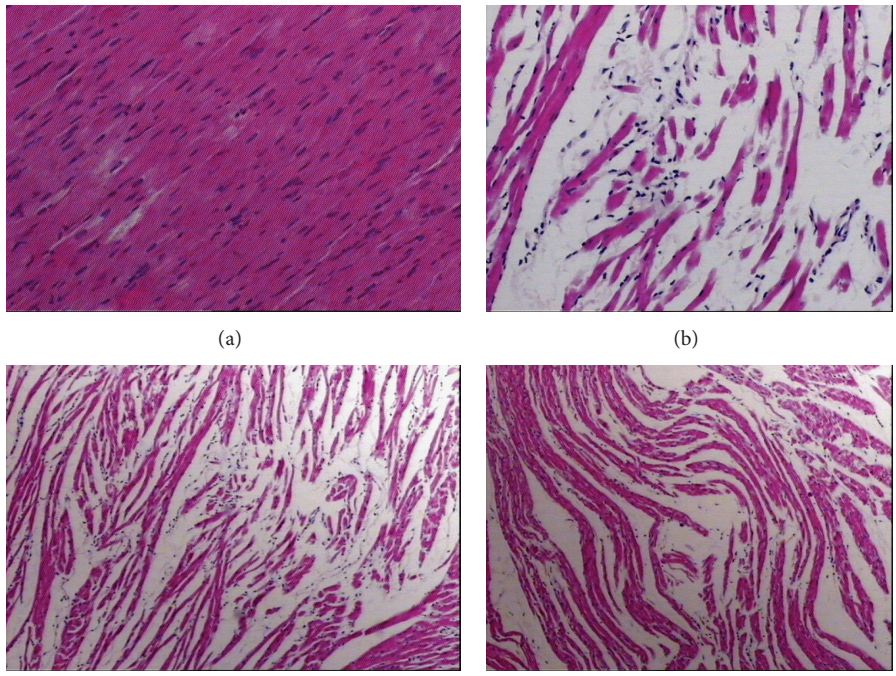

Figure 1: The effect of exhaustive exercise and SAL on the myocardial morphology. Hematoxylin and eosin (H&E) staining (×400); (a) the C group, (b) the EE group, (c) the LS group, and (d) the HS group.

crest of the mitochondria partially fused and became blurry or missing, and a small amount of muscle fiber was necrotic. Figures 2(c) and 2(d) showed the myocardial structure of the LS and HS group rats, which was as follows: the myocardial cell matrix had edema and the membrane and mitochondrial crest partially fused and became blurry or absent.

3.2. The Effect of EE and SAL Interference on Enzyme Markers of Heart Injury. As shown in Table 2, compared to the C group, LDH, CK-MB, CK, CTN-I, and MB in the EE group increased significantly ($P < 0.05$); compared to the EE group, LDH, CK-MB, CK, CTN-I, and MB of the LS group were reduced significantly ($P < 0.05$); and compared to the LS group, LDH, CK-MB, CK, and MB of the HS group were also reduced significantly ($P < 0.05$).

3.3. The Effect of EE and SAL Interference on Mitochondrial Respiration Function. As illustrated in Figure 3, titration of cytochrome c did not alter the flux, indicating that the mitochondrial outer membrane was intact. With glutamate and malate as electron donors for complex I, compared to the C group, the state 3 respiration rate of the EE group was reduced significantly ($P < 0.05$); compared to the EE group, the LS was increased significantly ($P < 0.05$); and compared to the LS group, HS was increased significantly ($P < 0.05$). Compared to the C group, the RCR of the EE group was reduced significantly ($P < 0.05$); compared to the EE group, the RCR of LS and HS groups were both increased significantly ($P < 0.05$).

Using succinate as a substrate for complex II, compared to the C group, the state 3 respiration rate of the EE group was reduced significantly ($P < 0.05$); compared to the EE group, the LS was increased insignificantly ($P > 0.05$) and the HS was increased significantly ($P < 0.05$); and compared to the LS groups, the HS was increased significantly ($P < 0.05$).

With ascorbate/TMPD being used as substrates for complex IV, compared to the C group, the state 3 respiratory rate of the EE group was reduced significantly ($P < 0.05$); compared to the EE group, the LS was increased insignificantly ($P > 0.05$) and the HS was increased significantly ($P < 0.05$); and compared to the LS group, the HS was increased significantly ($P < 0.05$).

3.4. The Effects of EE and SAL Interference on PGC-1α, NRF1, and NRF2 Gene Expression Levels. As shown in Figure 4, compared to the C group, *PGC-1α*, *NRF1*, and *NRF2* mRNA expression levels in the EE group were all significantly elevated ($P < 0.05$); compared to the EE group, *PGC-1α*, *NRF1*, and *NRF2* mRNA expression levels in the LS group were elevated significantly ($P < 0.05$); and compared to the LS group, *PGC-1α*, *NRF1*,and *NRF2* mRNA expression levels in HS group were all significantly elevated ($P < 0.05$).

3.5. The Effect of Exhaustive Exercise and Salidroside Interference on PGC-1α, NRF1, and NRF2 Protein Expression. As shown in Figure 5, compared to the C group, *PGC-1α*, *NRF1*, and *NRF2* protein levels in the EE group were reduced significantly ($P < 0.05$); compared to the EE group, *PGC-1α*,

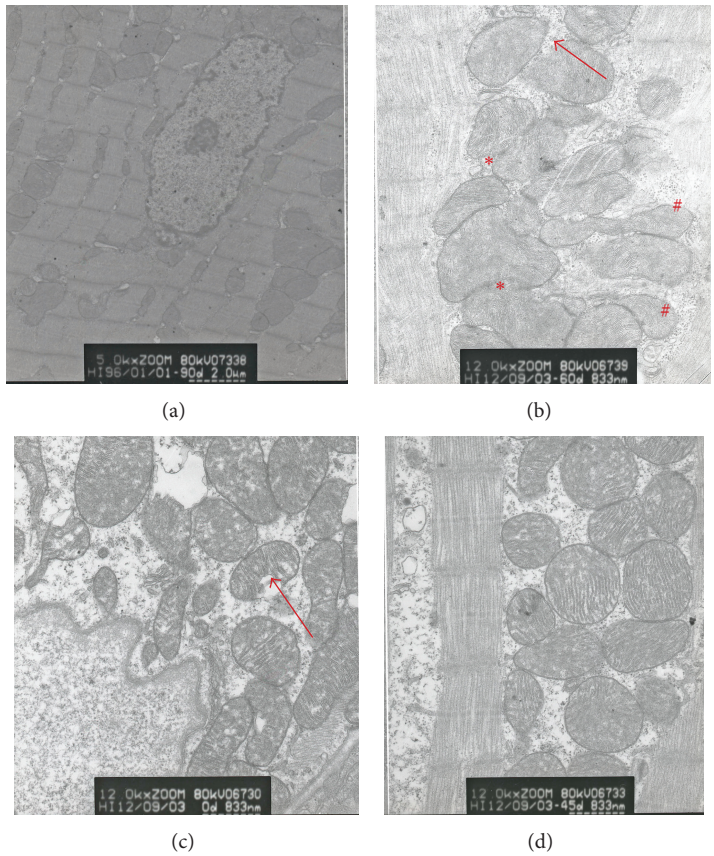

Figure 2: The effect of SAL on cardiomyocyte ultrastructure (×20,000); (a) the C group, (b) the EE group, (c) the LS group, and (d) the HS group. Note the disrupted mitochondrial membrane (arrows), mitochondrial swelling and fusion (∗), and mitochondrial malformation (#).

Table 2: A comparison of heart injury serum markers in different groups.

Groups	LDH	CK-MB	CK	CTN-I	MB
C	0.92 ± 0.04	2.11 ± 0.18	11.70 ± 0.46	144.61 ± 12.71	3.32 ± 0.49
EE	1.08 ± 0.09*	3.23 ± 0.19*	16.93 ± 0.41*	172.00 ± 12.83*	4.90 ± 0.41*
LS	1.04 ± 0.06$^{\#}$	3.14 ± 0.24	14.56 ± 0.53$^{\#}$	157.18 ± 16.95	4.22 ± 0.43$^{\#}$
HS	1.02 ± 0.10$^{\#}$	2.57 ± 0.21$^{\#\Delta}$	13.19 ± 1.91$^{\#\Delta}$	159.26 ± 8.93	3.98 ± 0.54$^{\#\Delta}$

Data are expressed as means ± SD; $n = 8$ for each group; $^{*}P < 0.05$ versus the C group, $^{\#}P < 0.05$ versus the EE group, and $^{\Delta}P < 0.05$ versus the LS group.

NRF1, and *NRF2* protein levels in the LS group were significantly elevated ($P < 0.05$); and compared to the LS group, *PGC-1α*, *NRF1*, and *NRF2* protein levels in the HS group were increased significantly ($P < 0.05$).

4. Discussion

In this study, we investigated the protective effect and underlying mechanism of SAL on exhaustive exercise-induced heart injury with a focus on energy metabolism. We mainly observed alterations of myocardial structure, myocardial injury enzyme markers, and mitochondrial respiratory function in permeabilized fibers in response to exhaustive exercise. We also observed the expression of the key mitochondrial biogenesis signaling pathway *PGC-1α–NRF1/NRF2* to characterize the cellular and molecular mechanism of exhaustive exercise-induced heart injury.

The serum marker analyses suggest that CK, CK-MB, LDH, cTn-I, and MB were released into blood, so the contents of these enzymes in the serum increased significantly, indicating that the cardiomyocytes were injured. Applying morphometric analysis to optical and electron microscopy specimens, we found that the characteristics of the EE group rat myocardia were nuclear matrix edema, nuclear gap widening, an increased number of mitochondria and amount of glycogen, partial membrane and mitochondrial crest fusion that became blurry or absent, and a small amount of muscle fiber necrosis. Those findings indicate that cardiomyocyte structure was damaged as a consequence of exhaustive exercise.

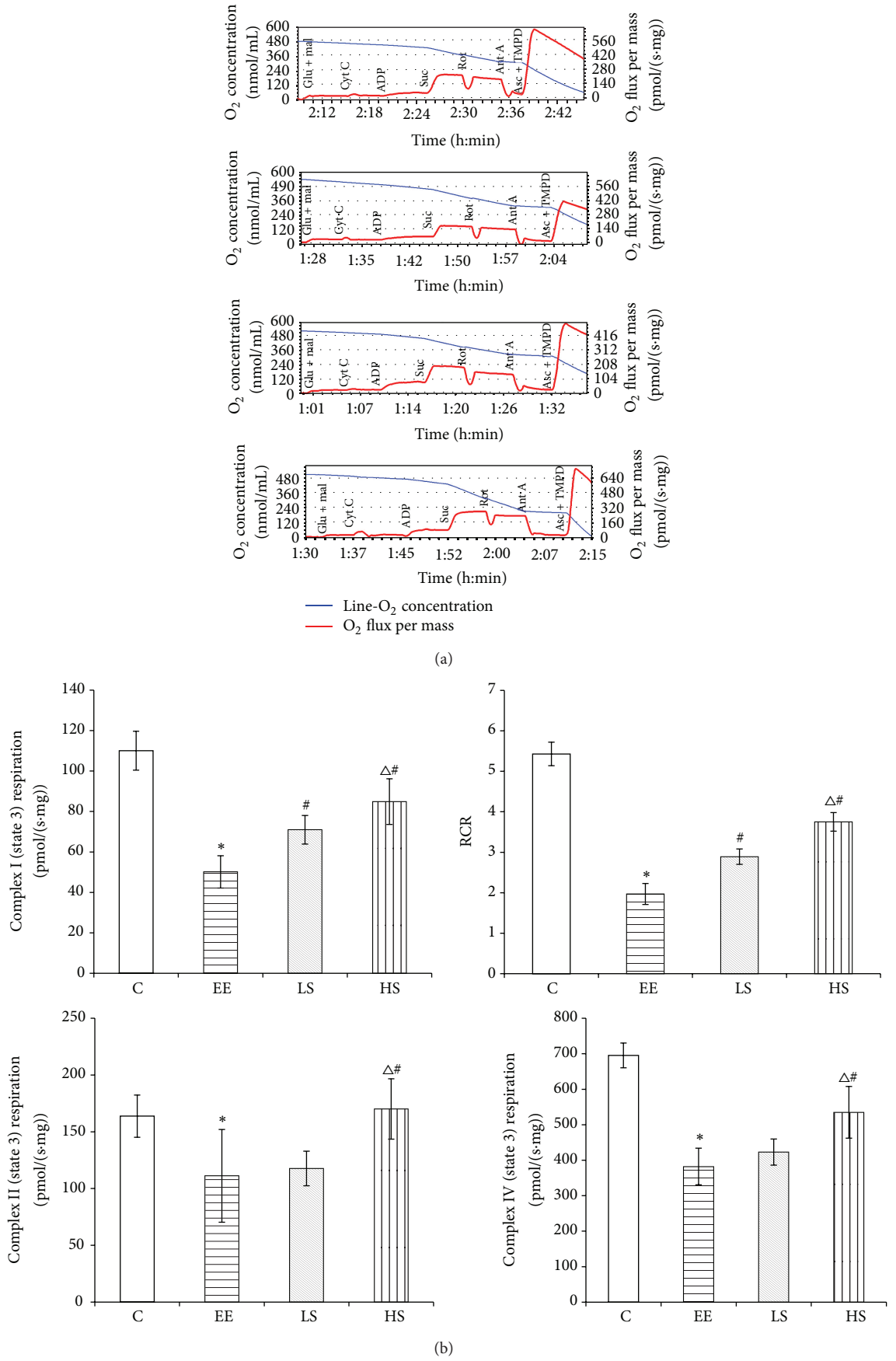

FIGURE 3: Maximal respiratory capacity (state 3 respiration) in permeabilized myocardial fibers. (a) Original recording. (b) Comparison. Glu, glutamate; Mal, malate; Cyt C, cytochrome C; Suc, succinate; Rot, rotenone; Ant A, antimycin A; and Asc, ascorbate. Data were expressed as means ± SD; $n = 8$ per group; $^{*}P < 0.05$ versus the C group; $^{\#}P < 0.05$ versus the EE group; and $^{\Delta}P < 0.05$ versus the LS group.

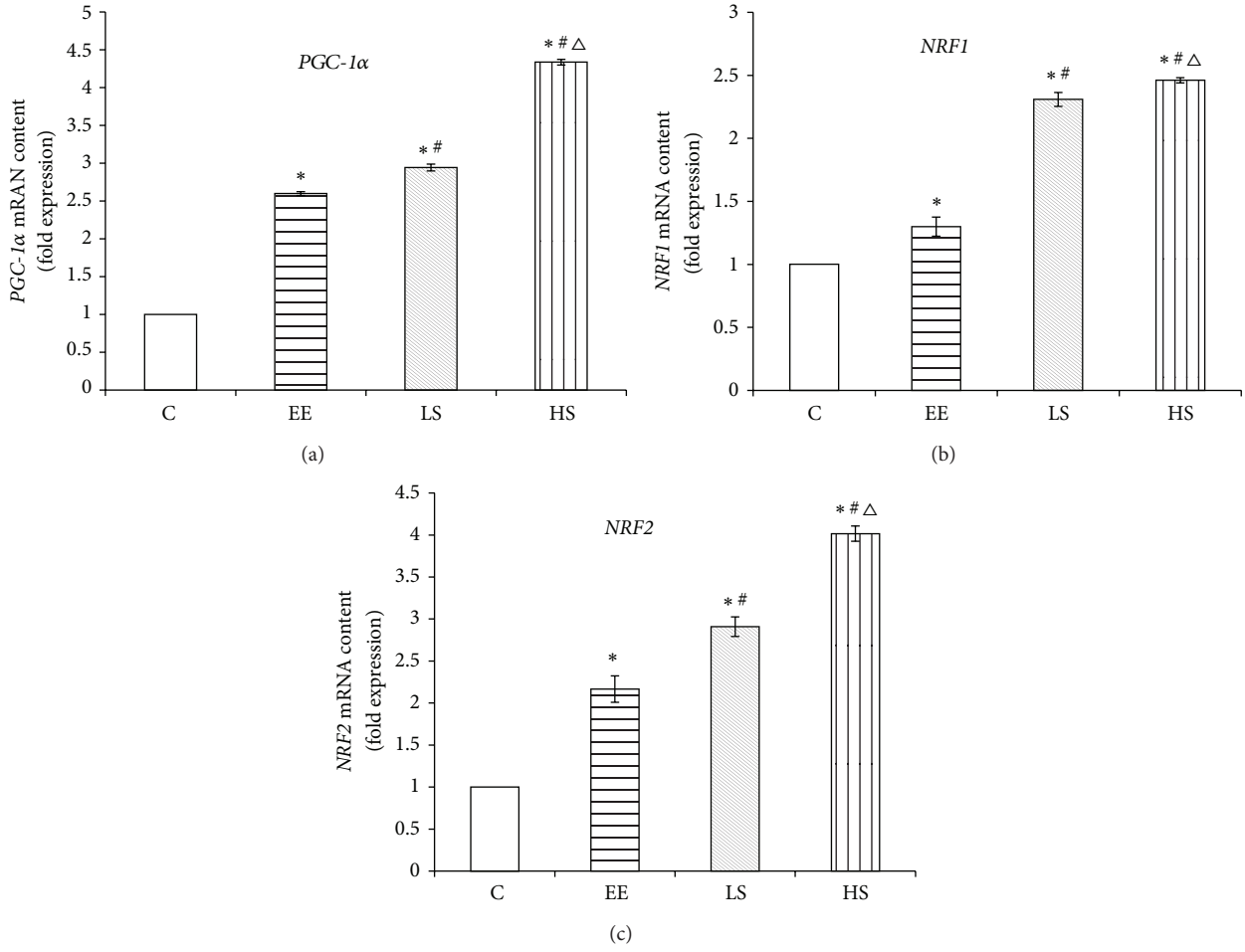

Figure 4: *PGC-1α*, *NRF1*, and *NRF2* mRNA expression levels in different groups. Data were expressed as means ± SD; $n = 8$ per group; $^{*}P < 0.05$ versus the C group; $^{\#}P < 0.05$ versus the EE group; and $^{\Delta}P < 0.05$ versus the LS group.

Muscle oxidative capacities have been assessed by measuring respiration of mitochondria in permeabilized fibres with no limitation of substrates, ADP, or oxygen [13]. Results showed that the state 3 of ETS complexes I, II, and IV was decreased 55%, 32%, and 45%, respectively. This suggests that exhaustive exercise induced depression of myocardial mitochondrial respiration function. In order to fulfill the energy needs of myocytes, the ETS would compensate with producing large amount of superoxide which in turn injures myocardium [14–16] and causes the respiration apparatus damage and energy production failure. In contrast, the treated group showed improvements for the above indicators, particularly for the high SAL dose group that had clearly showed improved energy metabolism. These data indicate that SAL can protect from exhaustive exercise-induced heart injury by improving mitochondrial respiratory function and energy metabolism.

The coactivator *PGC-1α* plays a central role in a regulatory network that governs the transcriptional control of mitochondrial biogenesis and respiratory function. Through its interaction with multiple transcription factors, *PGC-1α* enhances mitochondrial capacity for oxidative phosphorylation and triggers the coordinate expression of nuclear- and mitochondrial-encoded genes driving mitochondrial biogenesis [17].

Actually, two distinct classes of regulatory proteins govern mitochondrial biogenesis at the transcriptional level in mammalian systems. The first class comprises transcription factors mitochondrial transcription factor A (Tfam) and the mitochondrial transcription factor B (mtTFB) isoforms TFB1M and TFB2M, which direct transcription from divergent heavy- and light-strand promoters within the mitochondrial D-loop regulatory region. A second group of transcription factors act on the majority of nuclear genes whose products are required for respiratory chain expression and biological function. Among these are the nuclear respiratory factors *NRF1* and *NRF2* [18]. Since we mainly observed the mitochondrial respiration function performance in this research, we attached more importance to *NRF1* and *NRF2*.

In this research, expression levels of *PGC-1α*, *NRF1*, and *NRF2* mRNA were upregulated compared to the control groups immediately after the exercise; however, *PGC-1α*, *NRF1*, and *NRF2* proteins were reduced 1.6-fold, 14.6%, and 52%, respectively. This inconsistency between mRNA and protein expression levels might indicate that exhaustive exercise caused mitochondrial biogenesis protein synthesis or

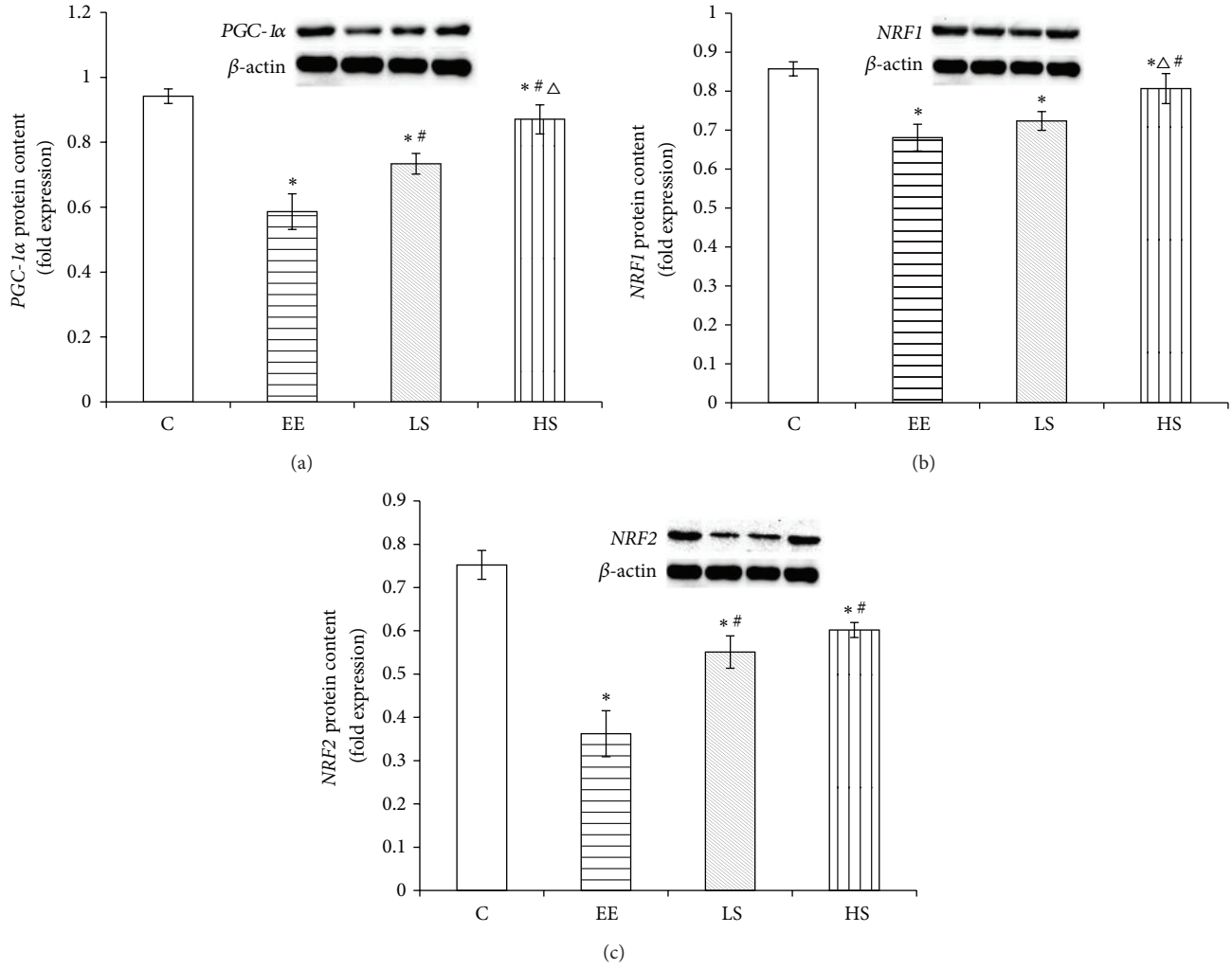

Figure 5: *PGC-1α, NRF1*, and *NRF2* protein expression levels in different groups. Data were expressed as means ± SD; $n = 8$ per group; $^{*}P < 0.05$ versus the C group; $^{\#}P < 0.05$ versus the EE group; and $^{\Delta}P < 0.05$ versus the LS group.

assembly processes dysfunction. The downregulation of *NRF1* and *NRF2* proteins is also involved in dysfunctional synthesis of mitochondrial respiration complex subunits, resulting in reduced mitochondrial respiration function [19, 20]. Therefore, decreased *PGC-1α* and its downstream transcription factors *NRFs* proteins contribute to deficiency in myocardial oxidative capacity and energy production [1]. These results indicate that exhaustive exercise is such an intense stress that it damages mitochondrial respiration function which is responsible for energy production by downregulating the mitochondrial biogenesis key regulatory factors *PGC-1α–NRF1/NRF2* signaling pathway. The duration of the stress will in turn worsen the imbalance between energy production and energy demand to satisfy the contractile function of cardiac muscle, which will lead to irreversible myocardial damage and energy failure. In contrast, the SAL treated group particularly the high-dose group significantly upregulated *PGC-1α*, *NRF1*, and *NRF2*, indicating that SAL can improve energy metabolism by upregulating mitochondrial biogenesis regulators and ameliorate myocardial injury induced by intense exercise.

To date, studies have examined changes in *PGC-1α* in a variety of exercise models of heart. Botta et al. [3] reported that short-term and moderate-intensity exercise upregulated *PGC-1α*. A five-week high-intensity exercise training regimen resulted in a 41.5% increase in the *PGC-1α* mRNA expression levels [21]. Those controversial results probably vary depending on exercise intensity.

In this study, SAL significantly reduces the levels of myocardial injury enzymes in the serum, relieves the myocardium ultrastructure injury, improves the activity of mitochondrial ETS complexes I, II, and IV, and increases expression of key mitochondrial biogenesis factors *PGC-1α*, *NRF1*, and *NRF2*. All of these findings indicate that SAL can protect the heart from exhaustive exercise-induced injury by improving mitochondrial respiratory function and mitochondrial biogenesis.

In conclusion, exhaustive exercise can induce heart injury, including structural injury, enzyme abnormalities, reduced respiratory function, and the downregulation of mitochondrial biogenesis. The accumulation of these maladaptive traits initiates a vicious cycle that can further cause

myocardial metabolic dysfunction, thereby contributing to myocardial injury and heart failure. SAL, one of the major effective components of extracts from the traditional Chinese medicine *R. crenulata*, appears to protect the myocardium from exhaustive exercise-induced injury by improving respiratory function and upregulating mitochondrial biogenesis.

Conflict of Interests

The authors declare that there is no conflict of interests regarding the publication of this paper.

Acknowledgments

This research was supported by grants from the Natural Science Foundation of China (no. 81173585) and the Hebei Province Natural Science Foundation of China (no. C2014104010).

References

[1] R. Ventura-Clapier, A. Garnier, V. Veksler, and F. Joubert, "Bioenergetics of the failing heart," *Biochimica et Biophysica Acta: Molecular Cell Research*, vol. 1813, no. 7, pp. 1360–1372, 2011.

[2] R. Ventura-Clapier, A. Garnier, and V. Veksler, "Transcriptional control of mitochondrial biogenesis: the central role of PGC-1alpha," *Cardiovascular Research*, vol. 79, no. 2, pp. 208–217, 2008.

[3] A. Botta, I. Laher, J. Beam et al., "Short term exercise induces *PGC-1α*, ameliorates inflammation and increases mitochondrial membrane proteins but fails to increase respiratory enzymes in aging diabetic hearts," *PLoS ONE*, vol. 8, no. 8, Article ID e70248, 2013.

[4] A. V. Kuznetsov, V. Veksler, F. N. Gellerich, V. Saks, R. Margreiter, and W. S. Kunz, "Analysis of mitochondrial function in situ in permeabilized muscle fibers, tissues and cells," *Nature Protocols*, vol. 3, no. 6, pp. 965–976, 2008.

[5] F. Colleoni, A. J. Morash, T. Ashmore, M. Monk, G. J. Burton, and A. J. Murray, "Cryopreservation of placental biopsies for mitochondrial respiratory analysis," *Placenta*, vol. 33, no. 2, pp. 122–123, 2012.

[6] X. Lan, K. Chang, L. Zeng et al., "Engineering salidroside biosynthetic pathway in hairy root cultures of *Rhodiola crenulata* based on metabolic characterization of tyrosine decarboxylase," *PLoS ONE*, vol. 8, no. 10, Article ID e75459, 2013.

[7] M.-C. Xu, H.-M. Shi, X.-F. Gao, and H. Wang, "Salidroside attenuates myocardial ischemia-reperfusion injury via PI3K/Akt signaling pathway," *Journal of Asian Natural Products Research*, vol. 15, no. 3, pp. 244–252, 2013.

[8] X.-F. Gao, H.-M. Shi, T. Sun, and H. Ao, "Effects of Radix et Rhizoma Rhodiolae Kirilowii on expressions of von Willebrand factor, hypoxia-inducible factor 1 and vascular endothelial growth factor in myocardium of rats with acute myocardial infarction," *Zhong Xi Yi Jie He Xue Bao*, vol. 7, no. 5, pp. 434–440, 2009.

[9] Y. Wang, P. Xu, H. Liu, Y. Zhou, and X. Cao, "The protection of salidroside of the heart against acute exhaustive injury and molecular mechanism in rat," *Oxidative Medicine and Cellular Longevity*, vol. 2013, Article ID 507832, 8 pages, 2013.

[10] Y. Zhang and X. Cao, "The effect of salidroside on cardiac myocyte metabolic enzyme of hypoxia-induced neonate rat," *Chinese Medicine*, vol. 124-125, supplement 1, p. 216, 2011.

[11] C. F. Ji, X. Geng, and Y. B. Ji, "Effect of salidroside on energy metabolism in exhausted rats," *Journal of Clinical Rehabilitative Tissue Engineering Research*, vol. 11, no. 45, pp. 9149–9151, 2007.

[12] D. P. Thomas and K. I. Marshall, "Effects of repeated exhaustive exercise on myocardial subcellular membrane structures," *International Journal of Sports Medicine*, vol. 9, no. 4, pp. 257–260, 1988.

[13] D. Pesta and E. Gnaiger, "High-resolution respirometry: OXPHOS protocols for human cells and permeabilized fibers from small biopsies of human muscle," *Methods in Molecular Biology*, vol. 810, pp. 25–58, 2012.

[14] C. Gao, X. Chen, J. Li et al., "Myocardial mitochondrial oxidative stress and dysfunction in intense exercise: regulatory effects of quercetin," *European Journal of Applied Physiology*, vol. 114, no. 4, pp. 695–705, 2014.

[15] Q. Fan, L. Chen, S. Cheng et al., "Aging aggravates nitrate-mediated ROS/RNS changes," *Oxidative Medicine and Cellular Longevity*, vol. 2014, Article ID 376515, 7 pages, 2014.

[16] M. Sebastiani, C. Giordano, C. Nediani et al., "Induction of mitochondrial biogenesis is a mala daptive mechanism in mitochondrial cardiomyopathies," *Journal of the American College of Cardiology*, vol. 50, no. 14, pp. 1362–1369, 2007.

[17] R. Ventura-Clapier, A. Garnier, and V. Veksler, "Transcriptional control of mitochondrial biogenesis: the central role of PGC-1α," *Cardiovascular Research*, vol. 79, no. 2, pp. 208–217, 2008.

[18] R. C. Scarpulla, "Nuclear control of respiratory chain expression by nuclear respiratory factors and PGC-1-related coactivator," *Annals of the New York Academy of Sciences*, vol. 1147, pp. 321–334, 2008.

[19] M. Liu, B. Zhou, Z.-Y. Xia et al., "Hyperglycemia-induced inhibition of DJ-1 expression compromised the effectiveness of ischemic postconditioning cardioprotection in rats," *Oxidative Medicine and Cellular Longevity*, vol. 2013, Article ID 564902, 8 pages, 2013.

[20] P.-H. Ducluzeau, M. Priou, M. Weitheimer et al., "Dynamic regulation of mitochondrial network and oxidative functions during 3T3-L1 fat cell differentiation," *Journal of Physiology and Biochemistry*, vol. 67, no. 3, pp. 285–296, 2011.

[21] D. Ramos, E. G. Martins, D. Viana-Gomes, G. Casimiro-Lopes, and V. P. Salerno, "Biomarkers of oxidative stress and tissue damage released by muscle and liver after a single bout of swimming exercise," *Applied Physiology, Nutrition and Metabolism*, vol. 38, no. 5, pp. 507–511, 2013.

Hindawi Publishing Corporation
Oxidative Medicine and Cellular Longevity
Volume 2015, Article ID 364020, 8 pages
http://dx.doi.org/10.1155/2015/364020

Research Article

Mechanical Ventilation Induces an Inflammatory Response in Preinjured Lungs in Late Phase of Sepsis

Wei Xuan, Quanjun Zhou, Shanglong Yao, Qingzhu Deng, Tingting Wang, and Qingping Wu

Department of Anesthesiology, Union Hospital, Tongji Medical College, Huazhong University of Science and Technology, Wuhan 430022, China

Correspondence should be addressed to Tingting Wang; wangtingting721@yahoo.com and Qingping Wu; wqp1968@126.com

Received 21 July 2014; Revised 9 October 2014; Accepted 16 October 2014

Academic Editor: Zhengyuan Xia

Mechanical ventilation (MV) may amplify the lung-specific inflammatory response in preinjured lungs by elevating cytokine release and augmenting damage to the alveolar integrity. In this study, we test the hypothesis that MV exerts different negative impacts on inflammatory response at different time points of postlung injury. Basic lung injury was induced by cecal ligation and puncture (CLP) surgery in rats. Physiological indexes including blood gases were monitored during MV and samples were assessed following each experiment. Low V_T (tidal volume) MV caused a slight increase in cytokine release and tissue damage at day 1 and day 4 after sepsis induced lung injury, while cytokine release from the lungs in the two moderately ventilated V_T groups was amplified. Interestingly, in the two groups where rats received low V_T MV, we found that infiltration of inflammatory cells was only profound at day 4 after CLP. Marked elevation of protein leakage indicated a compromise in alveolar integrity in rats that received moderate V_T MV at day 4 following CLP, correlating with architectural damage to the alveoli. Our study indicates that preinjured lungs are more sensitive to mechanical MV at later phases of sepsis, and this situation may be a result of differing immune status.

1. Introduction

Patients suffering from acute lung injury (ALI) or acute aspiratory distress syndrome (ARDS) are likely to receive mechanical ventilation (MV) treatment as a therapeutic intervention [1]. Although MV is necessary and life-saving, it may cause lung injury or exacerbate preexisting lung injury, a condition known as ventilator-associated lung injury (VILI) [2, 3]. Curative strategy of MV can cause VILI via the induction of oxidant stress and neutrophil infiltration in a rat model [4].

Sepsis is a critical state of inflammation with high morbidity and mortality rates in the intensive care unit (ICU) [5]. Certain factors, such as overgeneration of reactive oxygen species (ROS), play important roles between sepsis and VILI. Both in vivo and in vitro studies have demonstrated that oxidative stress, plus dysfunction of antioxidant system, leads to the onset or deterioration of ALI after sepsis and VILI [6, 7]. On the other hand, sepsis can overwhelm the body resulting in immune suppression, leaving patients more susceptible to secondary infections due to an inability to mount an effective inflammatory response [8–10]. The generation of reactive oxygen species by immune cells can be changed depending on different phase of sepsis [11], in which persistence indicates a poor result and may affect the outcome of VILI due to the modulation of ROS elimination. Previous studies have shown that MV had a negative impact on preinjured lungs or other organs affected by sepsis [12–14].

The purpose of this study was to investigate how MV impacts upon preinjured lung function at different time points after sepsis induction. We used a clinically relevant septic rat model to assess prolonged lung injury. We hypothesized that the negative impacts of MV on preinjured lung at the later phase of sepsis may be more severe than those observed in the early phase. We did not include a high V_T (more than 12 mL/kg) of MV in our current study due to the fact that it was not clinically relevant and this method results in V_T-induced serious lung injury in patients and a range of animal models [15–17]. To evaluate the effects of MV on preexisting lung injury, we examined the physiological

response, lung injury, inflammatory cell accumulation and infiltration, and cytokine release using septic rat model.

2. Materials and Methods

2.1. Animals and Experimental Sepsis. We used pathogen-free male Sprague-Dawley rats (weighing 250–300 g). All rats in the sepsis groups received cecal ligation and puncture (CLP) surgery. In brief, rats were fasted 16 h before surgery and then anesthetized by an injection of 1 mL of 2% pentobarbital in the peritoneal cavity. Under sterile conditions, a 2 cm incision was made on the midline of the abdomen, before exposing the cecum. The cecum was ligated one-third along its distal position and punctured twice with a 16-gauge needle. This operation caused ALI and had a 95% survival rate in our preliminary study (data not shown). The cecum was returned to the peritoneal cavity and the incision was closed in two layers by suture. All the animals received subcutaneous application of 10 mL/kg sterile saline for fluid resuscitation. The experimental protocol was approved by the Animal Care and Scientific Committee of Tongji Medical College, Huazhong University of Science and Technology.

2.2. Mechanical Ventilation (MV) Protocol. All rats were randomly allocated into seven groups as follows (four MV groups were ventilated for 4 hours with room air): control group: control rats ($n = 6$); group CLP1day: septic rats were sacrificed at day 1 after CLP without MV ($n = 6$); group CLP1day + LMV: septic rats received MV at day 1 after CLP, low V_T (6 mL/kg), 4 cm H_2O ZEEP ($n = 8$); group CLP1day + MMV: septic rats received MV at day 1 after CLP, moderate V_T (12 mL/kg), 2 cm H_2O ZEEP ($n = 8$); group CLP4day: septic rats were sacrificed at day 4 after CLP without MV ($n = 6$); group CLP4day + LMV: septic rats received MV at day 4 after CLP, low V_T (6 mL/kg), 4 cm H_2O ZEEP ($n = 8$); group CLP4day + MMV: septic rats received MV at day 4 after CLP, moderate V_T (12 mL/kg), 2 cm H_2O ZEEP ($n = 8$). All rats were anesthetized by intraperitoneal injection of 2% pentobarbital (1 mL) before undergoing tracheotomy and were connected to a small-animal ventilator (Harvard Apparatus, Holliston, MA, USA). Anesthesia was maintained by constant injection of pentobarbital (80 mg/kg/h) and fluids were administered at a rate of 10 mL/kg/h by jugular vein intubation. A catheter was inserted into the left carotid artery for blood pressure measurements and blood gas analysis every two hours. We kept partial pressure of arterial carbon dioxide (P_aCO_2) between 35 and 45 mmHg by changing breathing rate. Body temperature was monitored rectally and regulated automatically by a heating pad. All animals were sacrificed by abdominal aorta exsanguination at experiment completion.

2.3. Histology of the Lung. The superior lobe of the right lung was fixed in 10% pH neutral formalin for 24 h, cut into 10 μm sections, and mounted on glass slides. The tissue sections were stained with hematoxylin and eosin (H&E) and examined by light microscopy. The histological alterations were scored in five grades from 0 to 4 depending on the degree of microscopic damage of architectural integrity, inflammatory cell infiltration, interstitial edema, and hemorrhage.

2.4. Cell Counts. Lung lavages were performed with 3 × 2 mL cold sterile PBS; the fluid was centrifuged at 150 ×g at 4°C for 10 min. After centrifugation, the supernatant was collected and frozen at −70°C for further analysis. The cell pellet was resuspended in 0.5 mL cold PBS. Total cell counts of bronchoalveolar lavage fluid (BALF) were determined using a cell counting chamber. Slides of the differential counts were performed using a cytocentrifuge at 150 ×g for 5 min, followed by Wright staining.

2.5. Cytokine Assays. Level of interleukin- (IL-) 6 in the supernatant of BALF was measured by enzyme-linked immunosorbent assay (ELISA) according to the manufacturer's protocol. Briefly, samples or standards were pipetted into microplate wells precoated with monoclonal antibody. After washing away unbound substances, an enzyme-linked polyclonal antibody specific for rat IL-6 (BD Biosciences Pharmingen, San Diego, CA, USA) was added to the microplate wells. Following a wash to remove any unbound antibody-enzyme reagent, substrate solution was added to the wells. The enzyme reaction yielded a blue product that turned yellow when the phosphoric acid stop solution was added. The intensity of the color was proportionate to the amount of total rat IL-6 bound in the initial step and the sample values were then extrapolated from the standard curve. Total protein levels in BALF were determined by Pierce BCA Protein Assay kit (Thermo Scientific, Rockford, IL, USA) according to the manufacturer's instructions with bovine serum albumin (BSA) as a standard.

2.6. Statistical Analysis. Data are expressed as mean ± SD (standard deviation). All parameters were analyzed by one-way analysis of variance (ANOVA) with least significant difference (LSD) posttest. The histological injury scores comparisons were made by the nonparametric Mann-Whitney test. P values of <0.05 were considered to be statistically significant.

3. Results

Two rats died from cardiovascular collapse: one in group two and one in group 3. Therefore, only 48 rats out of 50 were studied.

3.1. MV Impacts on Physical Signs. There was no statistically significant difference in P_aO_2/FiO_2 among the four MV groups at the start of ventilation. Furthermore, the oxygen index (OI) was only slightly higher in the two CLP day-four groups (Figure 1(a)). The OI differed over time in all groups with the lowest P_aO_2/FiO_2 occurring in group CLP1day + LMV, while the highest OI occurred in group CLP4day + MMV.

The initial mean arterial pressure (MAP) was similar and gradually decreased over time in all groups (Figure 1(b)). The lowest blood pressure measurement was observed in group

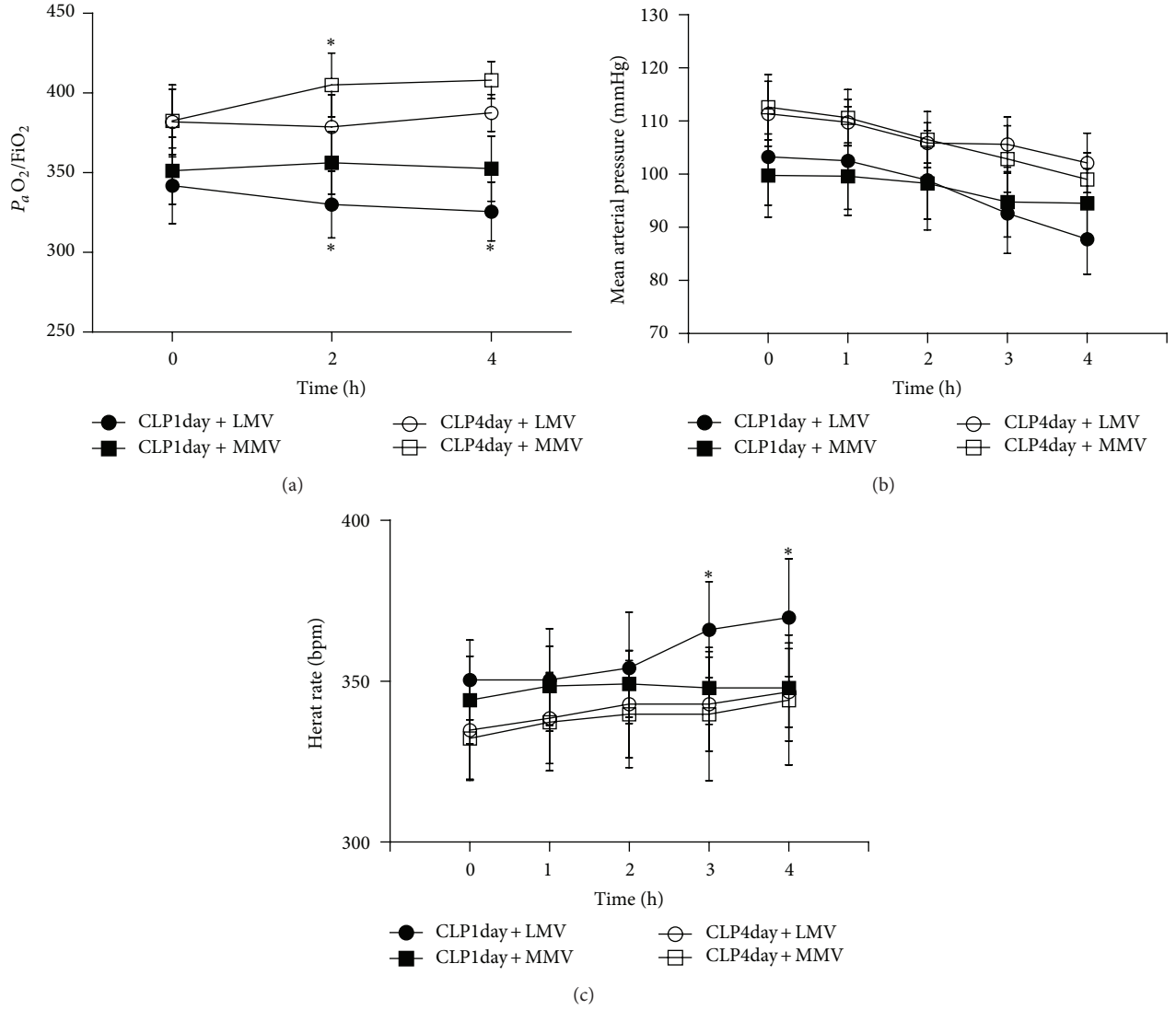

Figure 1: Physiological response to mechanical ventilation following induction of sepsis over time. P_aO_2/FiO_2 (a), mean arterial pressure (b), and heart rate (c) were measured. P values are calculated by repeated-measures ANOVA. Significant differences are highlighted between groups receiving MV on the same day. *The same time point at which the group received MV at the same day after CLP. Data are presented as mean ± SD.

CLP1day + LMV, but this drop was not statistically significant. Heart rate (HR) was steady in the other three MV groups but had a statistically significant rise in group CLP1day + LMV after 2 h MV (Figure 1(c)).

Although there was a trend of lower pH in groups CLP1day + LMV and CLP1day + MMV, the pH values generally matched those in groups CLP4day + LMV and CLP4day + MMV (data not shown).

3.2. Lung Injury. CLP surgery caused moderate structural damage of lung, slight cellular infiltration, and edema at days one and four after operation (Figures 2(a) and 2(d)). We saw more severe accumulation of inflammatory cells in groups CLP1day + LMV and CLP4day + LMV (Figures 2(b) and 2(e)). For moderate V_T MV one day after sepsis, these histological changes were similar to those in two low V_T groups (Figure 2(c)). The impacts of MV were most evident in group CLP4day + MMV, with partial interstitial edema and areas of alveolar hemorrhage (Figure 2(f)), which showed that relatively higher tidal volume MV exerted more negative impact on preinjured lung at day four after CLP compared with day one following CLP.

3.3. Cell Counts. BALF total cell counts are an important indicator of the integrity of lung capillary. From the results, we can see that CLP surgery increased the total cell counts in BALF (Figure 3(a)). There were large increases in groups of CLP4day + LMV and CLP4day + MMV, while in the groups of day one after CLP, only MMV caused a significant increase of total cell counts. Differential analysis revealed similar increases of polymorphonuclear (PMN) cells in BALF except in group CLP1day + LMV (Figures 3(b) and 4). Examination

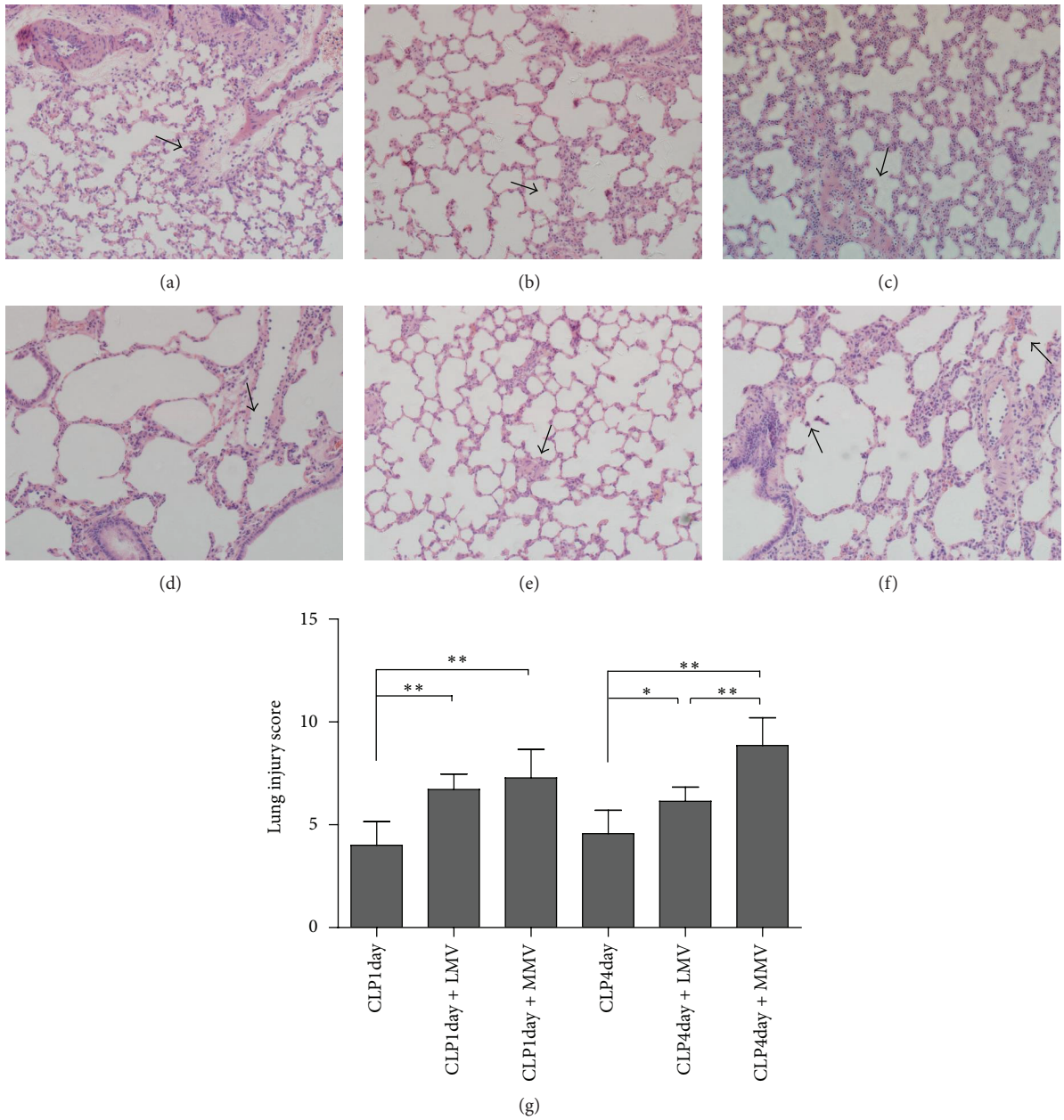

Figure 2: Representative hematoxylin and eosin-stained 5 μm lung sections at 400x magnification. CLP at day one without MV (a), with low V_T MV (b), and with moderate V_T MV (c). CLP at day four without MV (d), with low V_T MV (e), and with moderate V_T MV (f) are shown. Lung injuries according to the scoring system are pointed with black arrow in the figures. Lung injury score is presented as bar chart on the right (g). Data are presented as mean ± SD.

of tissue slides under light microscopy validated these observations. Additionally, MV magnified the inflammatory cells infiltration to a deeper extent at day four after CLP compared with day one after CLP. These data are in accordance with the findings from histological sections.

3.4. Total Protein and IL-6 Levels. BALF total protein level was quantified to identify the status of capillary permeability and IL-6 was selected as a representative inflammatory cytokine. Studies have shown that moderate V_T can augment rabbit lung cytokine release, such as TNF-α and IL-8, after the systemic of systemic LPS [18]. IL-6 is regarded as an active factor and an ongoing inflammatory marker of many lung diseases [19]. The synergistic role of IL-6 in pathologic mechanical stretch induced lung endothelial cell injury has also been demonstrated in vitro [20]. As shown in Figure 5, both total protein and IL-6 were significantly higher in group CLP4day + MMV when compared to groups CLP4day and CLP4day + LMV, which indicated

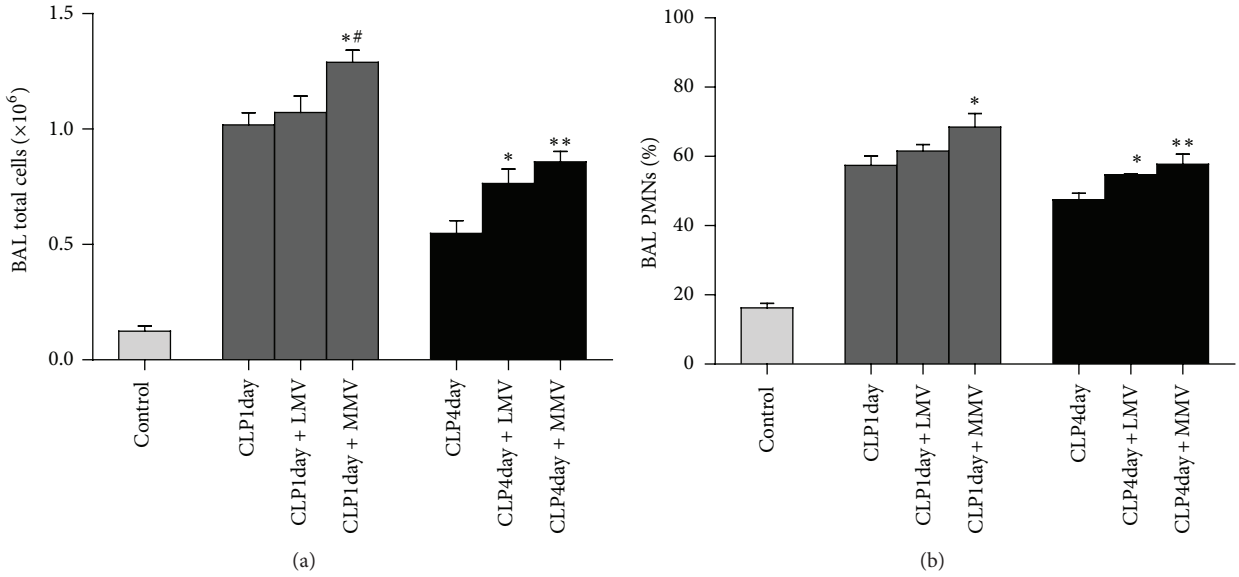

Figure 3: Total cell counts (a) and polymorphonuclear cell count (PMN) (b) in BAL for each of the seven groups. *Without MV at the same day after CLP; #low V_T MV at the same day after CLP. Data are presented as mean ± SD.

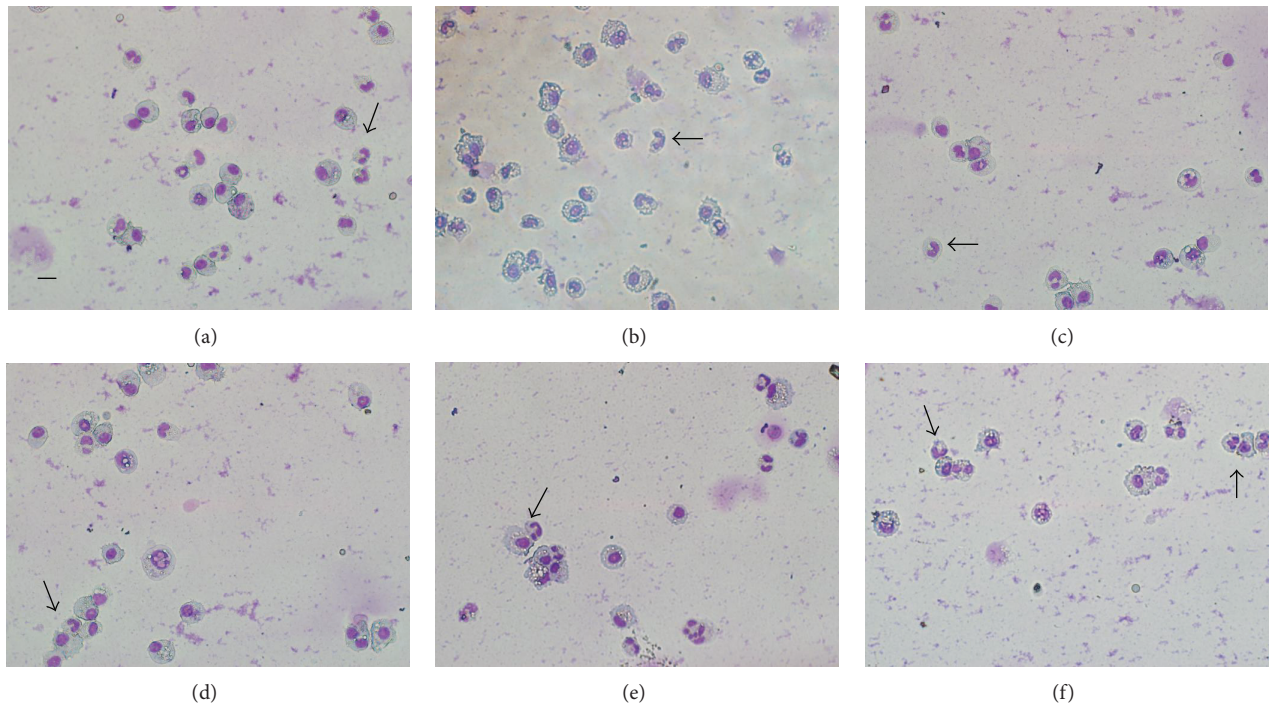

Figure 4: Differential analysis of PMNs is presented at 400x magnification. CLP at day one without MV (a), with low V_T MV (b), and with moderate V_T MV (c). CLP at day four without MV (d), with low V_T MV (e), and with moderate V_T MV (f). Polymorphonuclear neutrophils are pointed with black arrow. Bar = 50 μm.

that, on the fourth day after initiation of CLP, relatively higher volume of MV severely increases both lung capillary permeability and cytokine release. Furthermore, IL-6 was significantly higher in group CLP1day + MMV compared with groups CLP1day and CLP1day + LMV, while there were no statistically significant differences in total levels of protein observed between these groups (Figure 5). These results suggested that, at the early stage of sepsis (day one after CLP), when compared to low tidal volume, moderate tidal volume of MV changed inflammatory cytokine release but had no effect on lung capillary permeability.

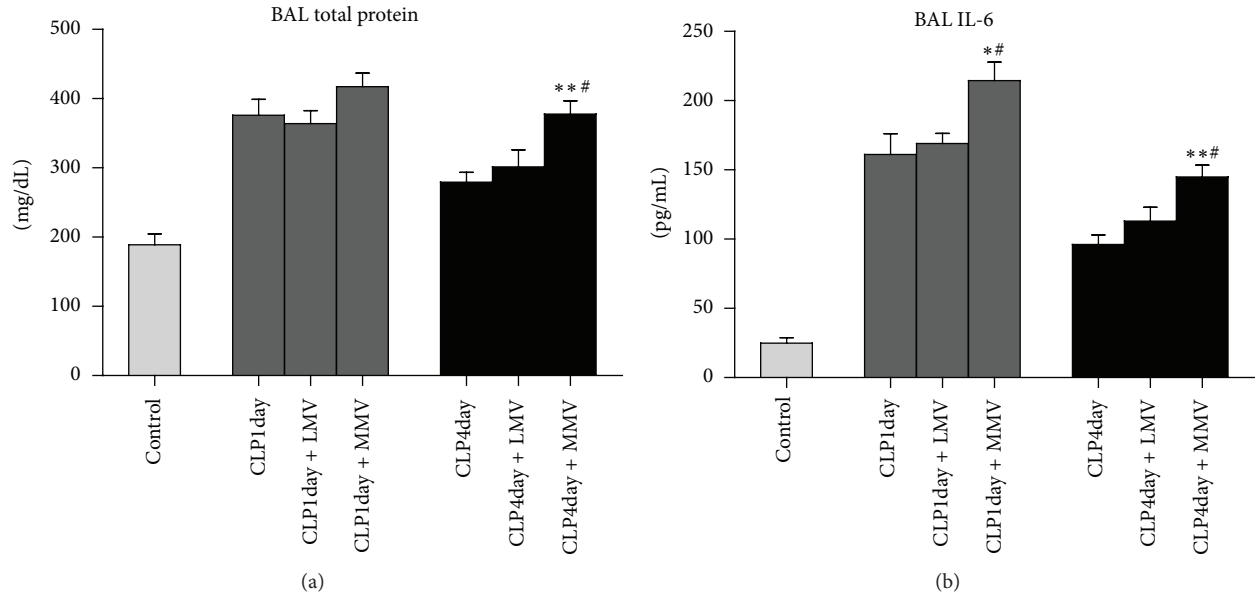

Figure 5: Total protein (a) and IL-6 (b) in BAL for each of the seven groups. *Without MV at the same day after CLP; #low V_T MV at the same day after CLP. Data are presented as mean ± SD.

4. Discussion

The aim of this study was to investigate whether MV exerts distinct effects on lungs at different time after lung injury. We hypothesized that MV would induce an inflammatory response following induction of sepsis by CLP surgery and that this response would be amplified over time. According to our findings, no changes could be found in the inflammatory response at one day after sepsis induction by LMV, but both LMV and MMV did show more severe inflammatory cytokine release and lung injury at a later phase of sepsis.

Acute lung injury (ALI) is a common life-threatening condition that often needs the treatment of MV [1]. Nevertheless, MV can amplify the inflammatory response of preinjured lungs or induce massive release of cytokines from healthy lungs [21, 22], a finding that was validated in our current study. In patients with ARDS, higher tidal volume of MV increases mortality [23]. A recent study showed that MV with a low tidal volume (6 mL/kg) reduced the incidence of mechanical associated lung injury in patients without preexisting lung injury [24]. Therefore, it is now a common view among experts that MV with a low tidal volume protects lungs for patients with and without preexisting lung injury. However, no studies have investigated whether preinjured lungs responded differently to MV at different periods of sepsis. We believe that this information will be meaningful for the determination of the proper tidal volume on a case-by-case basis.

Negative synergistic effects of MV at single time points after sepsis have been found and higher tidal volume tends to be more detrimental [16, 25, 26]. We examined whether moderate tidal volume could be more detrimental to preinjured lungs when compared to low tidal volume in two typical phases of sepsis (one day versus four days) in this study. Furthermore, we examined the effects of two settings (low versus moderate tidal volume) of MV on lungs at different days after initiation of lung injury induced by sepsis.

Low V_T MV caused some heart rate fluctuation and insufficient oxygen index in the first day in the CLP group, where early phase of sepsis was used. Moderate tidal volume MV provided better oxygenation and hemodynamic stability. We found that BALF total protein concentrations were not significantly different among the groups except on the fourth day with moderate MV, which caused a significant increase in total protein concentration. This could be explained by the more severe histological alterations observed in the same group, in which the loss of alveolar integrity would cause more protein leakage.

In terms of BALF total cell counts and PMN differential counts, we observed that effects of moderate V_T MV were similar at different days following sepsis. However, low V_T MV attracted more inflammatory cells and induced more PMN differentiation at the fourth day after sepsis. The concentrations of IL-6 were greater in the group receiving moderate V_T MV at the first and fourth day. This trend was more evident in group 7 on the fourth day after CLP.

These results suggest that although there are some differences between low and moderate V_T MV at the first day of sepsis in our model, moderate V_T MV four days after sepsis are more likely to exert a negative impact on inflammatory lungs responses. Furthermore, for rats receiving low V_T MV, only after four days were synergistic effects on total cell and PMN differential counts observed. This consequence may result from diverse functions of immune cells during sepsis. The immune system plays an important role in the host-pathogen relationship, particularly during sepsis, since sepsis can cause immune suppression that affects the response to other infectious threats [27]. Patients suffering from sepsis

undergo certain adaptive responses including a phase of immunosuppression [28–30], and animals are susceptible to infections in the lung or peripheral blood [31, 32]. This situation may be induced by impaired function of immune cells or dysfunctional cell signaling pathways [10, 33, 34]. Since MV can influence immune cells such as macrophages or alveolar epithelial cells to cause trauma [35, 36], different immune cell states determine different influences of MV. Furthermore, due to the influence of a number of perioperative factors, certain cell functions can be modulated via ROS system [37]. The expression of toll-like receptors (TLRs) is also associated with mechanical induction of lung injury [38, 39]. Previous studies have shown that signal transduction of TLRs can be modulated by sepsis [10]. Taking this into consideration, TLR4 may directly alter the interaction between MV and lungs that were preinjured by sepsis. At the early phase of sepsis, immune cells may not be sensitive to MV due to immunosuppression; thus MV only cause mild inflammatory response.

The function of immune system and ROS generation are variable at a different time point during the process of sepsis [12]. Campos et al. revealed that antioxidant *N*-acetylcysteine could alleviate ALI after CLP followed by low V_T MV in a rat, and this protective effect was attributed to the decrease of oxidative stress [13]. ROS also has the property to increase TLR expression of alveolar macrophages in a mice hemorrhagic shock model [40]. Based on the interaction between MV and immune cells mentioned above, it is reasonable to link the variation of VILI to the production of ROS that at the later phase of sepsis, the fourth day after CLP. In our current experiment, more severe lung injury can be found after the treatment of MV.

Our results confirm that although lung-protective MV with low V_T is important in minimizing the negative impact of MV on lungs, sometimes it cannot meet all physiological requirements in the septic rat model. It may be beneficial to increase the tidal volume in certain periods after sepsis to improve the oxygenation or stabilize the circulation system, without worrying about the consequent inflammatory response. However, our study suggests that a specific window of time exists at the later phase of sepsis to consider the changes to MV as an intervention.

5. Conclusions

We have found that moderate V_T MV causes a more severe inflammatory response when compared to low V_T MV in preinjured lungs, and this effect is more evident at a later phase (fourth day) of sepsis. Furthermore, low V_T MV causes greater synergistic inflammatory effects at later period of sepsis. It will be important to investigate if the different status of ROS generation of immune cells contributes to these phenomena in future studies.

Conflict of Interests

The authors declare that there is no conflict of interests regarding the publication of this paper.

Authors' Contribution

Wei Xuan and Quanjun Zhou contributed equally to this work.

Acknowledgment

The study was supported by a grant from the National Natural Science Foundation of China (no. 81370112 and no. 81200609).

References

[1] M. A. Matthay and R. L. Zemans, "The acute respiratory distress syndrome: pathogenesis and treatment," *Annual Review of Pathology: Mechanisms of Disease*, vol. 6, pp. 147–163, 2011.

[2] D. Dreyfuss and G. Saumon, "Ventilator-induced lung injury: lessons from experimental studies," *The American Journal of Respiratory and Critical Care Medicine*, vol. 157, no. 1, pp. 294–323, 1998.

[3] J. A. Frank, P. E. Parsons, and M. A. Matthay, "Pathogenetic significance of biological markers of ventilator-associated lung injury in experimental and clinical studies," *Chest*, vol. 130, no. 6, pp. 1906–1914, 2006.

[4] L.-F. Li, C.-T. Yang, C.-C. Huang, Y.-Y. Liu, K.-C. Kao, and H.-C. Lin, "Low-molecular-weight heparin reduces hyperoxia-augmented ventilator-induced lung injury via serine/threonine kinase-protein kinase B," *Respiratory Research*, vol. 12, article 90, 2011.

[5] G. S. Martin, D. M. Mannino, S. Eaton, and M. Moss, "The epidemiology of sepsis in the United States from 1979 through 2000," *The New England Journal of Medicine*, vol. 348, no. 16, pp. 1546–1554, 2003.

[6] S. Tasaka, F. Amaya, S. Hashimoto, and A. Ishizaka, "Roles of oxidants and redox signaling in the pathogenesis of acute respiratory distress syndrome," *Antioxidants and Redox Signaling*, vol. 10, no. 4, pp. 739–753, 2008.

[7] K. E. Chapman, S. E. Sinclair, D. Zhuang, A. Hassid, L. P. Desai, and C. M. Waters, "Cyclic mechanical strain increases reactive oxygen species production in pulmonary epithelial cells," *American Journal of Physiology—Lung Cellular and Molecular Physiology*, vol. 289, no. 5, pp. L834–L841, 2005.

[8] J. Wynn, T. T. Cornell, H. R. Wong, T. P. Shanley, and D. S. Wheeler, "The host response to sepsis and developmental impact," *Pediatrics*, vol. 125, no. 5, pp. 1031–1041, 2010.

[9] J. Cohen, "The immunopathogenesis of sepsis," *Nature*, vol. 420, no. 6917, pp. 885–891, 2002.

[10] J. C. Deng, G. Cheng, M. W. Newstead et al., "Sepsis-induced suppression of lung innate immunity is mediated by IRAK-M," *The Journal of Clinical Investigation*, vol. 116, no. 9, pp. 2532–2542, 2006.

[11] S. S. Santos, M. K. C. Brunialti, O. Rigato, F. R. MacHado, E. Silva, and R. Salomao, "Generation of nitric oxide and reactive oxygen species by neutrophils and monocytes from septic patients and association with outcomes," *Shock*, vol. 38, no. 1, pp. 18–23, 2012.

[12] M. T. Herrera, C. Toledo, F. Valladares et al., "Positive end-expiratory pressure modulates local and systemic inflammatory responses in a sepsis-induced lung injury model," *Intensive Care Medicine*, vol. 29, no. 8, pp. 1345–1353, 2003.

[13] R. Campos, M. H. M. Shimizu, R. A. Volpini et al., "N-acetylcysteine prevents pulmonary edema and acute kidney injury in rats with sepsis submitted to mechanical ventilation," *The American Journal of Physiology—Lung Cellular and Molecular Physiology*, vol. 302, no. 7, pp. L640–L650, 2012.

[14] M. C. J. Kneyber, R. P. Gazendam, H. W. M. Niessen et al., "Mechanical ventilation during experimental sepsis increases deposition of advanced glycation end products and myocardial inflammation," *Critical Care*, vol. 13, no. 3, article R87, 2009.

[15] F. Lellouche, S. Dionne, S. Simard, J. Bussières, and F. Dagenais, "High tidal volumes in mechanically ventilated patients increase organ dysfunction after cardiac surgery," *Anesthesiology*, vol. 116, no. 5, pp. 1072–1082, 2012.

[16] N. Nin, J. A. Lorente, P. Fernández-Segoviano, M. De Paula, A. Ferruelo, and A. Esteban, "High-tidal volume ventilation aggravates sepsis-induced multiorgan dysfunction in a dexamethasone-inhibitable manner," *Shock*, vol. 31, no. 4, pp. 429–434, 2009.

[17] C. Menendez, L. Martinez-Caro, L. Moreno et al., "Pulmonary vascular dysfunction induced by high tidal volume mechanical ventilation," *Critical Care Medicine*, vol. 41, no. 8, pp. E149–E155, 2013.

[18] W. A. Altemeier, G. Matute-Bello, C. W. Frevert et al., "Mechanical ventilation with moderate tidal volumes synergistically increases lung cytokine response to systemic endotoxin," *American Journal of Physiology: Lung Cellular and Molecular Physiology*, vol. 287, no. 3, pp. L533–L542, 2004.

[19] M. Rincon and C. G. Irvin, "Role of IL-6 in asthma and other inflammatory pulmonary diseases," *International Journal of Biological Sciences*, vol. 8, no. 9, pp. 1281–1290, 2012.

[20] A. A. Birukova, Y. Tian, A. Meliton, A. Leff, T. Wu, and K. G. Birukov, "Stimulation of Rho signaling by pathologic mechanical stretch is a "second hit" to Rho-independent lung injury induced by IL-6," *American Journal of Physiology: Lung Cellular and Molecular Physiology*, vol. 302, no. 9, pp. L965–L975, 2012.

[21] T. C. Whitehead, H. Zhang, B. Mullen, and A. S. Slutsky, "Effect of mechanical ventilation on cytokine response to intratracheal lipopolysaccharide," *Anesthesiology*, vol. 101, no. 1, pp. 52–58, 2004.

[22] M. Vaneker, F. J. Halbertsma, J. van Egmond et al., "Mechanical ventilation in healthy mice induces reversible pulmonary and systemic cytokine elevation with preserved alveolar integrity: an in vivo model using clinical relevant ventilation settings," *Anesthesiology*, vol. 107, no. 3, pp. 419–426, 2007.

[23] R. G. Brower, M. A. Matthay, A. Morris, D. Schoenfeld, B. T. Thompson, and A. Wheeler, "Ventilation with lower tidal volumes as compared with traditional tidal volumes for acute lung injury and the acute respiratory distress syndrome," *The New England Journal of Medicine*, vol. 342, no. 18, pp. 1301–1308, 2000.

[24] R. M. Determann, A. Royakkers, E. K. Wolthuis et al., "Ventilation with lower tidal volumes as compared with conventional tidal volumes for patients without acute lung injury: a preventive randomized controlled trial," *Critical Care*, vol. 14, no. 1, article 1, 2010.

[25] J. Villar, N. Cabrera, M. Casula et al., "Mechanical ventilation modulates Toll-like receptor signaling pathway in a sepsis-induced lung injury model," *Intensive Care Medicine*, vol. 36, no. 6, pp. 1049–1057, 2010.

[26] T. Nakamura, J. Malloy, L. McCaig et al., "Mechanical ventilation of isolated septic rat lungs: effects on surfactant and inflammatory cytokines," *Journal of Applied Physiology*, vol. 91, no. 2, pp. 811–820, 2001.

[27] T. van der Poll and S. M. Opal, "Host-pathogen interactions in sepsis," *The Lancet Infectious Diseases*, vol. 8, no. 1, pp. 32–43, 2008.

[28] N. V. Gorbunov, B. R. Garrison, D. P. McDaniel et al., "Adaptive redox response of mesenchymal stromal cells to stimulation with lipopolysaccharide inflammagen: mechanisms of remodeling of tissue barriers in sepsis," *Oxidative Medicine and Cellular Longevity*, vol. 2013, Article ID 186795, 16 pages, 2013.

[29] H. D. Volk, P. Reinke, and W. D. Docke, "Clinical aspects: from systemic inflammation to 'immunoparalysis'," in *Cd14 in the Inflammatory Response*, vol. 74, pp. 162–177, 2000.

[30] R. S. Hotchkiss and D. W. Nicholson, "Apoptosis and caspases regulate death and inflammation in sepsis," *Nature Reviews Immunology*, vol. 6, no. 11, pp. 813–822, 2006.

[31] C. G. Davis, K. Chang, D. Osborne, A. H. Walton, W. M. Dunne, and J. T. Muenzer, "Increased susceptibility to Candida infection following cecal ligation and puncture," *Biochemical and Biophysical Research Communications*, vol. 414, no. 1, pp. 37–43, 2011.

[32] C. F. Benjamim, C. M. Hogaboam, N. W. Lukacs, and S. L. Kunkel, "Septic mice are susceptible to pulmonary aspergillosis," *The American Journal of Pathology*, vol. 163, no. 6, pp. 2605–2617, 2003.

[33] A. L. Coelho, M. A. Schaller, C. F. Benjamim, A. Z. Orlofsky, C. M. Hogaboam, and S. L. Kunkel, "The chemokine CCL6 promotes innate immunity via immune cell activation and recruitment," *Journal of Immunology*, vol. 179, no. 8, pp. 5474–5482, 2007.

[34] C. F. Benjamim, S. K. Lundy, N. W. Lukacs, C. M. Hogaboam, and S. L. Kunkel, "Reversal of long-term sepsis-induced immunosuppression by dendritic cells," *Blood*, vol. 105, no. 9, pp. 3588–3595, 2005.

[35] M. T. Kuipers, H. Aslami, J. R. Janczy et al., "Ventilator-induced lung injury is mediated by the NLRP3 inflammasome," *Anesthesiology*, vol. 116, no. 5, pp. 1104–1115, 2012.

[36] T. S. Cohen, G. G. Lawrence, A. Khasgiwala, and S. S. Margulies, "MAPk activation modulates permeability of isolated rat alveolar epithelial cell monolayers following cyclic stretch," *PLoS ONE*, vol. 5, no. 4, Article ID e10385, 2010.

[37] J. Tang, J. J. Hu, C. H. Lu et al., "Propofol inhibits lipopolysaccharide-induced tumor necrosis factor-alpha expression and myocardial depression through decreasing the generation of superoxide anion in cardiomyocytes," *Oxidative Medicine and Cellular Longevity*, vol. 2014, Article ID 157376, 12 pages, 2014.

[38] M. Vaneker, L. A. Joosten, L. M. A. Heunks et al., "Low-tidal-volume mechanical ventilation induces a toll-like receptor 4-dependent inflammatory response in healthy mice," *Anesthesiology*, vol. 109, no. 3, pp. 465–472, 2008.

[39] P. E. Charles and S. D. Barbar, "Toll-like receptors: a link between mechanical ventilation, innate immunity and lung injury?" *Intensive Care Medicine*, vol. 36, no. 6, pp. 909–911, 2010.

[40] J. Fan, Y. Li, Y. Vodovotz, T. R. Billiar, and M. A. Wilson, "Neutrophil NAD(P)H oxidase is required for hemorrhagic shock-enhanced TLR2 up-regulation in alveolar macrophages in response to LPS," *Shock*, vol. 28, no. 2, pp. 213–218, 2007.

Hindawi Publishing Corporation
Oxidative Medicine and Cellular Longevity
Volume 2015, Article ID 590987, 14 pages
http://dx.doi.org/10.1155/2015/590987

Review Article

Oxidative Stress and Lung Ischemia-Reperfusion Injury

Renata Salatti Ferrari[1,2] and Cristiano Feijó Andrade[1,2]

[1] *Thoracic Surgery Department, Laboratory of Airways and Lung, Hospital of Clínicas of Porto Alegre, Ramiro Barcelos 2.350, 90035-903 Porto Alegre, RS, Brazil*
[2] *Federal University of Rio Grande of Sul (FRGS), Rua Ramiro Barcelos 2400, 2° andar Bairro Santana, 90035-003 Porto Alegre, RS, Brazil*

Correspondence should be addressed to Cristiano Feijó Andrade; cristianofa@gmail.com

Received 19 October 2014; Revised 19 January 2015; Accepted 20 January 2015

Academic Editor: Zhengyuan Xia

Ischemia-reperfusion (IR) injury is directly related to the formation of reactive oxygen species (ROS), endothelial cell injury, increased vascular permeability, and the activation of neutrophils and platelets, cytokines, and the complement system. Several studies have confirmed the destructiveness of the toxic oxygen metabolites produced and their role in the pathophysiology of different processes, such as oxygen poisoning, inflammation, and ischemic injury. Due to the different degrees of tissue damage resulting from the process of ischemia and subsequent reperfusion, several studies in animal models have focused on the prevention of IR injury and methods of lung protection. Lung IR injury has clinical relevance in the setting of lung transplantation and cardiopulmonary bypass, for which the consequences of IR injury may be devastating in critically ill patients.

1. Introduction

The process of ischemia and subsequent reperfusion is present in many medical situations such as major surgical procedures and organ transplantation. This event may lead to devastating consequences in some patients; therefore, the understanding of this process is extremely important in the search for new therapies and procedures that could reduce tissue injury [1].

Tissue damage to a particular organ when subjected to ischemia is exacerbated at the moment of its reoxygenation during reperfusion, a process that is considered to be more harmful than ischemia itself [2]. This mechanism of tissue injury is called reperfusion injury or ischemia-reperfusion (IR) injury and consists of a complex pathophysiological phenomenon requiring the presence of oxygen for its genesis, as well as the maintenance and activation of vascular, humoral, and cellular factors.

In its classical manifestation, occlusion of the arterial supply is caused by an embolus or a plug, resulting in ischemia and consequently a serious imbalance between the supply and metabolic demand, causing tissue hypoxia. During reperfusion, the restoration of blood flow is often associated with an exacerbation of tissue injury and an intense inflammatory response [3].

Ischemia directly affects cells and triggers a series of events due to a lack of oxygen, resulting in different intensities of cellular damage and the consequent activation of cytotoxic enzymes, ultimately culminating in cell death.

Oxidative phosphorylation does not occur in mitochondria during oxygen deprivation; anaerobic glycolysis then begins to provide energy but is not suitable for the replenishment of adenosine triphosphate (ATP). This ATP deficit affects the active transport of ions across the membrane, leading to an accumulation of sodium and, by diffusion, water inside the cell, with subsequent edema. This imbalance also occurs within organelles, leading to the swelling and disintegration of mitochondria and the expansion and formation of vesicles in the endoplasmic reticulum. The rupture of lysosomes and release of enzymes contained therein represent the final events prior to cell death [4].

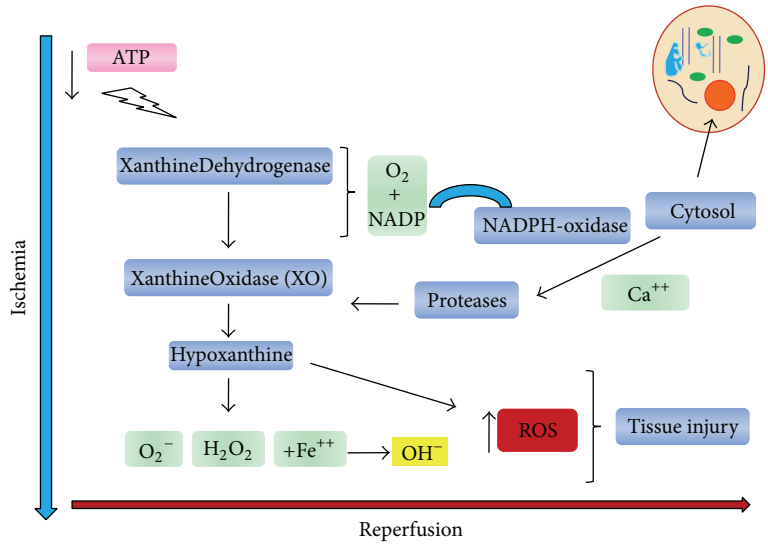

Figure 1: Formation of oxygen-free radicals during lung ischemia and reperfusion injury.

Reperfusion injury is directly related to the formation of reactive oxygen species (ROS), endothelial cell injury, increased vascular permeability, and the activation of neutrophils and platelets, cytokines, and the complement system [5].

When exposed to hypoxia, endothelial cells alter their cytoskeletal morphology, forming small intercellular pores, and the presence of these pores provides increased permeability of the endothelium, with the formation of tissue edema [6]. The worsening of perfusion is enhanced by an imbalance in the production of vasoconstrictor and vasodilator factors. Hypoxic endothelium shows increased production of potent vasoconstrictors (endothelin types 1, 2, and 3) and decreased production of vasodilators (nitric oxide) [2]. These changes initiated during ischemia, particularly in endothelial cells and leukocytes, not only cause tissue injury but also create conditions that favor future injury with the occurrence of reperfusion. Another effect that has been demonstrated after a period of ischemia reperfusion is the impairment of certain segments of the microcirculation, generating heterogeneity in the distribution of blood flow, with focal tissue hypoxia. This phenomenon, called nonreperfusion (no-reflow), is another mechanism of tissue injury after reperfusion [7].

Due to the complications of IR-induced injury, as well as its high morbidity and mortality, several studies have investigated the pathophysiology of IR injury in an attempt to prevent or reverse its deleterious effects.

2. Oxidative Stress and Ischemia-Reperfusion

Oxidative stress has a role in the pathogenesis of several clinical conditions, such as malignancy, diabetes mellitus, atherosclerosis, chronic inflammation, infection with the human immunodeficiency virus, and IR injury [8]. There are different pathways for the production of reactive oxygen species [9], especially via xanthine oxidase as the primary source of production in most organs with systemic vasculature [10]. ROS formation occurs in the mitochondrial matrix through the electron transport chain due to the reduction of molecular oxygen to superoxide radical (O_2^-) [11].

When a tissue is subjected to ischemia, a sequence of chemical reactions is initiated. Despite the lack of identification of a critical event responsible for tissue damage, most studies have shown that the depletion of energy and the accumulation of toxic oxygen metabolites (oxidative stress) can contribute to cell death. Paradoxically, reperfusion quickly restores the energy supply by removing toxic metabolites and preventing organ failure; however, it also contributes to and amplifies the mechanisms involved in ischemic tissue damage [5].

During tissue ischemia, a reduction in the availability of ATP as a result of the degradation on adenosine diphosphate (ADP), adenosine monophosphate [12], adenosine, inosine, and hypoxanthine occurs. Furthermore, xanthine dehydrogenase is converted to xanthine oxidase.

This reaction can occur through two mechanisms: (1) xanthine dehydrogenase can be reversibly converted to xanthine oxidase via the oxidation of sulfhydryl groups; or (2) xanthine dehydrogenase can be irreversibly converted to xanthine oxidase via proteolysis through proteases activated by calcium, which is increased in the cytosol and derived from the extracellular environment [5].

Xanthine oxidase relies on oxygen to metabolize hypoxanthine, and when this is provided by reperfusion (reoxygenation), ROS molecules are formed, with a large capacity to cause injury to tissue [5].

NADPH oxidase, an enzyme expressed in virtually all inflammatory cells, contributes to the formation of cytotoxic peroxynitrite. Furthermore, hydrogen peroxide (H_2O_2) derived from the dismutation of O_2 results in highly toxichydroxyl radical (OH^-) by the Haber-Weiss reaction, which is facilitated by the increased availability of free iron during ischemia [13] (Figure 1).

Xanthine dehydrogenase uses nicotinamide dinucleotide phosphate (NADP) and may be irreversibly converted to xanthine oxidase. Additionally, proteases are activated by calcium, which are increased in the cytosol. In the presence of oxygen resulting from reperfusion, xanthine oxidase (XO) metabolizes hypoxanthine, forming ROS. Hydrogen peroxide (H_2O_2) generates hydroxyl radical (OH), which is highly toxic, by the Haber-Weiss reaction, which is facilitated by the increased availability of free iron during ischemia. The increase in ROS results in major pulmonary tissue damage.

The importance of oxygen radicals in the pathophysiology of IR injury was demonstrated after the injection of free radical scavengers or enzymes, such as superoxide dismutase (SOD), catalase (CAT), and glutathione peroxidase (GPX), preventing the damage that occurs during reperfusion [14, 15].

Several studies have confirmed the destructiveness of the derived toxic oxygen metabolites and their role in the pathophysiology of different processes, such as oxygen poisoning, inflammation, and ischemic injury [16].

3. Oxidative Stress and Lung Ischemia-Reperfusion Injury

The mechanisms of IR injury in the pulmonary parenchyma are similar to reperfusion injury in other organs and include a significant involvement of ROS, intracellular calcium influx, endothelial cell injury, leukocyte sequestration and activation in the pulmonary circulation, activation of the complement system, and the release of inflammatory mediators such as arachidonic acid metabolites [2].

Pulmonary IR injury can occur due to trauma, atherosclerosis, pulmonary embolism, and surgical procedures, such as cardiopulmonary bypass (CPB) and lung transplantation [17]. The latter is the most studied situation because it is directly related to the incidence of early graft dysfunction and is responsible for up to 20% of mortality in the early postoperative period [18, 19].

The IR-induced lung injury that occurs in the setting of lung transplantation is characterized by edema, hypoxemia, and pulmonary infiltrates on chest X-ray [20].

This occurs mainly in postcapillary venules, increasing hydrostatic pressure, and favoring the formation of edema, which is facilitated by the increased capillary permeability caused by endothelial injury. ROS have a key role in the development of pulmonary injury (IR) [21, 22], which is characterized by increases in ROS and other free radicals, with a crucial role in the sequence of events leading to lung failure [23].

The IR phenomenon occurs in the heart, liver, kidney, gut, central nervous system, skeletal muscles, and other organs [8]. In these organs, ischemia is accompanied by tissue anoxia until the reintroduction of oxygen during reperfusion and is thus the equivalent to IR anoxia-reoxygenation. Unlike other organs, the lung is considered the only organ that can suffer ischemia without hypoxia because alveolar oxygen helps to maintain aerobic metabolism, thereby preventing hypoxia. Thus, the oxidative stress in the lung resulting from ischemia should be distinguished from that resulting from hypoxia itself [24].

In the setting of lung transplantation, factors present in the prereperfusion phase of the graft, such as brain death, pneumonia, mechanical ventilation, aspiration, contusion, hypotension, and cold ischemia, have been recognized as aggravating IR injury through the activation of inflammatory factors [24, 25].

Hypoxia and consequently anoxia result in a decrease in intracellular ATP and an increase in ATP degradation products, such as hypoxanthine, which generates ROS production when oxygen is reintroduced during reperfusion and/or ventilation. During ischemia, this phenomenon may occur in the lung if the alveolar oxygen tension drops below 7 mmHg [26, 27]. The absence of pulmonary blood flow leads to lipid peroxidation, even in the presence of oxygen. The mechanism of oxidative stress is different from what occurs during anoxia-reoxygenation because it is not associated with decreased ATP, and it may occur even during the period of cold ischemia in an organ stored for transplantation [28].

In the lungs, ROS are related to the activation of inflammatory processes through transcription factors such as nuclear factor-kappa B (NF-κB), leading to chromatin remodeling and the expression of proinflammatory mediator genes [29, 30]. Intracellular ROS production has been observed in various cell types of lung tissue, including endothelial cells, alveolar type II epithelial cells, clara cells, ciliated epithelial cells, and alveolar macrophages [31]. It is believed that IR pulmonary injury is due to an increase in ROS, which triggers a response from the graft, resulting in the activation of the adaptive immune response (acute rejection) through the activation of antigen-presenting cells [32]. Additionally, the use of LPD (low-potassium dextran), a lung preservation solution, appears to decrease ROS production [33] and reduce the incidence of primary graft failure through a reduction in ROS production from the pulmonary vasculature [34].

4. Systemic Effects of Ischemia-Reperfusion Injury

IR injury and multiple organ failure contribute significantly to mortality and postoperative morbidity, and reperfusion induces the oxidative stress that plays a key role in this pathology. Pulmonary IR injury induces systemic effects in the liver and heart and is characterized by neutrophil sequestration and the release of significant amounts of ROS into the circulation [35, 36].

However, the pulmonary system may also suffer consequences from IR tissue located remotely [37]: a single organ exposed to IR can subsequently cause inflammatory activation in other organs, leading to the failure on multiple systems. Importantly, ischemic syndromes are a heterogeneous group of conditions. Although there are some similarities in biological responses between these syndromes that occur in different organs, there are important differences between a reduction in systemic perfusion, for example, during shock,

compared with regional ischemia and the reperfusion of a single organ [38].

During IR injury in the liver or kidney, the activation of intestinal inflammatory responses triggers a sequence of events that leads to multiorgan failure. The IR of peripheral organs (such as the liver) results in the activation of intestinal Paneth cells and the subsequent release of cytokines such as IL-17, causing failure in other systems, including the pulmonary system [39, 40].

The systemic inflammatory responses of mesenteric IR represent an important model of severe disease because deficits in the intestinal mucosa appear to be critical in the initiation and propagation of multiple organ failure [41].

Using a mouse model of intestinal IR injury, Mura et al. reported that nearly 50% of the IR group animals died during the experimental period of 4 h. The combined effects of intestinal IR, surgical procedure, the application of a high oxygen concentration, and mechanical ventilation may be responsible for this high mortality rate. In this model, the lung was the most severely injured remote organ [4]. Additionally, a recent clinical study confirmed that respiratory dysfunction following traumatic injury is an obligatory event that precedes heart, kidney, and liver failure [4, 42].

Recent studies also report that activated neutrophils aggregate in the subendothelial space, where they release reactive oxygen species (ROS), enzymes, and cytokines, causing direct renal injury and the recruitment of monocytes and macrophages leading to further aggravation of the oxidative injury [43, 44].

5. The Antioxidant Defense System

An antioxidant is any substance that, even at low concentrations, significantly delays or inhibits the oxidation of a substrate in an enzymatic or nonenzymatic manner [45].

The organism's defense against ROS ranges from the prevention of ROS formation to interception of the formed radicals to cell repair. Enzymes that control the levels of ROS are glutathione peroxidase (GPx), superoxide dismutase (SOD), and catalase (CAT), leading to the sequestration and deactivation of ROS, which are neutralized to prevent the further oxidation of other molecules. The final neutralization of a compound with one or more unpaired electrons is the formation of another nonradical product.

Water-soluble radical compounds transfer the radical function away from the potential target site and are called free radical scavengers. The combination of a substance with a free radical leads to the formation of a nonradical or a radical that is less harmful, for example, tocopherols and carotenoids [45].

Antioxidant therapy can be performed by the replacement of endogenous antioxidants, such as recombinant superoxide dismutase [46] or by exogenous supplementation of antioxidant agents, such as N-acetylcysteine [47].

However, the use of antioxidants in animal models of lung injury has been little exploited in experimental and clinical studies, for example, the use of N-acetylcysteine [48], which has proven to be an important therapeutic potential for use in IR lesion [42].

6. N-Acetylcysteine

Several authors have described different ways to increase the viability of lung graft posttransplantation and to reduce the undesirable effects of IR injury, including the use of antioxidants such as NAC and melatonin [42, 49].

NAC (chemical formula $C_5H_9NO_3S$; molecular weight 163.2) is a thiol compound that contains a sulfhydryl group and is widely used in clinical medicine [50].

NAC is a mucolytic that was first implemented for treating congestive and obstructive lung diseases associated with hypersecretion. NAC is also used in the treatment of adult respiratory distress syndrome and in cases of acquired immunodeficiency in HIV infection [51]. Its antioxidant activity is mainly governed by two mechanisms: (1) direct reduction of H_2O_2 and $O_2^{\bullet-}$ into less reactive species, forming sulfur or cysteine radicals; (2) promotion of the biosynthesis of GSH, which acts as a scavenger of free radicals and as a substrate in the redox cycle of glutathione [52].

The loss of antioxidant capacity in an oxidized cell is mainly due to a decrease in glutathione, which is the most abundant intracellular free thiol. Oxidative stress in vivo is translated as a deficiency in glutathione or its precursor, cysteine, and the most effective antioxidant that has been studied is the NAC, a glutathione precursor [46].

Chemically, NAC is similar to cysteine, and the presence of this acetyl environment reduces thiol reactivity compared to cysteine. Moreover, NAC is less toxic and less susceptible to oxidation and dimerization and is more soluble in water, making it a better source of cysteine than the parenteral administration of cysteine [53]. NAC provides protection mediated by administration of lipopolysaccharide endotoxemia, resulting in a decrease in H_2O_2, and this was directly related to its ability to reduce ROS rather than its function of promoting the biosynthesis of glutathione [54]. Many studies have demonstrated the effects of NAC, mainly with regard to modulating the activity of inducible nitric oxide synthase (iNOS), reducing the formation of inflammatory cytokines and inhibiting the action of neutrophils [55–58]. Furthermore, NAC acts as a "scavenger" of free radicals by inhibiting oxidative stress and preventing cell death [59].

Studies have demonstrated that treatment with NAC prior to lung warm ischemia significantly attenuates inflammatory changes in both the ischemic and reperfusion periods [60]. NAC reduces the phosphorylation of IκB-α and p-65, resulting in a decrease in apoptosis and inflammatory responses. The intravenous administration of NAC demonstrates protective properties against lung IR injury, and the use of NAC immediately after reperfusion potentiates its protective effects [61].

Study of Wu et al., demonstrated that the NAC administration reduced lung I/R-induced increases in myocardial hydroxyl radical production and lipid peroxidation and ameliorated LV contractility and stiffening [62].

This protective effect could be explained by NAC increasing GSH synthesis or eliminating free radicals directly or both. The observed reduction in malondialdehyde (MDA) levels is consistent with the potent antioxidant effects of NAC, with a significant reduction in lipid peroxidation being reported by many researchers [63–65].

Current studies suggest the use of isoprostane as a more specific index of oxidative stress induced by ROS [66–68].

In experimental studies, treatment with NAC resulted in higher levels of tissue GSH, which led to improved lung graft function [46, 69].

7. Calcium and Sodium Pump in Ischemia-Reperfusion Injury

Ischemia causes an increase in calcium permeability by promoting its entry into cells. Such an increase in intracellular calcium, which is enhanced by a decrease in its active, ATP-dependent transport to the extracellular environment, has several deleterious effects: a change in cell shape by contraction of the cytoskeleton and phospholipase activation, with the consequent release of the metabolite arachidonic acid from cell membranes and organelles and the production of free radicals. All these effects contribute to cell death [70].

In addition to the increase in intracellular calcium as a result of ischemia, intracellular consumption occurs during the "storage" of ATP; hence, there is an increase in anaerobic glycolysis products. Such an event impairs the transmembrane ion gradient, with the consequent accumulation of sodium (Na^+) and water, leading to cellular edema and the swelling of organelles, such as the mitochondria, culminating in cell lysis. Furthermore, the sodium pump (Na^+/K^+ATPase) is inactive during ischemia, contributing to the disruption of the ion gradient [71].

The accumulation of calcium ions (Ca^{++}) intracellularly as a consequence of changes in the permeability of the plasma membrane and the decrease in its active ATP-dependent transport results in the activation of phospholipases and proteases [72]. Proteases potentiate the effects of ROS on organelles by converting xanthine dehydrogenase to xanthine oxidase, and phospholipases activate the transformation of arachidonic acid into products such as leukotrienes, prostaglandins, and thromboxane [72].

8. Endothelium in Lung IR Injury

The endothelium is the main source of ROS during nonhypoxic pulmonary ischemia through the activation of NADPH oxidase. This enzyme complex is also found in other lung cells, but its concentration is more evident in neutrophils, monocytes, and alveolar macrophages. Cell stimulation during ischemia results in the translocation of NADPH oxidase components to the cell membrane, a site where integration occurs with membrane components to form a system of electron transfer that catalyzes the reduction of molecular oxygen (O_2) to superoxide radical (O_2^-) while oxidizing NADPH. This increase in the consumption of O_2 and production of O_2^- is responsible for the "oxidative burst" that results from the activation of NADPH. The O_2^- generated can be subsequently transformed into H_2O_2 in a reaction catalyzed by SOD. Oxidizing compounds are also produced by enzymes contained in intracellular granules. Azurophilic granules release the enzyme myeloperoxidase [12], which during neutrophil activation catalyzes the reaction between H_2O_2 and chlorine to produce hydrochloridric acid, which is considered to be an extremely potent oxidant. Furthermore, hydrochloridric acid can react with amines, generating chloramines, which are considered potent oxidants [73].

Based on previous studies that demonstrated the presence of the enzyme xanthine dehydrogenase in endothelial cells and the ability of the cells to release ROS, these authors studied the effect of the presence of activated neutrophils in contact with these cells. They demonstrated that activated neutrophils induce the conversion of xanthine dehydrogenase into xanthine oxidase in endothelium [74].

9. Iron

Although iron is an essential element for all cells, it may be highly toxic under pathophysiological conditions, such as in the presence of oxidative stress, due to its oxidation-reduction properties [41].

The iron is mostly stored in ferritin molecules and is transported by transferrin molecules. However, "free" iron exists and can participate in Fenton's reaction, in which O_2 and H_2O_2 react with iron and produce OH radicals. Iron is released from ferritin and cytochrome P-450 during ischemia due to the effect of acidosis and through the action of superoxide radical and proteolysis. Moreover, when released into the circulation, iron can activate platelet aggregation. An experimental model of lung IR injury using 3 hours of warm ischemia in dogs showed that a new type of lazaroid is able to reduce iron-dependent lipid peroxidation [75].

10. Inflammatory Mediators

Some inflammatory mediators released as a consequence of the reperfusion of an organ or similar such region can activate endothelial cells in distant organs that were not exposed to the ischemic insult but are injured as a result of reperfusion injury.

Moreover, reperfusion injury is characterized by autoimmune responses, including the recognition of natural antibodies and neoantigens and the subsequent activation of the complement (autoimmunity) system [76]. Despite the fact that IR typically occurs in a sterile environment, the activation of innate and adaptive immune response occurs and contributes to the injury, including the activation of pattern recognition molecules, such as toll-like receptors (TLR), and the inflow of inflammatory cells in the injured organ [77].

For example, when TLRs recognize specific molecules, they trigger the activation of signaling pathways, including the NF-κB activation of protein kinase (MAPK) pathways and type I interferon, which results in the induction of proinflammatory cytokines and chemokines. These receptors can also be activated by endogenous molecules in the absence of microbial compounds, particularly within the context of cell damage or death, as occurs during IR [78] (Figure 2).

The recognition of "danger signals" by toll-like receptors (TLRs) on the surface of inflammatory cells leads to the activation of different signaling pathways, including the NF-κB activation of protein kinase (MAPK) pathways and type I

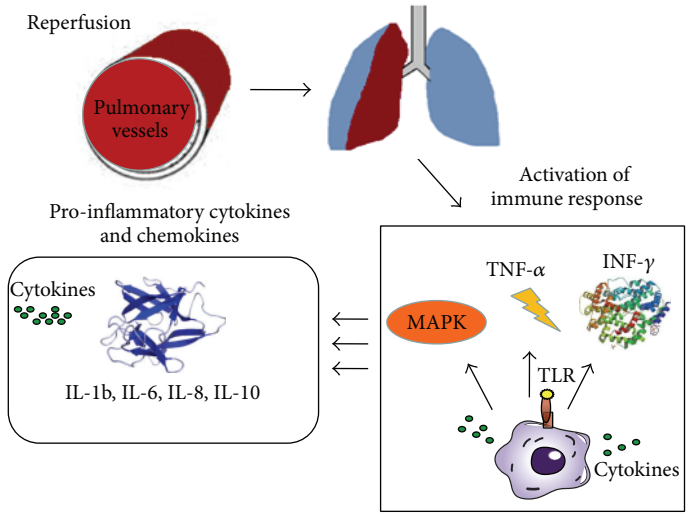

Figure 2: Activation of the immune response and trafficking of inflammatory cells in the diseased organ during reperfusion.

interferon, which results in the induction of proinflammatory cytokines and chemokines.

Specifically, the activation of TLR4 may be aggravated by the oxidative stress generated during IR, which when recognized by inflammatory cells increases responsiveness to subsequent stimuli. Alveolar macrophages from rodents subjected to hemorrhagic shock and resuscitation express increased levels of TLR4, an effect that was inhibited by the addition of the antioxidant NAC with fluid resuscitation [77]. Andrade et al. examined the levels of TLR mRNA expression in lung tissue collected during IR in human lung transplantation and found that the mRNA levels of most TLRs correlate with the mRNA levels of cytokines (IL-1b, IL-6, IL-8, IL-10, and IFN-gamma) in the lungs of donors during hypothermic storage. These observations suggest that inflammatory responses in the donor organ can affect the expression and activity of TLR genes; alternatively, the levels of expression and activation of TLRs may contribute to the regulation of cytokine gene expression. In addition, a close correlation between TL4 and IL-8 before and after reperfusion was found, suggesting that this cytokine may be involved in the regulation of TLR4 gene expression in the setting of lung transplantation [79].

TNF-α (tumor necrosis factor α), ROS, and interleukin-6 (IL-6) are involved in the tissue damage that occurs during IR because they are toxic molecules that alter cellular proteins, lipids and ribonucleic acids, leading to cellular dysfunction or death [80]. A further contribution to tissue injury occurs when the worsening of perfusion is potentiated by an imbalance in the production of vasoconstrictor and vasodilator factors. The hypoxic endothelium shows an increased production of potent vasoconstrictors (endothelin types 1, 2, and 3) and a decreased production of vasodilators (nitric oxide) [2].

The cellular damage generated by ROS in the lipid membrane promotes the activation of phospholipase A2 by inducing the production of platelet activating factor (PAF), which promotes the mobilization of arachidonic acid from the phospholipids of cell membrane. Arachidonic acid is the substrate for numerous enzymes and inside the lungs is primarily metabolized by two enzymes, cyclooxygenase and 5-lipoxygenase, producing inflammatory mediators. The cyclooxygenase pathway generates prostaglandins (PGE1 and PGI2) and thromboxane (TXA2), and the 5-lipoxygenase pathway produces leukotrienes, such as leukotriene B4, C4, D4, and E4 [81, 82].

Pulmonary vascular resistance depends on the interaction between vasoconstrictor and vasodilator factors. Most of the metabolites of arachidonic acid are derived from endothelial cells and contribute to maintaining low vascular resistance in the lung. The effects of prostaglandins and thromboxanes are antagonistic. Prostacyclin (PGI2) is a bronchodilator and a pulmonary vasodilator and prevents platelet aggregation, whereas thromboxane A2 (TXA2) is a broncho- and vasoconstrictor and induces platelet aggregation [82].

Prostaglandins (PGE1 and PGI2) are associated with the following effects: vasodilation and bronchodilation; the inhibition of platelet aggregation, leukocyte adhesion, and sequestration; and the suppression of proinflammatory cytokine (TNF-α, IL-1, and IL-6) production [12, 83, 84].

PAF can be released from various cells, such as macrophages, platelets, mast cells, endothelial cells, and neutrophils, and is responsible for leukocyte activation, platelet aggregation, cytokine release, and adhesion molecule expression [85]. PAF acetylhydrolase is responsible for the degradation and regulation of the activity of PAF, and high levels of this enzyme were found in the bronchoalveolar lavage of patients with ARDS [86]. Furthermore, it has been observed that when added to a lung preservation solution in an isolated perfused rat model, the substance has the ability to reduce pulmonary capillary permeability [87].

Leukotrienes, products of arachidonic acid metabolism by the 5-lipoxygenase pathway, are divided into two classes: cysteine LTC4, LTD4, and (LTE4) and noncysteine (LTB4). LTB4, a potent proinflammatory activator of leukocyte chemotaxis that has an important role in lung IR injury, is

produced by monocytes, lymphocytes, mast cells, and lung macrophages [88].

Vascular endothelial growth factor (VEGF) and its receptor are central to the regulation of vascular permeability and the survival of endothelial cells. Mura et al. suggested that VEGF may have dual roles in LPA-induced intestinal IR. The early release of VEGF can increase pulmonary permeability, whereas a decrease in the expression of VEGF and VEGFR-1 in lung tissue could contribute to the death of alveolar epithelial [4].

11. Nitric Oxide

Nitric oxide (NO) plays an important role in vascular homeostasis due to its potent vasoregulatory and immunomodulatory properties. It is known that NO attenuates the capillary overflow and tissue damage observed in animal models of pulmonary IR, myocardial and cerebral ischemia by inhibiting the adhesion of neutrophils, and the production of superoxide by neutrophils [89].

NO is considered to be an optimal transcellular messenger due to its lipophilic nature and short half-life in biological systems, approximately 3 to 30 seconds [90].

NO is also a key biological mediator produced by various cell types, including vascular endothelium, is an inhibitor of platelet aggregation and neutrophil adhesion, and modulates vascular permeability. Additionally, NO acts as a bronchodilator and neurotransmitter [84].

After pulmonary IR, the levels of endogenous NO are reduced. This may be associated with the increased expression of eNOS, which may suggest that endogenous NO production can be readily attenuated by free radicals after reperfusion and/or because IR can induce the generation of NOS inhibitors [91, 92].

The decreased production of endogenous NO by the immediate reaction of NO with the radical superoxide results in the production of a powerful oxidant, peroxynitrite (OONO). Such a loss of the protective action of NO will result in endothelial dysfunction [90].

12. Leukocyte Activation

IR injury in lung transplantation has a biphasic pattern. The early phase of reperfusion is mainly dependent on the characteristics of the donor, whereas the late phase is dependent on the characteristics of the recipient, lasting 24 hours. Donor macrophages activated during ischemia are the mediators of the early phase; lymphocytes and neutrophils from the recipient are mainly involved in the late phase. The recruitment of these cells occurs through the release of cytokines and other inflammatory mediators before and after reperfusion [93].

Alveolar macrophages produce large amounts of cytokines and procoagulant factors in response to oxidative stress. The importance of tumor necrosis factor alpha (TNF-α), interferon gamma (INF-γ), and chemoattractant protein-1 macrophage (equivalent to human IL-8) in the early phase of graft reperfusion was shown in a rat lung IR model [94].

Lymphocytes play an important role in pulmonary IR injury. The lung contains a large amount of donor macrophages and activated lymphocytes represented by T and natural killer cells, which are responsible for the graft-host immune response but also have beneficial immunomodulatory effects [95]. In a rat lung transplant model, it was observed that CD4+ T lymphocytes are the mediators of IR injury and infiltrate the graft an hour after reperfusion, consequently increasing the production of IFN-γ; furthermore, it was suggested that this effect is independent of neutrophil recruitment and activation [24].

The role of leukocytes in lung reperfusion injury is due to the release of substances during their own degranulation, some of which are free radicals. Polymorphonuclear neutrophils possess nicotinamide adenine dinucleotide phosphate oxidase (NADPH oxidase), which is capable of reducing molecular oxygen and generating superoxide anion [96].

These cells also secrete myeloperoxidase enzyme, which catalyzes the formation of hypochlorous acid (HOCl) from the oxidation of chloride ion in the presence of hydrogen peroxide. HOCl reacts with amines, generating chloramines, potent oxidants [97].

Neutrophils have the characteristic of infiltrating the transplanted lung progressively during the first 24 hours after reperfusion. Although these cells have an important role in the late phase of reperfusion injury, their role in the early phase is less well known. Deeb et al. demonstrated that reperfusion injury in the first four hours depends of the presence of neutrophils, with macrophages also having an important role at this stage; none the less, after this period, neutrophils are the primary mediators [98].

13. Apoptosis and Lung Ischemia-Reperfusion Injury

Apoptosis is an active process, the hall mark of which is the controlled autodigestion of cellular constituents due to the activation of endogenous proteases and can be metaphorically compared to "cell suicide." The activation of these proteases compromises the integrity of the cytoskeleton, causing the collapse of the cell structure. In response to the contraction of the cytoplasmic volume, the cell membrane forms bubbles, with changes in the positioning of the lipid components [99].

Nuclear NF-κB transcription is regulated by the inhibitory action of inhibitor of κB (IκB), which is targeted for degradation via phosphorylation by the action of IκB kinases (IKKα, IKKβ) [100]. Inflammatory signaling activates a cascade of events, such as the phosphorylation of the TNF receptor, leading to the activation of transforming-growth factor b-activated kinase 1 (TAK1). TAK1 phosphorylates the IKK complex and then phosphorylates IκBα, resulting in the ubiquitination and dissociation of IκBα from NF-κB and IκBα degradation by the proteasome. NF-κB translocates to the nucleus and binds to specific DNA regions, initiating the transcription of multiple genes, including cytokines, chemokines, and other inflammatory mediators [101].

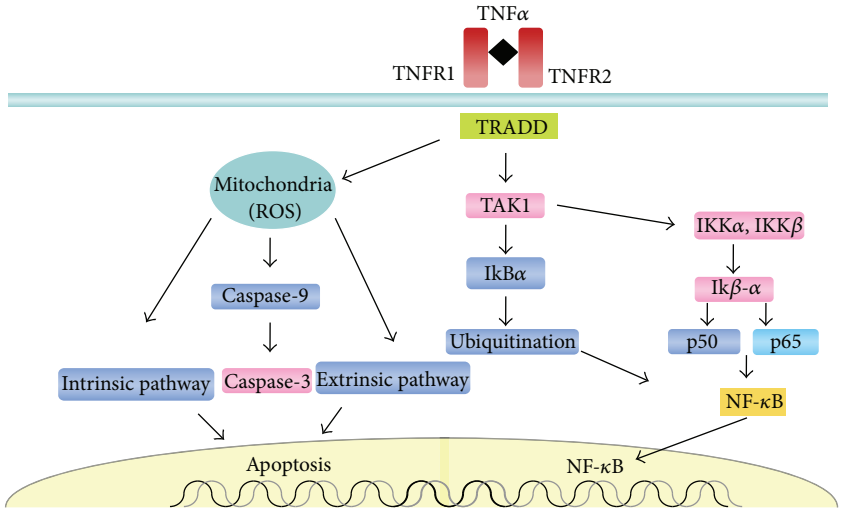

Figure 3: The transcription of nuclear NF-κB is regulated by the inhibitory action of the inhibitor protein IκB during ischemia-reperfusion injury.

Unlike what occurs with necrosis, apoptosis or programmed cell death does not occur during ischemia, but a peak of it does occur during reperfusion [100]. The induction of apoptosis can occur through two pathways. The intrinsic pathway is dependent on mitochondria and is activated by ROS, whereas the extrinsic pathway is dependent on inflammatory molecules, such as TNF-α. However, by activating the production of ROS via the NADPH oxidase pathway, TNF would also contribute to the intrinsic pathway [102]. Both pathways promote the activation of caspases and proteases responsible for the cleavage of specific cellular substrates, which results in changes in cellular configuration, changes in membrane permeability, and DNA fragmentation, with consequent cell death [103]. The intrinsic pathway is activated in the early phase of reperfusion, and the extrinsic pathway can be activated up to a few hours after reperfusion [104] (Figure 3).

Phosphorylation of the TNF receptor (TNFR1 and TNFR2) leads to the activation of transforming-growth factor b-activated kinase 1 (TAK1), which phosphorylates the protein IκBα, resulting in ubiquitination and leading to the dissociation of IκBα from NF-κB. TAK1 also leads to degradation of IKKa and IKKb, releasing two subunits of p50 and p65; NF-κB translocates to the nucleus, initiating the transcription of multiple genes, including cytokines, chemokines, and other inflammatory mediators. This occurs to be concomitant with the induction of apoptosis by the activation and induction of two pathways: the mitochondria-dependent intrinsic pathway is activated by ROS, and the extrinsic pathway is dependent on inflammatory molecules, such as TNF-α. The intrinsic pathway is activated in the early phase of reperfusion; the extrinsic pathway can be activated up to a few hours after pulmonary IR.

Apoptosis is regulated by a cascade of proteins called caspases, which are apoptosis effector proteins present in all cells. After cleavage, caspases become active and initiate pathways leading to apoptosis [105].

The following are features of apoptosis: chromatin condensation, phosphatidylserine exposure on the cell surface, cytoplasmic shrinkage, the formation of apoptotic bodies, and fragmentation of DNA [106]. As opposed to necrosis, which also occurs in the absence of ATP, apoptosis is an energy-dependent process [107].

Forgiarini et al. demonstrated that the duration of ischemia has a direct effect on the viability of lung cells using an experimental model of lung IR. The increase in caspase 3 activity reflected a larger number of apoptotic cells after 45 minutes of ischemia [108].

The signaling pathway that leads to programmed cell death is maintained by positive and negative regulators, and the balance between these factors decides whether the cell survives or undergoes apoptosis. The proteins that promote survival are the antiapoptotic proteins Bcl-2 and Bcl-xL, whereas proapoptotic proteins Bax, Bad, Bak, and Bid induce programmed cell death [109].

An important regulator of apoptosis following DNA damage is p53, which can induce Bax and Bak, regulating the release of cytochrome C from mitochondria and thereby initiating the cascade leading to apoptosis [110]. Cytochrome C binds to apoptotic protease activating factor 1 (Apaf-1), activating caspase 9, which in turn cleaves caspases 3 and 6 [111, 112], leading to cell death (Figure 4).

An important regulator of apoptosis is p53, which can induce Bax and Bak, which regulate the release of cytochrome C from mitochondria, thereby initiating the cascade that leads to apoptosis. Cytochrome C binds to apoptotic protease activating factor 1 (Apaf-1) to activate caspase 9, which cleaves caspases 3 and 6, leading to cell death.

14. Prevention and Treatment of Pulmonary IR Injury

Major advances in our understanding of the mechanisms of reperfusion injury and the development of strategies to

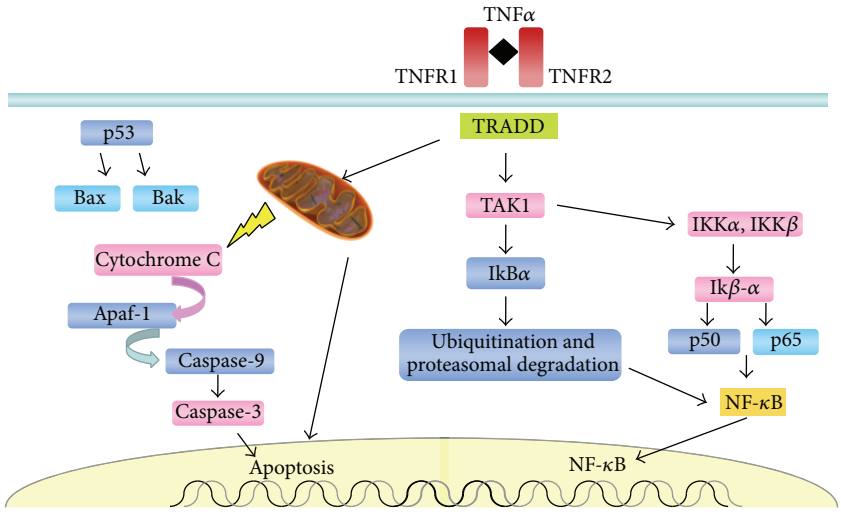

Figure 4: Release of cytochrome C from mitochondria triggers the activation of caspase 9, which cleaves caspases 3 and 6, leading to apoptosis.

increase tissue resistance to ischemia or to attenuate reperfusion injury have occurred. For example, experimental studies of adaptive responses induced by hypoxia have provided strong evidence for new treatment approaches in IR [38].

The tissue damage is not limited only to ischemia and may extend or worsen with reperfusion, and recognizing this is important for carefully reversing ischemia, which is a critical point for maintaining tissue viability under damaging conditions [20].

Because of the pulmonary damage that IR causes, many studies in animal models have focused on the prevention of IR injury and the improvement of lung preservation methods [113–115], such as the use of lung hyperinflation [26, 116], hypothermic preservation [117], different lung preservation solutions [118, 119], retrograde pulmonary perfusion [118, 119], liquid ventilation [120], and perfluorocarbon [121, 122]. These are in addition to the use of vasodilators [123, 124] antioxidants [125] gene therapy [126], inhaled nitric oxide [89], and ischemic preconditioning (PCI) [127].

All therapeutic options tested by different methods attempt to minimize or prevent the cell death that occurs during IR and consequently activate the various pathways of cell death, which can be categorized as necrosis, apoptosis, or cell death associated with autophagy. Necrosis is characterized by the swelling of cells and organelles with the subsequent rupture of membranes and the surface and the shedding of intracellular contents [128].

Necrotic cells are highly immunostimulatory and cause inflammatory cell infiltration and cytokine production. In contrast, apoptosis involves a cascade of caspase signaling that induces programmed cell death, which is characterized by cell and nuclear shrinkage, though the integrity of the plasma membrane persists until the end of the process. Different studies have investigated whether the inhibition of apoptosis may become a promising therapeutic strategy for lung ischemia-reperfusion injury [129, 130].

Some studies have investigated whether mice with a disruption in the gene encoding IKKb, the catalytic subunit of IKK that is essential for the activation of NF-κB, can provide an opportunity to study the effects of preventing the activation of NF-κB. However, this manipulation results in embryonic lethality due to massive apoptosis in the developing liver driven by NF-κB [131]. Ishiyama et al. [132] studied the inhibition of NF-κB activation by applying inhibitors that prevented IκB phosphorylation and showed an increase in the oxygenation of the transplanted lung and reductions in pulmonary edema, neutrophil aggregation, and apoptotic cells after experimental lung transplantation.

Chang and Yang [103] demonstrated that the inhibition of NF-κB attenuates IR injury, as it is responsible for a reduction in cytokine production. In their study, the activation of NF-κB was responsible for the increased expression of caspase 3 and iNOS.

Another study on intestinal ischemia and reperfusion showed that although IKKb deficiency in enterocytes is associated with a reduction in inflammation, severe apoptotic damage occurs in the mucosa. Thus, attempts to inhibit the activation the NF-κB pathway are associated with the prevention of systemic injury but consequently increase local inflammation injury [133].

Certain calcium channel blockers are also used, such as verapamil, which has a protective effect during lung ischemia-reperfusion [134].

Torres et al. suggested that the presence of LPD preservation solution in the systemic blood increases the plasma's total antioxidant potential, both in the presence and absence of a lung ischemic event. A decrease in erythrocyte LPD was also observed in the presence of lung ischemia [33].

Other evidence suggests that TLRs are involved in IR injury of different organs. In a study of myocardial ischemia-reperfusion injury, two strains of TLR4-deficient mice (C57/BL10 SCCR and C3H/HeJ) showed significantly smaller areas of myocardial infarction than control strains (C57/BL10 ScSn and C3H/OuJ). The TLR4-deficient mice also showed reduced neutrophil infiltration, reduced lipid peroxidation, and reduced complement deposition in cardiac tissues [120, 135].

Some studies have used NO as an additional substance for lung preservation, and this has been shown to be effective in reducing the damage of reperfusion injury in various animal models [136–139]. However, the use of NO during lung reperfusion did not decrease pulmonary edema in a randomized clinical trial [89]. In another study of 84 patients undergoing lung transplantation, the use of NO during reperfusion showed no benefit with respect to hemodynamics, extubation, the incidence of IR injury, or the length of hospital and ICU stay [140]. Ardehali and colleagues [141] demonstrated a benefit with the use of inhaled NO postoperatively a subgroup of patients who developed IR injury despite not decreasing its incidence [141].

15. Conclusion

Over the years, several studies have investigated possible therapeutic alternatives that are deemed safe and with proven clinical efficacy. Although these alternatives may act directly on tissue damage triggered by ischemia and reperfusion, clear safety and effective evidence have yet been clinically demonstrated.

Future Perspectives

The search for different methods of lung protection is necessary and indispensable for testing different pharmacological approaches in an attempt to provide better therapeutic strategies for IR injury.

Conflict of Interests

The authors declare that there is no conflict of interests regarding the publication of this paper.

Acknowledgments

This research was supported by grants from FIPE/HCPA (Hospital de Clinicas of Porto Alegre Institutional Research Fund). The authors acknowledge the expert proofreading of this paper reviewing provided by the American Journal Expert.

References

[1] W. G. S. Bonservizi, M. K. Koike, R. Saurim et al., "Ischemic preconditioning and atenolol on lung injury after intestinal ischemia and reperfusion in rats," *Transplantation Proceedings*, vol. 46, no. 6, pp. 1862–1866, 2014.

[2] B. V. Pinheiro, M. A. Holanda, F. G. Araujo, and H. Romaldini, "Lesão pulmonar de reperfusão," *Jornal Brasileiro de Pneumologia*, vol. 25, no. 2, pp. 124–136, 1999.

[3] D. M. Yellon and D. J. Hausenloy, "Myocardial reperfusion injury," *The New England Journal of Medicine*, vol. 357, no. 11, pp. 1121–1135, 2007.

[4] M. Mura, C. F. Andrade, B. Han et al., "Intestinal ischemia-reperfusion-induced acute lung injury and oncotic cell death in multiple organs," *Shock*, vol. 28, no. 2, pp. 227–238, 2007.

[5] B. J. Zimmerman and D. N. Granger, "Mechanisms of reperfusion injury," *The American Journal of the Medical Sciences*, vol. 307, no. 4, pp. 284–292, 1994.

[6] S. Ogawa, H. Gerlach, C. Esposito, A. Pasagian-Macaulay, J. Brett, and D. Stern, "Hypoxia modulates the barrier and coagulant function of cultured bovine endothelium. Increased monolayer permeability and induction of procoagulant properties," *Journal of Clinical Investigation*, vol. 85, no. 4, pp. 1090–1098, 1990.

[7] M. D. Menger, "Microcirculatory disturbances secondary to ischemia-reperfusion," *Transplantation Proceedings*, vol. 27, no. 5, pp. 2863–2865, 1995.

[8] W. Dröge, "Free radicals in the physiological control of cell function," *Physiological Reviews*, vol. 82, no. 1, pp. 47–95, 2002.

[9] S. N. Jerome, M. Dore, J. C. Paulson, C. W. Smith, and R. J. Korthuis, "P-selectin and ICAM-1-dependent adherence reactions: role in the genesis of postischemic no-reflow," *The American Journal of Physiology—Heart and Circulatory Physiology*, vol. 266, part 2, no. 4, pp. H1316–H1321, 1994.

[10] S. Cuzzocrea, D. P. Riley, A. P. Caputi, and D. Salvemini, "Antioxidant therapy: a new pharmacological approach in shock, inflammation, and ischemia/reperfusion injury," *Pharmacological Reviews*, vol. 53, no. 1, pp. 135–159, 2001.

[11] T. P. Dalton, H. G. Shertzer, and A. Puga, "Regulation of gene expression by reactive oxygen," *Annual Review of Pharmacology and Toxicology*, vol. 39, pp. 67–101, 1999.

[12] K. N. DeCampos, S. Keshavjee, M. Liu, and A. S. Slutsky, "Prevention of rapid reperfusion-induced lung injury with prostaglandin E1 during the initial period of reperfusion," *Journal of Heart and Lung Transplantation*, vol. 17, no. 11, pp. 1121–1128, 1998.

[13] C. Iadecola and J. Anrather, "The immunology of stroke: from mechanisms to translation," *Nature Medicine*, vol. 17, no. 7, pp. 796–808, 2011.

[14] K. E. De Greef, D. K. Ysebaert, M. Ghielli et al., "Neutrophils and acute ischemia-reperfusion injury," *Journal of Nephrology*, vol. 11, no. 3, pp. 110–122, 1998.

[15] S. Oredsson, G. Plate, and P. Qvarfordt, "Experimental evaluation of oxygen free radical scavengers in the prevention of reperfusion injury in skeletal muscle," *European Journal of Surgery*, vol. 160, no. 2, pp. 97–103, 1994.

[16] P. A. Southorn and G. Powis, "Free radicals in medicine. II. Involvement in human disease," *Mayo Clinic Proceedings*, vol. 63, no. 4, pp. 390–408, 1988.

[17] G. Ambrosio and I. Tritto, "Reperfusion injury: experimental evidence and clinical implications," *American Heart Journal*, vol. 138, no. 2, part 2, pp. S69–S75, 1999.

[18] R. C. King, O. A. R. Binns, F. Rodriguez et al., "Reperfusion injury significantly impacts clinical outcome after pulmonary transplantation," *Annals of Thoracic Surgery*, vol. 69, no. 6, pp. 1681–1685, 2000.

[19] J. D. Cooper, G. A. Patterson, E. P. Trulock et al., "Results of single and bilateral lung transplantation in 131 consecutive recipients," *Journal of Thoracic and Cardiovascular Surgery*, vol. 107, no. 2, pp. 460–471, 1994.

[20] P. M. Reilly, H. J. Schiller, and G. B. Bulkley, "Pharmacologic approach to tissue injury mediated by free radicals and other reactive oxygen metabolites," *American Journal of Surgery*, vol. 161, no. 4, pp. 488–503, 1991.

[21] J. V. Conte and W. A. Baumgartner, "Overview and future practice patterns in cardiac and pulmonary preservation," *Journal of Cardiac Surgery*, vol. 15, no. 2, pp. 91–107, 2000.

[22] C.-K. Sun, C.-H. Yen, Y.-C. Lin et al., "Autologous transplantation of adipose-derived mesenchymal stem cells markedly reduced acute ischemia-reperfusion lung injury in a rodent model," *Journal of Translational Medicine*, vol. 9, no. 1, article 118, 2011.

[23] G. Ucar, E. Topaloglu, H. B. Kandilci, and B. Gümüsel, "Effect of ischemic preconditioning on reactive oxygen species-mediated ischemia-reperfusion injury in the isolated perfused rat lung," *Clinical Biochemistry*, vol. 38, no. 7, pp. 681–684, 2005.

[24] M. de Perrot, M. Liu, T. K. Waddell, and S. Keshavjee, "Ischemia-reperfusion-induced lung injury," *American Journal of Respiratory and Critical Care Medicine*, vol. 167, no. 4, pp. 490–511, 2003.

[25] R. J. Novick, K. E. Gehman, I. S. Ali, and J. Lee, "Lung preservation: the importance of endothelial and alveolar type II cell integrity," *Annals of Thoracic Surgery*, vol. 62, no. 1, pp. 302–314, 1996.

[26] J. D. Puskas, T. Hirai, N. Christie, E. Mayer, A. S. Slutsky, and G. A. Patterson, "Reliable thirty-hour lung preservation by donor lung hyperinflation," *Journal of Thoracic and Cardiovascular Surgery*, vol. 104, no. 4, pp. 1075–1083, 1992.

[27] H. Date, A. Matsumura, J. K. Manchester et al., "Evaluation of lung metabolism during successful twenty-four-hour canine lung preservation," *Journal of Thoracic and Cardiovascular Surgery*, vol. 105, no. 3, pp. 480–491, 1993.

[28] R. G. Eckenhoff, C. Dodia, Z. Tan, and A. B. Fisher, "Oxygen-dependent reperfusion injury in the isolated rat lung," *Journal of Applied Physiology*, vol. 72, no. 4, pp. 1454–1460, 1992.

[29] C.-H. Chiang, H.-I. Pai, and S.-L. Liu, "Ventilator-induced lung injury (VILI) promotes ischemia/reperfusion lung injury (I/R) and NF-kB antibody attenuates both injuries," *Resuscitation*, vol. 79, no. 1, pp. 147–154, 2008.

[30] I. Rahman, J. Marwick, and P. Kirkham, "Redox modulation of chromatin remodeling: impact on histone acetylation and deacetylation, NF-κB and pro-inflammatory gene expression," *Biochemical Pharmacology*, vol. 68, no. 6, pp. 1255–1267, 2004.

[31] A. B. Al-Mehdi, H. Shuman, and A. B. Fisher, "Intracellular generation of reactive oxygen species during nonhypoxic lung ischemia," *American Journal of Physiology—Lung Cellular and Molecular Physiology*, vol. 272, no. 2, part 1, pp. L294–L300, 1997.

[32] W. G. Land, "The role of postischemic reperfusion injury and other nonantigen-dependent inflammatory pathways in transplantation," *Transplantation*, vol. 79, no. 5, pp. 505–514, 2005.

[33] R. L. Torres, L. K. Martins, M. Picoral et al., "The potential protective effect of low potassium dextran against lipid peroxidation in a rat lung transplantation model," *The Thoracic and Cardiovascular Surgeon*, vol. 57, no. 5, pp. 309–311, 2009.

[34] R. F. Kelly, J. Murar, Z. Hong et al., "Low potassium dextran lung preservation solution reduces reactive oxygen species production," *Annals of Thoracic Surgery*, vol. 75, no. 6, pp. 1705–1710, 2003.

[35] H. Esme, H. Fidan, T. Koken, and O. Solak, "Effect of lung ischemia-reperfusion on oxidative stress parameters of remote tissues," *European Journal of Cardio-Thoracic Surgery*, vol. 29, no. 3, pp. 294–298, 2006.

[36] M. A. McMillen, M. Huribal, and B. Sumpio, "Common pathway of endothelial-leukocyte interaction in shock, ischemia, and reperfusion," *The American Journal of Surgery*, vol. 166, no. 5, pp. 557–562, 1993.

[37] R. S. Ferrari, D. P. da Rosa, L. F. Forgiarini, S. Bona, A. S. Dias, and N. P. Marroni, "Oxidative stress and pulmonary changes in experimental liver cirrhosis," *Oxidative Medicine and Cellular Longevity*, vol. 2012, Article ID 486190, 8 pages, 2012.

[38] H. K. Eltzschig and T. Eckle, "Ischemia and reperfusion-from mechanism to translation," *Nature Medicine*, vol. 17, no. 11, pp. 1391–1401, 2011.

[39] A. Grenz, E. Clambey, and H. K. Eltzschig, "Hypoxia signaling during intestinal ischemia and inflammation," *Current Opinion in Critical Care*, vol. 18, no. 2, pp. 178–185, 2012.

[40] S. W. Park, M. Kim, K. M. Brown, V. D. D'Agati, and H. T. Lee, "Paneth cell-derived interleukin-17A causes multiorgan dysfunction after hepatic ischemia and reperfusion injury," *Hepatology*, vol. 53, no. 5, pp. 1662–1675, 2011.

[41] G. Zhao, I. S. Ayene, and A. B. Fisher, "Role of iron in ischemia-reperfusion oxidative injury of rat lungs," *American Journal of Respiratory Cell and Molecular Biology*, vol. 16, no. 3, pp. 293–299, 1997.

[42] I. Inci, B. Erne, S. Arni et al., "Prevention of primary graft dysfunction in lung transplantation by N-acetylcysteine after prolonged cold ischemia," *Journal of Heart and Lung Transplantation*, vol. 29, no. 11, pp. 1293–1301, 2010.

[43] H. T. Lee, S. W. Park, M. Kim, and V. D. D'Agati, "Acute kidney injury after hepatic ischemia and reperfusion injury in mice," *Laboratory Investigation*, vol. 89, no. 2, pp. 196–208, 2009.

[44] L. E. C. Miranda, V. K. Capellini, G. S. Reis, A. C. Celotto, C. G. Carlotti Jr., and P. R. B. Evora, "Effects of partial liver ischemia followed by global liver reperfusion on the remote tissue expression of nitric oxide synthase: lungs and kidneys," *Transplantation Proceedings*, vol. 42, no. 5, pp. 1557–1562, 2010.

[45] B. Halliwell, "Biochemistry of oxidative stress," *Biochemical Society Transactions*, vol. 35, part 5, pp. 1147–1150, 2007.

[46] M. Zafarullah, W. Q. Li, J. Sylvester, and M. Ahmad, "Molecular mechanisms of *N*-acetylcysteine actions," *Cellular and Molecular Life Sciences*, vol. 60, no. 1, pp. 6–20, 2003.

[47] R. L. Paterson, H. F. Galley, and N. R. Webster, "The effect of N-acetylcysteine on nuclear factor-κB activation, interleukin-6, interleukin-8, and intercellular adhesion molecule-1 expression in patients with sepsis," *Critical Care Medicine*, vol. 31, no. 11, pp. 2574–2578, 2003.

[48] J. L. Farber, K. R. Chien, and S. Mittnacht Jr., "Myocardial ischemia: the pathogenesis of irreversible cell injury in ischemia," *The American Journal of Pathology*, vol. 102, no. 2, pp. 271–281, 1981.

[49] G. Sener, O. Tosun, A. Ö. Şehirli et al., "Melatonin and N-acetylcysteine have beneficial effects during hepatic ischemia and reperfusion," *Life Sciences*, vol. 72, no. 24, pp. 2707–2718, 2003.

[50] I. Ziment, "Acetylcysteine: a drug that is much more than a mucokinetic," *Biomedicine and Pharmacotherapy*, vol. 42, no. 8, pp. 513–519, 1988.

[51] B. Särnstrand, A. Tunek, K. Sjödin, and A. Hallberg, "Effects of *N*-acetylcysteine stereoisomers on oxygen-induced lung injury in rats," *Chemico-Biological Interactions*, vol. 94, no. 2, pp. 157–164, 1995.

[52] O. I. Aruoma, B. Halliwell, B. M. Hoey, and J. Butler, "The antioxidant action of N-acetylcysteine: its reaction with hydrogen peroxide, hydroxyl radical, superoxide, and hypochlorous acid," *Free Radical Biology & Medicine*, vol. 6, no. 6, pp. 593–597, 1989.

[53] L. Bonanomi and A. Gazzaniga, "Toxicological, pharmacokinetic and metabolic studies on acetylcysteine," *European Journal of Respiratory Diseases*, vol. 61, no. 111, pp. 45–51, 1980.

[54] R. C. Sprong, A. Miranda, L. Winkelhuyzen-Janssen et al., "Low-dose N-acetylcysteine protects rats against endotoxin-mediated oxidative stress, but high-dose increases mortality," *The American Journal of Respiratory and Critical Care Medicine*, vol. 157, no. 4, part 1, pp. 1283–1293, 1998.

[55] J. Bakker, H. Zhang, M. Depierreux, S. van Asbeck, and J.-L. Vincent, "Effects of *N*-acetylcysteine in endotoxic shock," *Journal of Critical Care*, vol. 9, no. 4, pp. 236–243, 1994.

[56] S. Bergamini, C. Rota, R. Canali et al., "*N*-acetylcysteine inhibits *in vivo* nitric oxide production by inducible nitric oxide synthase," *Nitric Oxide*, vol. 5, no. 4, pp. 349–360, 2001.

[57] S. Cuzzocrea, E. Mazzon, G. Costantino, I. Serraino, A. De Sarro, and A. P. Caputi, "Effects of n-acetylcysteine in a rat model of ischemia and reperfusion injury," *Cardiovascular Research*, vol. 47, no. 3, pp. 537–548, 2000.

[58] H. Türüt, H. Ciralik, M. Kilinc, D. Ozbag, and S. S. Imrek, "Effects of early administration of dexamethasone, N-acetylcysteine and aprotinin on inflammatory and oxidant-antioxidant status after lung contusion in rats," *Injury*, vol. 40, no. 5, pp. 521–527, 2009.

[59] Y.-S. Kim, D.-Y. Jhon, and K.-Y. Lee, "Involvement of ROS and JNK1 in selenite-induced apoptosis in chang liver cells," *Experimental & Molecular Medicine*, vol. 36, no. 2, pp. 157–164, 2004.

[60] N. Geudens, C. van de Wauwer, A. P. Neyrinck et al., "N-acetyl cysteine pre-treatment attenuates inflammatory changes in the warm ischemic murine lung," *Journal of Heart and Lung Transplantation*, vol. 26, no. 12, pp. 1326–1332, 2007.

[61] L. F. Forgiarini, L. A. Forgiarini Jr., D. P. da Rosa, M. B. Silva, R. Mariano, and A. D. Paludo, "N-acetylcysteine administration confers lung protection in different phases of lung ischemia-reperfusion injury," *Interactive CardioVascular and Thoracic Surgery*, vol. 19, no. 6, pp. 894–899, 2014.

[62] N.-C. Wu, T.-H. Chen, Y.-C. Yang, F.-T. Liao, J.-C. Wang, and J.-J. Wang, "N-acetylcysteine improves cardiac contractility and ameliorates myocardial injury in a rat model of lung ischemia and reperfusion injury," *Transplantation Proceedings*, vol. 45, no. 10, pp. 3550–3554, 2013.

[63] Ö. Çakir, A. Oruc, S. Kaya, N. Eren, F. Yildiz, and L. Erdinc, "*N*-acetylcysteine reduces lung reperfusion injury after deep hypothermia and total circulatory arrest," *Journal of Cardiac Surgery*, vol. 19, no. 3, pp. 221–225, 2004.

[64] S. Cuzzocrea, M. C. McDonald, E. Mazzon et al., "Beneficial effects of tempol, a membrane-permeable radical scavenger, in a rodent model of splanchnic artery occlusion and reperfusion," *Shock*, vol. 14, no. 2, pp. 150–156, 2000.

[65] C. J. Davreux, I. Soric, A. B. Nathens et al., "N-acetyl cysteine attenuates acute lung injury in the rat," *Shock*, vol. 8, no. 6, pp. 432–438, 1997.

[66] Z.-Y. Huang, Z.-Y. Xia, D. M. Ansley, and B. S. Dhaliwal, "Clinical significance of plasma free 15-F2t-isoprostane concentration during coronary artery bypasses graft surgery," *Zhongguo Wei Zhong Bing Ji Jiu Yi Xue*, vol. 16, no. 3, pp. 165–168, 2004.

[67] X. Mao, T. Wang, Y. Liu et al., "N-acetylcysteine and allopurinol confer synergy in attenuating myocardial ischemia injury via restoring HIF-1alpha/HO-1 signaling in diabetic rats," *PLoS ONE*, vol. 8, no. 7, Article ID e68949, 2013.

[68] T. Wang, X. Mao, H. Li et al., "*N*-acetylcysteine and allopurinol up-regulated the Jak/STAT3 and PI3K/Akt pathways via adiponectin and attenuated myocardial postischemic injury in diabetes," *Free Radical Biology and Medicine*, vol. 63, pp. 291–303, 2013.

[69] H. Nakano, K. Boudjema, E. Alexandre et al., "Protective effects of N-acetylcysteine on hypothermic ischemia-reperfusion injury of rat liver," *Hepatology*, vol. 22, no. 2, pp. 539–545, 1995.

[70] K. Waxman, "Shock: ischemia, reperfusion, and inflammation," *New Horizons: Science and Practice of Acute Medicine*, vol. 4, no. 2, pp. 153–160, 1996.

[71] L. B. Ware, J. A. Golden, W. E. Finkbeiner, and M. A. Matthay, "Alveolar epithelial fluid transport capacity in reperfusion lung injury after lung transplantation," *American Journal of Respiratory and Critical Care Medicine*, vol. 159, no. 3, pp. 980–988, 1999.

[72] M. Okuda, H.-C. Lee, B. Chance, and C. Kumar, "Role of extracellular Ca^{2+} in ischemia-reperfusion injury in the isolated perfused rat liver," *Circulatory Shock*, vol. 37, no. 3, pp. 209–219, 1992.

[73] S. Chatterjee and A. B. Fisher, "ROS to the rescue," *American Journal of Physiology—Lung Cellular and Molecular Physiology*, vol. 287, no. 4, pp. L704–L705, 2004.

[74] G. M. Rosen and B. A. Freeman, "Detection of superoxide generated by endothelial cells," *Proceedings of the National Academy of Sciences of the United States of America*, vol. 81, no. 23, pp. 7269–7273, 1984.

[75] I. Takeyoshi, K. Iwanami, N. Kamoshita et al., "Effect of lazaroid U-74389G on pulmonary ischemia-reperfusion injury in dogs," *Journal of Investigative Surgery*, vol. 14, no. 2, pp. 83–92, 2001.

[76] M. C. Carroll and V. M. Holers, "Innate autoimmunity," *Advances in Immunology*, vol. 86, pp. 137–157, 2005.

[77] G. Y. Chen and G. Nuñez, "Sterile inflammation: Sensing and reacting to damage," *Nature Reviews Immunology*, vol. 10, no. 12, pp. 826–837, 2010.

[78] D. N. Granger, M. E. Hollwarth, and D. A. Parks, "Ischemia-reperfusion injury: role of oxygen-derived free radicals," *Acta Physiologica Scandinavica*, vol. 126, no. 548, pp. 47–63, 1986.

[79] C. F. Andrade, H. Kaneda, S. Der et al., "Toll-like receptor and cytokine gene expression in the early phase of human lung transplantation," *Journal of Heart and Lung Transplantation*, vol. 25, no. 11, pp. 1317–1323, 2006.

[80] J. T. Ambros, I. Herrero-Fresneda, O. G. Borau, and J. M. G. Boira, "Ischemic preconditioning in solid organ transplantation: from experimental to clinics," *Transplant International*, vol. 20, no. 3, pp. 219–229, 2007.

[81] S. Uhlig, R. Göggel, and S. Engel, "Mechanisms of platelet-activating factor (PAF)-mediated responses in the lung," *Pharmacological Reports*, vol. 57, supplement, pp. 206–221, 2005.

[82] I. S. Farrukh, J. R. Michael, S. P. Peters et al., "The role of cyclooxygenase and lipoxygenase mediators in oxidant-induced lung injury," *American Review of Respiratory Disease*, vol. 137, no. 6, pp. 1343–1349, 1988.

[83] M. de Perrot, S. Fischer, M. Liu et al., "Prostaglandin E1 protects lung transplants from ischemia-reperfusion injury: a shift from pro- to anti-inflammatory cytokines," *Transplantation*, vol. 72, no. 9, pp. 1505–1512, 2001.

[84] Y. Matsuzaki, T. K. Waddell, J. D. Puskas et al., "Amelioration of post-ischemic lung reperfusion injury by prostaglandin E_1," *American Review of Respiratory Disease*, vol. 148, no. 4, part 1, pp. 882–889, 1993.

[85] E. M. Drost and W. MacNee, "Potential role of IL-8, platelet-activating factor and TNF-alpha in the sequestration of neutrophils in the lung: effects on neutrophil deformability, adhesion receptor expression, and chemotaxis," *European Journal of Immunology*, vol. 32, no. 2, pp. 393–403, 2002.

[86] C. K. Grissom, J. F. Orme Jr., L. D. Richer, T. M. McIntyre, G. A. Zimmerman, and M. R. Elstad, "Platelet-activating factor acetylhydrolase is increased in lung lavage fluid from patients with acute respiratory distress syndrome," *Critical Care Medicine*, vol. 31, no. 3, pp. 770–775, 2003.

[87] S.-H. Back, J.-Y. Kim, J.-H. Choi et al., "Reduced glutathione oxidation ratio and 8 ohdG accumulation by mild ischemic pretreatment," *Brain Research*, vol. 856, no. 1-2, pp. 28–36, 2000.

[88] K. Yoshimura, S. Nakagawa, S. Koyama, T. Kobayashi, and T. Homma, "Roles of neutrophil elastase and superoxide anion in leukotriene B4- induced lung injury in rabbit," *Journal of Applied Physiology*, vol. 76, no. 1, pp. 91–96, 1994.

[89] G. Perrin, A. Roch, P. Michelet et al., "Inhaled nitric oxide does not prevent pulmonary edema after lung transplantation measured by lung water content: a randomized clinical study," *Chest*, vol. 129, no. 4, pp. 1024–1030, 2006.

[90] C. M. Hart, "Nitric oxide in adult lung disease," *Chest*, vol. 115, no. 5, pp. 1407–1417, 1999.

[91] N. Marczin, B. Riedel, J. Gal, J. Polak, and M. Yacoub, "Exhaled nitric oxide during lung transplantation," *The Lancet*, vol. 350, no. 9092, pp. 1681–1682, 1997.

[92] T. D. le Cras and I. F. McMurtry, "Nitric oxide production in the hypoxic lung," *The American Journal of Physiology—Lung Cellular and Molecular Physiology*, vol. 280, no. 4, pp. L575–L582, 2001.

[93] S. M. Fiser, C. G. Tribble, S. M. Long et al., "Lung transplant reperfusion injury involves pulmonary macrophages and circulating leukocytes in a biphasic response," *Journal of Thoracic and Cardiovascular Surgery*, vol. 121, no. 6, pp. 1069–1075, 2001.

[94] M. J. Eppinger, G. M. Deeb, S. F. Bolling, and P. A. Ward, "Mediators of ischemia-reperfusion injury of rat lung," *The American Journal of Pathology*, vol. 150, no. 5, pp. 1773–1784, 1997.

[95] N. Richter, G. Raddatz, G. Steinhoff, H.-J. Schafers, and H. J. Schlitt, "Transmission of donor lymphocytes in clinical lung transplantation," *Transplant International*, vol. 7, no. 6, pp. 414–419, 1994.

[96] J. Sperling, J. Chebath, H. Arad-Dann et al., "Possible involvement of (2′-5′)oligoadenylate synthetase activity in pre-mRNA splicing," *Proceedings of the National Academy of Sciences of the United States of America*, vol. 88, no. 23, pp. 10377–10381, 1991.

[97] C. R. B. Welbourn, G. Goldman, I. S. Paterson, C. R. Valeri, D. Shepro, and H. B. Hechtman, "Neutrophil elastase and oxygen radicals: Synergism in lung injury after hindlimb ischemia," *The American Journal of Physiology—Heart and Circulatory Physiology*, vol. 260, no. 6, part 2, pp. H1852–H1856, 1991.

[98] G. M. Deeb, C. M. Grum, M. J. Lynch et al., "Neutrophils are not necessary for induction of ischemia-reperfusion lung injury," *Journal of Applied Physiology*, vol. 68, no. 1, pp. 374–381, 1990.

[99] M. B. Parolin and I. J. Messias Reason, "Apoptosis as a mechanism of tissue injury in hepatobiliary diseases," *Arquivos de Gastroenterologia*, vol. 38, no. 2, pp. 138–144, 2001.

[100] U. Stammberger, A. Gaspert, S. Hillinger et al., "Apoptosis induced by ischemia and reperfusion in experimental lung transplantation," *Annals of Thoracic Surgery*, vol. 69, no. 5, pp. 1532–1536, 2000.

[101] J. A. C. de Souza, C. Rossa Junior, G. P. Garlet, A. V. B. Nogueira, and J. A. Cirelli, "Modulation of host cell signaling pathways as a therapeutic approach in periodontal disease," *Journal of Applied Oral Science*, vol. 20, no. 2, pp. 128–138, 2012.

[102] D. Rossi and G. Gaidano, "Messengers of cell death: apoptotic signaling in health and disease," *Haematologica*, vol. 88, no. 2, pp. 212–218, 2003.

[103] H. Y. Chang and X. Yang, "Proteases for cell suicide: functions and regulation of caspases," *Microbiology and Molecular Biology Reviews*, vol. 64, no. 4, pp. 821–846, 2000.

[104] K. Kuwano and N. Hara, "Signal transduction pathways of apoptosis and inflammation induced by the tumor necrosis factor receptor family," *The American Journal of Respiratory Cell and Molecular Biology*, vol. 22, no. 2, pp. 147–149, 2000.

[105] A. E. Greijer and E. van der Wall, "The role of hypoxia inducible factor 1 (HIF-1) in hypoxia induced apoptosis," *Journal of Clinical Pathology*, vol. 57, no. 10, pp. 1009–1014, 2004.

[106] H. A. de Schepop, J. S. de Jong, P. J. van Diest, and J. P. A. Baak, "Counting of apoptotic cells: a methodological study in invasive breast cancer," *Journal of Clinical Pathology—Clinical Molecular Pathology*, vol. 49, no. 4, pp. M214–M217, 1996.

[107] D. S. McClintock, M. T. Santore, V. Y. Lee et al., "Bc1-2 family members and functional electron transport chain regulate oxygen deprivation-induced cell death," *Molecular and Cellular Biology*, vol. 22, no. 1, pp. 94–104, 2002.

[108] L. A. Forgiarini, G. Grün, N. A. Kretzmann et al., "When is injury potentially reversible in a lung ischemia-reperfusion model?" *Journal of Surgical Research*, vol. 179, no. 1, pp. 168–174, 2013.

[109] A. Gross, X. M. Yin, K. Wang et al., "Caspase cleaved BID targets mitochondria and is required for cytochrome c release, while BCL-X(L) prevents this release but not tumor necrosis factor-R1/Fas death," *The Journal of Biological Chemistry*, vol. 274, no. 2, pp. 1156–1163, 1999.

[110] M. C. Wei, W. X. Zong, E. H. Y. Cheng et al., "Proapoptotic BAX and BAK: a requisite gateway to mitochondrial dysfunction and death," *Science*, vol. 292, no. 5517, pp. 727–730, 2001.

[111] P. Li, D. Nijhawan, I. Budihardjo et al., "Cytochrome c and dATP-dependent formation of Apaf-1/caspase-9 complex initiates an apoptotic protease cascade," *Cell*, vol. 91, no. 4, pp. 479–489, 1997.

[112] D. W. Nicholson and N. A. Thornberry, "Caspases: killer proteases," *Trends in Biochemical Sciences*, vol. 22, no. 8, pp. 299–306, 1997.

[113] L. de Kerchove, M. Boodhwani, P.-Y. Etienne et al., "Preservation of the pulmonary autograft after failure of the Ross procedure," *European Journal of Cardio-Thoracic Surgery*, vol. 38, no. 3, pp. 326–332, 2010.

[114] M. de Perrot and S. Keshavjee, "Lung preservation," *Seminars in Thoracic and Cardiovascular Surgery*, vol. 16, no. 4, pp. 300–308, 2004.

[115] Y. X. Zhang, H. Fan, Y. Shi et al., "Prevention of lung ischemia-reperfusion injury by short hairpin RNA-mediated caspase-3 gene silencing," *Journal of Thoracic and Cardiovascular Surgery*, vol. 139, no. 3, pp. 758–764, 2010.

[116] A. M. D'Armini, C. S. Roberts, P. K. Griffith, J. J. Lemasters, and T. M. Egan, "When does the lung die? I. Histochemical evidence of pulmonary viability after 'death'," *Journal of Heart and Lung Transplantation*, vol. 13, no. 5, pp. 741–747, 1994.

[117] S. Chien, F. Zhang, W. Niu, M. T. Tseng, and L. Gray Jr., "Comparison of university of wisconsin, euro-collins, low-potassium dextran, and krebs-henseleit solutions for hypothermic lung preservation," *Journal of Thoracic and Cardiovascular Surgery*, vol. 119, no. 5, pp. 921–930, 2000.

[118] A. Alvarez, A. Salvatierra, R. Lama et al., "Preservation with a retrograde second flushing of eurocollins in clinical lung transplantation," *Transplantation Proceedings*, vol. 31, no. 1-2, pp. 1088–1090, 1999.

[119] C. Z. Chen, R. C. Gallagher, P. Ardery, W. Dyckman, and H. B. C. Low, "Retrograde versus antegrade flush in canine left lung preservation for six hours," *Journal of Heart and Lung Transplantation*, vol. 15, no. 4, pp. 395–403, 1996.

[120] J.-I. Oyama, C. Blais Jr., X. Liu et al., "Reduced myocardial ischemia-reperfusion injury in toll-like receptor 4-deficient mice," *Circulation*, vol. 109, no. 6, pp. 784–789, 2004.

[121] L. A. Forgiarini Jr., L. F. Forgiarini, D. P. Da Rosa, R. Mariano, J. M. Ulbrich, and C. F. Andrade, "Endobronchial perfluorocarbon administration decreases lung injury in an experimental model of ischemia and reperfusion," *Journal of Surgical Research*, vol. 183, no. 2, pp. 835–840, 2013.

[122] L. A. Forgiarini Junior, A. R. R. Holand, L. F. Forgiarini et al., "Endobronchial perfluorocarbon reduces inflammatory activity before and after lung transplantation in an animal experimental model," *Mediators of Inflammation*, vol. 2013, Article ID 193484, 9 pages, 2013.

[123] M. S. Bhabra, D. N. Hopkinson, T. E. Shaw, and T. L. Hooper, "Relative importance of prostaglandin/cyclic adenosine monophosphate and nitric oxide/cyclic guanosine monophosphate pathways in lung preservation," *Annals of Thoracic Surgery*, vol. 62, no. 5, pp. 1494–1499, 1996.

[124] R. S. Bonser, L. S. Fragomeni, S. W. Jamieson et al., "Effects of prostaglandin E1, in twelve-hour lung preservation," *Journal of Heart and Lung Transplantation*, vol. 10, no. 2, pp. 310–316, 1991.

[125] T. M. Egan, K. S. Ulicny, C. J. Lambert, and B. R. Wilcox, "Effect of a free radical scavenger on cadaver lung transplantation," *The Annals of Thoracic Surgery*, vol. 55, no. 6, pp. 1453–1459, 1993.

[126] H. Itano, W. Zhang, J. H. Ritter, T. J. McCarthy, T. Mohanakumar, and G. A. Patterson, "Adenovirus-mediated gene transfer of human interleukin 10 ameliorates reperfusion injury of rat lung isografts," *The Journal of Thoracic and Cardiovascular Surgery*, vol. 120, no. 5, pp. 947–956, 2000.

[127] E. S. Pilla, G. S. Vendrame, P. G. Sánchez et al., "Ischemic preconditioning by selective occlusion of the pulmonary artery in rats," *Jornal Brasileiro de Pneumologia*, vol. 34, no. 8, pp. 583–589, 2008.

[128] R. S. Hotchkiss, A. Strasser, J. E. McDunn, and P. E. Swanson, "Mechanisms of disease: cell death," *The New England Journal of Medicine*, vol. 361, no. 16, pp. 1570–1583, 2009.

[129] C. V. Thakar, K. Zahedi, M. P. Revelo et al., "Identification of thrombospondin 1 (TSP-1) as a novel mediator of cell injury in kidney ischemia," *The Journal of Clinical Investigation*, vol. 115, no. 12, pp. 3451–3459, 2005.

[130] Z. Tang, P. Arjunan, C. Lee et al., "Survival effect of PDGF-CC rescues neurons from apoptosis in both brain and retina by regulating GSK3β phosphorylation," *Journal of Experimental Medicine*, vol. 207, no. 4, pp. 867–880, 2010.

[131] I. M. Verma, "Severe liver degeneration in mice lacking the IκB kinase 2 gene," *Science*, vol. 284, no. 5412, pp. 321–325, 1999.

[132] T. Ishiyama, S. Dharmarajan, M. Hayama, H. Moriya, K. Grapperhaus, and G. A. Patterson, "Inhibition of nuclear factor κB by IκB superrepressor gene transfer ameliorates ischemia-reperfusion injury after experimental lung transplantation," *Journal of Thoracic and Cardiovascular Surgery*, vol. 130, no. 1, pp. 194–201, 2005.

[133] L.-W. Chen, L. Egan, Z.-W. Li, F. R. Greten, M. F. Kagnoff, and M. Karin, "The two faces of IKK and NF-κB inhibition: prevention of systemic inflammation but increased local injury following intestinal ischemia-reperfusion," *Nature Medicine*, vol. 9, no. 5, pp. 575–581, 2003.

[134] L. Swoboda, D. E. Clancy, M. A. Donnebrink, and C. M. Rieder-Nelissen, "The influence of verapamil on lung preservation. A study on rabbit lungs with a reperfusion model allowing physiological loading," *Thoracic and Cardiovascular Surgeon*, vol. 41, no. 2, pp. 85–92, 1993.

[135] C. F. Andrade, T. K. Waddell, S. Keshavjee, and M. Liu, "Innate immunity and organ transplantation: the potential role of toll-like receptors," *The American Journal of Transplantation*, vol. 5, no. 5, pp. 969–975, 2005.

[136] H. Yamagishi, C. Yamashita, and M. Okada, "Preventive influence of inhaled nitric oxide on lung ischemia-reperfusion injury," *Surgery Today*, vol. 29, no. 9, pp. 897–901, 1999.

[137] A. V. Ovechkin, D. Lominadze, K. C. Sedoris, E. Gozal, T. W. Robinson, and A. M. Roberts, "Inhibition of inducible nitric oxide synthase attenuates platelet adhesion in subpleural arterioles caused by lung ischemia-reperfusion in rabbits," *Journal of Applied Physiology*, vol. 99, no. 6, pp. 2423–2432, 2005.

[138] H. Esme, H. Fidan, O. Solak, F. H. Dilek, R. Demirel, and M. Unlu, "Beneficial effects of supplemental nitric oxide donor given during reperfusion period in reperfusion-induced lung injury," *Thoracic and Cardiovascular Surgeon*, vol. 54, no. 7, pp. 477–483, 2006.

[139] H. Yamashita, S. Akamine, Y. Sumida et al., "Inhaled nitric oxide attenuates apoptosis in ischemia-reperfusion injury of the rabbit lung," *Annals of Thoracic Surgery*, vol. 78, no. 1, pp. 292–297, 2004.

[140] M. O. Meade, J. T. Granton, A. Matte-Martyn et al., "A randomized trial of inhaled nitric oxide to prevent ischemia-reperfusion injury after lung transplantation," *The American Journal of Respiratory and Critical Care Medicine*, vol. 167, no. 11, pp. 1483–1489, 2003.

[141] A. Ardehali, H. Laks, M. Levine et al., "A prospective trial of inhaled nitric oxide in clinical lung transplantation," *Transplantation*, vol. 72, no. 1, pp. 112–115, 2001.

Hindawi Publishing Corporation
Oxidative Medicine and Cellular Longevity
Volume 2015, Article ID 624819, 8 pages
http://dx.doi.org/10.1155/2015/624819

Research Article

Neuroprotective Effect of Ulinastatin on Spinal Cord Ischemia-Reperfusion Injury in Rabbits

Bingbing Liu,[1] Weihua Huang,[1] Xiaoshan Xiao,[1] Yao Xu,[1,2] Songmei Ma,[1,3] and Zhengyuan Xia[4,5]

[1]*Department of Anesthesiology, The 2nd People's Hospital of Guangdong Province, Guangdong Provincial Emergency Hospital, Guangzhou 510317, China*
[2]*Department of Anesthesiology, Huizhou Municipal Central Hospital, Huizhou 516001, China*
[3]*Department of Anesthesiology, The First People's Hospital of Shangqiu, Shangqiu 476000, China*
[4]*Department of Anesthesiology, Affiliated Hospital of Guangdong Medical College, Zhanjiang 524003, China*
[5]*Department of Anesthesiology, The University of Hong Kong, Hong Kong*

Correspondence should be addressed to Xiaoshan Xiao; mzkgd177@126.com

Received 17 September 2014; Revised 8 January 2015; Accepted 8 January 2015

Academic Editor: Mengzhou Xue

Ulinastatin (UTI), a trypsin inhibitor, is isolated and purified from human urine and has been shown to exert protective effect on myocardial ischemia reperfusion injury in patients. The present study was aimed at investigating the effect of ulinastatin on neurologic functions after spinal cord ischemia reperfusion injury and the underlying mechanism. The spinal cord IR model was achieved by occluding the aorta just caudal to the left renal artery with a bulldog clamp. The drugs were administered immediately after the clamp was removed. The animals were terminated 48 hours after reperfusion. Neuronal function was evaluated with the Tarlov Scoring System. Spinal cord segments between L_2 and L_5 were harvested for pathological and biochemical analysis. Ulinastatin administration significantly improved postischemic neurologic function with concomitant reduction of apoptotic cell death. In addition, ulinastatin treatment increased SOD activity and decreased MDA content in the spinal cord tissue. Also, ulinastatin treatment suppressed the protein expressions of Bax and caspase-3 but enhanced Bcl-2 protein expression. These results suggest that ulinastatin significantly attenuates spinal cord ischemia-reperfusion injury and improves postischemic neuronal function and that this protection might be attributable to its antioxidant and antiapoptotic properties.

1. Introduction

Spinal cord injury is mainly divided into primary and secondary injuries according to pathophysiologic features. Primary injury mainly includes direct injury and ischemic injury, and it often occurs in a relatively short time after injury (generally after 4 hours of injury), with the irreversible nerve damage [1]. The secondary injury often takes place in the process of perfusion after spinal cord ischemia, causing spinal cord ischemia-reperfusion injury (SCIRI) which aggravates the neurofunctional damages of limbs. Spinal cord ischemia-reperfusion injury remains to be a devastating complication of thoracic aortic intervention, which may cause delayed paraplegia [2, 3]. The reasons for SCIRI were generally considered to be attributable to oxygen free radical-induced lipid peroxidation, leukocyte activation, inflammatory and neuronal apoptosis, and so on. Although technological advancements in surgery, such as hypothermic circulatory arrest, left heart bypass, intercostal artery reimplantation, and lumbar drains, have partly reduced complications of spinal cord injury, the incidence of paraplegia (immediate and delayed combined) after thoracic aortic intervention still ranges between 4% and 11% [4, 5]. Unfortunately, a reliable preventive method has not proven clinically efficacious in attenuating this injury until now. The mechanisms associated with delayed paraplegia are still not fully defined. Existing

studies indicated that the apoptosis of motor neurons may cause the delayed paraplegia [6], and other studies showed that the cytokine interleukin- (IL-) 17 may play an important role in promoting spinal cord neuroinflammation after SCI via activation of STAT3 [7]. Therefore, it is necessary to formulate treatment tragedy for inhibiting the motor neurons apoptosis.

The urinary trypsin inhibitor, also called ulinastatin, is a protease inhibitor that is purified from human urine with a molecular weight of 67 kDa and it has been shown to have anti-inflammatory effect by suppressing the production of proinflammatory cytokines [8–10] and attenuated postoperative clinical outcome after myocardial ischemia-reperfusion in patients [11]. Ulinastatin significantly reduced pulmonary vascular permeability index (PVPI) and extravascular lung water index (ELWI) through inhibition of lipid peroxidation [12]. Experimental studies have shown organ protective effect of ulinastatin on ischemia-reperfusion injury of the lung, liver, heart, and kidney [13–16]. Ulinastatin also attenuates focal ischemia-reperfusion injury in rat brain, decreasing neutrophil infiltration in the ischemic hemisphere [17]. To the best of our knowledge, it is unknown whether ulinastatin has neuroprotective effects on spinal cord ischemia-reperfusion injury.

The aim of this study was to investigate the potential protective effects of ulinastatin on spinal cord ischemia-reperfusion injury and to explore its mechanism in relation to inhibiting neuron apoptosis in a rabbit model.

2. Materials and Methods

2.1. Animals. Adult male New Zealand White rabbits weighing 2.5–3.0 kg were provided by the Laboratory Animal Center of Southern Medical University (Guangzhou, China). Animals were housed at 22–25°C with a 12 h light/dark cycle before and after surgery. Standard animal chow and water were freely accessible. All experimental protocols were approved by the Institutional Animal Care and Use Committee of Southern Medical University and performed in accordance with the National Institutes of Health (NIH, USA) guidelines for the use of experimental animals. The rabbits were randomized and blindly assigned to three groups, with eight rabbits per group.

2.2. Experimental Grouping. The groups were as follows.

Sham control group (Sham, $n = 8$): rabbits underwent laminectomy and abdominal aorta was exposed but with no aortic occlusion clamp.

Ischemia-reperfusion (IR) group (IR, $n = 8$): rabbits underwent transient global spinal cord ischemia; the saline (0.9% NaCl, 5 mL/kg) was injected intravenously immediately after the occlusion clamp was removed.

Ulinastatin group (IR + UTI, $n = 8$): as for ischemia group, but ulinastatin at the dose of 50,000 U/kg (diluted with saline (0.9% NaCl) to 5 mL per kilogram) was injected intravenously immediately after the occlusion clamp was removed.

2.3. Experimental Protocols. Anesthesia was induced by intraperitoneal administration of 30 mg/kg ketamine. When necessary, additional dose of ketamine was administrated. A 22 G catheter was inserted into ear artery for measuring the arterial pressure. An ear vein catheter was placed for administration of additional medications and fluids. The anesthesia was maintained by intermittent intravenous injection of ketamine. The lactated Ringer's solution (10 mL/kg/h) was intravenously infused. The animals were intubated, placed supine on a heated operating table, and ventilated with 90% oxygen. Core body temperature was maintained at 36 ± 0.5°C. Animals were placed in the supine position for the surgery. After sterile preparation, a 10 cm midline incision was made, and the abdominal aorta was exposed through a transperitoneal approach. Heparin (130 U/kg) was administered intravenously 5 min before clamping for anticoagulation. Approximately 1 cm below the left renal artery, the aorta was clamped using a bulldog clamp. Ischemia-reperfusion injury was achieved via occlusion of the abdominal aorta for 40 min, and then the clamp was removed. After the surgical and ischemic interventions, the surgical wound was closed in layers with 3-0 silk sutures. The animals were given free access to water and food at room temperature.

At 48 hours after reperfusion, the animals were euthanized under deep anesthesia and transcardiac perfusion with 500 mL ice-cold saline was performed. The lumbar spinal cord (L_{3-5} segments) of all animals was removed. Spinal cord samples were carefully dissected and divided into two sections. One of the sections was placed in 4% paraformaldehyde for 24 hours. Following fixation, tissue sample was embedded in paraffin. The other part of tissue sample was flash frozen in liquid nitrogen and stored at −80°C until further analysis.

2.4. Functional Assessment. Neurologic function was scored at 4, 12, 24, and 48 hours after reperfusion by assessing hindlimb neurologic function using the Tarlov Scoring System. A score of 0 to 4 was assigned to each animal as follows: 0 = spastic paraplegia and no movement of the lower limbs, 1 = spastic paraplegia and slight movement of the lower limbs, 2 = good movement of the lower limbs but unable to stand, 3 = able to stand but unable to walk normally, and 4 = complete recovery and normal gait-hopping. Neurologic function evaluation was performed by a medical doctor who was blinded to the experimental groups.

2.5. Assay of SOD and MDA Activities. For biochemical analysis, spinal cord tissues were washed two times with cold saline solution and stored in −80°C until analysis. Tissue malondialdehyde (MDA) levels were determined as described [18]. Briefly, MDA was reacted with thiobarbituric acid by incubating for 1 hour at 95–100°C and fluorescence intensity was measured in the n-butanol phase with a fluorescence spectrophotometry (Hitachi, Mode l F-4010, Japan), by comparing with a standard solution of 1,1,3,3-tetramethoxypropane. The results were expressed in terms of nmol/g wet tissue. Total (Cu–Zn and Mn) superoxide

dismutase (SOD) activity was measured according to reduction of nitro-blue tetrazolium by xanthine-xanthine oxidase system as described previously. Enzyme activity leading to 50% inhibition was regarded as one unit. The results were expressed as U/mg of protein. Protein concentrations were determined according to Lowry's method [19].

2.6. Determination of the Expression of Bcl-2, Bax, and Caspase-3 by Immunohistochemistry. The spinal cord tissue sections were deparaffinized in xylene and immersed in graded ethanol and distilled water. Immunohistochemical staining was performed using the avidin-biotin peroxidase complex (ABC) method according to the manufacturer's instructions (Dako, Carpinteria, CA, USA). The sections were incubated with a mouse monoclonal anti-Bax IgG2b antibody (1 : 500, sc-7480, Santa Cruz Biotechnology, CA, USA), a mouse monoclonal anti-Bcl-2 IgG1 antibody (1 : 20, sc-8392, Santa Cruz Biotechnology, CA, USA), and caspase-3 (1 : 500, Santa Cruz Biotechnology, Inc. Santa Cruz, CA, USA). The primary antibody was omitted as a negative control for the immunostaining. An image of each section was captured using a light microscope (Canon, Tokyo, Japan) at ×400 magnification and the integrated optical density (IOD) of the positively stained tissue in each image was determined using Image Pro Plus software, version 6.0 (Media Cybernetics, Silver Spring, MD, USA).

2.7. Determination of the Expression of Bcl-2, Bax, and Caspase-3 Protein by Western Blot. Frozen spinal cord samples were processed for protein assays using standard Western blotting analysis as described [20, 21]. In brief, the samples were homogenized in 5 v of buffer containing buffer containing sucrose 300 mM, HEPES 4 mM, EGTA 2 mM, phenylmethylsulphonyl fluoride (PMSF) 1 mM, and leupeptin 20 mM using a polytron homogenizer at the maximum speed in five 5 s bursts. The homogenates were incubated at 4°C for 30 min and then centrifuged at 10,000 ×g for 30 min at 4°C. The lysates were collected and the protein concentration was determined using the BCA Protein Assay kit. Equal amounts of proteins were separated by SDS-PAGE and transferred to polyvinylidene difluoride membranes (GE Healthcare Biosciences). The blots were initially blocked overnight with 5% milk in buffer containing Tris-HCl 20 mM (pH 7.4), NaCl 137 mM, 0.05% Tween-20, and then incubated for 1 h with anti-Bcl-2 antibody (1 : 1000), anti-Bax antibody (1 : 1000), anti-caspase-3 antibody (1 : 1000), all from Santa Cruz Biotechnology, CA, USA. After washing, the blots were incubated for 1 h at room temperature with a peroxidase-linked, goat anti-mouse secondary antibody (1 : 1000 dilution). The internal control was monoclonal anti-actin antibody (Sigma, St. Louis, USA) diluted 1 : 250. The bound antibody was then visualized using an enhanced chemiluminescence (ELC) kit (Amersham). Bcl-2, Bax, and caspase-3 were quantified densitometrically using suitable autoradiographs sucrose 300 mM, HEPES 4 mM, EGTA. Immunoblot results were quantified with Gel-Pro Analyzer 4.0 software (Media Cybernetics, Silver Spring, MD, USA).

2.8. Terminal Deoxynucleotidyl Transferase-Mediated dUTP-Biotin Nick End Labeling (TUNEL) Assay. Fixed spinal cord slices were embedded in paraffin, and 4 mm thick sections were deparaffinized by washing in 100% xylene and a descending ethanol series (from 100% ethanol two times to 80% ethanol once and 60% ethanol once). The sections were stained with haematoxylin and processed as described [22]. DNA fragments were determined using an ApopTag *in situ* apoptosis detection kit (ApopTag, Oncor, USA). The DNA nick was labelled according to the manufacturer's instructions. Following TUNEL, the sections were counterstained with haematoxylin. Neurons in which the nucleus was obviously labeled with diaminobenzidine were defined as TUNEL-positive. The apoptotic index (AI) was used to quantify the number of TUNEL positive cells. Five nonadjacent fields in each section were randomly chosen to count the total number of neurons and positive cells. The AI was calculated as follows: AI = (number of apoptotic cells/total number counted) × 100%.

2.9. Statistical Analysis. All data are expressed as the mean ± standard deviation (SD). Parametric statistics analyses were performed by ANOVA followed by Dennett's test for multiple comparisons or by Student's t-test. Nonparametric statistics analyses were performed by Kruskal-Wallis test followed by the Mann-Whitney U test with Bonferroni correction. P values less than 0.05 were considered significant. Statistical analysis was performed using the Statistical Package for the Social Sciences version 13.0 program (SPSS, Chicago, IL, USA).

3. Results

3.1. Neurologic Function. Hind-limb function was recorded using the Tarlov Scoring System (Figure 1). In the Sham group, the scores from 4 to 48 h after reperfusion did not significantly change ($P > 0.05$), but in the UTI + IR group the scores were higher at 24 h and 48 h time points than at 4 h and 12 h time points ($P < 0.05$). The score in the IR group was higher 4 h after reperfusion than 12 to 48 h ($P < 0.05$). At 24 h and 48 h time points, the hind-limb function of UTI + IR group animals was improved compared to that of IR group animals ($P < 0.01$), but it did not reach the level of Sham group ($P < 0.05$).

3.2. Effect of Ulinastatin on MDA, SOD Levels. To determine the local oxidative/antioxidative levels, we detected the MDA content and SOD activities in spinal cord tissue. Spinal cord IR was associated with significant elevation in MDA production with concomitant reduction in SOD activity. Following ischemia-reperfusion injury, the SOD activity in the UTI + IR group was significantly higher than that in the IR group, but MDA content in spinal cord tissue was decreased significantly compared with IR group (Figure 2).

3.3. Immunohistochemistry of Bcl-2, Bax, and Caspase-3 Proteins. As shown in Figure 3, spinal cord ischemia-reperfusion resulted in significant increase of Bax and

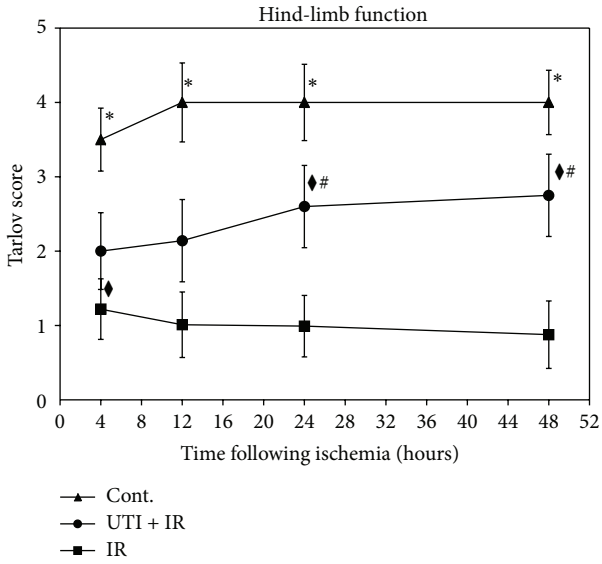

Figure 1: Hind-limb function indicated a progressive decline in function of ischemia-reperfusion IR controls. The scores of Sham group at the same time point were higher than UTI + IR and IR groups ($^{*}P < 0.05$). The scores of hind-limb function in IR group declined from 4 h to 48 h, but rabbits treated with UTI (UTI + IR group) did not decline; their function stabilized and was significantly greater ($^{\#}P < 0.01$) than that in the IR controls at 24 h and 48 h after reperfusion. In UTI + IR group, function score was higher at 24 h and 48 h time points than at 4 h and 12 h time points ($^{\blacklozenge}P < 0.05$), but the score of IR group was higher at 4 h time point than at the other time points ($^{\blacklozenge}P < 0.05$). Values are the means ± SD, $n = 8$ per group.

caspase-3 protein expression and decrease of Bcl-2 protein expression as compared with the Sham group. The number of the positive cells containing Bcl-2 protein expression (brown stain) increased in the UTI + IR group compared to the IR control group. The number of positive cells containing Bax and caspase-3 protein expression (brown stain) decreased in the UTI + IR group compared with the IR group.

3.4. Western Blot Analysis of Bcl-2, Bax, and Caspase-3 Proteins. The expression of Bax protein was significantly upregulated in the IR control group as compared to the Sham group. However, this upregulation of the expression of Bax protein was significantly inhibited in the IR + UTI group. With respect to Bcl-2, the expression level in the IR + UTI group significantly increased as compared with the Sham group and the IR group, respectively. The expression of caspase-3 decreased in the IR + UTI group, but increased in the IR control group (Figure 4).

3.5. Apoptotic Cell Death Assessed by TUNEL Staining. TUNEL-positive cells were minimally detectable in the Sham group, whereas the IR group showed a significant number of TUNEL-positive cells. Ulinastatin intervention significantly decreased the number of TUNEL-positive cells compared to the IR group ($P < 0.05$, Figure 5).

4. Discussion

The aim of this study was to investigate the potential protective effects of ulinastatin on spinal cord ischemia-reperfusion injury and to explore the underlying mechanisms. The present study showed that ulinastatin improved the neurological outcome and reduced the postischemic apoptotic cell death in neurons by way of decreasing the levels of MDA, increasing SOD activities, suppressing the upregulation of the proapoptotic protein expression and the downregulation of antiapoptotic protein expression.

Spinal cord ischemia and reperfusion injury is a common postoperative complication following surgeries implicating the descending and thoracoabdominal aorta, which may lead to catastrophic consequences, such as paraplegia. Spinal cord ischemia due to hypoperfusion during aortic cross clamping is largely responsible for spinal cord injury. This injury is followed by a secondary injury caused by blood reperfusion [23]. The lack of the nutrients and oxygen activates devastating biochemical cascades, which causes spinal cord ischemia and reperfusion injury, namely, primary injury [24]. The primary injury followed by blood reperfusion may cause additional spinal cord damage, which impairs neuron function and generates the secondary damage. Secondary damage to the spinal cord is primarily responsible for many negative effects of the spinal cord injury (SCI) and most researches however have focused on understanding the pathophysiology of the secondary damage and reducing the amount of delayed cell loss following SCI [25, 26]. It has been reported that production of reactive oxygen species (ROS) is a well characterized pathological process during the reperfusion [27]. The event triggers accumulation of intracellular calcium levels, mitochondrial dysfunction [23]. ROS causes lipid peroxidation as well as oxidative and nitrative damage to proteins and nucleic acids [28, 29]. The central nervous system is primarily composed of lipids, which makes it easily damaged by free-radical-induced lipid peroxidation [30]. Lipid peroxidation is believed to be one of the primary pathophysiological mechanisms, which is also implicated in secondary damage [31]. Under the normal conditions, there is a balance between the production of ROS and the defense system, the antioxidants. Once the production of ROS is beyond the capacity of those antioxidant enzymes (such as SOD) as happened during reperfusion, oxidative damage occurred.

Ulinastatin, a protease inhibitor, was a glycoprotein, which was obtained from human urine with a molecular weight of 67 kDa [32], and it has been showed to reduce lipid peroxidation in various models of ischemia-reperfusion or sepsis [33]. In the present study, ulinastatin treatment attenuated lipid peroxidation by decreasing MDA content and elevating SOD activity in the spinal cord tissue, suggesting that ulinastatin can attenuate oxidative stress of the spinal cord tissue. Ulinastatin produced dose-dependent attenuation of the systemic inflammatory response of rats following lung I/R injury [34], and the doses of ulinastatin had been used from 5000 U/kg to 300000 U/kg [17, 34]. Therefore, we chose 50000 U/kg as the treatment dose, and our data further confirm that ulinastatin inhibits free radicals induced

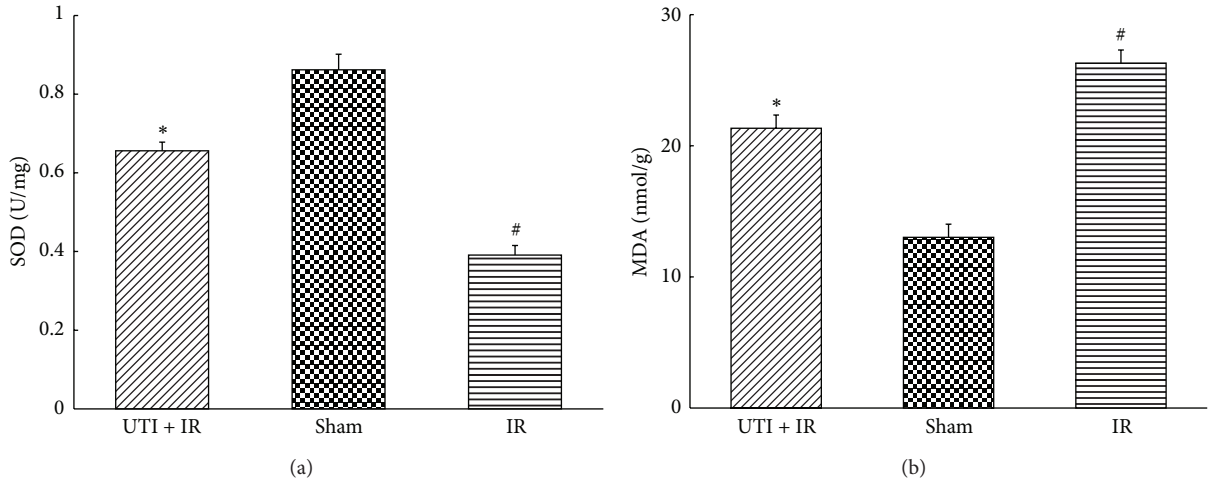

Figure 2: (a) SOD activities and MDA levels in rabbit spinal cord. *Compared with IR group ($P < 0.01$). #Compared with Sham group ($P < 0.01$). Values are the means ± SD, $n = 8$ per group.

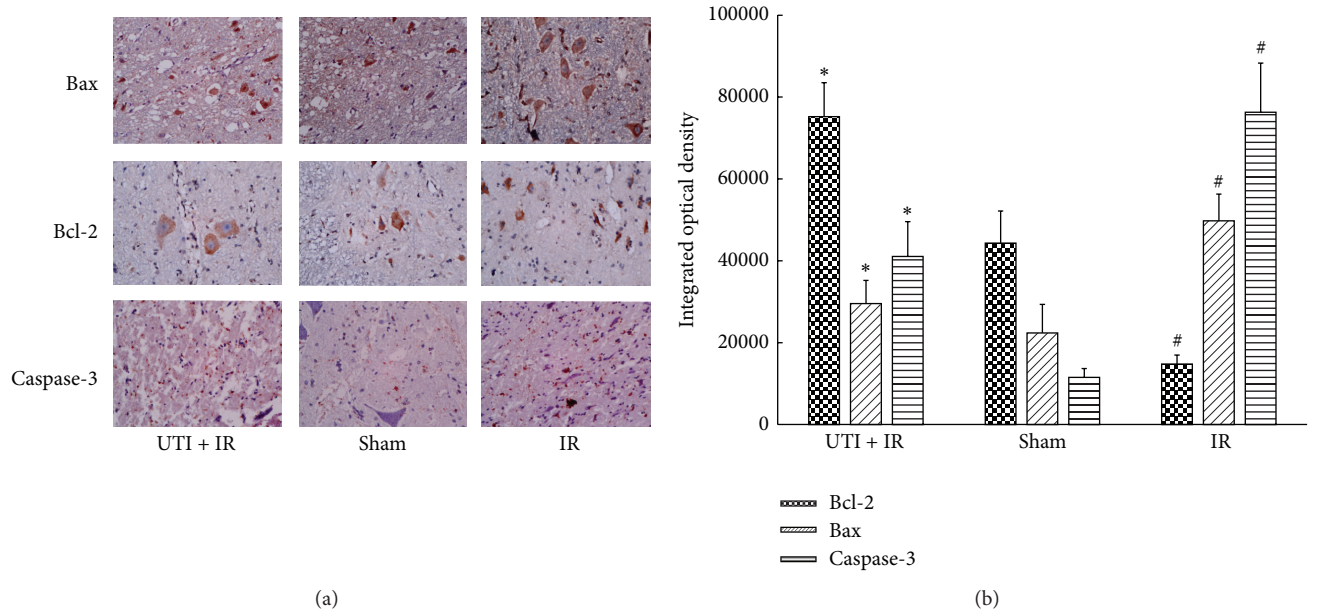

Figure 3: The expression of Bax, Bcl-2, and caspase-3 detected by immunohistochemistry. IR injury promoted Bax and caspase-3 expression but suppressed Bcl-2 expression. However, ulinastatin suppressed Bax and caspase-3 expression and promoted Bcl-2 expression. *Compared with IR group ($P < 0.01$). #Compared with Sham group ($P < 0.01$). Values are the means ± SD, $n = 8$ per group.

oxidative stress by accelerating its scavenging and thus plays a protective role after spinal cord ischemia reperfusion.

Evaluation of neurologic function is a current means for accessing the degree of the injury and the outcome of a medication treatment. The Sham group did not have nerve function impairment as assessed by using the Basso, Beattie, and Bresnahan (BBB) hind-limb locomotor rating scale test. However, in the SCI group the animals became unconscious at 1 hour time point and their BBB scores increased from 1.41 at 24 h to 4.51 at 72 h [7]. Similarly, in the present study the Sham group hind-limb function was also normal at the different time points, but the function in the IR group was impaired from 12 h to 48 h after reperfusion.

Apoptosis is the process of programmed cell death, which is indispensable for the normal development and homeostasis of all multicellular organisms [35]. It was believed that neuron apoptosis played a pivotal role in the second injury after spinal cord ischemia reperfusion. Previous research has demonstrated that a line of genes are involved in the development of apoptosis, such as the Bcl-2 gene family. The Bcl-2 gene family consists of 12 different gene products with pro- and antiapoptotic mechanisms. These pro- and

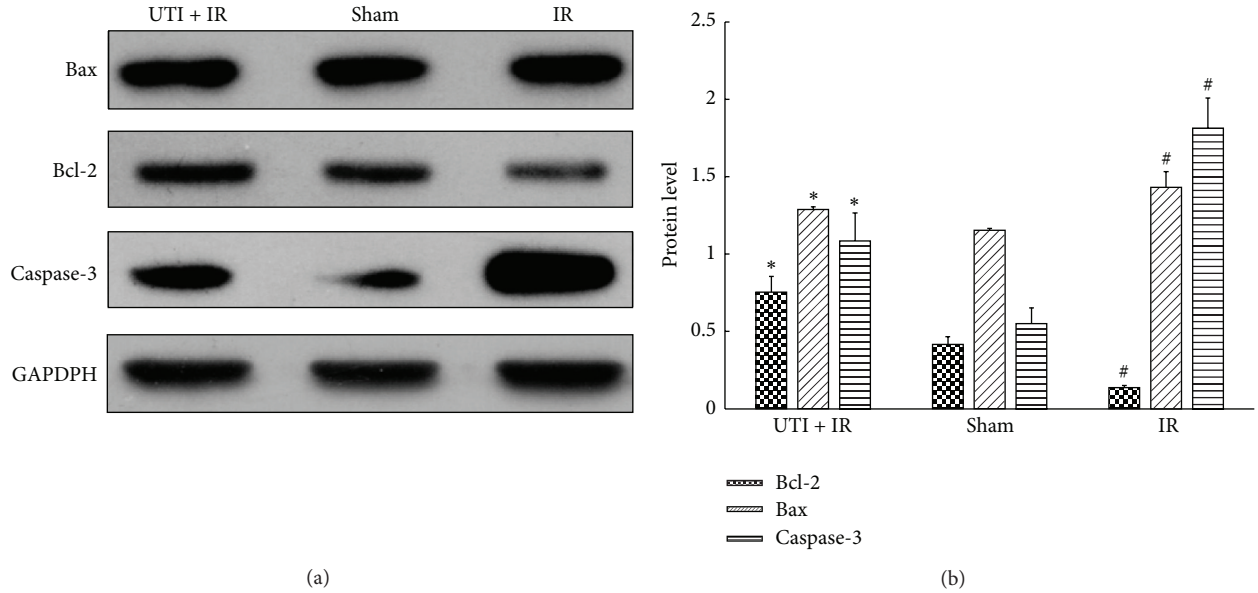

Figure 4: Expression level of apoptosis relevant proteins. (a) Western blot identified the expression level of apoptosis relevant proteins: Bax, Bcl-2, and caspase-3 in the spinal cord after 48 hours of reperfusion. (b) Compared with the Sham group, the IR group showed a significant increase of Bax, caspase-3 but decrease of Bcl-2. Compared with the IR group, the UTI + IR group demonstrated a significant decreased of Bax and caspase-3 but increase of Bcl-2. *Compared with IR group ($P < 0.01$). #Compared with Sham group ($P < 0.01$). Values are the means ± SD, $n = 8$ per group.

antiapoptotic proteins are different with regard to structure and tissue distribution and exert different functional effects. Bcl-2 and Bax are essentially involved in the regulation of cell apoptosis [36]. The antiapoptotic protein Bcl-2 is localized mainly in the outer mitochondrial membrane. In contrast, the proapoptotic proteins Bax reside mainly in the cytoplasm and are activated by various apoptotic stimuli. Bax translocates to the mitochondria, where it forms a complex with Bcl-2. An increased ratio of Bax/Bcl-2 leads to the formation of pores in the mitochondria, release of cytochrome c, and activation of the apoptotic pathway. Bcl-2 can prevent the release of cytochrome c, along with dATP and Apaf-1, and thus protect from apoptosis [37]. Chen et al. [38] reported that ulinastatin reduced the renal dysfunction and injury associated with ischemia-reperfusion of the kidney by upregulating of Bcl-2 expression. In our study, the TUNEL staining indicated that ulinastatin significantly reduced neuronal apoptosis in spinal cord after spinal cord ischemia reperfusion. Ulinastatin significantly upregulated Bcl-2 expression while suppressing the overexpression of Bax, suggesting that ulinastatin has an antiapoptosis property that plays a protective role attenuating postischemic spinal cord injury.

Caspases are a family of inactive proenzymes that play a crucial role in cell apoptosis, which is the scheduled death of cells. Caspase-3 is a protein that regulates apoptosis by inducing the cleavage of the key cellular proteins and alters cell integrity [39]. The role of caspase-3 in apoptosis is to activate the stages of cellular death in a nontraumatic manner. The intrinsic apoptosis is triggered by a wide range of stimuli that leads to release of cytochrome c from the mitochondria. This results in the formation of the apoptosome. The apoptosome then activates initiator caspase, typically caspase-9, which leads to the activation of the executioner caspase-3, and apoptosis finally occurs. Caspase-3 as the executioner is the common pathway which must be passed through in the apoptosis cascade, and it is the key one in mammalian cell apoptosis [40]. Caspase-3 is vital to this process because it allows the process to progress in sequence, which prevents undue damage to the remaining cells. In the present study, we found that the expression of caspase-3 was elevated in the IR group, but ulinastatin could decrease it significantly; thus the protective effect of ulinastatin may be in part due to inhibition of caspase-3 protein expression.

In summary, our results demonstrate that ulinastatin improves postischemic neurological function. To be best of our knowledge, the current study is the first to investigate the effects and mechanisms of ulinastatin in attenuating spinal cord ischemia-reperfusion injury. We have shown that ulinastatin increases SOD activity and decreases MDA content. Finally, we have revealed that ulinastatin can inhibit the neuronal apoptosis by regulating the expression of apoptosis proteins including Bcl-2, Bax, and caspase-3. Therefore, we propose that ulinastatin has a protective role and improves neurological outcome due to its beneficial effects including antioxidant and antiapoptosis effects. Findings obtained from the current study may have significant clinical implications given that ulinastatin is in use clinically.

Conflict of Interests

The authors declare that there is no conflict of interests regarding the publication of this paper.

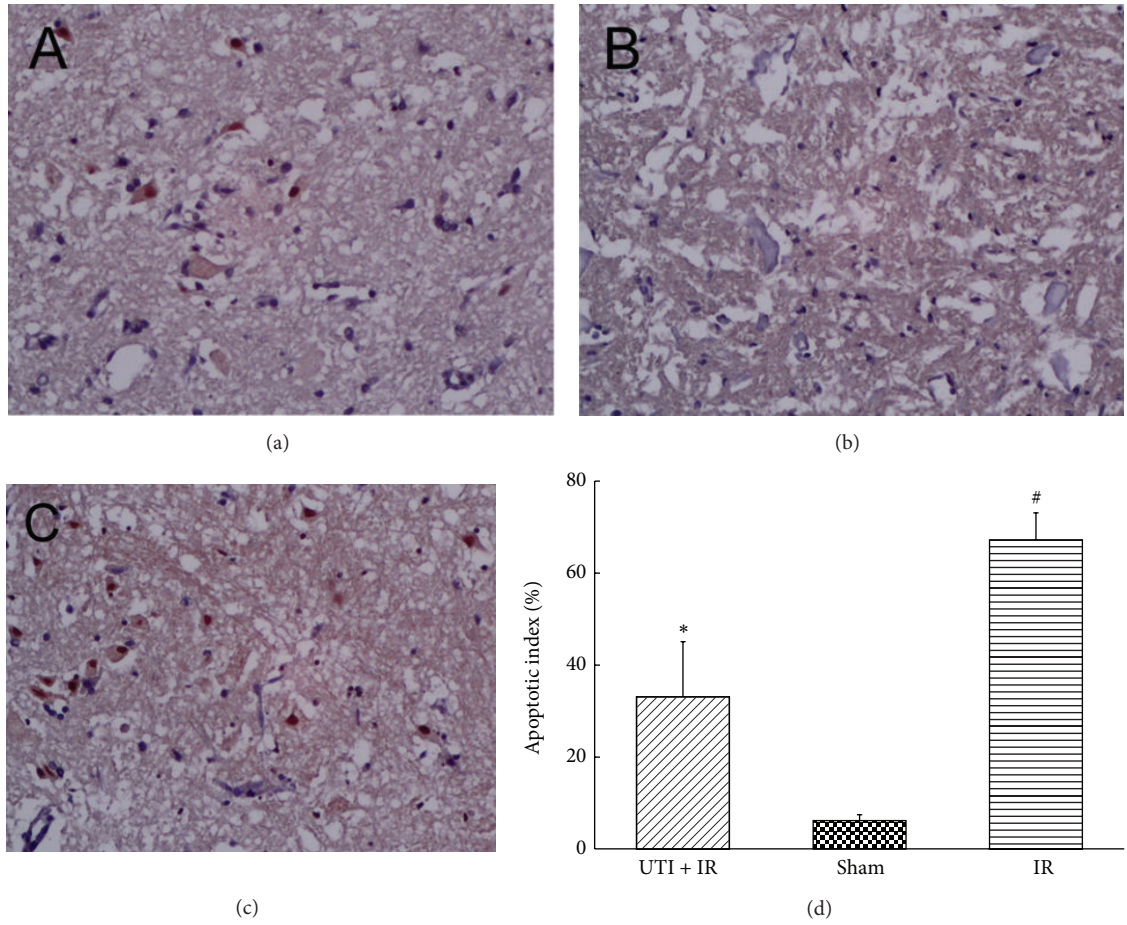

Figure 5: TUNEL staining and the apoptotic index of spinal cord neurons. (a) In the UTI + IR group, the number of apoptotic cells was far less than that in the IR group, which suggested that UTI decreased cell apoptosis caused by IR. (b) In the Sham group, a very few apoptotic cells were found. (c) In the IR group, the apoptotic cells increased significantly. *Compared with IR group ($P < 0.01$). #Compared with Sham group ($P < 0.01$). Values are the means ± SD, $n = 8$ per group.

Acknowledgment

This study was supported by Administration of Traditional Chinese Medicine of Guangdong Province, China (no. 20141010).

References

[1] C. B-Rao and J. Stewart, "Inverse analysis of empirical matrices of idiotypic network interactions," *Bulletin of Mathematical Biology*, vol. 58, no. 6, pp. 1123–1153, 1996.

[2] P. D. Smith, F. Puskas, X. Meng et al., "The evolution of chemokine release supports a bimodal mechanism of spinal cord ischemia and reperfusion injury," *Circulation*, vol. 126, pp. S110–S117, 2012.

[3] M. Kakinohana, K. Kida, S. Minamishima et al., "Delayed paraplegia after spinal cord ischemic injury requires caspase-3 activation in mice," *Stroke*, vol. 42, no. 8, pp. 2302–2307, 2011.

[4] L. Lang-Lazdunski, K. Matsushita, L. Hirt, C. Waeber, J.-P. G. Vonsattel, and M. A. Moskowitz, "Spinal cord ischemia: development of a model in the mouse," *Stroke*, vol. 31, no. 1, pp. 208–213, 2000.

[5] M. F. Conrad, J. Y. Ye, T. K. Chung, J. K. Davison, and R. P. Cambria, "Spinal cord complications after thoracic aortic surgery: long-term survival and functional status varies with deficit severity," *Journal of Vascular Surgery*, vol. 48, no. 1, pp. 47–53, 2008.

[6] T. Hayashi, M. Sakurai, K. Abe, M. Sadahiro, K. Tabayashi, and Y. Itoyama, "Apoptosis of motor neurons with induction of caspases in the spinal cord after ischemia," *Stroke*, vol. 29, no. 5, pp. 1007–1013, 1998.

[7] S. Zong, G. Zeng, Y. Fang et al., "The role of IL-17 promotes spinal cord neuroinflammation via activation of the transcription factor STAT3 after spinal cord injury in the rat," *Mediators of Inflammation*, vol. 2014, Article ID 786947, 10 pages, 2014.

[8] J. Oda, K. Yamashita, T. Inoue et al., "Resuscitation fluid volume and abdominal compartment syndrome in patients with major burns," *Burns*, vol. 32, no. 2, pp. 151–154, 2006.

[9] S. Endo, K. Inada, K. Taki, S. Hoshi, and M. Yoshida, "Inhibitory effects of ulinastatin on the production of cytokines: implications for the prevention of septicemic shock," *Clinical Therapeutics*, vol. 12, no. 4, pp. 323–326, 1990.

[10] Y.-Z. Cao, Y.-Y. Tu, X. Chen, B.-L. Wang, Y.-X. Zhong, and M.-H. Liu, "Protective effect of Ulinastatin against murine models

of sepsis: inhibition of TNF-α and IL-6 and augmentation of IL-10 and IL-13," *Experimental and Toxicologic Pathology*, vol. 64, no. 6, pp. 543–547, 2012.

[11] Q.-L. He, F. Zhong, F. Ye et al., "Does intraoperative ulinastatin improve postoperative clinical outcomes in patients undergoing cardiac surgery: a meta-analysis of randomized controlled trials," *BioMed Research International*, vol. 2014, Article ID 630835, 15 pages, 2014.

[12] H.-M. Luo, M.-H. Du, Z.-L. Lin et al., "Ulinastatin suppresses burn-induced lipid peroxidation and reduces fluid requirements in a swine model," *Oxidative Medicine and Cellular Longevity*, vol. 2013, Article ID 904370, 8 pages, 2013.

[13] Z.-L. Cao, Y. Okazaki, K. Naito, T. Ueno, M. Natsuaki, and T. Itoh, "Ulinastatin attenuates reperfusion injury in the isolated blood-perfused rabbit heart," *Annals of Thoracic Surgery*, vol. 69, no. 4, pp. 1121–1126, 2000.

[14] O. A. R. Binns, N. F. DeLima, S. A. Buchanan et al., "Neutrophil endopeptidase inhibitor improves pulmonary function during reperfusion after eighteen-hour preservation," *The Journal of Thoracic and Cardiovascular Surgery*, vol. 112, no. 3, pp. 607–613, 1996.

[15] Y. Kudo, T. Egashira, and Y. Yamanaka, "Protective effect of ulinastatin against liver injury caused by ischemia-reperfusion in rats," *Japanese Journal of Pharmacology*, vol. 60, no. 3, pp. 239–245, 1992.

[16] H. Nakahama, K. Obata, and M. Sugita, "Ulinastatin ameliorates acute ischemic renal injury in rats," *Renal Failure*, vol. 18, no. 6, pp. 893–898, 1996.

[17] T. Yano, S. Anraku, R. Nakayama, and K. Ushijima, "Neuroprotective effect of urinary trypsin inhibitor against focal cerebral ischemia-reperfusion injury in rats," *Anesthesiology*, vol. 98, no. 2, pp. 465–473, 2003.

[18] W. Yao, G. Luo, G. Zhu et al., "Propofol activation of the Nrf2 pathway is associated with amelioration of acute lung injury in a rat liver transplantation model," *Oxidative Medicine and Cellular Longevity*, vol. 2014, Article ID 258567, 9 pages, 2014.

[19] O. H. Lowry, N. J. Rosebrough, A. L. Farr, and R. J. Randall, "Protein measurement with the Folin phenol reagent," *The Journal of Biological Chemistry*, vol. 193, no. 1, pp. 265–275, 1951.

[20] T. Luo, Z. Xia, D. M. Ansley et al., "Propofol dose-dependently reduces tumor necrosis factor-α-induced human umbilical vein endothelial cell apoptosis: effects on Bcl-2 and bax expression and nitric oxide generation," *Anesthesia and Analgesia*, vol. 100, no. 6, pp. 1653–1659, 2005.

[21] M. Liu, B. Zhou, Z.-Y. Xia et al., "Hyperglycemia-induced inhibition of DJ-1 expression compromised the effectiveness of ischemic postconditioning cardioprotection in rats," *Oxidative Medicine and Cellular Longevity*, vol. 2013, Article ID 564902, 8 pages, 2013.

[22] H. Li, Z. Liu, J. Wang et al., "Susceptibility to myocardial ischemia reperfusion injury at early stage of type 1 diabetes in rats," *Cardiovascular Diabetology*, vol. 12, no. 1, article 133, 2013.

[23] N. T. Kouchoukos, J. R. Scharff, and C. F. Castner, "Repair of primary or complicated aortic coarctation in the adult with cardiopulmonary bypass and hypothermic circulatory arrest," *The Journal of Thoracic and Cardiovascular Surgery*, 2014.

[24] H. Kertmen, B. Gürer, E. R. Yilmaz et al., "The protective effect of low-dose methotrexate on ischemia-reperfusion injury of the rabbit spinal cord," *European Journal of Pharmacology*, vol. 714, no. 1–3, pp. 148–156, 2013.

[25] E. D. Hall and J. E. Springer, "Neuroprotection and acute spinal cord injury: a reappraisal," *NeuroRx*, vol. 1, no. 1, pp. 80–100, 2004.

[26] C. A. Oyinbo, "Secondary injury mechanisms in traumatic spinal cord injury: a nugget of this multiply cascade," *Acta Neurobiologiae Experimentalis*, vol. 71, no. 2, pp. 281–299, 2011.

[27] R. D. Azbill, X. Mu, A. J. Bruce-Keller, M. P. Mattson, and J. E. Springer, "Impaired mitochondrial function, oxidative stress and altered antioxidant enzyme activities following traumatic spinal cord injury," *Brain Research*, vol. 765, no. 2, pp. 283–290, 1997.

[28] Q. Fan, X.-C. Yang, Y. Liu et al., "Postconditioning attenuates myocardial injury by reducing nitro-oxidative stress in vivo in rats and in humans," *Clinical Science*, vol. 120, no. 6, pp. 251–261, 2011.

[29] S. Lei, H. Li, J. Xu et al., "Hyperglycemia-induced protein kinase C β2 activation induces diastolic cardiac dysfunction in diabetic rats by impairing caveolin-3 expression and Akt/eNOS signaling," *Diabetes*, vol. 62, no. 7, pp. 2318–2328, 2013.

[30] E. R. Yilmaz, H. Kertmen, H. Dolgun et al., "Effects of darbepoetin-alpha in spinal cord ischemia-reperfusion injury in the rabbit," *Acta Neurochirurgica*, vol. 154, no. 6, pp. 1037–1044, 2012.

[31] A. Diaz-Ruiz, C. Rios, I. Duarte et al., "Lipid peroxidation inhibition in spinal cord injury: cyclosporin-A vs methylprednisolone," *NeuroReport*, vol. 11, no. 8, pp. 1765–1767, 2000.

[32] Y. Yamauchi, Y. Izumi, M. Inoue et al., "Safety of postoperative administration of human urinary trypsin inhibitor in lung cancer patients with idiopathic pulmonary fibrosis," *PLoS ONE*, vol. 6, no. 12, Article ID e29053, 2011.

[33] Y. Koga, M. Fujita, R. Tsuruta et al., "Urinary trypsin inhibitor suppresses excessive superoxide anion radical generation in blood, oxidative stress, early inflammation, and endothelial injury in forebrain ischemia/reperfusion rats," *Neurological Research*, vol. 32, no. 9, pp. 925–932, 2010.

[34] L. Xu, B. Ren, M. Li, F. Jiang, Z. Zhanng, and J. Hu, "Ulinastatin suppresses systemic inflammatory response following lung ischemia-reperfusion injury in rats," *Transplantation Proceedings*, vol. 40, no. 5, pp. 1310–1311, 2008.

[35] K. Kannan and S. K. Jain, "Oxidative stress and apoptosis," *Pathophysiology*, vol. 7, no. 3, pp. 153–163, 2000.

[36] B. Antonsson and J. C. Martinou, "The Bcl-2 protein family," *Experimental Cell Research*, vol. 256, no. 1, pp. 50–57, 2000.

[37] D. R. Green and J. C. Reed, "Mitochondria and apoptosis," *Science*, vol. 281, no. 5381, pp. 1309–1312, 1998.

[38] C.-C. Chen, Z.-M. Liu, H.-H. Wang, W. He, Y. Wang, and W.-D. Wu, "Effects of ulinastatin on renal ischemia-reperfusion injury in rats," *Acta Pharmacologica Sinica*, vol. 25, no. 10, pp. 1334–1340, 2004.

[39] Y. Wang, X. Liu, D. Zhang, J. Chen, S. Liu, and M. Berk, "The effects of apoptosis vulnerability markers on the myocardium in depression after myocardial infarction," *BMC Medicine*, vol. 11, no. 1, article 32, 2013.

[40] G. M. Cohen, "Caspase: the executioners of apoptosis," *Biochemical Journal*, vol. 326, no. 1, pp. 1–16, 1997.

Hindawi Publishing Corporation
Oxidative Medicine and Cellular Longevity
Volume 2015, Article ID 380403, 9 pages
http://dx.doi.org/10.1155/2015/380403

Research Article

Preventive Treatment with Ketamine Attenuates the Ischaemia-Reperfusion Response in a Chronic Postischaemia Pain Model

Suryamin Liman,[1] Chi Wai Cheung,[1,2] Kar Lok Wong,[1,2,3] Wai Tai,[1,2] Qiu Qiu,[1,2] Kwok Fu Ng,[1,2] Siu Wai Choi,[1,2] and Michael Irwin[1,2]

[1]*Department of Anaesthesiology, The University of Hong Kong, Pokfulam, Hong Kong*
[2]*Laboratory and Clinical Research Institute for Pain, The University of Hong Kong, Pokfulam, Hong Kong*
[3]*Department of Anaesthesiology, China Medical University and Hospital, Taichung 40402, Taiwan*

Correspondence should be addressed to Chi Wai Cheung; cheucw@hku.hk

Received 18 September 2014; Accepted 21 December 2014

Academic Editor: Qian Fan

Ischemia and inflammation may be pathophysiological mechanisms of complex regional pain syndrome (CRPS). Ketamine has proposed anti-inflammatory effects and has been used for treating CRPS. This study aimed to evaluate anti-inflammatory and analgesic effects of ketamine after ischaemia-reperfusion injury in a chronic postischaemia pain (CPIP) model of CRPS-I. Using this model, ischemia was induced in the hindlimbs of male Sprague-Dawley rats. Ketamine, methylprednisolone, or saline was administered immediately after reperfusion. Physical effects, (oedema, temperature, and mechanical and cold allodynia) in the bilateral hindpaws, were assessed from 48 hours after reperfusion. Fewer (56%) rats in the ketamine group developed CPIP at the 48th hour after reperfusion (nonsignificant). Ketamine treated rats showed a significantly lower temperature in the ischaemic hindpaw compared to saline ($P < 0.01$) and methylprednisolone ($P < 0.05$) groups. Mechanical and cold allodynia were significantly lower in the ischaemic side in the ketamine group ($P < 0.05$). Proinflammatory cytokines TNF-α and IL-2 were significantly lower at the 48th hour after reperfusion in ketamine and methylprednisolone groups, compared to saline (all $P < 0.05$). In conclusion, immediate administration of ketamine after an ischaemia-reperfusion injury can alleviate pain and inflammation in the CPIP model and has potential to treat postischaemic pain.

1. Introduction

Complex regional pain syndrome (CRPS) is a chronic neuropathic pain disorder. Its key features in humans include spontaneous pain, hyperalgesia, allodynia, and abnormal vasomotor and sudomotor activities [1]. The incidence is about 26.2 per 100,000 persons and it is more prevalent among females than males [2]. CRPS is divided into two types: CRPS-II involves nerve injury while CRPS-I does not. The pathophysiological mechanisms of CRPS remain poorly understood but the clinical features suggest that the pathogenesis involves inflammation, ischaemia, nerve regeneration, and abnormal cross talk between affected nerves and blood vessels that are characterized by complicated cellular and molecular changes [3–5]. The blister fluid of CRPS patients has high levels of interleukin- (IL-) 6 and tumour necrosis factor-alpha (TNF-α) [6]. Interleukin- (IL-) 2 and TNF-α are also elevated systemically in patients with CRPS-I [7]. Thus, drugs modulating the cytokine system have started to be used for CRPS pain management in clinical trials [8].

Ketamine, an N-methyl-D-aspartate (NMDA) receptor antagonist and dissociative anaesthetic, has been shown to produce analgesia by inhibiting both normal and pathologic pain pathways [9]. Activated by glutamate, the NMDA receptor is believed to play an important role in the development of central sensitization, which can induce chronic pain, including CRPS. NMDA receptor antagonism may attenuate central sensitization and further reduce the symptoms of CRPS. In addition, ketamine has an anti-inflammatory effect [10], which may partially contribute to its analgesic properties. It

has been used to treat CRPS clinically and shows promise in this area [11]. However, to date, there has been no study conducted to evaluate its anti-inflammatory analgesic effects in pain conditions. In this study, we also compared the anti-inflammatory effects of ketamine with methylprednisolone (a glucocorticoid anti-inflammatory agent), which served as a positive control, to investigate whether ketamine had additional therapeutic effects compared to methylprednisolone on a postischaemic pain model.

We hypothesized that if administered early after ischaemia-reperfusion injury, ketamine would modify the postischaemic responses, including pain and inflammation, in the CPIP animal model established by Coderre and colleagues [12]. The model has been shown to mimic CRPS-I reliably by 3-hour inductions of ischaemia and reperfusion [12], presenting hyperaemia, plasma extravasation, mechanical and cold allodynia, and the induction of TNF-α, IL-2, IL-6, and nuclear factor kappa B (NFκB) [13].

2. Materials and Methods

All procedures were carried out according to the US National Institutes of Health Guide for the Care and Use of Laboratory Animals and were approved by the Committee on the Use of Live Animals in Teaching and Research at the University of Hong Kong. The license to conduct experiments was issued by the Department of Health, the Government of the Hong Kong Special Administrative Region.

2.1. Animal Preparation. There were three treatment groups in this study: a ketamine treatment group (group KE), a methylprednisolone (corticosteroid) treatment group (group MP), and a 0.9% saline treatment group (group NS). Ten 270~300 g adult male SD rats (Charles River Laboratories, USA) were used for each group based on our preliminary study (unpublished). The animals were housed individually in isolated cages with food and water available ad libitum, on a 12 : 12 h light : dark cycle in the laboratory animal unit at the University of Hong Kong. The room temperature was maintained at 23°C and humidity ranged between 25% and 45%.

2.2. CPIP Criteria. Successful development of CPIP relies on the existence of mechanical allodynia, which meets the criteria of a 30% decrease in the mechanical threshold of an ischaemic limb (ipsilateral side) at the forty-eighth hour after reperfusion [12]. Those fulfilling the criteria would be regarded as having successfully developed CPIP. The proportion of rats meeting the criteria for successful development of CPIP was calculated. Since effects on the modification of the postischaemic responses (anti-inflammatory and analgesic effects) of early ketamine administration were assessed, all of the rats in this study were recruited to evaluate physical signs, pain behaviour, and serum proinflammatory cytokine levels.

2.3. CPIP Model and Drug Administration. The rats were initially anaesthetised with intraperitoneal (i.p.) pentobarbital 40 mg/kg, followed by 13 mg per hour for the first hour and 6.5 mg for the second hour. Three doses were given in total. To induce ischaemia, a tourniquet (Nitrile 70 Durometer O-ring) with 7/32-inch internal diameter was placed around the rat's left hindlimb (ipsilateral) near the ankle joint and proximal to the medial malleolus. The O-rings were selected to produce a tight-fit that produced ischaemia similar to that produced by a blood pressure of 350 mmHg and were left on the limb for 3 hours. Blood flow to the limb was confirmed with laser Doppler [12]. Briefly, a laser Doppler probe (DP1T-V2; Moor Instruments, Axminster, UK) and a fibre were loosely taped to the plantar surface of the ipsilateral paw. Blood flow was recorded with a DRT4 monitor (Moor Instruments, Axminster, UK). At the third hour, the O-ring was cut and reperfusion occurred. The termination of sodium pentobarbital anaesthesia was timed so that the rats recovered fully within 30–60 minutes following reperfusion. The study drugs ketamine (100 mg/kg), methylprednisolone (30 mg/kg), and 0.9% saline in a bolus of 0.5 mL were given intraperitoneally, immediately after the removal of the O-ring tourniquet. Dose of ketamine was chosen according to a previous study on intestinal ischaemia-reperfusion injury [14]. Methylprednisolone was used as a positive control and the dose was determined according to a study of methylprednisolone on ischaemia-reperfusion injury in rat livers [15].

2.4. Physical Signs and Behaviour Assessment. The rats were taken to the laboratory platform for one hour per day for a total of two days prior to the experiment and 30 minutes before behaviour assessment on the experiment day to become accustomed to the laboratory environment. The investigator assessing the physical signs and pain behaviour of the rats was blinded to the study medications administered.

2.5. Hindpaw Temperature. Coderre's CPIP animal model showed an increase in skin temperature in the ischaemic hindpaw lasting for two hours after reperfusion [12]. A thermocouple wire was used to measure the baseline temperature of both hindpaws before ischaemia and from the fifth minute to the seventh day after the reperfusion. Three sites were tested over the dorsum of the hindpaw. These were the spaces between the first and second metatarsals (medial), the second and the third metatarsals (central), and the fourth and fifth metatarsals (lateral) in medial, central, and lateral sequence. The three measurements were averaged to obtain a mean temperature for each side.

2.6. Hindpaw Thickness. The thickness of the hindpaw was measured as an indication of hindpaw volume and oedema after induction of CPIP, as it has been reported that the hindpaw volume can be presented as hindpaw thickness [16]. In this experiment, a manual calliper was used to measure the ventral thickness of both hindpaws (maximum dorsal) at baseline before ischaemia and from the fifth minute to the seventh day after reperfusion. The calliper was lightly applied to the skin without tissue displacement.

2.7. Mechanical Allodynia. The criterion for successful development of CPIP is a 30% reduction in the mechanical allodynia threshold on the ipsilateral hindpaw. This was measured by assessing the hindpaw withdrawal threshold with a von Frey fibre of an Electrovonfrey apparatus (IITC/Life Science Instruments). A blunt fibre with a stiffness of 65 g was applied against the hindpaw plantar skin at approximately the midsole, avoiding the tori pads. It was pushed until it is slightly bent, and a hindpaw withdrawal within 6–8 seconds of the stimulus was considered a positive response. The force (in grams) that was needed to elicit a positive response was then recorded and shown on the screen of the Electrovonfrey apparatus. The withdrawal threshold was measured at 5- to 10-minute intervals, alternating between the right and left sides until each side had been tested twice. The readings of the ischaemic and contralateral sides were averaged to give a mean withdrawal threshold for each side. This was measured at baseline before ischaemia and from the sixth hour to the seventh day after reperfusion.

2.8. Cold Allodynia. Cold allodynia was measured as a decrease in withdrawal latency to acetone, according to Coderre et al. [12]. The measurements started at baseline before ischaemia and from the sixth hour to the seventh day after reperfusion. The rats were placed in a clear plastic cylinder on a glass surface maintained at a constant temperature of 23°C. After 15 minutes of acclimatization, a drop of acetone was placed on the skin of the heel. Unlike normal rats which usually ignore the stimulus, CPIP rats often respond to it with an exaggerated withdrawal that we were able to time. The hindpaw withdrawal latency was repeatedly measured at 5–10-minute intervals, alternating between the right and left sides until each side had been tested twice. The two withdrawal latencies of both ischemic and contralateral sides were averaged to give mean withdrawal latency.

2.9. Heat Threshold. Heat threshold was assessed by timing hindpaw withdrawal latency to radiant heat using a fabricated radiant heat device according to Vatine et al. [17]. The time measurements started at baseline before ischemia and from the sixth hour to the seventh day after reperfusion. Rats were placed in a clear plastic cylinder on a glass surface maintained at a constant temperature of 23°C. After 15 minutes of acclimatization, a radiant light source was focused on the heel of the ischaemic side hindpaw. The hindpaw withdrawal latency was measured at 5–10-minute intervals, alternating between the right and left sides, until each side had been tested twice. The two withdrawal latencies of both ischaemic and contralateral sides were averaged to give mean withdrawal latency.

2.10. Serum Proinflammatory Cytokines. An increase in proinflammatory cytokines can indicate the involvement of the inflammatory process in CPIP. Blood was collected from the tail vein forty-eight hours after reperfusion. After being stored overnight at 4°C, the blood was centrifuged at 1000 ×g for 20 minutes. The supernatant was taken and allocated for use. Serum TNF-α and IL-2 were measured by an enzyme-linked immunosorbent assay (ELISA) and commercial assays (R&D Systems, Inc., Minneapolis).

2.11. Statistical Analysis. A two-way repeated measures analysis of variance (ANOVA) was used to compare temperature, hindpaw thickness, withdrawal threshold to von Frey fibre and acetone, and heat thresholds in a manner that ensured the data were compared on a complete study time-course basis instead of individual time points. One-way ANOVA was used to test the serum inflammatory cytokines. When a significant result was obtained, Tukey's test was applied for post hoc comparisons. The proportions of mortality and CPIP development among groups were tested by Fisher's exact test. Data are presented as mean ± S.E.M, and differences are considered significant at a P value ≤ 0.05.

3. Results

3.1. Mortality Rate and Proportion of Rats with Successful Development of CPIP. One animal in the ketamine and two in the methylprednisolone treatment groups died after the injection of the study drug, making the residual number of each group $n = 9$ in group KE, $n = 8$ in group MP, and $n = 10$ in group NS with no significant difference in the mortality rate among the three groups.

Using the criteria of a 30% decrease in the withdrawal threshold of the von Frey fibre (mechanical allodynia) on the ischaemic side, the percentages of successful CPIP development were 56% in the KE group, 75% in the MP group, and 80% in the NS group. Although KE group had the least development rate of CPIP, no statistically significant difference among the three treatment groups could be found.

3.2. Hindpaw Temperature and Thickness. Our thermography study showed that the temperature on the ipsilateral side hindpaws of group KE rats was lower than in the NS and MP group rats ($P < 0.01$ and $P < 0.05$, resp., Figure 1(a)). Ketamine also attenuated the rise in the hindpaw temperature on the contralateral side during the same period compared with group NS ($P < 0.05$, Figure 1(b)). Although there was a clear difference, it was only obvious up to the sixth hour after reperfusion. We also monitored the hindpaw thickness but no obvious difference was found between all three treatment groups in the ipsilateral and contralateral sides (Figures 2(a) and 2(b)).

3.3. Mechanical and Cold Allodynia. Ketamine significantly alleviated both mechanical and cold allodynia in the ipsilateral hindpaw. On the ipsilateral side, the withdrawal threshold to the von Frey fibre in group KE was significantly higher than that in groups NS and MP ($P < 0.01$ and $P < 0.05$, resp., Figure 3(a)). On the contralateral sides, groups KE and MP also showed a higher withdrawal threshold to the von Frey fibre compared with group NS (all $P < 0.05$, Figure 3(b)). The withdrawal threshold to acetone in the ketamine treatment group was significantly higher on the

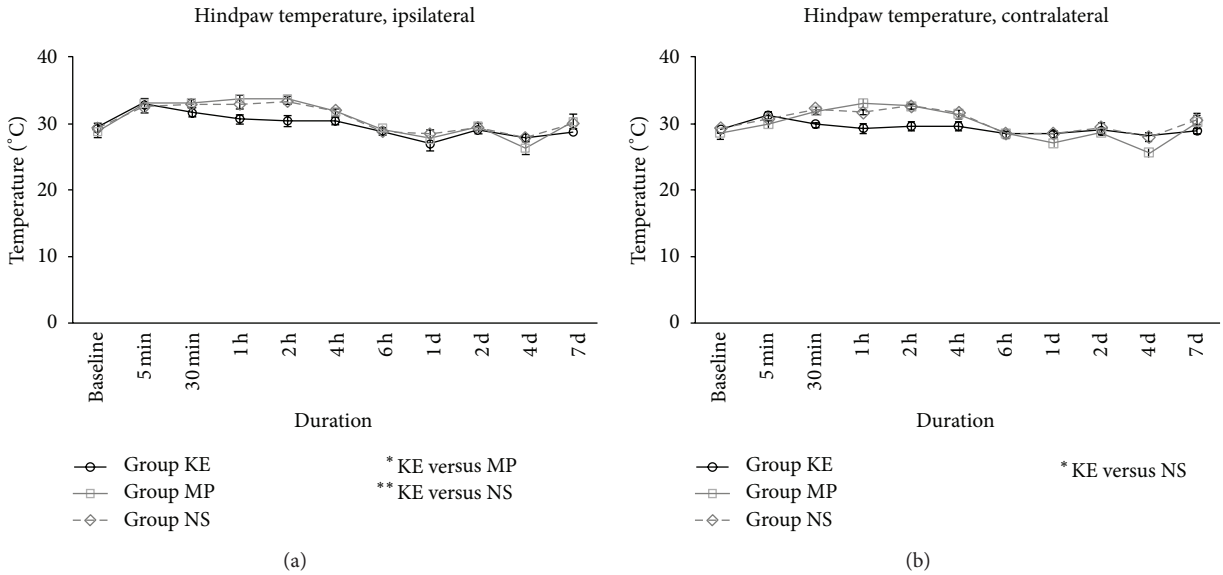

Figure 1: Hindpaw temperatures of KE, MP, and NS groups on the ipsilateral (a) and contralateral side (b) from baseline before ischaemia until the first 7 days after reperfusion. The temperature in group KE was lower in the ipsilateral side, compared with MP ($P < 0.05$) and NS ($P < 0.01$) groups. However, the difference was only obvious up to the 6th hour after reperfusion. Group KE also had decreased hindpaw temperature on the contralateral side during the same period, compared with group NS ($P < 0.05$); $^{*}P < 0.05$ and $^{**}P < 0.01$.

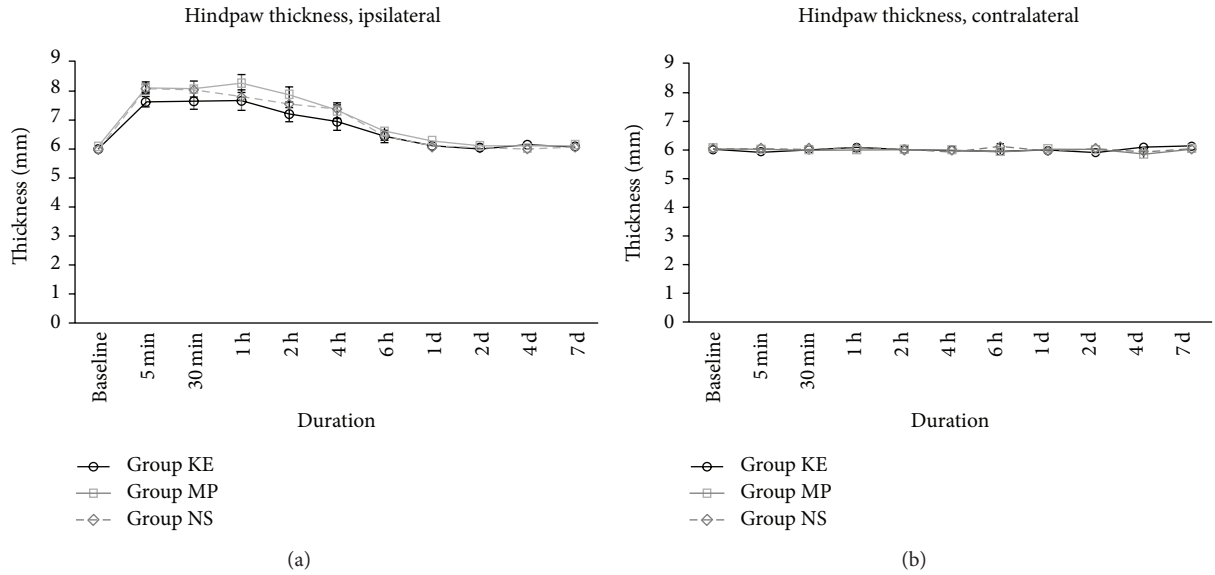

Figure 2: Hindpaw thickness of KE, MP, and NS groups on the ipsilateral (a) and contralateral side (b) from baseline before ischaemia until the first 7 days after reperfusion. There was no difference among all three treatment groups in the ipsilateral side during the 7-day study period.

ipsilateral side compared with group NS ($P < 0.05$) and group MP (all $P < 0.05$), as shown in Figure 4(a). For the contralateral sides, groups KE and MP also exhibited a significantly higher withdrawal threshold to acetone stimuli compared to group NS (all $P < 0.001$, Figure 4(b)).

3.4. Heat Threshold. Fabricated radiant heat measurements produced no obvious difference in withdrawal threshold among all three treatment groups, in both the ipsilateral and contralateral sides (Figures 5(a) and 5(b)).

3.5. Serum TNF-α and IL-2. Groups KE and MP were able to markedly attenuate the increase in serum TNF-α levels (all $P < 0.001$, Figure 6(a)) and serum IL-2 (all $P < 0.05$, Figure 6(b)) forty-eight hours after reperfusion, compared with group NS.

4. Discussion

The present study successfully reproduced Coderre's CPIP model by inducing CRPS-I-like symptoms such as hyperaemia and mechanical and cold allodynia in both the

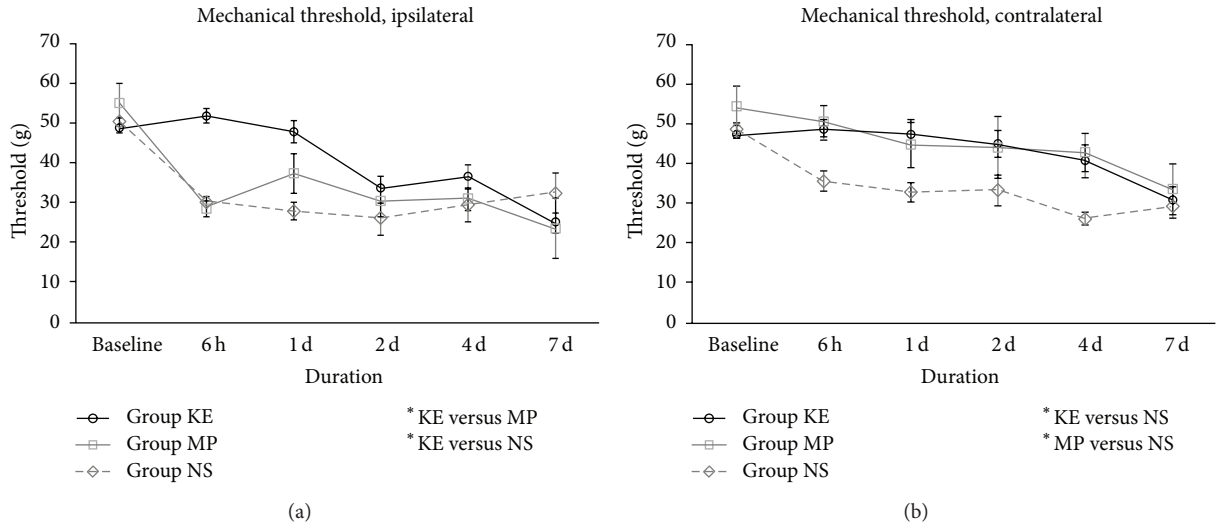

Figure 3: Mechanical allodynia of KE, MP, and NS groups on the ipsilateral (a) and contralateral side (b) from baseline before ischaemia until the first 7 days after reperfusion. On the ipsilateral side, the withdrawal threshold of group KE was significantly higher than that of NS ($P < 0.01$) and MP ($P < 0.05$). On the contralateral side, the withdrawal threshold was higher in both KE ($P < 0.05$) and MP ($P < 0.05$) groups than that in group NS; $^{*}P < 0.05$; $^{**}P < 0.01$.

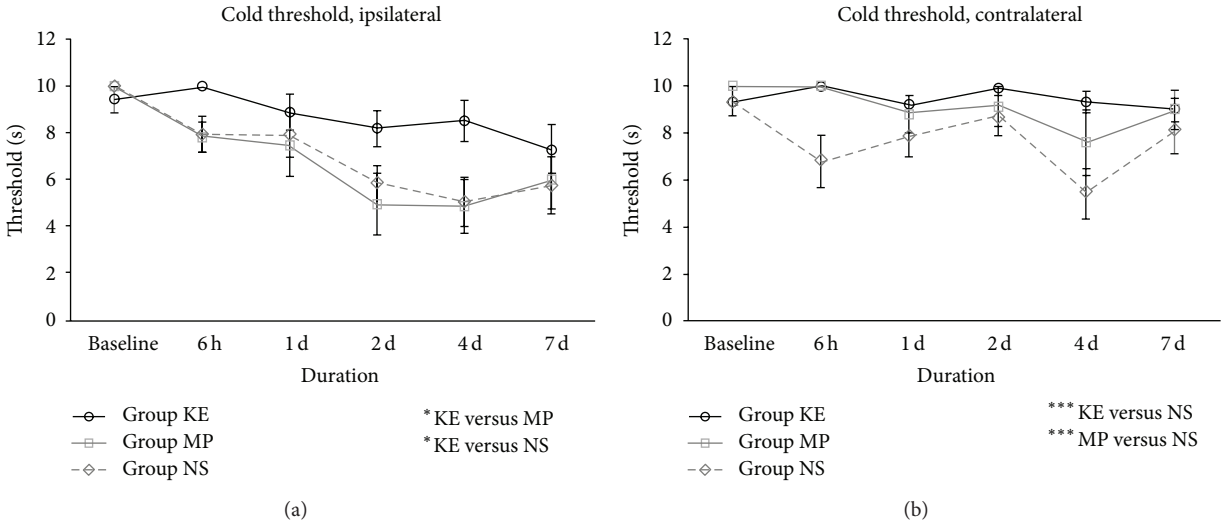

Figure 4: Cold allodynia of KE, MP, and NS groups on the ipsilateral (a) and contralateral side (b) from baseline before ischaemia until 7 days after reperfusion. On the ipsilateral side, the withdrawal threshold to acetone of group KE was significantly higher, compared with groups NS ($P < 0.05$) and MP ($P < 0.05$). On the contralateral side, the withdrawal threshold to acetone was significantly higher in KE ($P < 0.001$) and MP ($P < 0.001$) groups than that of NS; $^{*}P < 0.05$; $^{***}P < 0.001$.

ipsilateral and contralateral hindpaws of experimental SD rats. The appearance of bilateral symptoms has also been observed in other animal models of CRPS-I [18–21] and this is often a feature in patients with CRPS-I [22, 23]. The underlying mechanism of this contralateral effect may involve central sensitization caused by damage to muscle tissue [24]. It is thought that persistent inflammation after ischaemia-reperfusion injury may sensitize and activate afferent nociceptors in damaged tissue which may then lead to central sensitization contributing to the mechanical and cold allodynia observed in CPIP [12]. In this study, as medications were given immediately after induction of ischaemia, the treatment was essentially preventive of the acute phase of CPIP.

Ketamine is an NMDA receptor antagonist that also inhibits serotonin and dopamine reuptake, binds to μ-opioid receptors, and has effects on nerve growth factors and voltage-gated Na+ and K+ channels. It has been shown to produce analgesia by inhibiting normal and pathologic pain pathways, as NMDA receptor antagonism may attenuate central sensitization after tissue injury or inflammation [9, 25]. This may reduce secondary hyperalgesia and is reflected

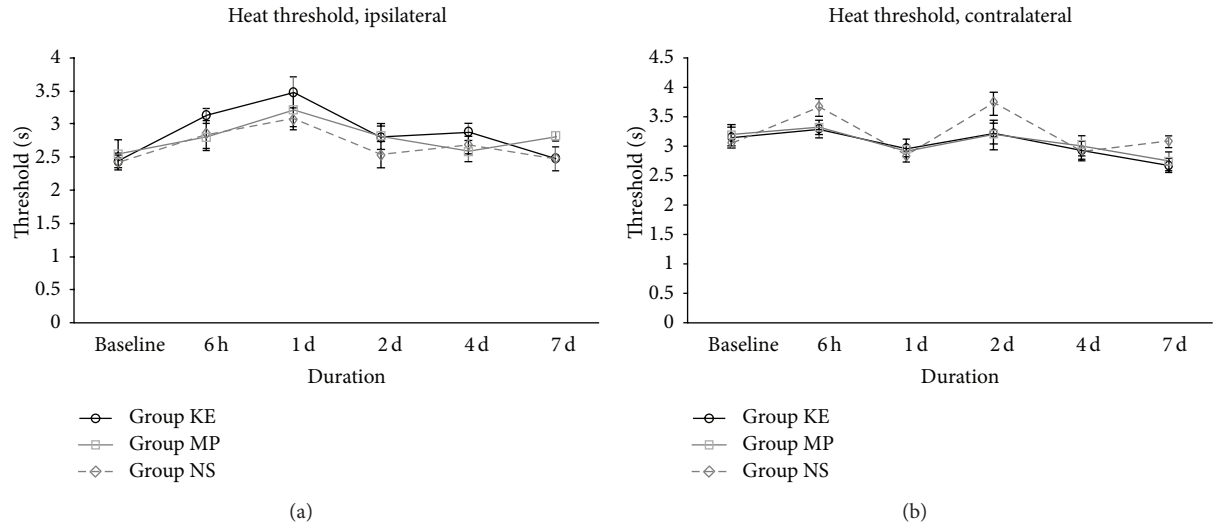

Figure 5: Heat thresholds of KE, MP, and NS groups on the ipsilateral (a) and contralateral side (b) from baseline before ischaemia to the first 7 days after reperfusion. There was no obvious difference of withdrawal threshold to fabricated radiant heat among all treatment groups in both ipsilateral and contralateral sides during the 7-day study period.

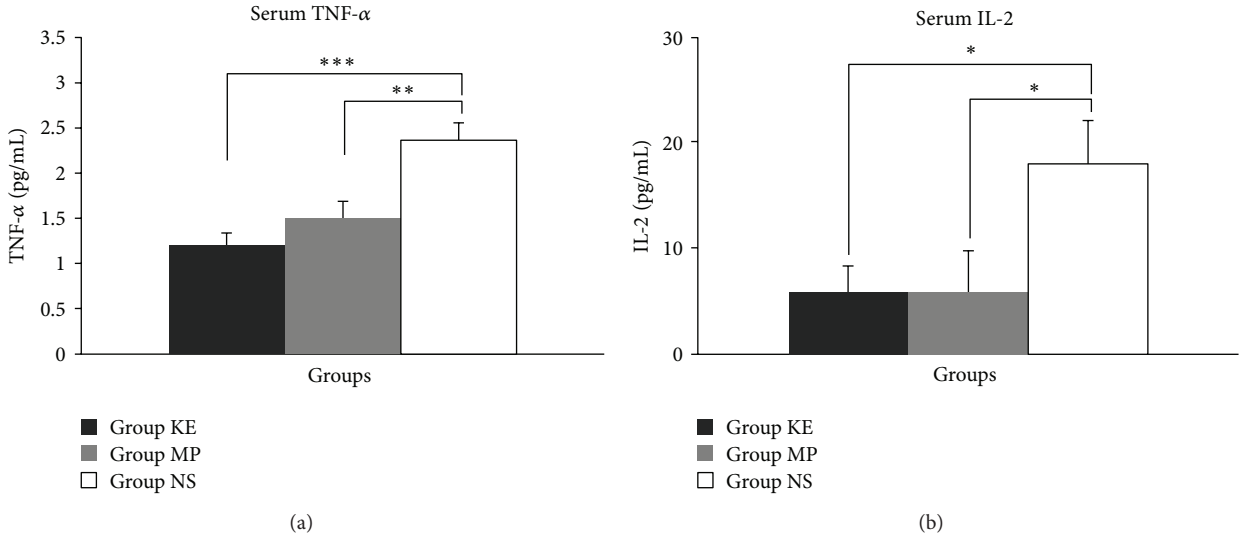

Figure 6: Serum TNF-α (a) and IL-2 (b) levels of KE, MP, and NS groups at the 48th hour after reperfusion. Compared with the NS group, serum TNF-α was significantly reduced in both KE ($P < 0.001$) and MP ($P < 0.01$) groups. Serum IL-2 was also significantly reduced in both KE and MP groups, compared with the NS group (all $P < 0.05$); $^{*}P < 0.05$; $^{**}P < 0.01$; $^{***}P < 0.001$.

at the transcriptional level by a decrease in c-fos-oncogene induction. Ketamine has also been found to have anti-inflammatory effects [10], which may partially explain the analgesic effect in pain conditions with an inflammatory component, such as CRPS-I. It has been used for treatment of CRPS clinically [26–28] and it has been shown that a single infusion of intravenous ketamine improved pain relief in patients with critical limb ischaemia [29]. However, there has been no laboratory study conducted prior to our study to evaluate the potential mechanisms of its action on the development of CRPS and its analgesic action on CPRS. In the present study, both ketamine and methylprednisolone were used to explore their effectiveness on CPIP-induced CRPS. Methylprednisolone (a glucocorticoid with powerful anti-inflammatory effects) was used as a positive control to determine whether ketamine had additional therapeutic effects on this ischemia-reperfusion pain model beyond any anti-inflammatory mechanism. Systemic TNF-α and IL-2 were assessed 48 hours after reperfusion because our preliminary data (unpublished) demonstrated that the difference in both TNF-α and IL-2 was significant when compared with the sham group (without ischemia-reperfusion). TNF-α was also shown to peak at this time point.

Based on the results of a previous study, glucocorticoid treatment appears to be associated with attenuation of pain symptoms by inhibiting inflammation and reducing

circulating inflammatory mediators [16]. Therefore, in this study, the mechanical and cold allodynia in the contralateral hindpaw were diminished by the administration of methylprednisolone. However, rats receiving methylprednisolone did not show a reduction in mechanical and cold allodynia in the ipsilateral (ischaemic) hindpaw when compared with the normal saline group. It seems that inflammation did contribute to postischaemic pain but that this was most likely to be only one of the mechanisms resulting in mechanical and cold allodynia in the ischaemic limb. Although it has been reported that glucocorticoids can inhibit symptoms of CRPS-II by preventing plasma extravasation [16, 29], oedema from local plasma extravasation was not significantly different between all three treatment groups in this study. Additional evidence indicates that inflammation is involved in the CRPS pathophysiologic mechanism. The pain produced by a low pH infusion into the normal, contralateral limb was similar to patients' who reported CRPS-I pain on the ipsilateral side [30]. Of the many pain-related inflammatory cytokines, only a limited number have been reported as being associated with neuropathic pain and CRPS. Willis proposed the involvement of inflammation in the CRPS pathophysiologic mechanism [31]. They demonstrated that the inflammatory mediators TNF-α and IL-2 were elevated in patients with CRPS-I [7]. In fact, TNF-α and IL-6 were also found in the local blister fluid of these patients [6].

In comparison with methylprednisolone, the therapeutic efficacy of ketamine has been shown to be superior in this study, and this finding most likely reflects its multimodal effects [14]. We found a decrease in serum proinflammatory cytokines TNF-α and IL-2, supporting an anti-inflammatory effect. Not only does ketamine relieve the major pain symptoms in most cases [32], but also it attenuates other inflammatory symptoms, including oedema and temperature [33]. Recently, a systematic review conducted by Dale and colleagues concluded that the intraoperative administration of ketamine could inhibit the early postoperative IL-6 inflammatory response [10]. However, pain relief was not one of the outcomes measured in the studies included in this review. Furthermore, in most studies ketamine was given at the induction of anaesthesia, but its role in modifying the ischemia-reperfusion response, including pain, has not been evaluated [10]. In this present study, we assessed whether the anti-inflammatory effects of ketamine could contribute to pain relief and preconditioning the early stage of CPIP after surgery to prevent further development of CRPS and confirmed the advantage of ketamine as an adjuvant analgesic.

Mechanismwise, Boettger and colleagues argued that dorsal root reflexes (DRR) might be linked to increased neuronal activity in the central terminal of primary afferent fibres and the aggravation of peripheral inflammation [34, 35]. Sensitization by inflammation leads to antidromic signalling in primary afferent neurons in DRR. Therefore, pain is being enhanced at one end, and neuropeptide release and inflammation are being aggravated at each cycle at the other [34, 35]. In addition, NMDA receptors were demonstrated to mediate responses of dorsal horn neurons to hindlimb ischemia in rat. NMDA receptors on the presynaptic membrane might act as autoreceptors for glutamate and enhance the incoming series of action potentials [36]. Furthermore, activation of postsynaptic NMDA receptors in the spinal cord by the increased release of glutamate from primary afferents can lead to central sensitization [37]. Thus, an NMDA antagonist such as ketamine blocks these receptors and might have significant effects in reducing the glutamate release from these terminals and further attenuating the inflammatory response [35].

In this study, ketamine administered soon after an ischaemia-reperfusion injury has been demonstrated to modify the postischaemic response with superior analgesic effects when compared to methylprednisolone and normal saline over the study period. Early hyperaemia followed by long lasting mechanical and cold allodynia resembles the two well-known phases of CRPS-I in humans [30, 38, 39]. We examined hyperaemia by measuring temperature in the hindpaws and there was an increase in temperature bilaterally in the first 4 hours after reperfusion which mimicked the sometimes brief hyperaemia seen in patients with CRPS-I. The fact that ketamine attenuated the increase in temperature in both hindpaws while methylprednisolone only affected the ipsilateral side suggests that ketamine has a more prominent effect on the hot oedematous stage in prevention of further progression of the disease. Apart from the anti-inflammatory effect, there are other mechanisms to explain these improved outcomes. Ketamine not only blocks the NMDA receptor [40], but also at a high dose blocks other receptors such as opioid and muscarinic cholinergic receptors [40]. It inhibits NMDA receptor-mediated central sensitization by blocking NMDA receptors, thereby reducing the mean opening time of the channel. It also decreases the frequency of channel opening by an allosteric mechanism [40]. Blockage of NMDA receptor-mediated sensitization results in attenuation of symptoms and signs, such as mechanical and cold allodynia. It is this action on the central nervous system that alleviates mechanical and cold allodynia, not only in the ipsilateral hindpaw but also in the contralateral hindpaw.

5. Conclusions

In conclusion, our study demonstrates that early treatment with ketamine can modify postischaemic responses resulting in less mechanical and cold allodynia and lower serum levels of proinflammatory cytokines including TNF-α and IL-2 in a CPIP model using SD rats. Although methylprednisolone can also reduce these cytokines, the analgesic efficacy was lower than that provided by ketamine. Early administration of ketamine can potentially be an effective approach in preventing further progression of pain conditions with an ischaemic and inflammatory pathogenesis, including CRPS. Clinical studies exploring the anti-inflammatory and analgesic effects of anaesthetic doses of ketamine after ischaemia-reperfusion injury are warranted.

Conflict of Interests

None of the authors have any conflict of interests to report.

Authors' Contribution

Suryamin Liman was involved in the design and execution of the experiments, Chi Wai Cheung was involved in the design of the study and proofreading the paper, Ka Lok Wong, Wai Tai, and Qiu Qiu were all involved in executing experiments and data analysis, and Kwok Fu Ng, Siu Wai Choi, and Michael Irwin were all involved in the write-up of the paper.

References

[1] H. M. Oerlemans, R. A. B. Oostendorp, T. De Boo, R. S. G. M. Perez, and R. J. A. Goris, "Signs and symptoms in complex regional pain syndrome type I/reflex sympathetic dystrophy: judgment of the physician versus objective measurement," *Clinical Journal of Pain*, vol. 15, no. 3, pp. 224–232, 1999.

[2] R. M. Atkins, "Complex regional pain syndrome," *The Journal of Bone and Joint Surgery—Series B*, vol. 85, no. 8, pp. 1100–1106, 2003.

[3] R. J. A. Goris, "Reflex sympathetic dystrophy: model of a severe regional inflammatory response syndrome," *World Journal of Surgery*, vol. 22, no. 2, pp. 197–202, 1998.

[4] C. Schinkel, A. Gaertner, J. Zaspel, S. Zedler, E. Faist, and M. Schuermann, "Inflammatory mediators are altered in the acute phase of posttraumatic complex regional pain syndrome," *Clinical Journal of Pain*, vol. 22, no. 3, pp. 235–239, 2006.

[5] N. Üçeyler, T. Eberle, R. Rolke, F. Birklein, and C. Sommer, "Differential expression patterns of cytokines in complex regional pain syndrome," *Pain*, vol. 132, no. 1-2, pp. 195–205, 2007.

[6] F. J. P. M. Huygen, A. G. J. de Bruijn, M. T. de Bruin, J. George Groeneweg, J. Klein, and F. J. Zijlstra, "Evidence for local inflammation in complex regional pain syndrome type 1," *Mediators of Inflammation*, vol. 11, no. 1, pp. 47–51, 2002.

[7] C. Schinkel, A. Scherens, M. Köller, G. Roellecke, G. Muhr, and C. Maier, "Systemic inflammatory mediators in post-traumatic complex regional pain syndrome (Crps I)—longitudinalinvestigations and differences to control groups," *European Journal of Medical Research*, vol. 14, no. 3, pp. 130–135, 2009.

[8] C. Sommer, "The role of cytokines in pain," in *Current Topics in Pain: 12th World Congress on Pain*, J. Castro-Lopes, Ed., pp. 95–113, IASP Press, 2009.

[9] G. Hocking and M. J. Cousins, "Ketamine in chronic pain management: an evidence-based review," *Anesthesia & Analgesia*, vol. 97, no. 6, pp. 1730–1739, 2003.

[10] O. Dale, A. A. Somogyi, Y. Li, T. Sullivan, and Y. Shavit, "Does intraoperative ketamine attenuate inflammatory reactivity following surgery? A systematic review and meta-analysis," *Anesthesia and Analgesia*, vol. 115, no. 4, pp. 934–943, 2012.

[11] P. Azari, D. R. Lindsay, D. Briones, C. Clarke, T. Buchheit, and S. Pyati, "Efficacy and safety of ketamine in patients with complex regional pain syndrome: a systematic review," *CNS Drugs*, vol. 26, no. 3, pp. 215–228, 2012.

[12] T. J. Coderre, D. N. Xanthos, L. Francis, and G. J. Bennett, "Chronic post-ischemia pain (CPIP): a novel animal model of complex regional pain syndrome-Type I (CRPS-I; reflex sympathetic dystrophy) produced by prolonged hindpaw ischemia and reperfusion in the rat," *Pain*, vol. 112, no. 1-2, pp. 94–105, 2004.

[13] A. Laferriere, M. Millecamps, D. N. Xanthos, W. Xiao, G. J. Bennett, and T. J. Coderre, "142 chronic post-ischemia pain: a novel animal model suggests that ischemia-reperfusion (I-R) injury, no-reflow and chronic tissue ischemia contribute to CRPS-I," *European Journal of Pain*, vol. 11, supplement 1, pp. S61–S62, 2007.

[14] C. R. Cámara, F. J. Guzmán, E. A. Barrera et al., "Ketamine anesthesia reduces intestinal ischemia/reperfusion injury in rats," *World Journal of Gastroenterology*, vol. 14, no. 33, pp. 5192–5196, 2008.

[15] G. Subhas, A. Gupta, D. Bakston et al., "Protective effect of methylprednisolone on warm ischemia-reperfusion injury in a cholestatic rat liver," *American Journal of Surgery*, vol. 199, no. 3, pp. 377–381, 2010.

[16] K. Hargreaves, R. Dubner, F. Brown, C. Flores, and J. Joris, "A new and sensitive method for measuring thermal nociception in cutaneous hyperalgesia," *Pain*, vol. 32, no. 1, pp. 77–88, 1988.

[17] J.-J. Vatine, R. Argov, and Z. Seltzer, "Brief electrical stimulation of c-fibers in rats produces thermal hyperalgesia lasting weeks," *Neuroscience Letters*, vol. 246, no. 3, pp. 125–128, 1998.

[18] L. van der Laan, P. Kapitein, A. Verhofstad, T. Hendriks, and R. J. A. Goris, "Clinical signs and symptoms of acute reflex sympathetic dystrophy in one hindlimb of the rat, induced by infusion of a free-radical donor," *Acta Orthopaedica Belgica*, vol. 64, no. 2, pp. 210–217, 1998.

[19] L. van der Laan, P. J. C. Kapitein, W. J. G. Oyen, A. A. J. Verhofstad, T. Hendriks, and R. J. A. Goris, "A novel animal model to evaluate oxygen derived free radical damage in soft tissue," *Free Radical Research*, vol. 26, no. 4, pp. 363–372, 1997.

[20] L. van der Laan, W. J. G. Oyen, A. A. J. Verhofstad et al., "Soft tissue repair capacity after oxygen-derived free radical-induced damage in one hindlimb of the rat," *Journal of Surgical Research*, vol. 72, no. 1, pp. 60–69, 1997.

[21] G. Allen, B. S. Galer, and L. Schwartz, "Epidemiology of complex regional pain syndrome: a retrospective chart review of 134 patients," *Pain*, vol. 80, no. 3, pp. 539–544, 1999.

[22] J. Maleki, A. A. LeBel, G. J. Bennett, and R. J. Schwartzman, "Patterns of spread in complex regional pain syndrome, type I (reflex sympathetic dystrophy)," *Pain*, vol. 88, no. 3, pp. 259–266, 2000.

[23] C. J. Woolf and P. D. Wall, "Relative effectiveness of C primary afferent fibers of different origins in evoking a prolonged facilitation of the flexor reflex in the rat," *The Journal of Neuroscience*, vol. 6, no. 5, pp. 1433–1442, 1986.

[24] R. A. Sunder, G. Toshniwal, and G. P. Dureja, "Ketamine as an adjuvant in sympathetic blocks for management of central sensitization following peripheral nerve injury," *Journal of Brachial Plexus and Peripheral Nerve Injury*, vol. 3, article 22, 2008.

[25] T.-Z. Guo, T. Wei, and W. S. Kingery, "Glucocorticoid inhibition of vascular abnormalities in a tibia fracture rat model of complex regional pain syndrome type I," *Pain*, vol. 121, no. 1-2, pp. 158–167, 2006.

[26] F. Birklein, M. Weber, and B. Neundörfer, "Increased skin lactate in complex regional pain syndrome: evidence for tissue hypoxia?" *Neurology*, vol. 55, no. 8, pp. 1213–1215, 2000.

[27] C. Schinkel and M. H. Kirschner, "Status of immune mediators in complex regional pain syndrome type I," *Current Pain and Headache Reports*, vol. 12, no. 3, pp. 182–185, 2008.

[28] F. J. Guzmán-De la Garza, C. R. Cámara-Lemarroy, R. G. Ballesteros-Elizondo, G. Alarcón-Galván, P. Cordero-Pérez,

and N. E. Fernández-Garza, "Ketamine reduces intestinal injury and inflammatory cell infiltration after ischemia/reperfusion in rats," *Surgery Today*, vol. 40, no. 11, pp. 1055–1062, 2010.

[29] G. Tornero-Campello and J. M. Ramón, "Ketamine infusion for complex regional pain syndrome," *European Journal of Pain*, vol. 10, no. S1, p. S164, 2006.

[30] P. Shirani, A. R. Salamone, P. E. Schulz, and E. A. Edmondson, "Ketamine treatment for intractable pain in a patient with severe refractory complex regional pain syndrome: a case report," *Pain Physician*, vol. 11, no. 3, pp. 339–342, 2008.

[31] W. D. Willis Jr., "Dorsal root potentials and dorsal root reflexes: a double-edged sword," *Experimental Brain Research*, vol. 124, no. 4, pp. 395–421, 1999.

[32] M. K. Boettger, K. Weber, M. Gajda, R. Bräuer, and H.-G. Schaible, "Spinally applied ketamine or morphine attenuate peripheral inflammation and hyperalgesia in acute and chronic phases of experimental arthritis," *Brain, Behavior, and Immunity*, vol. 24, no. 3, pp. 474–485, 2010.

[33] H. Liu, H. Wang, M. Sheng, L. Y. Jan, Y. N. Jan, and A. I. Basbaum, "Evidence for presynaptic N-methyl-D-aspartate autoreceptors in the spinal cord dorsal horn," *Proceedings of the National Academy of Sciences of the United States of America*, vol. 91, no. 18, pp. 8383–8387, 1994.

[34] P. M. Dougherty, J. Palecek, V. Paleckova, L. S. Sorkin, and W. D. Willis, "The role of NMDA and non-NMDA excitatory amino acid receptors in the excitation of primate spinothalamic tract neurons by mechanical, chemical, thermal, and electrical stimuli," *The Journal of Neuroscience*, vol. 12, no. 8, pp. 3025–3041, 1992.

[35] F. Birklein, B. Riedl, N. Sieweke, M. Weber, and B. Neundörfer, "Neurological findings in complex regional pain syndromes—analysis of 145 cases," *Acta Neurologica Scandinavica*, vol. 101, no. 4, pp. 262–269, 2000.

[36] G. Wasner, J. Schattschneider, K. Heckmann, C. Maier, and R. Baron, "Vascular abnormalities in reflex sympathetic dystrophy (CRPS I): mechanisms and diagnostic value," *Brain*, vol. 124, no. 3, pp. 587–599, 2001.

[37] B. A. Orser, P. S. Pennefather, and J. F. MacDonald, "Multiple mechanisms of ketamine blockade of N-methyl-D-aspartate receptors," *Anesthesiology*, vol. 86, no. 4, pp. 903–917, 1997.

[38] K. Hirota, K. S. Sikand, and D. G. Lambert, "Interaction of ketamine with μ2 opioid receptors in SH-SY5Y human neuroblastoma cells," *Journal of Anesthesia*, vol. 13, no. 2, pp. 107–109, 1999.

[39] M. Narita, K. Yoshizawa, K. Aoki, M. Takagi, M. Miyatake, and T. Suzuki, "A putative sigma1 receptor antagonist NE-100 attenuates the discriminative stimulus effects of ketamine in rats," *Addiction Biology*, vol. 6, no. 4, pp. 373–376, 2001.

[40] J. Sleigh, M. Harvey, L. Voss, and B. Denny, "Ketamine—more mechanisms of action than just NMDA blockade," *Trends in Anaesthesia and Critical Care*, vol. 4, no. 2-3, pp. 76–81, 2014.

Hindawi Publishing Corporation
Oxidative Medicine and Cellular Longevity
Volume 2015, Article ID 585297, 8 pages
http://dx.doi.org/10.1155/2015/585297

Research Article

Adenosine 2B Receptor Activation Reduces Myocardial Reperfusion Injury by Promoting Anti-Inflammatory Macrophages Differentiation via PI3K/Akt Pathway

Yikui Tian,[1,2] Bryan A. Piras,[3] Irving L. Kron,[1] Brent A. French,[3] and Zequan Yang[1,3]

[1]*Department of Surgery, University of Virginia, P.O. Box 800709, Charlottesville, VA 22908, USA*
[2]*Department of Cardiovascular Surgery, Tianjin Medical University General Hospital, Tianjin 300052, China*
[3]*Department of Biomedical Engineering, University of Virginia, Charlottesville, VA 22908, USA*

Correspondence should be addressed to Zequan Yang; zy6b@virginia.edu

Received 18 September 2014; Revised 9 December 2014; Accepted 11 December 2014

Academic Editor: Zhengyuan Xia

Background. Activation of the adenosine A_{2B} receptor ($A_{2B}R$) can reduce myocardial ischemia/reperfusion (IR) injury. However, the mechanism underlying the $A_{2B}R$-mediated cardioprotection is less clear. The present study was designed to investigate the potential mechanisms of cardioprotection mediated by $A_{2B}R$. *Methods and Results*. C57BL/6 mice underwent 40-minute ischemia and 60-minute reperfusion. ATL-801, a potent selective $A_{2B}R$ antagonist, could not block ischemic preconditioning induced protection. BAY 60-6583, a highly selective $A_{2B}R$ agonist, significantly reduced myocardial infarct size, and its protective effect could be blocked by either ATL-801 or wortmannin. BAY 60-6583 increased phosphorylated Akt (p-Akt) levels in the heart at 10 min of reperfusion, and this phosphorylation could also be blocked by ATL-801 or wortmannin. Furthermore, BAY 60-6583 significantly increased M2 macrophages and decreased M1 macrophage and neutrophils infiltration in reperfused hearts, which also could be blocked by wortmannin. Meanwhile, confocal imaging studies showed that the majority of Akt phosphorylation in the heart was colocalized to CD206+ cells in both control and BAY 60-6583 pretreated hearts. *Conclusion*. Our results indicated that pretreatment with BAY 60-6583 protects the heart against myocardial IR injury by its anti-inflammatory effects, probably by modulating macrophages phenotype switching via a PI3K/Akt pathway.

1. Introduction

The adenosine receptor (AR) family comprises four subtypes: A_1, A_{2A}, A_{2B}, and A_3. They are widely distributed in mammalian species. The $A_{2B}R$ is the fourth AR subtype identified, and to date there is much less information available on the precise role of this receptor compared to the other AR subtypes. This notwithstanding an increasing body of evidence demonstrates that activation of $A_{2B}Rs$ by the selective $A_{2B}R$ agonist, BAY 60-6583, either before ischemia [1, 2] or before reperfusion [3, 4] reduces myocardial infarct size. Thus, pharmaceutical preconditioning with $A_{2B}R$ activation has been shown to protect against myocardial I/R injury, but the role of $A_{2B}Rs$ in IPC remains controversial.

Using an *in vivo* mouse model of IPC and genetic knockouts of ARs, Eckle et al. challenged the mechanism of A_1R-mediated IPC [5–7] by proposing that $A_{2B}Rs$, not A_1Rs, are essential in mediating IPC via an adenosine signaling pathway involving ecto-5′-nucleotidase [1]. However, Maas et al. reported that $A_{2B}R$ activation is not required for IPC in either rat or mouse models. Nevertheless, they did find that pretreatment prior to index ischemia with an $A_{2B}R$ agonist did reduce IR injury, but to a lesser degree compared to that of IPC [2]. Interestingly, another study reported by Eckle's group [8] recently demonstrated that BAY 60-6583 protected the heart against IR injury not by acting on cardiomyocytes but by activating the $A_{2B}R$ on bone marrow derived cells and reducing inflammatory cell infiltration in reperfused heart. The discrepancies between these published results call for more studies to clarify the role of $A_{2B}Rs$ in IPC and to explore the mechanisms underlying the $A_{2B}R$-mediated cardioprotection against IR injury.

By using a well-established intact mouse model with myocardial IR injury, the current study was undertaken to further define the roles of the $A_{2B}R$ in IPC and its anti-inflammatory effects during myocardial IR injury.

2. Materials and Methods

This study conformed to the Guide for the Care and Use of Laboratory Animals published by the National Institutes of Health (Eighth Edition, revised 2011) and was conducted under protocols approved by the University of Virginia's Institutional Animal Care and Use Committee.

2.1. Agents and Chemicals. 2,3,5-Triphenyltetrazolium chloride (TTC) and wortmannin were purchased from Sigma-Aldrich (St. Louis, MO). Phthalo blue was purchased from Heucotech Ltd. (Fairless Hills, PA). BAY 60-6583 was purchased from Tocris Bioscience (Bristol, UK). ATL-801 was kindly provided by Lewis and Clark Pharmaceuticals, Inc. (Charlottesville, VA). Antibodies against phospho-Akt and total Akt were purchased from Cell Signaling Technology (Beverly, MA). Ly-6B.2 and CD206 antibodies for neutrophils staining were from ABDSerotec (Oxford, UK). CD45 antibody was from BD Biosciences (San Jose, CA). All fluorochrome-conjugated secondary antibodies and Prolong Gold antifade reagent with DAPI were from Life Technologies (Grand Island, NY).

2.2. Animals and Experimental Protocol. C57BL/6 mice (9-13 weeks old, purchased from Jackson Laboratories) were assigned to 6 different groups as shown in Figure 1. These mice underwent 40 min of LAD occlusion followed by 60 min of reperfusion with or without IPC. IPC was applied to mice with two cycles of 5- minute ischemia and 5-minute reperfusion. In the treated groups, BAY 60-6583 (100 μg/kg, iv) was administered 15 minutes before index LAD occlusion. ATL-801 (100 μg/kg, iv) was administered 5 minutes before either BAY 60-6583 injection or IPC. Wortmannin (25 μg/kg, iv) was administered 5 minutes before BAY 60-6583 injection. The doses of the BAY 60-6583, ATL-801, and wortmannin used in this study were equal to or less than those used in the literature, which reported no significant effect on hemodynamics. Additional 3 mice from each group were undergoing sham surgery. We monitored heart rate and found no significant difference when compared to control groups (Table 1). The hearts were harvested at the end of the experiments for infarct size measurement or immunostaining. Effects of BAY 60-6583 on phosphorylated-Akt (p-Akt) levels in hearts which underwent 40 minutes of ischemia followed by 10 minutes of reperfusion were tested by western blot. The hearts from BAY 60-6583 + ATL-801 or BAY 60-6583 + wortmannin groups were also harvested for p-Akt analysis.

2.3. Myocardial Ischemia/Reperfusion Injury and Measurement of Infarct Size. Mice were subjected to 40 minutes of coronary occlusion followed by 60 minutes of reperfusion as detailed previously [5, 9–11]. Briefly, mice were anesthetized with sodium pentobarbital (100 mg/kg i.p.) and orally intubated. Artificial respiration was maintained with a FiO_2 of 0.80, 100 strokes per minute, and a 0.2 to 0.5 mL stroke volume. The heart was exposed through a left thoracotomy. A 7-0 silk suture was placed around LAD at a level 1 mm inferior to the left auricle and a miniature balloon occluder fashioned from Microbore Tygon tubing (Small Parts Inc., Seattle, WA) was affixed over the LAD. Ischemia and reperfusion were induced by inflating or deflating the balloon, respectively. ECG was monitored perioperatively using PowerLab instrumentation (ADInstruments, Colorado Springs, CO). The mice were euthanized 60 minutes after reperfusion, and the hearts were cannulated through the ascending aorta for perfusion with 3 to 4 mL of 1.0% TTC. The LAD was then reoccluded with the same suture used for coronary occlusion prior to 10% Phthalo blue perfusion to determine risk region (RR). The left ventricle was then cut into 5 to 7 transverse slices that were weighed and digitally photographed to determine infarct size as a percent of RR.

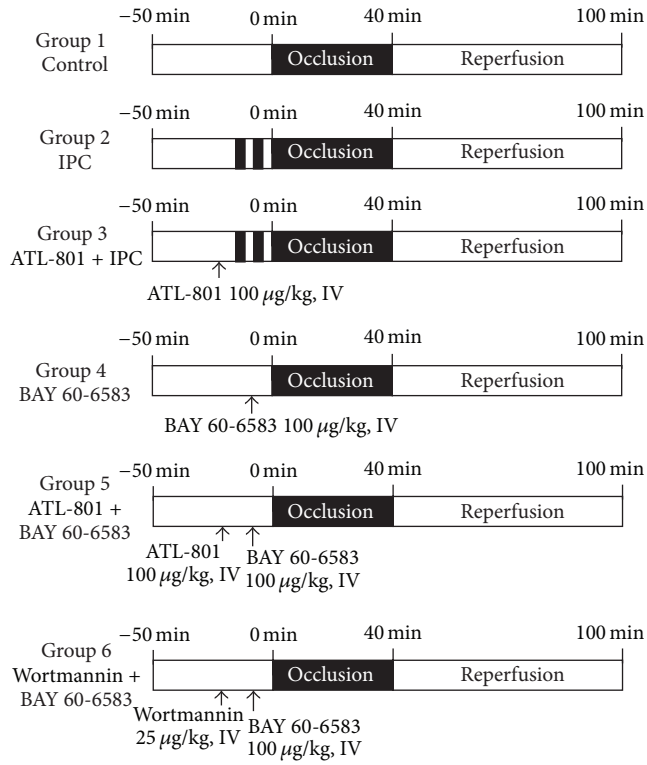

Figure 1: Experimental protocol. All mice underwent 40 min ischemia followed by 60 min reperfusion. At the end of experiments, hearts were harvested for TTC staining to determine the myocardial infarct size. IPC: ischemic preconditioning.

2.4. Western Blot Analysis. The total protein was extracted from the indicated experimental groups using RIPA buffer and protein concentration was determined by BCA protein assay (Thermo Scientific, Rockford, IL). All western blots were performed according to standard procedures. Twenty micrograms of protein was separated by 10% SDS-PAGE. After transfer, nitrocellulose membranes (BioRad, Hercules,

Table 1: Perioperative heart rates.

Groups	Baseline	During ischemia	Reperfusion
Control	437 ± 20	479 ± 18*	480 ± 20*
IPC	438 ± 9	492 ± 8*	494 ± 6*
ATL + IPC	440 ± 8	486 ± 6*	496 ± 5*
BAY	431 ± 13	485 ± 11*	481 ± 13*
ATL + BAY	411 ± 10	503 ± 15*	501 ± 11*
Wort + BAY	433 ± 6	502 ± 9*	501 ± 8*

IPC: ischemic preconditioning; ATL: ATL-801; BAY: BAY 60-6583; Wort: wortmannin.
*$P < 0.05$ versus baseline.

CA) were probed with primary antibodies against total Akt (t-Akt) or S473 (p-Akt) at a 1 : 2,000 dilution and secondary antibodies (Promega, Madison, WI) at a 1 : 5,000 dilution in blocking solution (0.5% BSA in TBS-T). Proteins were visualized with enhanced chemiluminescent substrate (Thermo Scientific, Rockford, IL), followed by densitometry analysis using Fluorchem 8900 imaging system (Alpha Innotech, Santa Clara, CA).

2.5. Immunohistochemistry for Neutrophils. The hearts were harvested and immediately fixed in 4% paraformaldehyde in PBS (pH 7.4) for paraffin embedding. Paraffin-embedded sections (5 μm) were rehydrated and incubated with 1% hydrogen peroxide. After being rinsed in PBS, the sections were incubated with 10% blocking serum. Immunostaining was performed with rat anti-mouse Ly-6B.2 antibody. Biotinylated secondary antibody was then applied for 1 hour at room temperature. After incubation with avidin-biotin complex, immunoreactivity was visualized by incubating the sections with 3,3-diaminobenzidine tetrahydrochloride to produce a brown precipitate.

2.6. Immunofluorescence Staining. In order to determine the localization of p-Akt expression, immunofluorescence staining was performed on hearts after 40 minutes of ischemia and 10 minutes of reperfusion in control or BAY 60-6583 treated groups. Cardiac macrophage polarization was detected after 60 minutes of reperfusion by defining M1 and M2 subsets of macrophages. Hearts were fixed in 4% paraformaldehyde in PBS (pH 7.4) for 1 hour at room temperature and then incubated in 30% sucrose overnight at 4°C before freezing in OCT. Frozen sections were cut and permeabilized by 0.3% TritonX-100 in PBS. After blocking with 10% normal serum for 1 hour, specimens were colabeled with anti-p-Akt and anti-CD45 or anti-CD206 antibody overnight at 4°C for colocalization detection. For macrophage staining, specimens were incubated with CD86 or CD163 antibodies to identify the M1 and M2 macrophages, respectively. After washing, sections were incubated with a mixture of Alexa Fluor 488- and Alexa Fluor 594-conjugated secondary antibodies for 1 hour. Prolong Gold antifade reagent with DAPI was used to mount the specimens. All images were acquired under the same parameters for each fluorochrome using an Olympus BX-41 Microscope (Olympus, America, Inc., Center Valley, PA) with a Retiga-2000R camera (QImaging, Surrey, BC). Further image processing was performed using Image J software (NIH).

2.7. Statistical Analysis. All data are presented as the mean ± SEM (standard error of the mean). Peri-ischemic heart rate changes were analyzed using a repeated measures ANOVA followed by Bonferroni pairwise comparisons. All other data were compared using one-way ANOVA followed by t-test for unpaired data with Bonferroni correction.

3. Results

3.1. Perioperative Heart Rate Changes. Table 1 shows changes in heart rate before, during, and after LAD occlusion. Consistent with previous reports, heart rate was increased significantly after LAD occlusion and remained elevated until early reperfusion compared with baseline in all groups. There was no significant difference in heart rates between control and treated mice.

3.2. Role of $A_{2B}R$ in IPC-Induced Infarct-Sparing Effect. Three groups of mice which underwent 40 minutes of LAD occlusion followed by 60 minutes of reperfusion were designed to investigate the role of $A_{2B}R$ in IPC phenomenon. There was no significant difference of risk region (RR) among the three groups. Infarct size in the IPC-treated group (19.2 ± 2.7% of RR) was significantly reduced compared with the control group (49.6 ± 1.4% of RR, $P < 0.05$). Administration of $A_{2B}R$ selective antagonist, ATL-801, 5 minutes before IPC could not block the cardioprotective effects (18.7 ± 1.4% versus 19.2 ± 2.7% of RR, $P > 0.05$) (Figure 2).

3.3. Activation of $A_{2B}R$ Reduced Myocardial IR Injury Is Mediated by PI3K/Akt Pathway. BAY 60-6583 had no effects on heart rate during the peri-ischemic phase (Table 1). Administration of BAY 60-6583 15 minutes before LAD occlusion had significant infarct-sparing effects against myocardial reperfusion injury (21.0 ± 1.3% versus 49.6 ± 1.4% of RR, $P < 0.05$). Pretreating the mice with ATL-801 before BAY 60-6583 administration completely blocked the cardioprotective effect (48.6 ± 2.4% of RR, $P < 0.05$, compared with BAY group) (Figure 3). As shown in Figure 3, the infarct-sparing effect of BAY 60-6583 was completely abrogated by wortmannin, a selective PI3K inhibitor, administered 5 minutes before BAY administration (45.0 ± 3.2% of RR, $P < 0.05$ compared with BAY group). Furthermore, western blot results showed that BAY 60-6583 significantly increased p-Akt levels in heart tissue undergoing 40 minutes of ischemia and 10 minutes of reperfusion. This effect was completely abolished by pretreating the mice with either ATL-801 or wortmannin 5 minutes before BAY 60-6583 administration (Figure 4).

3.4. Administration of $A_{2B}R$ Agonist Presents Local Anti-Inflammatory Effects after Myocardial IR Injury. It has been reported that activation of $A_{2B}R$ has anti-inflammatory effects by promoting macrophages phenotype switching. Also activated PI3K/Akt pathway has been shown to modulate

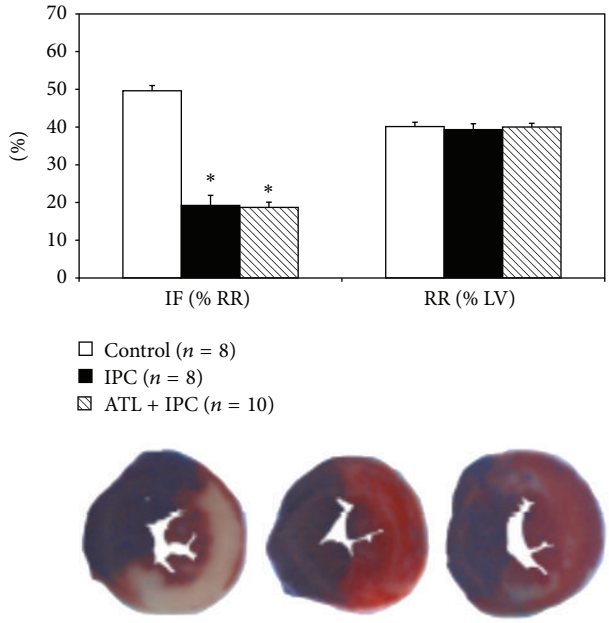

Figure 2: Role of $A_{2B}R$ antagonist in ischemic preconditioning. Pretreating mice with ATL-801, an $A_{2B}R$ selective antagonist, did not block the cardioprotective effect of IPC as compared with the control group ($^*P < 0.05$). IF: infarct size; RR: risk region; LV: left ventricle; IPC: ischemic preconditioning; ATL: ATL-801.

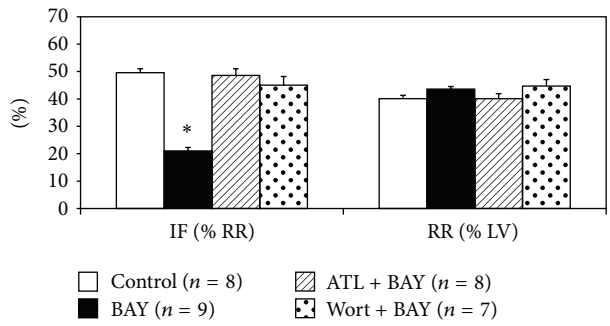

Figure 3: Role of $A_{2B}R$ in myocardial IR injury. Pretreating mice with BAY 60-6583, a potent $A_{2B}R$ agonist, reduced myocardial infarct size, an effect that was abolished by either ATL-801 or the PI3K inhibitor: wortmannin. IF: infarct size; RR: risk region; BAY: BAY 60-6583; ATL: ATL-801; Wort: wortmannin. $^*P < 0.05$ compared with control group.

macrophages to M2 anti-inflammatory subset. Thus, we hypothesized that BAY 60-6583 may protect the heart by regulating cardiac macrophages phenotype via PI3K/Akt pathway and presenting anti-inflammatory effects. Immunofluorescence staining was used to identify macrophage subsets. In sham mouse heart, there were few M1 macrophages (CD86+) but more M2 macrophages (CD163+). IR significantly increased the M1 and decreased the M2 macrophages number. Compared with the IR group, BAY 60-6583 restored the macrophage polarization to a M2 phenotype (Figure 5), which could also be abolished by wortmannin. In addition, confocal staining results showed that remarkable p-Akt

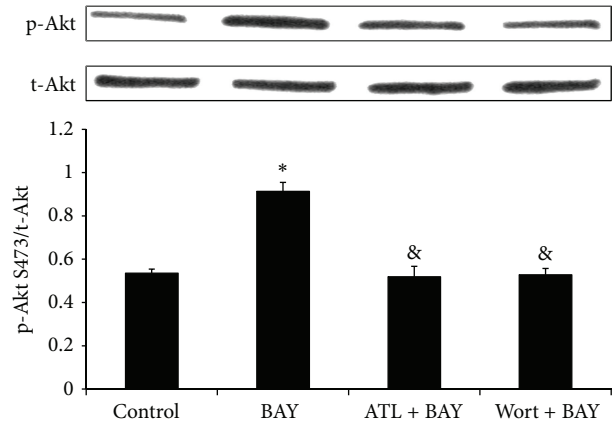

Figure 4: Phospho-Akt to total Akt ratio in heart tissue. The ratio of phospho-Akt S473 to total Akt (the bar graph) was measured by densitometry, where the total Akt inputs were normalized to 1. BAY 60-6583 pretreatment increased p-Akt level after 10 minutes of reperfusion, which was blocked by either ATL-801 or wortmannin. BAY: BAY 60-6583; ATL: ATL-801; Wort: wortmannin. $^*P < 0.05$ compared with control group; $^{\&}P < 0.05$ compared with BAY group.

expressions were colocalized with CD45+ cells (Figure 6(a)). In order to further identify these CD45+ cells, we performed additional confocal microscopy studies on tissue sections immunostained with p-Akt and CD206 antibodies, another specific marker of M2 macrophages. As shown in Figure 6(b), although a few of the p-Akt+ cells were CD206 negative, the majority of the p-Akt expression colocalized with M2 macrophages. These results suggest that BAY 60-6583 may protect the heart by promoting macrophage phenotype switching to anti-inflammatory subsets via the PI3K/Akt pathway. Immunohistochemistry was used to stain neutrophils in hearts undergoing 40 minutes of ischemia and 60 minutes of reperfusion. When pretreated with BAY 60-6583 before IR, neutrophil infiltration was significantly reduced. Consistent with the infarct size results, this anti-inflammatory effect of BAY 60-6583 could be blocked by both ATL-801 and wortmannin, respectively (Figure 7).

4. Discussion

For over a decade, abundant evidence has accumulated to demonstrate that brief periods of myocardial ischemia (IPC) activate the A1R to protect the heart against the subsequent prolonged ischemia [5, 12–15]. Activation of A1Rs triggers the survival signal transduction pathway through the enhanced phosphorylation of Akt [15–17]. This event mostly likely occurs inside cardiomyocytes, thus rendering them more resistant to the subsequent ischemic insult [5, 12]. Eckle and colleagues [1] recently proposed that cardioprotective effect of IPC was mediated via CD73-dependent generation of extracellular adenosine and signaling through the $A_{2B}R$, the lowest-affinity receptor among the 4 subtypes of adenosine receptor. $A_{2B}R$KO mice demonstrate increased susceptibility to acute IR injury and are not protected by IPC. However, Maas and colleagues evaluated the role of $A_{2B}R$ activation

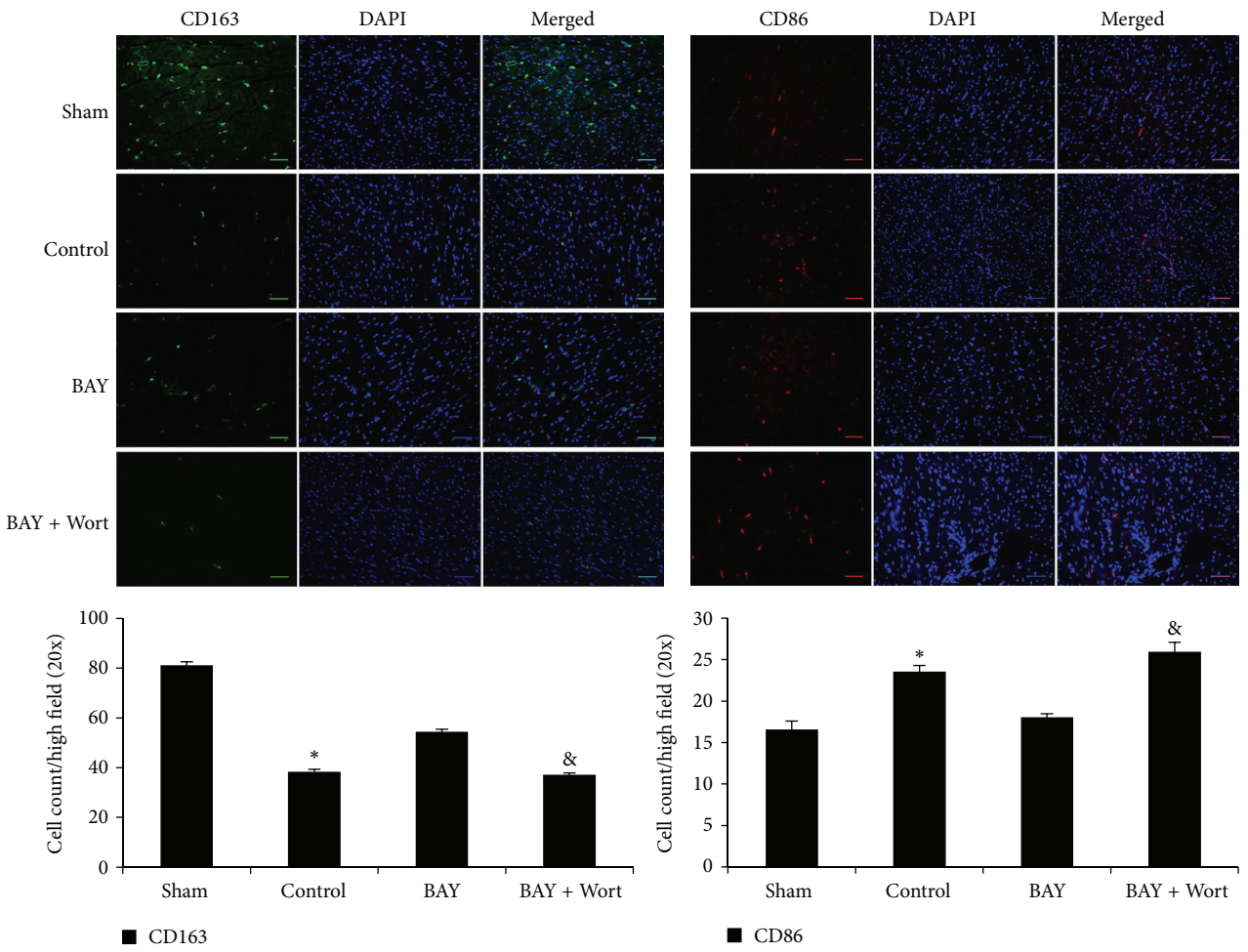

Figure 5: Cardiac macrophages polarization after IR injury. There are mainly M2 subsets macrophages in normal heart. IR reduced the number of M2 subset (CD163, green staining) macrophages and increased M1 subset (CD86, red staining). BAY 60-6583 pretreatment significantly restored the macrophage polarization during reperfusion. Wortmannin, a PI3K inhibitor, blocked the effects of BAY 60-6583. DAPI was used to stain the nuclei. Scale bar: 50 μm. IR: ischemia and reperfusion injury; BAY: BAY 60-6583; Wort: wortmannin. $^{*}P < 0.05$ compared with sham or BAY groups; $^{\&}P < 0.05$ compared with BAY groups.

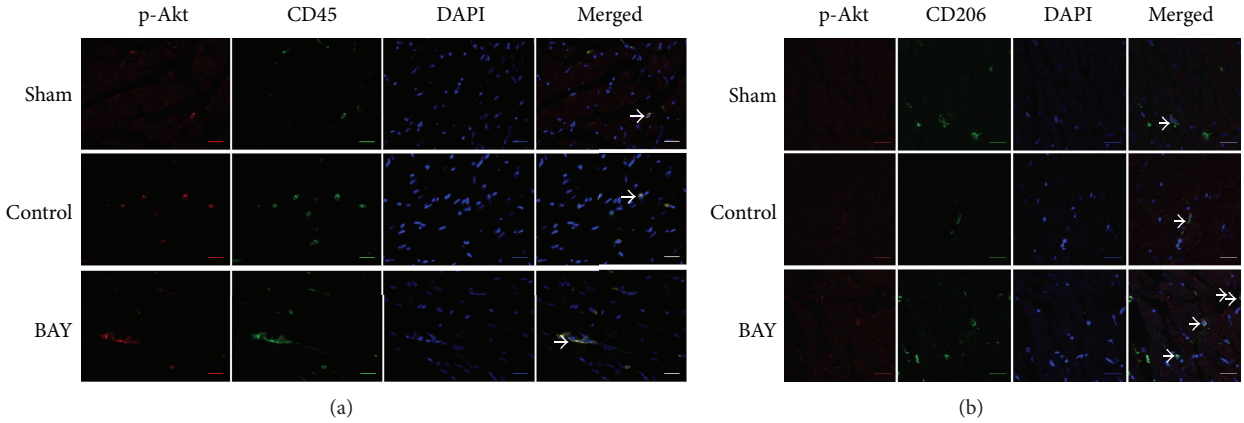

Figure 6: Confocal staining of p-Akt and immune cells in the heart. Hearts were harvested from mice with 40 min/10 min IR injury for staining to determine the localization of p-Akt expression. (a) In the ischemic area or lower anterior wall of the left ventricle, higher p-Akt expression (red staining) was colocalized with CD45 signal (green staining) in all groups. Scale bar: 20 μm. (b) The majority of strong p-Akt expression (red staining) was colocated with CD206 expression (green staining), which is a specific marker of M2 macrophages. Scale bar: 20 μm. Arrows indicate coexpression of p-Akt and CD45 or CD206. 4′,6-Diamidino-2-phenylindole (DAPI, blue staining) was used to stain the nuclei. IR: ischemia and reperfusion injury; BAY: BAY 60-6583.

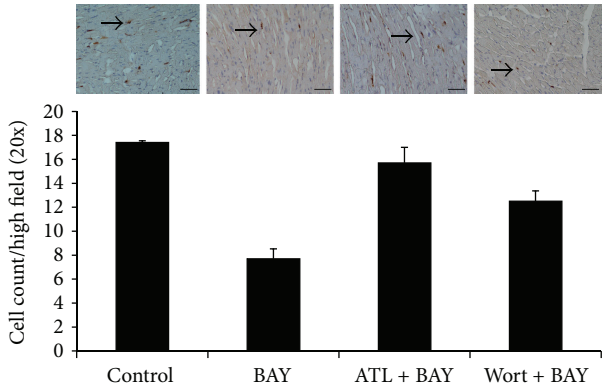

Figure 7: Neutrophils infiltration after IR injury. BAY 60-6583 significantly reduced neutrophil infiltration (brown staining) after IR injury, which could be blocked by either ATL-801 or wortmannin. Scale bar: 50 μm. Arrows indicate neutrophils. BAY: BAY 60-6583; ATL: ATL-801; Wort: wortmannin. $^{*}P < 0.05$ compared with other groups.

or inhibition in both *ex vivo* and *in vivo* mouse/rat models with myocardial IR injury and found that IPC-induced cardioprotection was not dependent upon $A_{2B}R$ activation and also existed in a different strain of A_{2B}RKO mice [2]. It should be noted that the lowest affinity for adenosine could make $A_{2B}R$ be the last receptor activated by endogenous adenosine, which is the core mechanism of IPC [18], although $A_{2B}R$ might be sensitized by PKC at reperfusion phase [19]. Also $A_{2B}R$ expression at the mRNA level is very low in the heart when compared to other organs [20] or other adenosine receptors [21]. Moreover, there has been no physical evidence so far to demonstrate that A_{2B}Rs can be detected on the sarcolemma of cardiomyocytes, but increased $A_{2B}R$ mRNA expression has been reported after IR injury [22], which may be derived from infiltrating inflammatory cells. By employing the same *in vivo* mouse model we used previously [9, 11, 17, 23], the current study demonstrated activation of A_{2B}Rs before ischemia reduced myocardial infarct size, probably by inhibiting inflammatory responses during reperfusion, not by preconditioning cardiomyocytes (Figures 2 and 3).

Accumulating evidences have shown that inflammatory responses play important roles during myocardial reperfusion injury [10, 11, 24, 25]. $A_{2B}R$ has been shown to have anti-inflammatory effects in several *in vitro* and *in vivo* animal models. Yang and colleagues [26] found that A_{2B}RKO mice present proinflammatory phenotype. They found that more inflammatory cytokines, such as TNF-alpha and IL-6, increased in serum of A_{2B}RKO mice compared with wild-type mice. Konrad and colleagues [27] reported that BAY 60-6583, a specific $A_{2B}R$ agonist, acts on hematopoietic cells to inhibit PMN migration into lung interstitium. BAY 60-6583 also has been shown to inhibit TNF-alpha secretion from macrophages after vascular injury [28]. Consistent with these studies, we found that BAY 60-6583 significantly promoted macrophages phenotype switching to a M2 (anti-inflammatory) subset and reduced neutrophils infiltration after myocardial IR injury (Figures 5 and 7). Indeed, $A_{2B}R$ has been shown to be able to modulate macrophage phenotype to an anti-inflammatory M2 subset and increase IL-10 expression in both cultured macrophage and dendritic cell [29, 30], which are consistent with our findings that $A_{2B}R$ agonist promoted the cardiac macrophage transforming to an anti-inflammatory M2 phenotype. Indeed, previous studies have shown that BAY 60-6583 provided potent cardioprotection in a Krebs-perfused isolated heart model. However, it is worthwhile to note that there actually are several residential macrophages and dendritic cells in the heart, which may mediate the cardioprotection of the $A_{2B}R$ agonist. Further study is warranted to investigate the mechanism of how these residential immune cells regulate myocardial IR injury.

Activation of PI3K/Akt pathway in immune cells has been reported providing anti-inflammatory effect by upregulating IL-10 expression [31, 32]. The relationship between $A_{2B}R$ activation and PI3K/Akt pathway is not well established. Kuno and colleagues [3] reported that activation of $A_{2B}R$ increased p-Akt levels in a rabbit model, although a nonselective adenosine receptor agonist was used. It is also reported that activation of $A_{2B}R$ contributes to PI3K/Akt activation and subsequent eNOS phosphorylation in penile endothelia [33]. In present study, we found that after 40 minutes of ischemia and 10 minutes of reperfusion, phosphorylation of Akt in the heart was significantly increased in mice treated with $A_{2B}R$ agonist, which could be blocked by either ATL-801, a selective $A_{2B}R$ antagonist, or wortmannin, a PI3K inhibitor (Figure 4). Since activation of PI3K/Akt pathway in nonimmune cells, such as cardiomyocytes [34] or endothelial cells [35], could enhance cellular survival or inhibit oxidative stress, we further performed confocal imaging analysis to determine the location of p-Akt expression. The results showed that the majority of p-Akt expression was localized to CD206+ cells, a specific marker for M2 macrophages, in both control and BAY 60-6583 pretreated mice. In addition, the PI3K inhibitor attenuated the anti-inflammatory effects of BAY 60-6583 (Figures 5–7). These findings strongly suggest that BAY 60-6583 exerts its infarct-limiting effect not by acting on cardiomyocytes but possibly by acting on macrophages via a PI3K/Akt pathway.

It should be noted that a regulatory inflammation environment could promote macrophages phenotype switch to M2 subset [36]. Although our results strongly indicated BAY 60-6583 modulates macrophages phenotype switching after myocardial IR injury, there are several cell types other than macrophages which may mediate BAY 60-6583 induced cardioprotection, which warrants further studies. Koeppen and his colleagues [8] demonstrated that BAY 60-6583 protects heart from myocardial ischemia and reperfusion injury by acting on bone marrow derived cells. They found that BAY 60-6583 inhibited tumor necrosis factor α release of PMNs, which limited myocardial injury. van der Hoeven and his colleagues [37] showed that $A_{2B}R$ activation suppressed oxidase activity in neutrophils. Moreover, $A_{2B}R$ was also found in dendritic cells and lymphocytes. Studies are needed to define the roles of these cells during myocardial IR injury and the cardioprotection effects of $A_{2B}R$.

In present study, we did not analyze the cardiac function after myocardial reperfusion injury. However, it is well known that histological determination of myocardial infarction has

been widely used to estimate the cardiac injury in animal models [38] and utilized as the golden standard to validate novel imaging methods of infarction quantification, including cardiac MRI [39] and contrast echocardiography [40]. Moreover, using a cardiac MRI imaging technique, we have defined in our previous publication that left ventricular function is depressed proportionally to the size of infarction, which was determined by the same TTC staining technique in the present study [41]. Hence, it is reasonable to speculate that BAY 60-6583 could improve the cardiac function after reperfusion injury. However, further study is warranted to determine the role of $A_{2B}R$ activation during long-term ventricular remodeling after myocardial infarction.

In summary, our work demonstrates that the $A_{2B}R$ agonists reduce myocardial IR injury by inhibiting inflammatory responses in reperfused heart, probably by promoting macrophage phenotype switching to an anti-inflammatory M2 subset.

Conflict of Interests

The authors declare that there is no conflict of interests regarding the publication of this paper.

Acknowledgments

This study was funded in part by NIH R01 HL 092305 to Irving L. Kron and Brent A. French and The National Natural Science Foundation of China (NSFC 81400213) to Yikui Tian.

References

[1] T. Eckle, T. Krahn, A. Grenz et al., "Cardioprotection by ecto-5′-nucleotidase (CD73) and A_{2B} adenosine receptors," *Circulation*, vol. 115, no. 12, pp. 1581–1590, 2007.

[2] J. E. Maas, T. C. Wan, R. A. Figler, G. J. Gross, and J. A. Auchampach, "Evidence that the acute phase of ischemic preconditioning does not require signaling by the A_{2B} adenosine receptor," *Journal of Molecular and Cellular Cardiology*, vol. 49, no. 5, pp. 886–893, 2010.

[3] A. Kuno, S. D. Critz, L. Cui et al., "Protein kinase C protects preconditioned rabbit hearts by increasing sensitivity of adenosine A_{2b}-dependent signaling during early reperfusion," *Journal of Molecular and Cellular Cardiology*, vol. 43, no. 3, pp. 262–271, 2007.

[4] C. Methner, K. Schmidt, M. V. Cohen, J. M. Downey, and T. Krieg, "Both A_{2a} and A_{2b} adenosine receptors at reperfusion are necessary to reduce infarct size in mouse hearts," *American Journal of Physiology—Heart and Circulatory Physiology*, vol. 299, no. 4, pp. H1262–H1264, 2010.

[5] A. R. Lankford, J.-N. Yang, R. Rose'Meyer et al., "Effect of modulating cardiac A1 adenosine receptor expression on protection with ischemic preconditioning," *The American Journal of Physiology—Heart and Circulatory Physiology*, vol. 290, no. 4, pp. H1469–H1473, 2006.

[6] J. A. Auchampach and G. J. Gross, "Adenosine A1 receptors, K(ATP) channels, and ischemic preconditioning in dogs," *The American Journal of Physiology—Heart and Circulatory Physiology*, vol. 264, no. 5, pp. H1327–H1336, 1993.

[7] M. E. Reichelt, A. Shanu, L. Willems et al., "Endogenous adenosine selectively modulates oxidant stress via the A1 receptor in ischemic hearts," *Antioxidants and Redox Signaling*, vol. 11, no. 11, pp. 2641–2650, 2009.

[8] M. Koeppen, P. N. Harter, S. Bonney et al., "Adora2b signaling on bone marrow derived cells dampens myocardial ischemia-reperfusion injury," *Anesthesiology*, vol. 116, no. 6, pp. 1245–1257, 2012.

[9] Z. Yang, V. E. Laubach, B. A. French, and I. L. Kron, "Acute hyperglycemia enhances oxidative stress and exacerbates myocardial infarction by activating nicotinamide adenine dinucleotide phosphate oxidase during reperfusion," *The Journal of Thoracic and Cardiovascular Surgery*, vol. 137, no. 3, pp. 723–729, 2009.

[10] Z. Yang, Y.-J. Day, M.-C. Toufektsian et al., "Infarct-sparing effect of A2A-adenosine receptor activation is due primarily to its action on lymphocytes," *Circulation*, vol. 111, no. 17, pp. 2190–2197, 2005.

[11] Z. Yang, Y.-J. Day, M.-C. Toufektsian et al., "Myocardial infarct-sparing effect of adenosine A2A receptor activation is due to its action on $CD4^+$ T lymphocytes," *Circulation*, vol. 114, no. 19, pp. 2056–2064, 2006.

[12] C. Dougherty, J. Barucha, P. R. Schofield, K. A. Jacobson, and B. T. Liang, "Cardiac myocytes rendered ischemia resistant by expressing the human adenosine A1 or A3 receptor," *The FASEB Journal*, vol. 12, no. 15, pp. 1785–1792, 1998.

[13] Z. Yang, R. L. J. Cerniway, A. M. Byford, S. S. Berr, B. A. French, and G. Paul Matherne, "Cardiac overexpression of A_1-adenosine receptor protects intact mice against myocardial infarction," *American Journal of Physiology—Heart and Circulatory Physiology*, vol. 282, no. 3, pp. H949–H955, 2002.

[14] Z.-Q. Zhao, K. Nakanishi, D. Scott McGee, P. Tan, and J. Vinten-Johansen, "A1 receptor mediated myocardial infarct size reduction by endogenous adenosine is exerted primarily during ischaemia," *Cardiovascular Research*, vol. 28, no. 2, pp. 270–279, 1994.

[15] J. D. Joo, M. Kim, V. D. D'Agati, and H. T. Lee, "Ischemic preconditioning provides both acute and delayed protection against renal ischemia and reperfusion injury in mice," *Journal of the American Society of Nephrology*, vol. 17, no. 11, pp. 3115–3123, 2006.

[16] N. V. Solenkova, V. Solodushko, M. V. Cohen, and J. M. Downey, "Endogenous adenosine protects preconditioned heart during early minutes of reperfusion by activating Akt," *American Journal of Physiology—Heart and Circulatory Physiology*, vol. 290, no. 1, pp. H441–H449, 2006.

[17] Z. Yang, Y. Tian, Y. Liu, S. Hennessy, I. L. Kron, and B. A. French, "Acute hyperglycemia abolishes ischemic preconditioning by inhibiting Akt phosphorylation: normalizing blood glucose before ischemia restores ischemic preconditioning," *Oxidative Medicine and Cellular Longevity*, vol. 2013, Article ID 329183, 8 pages, 2013.

[18] K. Mubagwa and W. Flameng, "Adenosine, adenosine receptors and myocardial protection: an updated overview," *Cardiovascular Research*, vol. 52, no. 1, pp. 25–39, 2001.

[19] X. Yang, M. V. Cohen, and J. M. Downey, "Mechanism of cardioprotection by early ischemic preconditioning," *Cardiovascular Drugs and Therapy*, vol. 24, no. 3, pp. 225–234, 2010.

[20] A. K. Dixon, A. K. Gubitz, D. J. S. Sirinathsinghji, P. J. Richardson, and T. C. Freeman, "Tissue distribution of adenosine receptor mRNAs in the rat," *British Journal of Pharmacology*, vol. 118, no. 6, pp. 1461–1468, 1996.

[21] P. C. Chandrasekera, V. J. McIntosh, F. X. Cao, and R. D. Lasley, "Differential effects of adenosine A_{2a} and A_{2b} receptors on cardiac contractility," *American Journal of Physiology—Heart and Circulatory Physiology*, vol. 299, no. 6, pp. H2082–H2089, 2010.

[22] R. R. Morrison, B. Teng, P. J. Oldenburg, L. C. Katwa, J. B. Schnermann, and S. J. Mustafa, "Effects of targeted deletion of A_1 adenosine receptors on postischemic cardiac function and expression of adenosine receptor subtypes," *American Journal of Physiology—Heart and Circulatory Physiology*, vol. 291, no. 4, pp. H1875–H1882, 2006.

[23] Z. Yang, Y.-J. Day, M.-C. Toufektsian et al., "Infarct-sparing effect of A_{2A}-adenosine receptor activation is due primarily to its action on lymphocytes," *Circulation*, vol. 111, no. 17, pp. 2190–2197, 2005.

[24] J. Han, D. Wang, B. Yu et al., "Cardioprotection against ischemia/reperfusion by licochalcone B in isolated rat hearts," *Oxidative Medicine and Cellular Longevity*, vol. 2014, Article ID 134862, 11 pages, 2014.

[25] J. Li, C. Xie, J. Zhuang et al., "Resveratrol attenuates inflammation in the rat heart subjected to ischemia-reperfusion: role of the TLR4/NF-κB signaling pathway," *Molecular Medicine Reports*, 2014.

[26] D. Yang, Y. Zhang, H. G. Nguyen et al., "The A2B adenosine receptor protects against inflammation and excessive vascular adhesion," *Journal of Clinical Investigation*, vol. 116, no. 7, pp. 1913–1923, 2006.

[27] F. M. Konrad, E. Witte, I. Vollmer, S. Stark, and J. Reutershan, "Adenosine receptor A_{2b} on hematopoietic cells mediates LPS-induced migration of PMNs into the lung interstitium," *American Journal of Physiology—Lung Cellular and Molecular Physiology*, vol. 303, no. 5, pp. L425–L438, 2012.

[28] H. Chen, D. Yang, S. H. Carroll, H. K. Eltzschig, and K. Ravid, "Activation of the macrophage A2b adenosine receptor regulates tumor necrosis factor-α levels following vascular injury," *Experimental Hematology*, vol. 37, no. 5, pp. 533–538, 2009.

[29] J. Ham and D. A. Rees, "The adenosine A2b receptor: its role in inflammation," *Endocrine, Metabolic and Immune Disorders: Drug Targets*, vol. 8, no. 4, pp. 244–254, 2008.

[30] E. Sciaraffia, A. Riccomi, R. Lindstedt et al., "Human monocytes respond to extracellular cAMP through A2A and A2B adenosine receptors," *Journal of Leukocyte Biology*, vol. 96, no. 1, pp. 113–122, 2014.

[31] W. Zhang, W. Xu, and S. Xiong, "Macrophage differentiation and polarization via phosphatidylinositol 3-kinase/Akt-ERK signaling pathway conferred by serum amyloid P component," *Journal of Immunology*, vol. 187, no. 4, pp. 1764–1777, 2011.

[32] L. Tarassishin, H.-S. Suh, and S. C. Lee, "Interferon regulatory factor 3 plays an anti-inflammatory role in microglia by activating the PI3K/Akt pathway," *Journal of Neuroinflammation*, vol. 8, article 187, 2011.

[33] J. Wen, A. Grenz, Y. Zhang et al., "A_{2B} adenosine receptor contributes to penile erection via PI3K/AKT signaling cascade-mediated eNOS activation," *The FASEB Journal*, vol. 25, no. 8, pp. 2823–2830, 2011.

[34] Y. Cao, Y. Ruan, T. Shen et al., "Astragalus polysaccharide suppresses doxorubicin-induced cardiotoxicity by regulating the PI3k/Akt and p38MAPK pathways," *Oxidative Medicine and Cellular Longevity*, vol. 2014, Article ID 674219, 12 pages, 2014.

[35] S. Xing, X. Yang, W. Li et al., "Salidroside stimulates mitochondrial biogenesis and protects against H_2O_2-induced endothelial dysfunction," *Oxidative Medicine and Cellular Longevity*, vol. 2014, Article ID 904834, 13 pages, 2014.

[36] M. Nahrendorf and F. K. Swirski, "Monocyte and macrophage heterogeneity in the heart," *Circulation Research*, vol. 112, no. 12, pp. 1624–1633, 2013.

[37] D. van der Hoeven, T. C. Wan, E. T. Gizewski et al., "A role for the low-affinity A2B adenosine receptor in regulating superoxide generation by murine neutrophils," *Journal of Pharmacology and Experimental Therapeutics*, vol. 338, no. 3, pp. 1004–1012, 2011.

[38] J. P. Borges, K. S. Verdoorn, A. Daliry et al., "Delta opioid receptors: the link between exercise and cardioprotection," *PLoS ONE*, vol. 9, no. 11, Article ID e113541, 2014.

[39] S. M. Grieve, J. Mazhar, F. Callaghan et al., "Automated quantification of myocardial salvage in a rat model of ischemia-reperfusion injury using 3D high-resolution magnetic resonance imaging (MRI)," *Journal of the American Heart Association*, vol. 3, no. 4, 2014.

[40] A. Filusch, S. Buss, S. Hardt, H. A. Katus, H. F. Kuecherer, and A. Hansen, "Evaluation cardioprotective effects of atorvastatin in rats by real time myocardial contrast echocardiography," *Echocardiography*, vol. 25, no. 9, pp. 974–981, 2008.

[41] Z. Yang, J. Linden, S. S. Berr, I. L. Kron, G. A. Beller, and B. A. French, "Timing of adenosine 2A receptor stimulation relative to reperfusion has differential effects on infarct size and cardiac function as assessed in mice by MRI," *American Journal of Physiology—Heart and Circulatory Physiology*, vol. 295, no. 6, pp. H2328–H2335, 2008.

Hindawi Publishing Corporation
Oxidative Medicine and Cellular Longevity
Volume 2015, Article ID 683197, 11 pages
http://dx.doi.org/10.1155/2015/683197

Research Article

OGG1 Involvement in High Glucose-Mediated Enhancement of Bupivacaine-Induced Oxidative DNA Damage in SH-SY5Y Cells

Zhong-Jie Liu, Wei Zhao, Qing-Guo Zhang, Le Li, Lu-Ying Lai, Shan Jiang, and Shi-Yuan Xu

Department of Anesthesiology, Zhujiang Hospital, Southern Medical University, No. 253 Middle Gongye Street, Guangzhou, Guangdong 510282, China

Correspondence should be addressed to Shi-Yuan Xu; xushiyuan355@163.com

Received 21 September 2014; Revised 13 December 2014; Accepted 15 December 2014

Academic Editor: Mengzhou Xue

Hyperglycemia can inhibit expression of the 8-oxoG-DNA glycosylase (OGG1) which is one of the key repair enzymes for DNA oxidative damage. The effect of hyperglycemia on OGG1 expression in response to local anesthetics-induced DNA damage is unknown. This study was designed to determine whether high glucose inhibits OGG1 expression and aggravates bupivacaine-induced DNA damage via reactive oxygen species (ROS). SH-SY5Y cells were cultured with or without 50 mM glucose for 8 days before they were treated with 1.5 mM bupivacaine for 24 h. OGG1 expression was measured by quantitative real-time polymerase chain reaction (qRT-PCR) and western blot. ROS was estimated using the redox-sensitive fluorescent dye DCFH-DA. DNA damage was investigated with immunostaining for 8-oxodG and comet assays. OGG1 expression was inhibited in cells exposed to high glucose with concomitant increase in ROS production and more severe DNA damage as compared to control culture conditions, and these changes were further exacerbated by bupivacaine. Treatment with the antioxidant N-acetyl-L-cysteine (NAC) prevented high glucose and bupivacaine mediated increase in ROS production and restored functional expression of OGG1, which lead to attenuated high glucose-mediated exacerbation of bupivacaine neurotoxicity. Our findings indicate that subjects with diabetes may experience more detrimental effects following bupivacaine use.

1. Introduction

The risk of severe postoperative neurologic dysfunction is increased in patients with diabetic polyneuropathy undergoing neuraxial anesthesia or analgesia [1], but the mechanism by which high glucose conditions enhance the neurotoxicity of local anesthetics is not fully understood. Clinical trials and basic studies have provided strong evidence that both local anesthetics such as bupivacaine and hyperglycemia can cause neurotoxicity and apoptosis by inducing DNA oxidative damage via enhancing reactive oxygen species (ROS) generation [2–5]. Bupivacaine can uncouple oxidative phosphorylation, inhibit ATP production, and collapse the mitochondrial membrane potential. The decrease in ATP can activate AMPK which results in a marked increase in intracellular ROS [4]. Hyperglycemia can induce ROS overproduction through multiple pathways such as redox imbalances secondary to enhanced aldose reductase activity, altered protein kinase C activity, increased advanced glycation end products, and prostanoid imbalances [6]. Because it results in membrane lipid peroxidation, nitration of proteins, and degradation of DNA, ROS could be an apoptotic trigger in neuronal cell DNA oxidative damage. It is indispensable for the development and progression of neuronal neuropathy, because of the high content of phospholipids and relatively insufficient free-radical defense of nerves [7]. Whether ROS-mediated oxidative DNA damage plays an important role in enhancing the neurotoxicity of the bupivacaine under high glucose condition needs further study to reveal it.

DNA repair pathways are activated to allow damaged cells to survive [8, 9]. Ineffective DNA repair may cause cell apoptosis or disease, which implies that cell fate is influenced by the cell's ability to repair DNA [10]. Apoptosis occurred as a result of irreparable or incompletely repaired genomic DNA, which is constantly subject to assault from intrinsic and environmental insults. ROS are continuously generated as

respiration byproducts in mitochondria and are endogenous toxic agents [11]. Oxidized forms of DNA in particular are produced as a byproduct of normal metabolism or in response to exogenous sources of ROS. Base excision repair (BER) pathway is active against much of the damage formed in DNA as a result of cell self-defense mechanism. It is one of the most active DNA repair processes that allows the specific recognition and excision of a damaged DNA base. Oxidative stress is the development of DNA damage, which includes not only a multitude of base modifications, but also base loss and single or double-strand breaks containing sugar fragments or phosphates. All of these lesions are invariably cytotoxic or mutagenic. The majority of damage processed by the BER pathway is generated by the attack of ROS [12, 13]. 8-Oxo-deoxyguanine (8-oxodG) is one of the major base lesions formed after oxidative damage to DNA. 8-OxodG pairs with adenine during DNA synthesis, increasing G:C to T:A transversions. 8-OxodG in DNA is repaired primarily via the DNA base excision repair pathway. The gene encoding the DNA repair enzyme that recognizes and excises 8-oxodG is 8-oxoG-DNA glycosylase (OGG1) [14]. OGG1 deficiency or low expression can limit a cell's ability to repair DNA, leading to the accumulation of DNA damage and eventually to cell apoptosis [15, 16]. Chronic hyperglycemia leads to phosphorylation/inactivation of tuberin and downregulation of OGG1 via a redox-dependent activation of akt, resulting in accumulating cell DNA damage [17]. There is extensive evidence showing that damaged DNA and RNA accumulate in the context of diabetes [18–20]. However, little is known about whether hyperglycemia can aggravate bupivacaine-induced DNA damage and whether hyperglycemia is associated with OGG1 expression in response to DNA damage when diabetic patients receive nerve block anesthesia.

SH-SY5Y cells biological characteristic is similar to normal neural cells. So it is used to research local anesthetic neurotoxicity [2, 4]. We used an in vitro model to investigate OGG1 expression and DNA damage induced by bupivacaine in SH-SY5Y cells treated with high glucose. Our findings may provide a model that is useful for exploring the molecular mechanisms of OGG1 involvement in chronic hyperglycemia-aggravated neurotoxicity in diabetic patients treated with bupivacaine.

2. Materials and Methods

2.1. Reagents. The human dopaminergic neuroblastoma SH-SY5Y cell line was purchased from the Shanghai Institutes for Biological Sciences. Bupivacaine hydrochloride (purity 99.9%), glucose (purity 99.5%), and N-acetyl-L-cysteine (NAC) were purchased from Sigma (St. Louis, MO). Other reagents used included Dulbecco's modified Eagle medium (DMEM)/F12 (including 17.5 mM glucose) and fetal bovine serum (FBS: Gibco, Grand Island, NY); Cell Counting Kit-8 (CCK8) assay kit (Dojindo, Kumamoto, Japan); 2′,7′-dichlorofluorescein diacetate (DCFH-DA) (Beyotime, China); 4′,6-diamidino-2-phenylindole dihydrochloride n-hydrate (DAPI) which were purchased from Wako Pure Chemical Industries Ltd. (Osaka, Japan); comet assay (Trevigen, Inc., Gaithersburg, MD); anti-OGG1 and anti-8-oxodG (Abcam, Cambridge, UK, ab115841 and ab62623); anti-caspase-9 (CST, USA, 9508) and anti-β-actin (KangChen Bio-tech, China, KC-5A08). All reagents were obtained from commercial suppliers and were of standard biochemical quality.

2.2. Cell Culture. SHSY-5Y cells were maintained at 37°C in 5% CO_2 in DMEM/F12 medium, supplemented with 10% FBS and penicillin/streptomycin. Culture medium was renewed once a day during cell growth.

2.3. Measurement of Cell Viability. Cells were seeded onto 96-well plates at a concentration of 5×10^3 cells in 200 μL culture medium per well. After serum starvation in DMEM/F12 medium for 24 h, the cells were exposed to 0.5, 1.0, 1.5, 2.0, 2.5, or 3.0 mM bupivacaine for 24 h. Next, 20 μL CCK-8 was added to each well for another 2.5 h at 37°C. Optical density (OD) was read at 450 nm on a spectrophotometer (Bio-Tek, Winooski, VT).

2.4. Western Blot Assay. Total proteins were harvested from SH-SY5Y cells with lysis buffer after incubation as described. After centrifugation, protein concentrations were determined by a bicinchoninic acid (BCA) protein assay kit (Beyotime, Haimen, China). Equal amounts of protein (40 μg) were separated by sodium dodecyl sulfate-polyacrylamide gel electrophoresis, electrotransferred to polyvinylidene difluoride (PVDF) membranes, and blocked with 5% nonfat dry milk in Tris-buffered saline. They were then immunoblotted with anti-OGG1 (1 : 500), anti-caspase-9 (1 : 500), or anti-β-actin antibody (1 : 1,000) diluted in blocking solution containing 5% nonfat dry milk and 0.1% Tween-20 in Tris-HCl-buffered saline overnight at 4°C. After they were rinsed, membranes were incubated with horseradish peroxidase-conjugated anti-rabbit immunoglobulin at 1 : 1,000 for 1 h. Specific proteins were detected by enhanced chemiluminescence. Finally, the immunocomplexes were visualized using chemiluminescence, and the optical densities of individual bands were quantified using the Chemi-Imager digital imaging system (Alpha Innotech, San Leandro, CA). Band densities were measured using a densitometer and analyzed with Quantity One analysis software (Bio-Rad, Hercules, CA). OGG1 and cleaved caspase-9 protein expression were normalized to their corresponding β-actin products.

2.5. Quantitative Real-Time PCR (qRT-PCR). OGG1 mRNA levels were measured by qRT-PCR. After high glucose treatment and bupivacaine administration, total RNA was extracted from SH-SY5Y cells using TRIzol (Invitrogen, Carlsbad, CA, USA). cDNA was synthesized from 2 μg total RNA using PrimeScript RT Master Mix (Takara, Otsu, Japan). Quantitative real-time PCR was performed on a Lightcycler 480 (Applied Biosystems, Foster City, CA) using the SYBR Green Master Mix Kit (Takara, Japan). Relative amounts of OGG1 mRNA were quantified using the $2^{-\Delta\Delta CT}$ method [21]. qRT-PCR was performed on an ABI Prism 7500 sequence detector (Applied Biosystems, Foster City, CA). The primers

were human OGG1 and β-actin (OGG1-forward: 5′-CCCTGGCTCAACTGTATCAC-3′; reverse: 5′-TCGCACACCTTGGAATTTC-3′, and β-actin-forward: 5′-TGGATCAGCAAGCAGGAGTA-3′; reverse: 5′-TCGGCCACATTGTGAACTTT-3′).

2.6. Measurement of ROS. Cells were seeded onto 24-well plates at 5×10^5 cells/well in 500 μL culture medium. Intracellular accumulation of ROS was estimated using the redox-sensitive fluorescent dye DCFH-DA. The cells of each group were incubated with 10 μmol/L DCFH-DA at 37°C during the last 20 min. DCFH-DA-stained cells were washed 3 times in PBS, harvested, and resuspended in PBS. Fluorescence intensity was determined by flow cytometry to estimate relative ROS accumulation.

2.7. Immunostaining for 8-OxodG and DAPI. The slices were fixed in 4% paraformaldehyde at 37°C for 30 min. After rinsing with PBS, cells were treated with proteinase K (10 mg/mL) at room temperature for 7 min. After rinsing with PBS, DNA was denatured by treatment with 4 N HCl for 7 min at room temperature. The pH was adjusted with 50 mM Tris-HCl for 5 min at room temperature. After rinsing with 0.2% Triton X in PBS, the cells were stained with a monoclonal anti-8-oxodG (1 : 2000). Alexa Fluor 488-conjugated goat anti-mouse IgG (1 : 200) was used as the secondary antibody. The slices were mounted with Aqua-Poly/Mount (Polysciences, Inc., PA, USA). Fluorescence images were captured using a fluorescence microscope (AX-80, Olympus, Tokyo, Japan), and 20 images per treatment were obtained. The cells immunostained for 8-oxodG were rinsed and then stained with DAPI (2 mg/mL) for 5 min. After rinsing with PBS, the slices were mounted with Aqua-Poly/Mount. Fluorescence images were captured using a fluorescence microscope (AX-80, Olympus, Tokyo, Japan) and merged with 8-oxodG. The positive expression of 8-oxodG was measured by the mean fluorescence intensity using an image analyzer ATTO densitograph (ATTO, Tokyo, Japan).

2.8. Comet Assay for DNA Damage. Single cell gel electrophoresis (SCGE), also known as the alkaline comet assay, was used to measure DNA damage [22]. To assess DNA damage products, SH-SY5Y cells were subjected to comet assays. This method measures the ability of damaged DNA to migrate out of the cell when exposed to an electrical field, thus creating a "comet" particle. Undamaged DNA remains in the nucleoid, leaving a spherical particle. Slides were scored for comets using fluorescence microscopy under an inverted microscope (Eclipse TE300, Nikon, Tokyo, Japan) at 200x magnification. Images were captured using Cool SNAPES CCD camera. Fifty cells per slide were analyzed and scored in triplicate using Comet Assay Software Project (CASP) image analysis software (CASP-6.0, University of Wroclaw, Poland). DNA damage is represented as olive tail moment (OTM), which is the product of tail length and percent tail DNA.

2.9. Statistical Analysis. Data are presented as means ± standard deviation (SD). Comparisons between two means were performed using independent-sample t-tests, and multiple comparisons among groups were analyzed using one-way analysis of variance (ANOVA) with SPSS software 13.0 (SPSS Inc., Chicago, IL). Statistical significance was set at $P < 0.05$.

3. Results

3.1. The Effect of High Glucose on OGG1 Protein Expression. We investigated OGG1 mRNA level of SH-SY5Y cells exposed to increasing glucose concentrations (25, 50, and 100 mM) for 2 or 8 days. The result showed that OGG1 mRNA level was associated with concentration and time exposed to high glucose. OGG1 mRNA level was elevated by high glucose at the 2nd day, the higher OGG1 mRNA level when cells exposed to the higher concentration glucose (Figure 1(a)). But OGG1 mRNA level was inhibited by high glucose (50 mM) at the 8th day, the lower OGG1 mRNA level when cells were exposed to the higher concentration glucose (Figure 1(b)). Simultaneously, we investigated OGG1 protein expression of cells exposed to 50 mM glucose for 2, 4, and 8 days and found that OGG1 protein expression was inhibited in a time-dependent manner. OGG1 expression was inhibited by high glucose at the 4th day and onward, with the maximum effect found at 8 d (Figure 1(c)). The results suggested that long-term exposure to high glucose could inhibit OGG1 expression.

3.2. Cell Toxicity Induced by Bupivacaine. We compared the cytotoxicity of bupivacaine (0.5, 1.0, 1.5, 2.0, 2.5, and 3.0 mM) using the CCK-8 assay. Our results showed that bupivacaine inhibited cell growth in a concentration-dependent manner. Cell viability was significantly inhibited by 1.5 mM bupivacaine (Figure 2(a)).

3.3. The Effect of Bupivacaine on OGG1 Protein Expression. We investigated OGG1 protein expression of SH-SY5Y cells exposed to 0.5, 1.0, or 2.0 mM bupivacaine for 24 h and found that OGG1 protein expression was elevated in a concentration-dependent manner (Figure 2(b)). From the result of cell toxicity, we knew that bupivacaine cytotoxicity was associated with concentration. This result suggested that OGG1 expression could be elevated parallel to increasing concentration of bupivacaine for repairing increasing DNA damage.

3.4. High Glucose Inhibited OGG1 mRNA Transcription and Protein Expression in Response to Bupivacaine-Induced DNA Damage. OGG1 mRNA expression was examined by qRT-PCR and protein expression level was measured by western blot. Compared to the control group, OGG1 mRNA levels and protein expression were reduced in SH-SY5Y cells cultured in 50 mM glucose for 8 d, while they were significantly elevated in SH-SY5Y cells treated with bupivacaine for 24 h. Compared to SH-SY5Y cells treated only with bupivacaine for 24 h, OGG1 mRNA levels and protein expression were significantly reduced in cells treated with high glucose and bupivacaine (Figures 3 and 4(a)).

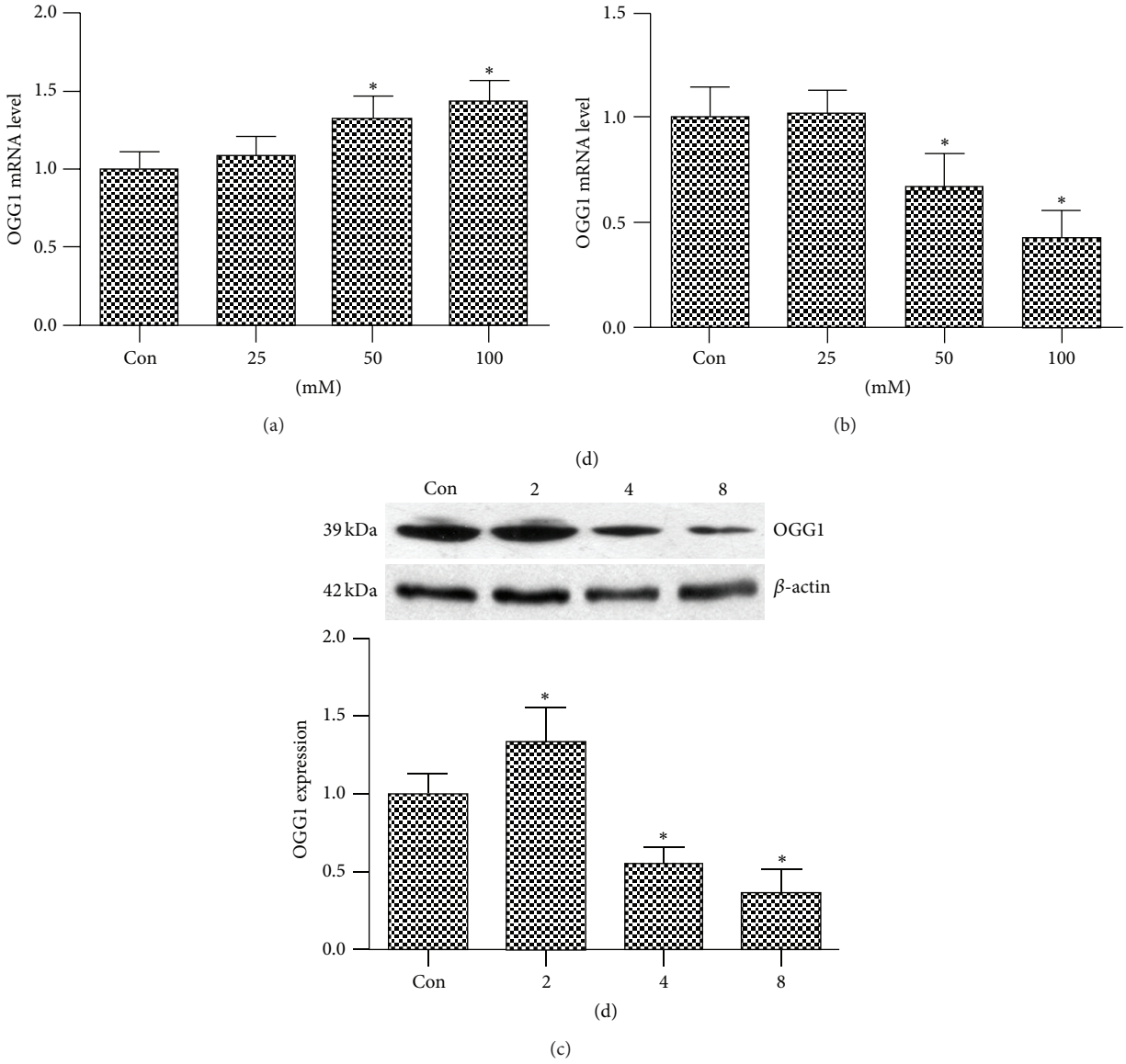

Figure 1: The effect of glucose on the OGG1 expression as detected by qRT-PCR (a, b) and western blot (c). (a) The OGG1 mRNA level in SH-SY5Y cells serum starved for 24 h, followed by incubation with increasing glucose concentrations (25, 50, and 100 mM) for 2 d. (b) The OGG1 mRNA level in SH-SY5Y cells serum starved for 24 h, followed by incubation with increasing glucose concentrations (25, 50, and 100 mM) for 8 d. (c) The OGG1 protein expression in SH-SY5Y cells serum starved for 24 h, followed by incubation with glucose concentration 50 mM for 2, 4, or 8 d. Data are presented as mean ± SD ($n = 3$). Compared with the group Con, $^{*}P < 0.05$.

3.5. High Glucose Enhanced ROS Production Induced by Bupivacaine. Treatment with either 50 mM glucose or 1.5 mM bupivacaine increased the intracellular ROS accumulation, indicated by DCFH-DA fluorescence, while high glucose pretreatment significantly enhanced ROS production induced by bupivacaine (Figure 5(a)).

3.6. High Glucose Aggravated Bupivacaine-Induced DNA Damage and Apoptosis. Oxidative DNA damage product accumulation was quantified by using immunofluorescence detection of 8-oxodG and the OTMs of comet assays. 8-OxodG relative expression and OTM values were increased in SH-SY5Y cells exposed to 50 mM glucose or 1.5 mM bupivacaine and were higher in cells exposed to both agents compared to those only exposed to bupivacaine. These results demonstrate that high glucose enhanced bupivacaine-induced DNA damage (Figure 6).

Cleaved caspase-9 protein expression was measured by western blot. High glucose or bupivacaine treatment resulted in significantly increased cleaved caspase-9 protein levels compared with the control group. Cleaved caspase-9 protein expression was significantly higher in cells treated with high glucose and bupivacaine than in cells treated only with bupivacaine (Figure 4(a)).

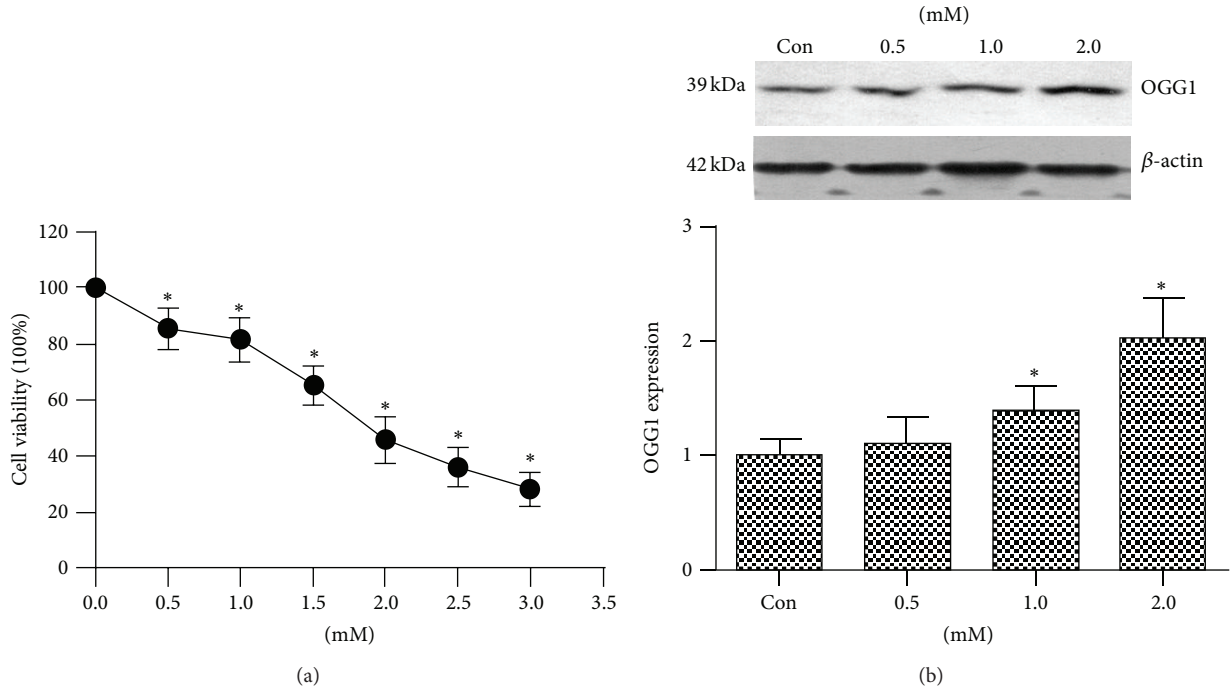

Figure 2: Proliferation effects of bupivacaine on SH-SY5Y cells and the effect of bupivacaine on the OGG1 protein expression. (a) After serum starved DMEM/F12 medium for 24 h, the cell was exposed to 0.5, 1.0, 1.5, 2.0, 2.5, or 3.0 mM bupivacaine for 24 h. Bupivacaine-induced cell injury was detected by CCK8 assay. (b) The OGG1 protein expression in SH-SY5Y cells serum starved for 24 h, followed by incubation with increasing bupivacaine concentrations (0.5, 1.0, and 2.0 mM) for 24 h. Data are presented as mean ± SD ($n = 3$). Compared with the group Con, $^{*}P < 0.05$.

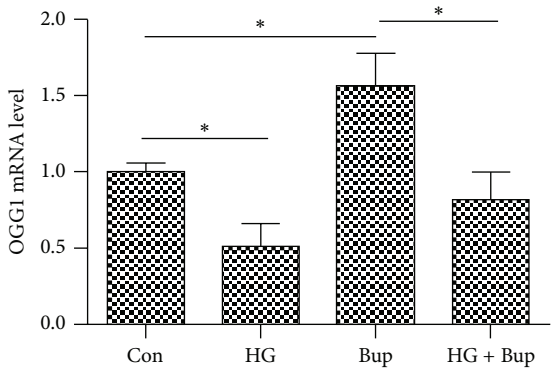

Figure 3: The effect of glucose or bupivacaine on the regulation of OGG1 mRNA level as detected by qRT-PCR. Con: SH-SY5Y cells of group control. HG: SH-SY5Y cells were exposed to 50 mM glucose for 8 d. Bup: SH-SY5Y cells were treated with 1.5 mM bupivacaine for 24 h. HG + Bup: SH-SY5Y cells were incubated with 50 mM glucose for 8 d and then treated with 1.5 mM bupivacaine for 24 h. Data are presented as mean ± SD ($n = 3$). $^{*}P < 0.05$.

Based on the above data, we hypothesized that high glucose could aggravate bupivacaine-induced neurotoxicity in SH-SY5Y cells.

3.7. NAC Attenuated DNA Damage Induced by High Glucose and Bupivacaine via Inhibited ROS Production and Increased OGG1 Expression. NAC pretreatment significantly reduced the ROS overproduction induced by high glucose and bupivacaine and increased OGG1 expression inhibited by high glucose (Figures 5(b) and 4(b)). Simultaneously, NAC attenuated DNA damage and apoptosis induced by high glucose and bupivacaine. However, compared to control group, NAC did not cancel glucose and bupivacaine-induced cell injury (Figures 7 and 4(b)). The above results suggested that high glucose enhanced DNA damage induced by bupivacaine via ROS and NAC could restore functional expression of OGG1.

4. Discussion

There are three main findings of the present study. First, long-term exposure to high glucose could inhibit the expression of OGG1 enzyme in SH-SY5Y cells. Second, long-term high glucose exposure inhibited the enhancement of OGG1 expression in response to bupivacaine-induced DNA damage in SH-SY5Y cells. Third, high glucose or bupivacaine can cause DNA damage and apoptosis in SH-SY5Y cells, and these effects were mediated via ROS in cells treated with both high glucose and bupivacaine. Collectively, our findings indicate that high glucose inhibited OGG1 expression in response to DNA damage induced by bupivacaine and aggravated the neurotoxic effects of bupivacaine in SH-SY5Y cells.

Bupivacaine induced depression of the cell respiration related to specific inhibition of complexes I and III, inhibited

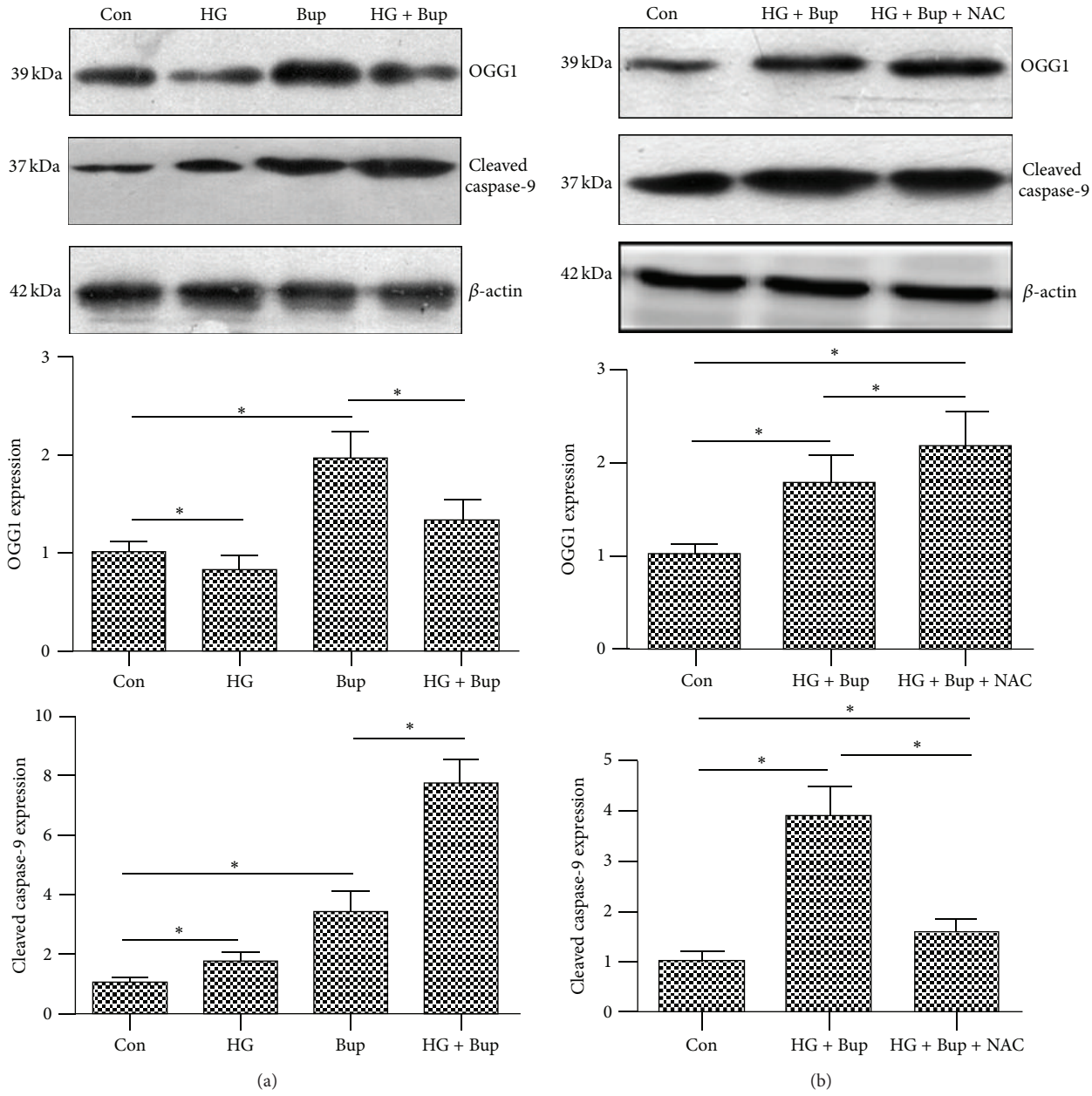

Figure 4: The effect of high glucose, bupivacaine, or NAC on OGG1 and cleaved caspase-9 protein expression as detected by western blot. Con: SH-SY5Y cells of group control. HG: SH-SY5Y cells were exposed to 50 mM glucose for 8 d. Bup: SH-SY5Y cells were treated with 1.5 mM bupivacaine for 24 h. HG + Bup: SH-SY5Y cells were incubated with 50 mM glucose for 8 d and then treated with 1.5 mM bupivacaine for 24 h. HG + Bup + NAC: cells treated with 50 mM glucose for 8 d and then pretreated with 5 mM NAC for 6 h prior to 1.5 mM bupivacaine exposure for 24 h. (a) The effect of high glucose on OGG1 and cleaved caspase-9 protein expression induced by bupivacaine. (b) The effect of NAC on OGG1 and cleaved caspase-9 protein expression induced by high glucose and bupivacaine. Data are presented as mean ± SD ($n = 3$) $^*P < 0.05$.

the production of ATP, and was accompanied with production of ROS. The decrease in ATP can activate AMPK. It can result in a marked increase in intracellular ROS. Overproduction of ROS could result in mitochondrial DNA oxidative damage, caspase activation, and apoptosis [2–4]. This study also showed that bupivacaine exerted concentration-dependent cell toxicity and induced DNA damage and apoptosis via enhancing ROS generation. Hyperglycemia could damage cellular DNA by generating ROS in patients with diabetes [23]. This conclusion is verified by our result showing that high glucose exerted time-dependent toxicity and induced DNA damage and apoptosis via enhancing ROS generation. Under high glucose condition, intracellular ROS production, DNA damage, and cell apoptosis induced by bupivacaine were enhanced. Importantly, cell injury was prevented by antioxidant treatment. It suggested an ROS-mediated

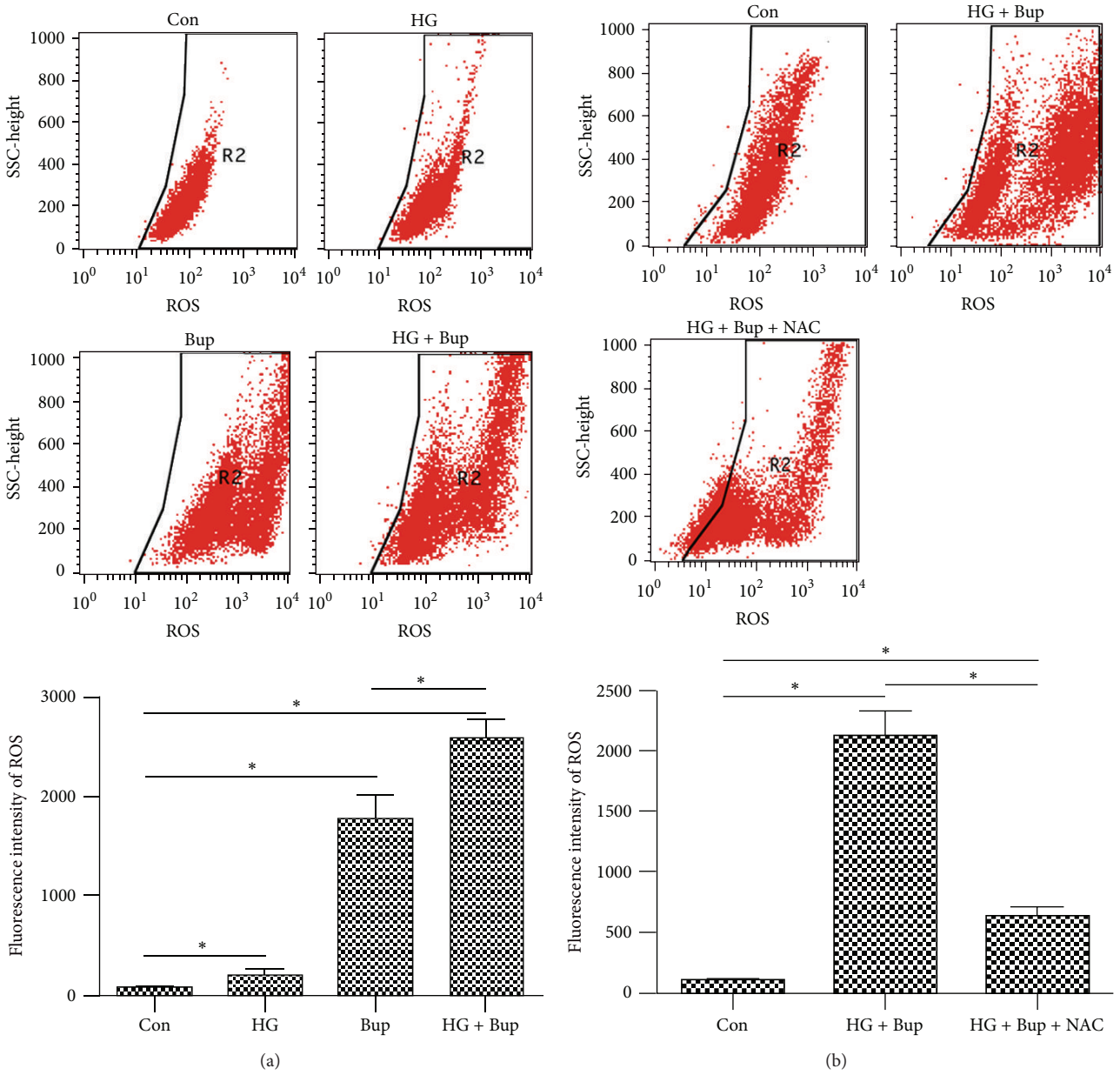

Figure 5: The levels of ROS were measured by flow cytometry. Con: SH-SY5Y cells of group control. HG: SH-SY5Y cells were exposed to 50 mM glucose for 8 d. Bup: SH-SY5Y cells were treated with bupivacaine for 24 h. HG + Bup: SH-SY5Y cells were incubated with 50 mM glucose for 8 d and then treated with bupivacaine for 24 h. HG + Bup + NAC: cells treated with 50 mM high glucose for 8 d and then pretreated with 5 mM NAC for 6 h prior to 1.5 mM bupivacaine exposure for 24 h. (a) The levels of ROS induced by high glucose or bupivacaine. High glucose enhanced ROS overproduction induced by bupivacaine. (b) NAC attenuated ROS overproduction induced by high glucose and bupivacaine. Summarized data shows the fluorescence intensity of ROS as detected by flow cytometry. Data represented are mean ± SD ($n = 6$), $^{*}P < 0.05$.

mechanism reinforcing the primary oxidative DNA damage of bupivacaine under high glucose condition. Antioxidant treatment may play an important role in preventing and curing hyperglycemia-aggravated neurotoxicity in diabetic patients treated with bupivacaine.

Accumulative ROS could cause DNA damage or mutation. Cells have evolved a diverse defense network to maintain genomic integrity and prevent permanent genetic damage induced by oxidative stress [24]. This results in changes in cellular transcription that, combined with oxidative damage to enzymes involved in processing and repairing DNA damage, might contribute to diabetic neuropathy [14]. 8-OxodG is a sensitive marker of ROS-induced DNA damage [25]. The steady state level of 8-oxodG in DNA reflects its rate of generation and of repairing. 8-OxodG in DNA is repaired primarily via the DNA base excision repair (BER) pathway [26]. One

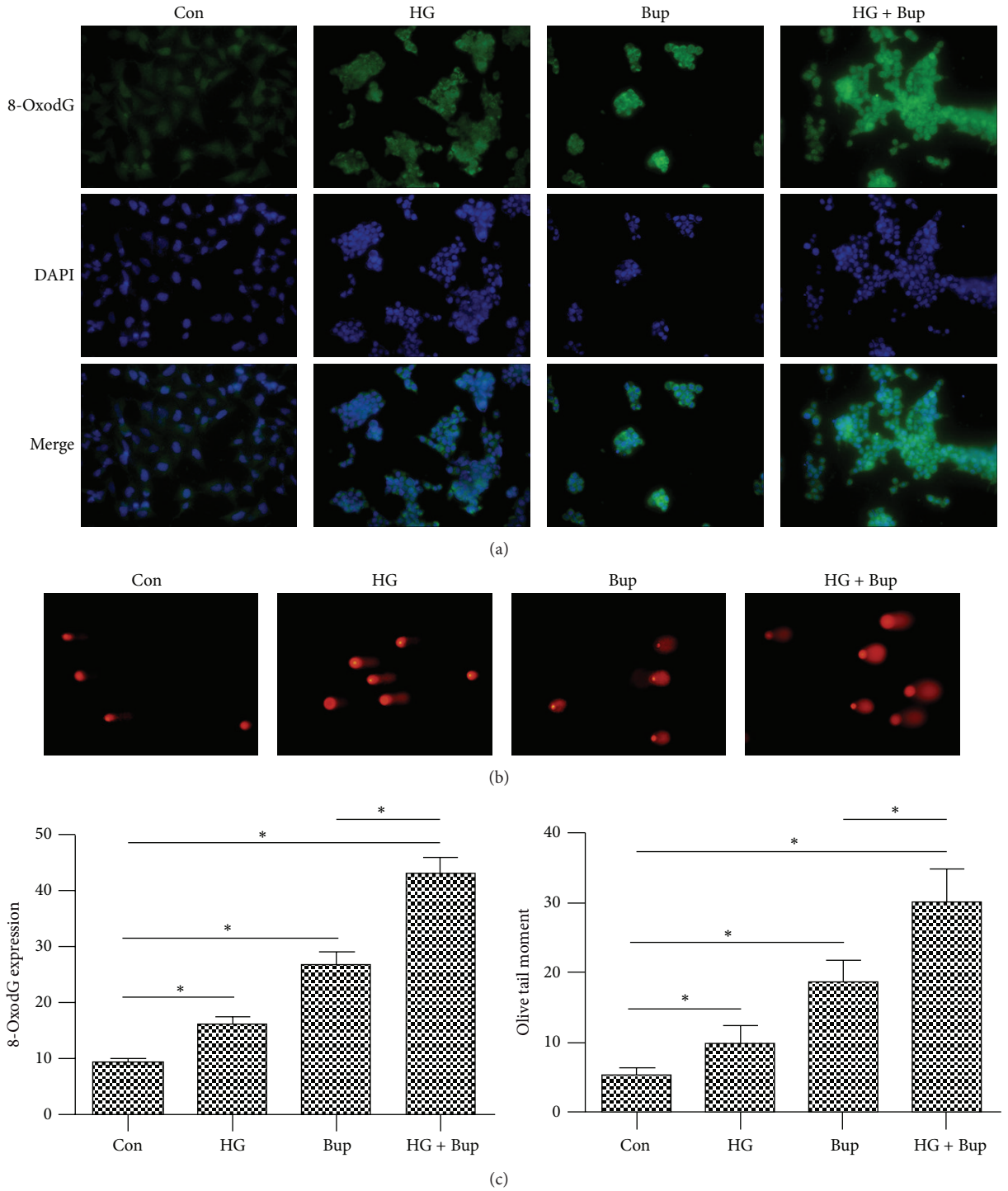

Figure 6: The effect of high glucose or bupivacaine on 8-oxodG expression and DNA damage. Con: SH-SY5Y cells of group control. HG: SH-SY5Y cells were exposed to 50 mM glucose for 8 d. Bup: SH-SY5Y cells were treated with 1.5 mM bupivacaine for 24 h. HG + Bup: SH-SY5Y cells were incubated with 50 mM glucose for 8 d and then treated with 1.5 mM bupivacaine for 24 h. (a) High glucose enhanced 8-oxodG expression induced by bupivacaine. (b) High glucose aggravated DNA damage induced by bupivacaine. (c) Summarized data show 8-oxodG expression as measured by the mean fluorescence intensity and DNA damage as detected by Olive tail moment. Data are presented as mean ± SD ($n = 3$), $^{*}P < 0.05$.

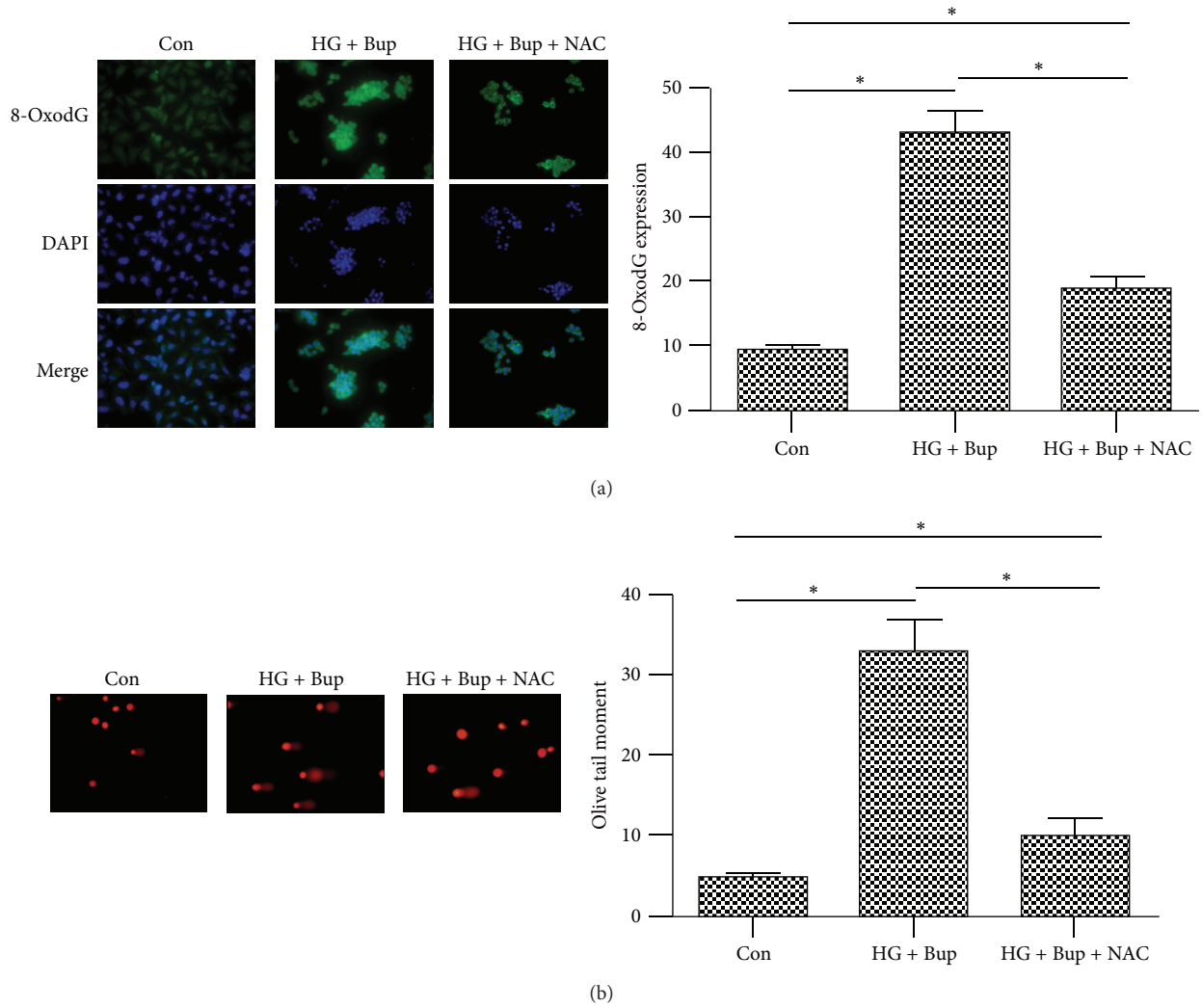

Figure 7: The effect of NAC on 8-oxodG expression and DNA damage induced by high glucose and bupivacaine. Con: SH-SY5Y cells of group control. HG + Bup: SH-SY5Y cells were incubated with 50 mM glucose for 8 d and then treated with bupivacaine for 24 h. HG + Bup + NAC: cells treated with 50 mM high glucose for 8 d and then pretreated with 5 mM NAC for 6 h prior to 1.5 mM bupivacaine exposure for 24 h. (a) NAC attenuated 8-oxodG expression induced by high glucose and bupivacaine. Summarized data show 8-oxodG expression as measured by the mean fluorescence intensity. (b) NAC attenuated DNA damage induced by high glucose and bupivacaine. Summarized data show DNA damage as detected by Olive tail moment. Data are presented as mean ± SD ($n = 3$), $^*P < 0.05$.

of the key BER enzymes is OGG1, which is necessary for the initial steps in the removal of the mutagenic lesion 8-oxoguanine. Because of its lyase activity, this enzyme may also play a critical role in cleaning the 3-end of oxidative lesions to the sugar-phosphate backbone. The present study showed that bupivacaine could induce ROS overproduction and cause cell DNA damage and apoptosis. 8-OxodG and OGG1 were significantly elevated when cells were exposed to bupivacaine. Bupivacaine-induced ROS resulted in a marked increase in intracellular 8-oxodG. For repairing it, DNA repair enzyme OGG1 was activated, what was cell diverse defense network to maintain genomic integrity and prevent permanent genetic damage induced by oxidative stress. This suggested that BER was involved in repairing bupivacaine-induced DNA damage via ROS in SH-SY5Y cells, and OGG1 might be a crucial factor.

DNA oxidative damage such as 8-oxodG was not effectively removed when OGG1 expression was reduced or inhibited and this could lead to damage accumulation, ultimately resulting in cells aging or apoptosis [27]. Extensive evidence in the literature indicates that diabetes is characterized by the accumulation of damaged DNA and RNA. However it remains unknown whether these lesions are due to inefficient removal by cellular DNA repair pathways [18–20]. Previous study has reported that chronic hyperglycemia could inhibit OGG1 expression via a redox-dependent activation of akt, resulting in accumulating cell DNA damage [17]. This results in deficient DNA repair function and, therefore, leads to the accumulation of DNA lesions. The importance of the OGG1 DNA glycosylase in the repair of oxidative damage was shown in OGG1-deficient mice [28]. These animals accumulate abnormally high levels of 8-oxodG in their genomes.

Furthermore, no cleavage of 8-oxoG: C-containing substrate was detected in tissue extracts from OGG1 knockout mice, indicating that OGG1 is the only mammalian glycosylase that can efficiently remove 8-oxodG from 8-oxoG: C pairs. In this study, OGG1 expression was reduced after long-term exposure to high glucose and then this leads to accumulating 8-oxodG. This result suggested that chronic hyperglycemia could result in DNA damage that overwhelmed the DNA repair defense system, which may induce genomic instability and cell dysfunction. Our study showed that SH-SY5Y cells cultured with high glucose and bupivacaine decreased OGG1 expression and resulted in more severe DNA damage and apoptosis. Under high glucose condition, OGG1 expression was inhibited, and it could not effectively repair increasing 8-oxodG induced by bupivacaine and high glucose. This leads to damage accumulation, ultimately resulting in cells apoptosis. NAC could restore functional expression of OGG1 inhibited by high glucose and attenuate this damage. It suggested that antioxidant could reverse hyperglycemia-induced inhibitory effect on OGG1. However, the way of NAC promoting OGG1 expression under high glucose condition remains unknown and needs further research to reveal it. This result demonstrated that under high glucose environment, the decrease in OGG1 was involved in enhanced DNA damage and apoptosis induced by bupivacaine. Antioxidant therapy could reverse these deleterious effects in part by restoring function of the DNA repair enzyme OGG1.

Some limitations of this study should be noted. First, we did not investigate the mechanism underlying the effect of bupivacaine on OGG1 in SH-SY5Y cells cultured in high glucose. Second, the bupivacaine concentration used in this study was 1.5 mM, which is equal to 0.045%. Local injection concentrations are generally 0.5% or 0.75%. So, this dosage is not precisely clinically relevant. Bupivacaine concentration-dependent cell toxicity did not allow us to determine whether bupivacaine at higher clinical concentration would kill all cells. However, in spinal or epidural anesthesia, the axons in the nerve roots of the cauda equina bear the brunt of the high initial bupivacaine concentration. So, the result of the study suggests that diabetic patients treated with bupivacaine may suffer from nerve or neuronal damage. Third, we did not perform in vivo experiments to validate our conclusions.

In conclusion, high glucose could inhibit OGG1 expression in response to bupivacaine-induced DNA damage and simultaneously aggravate the neurotoxic effects of bupivacaine via ROS in SH-SY5Y cells.

Abbreviations

OGG1:	8-OxoG-DNA glycosylase
8-oxodG:	8-Oxo-deoxyguanine
ROS:	Reactive oxygen species
NAC:	N-Acetyl-L-cysteine
OTM:	Olive tail moment.

Conflict of Interests

The authors do not declare any conflict of interests relevant to this paper.

Authors' Contribution

Zhong-Jie Liu, Wei Zhao, Qing-Guo Zhang, and Le Li contributed equally to this work.

Acknowledgments

This study was supported by the National Science Foundation of China (Grant no. 81271390) and Natural Science Foundation for the Youth (Grant no. 81400995).

References

[1] J. R. Hebl, S. L. Kopp, D. R. Schroeder, and T. T. Horlocker, "Neurologic complications after neuraxial anesthesia or analgesia in patients with preexisting peripheral sensorimotor neuropathy or diabetic polyneuropathy," *Anesthesia & Analgesia*, vol. 103, no. 5, pp. 1294–1299, 2006.

[2] L. Li, Q.-G. Zhang, L.-Y. Lai et al., "Neuroprotective effect of ginkgolide B on bupivacaine-induced apoptosis in SH-SY5Y cells," *Oxidative Medicine and Cellular Longevity*, vol. 2013, Article ID 159864, 11 pages, 2013.

[3] C. J. Park, S. A. Park, T. G. Yoon, S. J. Lee, K. W. Yum, and H. J. Kim, "Bupivacaine induces apoptosis via ROS in the Schwann cell line," *Journal of Dental Research*, vol. 84, no. 9, pp. 852–857, 2005.

[4] J. Lu, S. Y. Xu, Q. G. Zhang, and H. Y. Lei, "Bupivacaine induces reactive oxygen species production via activation of the AMP-Activated protein kinase-dependent pathway," *Pharmacology*, vol. 87, no. 3-4, pp. 121–129, 2011.

[5] M. Brownlee, "The pathobiology of diabetic complications: a unifying mechanism," *Diabetes*, vol. 54, no. 6, pp. 1615–1625, 2005.

[6] R. Pop-Busui, A. Sima, and M. Stevens, "Diabetic neuropathy and oxidative stress," *Diabetes/Metabolism Research and Reviews*, vol. 22, no. 4, pp. 257–273, 2006.

[7] H. B. Lee, M.-R. Yu, Y. Yang, Z. Jiang, and H. Ha, "Reactive oxygen species-regulated signaling pathways in diabetic nephropathy," *Journal of the American Society of Nephrology*, vol. 14, supplement 3, pp. S241–S245, 2003.

[8] D. M. S. Spencer, R. A. Bilardi, T. H. Koch et al., "DNA repair in response to anthracycline-DNA adducts: a role for both homologous recombination and nucleotide excision repair," *Mutation Research: Fundamental and Molecular Mechanisms of Mutagenesis*, vol. 638, no. 1-2, pp. 110–121, 2008.

[9] G. Wang and K. M. Vasquez, "Impact of alternative DNA structures on DNA damage, DNA repair, and genetic instability," *DNA Repair*, vol. 19, pp. 143–151, 2014.

[10] E. Y. So and T. Ouchi, "Decreased DNA repair activity in bone marrow due to low expression of DNA damage repair proteins," *Cancer Biology & Therapy*, vol. 15, no. 7, pp. 906–910, 2014.

[11] J. Cadet, T. Douki, D. Gasparutto, and J.-L. Ravanat, "Oxidative damage to DNA: formation, measurement and biochemical features," *Mutation Research: Fundamental and Molecular Mechanisms of Mutagenesis*, vol. 531, no. 1-2, pp. 5–23, 2003.

[12] M. Dizdaroglu, P. Jaruga, M. Birincioglu, and H. Rodriguez, "Free radical-induced damage to DNA: mechanisms and measurement," *Free Radical Biology & Medicine*, vol. 32, no. 11, pp. 1102–1115, 2002.

[13] M. D. Evans, M. Dizdaroglu, and M. S. Cooke, "Oxidative DNA damage and disease: induction, repair and significance," *Mutation Research: Reviews in Mutation Research*, vol. 567, no. 1, pp. 1–61, 2004.

[14] T. L. Scott, S. Rangaswamy, C. A. Wicker, and T. Izumi, "Repair of oxidative DNA damage and cancer: recent progress in DNA base excision repair," *Antioxidants & Redox Signaling*, vol. 20, no. 4, pp. 708–726, 2014.

[15] L. I. Rachek, V. I. Grishko, S. P. LeDoux, and G. L. Wilson, "Role of nitric oxide-induced mtDNA damage in mitochondrial dysfunction and apoptosis," *Free Radical Biology & Medicine*, vol. 40, no. 5, pp. 754–762, 2006.

[16] Y.-K. Lee, H.-G. Youn, H.-J. Wang, and G. Yoon, "Decreased mitochondrial OGG1 expression is linked to mitochondrial defects and delayed hepatoma cell growth," *Molecules and cells*, vol. 35, no. 6, pp. 489–497, 2013.

[17] S. Simone, Y. Gorin, C. Velagapudi, H. E. Abboud, and S. L. Habib, "Mechanism of oxidative DNA damage in diabetes: tuberin inactivation and downregulation of DNA repair enzyme 8-oxo-7,8-dihydro-2′-deoxyguanosine- DNA glycosylase," *Diabetes*, vol. 57, no. 10, pp. 2626–2636, 2008.

[18] E. Zherebitskaya, E. Akude, D. R. Smith, and P. Fernyhough, "Development of selective axonopathy in adult sensory neurons isolated from diabetic rats: role of glucose-induced oxidative stress," *Diabetes*, vol. 58, no. 6, pp. 1356–1364, 2009.

[19] N. Kilarkaje and M. M. Al-Bader, "Diabetes-induced oxidative DNA damage alters p53-p21$^{CIP1/Waf1}$ signaling in the rat testis," *Reproductive Sciences*, vol. 22, no. 1, pp. 102–112, 2014.

[20] T. Shimoike, T. Inoguchi, F. Umeda, H. Nawata, K. Kawano, and H. Ochi, "The meaning of serum levels of advanced glycosylation end products in diabetic nephropathy," *Metabolism*, vol. 49, no. 8, pp. 1030–1035, 2000.

[21] T. D. Schmittgen and K. J. Livak, "Analyzing real-time PCR data by the comparative C_T method," *Nature Protocols*, vol. 3, no. 6, pp. 1101–1108, 2008.

[22] S. Inturi, N. Tewari-Singh, C. Agarwal, C. W. White, and R. Agarwal, "Activation of DNA damage repair pathways in response to nitrogen mustard-induced DNA damage and toxicity in skin keratinocytes," *Mutation Research/Fundamental and Molecular Mechanisms of Mutagenesis*, vol. 763-764, pp. 53–63, 2014.

[23] C. Peng, J. Ma, X. Gao, P. Tian, W. Li, and L. Zhang, "High glucose induced oxidative stress and apoptosis in cardiac microvascular endothelial cells are regulated by FoxO3a," *PLoS ONE*, vol. 8, no. 11, Article ID e79739, 2013.

[24] P. A. Sontz, T. P. Mui, J. O. Fuss, J. A. Tainer, and J. K. Barton, "DNA charge transport as a first step in coordinating the detection of lesions by repair proteins," *Proceedings of the National Academy of Sciences of the United States of America*, vol. 109, no. 6, pp. E1856–E1861, 2012.

[25] C. F. Labuschagne and A. B. Brenkman, "Current methods in quantifying ROS and oxidative damage in *Caenorhabditis elegans* and other model organism of aging," *Ageing Research Reviews*, vol. 12, no. 4, pp. 918–930, 2013.

[26] D. J. Smart, J. K. Chipman, and N. J. Hodges, "Activity of OGG1 variants in the repair of pro-oxidant-induced 8-oxo-2′-deoxyguanosine," *DNA Repair*, vol. 5, no. 11, pp. 1337–1345, 2006.

[27] A. Bacsi, G. Chodaczek, T. K. Hazra, D. Konkel, and I. Boldogh, "Increased ROS generation in subsets of OGG1 knockout fibroblast cells," *Mechanisms of Ageing and Development*, vol. 128, no. 11-12, pp. 637–649, 2007.

[28] N. C. de Souza-Pinto, L. Eide, B. A. Hogue et al., "Repair of 8-oxodeoxyguanosine lesions in mitochondrial DNA depends on the oxoguanine DNA glycosylase (*OGG1*) gene and 8-oxoguanine accumulates in the mitochondrial DNA of OGG1-defective mice," *Cancer Research*, vol. 61, no. 14, pp. 5378–5381, 2001.

Hindawi Publishing Corporation
Oxidative Medicine and Cellular Longevity
Volume 2015, Article ID 843721, 12 pages
http://dx.doi.org/10.1155/2015/843721

Research Article

Ginsenoside Rb1 Treatment Attenuates Pulmonary Inflammatory Cytokine Release and Tissue Injury following Intestinal Ischemia Reperfusion Injury in Mice

Ying Jiang,[1] Zhen Zhou,[2] Qing-tao Meng,[1] Qian Sun,[1] Wating Su,[1] Shaoqing Lei,[1] Zhengyuan Xia,[3,4] and Zhong-yuan Xia[1]

[1]*Department of Anesthesiology, Renmin Hospital of Wuhan University, Wuhan 430060, China*
[2]*Department of Cardiovascular Surgery, Renmin Hospital of Wuhan University, Wuhan 430060, China*
[3]*Department of Anesthesiology, The University of Hong Kong, Pok Fu Lam, Hong Kong*
[4]*Department of Anesthesiology, Affiliated Hospital of Guangdong Medical College, Zhanjiang, Guangdong 524001, China*

Correspondence should be addressed to Zhong-yuan Xia; xiazhongyuan2005@aliyun.com

Received 18 September 2014; Revised 22 December 2014; Accepted 27 December 2014

Academic Editor: Yanfang Chen

Objective. Intestinal ischemia reperfusion (II/R) injury plays a critical role in remote organ dysfunction, such as lung injury, which is associated with nuclear factor erythroid 2-related factor 2 (Nrf2)/heme oxygenase-1 (HO-1) signaling pathway. In the present study, we tested whether ginsenoside Rb1 attenuated II/R induced lung injury by Nrf2/HO-1 pathway. *Methods*. II/R injury was induced in male C57BL/6J mice by 45 min of superior mesenteric artery (SMA) occlusion followed by 2 hours of reperfusion. Ginsenoside Rb1 was administrated prior to reperfusion with or without ATRA (all-transretinoic acid, the inhibitor of Nrf2/ARE signaling pathway) administration before II/R. *Results*. II/R induced lung histological injury, which is accompanied with increased levels of malondialdehyde (MDA), interleukin- (IL-) 6, and tumor necrosis factor- (TNF-) α but decreased levels of superoxide dismutase (SOD) and IL-10 in the lung tissues. Ginsenoside Rb1 reduced lung histological injury and the levels of TNF-α and MDA, as well as wet/dry weight ratio. Interestingly, the increased Nrf2 and HO-1 expression induced by II/R in the lung tissues was promoted by ginsenoside Rb1 treatment. All these changes could be inhibited or prevented by ATRA. *Conclusion*. Ginsenoside Rb1 is capable of ameliorating II/R induced lung injuries by activating Nrf2/HO-1 pathway.

1. Introduction

Intestinal ischemia reperfusion (II/R) injury is a life-threatening clinical surgical emergency, which is associated with the exacerbation of intestinal injury and a systemic inflammatory response leading to progressive distal organ impairment, finally resulting in cardiocirculatory, respiratory, hepatic, and renal failure. Acute respiratory distress syndrome (ARDS) induced by lung injury is one of the most serious complications. These clinical problems were involved in diverse causes such as intestinal barrier damage, bacteria translocation and oxidative stress, and activation of multiple inflammatory mediators [1, 2]. However, there still remain many doubts in the pathophysiology and therapeutics of II/R induced remote organ injury, especially lung injury.

Ginsenoside Rb1, a major active constituent of ginseng (*Panax ginseng*), has antioxidative effects and has been demonstrated to protect multiple organs from ischemia reperfusion injury [3–9]. However, it has not been fully elucidated whether it can also attenuate II/R induced acute lung injury. Nuclear factor erythroid 2-related factor 2 (Nrf2)/antioxidant response element (ARE) signaling pathway has been found as the most important endogenous antioxidative stress mechanism. It has been reported that Nrf2/ARE signaling pathway performs a fundamental role in protecting the body against the xenobiotics and oxidative injury in the pathophysiology of digestive system, circulation system, nervous system, and immune system diseases [10–13]. Nrf2 is a nuclear transcription factor that controls the expression and coordinates induction of a battery of defensive

genes encoding detoxifying enzymes and antioxidant proteins [14]. In response to stimulation of oxidative stress, Nrf2 translocates from the cytoplasm into the nucleus and then binds to a *cis*-acting enhancer sequence designated as ARE and regulates ARE mediated antioxidant enzyme gene such as heme oxygenase-1 (HO-1) expression and induction [15, 16]. HO-1 belongs to a member of the heat shock protein family and plays a significant protective role against inflammatory processes and oxidative tissue injury [17].

In this study, we established a superior mesenteric artery (SMA) occlusion/reperfusion mice model to induce lung injury. We used ATRA (all-transretinoic acid) as inhibitor of Nrf2/ARE signaling pathway, which interfered in the recruitment of Nrf2 to the ARE, thus disrupting the activation of ARE-driven genes [18]. With the treatment of ginsenoside Rb1, we aim to investigate whether ginsenoside Rb1 attenuates acute lung injury (ALI) induced by II/R in mice via Nrf2/ARE pathway.

2. Material and Methods

2.1. Mice. The current study was approved by the Animal Care Committee of Wuhan University, China, and was performed in accordance with National Institutes of Health guidelines for the use of experimental animals. Male C57BL/6 mice (9–12 weeks old; 17–22 g) were purchased from HUNAN SLAC JD Laboratory Animal Co. Ltd., China. They were housed under standard laboratory conditions at 22–24°C, relative humidity of 50 ± 15%, and kept on a 12 h day/night rhythm with free access to water and food. All experimental protocols conducted in the mice were carried out in accordance with the Guide for the Care and Use of Laboratory Animals by the National Institutes of Health (NIH Publication number 80-23).

2.2. Surgical Preparation. Animals were anesthetized intraperitoneally with pentobarbital sodium (50 mg/kg body weight). A midline laparotomy was performed; then the superior mesenteric artery (SMA) was isolated. The II/R injury was established by occluding SMA with a microvascular clip for 45 minutes followed by 2 hours of reperfusion as previously described [19]. Ischemia was recognized by the existence of pulseless or pale color of the small intestine. The return of pulses and the reestablishment of the pink color were assumed to indicate valid reperfusion of the intestine. The Sham group underwent the same surgical process, apart from occlusion of SMA. After 2 h reperfusion, the mice were killed. A median sternotomy was performed; the lung and intestine samples were obtained for further analysis.

2.3. Experimental Protocol. The mice were randomly allocated into eight groups ($n = 8$ in each group) (Figure 1): (1) Sham surgical preparation including isolation of the SMA without occlusion was performed (Sham); (2) mice were subjected to II/R without treatment (II/R); (3) mice were subjected to II/R with treatment of normal saline 10 minutes before reperfusion (II/R + NS); (4), (5) mice were treated with 30 mg/kg (II/R + Rb1-30) or 60 mg/kg (II/R + Rb1-60) ginsenoside Rb1, in which surgery was performed as in the II/R group with administration of the ginsenoside Rb1 intraperitoneally 10 minutes before reperfusion; (6) mice were subjected to Sham surgery and treated with ATRA (ATRA + Sham), which is the inhibitor of Nrf2/ARE signaling pathway; (7) mice were subjected to II/R and treated with ATRA (ATRA + II/R); (8) mice were subjected to II/R and treated with ATRA and 60 mg/kg ginsenoside Rb1 as group 5 (ATRA + II/R + Rb1-60). During the last two weeks before the operation, the mice in the group 6, 7, 8 received ATRA i.p. daily at 10 mg/kg and fed on a vitamin A-deficient diet, and the mice in the other groups received the equivalent volume of corn oil and fed on a control normal diet [18].

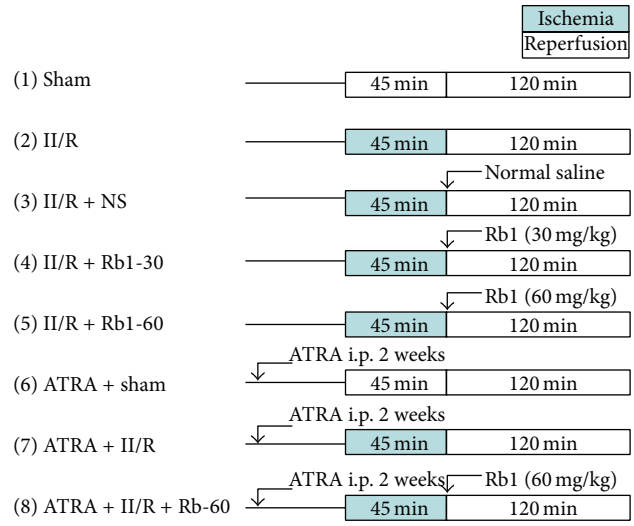

Figure 1: Experimental protocols. Mice were subjected to 45 min of SMA occlusion followed by 2 h of reperfusion. II/R: intestinal ischemia/reperfusion, NS: normal saline, Rb1: ginsenoside Rb1, and ATRA: all-transretinoic acid.

2.4. Lung Histology. The left lung was removed and fixed in 10% formalin. Following embedding in paraffin, the sections of 4 μm were stained with hematoxylin and eosin for light microscopy. Semiquantitative analysis of lung histopathology was performed by scoring the tissues based on lung edema, infiltration of inflammatory cells, alveolar hemorrhage, hyaline membrane, and atelectasis: no lesion, 0; injured area $\leqslant$ 25%, 1; injured area 26–50%, 2; injured area 51–70%, 3; injured area 71–90%, 4; injured area > 90%, 5. A total of three fields were randomly selected for each slide and the average was used as the histopathology score [20].

2.5. Histopathological Assessment of Intestines. After reperfusion, 1 cm of small intestine without adipose tissue was taken from the same place at the distal end of ileum and fixed in 4% formaldehyde. After embedding in paraffin, 4 μm sections were stained with hematoxylin and eosin before assessment by light microscopy (original magnification ×200, Olympus BX50; Olympus Optical, Tokyo, Japan).

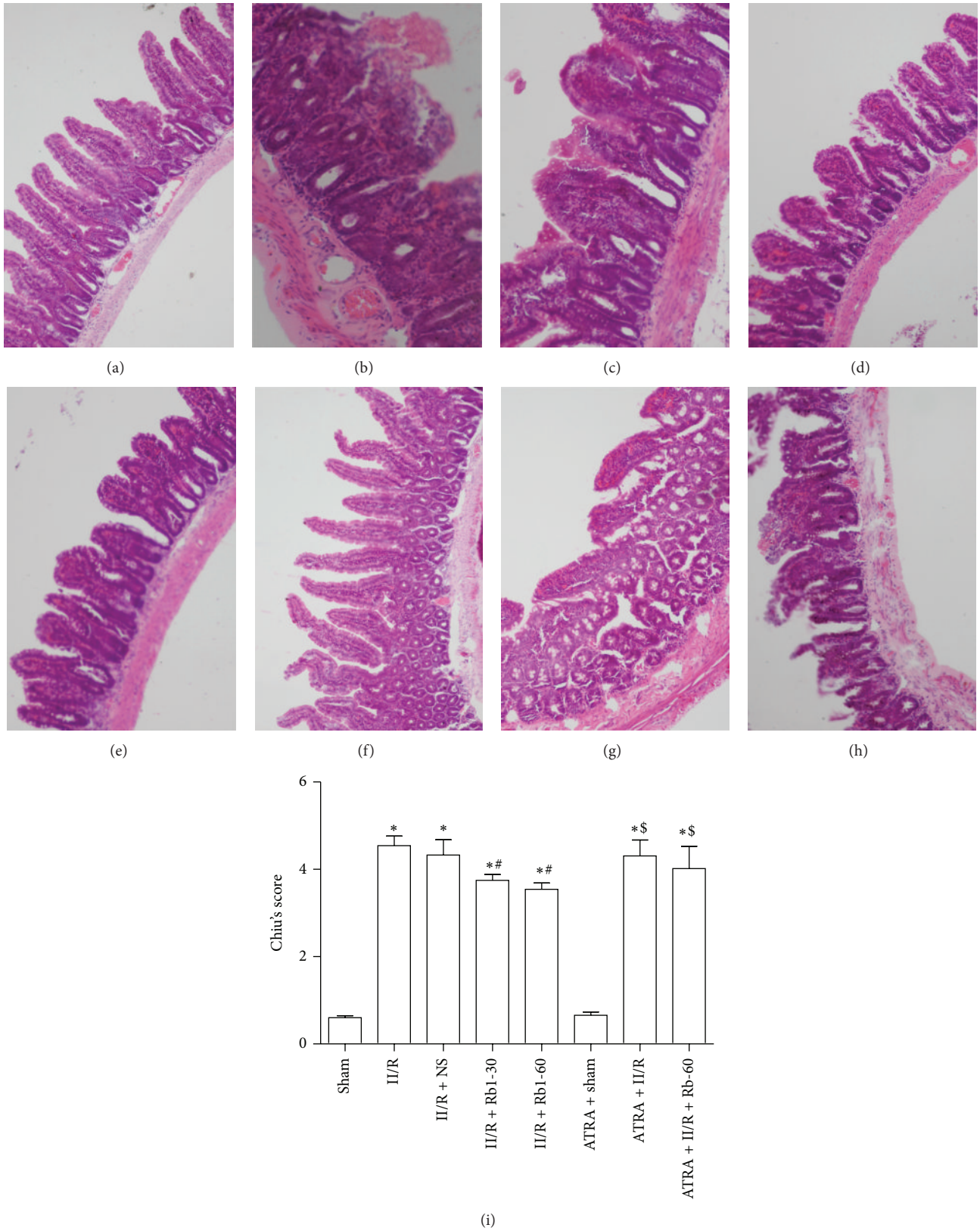

Figure 2: Intestinal histologic evaluation in the groups. ((a)–(h)) Histopathologic changes of the small-intestinal mucosa were observed under light microscopy (hematoxylin and eosin, ×200). (a) Sham group, (b) II/R group, (c) II/R + NS group, (d) II/R + Rb1-30 group, (e) II/R + Rb1-60 group, (f) ATRA + Sham group, (g) ATRA + II/R group, and (h) ATRA + II/R + Rb1-60 group. Data are mean ± SD, $n = 10$; $^{*}P < 0.05$ versus Sham group, $^{\#}P < 0.05$ versus II/R group, and $^{\$}P < 0.05$ versus II/R + Rb1-60 group.

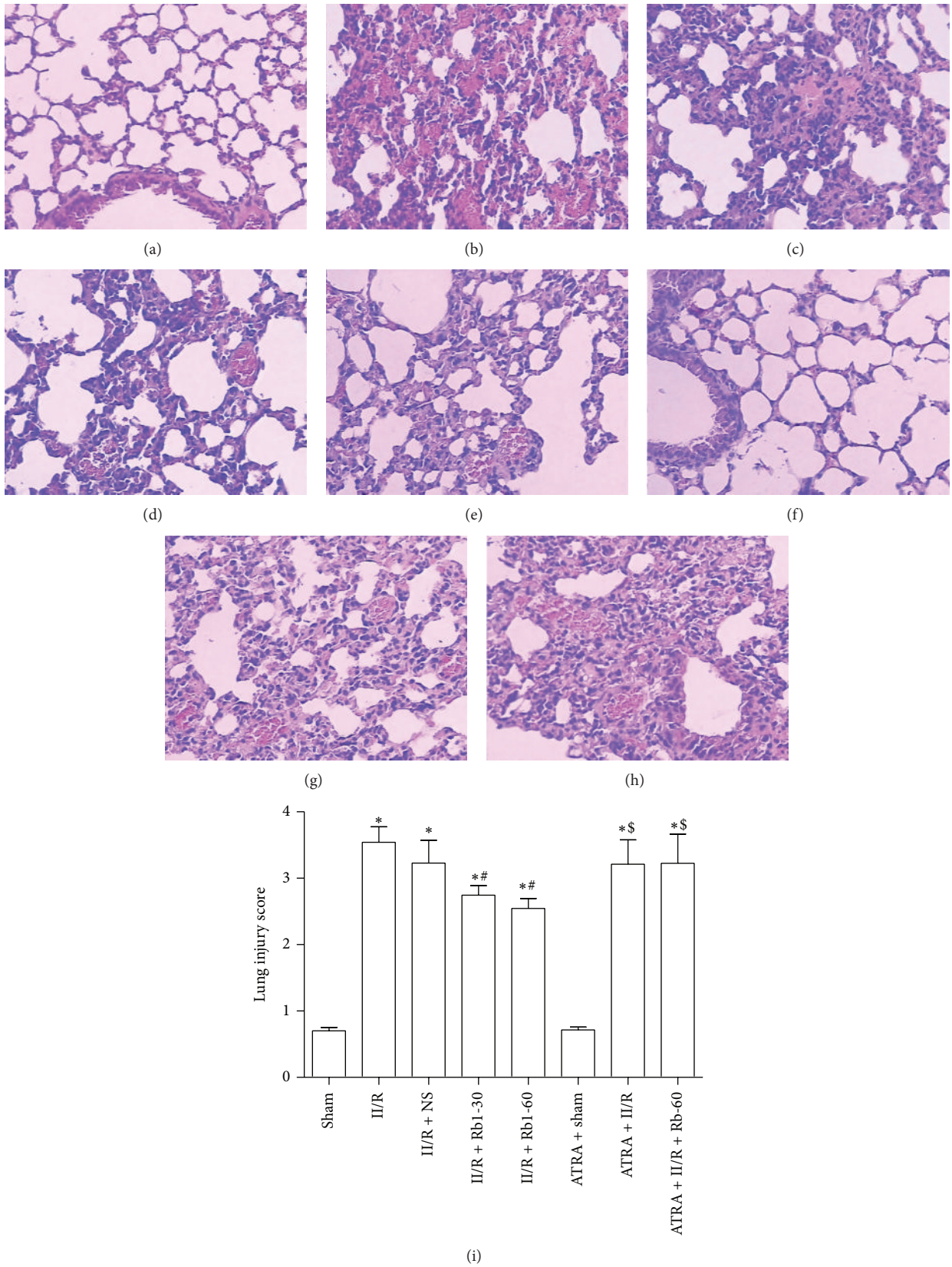

Figure 3: Histopathologic changes in mice lung under light microscopy (hematoxylin and eosin, ×200). (a) Sham group, (b) II/R group, (c) II/R + NS group, (d) II/R + Rb1-30 group, (e) II/R + Rb1-60 group, (f) ATRA + Sham group, (g) ATRA + II/R group, and (h) ATRA + II/R + Rb1-60 group. Data are mean ± SD, $n = 10$; $^{*}P < 0.05$ versus Sham group, $^{\#}P < 0.05$ versus II/R group, and $^{\$}P < 0.05$ versus II/R + Rb1-60 group.

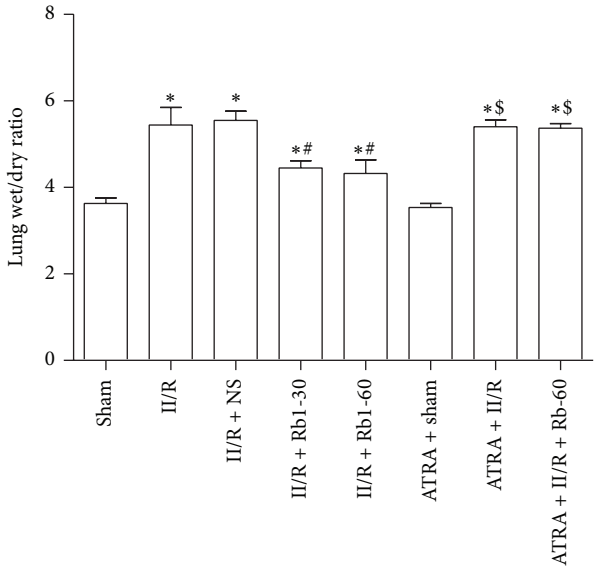

Figure 4: The effects of ginsenoside Rb1 on the lung wet/dry weight ratio. Data are mean ± SD, $n = 5$; $^{*}P < 0.05$ versus Sham group, $^{\#}P < 0.05$ versus II/R group, and $^{\$}P < 0.05$ versus II/R + Rb1-60 group.

Using the improved Chiu score method [21] to evaluate intestinal mucosal damage, higher scores are interpreted to indicate more severe damage. Criteria of Chiu grading system consist of 5 subdivisions according to the changes of villus and gland of intestinal mucosa: grade 0, normal mucosa; grade 1, development of subepithelial Gruenhagen's space at the tip of villus; grade 2, extension of the space with moderate epithelial lifting; grade 3, massive epithelial lifting with a few denuded villi; grade 4, denuded villi with exposed capillaries; and grade 5, disintegration of the lamina propria, ulceration, and hemorrhage.

2.6. Assessment of Pulmonary Edema. The left lung was harvested. After the lung wet weight was measured, the lungs were placed in a calorstat at 60°C for 48 h, and then the specimen was reweighed. The pulmonary edema was estimated by lung wet/dry weight ratio [22].

2.7. Immunohistochemical Assessment. Paraffin-embedded lung sections were stained using the streptavidin-biotin complex immunohistochemistry technique for HO-1 and Nrf2 detection. Brown staining in the cytoplasm and/or nucleus was considered an indicator of positive expression. With the Image-Pro Plus version 6.0, results were evaluated semiquantitatively according to optical density values of positive expression.

2.8. Western Blot Analysis. The right lungs were removed and nuclear fractions were prepared using a Nuclear and Cytoplasmic Protein Extraction Kit (Beyotime Institute of Biotechnology, China) according to the manufacturer's protocol. Western blot analysis was carried out as described [23]. Primary antibodies (working concentration) used were rabbit polyclonal antibodies against mice Nrf2 (1 : 2000, H-300, Santa Cruz Biotechnology, CA), HO-1 (1 : 1000, H-105, Santa Cruz Biotechnology, CA), and Lamin B1 (1 : 2000, H-90, Santa Cruz Biotechnology, CA). The HRP-conjugated secondary antibody was goat anti-rabbit IgG (Beyotime Institute of Biotechnology, China) used at 1 : 2000. Lamin B was used as an internal control. The ECL Western blotting detection reagents (Beyotime Institute of Biotechnology, China) were used for visualization of the protein bands. The intensities of the bands were analyzed with quantity one software (Bio-Rad, Hercules, CA).

2.9. Determination of Tissue Tumor Necrosis Factor Alpha (TNF-α), Interlukin-6 (IL-10), and Interlukin-6 (IL-6). Tissue levels of TNF-α, IL-10, and IL-6 were determined using commercially available ELISA kits (R&D, Minneapolis, MN) according to manufacturer's instructions. The results were expressed as pg/mL.

2.10. Determination of Tissue MDA Level and SOD Activity. The right lung tissues were homogenized on ice in normal saline. The homogenates were centrifuged at 4000 g·min^{-1} at 4°C for 10 min. The MDA level in the supernatants was determined by the measurement of thiobarbituric acid-reactive substances levels (assay kits were supplied by Nanjing Jiancheng Corp., China) as previously described [24]. The results were calculated as nmol·100 mg^{-1} protein. The SOD activity in the supernatants was evaluated by inhibition of nitroblue tetrazolium (NBT) reduction by O^{2-} generated by the xanthine/xanthine oxidase system (assay kits were supplied by Nanjing Jiancheng Corp., China) in accordance with the previous method [24]. The results were expressed by U·100 mg^{-1} protein.

2.11. Statistical Analysis. Data are presented as mean ± SD. Statistical comparison among multiple groups was performed by one-way analysis of variance (ANOVA) followed by Newman-Keuls multiple comparison test using the GraphPad Prism 5.0 software (GraphPad Software Inc., San Diego, CA, USA). A value of $P < 0.05$ was considered statistically significant.

3. Results

3.1. Histopathological Assessment of Intestines. The II/R group showed edema in the villi, inflammatory cells infiltration, and damaged areas interspersed with hemorrhage. In addition, the gap between epithelial cells significantly increased and capillaries and lymph vessels were markedly dilated. Normal villi were seen in the intestine of the Sham group and ATRA + Sham group under the light microscope. Ginsenoside Rb1 at the dose of 30 mg/kg and 60 mg/kg both significantly attenuated the histological intestine injury (Figure 2). However, there is little amelioration of the intestine injury induced by II/R in the ATRA + II/R + Rb1-60 group.

3.2. Pathologic Alternations of Lung Tissue. The lungs from II/R group showed damaged areas interspersed with hemorrhage, inflammatory cell infiltration, and pulmonary edema,

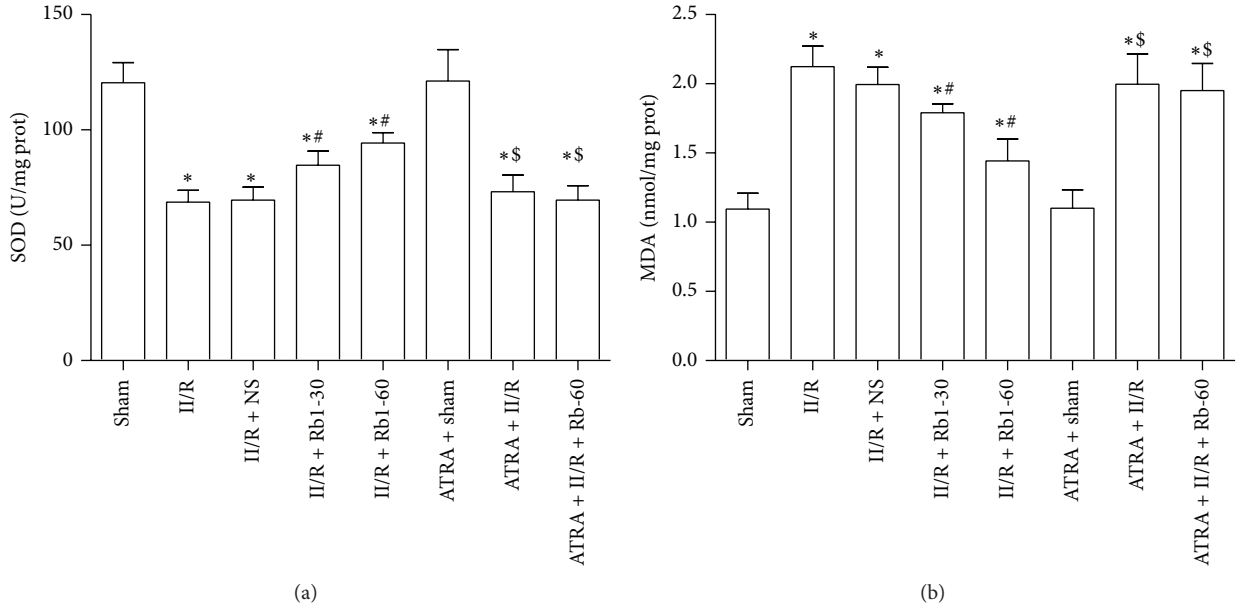

FIGURE 5: The changes of lung tissue SOD activity and MDA levels. Data are mean ± SD, $n = 10$; $^{*}P < 0.05$ versus Sham group, $^{\#}P < 0.05$ versus II/R group, and $^{\$}P < 0.05$ versus II/R + Rb1-60 group.

while little damage was seen in the lungs of the sham group and ATRA + Sham group under the light microscope. Ginsenoside Rb1 at the both doses of 30 mg/kg and 60 mg/kg significantly attenuated the histological lung injury (Figure 3). However, there is little amelioration of the lung injury induced by II/R in the ATRA + II/R + Rb1-60 group. This indicates that ATRA attenuated the protective action of ginsenoside Rb1 against II/R induced lung damage in the mice.

3.3. Changes of Lung Wet/Dry Weight Ratio. We next assessed the lung wet/dry weight ratio as indicators of lung permeability damage. As shown in Figure 4, the lung wet/dry weight ratio was significantly higher in the II/R group than the Sham group ($P < 0.05$). Compared with the II/R group, the lung wet/dry ratio was decreased significantly after the treatment of ginsenoside Rb1 ($P < 0.05$, II/R + Rb1-30 or II/R + Rb1-60 versus II/R). This decrease was reversed by administration of ATRA ($P > 0.05$, ATRA + II/R + Rb1-60 versus II/R). There was no significant difference between the Sham and ATRA + Sham group or II/R and II/R + NS group ($P > 0.05$).

3.4. Changes of the Level of MDA and the Activity of SOD. Oxidative stress has been proposed as an important mechanism of the development of II/R induced organ damage. Reperfusion or reoxygenation will activate recovery of aerobic metabolism and results in an overload of reactive oxygen species (ROS). Robust ROS generation generates excessive hydroxyl radicals, which are very unstable and have a high potential to damage cellular structures, enzymes, or channel proteins on the cellular membrane. We examined the effects of ginsenoside Rb1 on lung tissue lipidic peroxidation product (MDA) levels and the antioxidative SOD activity. As shown in Figure 5, treatment with 30 mg/kg and 60 mg/kg ginsenoside Rb1 significantly reduced MDA levels and increased SOD activity, and this effect was inhibited by administration of ATRA.

3.5. Changes of Tissue TNF-α, IL-10, and IL-6 Levels. In a number of clinical studies, microinflammation has been found to be associated with processes that may be related to II/R caused injury. As shown in Figure 6, the level of tissues TNF-α and IL-6 in the II/R group was significantly higher than that in the Sham group. However, the level of tissue IL-10 was significantly reduced in the II/R group compared to that in the Sham group. Treatment with 30 mg/kg and 60 mg/kg ginsenoside Rb1 significantly reduced TNF-α and IL-6 levels and increased IL-10 levels. After treatment with ATRA, this effect was inhibited.

3.6. Effects of Ginsenoside Rb1 on HO-1 and Nrf2 Expression in Lung Tissue by Immunohistochemical Detection. The lung tissue was obtained to measure the expression of Nrf2 and HO-1 by immunohistochemical assay. In the II/R group, both cytoplasm and nuclei of the lung tissue showed Nrf2 expression, but the expression of HO-1 was showed in the cytoplasm. Compared with the Sham group, the expression of Nrf2 and HO-1 in the II/R group increased significantly. After treatment with ginsenoside Rb1 at dose 30 or 60 mg/kg, the expression of Nrf2 and HO-1 was much higher than that in the II/R group. In the ATRA + II/R and ATRA + II/R + Rb1-60 groups, Nrf2 was also expressed obviously in the cytoplasm and nuclei, though mild expression of HO-1 could be seen in the cytoplasm of lung tissue in these groups (Figures 7 and 8).

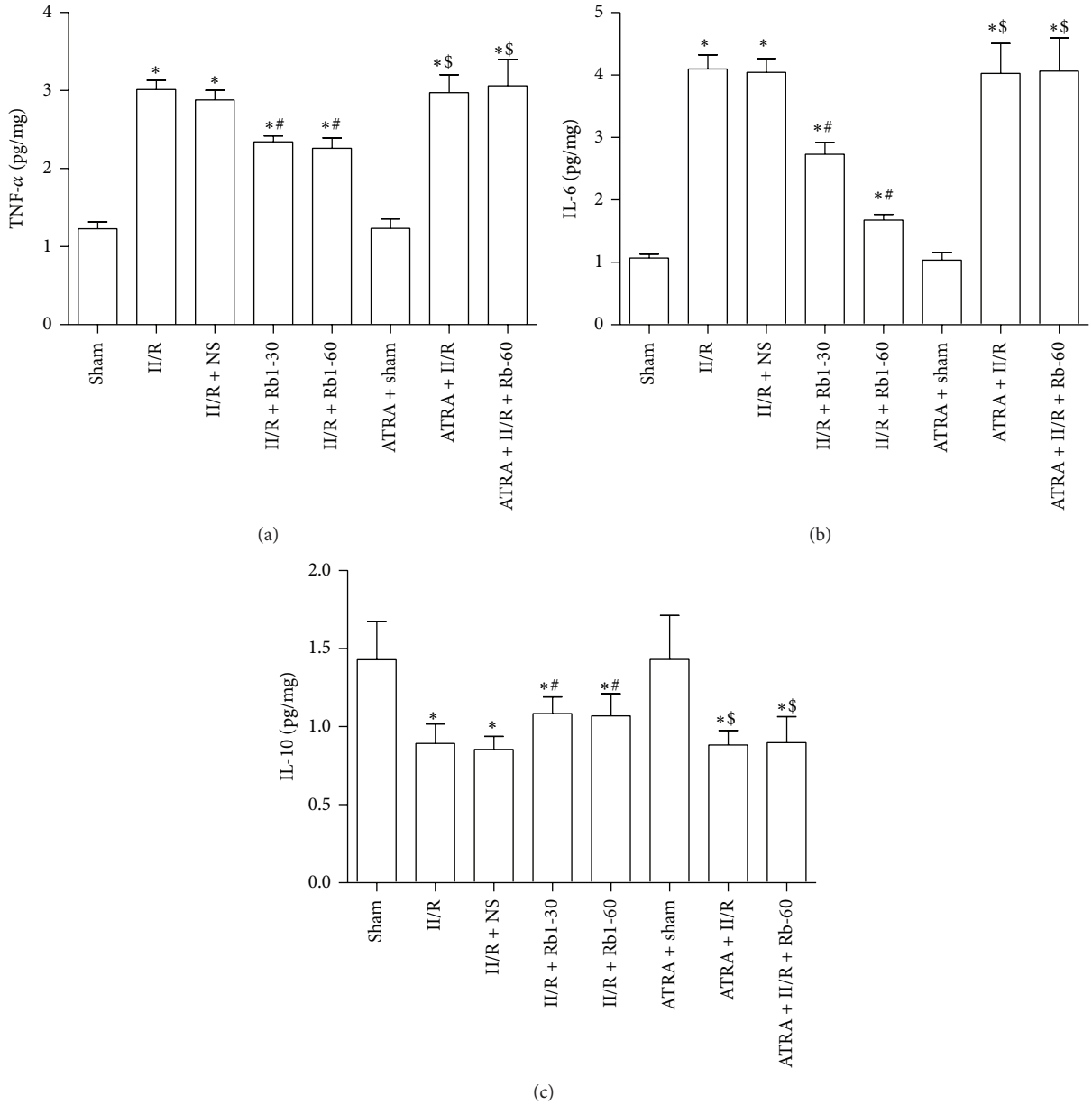

Figure 6: Cytokine levels in lung from mice. Cytokine levels were determined in lung homogenate using multiplex analysis: (a) TNF-α, (b) IL-6, and (c) IL-10. Data are mean ± SD, $n = 10$; $^{*}P < 0.05$ versus Sham group, $^{\#}P < 0.05$ versus II/R group, and $^{\$}P < 0.05$ versus II/R + Rb1-60 group.

3.7. Effects of Ginsenoside Rb1 on Cytoplasmic HO-1 and Nuclear Nrf2 Expression in Lung Tissue by Western Blotting Analysis. To further confirm the protective effect of ginsenoside Rb1 on the lung tissue against II/R injury, protein expression of nuclear Nrf2 and cytoplasmic HO-1 was examined by Western blot. As shown in Figure 9, Nrf2 and HO-1 expression were both increased markedly in the II/R group as compared with the Sham group. II/R with Rb1 intervention further increased the expression of Nrf2 and HO-1 significantly. ATRA administration has no effects on the cytoplasmic HO-1 expression as compared with the Sham group. This indicated that Rb1 induced cytoplasmic HO-1 expression was inhibited by ATRA. There was no significant difference in Nrf2 expression between the ATRA + II/R group and the II/R group or between the ATRA + II/R + Rb1-60 group and the II/R group.

4. Discussion

In this study, we have demonstrated in a mice model that 45 min occlusion of SMA followed by 2 h of reperfusion caused significant lung injury as evidenced by pathologic morphologic changes seen in the lung tissue, as well as the increased lung wet/dry ratio, which is in accordance with the previous reports [25]. We found that postischemia treatment

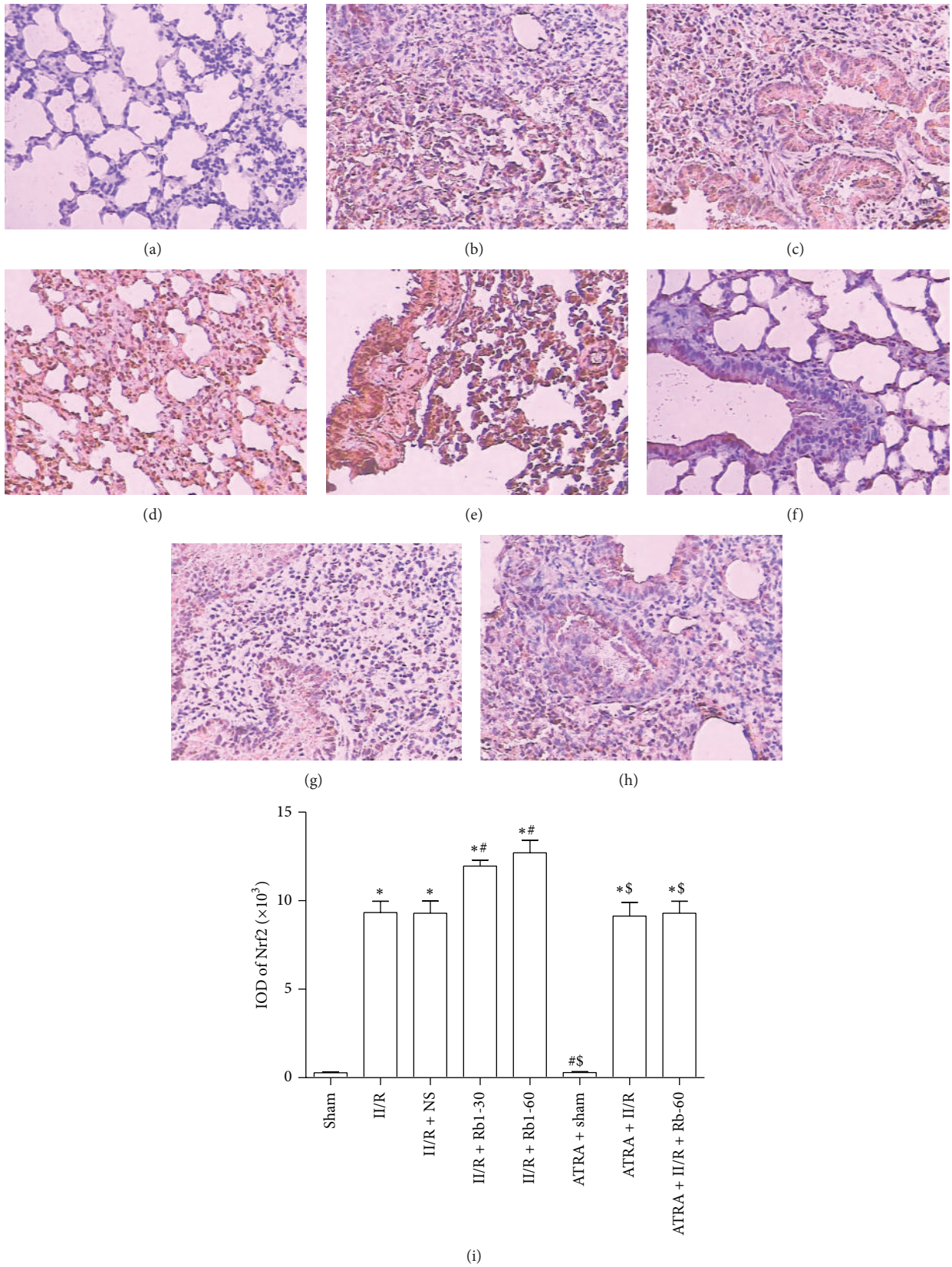

Figure 7: Expression of Nrf2 in the lung tissue under the light microscope (streptavidin-biotin complex immunohistochemistry, ×200). (a) Sham group, (b) II/R group, (c) II/R + NS group, (d) II/R + Rb1-30 group, (e) II/R + Rb1-60 group, (f) ATRA + Sham group, (g) ATRA + II/R group, and (h) ATRA + II/R + Rb1-60 group. Data are mean ± SD, $n = 5$; $^{*}P < 0.05$ versus Sham group, $^{\#}P < 0.05$ versus II/R group, and $^{\$}P < 0.05$ versus II/R + Rb1-60 group.

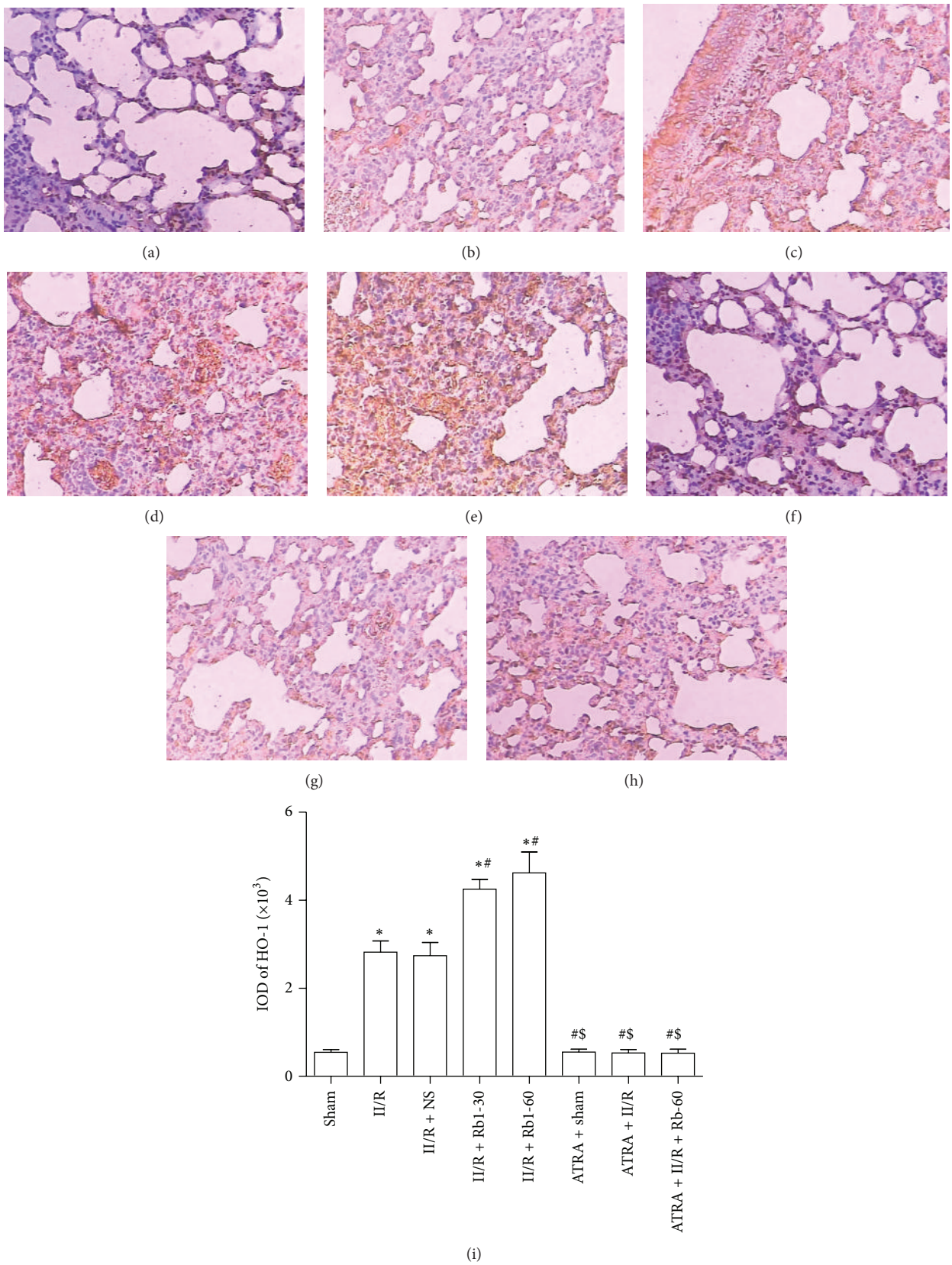

Figure 8: Expression of HO-1 in the lung tissue under the light microscope (streptavidin-biotin complex immunohistochemistry, ×200). (a) Sham group, (b) II/R group, (c) II/R + NS group, (d) II/R + Rb1-30 group, (e) II/R + Rb1-60 group, (F) ATRA + Sham group, (g) ATRA + II/R group, and (h) ATRA + II/R + Rb1-60 group. Data are mean ± SD, $n = 5$; $^{*}P < 0.05$ versus Sham group, $^{\#}P < 0.05$ versus II/R group, and $^{\$}P < 0.05$ versus II/R + Rb1-60 group.

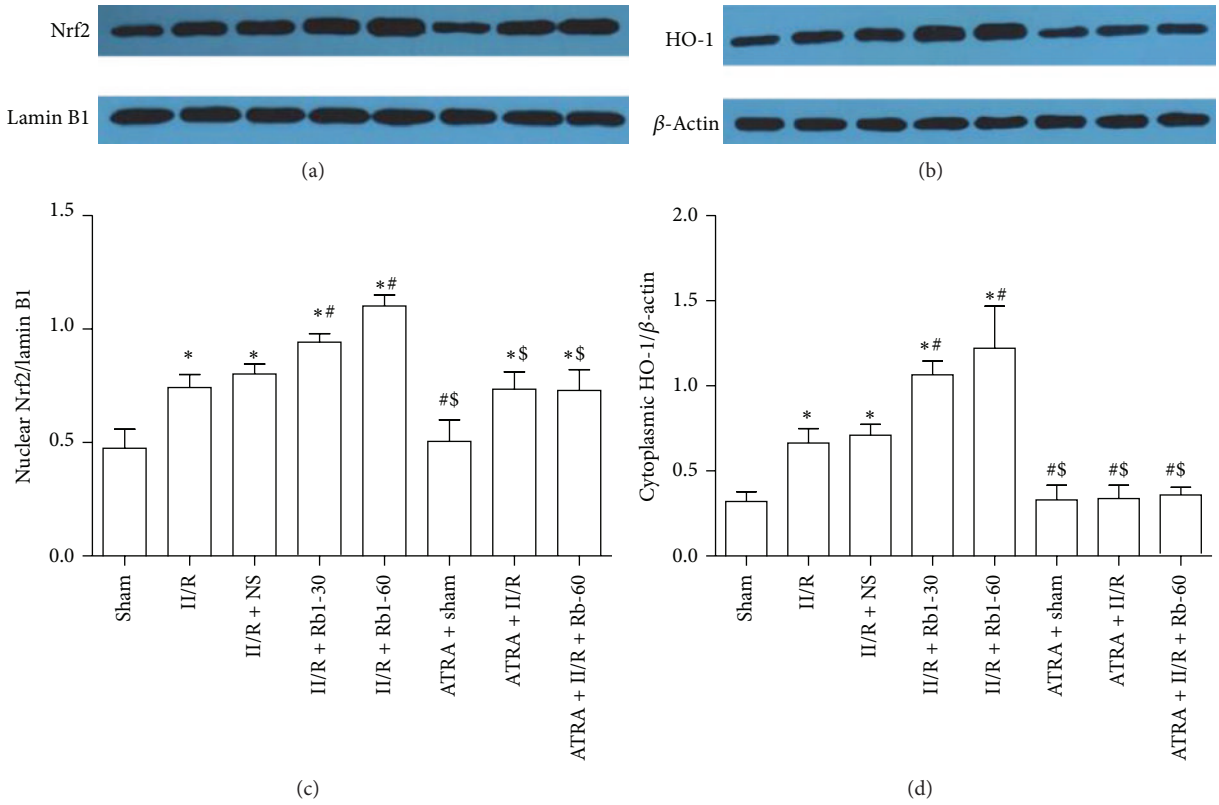

Figure 9: Western blotting analysis of the presence of Nrf2 in nuclear proteins and HO-1 in cytoplasmic proteins in the mice lung tissue. Data obtained from quantitative densitometry were presented as mean ± SD. $n = 10$, $^{*}P < 0.05$ versus Sham group, $^{\#}P < 0.05$ versus II/R group, and $^{\$}P < 0.05$ versus II/R + Rb1-60 group.

with ginsenoside Rb1 enhanced Nrf2 translocation to the nucleus in the lung tissues of mice and Rb1 treatment could reduce pulmonary morphologic damage, alleviate injuries induced by oxidative stress, and modulate inflammatory reactions. Further, Nrf2 function inhibition with ATRA reverted the pulmonary protective effects of ginsenoside Rb1, indicating that ginsenoside Rb1 confers its respiratory protection via Nrf2/ARE signaling in the II/R induced acute lung injury.

The mechanisms of acute lung injury induced by II/R are complex. It is thought that the damage of intestinal mucosal barrier following II/R causes the dislocation of bacteria or endogenous endotoxin, thus leading to increased oxidative stress and systemic inflammatory reaction, which is one of the main reasons for acute lung injury.

Ginseng is one of the most widely used herbal medicines. Ginsenosides, the major active ingredient of ginseng, have been noticed for their multiple pharmacological effects on antioxidation, signal transduction pathways, and interaction with receptors [26]. Oxidative stress refers to the mismatched redox equilibrium between the production of free radicals and the ability of cells to defend against them. One feasible way to prevent free radical mediated cellular injuries is to augment the oxidative defense capacity through intake of antioxidants. Moreover, the induction of endogenous phase II detoxifying enzymes or antioxidative proteins seems to be a reasonable strategy for delaying disease progression. Activation of Nrf2/ARE plays an important role in protecting cells from oxidative stress [27, 28]. The ability of Nrf2 to upregulate the expression of antioxidant genes via ARE suggests that increasing Nrf2 activity may provide a useful system for combating oxidative insults. Several recent reports have demonstrated that coordinate upregulation of ARE-driven genes protects organs from ischemia reperfusion injury [29–31]. Accumulating evidence also suggests that upregulation of HO-1 expression and the subsequent increase in HO activity may confer an adaptive survival response against oxidative insults. Our previous studies showed that Rb1 reduces renal apoptosis and alleviates renal dysfunction after II/R in part through the Nrf2/ARE pathway [32]. Wang et al. demonstrated that Rb1 attenuates lung injury induced by II/R via inhibiting NF-κB activation [33]. To determine the mechanism by which postischemia treatment with Rb1 reduces II/R-induced ROS generation, we examined the effect of ginsenoside Rb1 on Nrf2 and HO-1 expression in mice lung tissues. Our present study demonstrated that Rb1 increased nuclear Nrf2 protein and cytoplasmic HO-1 protein expressions in lung tissues of mice after II/R. The increase of HO-1 expression by Rb1 conferred cytoprotection against II/R induced oxidative stress. In addition, previous studies have shown that ATRA does not affect the half-life of Nrf2 or its nuclear translocation. ATRA inhibits Nrf2 function by stimulating the formation of Nrf2:RARα-containing complexes that do not bind to the ARE [18]. We showed that ATRA, as a

potent inhibitor for combination of Nrf2 with ARE, partially reversed the protective effects of Rb1, thus providing further evidence for Nrf2/ARE as a possible cytoprotective pathway for Rb1.

Ginseng extract was reported to have immunomodulatory effects [34]. Smolinski and Pestka [35] reported that immunologic effects include modulation of lipopolysaccharide-induced proinflammatory cytokine production in vitro and in vivo by ginsenoside Rb1. This was also confirmed with our study in which Rb1 significantly reduced the tissue level of TNF-α, IL-6, and IL-10. These results show that Rb1 may have multiple mechanisms of action that affect cytoprotection by both reducing ROS generation and increasing the anti-inflammatory effect.

In summary, our present study indicates that ginsenoside Rb1 alleviates acute lung injury following II/R via activating Nrf2/ARE pathway. The experiment data may help us further understand the pharmacological effects of Rb1 and also suggest a new therapeutic target to protect the body from II/R injury. However, further studies need to be performed in transfection of lung endothelial cells and intestinal epithelial cells with the siRNA and expressing plasmid for Nrf2 to confirm the findings of the current study.

Disclosure

All authors have no financial, personal, or other relationships with other people or organizations that could inappropriately influence the work.

Conflict of Interests

The authors declare that they have no conflict of interests.

Authors' Contribution

Ying Jiang and Zhen Zhou contributed equally to this work.

Acknowledgment

This study was mainly supported by a grant from the National Natural Science Foundation of China (NSFC) 81170768 and partly by NSFC 81471844 and 81300674.

References

[1] H. T. Hassoun, B. C. Kone, D. W. Mercer, F. G. Moody, N. W. Weisbrodt, and F. A. Moore, "Post-injury multiple organ failure: the role of the gut," *Shock*, vol. 15, no. 1, pp. 1–10, 2001.

[2] A. Pierro and S. Eaton, "Intestinal ischemia reperfusion injury and multisystem organ failure," *Seminars in Pediatric Surgery*, vol. 13, no. 1, pp. 11–17, 2004.

[3] T.-H. Lan, Z.-W. Xu, Z. Wang, Y.-L. Wu, W.-K. Wu, and H.-M. Tan, "Ginsenoside Rb1 prevents homocysteine-induced endothelial dysfunction via PI3K/Akt activation and PKC inhibition," *Biochemical Pharmacology*, vol. 82, no. 2, pp. 148–155, 2011.

[4] Y. P. Hwang and H. G. Jeong, "Ginsenoside Rb1 protects against 6-hydroxydopamine-induced oxidative stress by increasing heme oxygenase-1 expression through an estrogen receptor-related PI3K/Akt/Nrf2-dependent pathway in human dopaminergic cells," *Toxicology and Applied Pharmacology*, vol. 242, no. 1, pp. 18–28, 2010.

[5] Y. Wu, Z.-Y. Xia, J. Dou et al., "Protective effect of ginsenoside Rb1 against myocardial ischemia/reperfusion injury in streptozotocin-induced diabetic rats," *Molecular Biology Reports*, vol. 38, no. 7, pp. 4327–4335, 2011.

[6] Z. Jiang, Y. Wang, X. Zhang et al., "Preventive and therapeutic effects of ginsenoside Rb1 for neural injury during cerebral infarction in rats," *The American Journal of Chinese Medicine*, vol. 41, no. 2, pp. 341–352, 2013.

[7] L. Shen, Y. Xiong, D. Q.-H. Wang et al., "Ginsenoside Rb1 reduces fatty liver by activating AMP-activated protein kinase in obese rats," *Journal of Lipid Research*, vol. 54, no. 5, pp. 1430–1438, 2013.

[8] R. Hashimoto, J. Yu, H. Koizumi, Y. Ouchi, and T. Okabe, "Ginsenoside Rb1 prevents MPP^+-induced apoptosis in PC12 cells by stimulating estrogen receptors with consequent activation of ERK1/2, Akt and inhibition of SAPK/JNK, p38 MAPK," *Evidence-Based Complementary and Alternative Medicine*, vol. 2012, Article ID 693717, 8 pages, 2012.

[9] D. Liu, H. Zhang, W. Gu, Y. Liu, and M. Zhang, "Neuroprotective effects of ginsenoside rb1 on high glucose-induced neurotoxicity in primary cultured rat," *PLoS ONE*, vol. 8, no. 11, Article ID e79399, 2013.

[10] P. Yao, A. Nussler, L. Liu et al., "Quercetin protects human hepatocytes from ethanol-derived oxidative stress by inducing heme oxygenase-1 via the MAPK/Nrf2 pathways," *Journal of Hepatology*, vol. 47, no. 2, pp. 253–261, 2007.

[11] A. S. Pachori, L. G. Melo, L. Zhang, S. D. Solomon, and V. J. Dzau, "Chronic recurrent myocardial ischemic injury is significantly attenuated by pre-emptive adeno-associated virus heme oxygenase-1 gene delivery," *Journal of the American College of Cardiology*, vol. 47, no. 3, pp. 635–643, 2006.

[12] S. Lee and K. Suk, "Heme oxygenase-1 mediates cytoprotective effects of immunostimulation in microglia," *Biochemical Pharmacology*, vol. 74, no. 5, pp. 723–729, 2007.

[13] H. J. Kang, Y. B. Hong, H. J. Kim, and I. Bae, "CR6-interacting factor 1 (CRIF1) regulates NF-E2-related factor 2 (NRF2) protein stability by proteasome-mediated degradation," *Journal of Biological Chemistry*, vol. 285, no. 28, pp. 21258–21268, 2010.

[14] J. W. Kaspar, S. K. Niture, and A. K. Jaiswal, "Nrf2:INrf2 (Keap1) signaling in oxidative stress," *Free Radical Biology and Medicine*, vol. 47, no. 9, pp. 1304–1309, 2009.

[15] S. Dhakshinamoorthy, D. J. Long II, and A. K. Jaiswal, "Antioxidant regulation of genes encoding enzymes that detoxify xenobiotics and carcinogens," *Current Topics in Cellular Regulation*, vol. 36, pp. 201–216, 2001.

[16] D. Bloom, S. Dhakshinamoorthy, W. Wang, C. M. Celli, and A. K. Jaiswal, "Role of NFE2 related factors in oxidative stress," in *Cell and Molecular Responses to Stress. Volume 2: Protein Adaptation and Signal Transduction*, K. B. Storey and J. M. Storey, Eds., pp. 229–238, Elsevier, Amsterdam, The Netherlands, 2001.

[17] Y.-F. Liao, W. Zhu, D.-P. Li, and X. Zhu, "Heme oxygenase-1 and gut ischemia/reperfusion injury: a short review," *World Journal of Gastroenterology*, vol. 19, no. 23, pp. 3555–3561, 2013.

[18] X. J. Wang, J. D. Hayes, C. J. Henderson, and C. R. Wolf, "Identification of retinoic acid as an inhibitor of transcription factor Nrf2 through activation of retinoic acid receptor alpha," *Proceedings of the National Academy of Sciences of the United States of America*, vol. 104, no. 49, pp. 19589–19594, 2007.

[19] Q. Sun, Q. T. Meng, Y. Jiang, and Z.-Y. Xia, "Ginsenoside Rb1 attenuates intestinal ischemia reperfusion induced renal injury by activating Nrf2/ARE pathway," *Molecules*, vol. 17, no. 6, pp. 7195–7205, 2012.

[20] J. Shen, G. Fu, L. Jiang, J. Xu, L. Li, and G. Fu, "Effect of dexmedetomidine pretreatment on lung injury following intestinal ischemia-reperfusion," *Experimental and Therapeutic Medicine*, vol. 6, no. 6, pp. 1359–1364, 2013.

[21] C. J. Chiu, A. H. McArdle, R. Brown, H. J. Scott, and F. N. Gurd, "Intestinal mucosal lesion in low-flow states. I. A morphological, hemodynamic, and metabolic reappraisal," *Archives of Surgery*, vol. 101, no. 4, pp. 478–483, 1970.

[22] M. L. Pearce, J. Yamashita, and J. Beazell, "Measurement of pulmonary edema," *Circulation Research*, vol. 16, pp. 482–488, 1965.

[23] A. J. L. Chia, C. E. Goldring, N. R. Kitteringham, S. Q. Wong, P. Morgan, and B. K. Park, "Differential effect of covalent protein modification and glutathione depletion on the transcriptional response of Nrf2 and NF-κB," *Biochemical Pharmacology*, vol. 80, no. 3, pp. 410–421, 2010.

[24] K. X. Liu, Y. S. Li, W. Q. Huang, C. Li, and J.-X. Liu, "Immediate but not delayed postconditioning during reperfusion attenuates acute lung injury induced by intestinal ischemia/reperfusion in rats: comparison with ischemic preconditioning," *Journal of Surgical Research*, vol. 157, no. 1, pp. e55–e62, 2009.

[25] B. C. Guido, M. Zanatelli, W. Tavares-de-Lima, S. M. Oliani, and A. S. Damazo, "Annexin-A1 peptide down-regulates the leukocyte recruitment and up-regulates interleukin-10 release into lung after intestinal ischemia-reperfusion in mice," *Journal of Inflammation*, vol. 10, no. 1, article 10, 2013.

[26] J. M. Lü, Q. Yao, and C. Chen, "Ginseng compounds: an update on their molecular mechanisms and medical applications," *Current Vascular Pharmacology*, vol. 7, no. 3, pp. 293–302, 2009.

[27] W. F. Yao, G. J. Luo, G. S. Zhu et al., "Propofol activation of the Nrf2 pathway is associated with amelioration of acute lung injury in a rat liver transplantation model," *Oxidative Medicine and Cellular Longevity*, vol. 2014, Article ID 258567, 9 pages, 2014.

[28] H. R. Potteti, N. M. Reddy, T. K. Hei, D. V. Kalvakolanu, and S. P. Reddy, "The NRF2 activation and antioxidative response are not impaired overall during hyperoxia-induced lung epithelial cell death," *Oxidative Medicine and Cellular Longevity*, vol. 2013, Article ID 798401, 11 pages, 2013.

[29] B. Ke, X.-D. Shen, Y. Zhang et al., "KEAP1-NRF2 complex in ischemia-induced hepatocellular damage of mouse liver transplants," *Journal of Hepatology*, vol. 59, no. 6, pp. 1200–1207, 2013.

[30] W. Wang, J. Kang, H. Li et al., "Regulation of endoplasmic reticulum stress in rat cortex by p62/ZIP through the Keap1-Nrf2-ARE signalling pathway after transient focal cerebral ischaemia," *Brain Injury*, vol. 27, no. 7-8, pp. 924–933, 2013.

[31] B. F. Peake, C. K. Nicholson, J. P. Lambert et al., "Hydrogen sulfide preconditions the db/db diabetic mouse heart against ischemia-reperfusion injury by activating Nrf2 signaling in an Erk-dependent manner," *The American Journal of Physiology—Heart and Circulatory Physiology*, vol. 304, no. 9, pp. H1215–H1224, 2013.

[32] Q. Sun, Q. T. Meng, Y. Jiang et al., "Protective effect of ginsenoside Rb1 against intestinal ischemia-reperfusion induced acute renal injury in mice," *PLoS ONE*, vol. 8, no. 12, Article ID e80859, 2013.

[33] J. Wang, L. Qiao, S. Li, and G. Yang, "Protective effect of ginsenoside Rb1 against lung injury induced by intestinal ischemia-reperfusion in rats," *Molecules*, vol. 18, no. 1, pp. 1214–1226, 2013.

[34] A. Rhule, B. Rase, J. R. Smith, and D. M. Shepherd, "Toll-like receptor ligand-induced activation of murine DC2.4 cells is attenuated by *Panax notoginseng*," *Journal of Ethnopharmacology*, vol. 116, no. 1, pp. 179–186, 2008.

[35] A. T. Smolinski and J. J. Pestka, "Modulation of lipopolysaccharide-induced proinflammatory cytokine production in vitro and in vivo by the herbal constituents apigenin (chamomile), ginsenoside Rb_1 (ginseng) and parthenolide (feverfew)," *Food and Chemical Toxicology*, vol. 41, no. 10, pp. 1381–1390, 2003.

Hindawi Publishing Corporation
Oxidative Medicine and Cellular Longevity
Volume 2015, Article ID 287058, 6 pages
http://dx.doi.org/10.1155/2015/287058

Research Article

Effects of Cyclosporine on Reperfusion Injury in Patients: A Meta-Analysis of Randomized Controlled Trials

Kangxing Song,[1] Shuxia Wang,[2] and Dake Qi[3]

[1]*Department of Cardiology, The General Hospital of Chinese People's Liberation Army, No. 28, Fuxing Road, Beijing 100853, China*
[2]*Department of Geriatric Cardiology, The General Hospital of Chinese People's Liberation Army, No. 28, Fuxing Road, Beijing 100853, China*
[3]*Yale Cardiovascular Research Center, Department of Internal Medicine, Yale University School of Medicine, New Haven, CT 06511, USA*

Correspondence should be addressed to Dake Qi; dake.qi@yale.edu

Received 19 October 2014; Accepted 12 January 2015

Academic Editor: Mengzhou Xue

Mitochondrial permeability transition pore (mPTP) opening due to its role in regulating ROS generation contributes to cardiac reperfusion injury. In animals, cyclosporine (cyclosporine A, CsA), an inhibitor of mPTP, has been found to prevent reperfusion injury following acute myocardial infarction. However, the effects of CsA in reperfusion injury in clinical patients are not elucidated. We performed a meta-analysis using published clinical studies and electronic databases. Relevant data were extracted using standardized algorithms and additional data were obtained directly from investigators as indicated. Five randomized controlled blind trials were included in our meta-analysis. The clinical outcomes including infarct size (SMD: −0.41; 95% CI: −0.81, 0.01; $P = 0.058$), left ventricular ejection fraction (LVEF) (SMD: 0.20; 95% CI: −0.02, 0.42; $P = 0.079$), troponin I (TnI) (SMD: −0.21; 95% CI: −0.49, 0.07; $P = 0.149$), creatine kinase (CK) (SMD: −0.32; 95% CI: −0.98, 0.35; $P = 0.352$), and creatine kinase-MB isoenzyme (CK-MB) (SMD: −0.06; 95% CI: −0.35, 0.23; $P = 0.689$) suggested that there is no significant difference on cardiac function and injury with or without CsA treatment. Our results indicated that, unlike the positive effects of CsA in animal models, CsA administration may not protect heart from reperfusion injury in clinical patients with myocardial infarction.

1. Introduction

Ischemic heart disease is a leading cause of death and disability worldwide and it would continue to be the top reason of death till 2030 in both developing and developed countries [1]. Reperfusion therapy is the most important strategy to rescue ischemic myocardium and reduce infarction size [2]. However, it is often associated with a further cardiac injury functionally characterized by myocardial stunning, ventricular arrhythmias, and no-reflow [3, 4]. In histology, reperfusion injury leads to cell death in heart due to poor calcium handling in the sarcoplasmic reticulum-mitochondria system, calpain activation, oxidative stress, and mitochondrial damage [5, 6].

Mitochondrial dysfunction is a major factor leading to loss of cardiomyocyte function and viability [7]. The molecular mechanisms of mitochondrial dysfunction include a long-lasting opening of mitochondrial permeability transition pore (mPTPs) and oxidative stress resulting from reactive oxygen species (ROS) formation [6]. More recent studies indicated that mPTPs opening plays a crucial role in reperfusion injury [8]. The mPTPs opening during reperfusion could be regulated by several factors including high pH, Ca^{2+} overload, and burst of ROS at the onset of reperfusion [6, 9].

Cyclosporine, also known as cyclosporine A (CsA), is an inhibitor of mPTP opening, which has been proposed to prevent reperfusion injury following acute myocardial infarction [3, 10]. Some previous meta-analysis based on animal studies indicated that CsA might reduce myocardial infarct size [11]. However, the effects of CsA in clinical patients are largely unknown. A small pilot trial showed

that administration of CsA at the time of percutaneous coronary intervention (PCI) limited infarct size during acute myocardial infarction, suggesting a positive effect of CsA in reperfusion injury [12]. However, another study with a similar number of patients reported that CsA treatment did not produce any beneficial effect on either infarct size or other clinical outcomes [13].

So far based on any individual human study, it is hard to draw a conclusion that CsA benefits reperfusion injury due to limited patient number and race. Therefore, our present analysis was to identify and combine all published clinical trials that investigated CsA treatment in human patients. We hope to see a clearer picture about the therapeutic effects of CsA on reperfusion injury.

2. Methods

2.1. Literature Screening. We systematically searched PubMed, Cochrane Library, Embase, reviews, and reference lists of relevant papers before September 2014 by using Medical Subject Heading (MeSH) terms "Cyclosporine," "CSA" paired with the following terms: "reperfusion injury," "reperfusion," and "injury."

2.2. Study Selection. Studies were selected based on the following criteria: (1) randomized controlled studies; (2) patients with myocardial infarction or with aortic valve surgery or with coronary artery bypass graft surgery (CABG); (3) CsA treatment.

2.3. Quality Assessment. All the recruited studies were assessed and scored by the following five indicators including the quality of randomization, blinding, reporting of withdrawals, generation of random numbers, and concealment of allocation. The possible score is from 0 to 5 and score 5 represents the highest level of quality [14].

2.4. Data Extraction. The data extracted from each study include the first-author's name, year of publication, country, subject characteristics (race, gender, age, and so on), sample size, and endpoints of patients. Cardiac injury following infarction was evaluated by magnetic resonance imaging (MRI), release of cardiac enzymes (troponin I, creatine kinase, and creatine kinase-MB isoenzyme), and left ventricular ejection fraction (LVEF) performed with two independent investigators.

2.5. Statistics and Analysis. All the data were presented as mean ± standard deviation (SD). The value of SD was calculated from published data in the original articles. Briefly, a random effect model was performed in the data with P value less than 0.10 by heterogeneity test (χ^2-based Q-test), while a fixed-effect model was used when P value is higher than 0.10 [15]. Heterogeneity was also assessed by I^2 test. The I^2 value was classified by the percentage of observed study variability based on heterogeneity rather than chance (I^2 = 0–25%, no heterogeneity; I^2 = 25–50%, moderate heterogeneity; I^2 = 50–75%, large heterogeneity; I^2 = 75–100%, extreme heterogeneity) [16]. Since CK values have significant heterogeneity, the random effect models were performed. In addition, funnel plots were used to assess publication bias. Statistical analysis was carried out with Stata software (version 12.0; Stata Corporation, College Station, TX) and REVMAN software (version 5.0; Cochrane Collaboration, Oxford, UK).

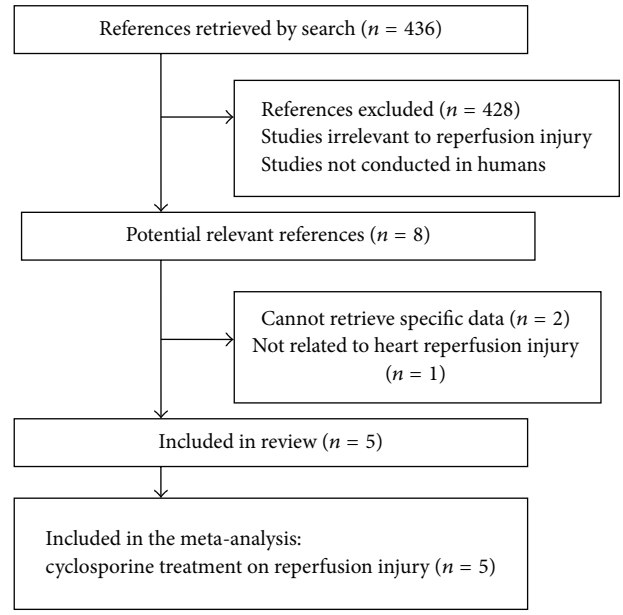

Figure 1: The flowchart outlining the process of search criteria and study selection.

3. Results

3.1. The Data Extracting from Literatures. A total of 436 articles were selected through the search and 428 of them were excluded due to the reasons like being irrelevant to reperfusion injury or nonhuman studies. A full text assessment in the eight potentially relevant articles led to a further exclusion of 3 studies (Figure 1). The exclusion was due to (1) failure to retrieve specific data for our meta-analysis [17, 18]; (2) being irrelevant to heart reperfusion injury [19]; or (3) lack of clinical data about left ventricular systolic dysfunction.

3.2. The Characteristics of Selected Studies. In the five recruited literatures [12, 13, 20–22], three studied patients with myocardial infarction [12, 13, 20], one studied patients following aortic valve surgery [21], and one studied patients following CABG surgery [22]. The CsA was given with an intravenous bolus dose (2.5 mg/kg) in all these studies. In addition, two studies were double-blinded [13, 22] and the other three were single-blinded [12, 20, 21]. The average age of patients varied from 58 to 67 years. The major characteristics of the selected studies have been listed in Table 1.

3.3. Data Quality. The quality scores of the trials varied from 3 to 5 (maximum score). All included trials were randomized, prospective, and placebo-controlled and blind design.

Table 1: Characteristics of the study population.

Reference	Year	Cyclosporine method	Cyclosporine dosage	Participants	Number of subjects	Age	Study design
Chiari et al. [21]	2014	Intravenous bolus	2.5 mg/kg	Patients accepting elective aortic valve surgery	30	67 ± 11	Prospective, monocentric, randomized, controlled, single-blind
Ghaffari et al. [13]	2013	Intravenous bolus	2.5 mg/kg	Patients with acute anterior STEMI receiving TLT	50	64.0 ± 11.2	Randomized, placebo-controlled, double-blinded
Hausenloy et al. [22]	2014	Intravenous bolus	2.5 mg/kg	Patients undergoing elective CABG surgery [1]	40	65.8 ± 10.7	Randomized, placebo-controlled, double-blinded
Mewton et al. [20]	2010	Intravenous bolus	2.5 mg/kg	Patients with AMI accepting PCI	15	60 ± 10	Prospective, multicenter, randomized, controlled, single-blind
Piot et al. [12]	2008	Intravenous bolus	2.5 mg/kg	Patients with [2] AMI accepting PCI	30	58 ± 2	Prospective, multicenter, randomized, controlled, single-blind

STEMI: ST-elevation myocardial infarction; CABG: coronary artery bypass graft; AMI: acute myocardial infarction; PCI: percutaneous coronary intervention; TLT: thrombolytic treatment.

3.4. The Evaluation of CsA Effects on Clinical Outcomes. The clinical indicators including infarct size, left ventricular ejection fraction (LVEF), troponin I (TnI), creatine kinase (CK), and creatine kinase-MB isoenzyme (CK-MB) were analyzed in our data.

3.4.1. Infarct Size. Infarct size was measured by MRI in one study, which was evaluated twice at the fifth day [12] and 6 months [20], respectively, following myocardial infarction. Myocardial infarction was identified by delayed hyperenhancement within myocardium and quantified by intensity of myocardial postcontrast signal. The significance was defined by more than two SD above that in a reference region of remote, noninfarct myocardium within the same slice [12]. The CsA treatment group appears to have a smaller infarct size compared to control group, but the difference is not statistically significant (SMD: −0.41; 95% CI: −0.81, 0.01; $P = 0.058$) (Figure 2). In addition, no significant calculated heterogeneity (heterogeneity $\chi^2 = 0.41$, $I^2 = 0\%$, and $P_{\text{heterogeneity}} = 0.52$) was found (Figure 2).

3.4.2. LVEF. LVEF was evaluated in three studies. One of them was measured at 5 days and 6 months following occurrence of myocardial infarction [20]. The second was assessed at the first day of admission and after hospital discharge [13]. The third was measured at hospital discharge [21]. There was no significant improvement on LVEF in CsA treatment group compared to control (SMD: 0.20; 95% CI: −0.02, 0.42; $P = 0.079$) (Figure 2). No significant heterogeneity in LVEF (heterogeneity $\chi^2 = 0.41$, $I^2 = 0\%$, and $P_{\text{heterogeneity}} = 0.52$) was found either (Figure 2).

3.4.3. TnI. TnI was also quantified in three studies. The plasma level of TnI following CsA treatment (SMD: −0.21; 95% CI: −0.49, 0.07; $P = 0.149$) was comparable to control group (Figure 2) and the heterogeneity of TnI was also unchanged (heterogeneity $\chi^2 = 2.19$, $I^2 = 8.6\%$, and $P_{\text{heterogeneity}} = 0.34$) (Figure 2).

3.4.4. CK and CK-MB. CK and CK-MB were evaluated in two studies, but none of them demonstrated changes following CsA treatment (CK: SMD: −0.32; 95% CI: −0.98, 0.35; $P = 0.352$) (CK-MB: SMD: −0.06; 95% CI: −0.35, 0.23; $P = 0.689$) (Figure 2). Interestingly, although a significant heterogeneity was observed in CK levels (heterogeneity $\chi^2 = 4.13$, $I^2 = 75.8\%$, and $P_{\text{heterogeneity}} = 0.042$), the heterogeneity of CK-MB was unchanged following CsA treatment (heterogeneity $\chi^2 = 0.01$, $I^2 = 0\%$, and $P_{\text{heterogeneity}} = 0.924$). The random effect models were subsequently performed to attenuate the effects of CK heterogeneity between the two studies.

3.5. Publication Bias. Funnel plots of the study are symmetric through visual examination and a statistical analysis of funnel plots also suggested there is no publication bias (Egger test, $P = 0.44$) (Figure 3).

4. Discussion

Reperfusion injury is associated with numerous cellular mechanisms including inflammatory responses, vascular leakage, free radical generation, and proapoptotic protein release [8]. Mitochondrial permeability transition pore (mPTP) plays a key role in regulating cell death and oxidative stress [8]. The mPTP opening allows small molecular solutes to freely move into the mitochondrial matrix leading to resultant mitochondrial swelling. This swelling then causes unfolding of cristae and release of intermembrane proteins that eventually trigger cell apoptosis [23, 24]. Therefore, the

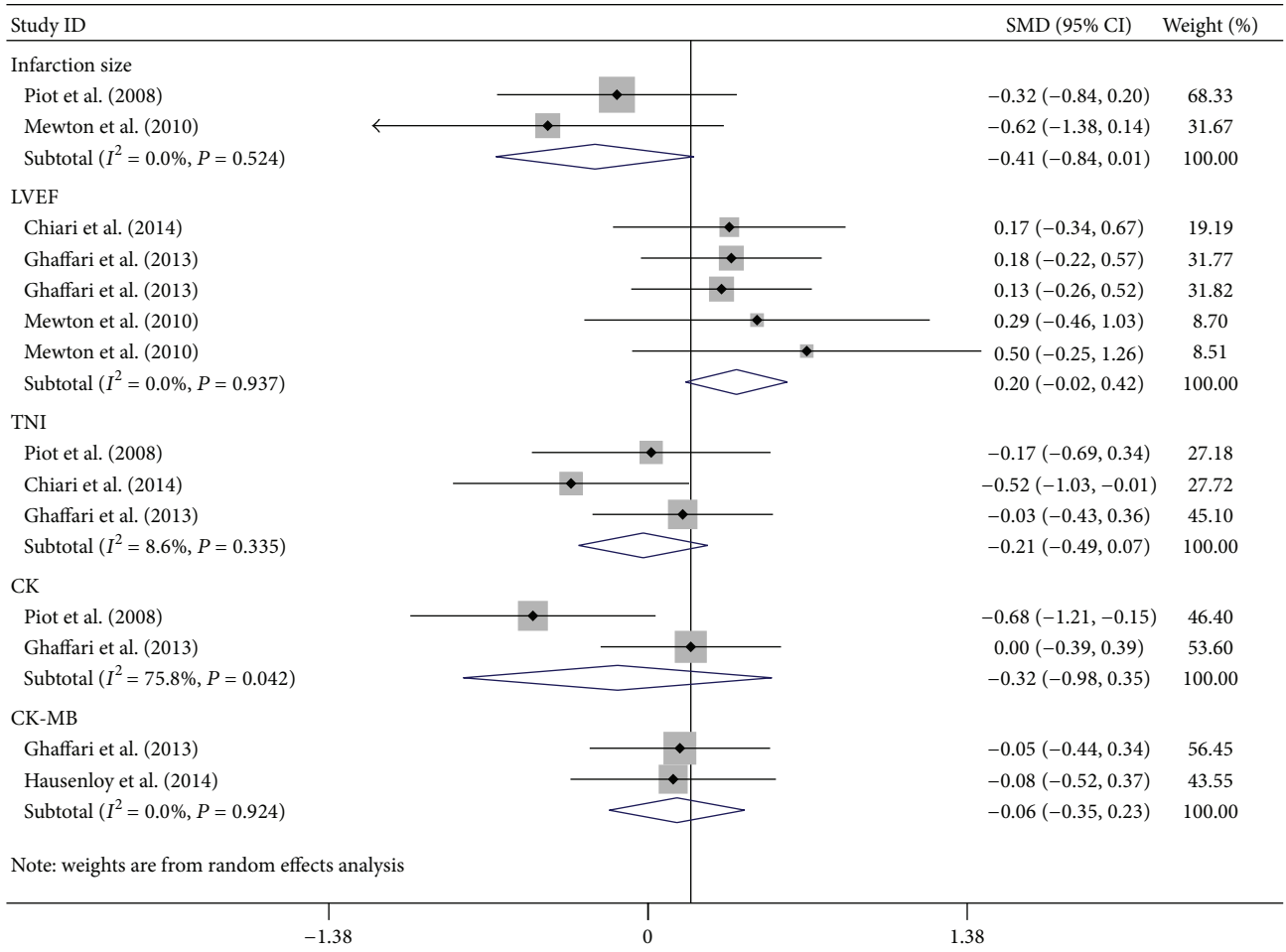

Figure 2: Random effect meta-analysis of standard mean differences (95% CI) on cardiac injury following cyclosporine treatment. The cardiac injury following reperfusion was quantified by infarct size, left ventricular ejection fraction (LVEF), creatine kinase (CK), and creatine kinase-MB (CK-MB) with and without cyclosporine treatment. The meta-analysis was performed on these data. Significance is $P < 0.05$.

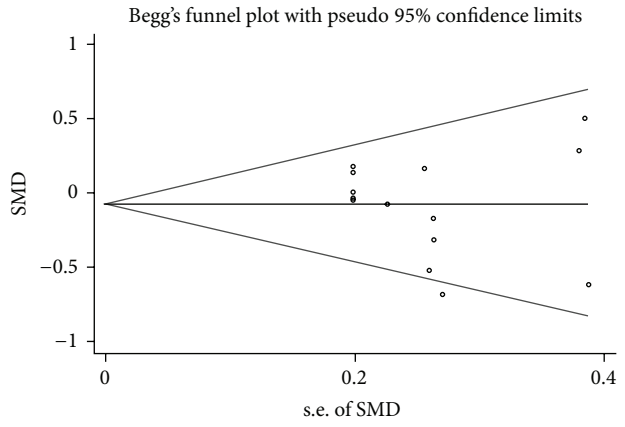

Figure 3: Begg's funnel plot (with pseudo 95% CIs) of all studies included in the meta-analysis.

mPTP opening may significantly contribute to cardiac reperfusion injury. Indeed, some previous studies have indicated that mPTP inhibitor, CsA, had a positive effect on reperfusion injury in animal models [25, 26]. The treatment of CsA in old rats is associated with decreased oxidative stress and improved mitochondrial function [27]. However, whether the inhibition of mPTP opening is also beneficial to ischemia-reperfusion injury in human being is still controversial.

In our meta-analysis, the five recruited studies have a randomized, controlled, and blind design. All the patients were intravenously injected with a bolus dose of CsA at 2.5 mg/kg before PCI, cardiac surgery, or thrombolytic treatment. Our aim was to evaluate the effects of CsA on reperfusion injury in human patients. Infarct size is a key indicator for postischemic injury in the heart and it is also a marker for cell death [28]. Cell death during reperfusion is associated with preapoptotic pathway c-Jun N terminal kinase (JNK) activation [29]. The mPTP opening facilitates ROS generation, which is a trigger of JNK upstream kinases [30]. Simultaneously, the increased JNK activation further upregulates ROS production [31]. Therefore, CsA administration may inhibit reperfusion injury through downregulating ROS production and JNK pathway activation. In our current analysis, two selected studies measured infarct size by MRI

at early (the fifth day after acute myocardial infarction) [12] and late reperfusion (6 months) [20]. The group with CsA treatment demonstrated a similar infarct size as control at both time points, suggesting that CsA regulated mitochondrial function is not a mechanism to stop the development of cell necrosis during reperfusion in the heart.

Cell necrosis leads to intracellular content release. Therefore, some cardiac specific enzymes including TnI, CK, and CK-MB have been widely used in clinical practice to identify cardiac injury. Our results indicated that CsA treatment did not alter TnI in clinical patients receiving PCI, CABG, or aortic valve surgery. However, plasma CK has a significant heterogeneity. We usually use the subgroup and metaregression analysis to explore heterogeneity in effects and influences of study characteristics or perform a random effect model to attenuate the effects of heterogeneity. In our current study, the CK analysis due to its small sample size is hard to run either subgroup or metaregression analysis. Random effect models assume that the treatment effects observed in the trials are random samples from a distribution of treatment effects with heterogeneity which typically produce more conservative estimates of the significance of the treatment effect than fixed-effect models [32]. Therefore, the random effect models were performed to reduce the effects of heterogeneity in our small sample studies. Eventually, our results indicated that plasma CK is not changed following CsA treatment, suggesting that CsA treatment did not affect reperfusion injury.

Overall, our current meta-analysis indicated that CsA may not protect heart from reperfusion injury in clinical patients. This conclusion is based on the tests from a small group of clinical patients. The restricted data leads to a result that no further subanalysis could be performed in patients with acute myocardial infarction or aortic valve surgery. In addition, a major confounding factor is the heterogeneity among cases and controls. Therefore, more careful selections of cases and controls in larger studies will be required to firmly establish the role of CsA in regulating reperfusion injury.

Conflict of Interests

The authors declare that there is no conflict of interests regarding the publication of this paper.

Authors' Contribution

Kangxing Song and Shuxia Wang contributed equally to this work.

Acknowledgment

This study was supported by the National Natural Science Foundation of China (Grants nos. 81470504 and 81100160).

References

[1] C. D. Mathers and D. Loncar, "Projections of global mortality and burden of disease from 2002 to 2030," *PLoS Medicine*, vol. 3, no. 11, article e442, 2006.

[2] J. L. Anderson, C. D. Adams, E. M. Antman et al., "2012 ACCF/AHA focused update incorporated into the ACCF/AHA 2007 guidelines for the management of patients with unstable angina/non-ST-elevation myocardial infarction: a report of the American College of Cardiology Foundation/American Heart Association Task Force on Practice Guidelines," *Circulation*, vol. 127, no. 23, pp. e663–e828, 2013.

[3] L. Gomez, B. Li, N. Mewton et al., "Inhibition of mitochondrial permeability transition pore opening: translation to patients," *Cardiovascular Research*, vol. 83, no. 2, pp. 226–233, 2009.

[4] E. Braunwald and R. A. Kloner, "Myocardial reperfusion: a double-edged sword?" *The Journal of Clinical Investigation*, vol. 76, no. 5, pp. 1713–1719, 1985.

[5] D. Garcia-Dorado, A. Rodríguez-Sinovas, M. Ruiz-Meana, and J. Inserte, "Protection against myocardial ischemia-reperfusion injury in clinical practice," *Revista Espanola de Cardiologia*, vol. 67, no. 5, pp. 394–404, 2014.

[6] X. Ma, H. Liu, S. R. Foyil et al., "Impaired autophagosome clearance contributes to cardiomyocyte death in ischemia/reperfusion injury," *Circulation*, vol. 125, no. 25, pp. 3170–3181, 2012.

[7] S. Gao, H. Li, X. Feng et al., "α-enolase plays a catalytically independent role in doxorubicin-induced cardiomyocyte apoptosis and mitochondrial dysfunction," *Journal of Molecular and Cellular Cardiology*, vol. 79, pp. 92–103, 2015.

[8] A. P. Halestrap and A. P. Richardson, "The mitochondrial permeability transition: a current perspective on its identity and role in ischaemia/reperfusion injury," *Journal of Molecular and Cellular Cardiology*, vol. 78, pp. 129–141, 2015.

[9] F. Di Lisa, N. Kaludercic, A. Carpi, R. Menabò, and M. Giorgio, "Mitochondrial pathways for ROS formation and myocardial injury: the relevance of p66Shc and monoamine oxidase," *Basic Research in Cardiology*, vol. 104, no. 2, pp. 131–139, 2009.

[10] P. Z. Gerczuk and R. A. Kloner, "An update on cardioprotection: a review of the latest adjunctive therapies to limit myocardial infarction size in clinical trials," *Journal of the American College of Cardiology*, vol. 59, no. 11, pp. 969–978, 2012.

[11] W. Y. Lim, C. M. Messow, and C. Berry, "Cyclosporin variably and inconsistently reduces infarct size in experimental models of reperfused myocardial infarction: a systematic review and meta-analysis," *British Journal of Pharmacology*, vol. 165, no. 7, pp. 2034–2043, 2012.

[12] C. Piot, P. Croisille, P. Staat et al., "Effect of cyclosporine on reperfusion injury in acute myocardial infarction," *The New England Journal of Medicine*, vol. 359, no. 5, pp. 473–481, 2008.

[13] S. Ghaffari, B. Kazemi, M. Toluey, and N. Sepehrvand, "The Effect of prethrombolytic cyclosporine-a injection on clinical outcome of acute anterior st-elevation myocardial infarction," *Cardiovascular Therapeutics*, vol. 31, no. 4, pp. e34–e39, 2013.

[14] D. Moher, B. Pham, A. Jones et al., "Does quality of reports of randomised trials affect estimates of intervention efficacy reported in meta-analyses?" *The Lancet*, vol. 352, no. 9128, pp. 609–613, 1998.

[15] R. DerSimonian and N. Laird, "Meta-analysis in clinical trials," *Controlled Clinical Trials*, vol. 7, no. 3, pp. 177–188, 1986.

[16] J. P. T. Higgins, S. G. Thompson, J. J. Deeks, and D. G. Altman, "Measuring inconsistency in meta-analyses," *British Medical Journal*, vol. 327, no. 7414, pp. 557–560, 2003.

[17] S. Morota, T. Manolopoulos, A. Eyjolfsson et al., " Functional and pharmacological characteristics of permeability transition in isolated human heart mitochondria," *PLoS ONE*, vol. 8, no. 6, Article ID e67747, 2013.

[18] E. Pahl, S. A. Miller, B. P. Griffith, and F. J. Fricker, "Occult restrictive hemodynamics after pediatric heart transplantation," *The Journal of Heart and Lung Transplantation*, vol. 14, pp. 1109–1115, 1995.

[19] L. A. Vricella, J. M. Karamichalis, S. Ahmad, R. C. Robbins, R. I. Whyte, and B. A. Reitz, "Lung and heart-lung transplantation in patients with end-stage cystic fibrosis: the Stanford experience," *Annals of Thoracic Surgery*, vol. 74, no. 1, pp. 13–18, 2002.

[20] N. Mewton, P. Croisille, G. Gahide et al., "Effect of cyclosporine on left ventricular remodeling after reperfused myocardial infarction," *Journal of the American College of Cardiology*, vol. 55, no. 12, pp. 1200–1205, 2010.

[21] P. Chiari, D. Angoulvant, N. Mewton et al., "Cyclosporine protects the heart during aortic valve surgery," *Anesthesiology*, vol. 121, no. 2, pp. 232–238, 2014.

[22] D. J. Hausenloy, G. Kunst, E. Boston-Griffiths et al., "The effect of cyclosporin-A on peri-operative myocardial injury in adult patients undergoing coronary artery bypass graft surgery: a randomised controlled clinical trial," *Heart*, vol. 100, no. 7, pp. 544–549, 2014.

[23] R. S. Gill, D. L. Bigam, and P.-Y. Cheung, "The role of cyclosporine in the treatment of myocardial reperfusion injury," *Shock (Augusta, Ga)*, vol. 37, no. 4, pp. 341–347, 2012.

[24] A. P. Halestrap, S. J. Clarke, and S. A. Javadov, "Mitochondrial permeability transition pore opening during myocardial reperfusion—a target for cardioprotection," *Cardiovascular Research*, vol. 61, no. 3, pp. 372–385, 2004.

[25] Q. Cai, G. F. Baxter, and D. M. Yellon, "Reduction of infarct size in isolated rat heart by CsA and FK506: possible role of phosphatase inhibition," *Cardiovascular Drugs and Therapy*, vol. 12, no. 5, pp. 499–501, 1998.

[26] J. Li, A. Iorga, S. Sharma et al., "Intralipid, a clinically safe compound, protects the heart against ischemia-reperfusion injury more efficiently than cyclosporine-A," *Anesthesiology*, vol. 117, no. 4, pp. 836–846, 2012.

[27] J. Zhu, M. J. Rebecchi, Q. Wang, P. S. A. Glass, P. R. Brink, and L. Liu, "Chronic Tempol treatment restores pharmacological preconditioning in the senescent rat heart," *The American Journal of Physiology—Heart and Circulatory Physiology*, vol. 304, no. 5, pp. H649–H659, 2013.

[28] R. J. Burns, R. J. Gibbons, Q. Yi et al., "The relationships of left ventricular ejection fraction, end-systolic volume index and infarct size to six-month mortality after hospital discharge following myocardial infarction treated by thrombolysis," *Journal of the American College of Cardiology*, vol. 39, no. 1, pp. 30–36, 2002.

[29] N. Krestnikova, A. Stulpinas, A. Imbrasaite, G. Sinkeviciute, and A. V. Kalvelyte, "JNK implication in adipocyte-like cell death induced by chemotherapeutic drug cisplatin," *The Journal of Toxicological Sciences*, vol. 40, no. 1, pp. 21–32, 2015.

[30] S. Wang, H. He, L. Chen, W. Zhang, X. Zhang, and J. Chen, "Protective effects of salidroside in the MPTP/MPP^+-induced model of parkinson's disease through ros-no-related mitochondrion pathway," *Molecular Neurobiology*, 2014.

[31] V. Appierto, P. Tiberio, M. G. Villani, E. Cavadini, and F. Formelli, "PLAB induction in fenretinide-induced apoptosis of ovarian cancer cells occurs via a ROS-dependent mechanism involving ER stress and JNK activation," *Carcinogenesis*, vol. 30, no. 5, pp. 824–831, 2009.

[32] R. DerSimonian and R. Kacker, "Random-effects model for meta-analysis of clinical trials: an update," *Contemporary Clinical Trials*, vol. 28, no. 2, pp. 105–114, 2007.

Hindawi Publishing Corporation
Oxidative Medicine and Cellular Longevity
Volume 2015, Article ID 568634, 15 pages
http://dx.doi.org/10.1155/2015/568634

Review Article

Organ-Protective Effects of Red Wine Extract, Resveratrol, in Oxidative Stress-Mediated Reperfusion Injury

Fu-Chao Liu,[1,2] Hsin-I Tsai,[1,2] and Huang-Ping Yu[1,2]

[1] *Department of Anesthesiology, Chang Gung Memorial Hospital, 5 Fu-Shin Street, Kwei-Shan, Taoyuan 333, Taiwan*
[2] *College of Medicine, Chang Gung University, Taoyuan, Taiwan*

Correspondence should be addressed to Huang-Ping Yu; yuhp2001@adm.cgmh.org.tw

Received 10 September 2014; Accepted 9 October 2014

Academic Editor: Zhengyuan Xia

Resveratrol, a polyphenol extracted from red wine, possesses potential antioxidative and anti-inflammatory effects, including the reduction of free radicals and proinflammatory mediators overproduction, the alteration of the expression of adhesion molecules, and the inhibition of neutrophil function. A growing body of evidence indicates that resveratrol plays an important role in reducing organ damage following ischemia- and hemorrhage-induced reperfusion injury. Such protective phenomenon is reported to be implicated in decreasing the formation and reaction of reactive oxygen species and pro-nflammatory cytokines, as well as the mediation of a variety of intracellular signaling pathways, including the nitric oxide synthase, nicotinamide adenine dinucleotide phosphate oxidase, deacetylase sirtuin 1, mitogen-activated protein kinase, peroxisome proliferator-activated receptor-gamma coactivator 1 alpha, hemeoxygenase-1, and estrogen receptor-related pathways. Reperfusion injury is a complex pathophysiological process that involves multiple factors and pathways. The resveratrol is an effective reactive oxygen species scavenger that exhibits an antioxidative property. In this review, the organ-protective effects of resveratrol in oxidative stress-related reperfusion injury will be discussed.

1. Introduction

Resveratrol, found in various plants, nuts, and fruits and especially abundant in grapes and red wine, is a naturally occurring plant antibiotic known as phytoalexins [1, 2]. Previous reports have demonstrated the protective effects of resveratrol in different pathological models and experimental conditions [3–6]. Many clinical studies indicate the beneficial effects of resveratrol in human diseases [7–12]. Recent report indicates that intake of a McDonald's meal with red wine could decrease oxidized low density lipoprotein level and increase antioxidative gene expression in healthy human [13]. A growing body of evidence indicates that resveratrol may play potential therapeutic roles in human health by its antioxidant, anti-inflammatory, antiaging, antidiabetic, and apoptotic properties [12, 14–17]. A number of target molecules mediating the abovementioned protective effects of resveratrol have been identified, including the endothelial nitric oxide synthase (eNOS) [18, 19], the mitogen-activated protein kinase (MAPK) [20, 21], the hemeoxygenase-1 (HO-1) [3], the estrogen receptor (ER) [20, 22–24], the histone deacetylase sirtuin 1 (SIRT1) [25–28], the nuclear factor E2-related factor-2 (Nfr2) [3, 29], and nuclear factor-kappa B (NF-κB) [30, 31]. A variety of laboratory and clinical studies also indicate that resveratrol may lead to tissue and organ protective effects against various injuries [6, 19, 32–35]. Ischemia-reperfusion (I/R) injury induces free radical formation and inflammation within hours and results in the excessive production of oxidants and proinflammatory mediators and that play a significant role in the development of multiple organ dysfunctions under those conditions [36–38]. Resveratrol has been suggested as an organ-protective agent to prevent and treat ischemia and shock-like and reperfusion injury due to its antioxidative activities [20, 39–49]. In this review, we summarize the protective effects and possible mechanisms of resveratrol on the preservation of organ function in oxidative stress-mediated I/R injury (Table 1).

Table 1: Protective effects and mechanisms of the resveratrol on different organs in oxidative stress-mediated reperfusion injury.

Species/targets	Model of reperfusion injury	Effective dose	Effects and mechanisms	References
Male Wistar rats rat/heart	Langendorff-perfused mode (ischemia 45 min, reperfusion 10 min).	25 mg/kg (pretreatment 7 days, IP)	MDA↓, CAT↓, peroxidase↑, and SOD↑	[80]
Spraque-Dawley rats/heart	Langendorff-perfused mode (ischemia 60 min, reperfusion 60 min)	20 mg/kg (pretreatment 14 days intragastric tube), 10 μM (30 min before ischemia)	MDA↓, LDH↓, carbonyl↓, and GSH↑	[68]
Male Sprague-Dawley rats/heart	Langendorff-perfused mode (ischemia 30 min, reperfusion 2 h)	10 μM (30 min before ischemia, IV perfused)	MDA↓ and infarct volume↓	[49]
Male Sprague Dawley rats/heart	Langendorff-perfused mode (ischemia 15 min, reperfusion 10 min).	resveratrol 1–100 μM (pretreatment 7 days, IP)	MDA↓ and no improvement in heart function	[82]
Sprague-Dawley/Brain	Right middle cerebral artery occlusion (ischemia 30 min, reperfusion 5.5 h)	0.1–1.0 μM (10 min before ischemia, IV)	Activation of ER-α and ER-β and infarct volume ↓	[23]
Male Wistar rats/brain	Bilateral common carotid occlusion (occlusion 4 h)	5–30 mg/kg (5 min before reperfusion, IP)	MDA↓, MPO↓, TNF-α ↓, IL-6↓, ICAM-I↓, Catalase↑, SOD↑, and IL-10↑	[99]
Male Sprague-Dawley rats/brain	Middle cerebral artery occlusion. (occlusion 2 h)	30 mg/kg (pretreatment 7 days, IP)	Adesonine↑, inosine↑, hypoxanthine↓, and xanthine↓	[92]
Male Wistar rats/Brain	Bilateral common carotid occlusion (occlusion 10 min)	30 mg/kg (pretreatment 7 days, IP)	ROS↓, MDA↓, NO↓, and Na^+K^+-aTPase↓	[61]
Male Wistar rats/brain	Bilateral common carotid occlusion (occlusion 10 min)	30 mg/kg (pretreatment 7 days, IP)	COX-2↓ and iNOS↓ and NF-kB and JNK activation↓	[100]
Male Sprague-Dawley rats/brain	Middle cerebral artery occlusion (occlusion 30 min)	15 and 30 mg/kg (pretreatment 7 days, IP)	MDA↓, SOD↑, Nrf2↑, HO-1↑, and caspase-3↓	[3]
Mongolian gerbils/brain	Bilateral common carotid occlusion (occlusion 5 min)	30 mg/kg (during occlusion, IP)	Neuronal cell death↓	[48]
Male Wistar rats/Brain	Middle cerebral artery occlusion (occlusion 2 h)	20 mg/kg (pretreatment 21 days, IP)	MDA↓, GSH↑, and infarct volume and motor impairment↓	[96]
Male New Zealand white rabbits/spinal cord	Occlusion of the infrarenal aorta (ischemia 30 min)	1–10 mg/kg (pretreatment 30 minutes, IV)	MDA↓ and NO↑	[101]
Male New Zealand white rabbits/spinal cord	Abdominal aorta clamp (ischemia 30 minute)	100 μg/kg (pretreatment 15 minutes before occluding, IV)	MPO↓, MDA↓, and spinal cord gray matter motor neurons injury↓	[46]
Male Wistar albino rats/intestine	Superior mesenteric artery occlusion (ischemia 60 min, reperfusion 60 min)	15 mg/kg (both before ischemia and before reperfusion, IP)	CAT↑, total antioxidant capacity↑, MPO↓, total oxidative status↓, and oxidative stress index (OSI) ↓	[105]
Male BALB/c mice/intestine	Superior mesenteric artery occlusion (ischemia 1 h, reperfusion 24 h)	50 mg/kg (pretreatment 10 days, PO)	NO↓, iNOS↓, MPO↓, MDA↓, SOD↑, GSH-Px↑, SIRT1↑, and NF-kB↓	[41]
Wistar albino rats/intestine	Superior mesenteric artery occlusion (ischemia 1 hour, reperfusion 24 h)	15 mg/kg (pretreatment 5 days and 15 min before occlusion, IP)	MPO↓, MDA↓, NO↓, and SOD↑	[43]

Table 1: Continued.

Species/targets	Model of reperfusion injury	Effective dose	Effects and mechanisms	References
Male Wistar rat/intestine	Superior mesenteric artery occlusion (ischemia 90 min h, reperfusion 120 min)	0.056 mg/kg (30 min before occlusion, IV)	Intestine damage score↓, MPO↓, and hemoglobin content↓	[42]
Male Wistar albino rats/spleen, ileum	Hepatic artery clamping (ischemia 45 min, reperfusion 30 min)	15 mg/kg (pretreatment 5 days and 15 min before occlusion, IP)	MDA↓, NO↓, and GSH↑	[107]
Male Wistar albino rats/kidney	Right nephrectomy and left renal pedicle clamping (ischemia 45 min, reperfusion 6 h)	30 mg/kg (30 min prior to ischemia and immediately before the reperfusion period, IP)	ROS↓, MDA↓, MPO↓, LDH↓, TNF-α ↓, SOD↑, and GSH↑	[112]
Male Wistar rats/kidney	Renal pedicles clamping (ischemia 45 min, reperfusion 24 h)	5 mg/kg, (pretrentment 30 minutes before surgery, PO)	NO↑, BUN↓, creatinine↓, SOD↑, GSH↑, and CAT↑	[117]
Male Wistar rats/kidney	Right nephrectomy and left renal pedicle clamping (ischemia 45 min, reperfusion 24 h)	5 mg/kg, (before I/R, PO)	BUN↓, creatinine↓, SOD↑, GSH↑, CAT↑, and NO↑	[45]
Male Wistar rats/kidney	Both renal pedicles cross-clamping (ischemia 40 min, reperfusion 24 h)	0.23 μg/kg (40 min before I/R, IV)	Mortality rate↓, renal damage↓, and NO↑	[113]
Male Sprague-Dawley rat/liver	Clamping the portal vein and hepatic artery (ischemia 1 h, reperfusion 3 h)	0.02 and 0.2 mg/kg (after reperfusion, IV)	IL-1β ↓, IL-6↓, MPO↓, TNF-α ↓, KC↓, and HO-1 mRNA↓	[122]
Male Sprague-Dawley rats/liver	Clamping the portal vein and hepatic artery (ischemia 45 min, reperfusion 45 min)	10 mg/kg (15 min before reperfusion, IV)	MDA↓, SOD↑, GSH↑, and CAT↑	[121]
Sprague-Dawley rat/lung	Left hilum (occlusion 60 min)	20 mg/kg (4 days and 15 min before ischemia, PO)	ROS↓, MDA↓, PGC1-α mRNA↑, and leukocyte infiltration↓	[126]
Male Sprague-Dawley rat/testis	Left testis torsion/detorsion (ischemia 4 h)	20 mg/kg (30 min before detorsion, IP)	MDA↓, H_2O_2 ↓, and oxidative stress index↓	[39]
Male Wistar rats/testis	Right testis torsion/detorsion (ischemia 4 h)	30 mg/kg (30 min before detorsion, IP; 7 days postoperatively, PO)	Improved contralateral spermatozoid production and some fertility parameters.	[133]
Wistar albino rat/ovary	Right unilateral adnexal torsion/detorsion (torsion 3 h, detorsion 3 h)	10 mg/kg (30 min before detorsion, IP)	MDA↓, XO↓, and GSH↑	[140]
Male Sprague Dawley rats/retinal	Anterior chamber saline bag (intraocular pressure 70–80 mm Hg for 45 min)	30 mg/kg (pretreatment 5 days, IP)	Reduce inner retinal layers thinning	[145]
Male Wistar rats rat/Retinal	Anterior chamber saline bag (intraocular pressure 120 mm Hg for 60 min)	0.5 nmole (pretreatment 15 min, IV)	MMP-9↓, iNOS↓, and HO-1↑	[149]
Male Spraque-Dawley rats/skeletal muscle	Abdominal aorta clamp (ischemia 120 min, reperfusion 60 min)	20 mg/kg (pretreatment for 14 days, gastric tube)	MDA↓, CPK↓, LDH↓, GSH↑ carbonyl↓, and myoglobin↓,	[157]
Sprague-Dawley rats/bladder	Abdominal aorta occlusion (ischemia 60 min, reperfusion 60 min)	10 mg/kg (15 min before I/R, IP)	MPO↓, MDA↓, and GSH↑	[164]

Abbreviations: I/R, ischemia-reperfusion; IP, intraperitonium; IV: intravenous; PO, Orally; MAP mean arterial pressure; ROS, reactive oxygen species; ER, estrogen receptor; HO-1, hemeoxygenase-1; PGC-1α, peroxisome proliferator-activated receptor-gamma coactivator 1 alpha; NF-kB, nuclear factor-kappa B; JNK, c-Jun N-terminal kinase; MMP-9, metallopeptidase 9; SOD, superoxide dismutase; CAT, catalase; GSH, glutathione; MDA, malondialdehyde; NOX, nicotinamide adenine dinucleotide phosphate-oxidase; XO, xanthine oxidase; H_2O_2, hydrogen peroxide; TNF-α, tumor necrosis factor-alpha; IL-6, interleukin 6; IL-10, interleukin 10; ICAM-1, intercellular adhesion molecule 1; MPO, myeloperoxidase; NO, nitric oxide; iNOS, inducible nitric oxide synthase.

2. The Organ-Protective Effects of Resveratrol in Ischemia and Reperfusion Injury

2.1. Oxidative Stress and Ischemia-Reperfusion Injury. The oxidative stress is still considered to be an important cause of I/R-induced tissue injury. There is a massive increase in oxidants and oxygen radicals during the initiation and progression of I/R injury [50–53]. Ischemia and reperfusion can promote production of ROS, such as superoxide anions (O_2^-), hydroxyl free radicals (HO^-), hydrogen peroxide (H_2O_2), and nitric oxide (NO), which is a major factor contributing to I/R-induced organ injury [50, 51, 54, 55]. I/R-induced reactive oxygen species (ROS) formation is the end result of several different oxidant-producing pathways, such as the mitochondria, xanthine oxidase (XO), and nicotinamide adenine dinucleotide phosphate-oxidase (NOX) [50, 52, 56, 57]. Oxygen radicals cause lipid peroxidation that can lead to cell membrane breakdown and mitochondrial damage triggering cell death [21, 58]. NO plays a protective role in I/R injury as increased NO expression can decrease I/R-induced organ injury [59, 60]. In controversy, previous studies have also shown that the inducible NO synthase is upregulated after I/R and can switch from NO to oxygen radical generation under oxidant stress [41, 61]. Oxidative stress could perturb the balance between oxidant and antioxidant status. In most cells, superoxide dismutase (SOD), catalase (CAT), and glutathione peroxidase (GSH-Px) are endogenous free radical scavenging enzymes induced by oxidative stress [62–64]. These antioxidant enzymes play a critical role in the prevention of oxidative damage during ischemia and reperfusion. In addition, the oxidant formation is generated through a series of interacting pathways in various organs and endothelial cells, triggering subsequent leukocyte chemotaxis and inflammation [20, 50, 65]. However, the pathophysiology of I/R injuries has not yet been fully elucidated due to complex interactions and signaling pathways. Previous evidence shows that resveratrol plays an important role organ protection against I/R injury via its antioxidative and anti-inflammatory properties [20, 66, 67]. The protective pathways and mechanisms of resveratrol in ischemia-reperfusion (I/R) will be further discussed in this paper.

2.2. The Cardioprotective Effect of Resveratrol in Ischemia-Reperfusion Injury. Myocardial ischemia-reperfusion injury is a complex pathophysiological process that involves various factors and pathways [68–71]. An excess amount of ROS is increased during I/R injury that results in myocardiocyte damage. Resveratrol exerts cardiovascular beneficial effects on atherosclerosis, ventricular arrhythmia, and myocardial I/R injury [4, 72, 73].

Resveratrol could reduce oxidative stress by inhibiting ROS production and has been reported to be a scavenger of hydroxyl, superoxide, metal-induced radicals, and H_2O_2 [31, 74–77]. However, the protective effects of resveratrol against oxidative injury are likely to be attributed to the upregulation of the endogenous cellular antioxidant systems rather than its direct ROS scavenging activity. Resveratrol also induces antioxidant enzymes in cardiovascular tissues including SOD, GSH, CAT [72, 74, 78], and NOX [74, 79], all of which are major ROS producing enzymes in the cardiovascular system.

Previous studies have shown that resveratrol-provided cardioprotection is achieved by preserving postischemic ventricular function and reducing myocardial infarct size and cardiomyocytes apoptosis [80]. Pretreatment of rats with resveratrol resulted in cardioprotection in the isolated heart following ischemia and reperfusion [49, 81, 82] and protected neonatal rat cardiomyocytes against anoxia/reoxygenation injury by antiapoptosis [31]. A recent study has shown that resveratrol improved diabetic cardiomyopathy and postischemic ventricular function through regulating myocardial lipoperoxidation and antioxidant enzyme activities [72, 77, 83]. The protective effect is related with an increased activity of peroxidase and superoxide dismutase and a decreased expression of catalase, malondialdehyde (MDA) and isoprostanes [80, 84]. However, MDA is not used as a relaible biomarker of oxidative stress. Instead, isoprostane is considered a specific marker of lipid peroxidation for monitoring oxidative stress [85–87].

NO has been identified as a crucial factor mediating the protective effects of resveratrol [18, 88]. Resveratrol enhances endothelial NO synthase (eNOS) expression in endothelial cells and improves the ventricular function during I/R [18, 88]. SIRT1 has been shown to regulate mammalian genes transcription and has a regulatory function of intracellular signaling in hypoxia or stress [26, 27]. Recent studies indicated that the upregulation of eNOS expression was mediated by SIRT1 [74, 75, 89]. SIRT1 activation may be necessary for the cardioprotective effect, which is mediated by NO signaling [90]. However, other studies have shown that acutely infused resveratrol had no beneficial effect in intestinal ischemia/reperfusion or stroke and it is not mediated by NO elevation [41, 61].

The cardioprotective mechanisms of resveratrol are complex in I/R injury. A previous report demonstrated that there was less myocardial injury and inflammation in Toll-like receptor 4- (TLR4-) deficient mice in I/R. This protective mechanism was possibly associated to the TLR4/nuclear factor-kappa B (NF-κB) signaling pathway [31, 41]. Furthermore, resveratrol attenuates postischemic leukocyte recruitment and subsequent endothelial dysfunction by superoxide-related proinflammatory stimulis, such as hypoxanthine (HX)/XO and platelet-activating factor (PAF) [91].

2.3. The Neuroprotective Effect of Resveratrol in Ischemia-Reperfusion Injury. The mechanisms of brain and spinal cord injuries are complex and multifactorial. Oxidative stress has been regarded as important pathogenesis for neurologic damage after cerebral I/R injury. ROS, like superoxide anions, hydroxyl free radicals, hydrogen peroxide, and nitric oxide, are produced during abnormal metabolic reactions or central nervous system activation in I/R [61, 92]. Previous experimental evidence has demonstrated that resveratrol exhibits neuroprotective effect in various cerebral ischemic stroke animal model [3, 93–95]. Treatment with transresveratrol

prevented motor impairment, reduced glutathione levels, and also significantly decreased the infarct size after middle cerebral artery occlusion and reperfusion in rat [96]. The neuroprotective effects of resveratrol were shown to be due to its antioxidative and NO promoting properties [48, 92, 97]. Wang and colleagues also showed that resveratrol decreased cerebral microglial activation and delayed neuronal cell death in gerbils, a beneficial effect attributed to its strong antioxidative activity [48]. Previous studies also showed that resveratrol significantly increased the basal levels of adesonine and inosine, inhibited the elevations of hypoxanthine and xanthine levels, remarkably decreased xanthine oxidase activity, and depressed oxidative biomarker (8-isoprostane) levels [84, 92].

Previous studies suggested that the cerebroprotective action of resveratrol could be mediated by both antioxidative and anti-inflammatory effects [98]. Resveratrol treatment decreased oxidative stress and inflammatory markers like isoprostane, tumor necrosis factor-alpha (TNF-α), interleukin 6 (IL-6), myeloperoxidase (MPO), and intercellular adhesion molecule 1 (ICAM-1) and increased antioxidative and anti-inflammatory markers like superoxide dismutase, catalase, and interleukin 10 (IL-10) levels in brain I/R injury [84, 99]. Resveratrol pretreatment also reduced astroglial and microglial cells activation by attenuating NF-κB and JNK activation associated with a decrease in inducible nitric oxide synthase (iNOS) and cyclooxygenase-2 (COX-2) production [100]. A recent study has shown that intracortical injection of resveratrol reduced rat cortex infarct volume. This neuroprotective effect was attenuated when resveratrol and a selective estrogen receptor- (ER-) α and ER-β antagonist injections were given in combination. These results indicated that neuroprotection of resveratrol is mediated via ER-α and ER-β subtypes [23].

In addition, the resveratrol also has protective effect in spinal cord I/R injury. In a rabbit study, prophylactic use of resveratrol decreased malondialdehyde and myeloperoxidase activity and reduced spinal cord gray matter motor neurons damage following abdominal aorta clamping and reperfusion [46]. Kiziltepe et al. [101] also showed that neuroprotective function of resveratrol in spinal cord I/R injury by scavenging free radicals, inhibiting oxidative stress, and upregulating NO.

2.4. The Intestinoprotective Effect of Resveratrol in Ischemia-Reperfusion Injury. Gastrointestinal tract is highly sensitive to I/R injury. Intestinal I/R could trigger the release of oxidants and tissue injurious factors, leading to interstitial edema, microvascular permeability change, vasoregulation impairment, mucosal barrier dysfunction, and inflammatory cell infiltration [65, 102–105].

Resveratrol plays a crucial role in intestinal I/R injuries. Previous study demonstrated that resveratrol exerted its broad spectrum of protective mechanisms through increasing its antioxidative capacity and reducing oxidative status and MPO in intestinal I/R injury [20, 42, 43, 105, 106]. Resveratrol ameliorated the intestinal tissue injury and decreased bacterial translocation in mesenteric lymph nodes via decreased MPO and NO levels and restored SOD activity [43].

Resveratrol at a dose of 0.056 mg/kg significantly decreased the hemoglobin content, the histopathologic score, and tissue myeloperoxidase activity in intestinal I/R injury, without improving the systemic and metabolic parameters [42]. One study showed that intraperitoneal administration of resveratrol reduced excessive NO formation and diminished rat spleen and ileum oxidative damage after hepatic I/R [107]. Furthermore, resveratrol rendered subacute intestinal protection in vivo. Resveratrol significantly ameliorated subacute intestinal I/R injury [41, 42], related to a reduction of NO production and the activation of the SIRT1-NF-κB pathway, which was associated with a decrease in iNOS expression as well as NO production [41]. NO is an important signaling molecule in antioxidative defense mechanisms and resveratrol relieved tissue I/R injuries through an NO-dependent manner [15, 16, 30, 108]. However, its protective or detrimental effect in intestinal I/R injury is still controversial. Some studies showed that an augmented NO production can protect the intestine following I/R injury [12, 109]. Other evidence indicated that a decreased production of NO may have a protective role via with the suppression of inducible NOS in the small intestine I/R [41, 98, 110].

2.5. The Renoprotective Effect of Resveratrol in Ischemia-Reperfusion Injury. Renal I/R causes an increase in ROS and isoprostane levels and a decrease of the antioxidant enzyme glutathione in the urological system [111]. Resveratrol may induce the GSH synthesis enzymes and maintain the GSH levels during oxidative stress [45, 112, 113]. It has been shown that resveratrol could maintain antioxidant defenses and reduce the oxidative damage of kidney [45, 113]. Pretreatment with resveratrol prevented the renal I/R-induced lipid peroxidation and protected the depletion of antioxidant enzyme in the renal I/R-treated rats. Moreover, oxidative injury of the kidneys was accompanied by neutrophil infiltration, as evidenced by the elevated tissue MPO levels. In addition, oxidative stress could be involved in renal glomerular lesions caused by a series of proinflammatory mediators, including cytokines and chemokines that lead to the ROS production, leukocyte activation, and glomerular damage [112]. ROS play an important role in the pathologic process of renal ischemia reperfusion injury. Previous study showed that the short-term treatment of resveratrol inhibited renal lipid peroxidation induced by IR. Resveratrol administration decreased renal cortex and medulla damage and reduced the mortality of ischemic rats from 50% to 10% [113].

NO expression is generated in renal tissue and plays an important role in the regulation of renal blood flow and glomerular filtration function. In kidney, resveratrol was found to exert its protective action through the upregulation of NO. Previous studies demonstrated that resveratrol could stimulate NO production during renal I/R [45, 113–116]. Preconditioning and resveratrol treatment also led to a marked increase in NO levels in kidneys and protect renal cells from I/R injury [117]. The protective phenomenon of resveratrol

was suggested to be through the NO-dependent mechanism [113]. Another report also evidenced that treatment with L-NAME (an NO synthase inhibitor) attenuated this protection afforded by resveratrol, indicating that resveratrol exerted its protective effect through the release of NO [45].

2.6. The Hepatoprotective Effect of Resveratrol in Ischemia-Reperfusion Injury. I/R stimulates the hepatic Kupffer cells and the residing macrophage activation, to generate ROS and proinflammatory cytokines and to upregulate iNOS [60, 118]. The activation of Kupffer cell (KC) with enhanced ROS production and secretion of inflammatory cytokines and proteolytic enzymes is considered to play an important role in liver reperfusion injury [40, 119]. Additionally, the activation of polymorphonuclear leukocytes migration and infiltration in the injury site may enhance the production of inflammatory cytokines, adhesion molecules, and ROS [40, 120].

Previous studies showed that resveratrol reduced liver damage after ischemia-reperfusion. This beneficial effect was due to the replacement of the depleted antioxidant defense system in hepatic I/R injury [121, 122]. Transresveratrol has also been suggested to decrease the superoxide and improve NO bioavailability. Postischemic treatment with lower dose transresveratrol (0.02 mg/kg) reduced TNF-α, interleukin 1β (IL-1β), keratinocyte chemoattractant (KC), and HO-1 hepatic mRNA expression and decreased hepatic neutrophil recruitment [122]. Gedik et al. [121] reported that resveratrol treatment decreased the lipid peroxidation and protected the depletion of antioxidant enzymes (SOD, CAT, and GSH) in rat model of common hepatic artery and portal vein clamping and reperfusion-induced hepatic injury.

2.7. The Pulmonoprotective Effect of Resveratrol in Ischemia-Reperfusion Injury. Lung I/R injury occurs in lung transplantation and cardiopulmonary surgery, resulting in an excessive production of reactive ROS [37, 123–125]. The exact mechanism in I/R-induced lung injury is not completely understood. However, an overproduction of ROS such as superoxide and peroxides, activation of macrophages, and infiltration of polymorphonuclear leukocytes are implicated in pulmonary injury [125]. Previous study [89] demonstrated that I/R-induced lung tissue damage was related to pulmonary mitochondrial dysfunction. Peroxisome proliferator-activated receptor-gamma coactivator 1 alpha (PGC-1α) was a coactivator controlling aerobic capacity and mitochondrial biogenesis, and an increase in PGC-1α mRNA expression was associated with a decreased pulmonary oxidative stress and improved aerobic capacity. Recent study [126] demonstrated that PGC-1α mRNA expression in the lungs was markedly improved with resveratrol, providing protection against pulmonary damage induced by contralateral lung I/R injury. Resveratrol treatment also effectively reduced the lipid peroxidation and alveolar neutrophils and maintained mitochondrial homeostasis. In addition, resveratrol could increase mitochondrial activity through upregulating PGC-1α and SIRT1 expression [89].

2.8. The Reproductive Organs Protective Effect of Resveratrol in Ischemia-Reperfusion Injury. Testicular torsion is urological emergency in which damaged germinal cells may lead to infertility [127–129]. Testicular torsion and detorsion may be regarded as an ischemia/reperfusion (I/R) injury. Oxidative stress is thought to be a major responsible in I/R injury; however, the mechanism involved in testicular injury has not been fully understood. Previous reports demonstrated that ipsilateral testicular torsion could affect the contralateral testis. The injuries caused by I/R were observed in the ipsilateral and contralateral testis [130, 131]. Resveratrol could decrease the cell injury by preventing lipid peroxidation in the cell membrane and DNA damage caused by excessive ROS production [39, 47, 132]. Previous study indicated that treatment with resveratrol improved fertility parameters and contralateral spermatozoid production [133]. A recent report showed that resveratrol pretreatment decreased tissue lipid peroxidation and had a protective effect in the prevention of apoptosis in rat testicular torsion/detorsion (T/D) model [39].

Ovarian torsion is also a gynecological emergency due to the twisting of the adnexa on its ligamentous support. Insufficiency in tissue blood flow due to various reasons such as torsion or embolism leads to ischemia [134, 135]. The levels of ROS and MDA are increased during the reperfusion period following ischemia. It is known that xanthine oxidase is an important source of the ROS production [136, 137] during I/R and GSH is an essential component of the cellular defense mechanism against oxidative cell damage [138, 139]. Hascalik et al. [140] reported that intraperitoneal resveratrol (10 mg/kg) administration reduced the tissue XO products, as well as restored GSH levels, and decreased rat ovarian damage following T/D injury.

2.9. The Ophthalmoprotective Effect of Resveratrol in Ischemia-Reperfusion Injury. The retina is a very sensitive neural structure that is easily damaged by free radicals and inflammation following ischemia-reperfusion injury [141, 142]. Retinal ischemia is a common cause of visual loss and impairment. I/R-induced neural injuries are associated with enhanced production of endogenous oxidants such as oxygen free radicals, NO, and calcium [141, 143, 144]. Previous studies showed that resveratrol was capable of crossing the blood-retina barrier and exerting its neuroprotective effects, including cerebral and retinal IR injuries. Vin et al. [145] reported that resveratrol prophylactic treatment attenuated ischemic-induced loss of retinal function and reduced ischemia-mediated thinning of inner retinal layers [145]. Li et al. also showed that pretreatment of resveratrol decreased retinal vascular degeneration by inhibiting endoplasmic reticulum stress in retinal ischemic injury; however, it did not prevent retinal neuronal cell loss [146].

Previous studies showed that matrix metallopeptidase 9 (MMP-9) expression was upregulated during brain ischemia [147] and HO-1 overexpression attenuated retinal cellular damage by intense light exposure [148]. In addition, resveratrol exerted retinal protective effects via modulation of NOS in oxygen-induced retinopathy. Recent study also evidenced

that the administration of resveratrol might protect the retina against ischemia by inhibiting iNOS and MMP-9 expression and upregulating HO-1 levels [149].

2.10. The Musculoprotective Effect of Resveratrol in Ischemia-Reperfusion Injury. I/R injuries of skeletal muscles are serious clinical problems and are commonly seen in a variety of injuries including traumatic damage, peripheral vascular surgery, plastic surgery, or limb surgery with long time tourniquet application [150–152]. I/R injury of skeletal muscle can increase free radicals production and activate ROS generation, with the ability to produce cell membrane damage and leukocyte infiltration [153–155]. Resveratrol is an effective scavenger of hydroxyl and superoxide and exhibits a protective effect to decrease cell membranes lipid peroxidation and free radicals induced DNA damage [153, 154, 156]. Previous studies have shown that dietary flavonoid resveratrol can protect the skeletal muscle tissue against ischemia and reperfusion injury because of its strong antioxidant properties [157]. Elmali et al. indicated that intraperitoneal resveratrol treatment could exert a protective effect against tourniquet-induced I/R injury in rat gastrocnemius muscle. However, resveratrol not only functioned as an antioxidant but also attenuated the neutrophil infiltration in damaged skeletal muscle [158].

2.11. The Vesicoprotective Effect of Resveratrol in Ischemia-Reperfusion Injury. Urinary bladder I/R injury is associated with vascular atherosclerotic disease or pelvic embolization operations [159, 160]. Bladder ischemia could result in detrusor contractility impairment and bladder dysfunction [161, 162]. Previous study showed that I/R injury induced a production of isoprostanes [85, 86] and a decrease in endogenous GSH, as well as an enhanced neutrophil infiltration in rat bladder [162, 163]. However, resveratrol treatment reduced bladder inflammatory cell infiltration, lipid peroxidation, and the myeloperoxidase activity in I/R injury. Resveratrol treatment also reversed the bladder contractile responses to carbachol and prevented oxidative tissue damage following I/R [164].

3. The Organ-Protective Effect of Resveratrol in Hemorrhage and Reperfusion Injury

Reperfusion injury after hemorrhage results in an excessive production of oxidants and proinflammatory mediators. The enhanced ROS and proinflammatory cytokines play important factors in the initiation and perpetuation of organ injury [67, 165]. Previous studies have shown that vascular endothelial cell dysfunction can lead to inadequate tissue perfusion, which occurs after hemorrhagic shock and persists despite fluid resuscitation [166, 167]. Oxidative stress and superoxide radical generation are believed to contribute to the pathogenesis of endothelial dysfunction in low-flow states [167, 168]. Endothelial NOX is a major source of ROS of the vasculature, and previous studies have shown that there is a marked increase in NOX-generated ROS by the endothelium under stressful conditions [169, 170]. Elevated ROS is considered a major contributing factor to endothelial dysfunction, and antioxidants have been found to attenuate ROS-induced injuries [168, 169]. Resveratrol has been shown to have broad antioxidative activities in a number of biological systems [170]. Our previous studies have shown that resveratrol prevented hemorrhagic shock-elicited oxidative stress and protected endothelium from subsequent functional damages [168]. The beneficial effects included the suppression of the NOX activity and direct scavenging of ROS. The inhibitory effect of resveratrol on the NOX activity appeared to be mediated through influence of the active NOX enzyme complex assembly in the cell membrane and the cytosol, as evidenced from reduced membrane-bound proteins p22phox and gp91phox and cytosolic protein p47phox [166, 168].

The SIRT1 transcription-modulating proteins showed a fine balance in response to intracellular cues such as hypoxia or stress signals. The beneficial effects of resveratrol mediated by SIRT1 activation can be contributed to by different organs [26, 171, 172]. Studies showed that resveratrol decreased oxidative stress-induce ROS elevation and reduced brain neuron injury by radiation through the activation of SIRT1 [171].

HO-1 appears to act as a protective agent in many organs against insults, such as ischemia and oxidative stress [173, 174]. Previous studies have shown that resveratrol binds and increases the transcriptional activity of ER-α and ER-β. Resveratrol can modulate HO-1 induction and previous studies have shown that estrogen or flutamide enhances HO-1 expression via ER [174–176]. Our previous studies suggested that the upregulation in HO-1 was associated with the prevention of endothelial dysfunction and the salutary effects of resveratrol on endothelial function, mediated in part by an upregulation of the HO-1-related pathway via ER [165]. The p38 MAPK and Akt have been reported to regulate inflammatory response after trauma hemorrhage [20, 174]. PI3K/Akt pathway is known to play a pivotal role in the ability of neutrophils to undergo chemotaxis. Blockade of Akt activation abolishes the salutary effects of resveratrol in the heart following reperfusion injury [177, 178]. Estrogen-mediated attenuation of the inflammatory response to shock-induced organ injury is abolished by the presence of a p38 MAPK inhibitor (SB-203580) [20, 174]. Previous study also showed that resveratrol administration after hemorrhagic shock upregulated p38 MAPK and Akt expression via HO-1-related pathway [20, 179]. Neutrophils are activated following hemorrhage/reperfusion injury and activated neutrophils appear to infiltrate the injured organs in parallel with increased expression of adhesion molecules on endothelial cells. Upregulation of HO-1 causes a reduction of cytokines, adhesion molecules, chemokines, and neutrophil accumulation and ameliorates organ injury in shock status [20, 180].

4. Conclusions

Resveratrol has been indicated to have many beneficial effects in various studies and experimental conditions. There is increasing evidence suggesting that resveratrol protects

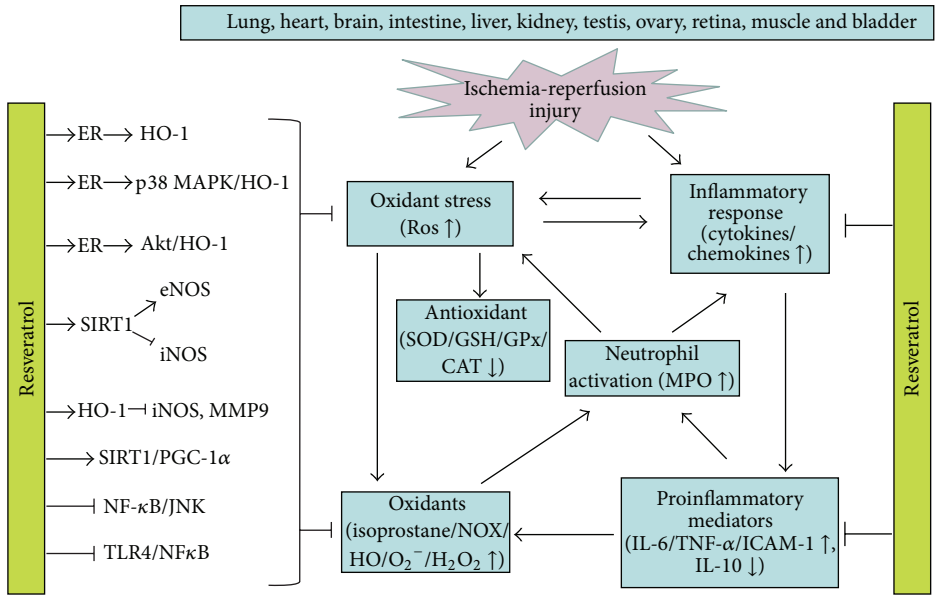

Figure 1: The mechanisms and pathways of resveratrol in oxidative stress-mediated ischemia-reperfusion injury. The protective benefits of resveratrol involved are its scavenging, antioxidant, and anti-inflammatory effect and the signaling mechanisms mediated may be via a variety of intracellular signaling pathways, including upregulation of ER-related MAPK/HO-1 and Sirt1/PGC-1α pathway and inhibition of the TLR4 and NF-κB dependent pathway. ROS, reactive oxygen species; ER, estrogen receptor; HO-1, hemeoxygenase 1; SIRT1, sirtuin 1; eNOS, endothelial nitric oxide synthase; iNOS, inducible nitric oxide synthase; TLR4, Toll-like receptor 4; PGC-1α, peroxisome proliferator-activated receptor-gamma coactivator 1 alpha; NF-κB, nuclear factor-kappa B; JNK, c-Jun N-terminal kinase; p38 MAPK, p38 mitogen-activated protein kinase; MMP-9, metallopeptidase 9; SOD, superoxide dismutase; CAT, catalase; GSH, glutathione; GSH-Px, glutathione peroxidase (GSH-Px); NOX, NADPH oxidase; XO, xanthine oxidase; O_2^-, superoxide anions; HO^-, hydroxyl free radicals; H_2O_2, hydrogen peroxide; TNF-α, tumor necrosis factor-alpha; IL-6, interleukin 6; IL-10, interleukin 10; ICAM-1, intercellular adhesion molecule 1; MPO, myeloperoxidase.

organ function after ischemia or shock-like reperfusion injury. Resveratrol can attenuate organs reperfusion injury through multiple pathways. However, the protective benefits of resveratrol may not simply be attributed by its scavenging, antioxidative, or anti-inflammatory effect. It is implicated that resveratrol is also mediated in part via a variety of intracellular signaling pathways including the regulation of the NOS, HO-1, SIRT1, ER, MAPK, PGC-1α, TLR4, and NF-κB (Figure 1). This complex network needs additional elucidation, more experimental studies, and clinical trials. Resveratrol might be a preventive and therapeutic agent to protect reperfusion-induced organ injury in future clinical treatment.

Abbreviations

I/R: Ischemia-reperfusion
IP: Intraperitonium
IV: Intravenous
PO: Orally
MAP: Mean arterial pressure
ROS: Reactive oxygen species
ER: Estrogen receptor
HO-1: Hemeoxygenase-1
PGC-1α: Peroxisome proliferator-activated receptor-gamma coactivator 1 alpha
NF-κB: Nuclear factor-kappa B
JNK: c-Jun N-terminal kinase
MMP-9: Metallopeptidase 9
SOD: Superoxide dismutase
CAT: Catalase; GSH: glutathione
NOX: Nicotinamide adenine dinucleotide phosphate-oxidase
XO: Xanthine oxidase
H_2O_2: hydrogen peroxide
TNF-α: tumor necrosis factor-alpha
IL-6: Interleukin 6
IL-10: Interleukin 10
ICAM-1: Intercellular adhesion molecule 1
MPO: Myeloperoxidase
NO: Nitric oxide
iNOS: inducible nitric oxide synthase.

Conflict of Interests

The authors declare that they have no competing interests.

Authors' Contribution

Huang-Ping Yu, MD, PhD, is the principle investigator for the studies providing oversight and contributed fundamental conceptualization for the research, writing a grant proposal

and paper. Fu-Chao Liu, MD, PhD contributed to paper preparation and data collection and assisted in writing the paper. Hsin-I Tsai, MD, assisted in writing the paper.

Acknowledgments

This work was partially supported by grants from the National Science Council (NSC102-2314-B-182A-051-MY3) and Chang Gung Memorial Hospital (CMRPG3B1052 and CMRPG3B1053) to Huang-Ping Yu. Support was also provided by the National Science Council (NSC103-2314-B-182-046-MY2) and Chang Gung Memorial Hospital (CMRPG3B1622) to Fu-Chao Liu.

References

[1] J. A. Santos, G. S. G. de Carvaho, V. Oliveira, N. R. B. Raposo, and A. D. Da Silva, "Resveratrol and analogues: a review of antioxidant activity and applications to human health," *Recent Patents on Food, Nutrition & Agriculture*, vol. 5, no. 2, pp. 144–153, 2013.

[2] R. F. Guerrero, M. C. Garcia-Parrilla, B. Puertas, and E. Cantos-Villar, "Wine, resveratrol and health: a review," *Natural Product Communications*, vol. 4, no. 5, pp. 635–658, 2009.

[3] J. Ren, C. Fan, N. Chen, J. Huang, and Q. Yang, "Resveratrol pretreatment attenuates cerebral ischemic injury by upregulating expression of transcription factor Nrf2 and HO-1 in Rats," *Neurochemical Research*, vol. 36, no. 12, pp. 2352–2362, 2011.

[4] P. K. Gupta, D. J. DiPette, and S. C. Supowit, "Protective effect of resveratrol against pressure overload-induced heart failure," *Food Science & Nutrition*, vol. 2, no. 3, pp. 218–229, 2014.

[5] L. Liu, H. Gu, H. Liu et al., "Protective effect of resveratrol against IL-1β-induced inflammatory response on human osteoarthritic chondrocytes partly via the TLR4/MyD88/NF-κB signaling pathway: an "in vitro study"," *International Journal of Molecular Sciences*, vol. 15, no. 4, pp. 6925–6940, 2014.

[6] M. Kitada and D. Koya, "Renal protective effects of resveratrol," *Oxidative Medicine and Cellular Longevity*, vol. 2013, Article ID 568093, 8 pages, 2013.

[7] J. Tome-Carneiro, M. Gonzalvez, M. Larrosa et al., "Resveratrol in primary and secondary prevention of cardiovascular disease: a dietary and clinical perspective," *Annals of the New York Academy of Sciences*, vol. 1290, no. 1, pp. 37–51, 2013.

[8] K. Legg, "Metabolic disease: identifying novel targets of resveratrol," *Nature Reviews Drug Discovery*, vol. 11, no. 4, article 273, 2012.

[9] K. Magyar, R. Halmosi, A. Palfi et al., "Cardioprotection by resveratrol: a human clinical trial in patients with stable coronary artery disease," *Clinical Hemorheology and Microcirculation*, vol. 50, no. 3, pp. 179–187, 2012.

[10] F. Li, Q. Gong, H. Dong, and J. Shi, "Resveratrol, a neuroprotective supplement for Alzheimer's disease," *Current Pharmaceutical Design*, vol. 18, no. 1, pp. 27–33, 2012.

[11] L. M. Chu, A. D. Lassaletta, M. P. Robich, and F. W. Sellke, "Resveratrol in the prevention and treatment of coronary artery disease," *Current Atherosclerosis Reports*, vol. 13, no. 6, pp. 439–446, 2011.

[12] L. G. Wood, P. A. B. Wark, and M. L. Garg, "Antioxidant and anti-inflammatory effects of resveratrol in airway disease," *Antioxidants & Redox Signaling*, vol. 13, no. 10, pp. 1535–1548, 2010.

[13] L. Di Renzo, A. Carraro, R. Valente, L. Iacopino, C. Colica, and A. De Lorenzo, "Intake of red wine in different meals modulates oxidized LDL level, oxidative and inflammatory gene expression in healthy people: a randomized crossover trial," *Oxidative Medicine and Cellular Longevity*, vol. 2014, Article ID 681318, 9 pages, 2014.

[14] W. Yu, Y.-C. Fu, and W. Wang, "Cellular and molecular effects of resveratrol in health and disease," *Journal of Cellular Biochemistry*, vol. 113, no. 3, pp. 752–759, 2012.

[15] A. Csiszar, "Anti-inflammatory effects of resveratrol: possible role in prevention of age-related cardiovascular disease," *Annals of the New York Academy of Sciences*, vol. 1215, no. 1, pp. 117–122, 2011.

[16] A. A. E. Bertelli, M. Migliori, V. Panichi et al., "Resveratrol, a component of wine and grapes, in the prevention of kidney disease," *Annals of the New York Academy of Sciences*, vol. 957, pp. 230–238, 2002.

[17] A. Gulcubuk, D. Haktanir, A. Cakiris et al., "The effects of resveratrol on tissue injury, oxidative damage, and pro-inflammatory cytokines in an experimental model of acute pancreatitis," *Journal of Physiology and Biochemistry*, vol. 70, no. 2, pp. 397–406, 2014.

[18] S. Wang, Y. Qian, D. Gong, Y. Zhang, and Y. Fan, "Resveratrol attenuates acute hypoxic injury in cardiomyocytes: correlation with inhibition of iNOS-NO signaling pathway," *European Journal of Pharmaceutical Sciences*, vol. 44, no. 3, pp. 416–421, 2011.

[19] B. Budak, M. Seren, N. N. Turan, Z. Sakaogullari, and A. T. Ulus, "The protective effects of resveratrol and L-NAME on visceral organs following aortic clamping," *Annals of Vascular Surgery*, vol. 23, no. 5, pp. 675–685, 2009.

[20] H.-P. Yu, T.-L. Hwang, P.-W. Hsieh, and Y.-T. Lau, "Role of estrogen receptor-dependent upregulation of P38 MAPK/heme oxygenase 1 in resveratrol-mediated attenuation of intestinal injury after trauma-hemorrhage," *Shock*, vol. 35, no. 5, pp. 517–523, 2011.

[21] P. Antonuccio, L. Minutoli, C. Romeo et al., "Lipid peroxidation activates mitogen-activated protein kinases in testicular ischemia-reperfusion injury," *The Journal of Urology*, vol. 176, no. 4, part 1, pp. 1666–1672, 2006.

[22] J. C. Nwachukwu, S. Srinivasan, N. E. Bruno et al., "Resveratrol modulates the inflammatory response via an estrogen receptor-signal integration network," *eLife*, vol. 3, Article ID e02057, 2014.

[23] M. C. Saleh, B. J. Connell, and T. M. Saleh, "Resveratrol induced neuroprotection is mediated via both estrogen receptor subtypes, ERα and ERβ," *Neuroscience Letters*, vol. 548, pp. 217–221, 2013.

[24] H.-P. Yu, J.-C. Hsu, T.-L. Hwang, C.-H. Yen, and Y.-T. Lau, "Resveratrol attenuates hepatic injury after trauma-hemorrhage via estrogen receptor-related pathway," *Shock*, vol. 30, no. 3, pp. 324–328, 2008.

[25] W. Xu, Y. Lu, J. Yao et al., "Novel role of resveratrol: suppression of HMGB1 nucleocytoplasmic translocation by the up-regulation of SIRT1 in sepsis-induced liver injury," *Shock*, 2014.

[26] B. Jian, S. Yang, I. H. Chaudry, and R. Raju, "Resveratrol restores sirtuin 1 (SIRT1) activity and pyruvate dehydrogenase kinase 1 (PDK1) expression after hemorrhagic injury in a rat model," *Molecular Medicine*, vol. 20, no. 1, pp. 10–16, 2014.

[27] T. Li, J. Zhang, J. Feng et al., "Resveratrol reduces acute lung injury in a LPS-induced sepsis mouse model via activation of Sirt1," *Molecular Medicine Reports*, vol. 7, no. 6, pp. 1889–1895, 2013.

[28] Y. Fu, Y. Wang, L. Du et al., "Resveratrol inhibits ionising irradiation-induced inflammation in MSCs by activating Sirt1 and limiting NLRP-3 inflammasome activation," *International Journal of Molecular Sciences*, vol. 14, no. 7, pp. 14105–14118, 2013.

[29] V. Kesherwani, F. Atif, S. Yousuf, and S. K. Agrawal, "Resveratrol protects spinal cord dorsal column from hypoxic injury by activating Nrf-2," *Neuroscience*, vol. 241, pp. 80–88, 2013.

[30] J. Zhang, J. Chen, J. Yang et al., "Resveratrol attenuates oxidative stress induced by balloon injury in the rat carotid artery through actions on the ERK1/2 and NF-kappa B pathway," *Cellular Physiology and Biochemistry*, vol. 31, no. 2-3, pp. 230–241, 2013.

[31] C. Zhang, G. Lin, W. Wan et al., "Resveratrol, a polyphenol phytoalexin, protects cardiomyocytes against anoxia/reoxygenation injury via the TLR4/NF-κB signaling pathway," *International Journal of Molecular Medicine*, vol. 29, no. 4, pp. 557–563, 2012.

[32] N. Atmaca, H. T. Atmaca, A. Kanici, and T. Anteplioglu, "Protective effect of resveratrol on sodium fluoride-induced oxidative stress, hepatotoxicity and neurotoxicity in rats," *Food and Chemical Toxicology*, vol. 70, pp. 191–197, 2014.

[33] W. Zhang, C. Guo, R. Gao, M. Ge, Y. Zhu, and Z. Zhang, "The protective role of resveratrol against arsenic trioxide-induced cardiotoxicity," *Evidence-Based Complementary and Alternative Medicine*, vol. 2013, Article ID 407839, 8 pages, 2013.

[34] H. X. Zhang, G. L. Duan, C. N. Wang et al., "Protective effect of resveratrol against endotoxemia-induced lung injury involves the reduction of oxidative/ nitrative stress," *Pulmonary Pharmacology and Therapeutics*, vol. 27, no. 2, pp. 150–155, 2014.

[35] G. Şimşek, Ş. Gürocak, N. Karadag et al., "Protective effects of resveratrol on salivary gland damage induced by total body irradiation in rats," *Laryngoscope*, vol. 122, no. 12, pp. 2743–2748, 2012.

[36] Y.-F. Liao, W. Zhu, D.-P. Li, and X. Zhu, "Heme oxygenase-1 and gut ischemia/reperfusion injury: a short review," *World Journal of Gastroenterology*, vol. 19, no. 23, pp. 3555–3561, 2013.

[37] P. D. Weyker, C. A. J. Webb, D. Kiamanesh, and B. C. Flynn, "Lung ischemia reperfusion injury: a bench-to-bedside review," *Seminars in Cardiothoracic and Vascular Anesthesia*, vol. 17, no. 1, pp. 28–43, 2013.

[38] A. J. Vardanian, R. W. Busuttil, and J. W. Kupiec-Weglinski, "Molecular mediators of liver ischemia and reperfusion injury: a brief review," *Molecular Medicine*, vol. 14, no. 5-6, pp. 337–345, 2008.

[39] E. Yulug, S. Türedi, E. Karagüzel, O. Kutlu, A. MenteSe, and A. Alver, "The short term effects of resveratrol on ischemia-reperfusion injury in rat testis," *Journal of Pediatric Surgery*, vol. 49, no. 3, pp. 484–489, 2014.

[40] R. D. Powell, J. H. Swet, K. L. Kennedy, T. T. Huynh, I. H. McKillop, and S. L. Evans, "Resveratrol attenuates hypoxic injury in a primary hepatocyte model of hemorrhagic shock and resuscitation," *Journal of Trauma and Acute Care Surgery*, vol. 76, no. 2, pp. 409–417, 2014.

[41] W. Dong, F. Li, Z. Pan et al., "Resveratrol ameliorates subacute intestinal ischemia-reperfusion injury," *Journal of Surgical Research*, vol. 185, no. 1, pp. 182–189, 2013.

[42] F. Petrat and H. De Groot, "Protection against severe intestinal ischemia/reperfusion injury in rats by intravenous resveratrol," *Journal of Surgical Research*, vol. 167, no. 2, pp. e145–e155, 2011.

[43] O. V. Ozkan, M. F. Yuzbasioglu, H. Ciralik et al., "Resveratrol, a natural antioxidant attenuates intestinal ischemia/reperfusion injury in rats," *The bTohoku Journal of Experimental Medicine*, vol. 218, no. 3, pp. 251–258, 2009.

[44] W. Dong, X. Zhang, D. Gao, and N. Li, "Cerebral angiogenesis induced by resveratrol contributes to relieve cerebral ischemic-reperfusion injury," *Medical Hypotheses*, vol. 69, no. 1, pp. 226–227, 2007.

[45] V. Chander and K. Chopra, "Protective effect of nitric oxide pathway in resveratrol renal ischemia-reperfusion injury in rats," *Archives of Medical Research*, vol. 37, no. 1, pp. 19–26, 2006.

[46] S. Kaplan, G. Bisleri, J. A. Morgan, F. H. Cheema, and M. C. Oz, "Resveratrol, a natural red wine polyphenol, reduces ischemia-reperfusion- induced spinal cord injury," *Annals of Thoracic Surgery*, vol. 80, no. 6, pp. 2242–2249, 2005.

[47] S. Uguralp, B. Mizrak, and A. B. Karabulut, "Resveratrol reduces ischemia reperfusion injury after experimental testicular torsion," *European Journal of Pediatric Surgery*, vol. 15, no. 2, pp. 114–119, 2005.

[48] Q. Wang, J. Xu, G. E. Rottinghaus et al., "Resveratrol protects against global cerebral ischemic injury in gerbils," *Brain Research*, vol. 958, no. 2, pp. 439–447, 2002.

[49] P. S. Ray, G. Maulik, G. A. Cordis, A. A. E. Bertelli, and D. K. Das, "The red wine antioxidant resveratrol protects isolated rat hearts from ischemia reperfusion injury," *Free Radical Biology & Medicine*, vol. 27, no. 1-2, pp. 160–169, 1999.

[50] Z. Xia, Y. Chen, Q. Fan, and M. Xue, "Oxidative stress-mediated reperfusion injury: mechanism and therapies," *Oxidative Medicine and Cellular Longevity*, vol. 2014, Article ID 373081, 2 pages, 2014.

[51] D. K. de Vries, K. A. Kortekaas, D. Tsikas et al., "Oxidative damage in clinical ischemia/reperfusion injury: a reappraisal," *Antioxidants & Redox Signaling*, vol. 19, no. 6, pp. 535–545, 2013.

[52] P. W. Kleikers, K. Wingler, J. J. Hermans et al., "NADPH oxidases as a source of oxidative stress and molecular target in ischemia/reperfusion injury," *Journal of Molecular Medicine*, vol. 90, no. 12, pp. 1391–1406, 2012.

[53] L. Ji, F. Fu, L. Zhang et al., "Insulin attenuates myocardial ischemia/reperfusion injury via reducing oxidative/nitrative stress," *The American Journal of Physiology—Endocrinology and Metabolism*, vol. 298, no. 4, pp. E871–E880, 2010.

[54] G. H. Heeba and A. A. El-Hanafy, "Nebivolol regulates eNOS and iNOS expressions and alleviates oxidative stress in cerebral ischemia/reperfusion injury in rats," *Life Sciences*, vol. 90, no. 11-12, pp. 388–395, 2012.

[55] S. C. Weight and M. L. Nicholson, "Nitric oxide and renal reperfusion injury: a review," *European Journal of Vascular and Endovascular Surgery*, vol. 16, no. 2, pp. 98–103, 1998.

[56] Y. Yang, W. Duan, Y. Lin et al., "SIRT1 activation by curcumin pretreatment attenuates mitochondrial oxidative damage induced by myocardial ischemia reperfusion injury," *Free Radical Biology & Medicine*, vol. 65, pp. 667–679, 2013.

[57] H. Okabe, "The role of xanthine dehydrogenase (xanthine oxidase) in ischemia-reperfusion injury in rat kidney," *Japanese Journal of Nephrology*, vol. 38, no. 12, pp. 577–584, 1996.

[58] F. Yaylak, H. Canbaz, M. Caglikulekci et al., "Liver tissue inducible nitric oxide synthase (iNOS) expression and lipid peroxidation in experimental hepatic ischemia reperfusion injury stimulated with lipopolysaccharide: the role of aminoguanidine," *Journal of Surgical Research*, vol. 148, no. 2, pp. 214–223, 2008.

[59] A. Folino, G. Losano, and R. Rastaldo, "Balance of nitric oxide and reactive oxygen species in myocardial reperfusion injury and protection," *Journal of Cardiovascular Pharmacology*, vol. 62, no. 6, pp. 567–575, 2013.

[60] M. Abu-Amara, S. Y. Yang, A. Seifalian, B. Davidson, and B. Fuller, "The nitric oxide pathway–evidence and mechanisms for protection against liver ischaemia reperfusion injury," *Liver International*, vol. 32, no. 4, pp. 531–543, 2012.

[61] F. Simão, A. Matté, C. Matté et al., "Resveratrol prevents oxidative stress and inhibition of Na^+K^+-ATPase activity induced by transient global cerebral ischemia in rats," *The Journal of Nutritional Biochemistry*, vol. 22, no. 10, pp. 921–928, 2011.

[62] A. M. Arent, L. F. D. Souza, R. Walz, and A. L. Dafre, "Perspectives on molecular biomarkers of oxidative stress and antioxidant strategies in traumatic brain injury," *BioMed Research International*, vol. 2014, Article ID 723060, 18 pages, 2014.

[63] P. O. Eghwrudjakpor and A. B. Allison, "Oxidative stress following traumatic brain injury: enhancement of endogenous antioxidant defense systems and the promise of improved outcome," *Nigerian Journal of Medicine*, vol. 19, no. 1, pp. 14–21, 2010.

[64] M. Sasaki and T. Joh, "Oxidative stress and ischemia-reperfusion injury in gastrointestinal tract and antioxidant, protective agents," *Journal of Clinical Biochemistry and Nutrition*, vol. 40, no. 1, pp. 1–12, 2007.

[65] H. Khastar, M. Kadkhodaee, H. R. Sadeghipour et al., "Liver oxidative stress after renal ischemia-reperfusion injury is leukocyte dependent in inbred mice," *Iranian Journal of Basic Medical Sciences*, vol. 14, no. 6, pp. 534–539, 2011.

[66] S. Bereswill, M. Muñoz, A. Fischer et al., "Anti-inflammatory effects of resveratrol, curcumin and simvastatin in acute small intestinal inflammation," *PLoS ONE*, vol. 5, no. 12, Article ID e15099, 2010.

[67] C. T. Wu, H. P. Yu, C. Y. Chung, Y. T. Lau, and S. K. Liao, "Attenuation of lung inflammation and pro-inflammatory cytokine production by resveratrol following trauma-hemorrhage," *The Chinese journal of physiology*, vol. 51, no. 6, pp. 363–368, 2008.

[68] S. Dernek, M. Ikizler, N. Erkasap et al., "Cardioprotection with resveratrol pretreatment: improved beneficial effects over standard treatment in rat hearts after global ischemia," *Scandinavian Cardiovascular Journal*, vol. 38, no. 4, pp. 245–254, 2004.

[69] V. Sharma, R. M. Bell, and D. M. Yellon, "Targeting reperfusion injury in acute myocardial infarction: a review of reperfusion injury pharmacotherapy," *Expert Opinion on Pharmacotherapy*, vol. 13, no. 8, pp. 1153–1175, 2012.

[70] E. Dongó, I. Hornyák, Z. Benko, and L. Kiss, "The cardioprotective potential of hydrogen sulfide in myocardial ischemia/reperfusion injury (review)," *Acta Physiologica Hungarica*, vol. 98, no. 4, pp. 369–381, 2011.

[71] S. K. Powers, Z. Murlasits, M. Wu, and A. N. Kavazis, "Ischemia-reperfusion-induced cardiac injury: a brief review," *Medicine & Science in Sports & Exercise*, vol. 39, no. 9, pp. 1529–1536, 2007.

[72] A. Movahed, L. Yu, S. J. Thandapilly, X. L. Louis, and T. Netticadan, "Resveratrol protects adult cardiomyocytes against oxidative stress mediated cell injury," *Archives of Biochemistry and Biophysics*, vol. 527, no. 2, pp. 74–80, 2012.

[73] S. Bradamante, L. Barenghi, and A. Villa, "Cardiovascular protective effects of resveratrol," *Cardiovascular Drug Reviews*, vol. 22, no. 3, pp. 169–188, 2004.

[74] Y. Tang, J. Xu, W. Qu et al., "Resveratrol reduces vascular cell senescence through attenuation of oxidative stress by SIRT1/NADPH oxidase-dependent mechanisms," *Journal of Nutritional Biochemistry*, vol. 23, no. 11, pp. 1410–1416, 2012.

[75] C.-L. Kao, L.-K. Chen, Y.-L. Chang et al., "Resveratrol protects human endothelium from H_2O_2-induced oxidative stress and senescence via SirT1 activation," *Journal of Atherosclerosis and Thrombosis*, vol. 17, no. 9, pp. 970–979, 2010.

[76] Y. Zheng, Y. Liu, J. Ge et al., "Resveratrol protects human lens epithelial cells against H_2O_2-induced oxidative stress by increasing catalase, SOD-1, and HO-1 expression," *Molecular Vision*, vol. 16, pp. 1467–1474, 2010.

[77] B. Wang, Q. Yang, Y. Y. Sun et al., "Resveratrol-enhanced autophagic flux ameliorates myocardial oxidative stress injury in diabetic mice," *Journal of Cellular and Molecular Medicine*, vol. 18, no. 8, pp. 1599–1611, 2014.

[78] G. Spanier, H. Xu, N. Xia et al., "Resveratrol reduces endothelial oxidative stress by modulating the gene expression of superoxide dismutase 1 (SOD1), glutathione peroxidase 1 (GPx1) and NADPH oxidase subunit (Nox4)," *Journal of Physiology and Pharmacology*, vol. 60, supplement 4, pp. 111–116, 2009.

[79] P.-W. Cheng, W.-Y. Ho, Y.-T. Su et al., "Resveratrol decreases fructose-induced oxidative stress, mediated by NADPH oxidase via an AMPK-dependent mechanism," *British Journal of Pharmacology*, vol. 171, no. 11, pp. 2739–2750, 2014.

[80] M. Mokni, S. Hamlaoui, I. Karkouch et al., "Resveratrol provides cardioprotection after ischemia/reperfusion injury via modulation of antioxidant enzyme activities," *Iranian Journal of Pharmaceutical Research*, vol. 12, no. 4, pp. 867–875, 2013.

[81] M. Shen, R.-X. Wu, L. Zhao et al., "Resveratrol attenuates ischemia/reperfusion injury in neonatal cardiomyocytes and its underlying mechanism," *PLoS ONE*, vol. 7, no. 12, Article ID e51223, 2012.

[82] M. Mokni, F. Limam, S. Elkahoui, M. Amri, and E. Aouani, "Strong cardioprotective effect of resveratrol, a red wine polyphenol, on isolated rat hearts after ischemia/reperfusion injury," *Archives of Biochemistry and Biophysics*, vol. 457, no. 1, pp. 1–6, 2007.

[83] M. Mohammadshahi, F. Haidari, and F. G. Soufi, "Chronic resveratrol administration improves diabetic cardiomyopathy in part by reducing oxidative stress," *Cardiology Journal*, vol. 21, no. 1, pp. 39–46, 2014.

[84] P. Toth, S. Tarantini, Z. Tucsek et al., "Resveratrol treatment rescues neurovascular coupling in aged mice: role of improved cerebromicrovascular endothelial function and downregulation of NADPH oxidase," *American Journal of Physiology: Heart and Circulatory Physiology*, vol. 306, no. 3, pp. H299–H308, 2014.

[85] E. Miller, A. Morel, L. Saso, and J. Saluk, "Isoprostanes and neuroprostanes as biomarkers of oxidative stress in neurodegenerative diseases," *Oxidative Medicine and Cellular Longevity*, vol. 2014, Article ID 572491, 10 pages, 2014.

[86] X. Qiao, J. Xu, Q.-J. Yang et al., "Transient acidosis during early reperfusion attenuates myocardium ischemia reperfusion injury VIA PI3K-AKT-eNOS signaling pathway," *Oxidative Medicine and Cellular Longevity*, vol. 2013, Article ID 126083, 6 pages, 2013.

[87] T. Wang, X. Mao, H. Li et al., "N-Acetylcysteine and allopurinol up-regulated the Jak/STAT3 and PI3K/Akt pathways via adiponectin and attenuated myocardial postischemic injury in diabetes," *Free Radical Biology and Medicine*, vol. 63, pp. 291–303, 2013.

[88] L.-M. Hung, M.-J. Su, and J.-K. Chen, "Resveratrol protects myocardial ischemia-reperfusion injury through both NO-dependent and NO-independent mechanisms," *Free Radical Biology and Medicine*, vol. 36, no. 6, pp. 774–781, 2004.

[89] M. Lagouge, C. Argmann, Z. Gerhart-Hines et al., "Resveratrol improves mitochondrial function and protects against metabolic disease by activating SIRT1 and PGC-1α," *Cell*, vol. 127, no. 6, pp. 1109–1122, 2006.

[90] M. Shalwala, S.-G. Zhu, A. Das, F. N. Salloum, L. Xi, and R. C. Kukreja, "Sirtuin 1 (SIRT1) activation mediates sildenafil induced delayed cardioprotection against ischemia-reperfusion injury in mice," *PLoS ONE*, vol. 9, no. 1, Article ID e86977, 2014.

[91] S. Shigematsu, S. Ishida, M. Hara et al., "Resveratrol, a red wine constituent polyphenol, prevents superoxide-dependent inflammatory responses induced by ischemia/reperfusion, platelet-activating factor, or oxidants," *Free Radical Biology and Medicine*, vol. 34, no. 7, pp. 810–817, 2003.

[92] H. Li, Z. Yan, J. Zhu, J. Yang, and J. He, "Neuroprotective effects of resveratrol on ischemic injury mediated by improving brain energy metabolism and alleviating oxidative stress in rats," *Neuropharmacology*, vol. 60, no. 2-3, pp. 252–258, 2011.

[93] X. M. Zhou, M. L. Zhou, X. S. Zhang, Z. Zhuang, T. Li, and J. X. Shi, "Resveratrol prevents neuronal apoptosis in an early brain injury model," *Journal of Surgical Research*, vol. 189, no. 1, pp. 159–165, 2014.

[94] J. W. Gatson, M.-M. Liu, K. Abdelfattah et al., "Resveratrol decreases inflammation in the brain of mice with mild traumatic brain injury," *Journal of Trauma and Acute Care Surgery*, vol. 74, no. 2, pp. 470–475, 2013.

[95] F. Karalis, V. Soubasi, T. Georgiou et al., "Resveratrol ameliorates hypoxia/ischemia-induced behavioral deficits and brain injury in the neonatal rat brain," *Brain Research*, vol. 1425, pp. 98–110, 2011.

[96] K. Sinha, G. Chaudhary, and Y. Kumar Gupta, "Protective effect of resveratrol against oxidative stress in middle cerebral artery occlusion model of stroke in rats," *Life Sciences*, vol. 71, no. 6, pp. 655–665, 2002.

[97] S.-K. Tsai, L.-M. Hung, Y.-T. Fu et al., "Resveratrol neuroprotective effects during focal cerebral ischemia injury via nitric oxide mechanism in rats," *Journal of Vascular Surgery*, vol. 46, no. 2, pp. 346–353, 2007.

[98] E. Barocelli, V. Ballabeni, P. Ghizzardi et al., "The selective inhibition of inducible nitric oxide synthase prevents intestinal ischemia-reperfusion injury in mice," *Nitric Oxide—Biology and Chemistry*, vol. 14, no. 3, pp. 212–218, 2006.

[99] P. Orsu, B. V. S. N. Murthy, and A. Akula, "Cerebroprotective potential of resveratrol through anti-oxidant and anti-inflammatory mechanisms in rats," *Journal of Neural Transmission*, vol. 120, no. 8, pp. 1217–1223, 2013.

[100] F. Simão, A. Matté, A. S. Pagnussat, C. A. Netto, and C. G. Salbego, "Resveratrol preconditioning modulates inflammatory response in the rat hippocampus following global cerebral ischemia," *Neurochemistry International*, vol. 61, no. 5, pp. 659–665, 2012.

[101] U. Kiziltepe, N. N. D. Turan, U. Han, A. T. Ulus, and F. Akar, "Resveratrol, a red wine polyphenol, protects spinal cord from ischemia-reperfusion injury," *Journal of Vascular Surgery*, vol. 40, no. 1, pp. 138–145, 2004.

[102] H. S. Ozacmak, V. H. Ozacmak, F. Barut, M. Arasli, and B. H. Ucan, "Pretreatment with mineralocorticoid receptor blocker reduces intestinal injury induced by ischemia and reperfusion: involvement of inhibition of inflammatory response, oxidative stress, nuclear factor κB, and inducible nitric oxide synthase," *Journal of Surgical Research*, vol. 191, no. 2, pp. 350–361, 2014.

[103] J. Cui, L. Liu, J. Zou et al., "Protective effect of endogenous hydrogen sulfide against oxidative stress in gastric ischemia-reperfusion injury," *Experimental and Therapeutic Medicine*, vol. 5, no. 3, pp. 689–694, 2013.

[104] P. R. Bertoletto, A. T. Ikejiri, F. S. Neto et al., "Oxidative stress gene expression profile in inbred mouse after ischemia/reperfusion small bowel injury," *Acta Cirurgica Brasileira*, vol. 27, no. 11, pp. 772–782, 2012.

[105] F. Yildiz, A. Terzi, S. Coban et al., "Protective effects of resveratrol on small intestines against intestinal ischemia-reperfusion injury in rats," *Journal of Gastroenterology and Hepatology*, vol. 24, no. 11, pp. 1781–1785, 2009.

[106] H. Namazi, "A novel molecular mechanism to account for the action of resveratrol against reperfusion injury," *Annals of Vascular Surgery*, vol. 22, no. 3, p. 492, 2008.

[107] A. B. Karabulut, V. Kirimlioglu, H. Kirimlioglu, S. Yilmaz, B. Isik, and O. Isikgil, "Protective effects of resveratrol on spleen and ileum in rats subjected to ischemia-reperfusion," *Transplantation Proceedings*, vol. 38, no. 2, pp. 375–377, 2006.

[108] L. Phillips, A. H. Toledo, F. Lopez-Neblina, R. Anaya-Prado, and L. H. Toledo-Pereyra, "Nitric oxide mechanism of protection in ischemia and reperfusion injury," *Journal of Investigative Surgery*, vol. 22, no. 1, pp. 46–55, 2009.

[109] M. Yamaguchi and M. Uchida, "α-Lactalbumin suppresses interleukin-6 release after intestinal ischemia/reperfusion via nitric oxide in rats," *Inflammopharmacology*, vol. 15, no. 1, pp. 43–47, 2007.

[110] L. Gu, N. Li, W. Yu et al., "Berberine reduces rat intestinal tight junction injury induced by ischemia-reperfusion associated with the suppression of inducible nitric oxide synthesis," *The American Journal of Chinese Medicine*, vol. 41, no. 6, pp. 1297–1312, 2013.

[111] M. Y. Kim, J. H. Lim, H. H. Youn et al., "Resveratrol prevents renal lipotoxicity and inhibits mesangial cell glucotoxicity in a manner dependent on the AMPK-SIRT1-PGC1α axis in db/db mice," *Diabetologia*, vol. 56, no. 1, pp. 204–217, 2013.

[112] G. Şener, H. Tuğtepe, M. Yüksel, Ş. Çetinel, N. Gedik, and B. Ç. Yeğen, "Resveratrol improves ischemia/reperfusion-induced oxidative renal injury in rats," *Archives of Medical Research*, vol. 37, no. 7, pp. 822–829, 2006.

[113] L. Giovannini, M. Migliori, B. M. Longoni et al., "Resveratrol, a polyphenol found in wine, reduces ischemia reperfusion injury in rat kidneys," *Journal of Cardiovascular Pharmacology*, vol. 37, no. 3, pp. 262–270, 2001.

[114] X. Fu, S. Li, G. Jia et al., "Protective effect of the nitric oxide pathway in L-citrulline renal ichaemia-reperfusion injury in rats," *Folia Biologica*, vol. 59, no. 6, pp. 225–232, 2013.

[115] A. Korkmaz and D. Kolankaya, "Inhibiting inducible nitric oxide synthase with rutin reduces renal ischemia/reperfusion injury," *Canadian Journal of Surgery*, vol. 56, no. 1, pp. 6–14, 2013.

[116] R. Schneider, M. Meusel, B. Betz et al., "Nitric oxide-induced regulation of renal organic cation transport after renal ischemia-reperfusion injury," *The American Journal of Physiology—Renal Physiology*, vol. 301, no. 5, pp. F997–F1004, 2011.

[117] V. Chander and K. Chopra, "Role of nitric oxide in resveratrol-induced renal protective effects of ischemic preconditioning," *Journal of Vascular Surgery*, vol. 42, no. 6, pp. 1198–1205, 2005.

[118] L. Y. Guan, P. Y. Fu, P. D. Li et al., "Mechanisms of hepatic ischemia-reperfusion injury and protective effects of nitric oxide," *World Journal of Gastrointestinal Surgery*, vol. 6, no. 7, pp. 122–128, 2014.

[119] G. K. Glantzounis, H. J. Salacinski, W. Yang, B. R. Davidson, and A. M. Seifalian, "The contemporary role of antioxidant therapy in attenuating liver ischemia-reperfusion injury: a review," *Liver Transplantation*, vol. 11, no. 9, pp. 1031–1047, 2005.

[120] F.-C. Liu, Y.-F. Tsai, and H.-P. Yu, "Maraviroc attenuates trauma-hemorrhage-induced hepatic injury through PPAR gamma-dependent pathway in rats," *PLoS ONE*, vol. 8, no. 10, Article ID e78861, 2013.

[121] E. Gedik, S. Girgin, H. Ozturk, B. D. Obay, H. Ozturk, and H. Buyukbayram, "Resveratrol attenuates oxidative stress and histological alterations induced by liver ischemia/reperfusion in rats," *World Journal of Gastroenterology*, vol. 14, no. 46, pp. 7101–7106, 2008.

[122] S. Hassan-Khabbar, M. Vamy, C.-H. Cottart et al., "Protective effect of post-ischemic treatment with trans-resveratrol on cytokine production and neutrophil recruitment by rat liver," *Biochimie*, vol. 92, no. 4, pp. 405–410, 2010.

[123] S. Gennai, C. Pison, and R. Briot, "Ischemia-reperfusion injury after lung transplantation," *La Presse Médicale*, vol. 43, no. 9, pp. 921–930, 2014.

[124] J. Rong, S. Ye, M.-Y. Liang et al., "Receptor for advanced glycation end products involved in lung ischemia reperfusion injury in cardiopulmonary bypass attenuated by controlled oxygen reperfusion in a canine model," *ASAIO Journal*, vol. 59, no. 3, pp. 302–308, 2013.

[125] R. Campos, M. H. M. Shimizu, R. A. Volpini et al., "N-acetylcysteine prevents pulmonary edema and acute kidney injury in rats with sepsis submitted to mechanical ventilation," *American Journal of Physiology—Lung Cellular and Molecular Physiology*, vol. 302, no. 7, pp. L640–L650, 2012.

[126] D. Y.-W. Yeh, Y. H. Fu, Y.-C. Yang, and J.-J. Wang, "Resveratrol alleviates lung ischemia and reperfusion-induced pulmonary capillary injury through modulating pulmonary mitochondrial metabolism," *Transplantation Proceedings*, vol. 46, no. 4, pp. 1131–1134, 2014.

[127] S. Çayan, B. Saylam, N. Tiftik et al., "Rho-kinase levels in testicular ischemia-reperfusion injury and effects of its inhibitor, Y-27632, on oxidative stress, spermatogenesis, and apoptosis," *Urology*, vol. 83, no. 3, pp. 675–678, 2014.

[128] S. M. Wei, Z. Z. Yan, and J. Zhou, "Protective effect of rutin on testicular ischemia-reperfusion injury," *Journal of Pediatric Surgery*, vol. 46, no. 7, pp. 1419–1424, 2011.

[129] D. Y. Woodruff, G. Horwitz, J. Weigel, and A. K. Nangia, "Fertility preservation following torsion and severe ischemic injury of a solitary testis," *Fertility and Sterility*, vol. 94, no. 1, pp. 352–355, 2010.

[130] H. Yildiz, A. S. Durmus, H. Şimşek, and M. Yaman, "Protective effect of sildenafil citrate on contralateral testis injury after unilateral testicular torsion/detorsion," *Clinics*, vol. 66, no. 1, pp. 137–142, 2011.

[131] R. M. Vigueras, G. Reyes, J. Rojas-Castañeda, P. Rojas, and R. Hernández, "Testicular torsion and its effects on the spermatogenic cycle in the contralateral testis of the rat," *Laboratory Animals*, vol. 38, no. 3, pp. 313–320, 2004.

[132] B. Etensel, S. Özkisacik, E. Özkara et al., "Dexpanthenol attenuates lipid peroxidation and testicular damage at experimental ischemia and reperfusion injury," *Pediatric Surgery International*, vol. 23, no. 2, pp. 177–181, 2007.

[133] C. T. Ribeiro, R. Milhomem, D. B. De Souza, W. S. Costa, F. J. B. Sampaio, and M. A. Pereira-Sampaio, "Effect of antioxidants on outcome of testicular torsion in rats of different ages," *Journal of Urology*, vol. 191, no. 5, pp. 1578–1584, 2014.

[134] H. G. Piper, S. C. Oltmann, L. Xu, S. Adusumilli, and A. C. Fischer, "Ovarian torsion: diagnosis of inclusion mandates earlier intervention," *Journal of Pediatric Surgery*, vol. 47, no. 11, pp. 2071–2076, 2012.

[135] S. Krishnan, H. Kaur, J. Bali, and K. Rao, "Ovarian torsion in infertility management—missing the diagnosis means losing the ovary: a high price to pay," *Journal of Human Reproductive Sciences*, vol. 4, no. 1, pp. 39–42, 2011.

[136] H. Jaeschke, "Xanthine oxidase-induced oxidant stress during hepatic ischemia-reperfusion: are we coming full circle after 20 years?" *Hepatology*, vol. 36, no. 3, pp. 761–763, 2002.

[137] P. E. Canas, "The role of xanthine oxidase and the effects of antioxidants in ischemia reperfusion cell injury," *Acta Physiologica Pharmacologica et Therapeutica Latinoamericana*, vol. 49, no. 1, pp. 13–20, 1999.

[138] T. A. Johnson, N. A. Stasko, J. L. Matthews et al., "Reduced ischemia/reperfusion injury via glutathione-initiated nitric oxide-releasing dendrimers," *Nitric Oxide—Biology and Chemistry*, vol. 22, no. 1, pp. 30–36, 2010.

[139] H. J. Stein, M. M. J. Oosthuizen, R. A. Hinder, and H. Lamprechts, "Oxygen free radicals and glutathione in hepatic ischemia/reperfusion injury," *Journal of Surgical Research*, vol. 50, no. 4, pp. 398–402, 1991.

[140] S. Hascalik, O. Celik, Y. Turkoz et al., "Resveratrol, a red wine constituent polyphenol, protects from ischemia-reperfusion damage of the ovaries," *Gynecologic and Obstetric Investigation*, vol. 57, no. 4, pp. 218–223, 2004.

[141] M. He, H. Pan, R. C.-C. Chang, K.-F. So, N. C. Brecha, and M. Pu, "Activation of the Nrf2/HO-1 antioxidant pathway contributes to the protective effects of lycium barbarum polysaccharides in the rodent retina after ischemia-reperfusion-induced damage," *PLoS ONE*, vol. 9, no. 1, Article ID e84800, 2014.

[142] N. Dilsiz, A. Sahaboglu, M. Z. Yildiz, and A. Reichenbach, "Protective effects of various antioxidants during ischemia-reperfusion in the rat retina," *Graefe's Archive for Clinical and Experimental Ophthalmology*, vol. 244, no. 5, pp. 627–633, 2006.

[143] O. Lewden, C. Garcher, C. Morales, A. Javouhey, L. Rochette, and A. M. Bron, "Changes of catalase activity after ischemia-reperfusion in rat retina," *Ophthalmic Research*, vol. 28, no. 6, pp. 331–335, 1996.

[144] M. E. Szabo, M. T. Droy-Lefaix, M. Doly, and P. Braquet, "Modification of ischemia/reperfusion-induced ion shifts (Na^+, K^+, Ca^{2+} and Mg^{2+}) by free radical scavengers in the rat retina," *Ophthalmic Research*, vol. 25, no. 1, pp. 1–9, 1993.

[145] A. P. Vin, H. Hu, Y. Zhai et al., "Neuroprotective effect of resveratrol prophylaxis on experimental retinal ischemic injury," *Experimental Eye Research*, vol. 108, pp. 72–75, 2013.

[146] C. Li, L. Wang, K. Huang, and L. Zheng, "Endoplasmic reticulum stress in retinal vascular degeneration: protective role of resveratrol," *Investigative Ophthalmology & Visual Science*, vol. 53, no. 6, pp. 3241–3249, 2012.

[147] D. Gao, X. Zhang, X. Jiang et al., "Resveratrol reduces the elevated level of MMP-9 induced by cerebral ischemia-reperfusion in mice," *Life Sciences*, vol. 78, no. 22, pp. 2564–2570, 2006.

[148] M. H. Sun, J. H. Pang, S. L. Chen et al., "Photoreceptor protection against light damage by AAV-mediated overexpression of heme oxygenase-1," *Investigative Ophthalmology & Visual Science*, vol. 48, no. 12, pp. 5699–5707, 2007.

[149] X. Q. Liu, B. J. Wu, W. H. Pan et al., "Resveratrol mitigates rat retinal ischemic injury: the roles of matrix metalloproteinase-9,

inducible nitric oxide, and heme oxygenase-1," *Journal of Ocular Pharmacology and Therapeutics*, vol. 29, no. 1, pp. 33–40, 2013.

[150] H. Yagmurdur, N. Ozcan, F. Dokumaci, K. Kilinc, F. Yilmaz, and H. Basar, "Dexmedetomidine reduces the ischemia-reperfusion injury markers during upper extremity surgery with tourniquet," *Journal of Hand Surgery*, vol. 33, no. 6, pp. 941–947, 2008.

[151] W. R. Carroll and R. M. Esclamado, "Ischemia/reperfusion injury in microvascular surgery," *Head & Neck*, vol. 22, no. 7, pp. 700–713, 2000.

[152] M. Mathru, D. J. Dries, L. Barnes, P. Tonino, R. Sukhani, and M. W. Rooney, "Tourniquet-induced exsanguination in patients requiring lower limb surgery: an ischemia-reperfusion model of oxidant and antioxidant metabolism," *Anesthesiology*, vol. 84, no. 1, pp. 14–22, 1996.

[153] A. Lejay, A. Meyer, A.-I. Schlagowski et al., "Mitochondria: mitochondrial participation in ischemia-reperfusion injury in skeletal muscle," *The International Journal of Biochemistry and Cell Biology*, vol. 50, no. 1, pp. 101–105, 2014.

[154] S. Gillani, J. Cao, T. Suzuki, and D. J. Hak, "The effect of ischemia reperfusion injury on skeletal muscle," *Injury*, vol. 43, no. 6, pp. 670–675, 2012.

[155] H. T. Hua, H. Al-Badawi, F. Entabi et al., "CXC chemokine expression and synthesis in skeletal muscle during ischemia/reperfusion," *Journal of Vascular Surgery*, vol. 42, no. 2, pp. 337–343, 2005.

[156] A. Kadambi and T. C. Skalak, "Role of leukocytes and tissue-derived oxidants in short-term skeletal muscle ischemia-reperfusion injury," *The American Journal of Physiology—Heart and Circulatory Physiology*, vol. 278, no. 2, pp. H435–H443, 2000.

[157] M. Ikizler, C. Ovali, S. Dernek et al., "Protective effects of resveratrol in ischemia-reperfusion injury of skeletal muscle: a clinically relevant animal model for lower extremity ischemia," *The Chinese Journal of Physiology*, vol. 49, no. 4, pp. 204–209, 2006.

[158] N. Elmali, I. Esenkaya, N. Karadağ, and F. Taş, "Effects of resveratrol on skeletal muscle in ischemia-reperfusion injury," *Ulusal Travma ve Acil Cerrahi Dergisi*, vol. 13, no. 4, pp. 274–280, 2007.

[159] M. Nomiya, O. Yamaguchi, K.-E. Andersson et al., "The effect of atherosclerosis-induced chronic bladder ischemia on bladder function in the rat," *Neurourology and Urodynamics*, vol. 31, no. 1, pp. 195–200, 2012.

[160] A. Ali, G. Nabi, S. Swami, and B. Somani, "Bladder necrosis secondary to internal iliac artery embolization following pelvic fracture," *Urology Annals*, vol. 6, no. 2, pp. 166–168, 2014.

[161] G. E. Senturk, K. Erkanli, U. Aydin et al., "The protective effect of oxytocin on ischemia/reperfusion injury in rat urinary bladder," *Peptides*, vol. 40, pp. 82–88, 2013.

[162] Y.-S. Juan, S. M. Chuang, B. A. Kogan et al., "Effect of ischemia/reperfusion on bladder nerve and detrusor cell damage," *International Urology and Nephrology*, vol. 41, no. 3, pp. 513–521, 2009.

[163] A. Yildirim, F. F. Onol, G. Haklar, and T. Tarcan, "The role of free radicals and nitric oxide in the ischemia-reperfusion injury mediated by acute bladder outlet obstruction," *International Urology and Nephrology*, vol. 40, no. 1, pp. 71–77, 2008.

[164] H. Toklu, I. Alican, F. Ercan, and G. Sener, "The beneficial effect of resveratrol on rat bladder contractility and oxidant damage following ischemia/reperfusion," *Pharmacology*, vol. 78, no. 1, pp. 44–50, 2006.

[165] H.-P. Yu, T.-L. Hwang, C.-H. Yen, and Y.-T. Lau, "Resveratrol prevents endothelial dysfunction and aortic superoxide production after trauma hemorrhage through estrogen receptor-dependent hemeoxygenase-1 pathway," *Critical Care Medicine*, vol. 38, no. 4, pp. 1147–1154, 2010.

[166] Z. F. Ba, J. F. Kuebler, L. W. Rue III, K. I. Bland, P. Wang, and I. H. Chaudry, "Gender dimorphic tissue perfusion response after acute hemorrhage and resuscitation: role of vascular endothelial cell function," *The American Journal of Physiology—Heart and Circulatory Physiology*, vol. 284, no. 6, pp. H2162–H2169, 2003.

[167] P. Wang, Z. F. Ba, and I. H. Chaudry, "Endothelial cell dysfunction occurs very early following trauma- hemorrhage and persists despite fluid resuscitation," *American Journal of Physiology—Heart and Circulatory Physiology*, vol. 265, no. 3, part 2, pp. H973–H979, 1993.

[168] H.-P. Yu, P.-W. Lui, T.-L. Hwang, C.-H. Yen, and Y.-T. Lau, "Propofol improves endothelial dysfunction and attenuates vascular superoxide production in septic rats," *Critical Care Medicine*, vol. 34, no. 2, pp. 453–460, 2006.

[169] L. Szalay, T. Shimizu, M. G. Schwacha et al., "Mechanism of salutary effects of estradiol on organ function after trauma-hemorrhage: upregulation of heme oxygenase," *American Journal of Physiology—Heart and Circulatory Physiology*, vol. 289, no. 1, pp. H92–H98, 2005.

[170] C.-C. Chang, C.-Y. Chang, J.-P. Huang, and L.-M. Hung, "Effect of resveratrol on oxidative and inflammatory stress in liver and spleen of streptozotocin-induced type 1 diabetic rats," *The Chinese Journal of Physiology*, vol. 55, no. 3, pp. 192–201, 2012.

[171] J. Li, L. Feng, Y. Xing et al., "Radioprotective and antioxidant effect of resveratrol in hippocampus by activating Sirt1," *International Journal of Molecular Sciences*, vol. 15, no. 4, pp. 5928–5939, 2014.

[172] B. Jian, S. Yang, I. H. Chaudry, and R. Raju, "Resveratrol improves cardiac contractility following trauma-hemorrhage by modulating Sirt1," *Molecular Medicine*, vol. 18, no. 2, pp. 209–214, 2012.

[173] J. T. Hsu, H. C. Yeh, T. H. Chen et al., "Role of Akt/HO-1 pathway in estrogen-mediated attenuation of trauma-hemorrhage-induced lung injury," *Journal of Surgical Research*, vol. 182, no. 2, pp. 319–325, 2013.

[174] J.-T. Hsu, W.-H. Kan, C.-H. Hsieh et al., "Mechanism of estrogen-mediated intestinal protection following trauma-hemorrhage: p38 MAPK-dependent upregulation of HO-1," *The American Journal of Physiology—Regulatory Integrative and Comparative Physiology*, vol. 294, no. 6, pp. R1825–R1831, 2008.

[175] J.-T. Hsu, W.-H. Kan, C.-H. Hsieh, M. A. Choudhry, K. I. Bland, and I. H. Chaudry, "Mechanism of salutary effects of estrogen on cardiac function following trauma-hemorrhage: Akt-dependent HO-1 up-regulation," *Critical Care Medicine*, vol. 37, no. 8, pp. 2338–2344, 2009.

[176] H. P. Yu, M. A. Choudhry, T. Shimizu et al., "Mechanism of the salutary effects of flutamide on intestinal myeloperoxidase activity following trauma-hemorrhage: up-regulation of estrogen receptor-β-dependent HO-1," *Journal of Leukocyte Biology*, vol. 79, no. 2, pp. 277–284, 2006.

[177] D. He, X. Liu, Y. Pang, and L. Liu, "Inhibitory effect of resveratol on ischemia reperfusion-induced cardiocyte apoptosis and its relationship with PI3K-Akt signaling pathway," *Zhongguo Zhong Yao Za Zhi*, vol. 37, no. 15, pp. 2323–2326, 2012.

[178] Y.-F. Tsai, F.-C. Liu, Y.-T. Lau, and H.-P. Yu, "Role of Akt-dependent pathway in resveratrol-mediated cardioprotection

after trauma-hemorrhage," *Journal of Surgical Research*, vol. 176, no. 1, pp. 171–177, 2012.

[179] H.-P. Yu, S.-C. Yang, Y.-T. Lau, and T.-L. Hwang, "Role of Akt-dependent up-regulation of hemeoxygenase-1 in resveratrol-mediated attenuation of hepatic injury after trauma hemorrhage," *Surgery*, vol. 148, no. 1, pp. 103–109, 2010.

[180] F. C. Liu, Y. J. Day, C. H. Liao, J. T. Liou, C. C. Mao, and H. P. Yu, "Hemeoxygenase-1 upregulation is critical for sirtinol-mediated attenuation of lung injury after trauma-hemorrhage in a rodent model," *Anesthesia and Analgesia*, vol. 108, no. 6, pp. 1855–1861, 2009.

Hindawi Publishing Corporation
Oxidative Medicine and Cellular Longevity
Volume 2015, Article ID 756576, 14 pages
http://dx.doi.org/10.1155/2015/756576

Research Article

Genome-Wide Expression Profiling of Anoxia/Reoxygenation in Rat Cardiomyocytes Uncovers the Role of MitoK_{ATP} in Energy Homeostasis

Song Cao,[1,2] Yun Liu,[2,3] Wenting Sun,[1,2] Li Zhao,[1,2] Lin Zhang,[1,2] Xinkui Liu,[1] and Tian Yu[1,2]

[1]*Department of Anesthesiology, Zunyi Medical College, Zunyi 563000, China*
[2]*Guizhou Key Laboratory of Anesthesiology and Organ Protection, Zunyi Medical College, Zunyi 563000, China*
[3]*Research Center for Medicine & Biology, Zunyi Medical College, Zunyi 563000, China*

Correspondence should be addressed to Tian Yu; zyyutian@126.com

Received 16 September 2014; Accepted 8 December 2014

Academic Editor: Yanfang Chen

Mitochondrial ATP-sensitive potassium channel (mitoK_{ATP}) is a common end effector of many protective stimuli in myocardial ischemia-reperfusion injury (MIRI). However, the specific molecular mechanism underlying its myocardial protective effect is not well elucidated. We characterized an anoxia/reoxygenation (A/R) model using freshly isolated adult rat cardiomyocytes. MitoK_{ATP} status was interfered with its specific opener diazoxide (DZ) or blocker 5-hydroxydecanote (5-HD). Digital gene expression (DGE) and bioinformatic analysis were deployed. Three energy metabolism related genes (*MT-ND6, Idh2,* and *Acadl*) were upregulated when mitoK_{ATP} opened. In addition, as many as 20 differentially expressed genes (DEGs) were significantly enriched in five energy homeostasis correlated pathways (PPAR, TCA cycle, fatty acid metabolism, and peroxisome). These findings indicated that mitoK_{ATP} opening in MIRI resulted in energy mobilization, which was confirmed by measuring ATP content in cardiomyocytes. These causal outcomes could be a molecular mechanism of myocardial protection of mitoK_{ATP} and suggested that the mitoK_{ATP} opening plays a physiologic role in triggering cardiomyocytes' energy homeostasis during MIRI. Strategies of modulating energy expenditure during myocardial ischemia-reperfusion may be promising approaches to reduce MIRI.

1. Introduction

Myocardial infarction has been a leading cause of death worldwide. The prognosis of acute myocardial infarction has been dramatically improved due to the advances of both catheterization techniques and reperfusion therapy by coronary mechanical and pharmacological intervention methods. However, strategies to limit myocardial ischemia-reperfusion injury (MIRI), thus reducing infarct size, have not been well applied in clinical settings.

Although myocardial ischemia-reperfusion (IR) induces lethal injury in the heart, after some artificial interventions, the cardiomyocytes and the heart tissue therein have powerful endogenous mechanisms to protect themselves from oxidative stress, energy deficiency, protein aggregation, and organelle malfunction, thereby minimizing MIRI [1]. For example, Murry et al. in 1990 [2, 3] first proposed that ischemic preconditioning (IPC) may protect the heart by reducing myocardial energy demand during myocardial ischemia and decreasing cell death by preserving ATP content and/or reducing catabolite accumulation. Following the discovery of the mitoK_{ATP} channel locating at the inner mitochondrial membrane in 1991 [4], Garlid et al. and Liu et al. [5, 6] demonstrated it as a trigger of IPC. Pharmacological intervention mimicking the IPC has currently been considered as a promising modality for the treatment of MIRI. Similar myocardial protection can be produced by drugs such as diazoxide (DZ) that open mitoK_{ATP} [5, 7]. Conversely, mitoK_{ATP} blockers (5-hydroxydecanote (5-HD) or glibenclamide) cancelled the effect of preconditioning and pharmacological cardioprotection [5, 6, 8]. It is also demonstrated that the pharmacological inhibition of the mitoK_{ATP} in early reperfusion abolished the infarct-limiting effects of IPost [9–11].

We have reported that mitoK$_{ATP}$ opening was cardioprotective in MIRI [12–14], but our understanding of its specific mechanism remained quite preliminary. To date, the main proposed mechanisms of cardioprotection by mitoK$_{ATP}$ were various: swelling of mitochondria increased fatty acid oxidation (FAO), mitochondrial respiration, and ATP production [15]; inhibition of ATP hydrolysis during ischemia [16, 17] preserved ATP and decreased Ca^{2+} uptake in the cardiomyocytes. However, other endogenous mechanisms of cardioprotection of mitoK$_{ATP}$ activation during IR remain to be elucidated.

Most of the *in vitro* studies used neonatal cardiac cells or immortal cardiac cell lines such as H9c2, which is physiologically different from adult cardiomyocytes [18]. For example, it is reported that neonatal cardiomyocytes were more resistant to hypoxia in comparison to adult ones [19, 20]. So, it may limit the extrapolation of the research results. We developed an A/R model using adult cardiomyocytes freshly isolated from rat to mimic the IR microenvironment *in vivo*; after all, MIRI is present almost exclusively in the adult population.

Compared with microarray and PCR-based technologies, digital gene expression (DGE) platform can provide adequate sequence coverage and quantitative accuracy to capture subtle changes resulting from mitoK$_{ATP}$ opening. In this study, a molecular and bioinformatic pipeline permitted comprehensive analysis of the myocardial mRNA expression. Next-generation sequencing technology was employed and the impact of mitoK$_{ATP}$ on the myocardial transcriptome signature of MIRI was explored to crystallize cardioprotective effects of mitoK$_{ATP}$.

2. Materials and Methods

2.1. Experimental Animals. Male Sprague-Dawley rats (250–300 g, 16–20 weeks) were provided by the Third Military Medical University (Chongqing, China) and maintained in specific pathogen free (SPF) animal facility in Zunyi Medical College under standardized conditions with 12 h light/dark cycles and free access to rat chow and water. All experimental procedures were performed according to the "Guide for the Care and Use of Laboratory Animals" in China (no. 14924, 2001) and approved by the Experimental Animal Care and Use Committee of Zunyi Medical College.

2.2. Isolation of Adult Cardiomyocytes. Rats were anesthetized with sodium pentobarbital (60 mg/kg, combined with 250 U/kg heparin, peritoneal injection). When rats had been successfully anesthetized, the chest cavity was opened and the heart excised rapidly. Ventricular cardiomyocytes were obtained by enzymatic digestion as previously described [24], with some necessary modification. Briefly, hearts were retrogradely perfused with 0.1% type 2 collagenase (Sigma, USA) at constant pressure (9 mL/min/g) on a Langendorff apparatus (Alcott Biotech, China); then the ventricle was scissored out and digested by type 2 collagenase solution in a beaker with manually shaking. Cells were filtered through a piece of gauze and washed 5 times to get rid of collagenase. Cardiomyocytes from one heart were evenly titrated into four

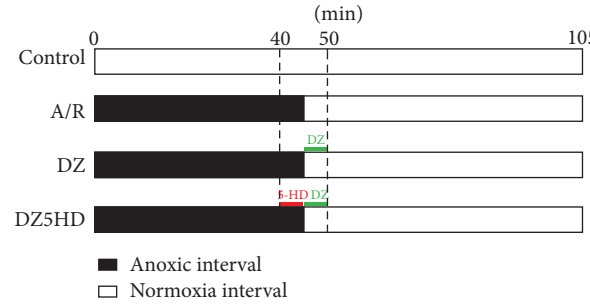

Figure 1: Illustration of the experimental A/R model protocols. Cardiomyocytes were cultured for 20 hours in normoxia incubator. Petri dishes were randomly distributed to 4 groups. Cardiomyocytes of Con were continuously cultured in normoxia environment for 105 min. Medium of A/R group was replaced with N_2 bubbled (95% N_2, 5% CO_2) modified M199 at the 40th min and then replaced with O_2 bubbled modified M199 at 45th and 50th min. Medium of DZ group was replaced with N_2 bubbled modified M199 at the 40th min; at 45th min, medium was replaced with O_2 bubbled modified M199 containing 50 μM DZ and at the 50th min it was replaced with O_2 bubbled modified M199 to remove DZ. Medium of DZ5HD group was replaced with N_2 bubbled modified M199 at 40th min containing 100 μM 5-HD; at 45th min, it was replaced with O_2 bubbled modified M199 containing 50 μM DZ and then replaced with O_2 bubbled modified M199 to remove DZ at 50th min.

60 mm laminin-precovered Petri dishes. Three mL serum free modified M199 medium (Hyclone, USA, with 2 mM carnitine, 2 mM glutamine, 5 mM taurine, 5 mM creatine, and 0.8 mM EGTA) was added. After 3 hours' incubation, the medium was replaced to get rid of noncardiomyocytes. Cell quality was confirmed with trypan blue exclusion test.

2.3. Anoxia/Reoxygenation and DZ Postconditioning in Adult Rat Cardiomyocytes. For each test, the 4 Petri dishes were placed in normoxia incubator for 20 hours before being randomly distributed to 4 groups: Control (Con), anoxia/reoxygenation (A/R), diazoxide (DZ), and DZ + blocker 5-hydroxydecanote (5-HD) (DZ5HD). Cardiomyocytes of Con were continuously cultured in normoxia environment for 105 min; A/R: under anoxia for 45 min and then reoxygenated for 60 min; DZ: anoxia for 45 minutes, reoxygenated with 50 μM DZ (Sigma, USA) for 5 min, and then reoxygenated without DZ for another 55 min; DZ5HD: anoxia for 40 min, anoxia with 100 μM 5-HD (Sigma, USA) for 5 min and then reoxygenated with DZ for 5 min and reoxygenated without DZ for another 55 min (Figure 1). Oxygen deprivation and reoxygenation were achieved by series of changes of the medium and incubators. Normoxia was set in a normoxia incubator (O_2/CO_2 incubator containing a humidified atmosphere of 5% CO_2 and 95% air at 37°C). Anoxia was achieved in an anoxic incubator (O_2/CO_2 incubator containing a humidified atmosphere of of 5% CO_2, 1% O_2, and 94% N_2 at 37°C) (Figure 1).

2.4. Intracellular Free Calcium ($[Ca^{2+}]_i$) Test. At the end of reoxygenation, $[Ca^{2+}]_i$ was detected as previously reported

[25]. Briefly, M199 was removed; cardiomyocytes of 4 groups were washed twice with PBS and loaded with Fluo-3 AM (Biotium, USA) at a final concentration of 10 μM and incubated for 30 min at 37°C in O_2/CO_2 incubator. The solution containing the Ca^{2+} probe was removed and cells were washed twice again with PBS. The average fluorescence intensity of $[Ca^{2+}]_i$ concentration in labeled cells was detected under a laser scanning confocal microscope (TCS SP2 AOBS, Leica, Germany). The wavelength of excitation was set at 488 nm and the emission wavelength was 525 nm for Fluo-3 fluorescence reading. More than 20 cells from each group were randomly chosen for data analysis; their outlines were circled out and the fluorescence density of Fluo-3 was calculated with Leica confocal software (Leica, Germany).

2.5. Cell Viability Detection. Adult cardiomyocytes' viability was detected with Cell Counting Kit-8 (CCK-8, Beyotime, China) in accordance with the manufacturer's instructions. The same amount of cells was seeded into 24-well plates. At the end point of reoxygenation, 30 μL WST-8 solution was added into M199 to form a 3% WST-8 final concentration. Cells were incubated for 1 h before the mixture's OD value was detected at 450 nm wavelength. The replicate size was 6 for each group.

2.6. RNA Extraction. At the end of reoxygenation (see Section 2.3), cardiomyocyte samples (3 replicates for 4 groups) were homogenized in TRIzol reagent (Invitrogen, USA) and vortexed with chloroform. The mixture was prepared at room temperature for 2 min and then centrifuged at 12000 ×g at 4°C. The aqueous phase was mixed with 100% ethanol and then filtered with a Qiagen RNeasy column. Subsequent steps for extraction of total RNAs were carried out as the Qiagen RNeasy kit (Qiagen, Germany) instructions described.

2.7. Tag Library Construction. The tag-seq library was constructed in accordance with the manufacturer's workflow as previously described [26]. Briefly, 6 mg extracted total RNA was used for mRNA capture with magnetic Oligo (dT) beads. Then cDNA was synthesized and the bead-bound cDNA was subsequently digested with NlaIII. Fragments attached to Oligo (dT) beads were washed away. GEX NlaIII adapter was ligated to the free 5′ end of the digested bead-bound cDNA fragments. Individual cDNA libraries were PCR amplified and purified on a 6% acrylamide gel. Attached DNA fragments were used to create a sequencing flow cell with millions of clusters, which contained about 1000 copies of the templates. Templates were sequenced by the Illumina HiSeq 2500 equipment using the four-color DNA sequencing-by-synthesis (SBS) technology. Each lane generated millions of raw reads.

2.8. Data Processing and Statistical Analysis. To obtain high quality and reliable data, raw reads were filtered to remove potentially erroneous reads. Briefly, the 3′ adaptor sequences were trimmed, low-quality tags containing N were abandoned, and small tags and only 1 copy tag were removed before obtaining the clean reads. After filtering, all reads were annotated to Rat Genome V3.4 Assembly (http://rgd.mcw.edu/). All the clean reads were mapped to the reference database; the unambiguous tags were annotated. Copy number of the clean tags of each gene was normalized with the RPKM (reads per kilobase of exon per million mapped reads) method [27] to get the final gene expression.

2.9. Identification of DEGs. According to the method by Tarazona et al. [28], the NOISeq-real algorithm was employed to determine the Q value (corresponding to the P value in differential gene expression detection) and screen genes [29, 30] differentially expressed between Con and A/R, A/R and DZ, and DZ and DZ5HD. In the present study, we considered a gene differentially expressed if the Q value was more than 0.8.

2.10. Gene Annotation with Gene Ontology and KEGG Pathway. GO (http://www.geneontology.org) provides a dynamic, controlled vocabulary. It comprises 3 independent ontologies: Biological Process, Molecular Function, and Cellular Component, each of which contains hundreds of terms. These terms reflect our understanding of the gene function.

KEGG Pathway database is for systematical analysis of gene functions, linking genomic information with higher order functional information. It provides an indication of the main biochemical and signal transduction pathways that DEGs are involved in.

Finally, the DEGs were enriched with GO (into ontologies and terms) and KEGG Pathway database.

2.11. RT-qPCR Analysis. Twenty-five DEGs were randomly selected for real-time quantitative PCR (RT-qPCR). The total RNA used for sequencing was reused to validate DGE sequencing. 500 ng RNA was reverse-transcribed into cDNA using a cDNA synthesis kit (Takara, Japan) in a final volume of 10 μL according to the manufacturer's protocol. RT-qPCR was performed with the CFX Connect Real-Time system (Bio-Rad, USA) using a SYBR green PrimeScript RT kit (Perfect Real Time, Takara, Japan) based on the manufacturer's instructions. The PCR conditions included predenaturing at 95°C for 30 s followed by 40 cycles of denaturation at 95°C for 10 s and combined annealing/extension at 58°C for 30 s. All the mRNA expression levels were calculated based on the comparative quantification method ($2^{-\Delta\Delta CT}$). The β-actin gene was used as an internal control. The primer sequences were listed in Table 4.

2.12. ATP Quantitation in Cardiomyocytes. At the end of reoxygenation, the cardiomyocytes were scraped off and centrifuged at 1000 ×g for 5 min; the supernatant (M199 medium) was abandoned. 1 mL precooled 0.4 M $HClO_4$ was added into the pellet and followed by ultrasonication and centrifugation at 10000 ×g for 20 min. The supernatant was collected and its pH was adjusted to 6.0 to 7.0 with 0.7 mL 1 M K_2HPO_4 before centrifugation again at 10000 ×g for another 20 min. All the above-mentioned procedures were conducted at 4°C. The supernatant was filtered through 0.22 μm

membrane before high performance liquid chromatography (HPLC) analysis. The chromatographic conditions were as follows: work station: LC 20A (Shimadzu, Japan); column: WondaSil C18-WR (150 mm × 4.6 mm, id = 5 μm; GL Sciences, Japan); column temperature: 25°C; mobile phase: buffered phosphate at pH 7.0; flow rate: 1 mL/min; detection wavelength: 254 nm; sample size: 10 μL. The ATP peaks of samples were determined in reference to the ATP standards (Sigma, USA). The amount of ATP was determined based on the standard curve and regression equation from ATP standard's concentration and peak area. Protein content was measured by using the same sample. ATP level of each sample is normalized to protein content.

2.13. Statistical Analysis. The quantitative data were expressed as mean ± SD. For experiments of cardiomyocytes of the four groups, one-way analysis of variance (ANOVA) was performed; LSD or Dunnett's T3 method was used to make multiple comparisons. A P value of less than 0.05 was considered to be statistically significant. All data analyses were carried out using SPSS v.19.0 (IBM, USA).

3. Results

3.1. Isolated Adult Rat Cardiomyocytes. A high percentage (70–80%) of rod-shaped adult cardiomyocytes with clear striations and sharp outlines without visible vesicles were obtained with our method (Figure 2(a)).

3.2. $[Ca^{2+}]_i$ and Cell Viability Detection. We used Fluo-3 AM to examine Ca^{2+} mobilizations in cardiomyocytes. In Con group, the level of $[Ca^{2+}]_i$ was the lowest. Compared with Con, $[Ca^{2+}]_i$ increased significantly in A/R ($P < 0.05$). After the applying of DZ, $[Ca^{2+}]_i$ fluorescence decreased dramatically ($P < 0.05$) compared with A/R while there was an apparent increase ($P < 0.05$) in DZ5HD compared with DZ (Figures 2(b) and 2(c)). It indicated that DZ strongly inhibited the $[Ca^{2+}]_i$ levels in adult rat cardiomyocytes.

Cardiomyocytes in A/R group possessed lower level of cell viability ($P < 0.05$) when compared with Con. DZ group contained higher level of cell viability ($P < 0.05$) when compared with A/R group, while DZ5HD group showed lower level of cell viability ($P < 0.05$) when compared with DZ group (Figure 2(d)).

3.3. Quality Evaluation of DGE Reads. A summary of the DGE reads and their mapping to the rat genome database is presented in Supplementary Table 1 available online at http://dx.doi.org/10.1155/2014/756576. For each group, more than 4.4 million clean reads were sequenced. Low-quality reads accounted for no more than 1.6% and modified Q30 bases rate no less than 97% in all the 12 libraries (Supplementary Table 1). Besides, perfect matched reads accounted for 60% and unique matched reads occupied more than 70% of all reads mapping to rat genome (Table 1), which revealed that the sample preparation and the sequencings were in perfect condition.

3.4. Sequencing Saturation Analysis. Samples with replicates of sequencing, sequencing saturation analysis can be performed to test whether the detected genes' percent increased with total reads number. As shown in Supplementary Figure 1, for 3 replicates of 4 groups, when the total tag number came to 3 million, the genes number started to level out. When the total tag number reached 4 million, gene number inclined to stabilization. It suggested that no more distinct genes would be identified when the total clean reads reached a certain number. For all of the 12 libraries, there were more than 4.4 million clean reads (Supplementary Table 1), which indicated that the deep sequencing results were comprehensive and saturated.

3.5. DEGs between Groups. All genes annotated to the rat genome (Supplementary Excel 1) were analyzed for an evidence of differential expression. A detailed description of DEGs between two groups was presented in Supplementary Excel 2 (Con versus A/R), Excel 3 (A/R versus DZ), and Excel 4 (DZ versus DZ5HD). Those genes were to some extent differentially expressed; they were considered significant with a Q value more than 0.8. A list of the top 10 DEGs between two groups was shown in Table 2. In these genes, *Mt-nd6*, *Acadl,* and *Idh2* are energy metabolism correlated and their expression status is listed in Table 3.

3.6. RT-qPCR Analysis. To confirm the DEGs revealed by the Illumina sequencing, 25 genes were randomly selected (Table 4) and assayed by SYBR green based RT-qPCR (Figure 3). Except *Cycs, Idh3B, Mgst3,* and *Pdk4*, 21 out of the 25 genes were expressed well in accordance with the results from Illumina sequencing (Table 4).

3.7. GO Enrichment Analysis. Ontology and term enrichment of DEGs in GO is listed in Figure 4. GO enrichment showed many of the DEGs from Con versus A/R (Figure 4(a)), A/R versus DZ (Figure 4(b)), and DZ versus DZ5HD (Figure 4(c)) participating in the Biological Process ontology. Histogram presentation of Gene Ontology functional classification and DEGs' enrichment is shown in Figures 4(d)–4(f) ((d) Con versus A/R; (e) A/R versus DZ; (f) DZ versus DZ5HD). The significantly enriched (corrected $P < 0.05$) terms for Con versus A/R (Supplementary Table 2), A/R versus DZ (Supplementary Table 3), and DZ versus DZ5HD (Supplementary Table 4) also listed.

3.8. Pathway Analysis. KEGG Pathway provides an indication of the main biochemical and signal transduction pathways that DEGs are involved in. Pathway enrichment for Con versus A/R, A/R versus DZ, and DZ versus DZ5HD were displayed in Supplementary Tables 5–7. For Con versus A/R, A/R versus DZ, and DZ versus DZ5HD, there were 40, 48, and 37 pathways highly enriched ($P < 0.01$, $Q < 0.05$), respectively.

In all the pathways, Metabolic Process was the DEGs most enriched one. It is not difficult to notice that many energy metabolism correlated pathways, such as fatty acid

Table 1: Summary of DGE profile and reads' mapping to the rat genome.

Library number	Total reads (%)	Total base pair (%)	Total mapped reads (%)	Perfect match (%)	≤2 bp mismatch (%)	Unique match (%)	Multiposition match (%)	Total unmapped reads (%)
Con-1	4350000, 100%	213120000, 100%	3690000, 84.92%	2690000, 61.92%	1000000, 23.00%	3470000, 79.81%	220000, 5.10%	650000, 15.08%
Con-2	5180000, 100%	253940000, 100%	4130000, 79.86%	3110000, 60.19%	1010000, 19.66%	3750000, 72.47%	380000, 7.38%	1040000, 20.14%
Con-3	4760000, 100%	233230000, 100%	3890000, 81.74%	2840000, 59.76%	1040000, 21.98%	3550000, 74.67%	330000, 7.07%	860000, 18.26%
A/R-1	5310000, 100%	260380000, 100%	4280000, 80.55%	3250000, 61.34%	1020000, 19.21%	3890000, 73.21%	390000, 7.34%	1030000, 19.45%
A/R-2	4600000, 100%	225450000, 100%	3760000, 81.85%	2800000, 61.07%	950000, 20.78%	3440000, 74.81%	320000, 7.03%	830000, 18.15%
A/R-3	5040000, 100%	246860000, 100%	4180000, 83.12%	3050000, 60.64%	1130000, 22.48%	3810000, 75.66%	370000, 7.46%	850000, 16.88%
DZ-1	5110000, 100%	250260000, 100%	4200000, 82.42%	3180000, 62.28%	1020000, 20.15%	3860000, 75.71%	340000, 6.72%	890000, 17.58%
DZ-2	5010000, 100%	245250000, 100%	4080000, 81.52%	3050000, 60.94%	1030000, 20.58%	3720000, 74.32%	360000, 7.20%	920000, 18.48%
DZ-3	4900000, 100%	240220000, 100%	4060000, 82.84%	2980000, 60.93%	1070000, 21.91%	3680000, 75.09%	380000, 7.76%	840000, 17.16%
DZ5HD-1	4900000, 100%	240100000, 100%	3940000, 80.58%	2960000, 60.58%	980000, 20.01%	3620000, 73.89%	320000, 6.69%	950000, 19.42%
DZ5HD-2	4720000, 100%	231050000, 100%	3770000, 80.12%	2860000, 60.80%	910000, 19.32%	3390000, 71.96%	380000, 8.16%	930000, 19.88%
DZ5HD-3	4470000, 100%	218750000, 100%	3670000, 82.37%	2680000, 60.21%	980000, 22.16%	3350000, 75.16%	320000, 7.21%	780000, 17.63%

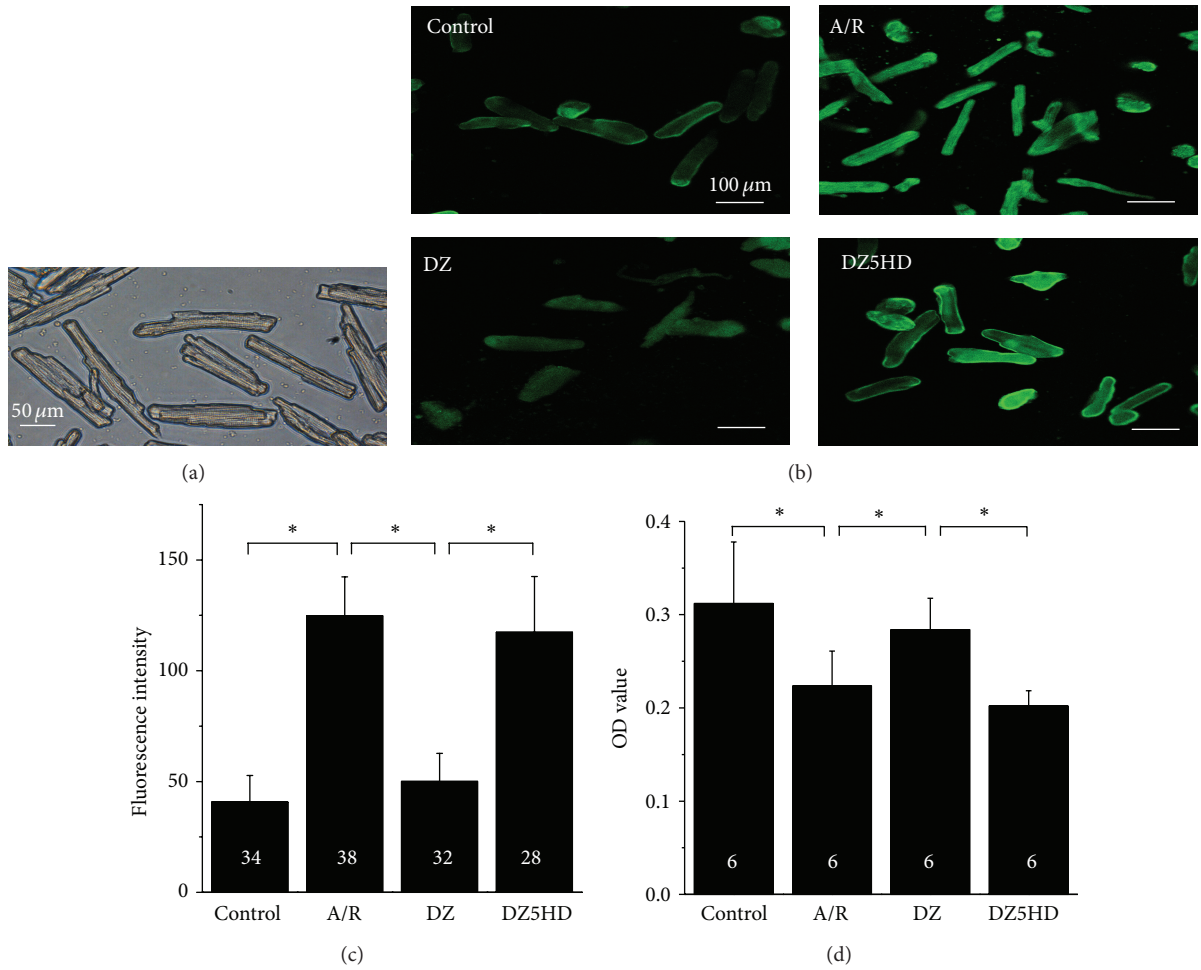

Figure 2: Adult rat cardiomyocytes and their status tests after mitoK$_{ATP}$ opening. (a) Light microscopic morphology of freshly isolated adult cardiomyocytes. They were rod-shaped, with sharp outlines and clear cross striations. (b-c) The effect of DZ and 5HD on the $[Ca^{2+}]_i$ in adult rat cardiomyocytes. At the end point of reoxygenation, cells of Con, A/R, DZ, and DZ5HD group were pretreated with 10 μM Fluo-3-AM and incubated for 60 min at 37°C and measured with a confocal laser microscope. (b) The $[Ca^{2+}]_i$ fluorescence image of cardiomyocytes in four groups. (c) The $[Ca^{2+}]_i$ fluorescence intensity comparison. $[Ca^{2+}]_i$ in A/R group was increased compared with the Con. Applying of DZ reduced the fluorescence intensity. After 5-HD administration, fluorescence intensity increased. (d) Cell viability test with CCK-8 kit. At the end point of reoxygenation, 30 μL CCK-8 was added into M199 to form a 3% CCK-8 resulting solution. Cells were incubated for 1 h before the mixture's OD value was detected at 450 nm. Cardiomyocytes of A/R group possessed lower level of cell viability when compared with Con. DZ group contained higher level of cell viability when compared with A/R group. Cells in DZ5HD showed the lowest level of cell viability in the 4 groups. Data are mean ± SD. Replication number for each group is marked on the columns. $^*P < 0.05$.

Table 2: Top 10 DEGs from Con versus A/R, A/R versus DZ, and DZ versus DZ5HD.

Number	Con versus A/R			A/R versus DZ			DZ versus DZ5HD		
	Gene name	$\log_2^{\text{Ratio (A/R/Con)}}$	Q value	Gene name	$\log_2^{\text{Ratio (DZ/A/R)}}$	Q value	Gene name	$\log_2^{\text{Ratio (DZ5HD/DZ)}}$	Q value
1	Pdlim2	4.95	0.84	Idh2	5.02	0.95	Ivd	4.22	0.92
2	MT-ND6	−4.94	0.94	Oxct1	4.92	0.95	MT-ND6	−3.95	0.91
3	Aldh1a7	−4.92	0.82	Acadl	4.87	0.94	Atf4	3.92	0.91
4	Idh2	−4.83	0.94	Mdh1	4.84	0.94	Ldhb	−3.85	0.91
5	Uba52	−4.71	0.93	Mdh2	4.73	0.94	Clu	3.84	0.90
6	Mdh2	−4.68	0.93	Aldh16a1	4.67	0.86	Idh2	−3.75	0.90
7	Podnl1	−4.65	0.80	Podnl1	4.61	0.83	Ankrd1	3.74	0.90
8	Mdh1	−4.63	0.93	Omg	4.60	0.82	Podnl1	−3.73	0.80
9	RGD1311224	−4.59	0.81	MT-ND6	4.56	0.93	Acadl	−3.69	0.90
10	Acadl	−4.58	0.93	Uba52	4.56	0.93	RGD1311224	−3.66	0.81

Table 3: Three energy metabolism related DEGs.

Gene name	Gene description	Con versus A/R		A/R versus DZ		DZ versus DZ5HD	
		$\log_2^{\text{Ratio (A/R/Con)}}$	Q value	$\log_2^{\text{Ratio (DZ/A/R)}}$	Q value	$\log_2^{\text{Ratio (DZ5HD/DZ)}}$	Q value
MT-ND6	NADH dehydrogenase subunit 6 (mitochondrion)	−4.94	0.94	4.56	0.93	−3.95	0.91
Idh2	Isocitrate dehydrogenase 2 (NADP+), mitochondrial	−4.83	0.94	5.02	0.95	−3.75	0.90
Acadl	Acyl-CoA dehydrogenase, long chain	−4.58	0.93	4.87	0.94	−3.69	0.90

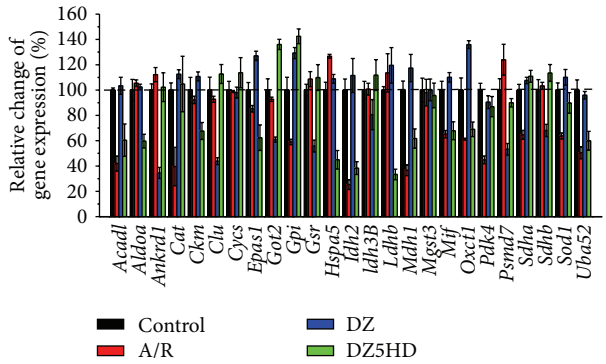

Figure 3: Validating DGE outcomes with RT-qPCR. 25 genes were randomly selected and RT-qPCR tests were carried out. Except *Cycs, Idh3B, Mgst3,* and *Pdk4*, all of the genes' expression was well in accordance with the results from Illumina sequencing (Table 4). Data are mean ± SD. All experiments were done in triplicate.

metabolism pathway, TCA cycle, proteasome, PPAR signaling pathway, and peroxisome pathway were highly enriched (Table 5).

3.9. ATP Detection. At the end of reoxygenation, the ATP levels of the A/R groups were much lower than Con ($P < 0.05$); ATP concentrations of DZ groups were much higher than A/R groups ($P < 0.05$). When 5-HD was applied, the beneficial effect of DZ was abolished in DZ5HD when compared with DZ ($P < 0.05$) (Figure 5).

4. Discussion

MIRI is always one of the leading causes of morbidity. *In vitro* experimental A/R model is a powerful tool to mimic *in vivo* ischemia-reperfusion injury. We developed an A/R model using freshly isolated adult rat cardiomyocytes, which are more relevant to the *in vivo* IR conditions.

In present study, DGE and bioinformatics technologies were employed to analyse molecular change after A/R and mitoK$_{ATP}$ opening. Our results demonstrated not only the robustness of next-generation sequencing in exploring the molecular change resulting from mitoK$_{ATP}$ opening but also the potential of the combine of next-generation sequencing and KEGG Pathway analysis to provide clues into target finding of molecular mechanisms underlying the myocardium protective effect of mitoK$_{ATP}$.

MitoK$_{ATP}$ opening or closing in cultured adult rat cardiomyocytes significantly resulted in gene expression change. Many of the genes were energy related. Metabolic Process was the DEGs most enriched GO ontology and energy metabolism correlated pathways were highly enriched too. We could not help doubting that mitoK$_{ATP}$ might have interfered with the energy metabolism and we confirmed that by directly measuring ATP content of four groups at the end of reoxygenation.

Three energy metabolism correlated genes, *Mt-nd6*, *Idh2,* and *Acadl,* were all upregulated (A/R versus DZ). *Mt-nd6* encodes NADH-quinone oxidoreductase (complex I) subunit 6 in mammal. In the respiratory chain, complex I is responsible for the oxidation of NADH and contributes to the formation of the proton gradient which drives ATP synthesis and passes electrons to ubiquinone [31]. Ischemia-reperfusion injury was characterized by decreased complex I respiration [32]. In this study, expression of *Mt-nd6* decreased after A/R treatment, while it was upregulated tremendously in DZ compared with A/R. Complex I is extremely susceptible to oxidative damage and subsequently produces more ROS [33], leading to extensive mitochondrial dysfunction and the depletion of ATP. MitoK$_{ATP}$ opening by DZ increased *Mt-nd6* expression, which might have contributed to ATP synthesis and resulted in its myocardial protection.

Idh2 encodes isocitrate dehydrogenase in mitochondria. In present study, expression of *Idh2* varyed: Con versus A/R downregulated; A/R versus DZ upregulated; DZ versus DZ5HD downregulated. Isocitrate dehydrogenase is the rate-limiting enzyme of TCA cycle, which catalyzes the oxidative decarboxylation of isocitrate to 2-oxoglutarate. Isocitrate dehydrogenase plays a role in intermediary metabolism and energy production. It had been reported that isocitrate dehydrogenase activity increased at the ischemia region when heart underwent ischemia [34, 35]; the authors deemed the increase that came from the increased need of energy.

Long Chain Acyl-CoA Dehydrogenase (*Acadl*) encodes long chain acyl-CoA dehydrogenase, which catalyzes the α- and β-dehydrogenation of acyl-CoA esters in fatty acid metabolism. It is the first rate-limiting enzyme in fatty acid β-oxidation reaction [36]. In present study, *Acadl* was downregulated after A/R, upregulated when mitoK$_{ATP}$ opened, and downregulated again when mitoK$_{ATP}$ was blocked by 5-HD. In physiological state, 60–70% of the total energy the heart needs comes from fatty acid β-oxidation [37]. In the ischemic condition, FAO is more indispensable. Ito et al. [38] demonstrated that high levels of fatty acids in the

Table 4: Genes selected for RT-qPCR confirmation.

Gene name	Primer sequences (5′ to 3′)		Reads number (RPKM, mean from 3 sequencings)			
	Forward	Reverse	Con	A/R	DZ	DZ5HD
Acadl	GGAATGAAAGCCCAGGACACAG	TCAAACATGAACTCACAGGCAGAAA	421.61	17.57	515.82	39.71
Aldoa	GGTGGTGTTGTGGGCATTAAGGT	ATGGCGAGGGACGAGGGAGTA	1171.38	1358.29	1300.62	121.90
Ankrd1	AAAATCAGTGCCCGAGACAAGC	ACCGAAGGTCATCAAGAGCCG	2875.32	3262.76	215.95	2890.14
Cat	GGCACACTTTGACAGAGAGCGG	CTGTGGAGAATCGGACGGCA	143.64	11.32	149.61	152.13
Ckm	AACCCACAGACAAGCATAAGACC	CTTCCACGGACAGCTTCTCTACA	862.02	929.51	903.35	139.07
Clu	ACTCAGAAGTCCCCTCTCGTGT	TTTCCTGCGGTATTCCTGTAGC	1009.00	1068.16	73.26	1050.66
Cycs	AAGCATAAGACTGGACCAAACCTC	GTGATACCTTTGTTCTTGTTGGCAT	230.49	289.74	129.06	283.52
Epas1	ACCTTCCCAGCCACCATCTACC	ACTTGCCACTCCTGACCCCTTT	10.16	10.53	10.68	1.89
Got2	GGGACTGGCTGATTTTTGTAAGG	CAGAAAGACATCTCGGCTGAACT	241.93	277.84	54.72	275.22
Gpi	ACCCAGGAGACCATCACCAAC	CTACCCAATCCCAGAACTCGAAC	137.57	10.77	146.16	141.82
Gsr	GTTGTGTTTTTCTTGCTTTGGC	GGAGGATTCTGAGTTGTTTGAGG	15.80	21.76	4.91	22.58
Hspa5	ACACTTGGTATTGAAACTGTGGGAG	CTTGATTGTTACGGTGGGCTG	132.59	171.78	157.12	27.08
Idh2	CCCATCACCATTGGCAGACAC	CCTCCGGCAGGGAAGTTATACA	718.92	25.15	816.33	60.47
Idh3B	ATTCGAGAACAGACAGAAGGGGAGT	CTCTGAGACTTGGTTCGAGTGACG	170.23	210.25	28.79	205.45
Ldhb	ACCAGAAGCTGAAGGACGATGAG	TGACCTACGTACAAGGCCGAAGA	1337.06	1599.30	1535.85	106.07
Mdh1	TCTCCTCCGCATGACTACACAG	TAGATCGCAGCACTAACAACGT	445.93	17.92	513.76	130.68
Mgst3	AAAGCCCGCAAGAAGTACAAGGT	CACGGTTAGGAAGAATAGGAAGGG	175.29	183.50	178.22	75.55
Mif	TATTACGACATGAACGCAGCCAA	TCAAACCATTTATTTCTCCCGACC	75.60	19.21	82.05	22.40
Oxct1	ATTGTAGACATTGGCTCGTTTGCTC	TTGGCTTTTCCTTCACCTTCCTTT	224.68	10.00	303.23	43.54
Pdk4	CAAGTCAGCCTTCAAACATTATCA	AAACAAGAGTCCACACACATTCA	184.97	14.36	193.38	32.08
Psmd7	AAGAGCGATGCGAAGAAAGAGGA	AAGGGTGACCAGGGCAGAGAG	74.87	82.47	13.07	59.27
Sdha	CTCTTTCCTACCCGCTCACATAC	TGTCATAGAAATGCCATCTCCAG	209.87	17.69	263.44	254.47
Sdhb	TCAACGGAGGCAACACGCT	GCATAGAAGTTACTCAAGTCAGGGA	378.70	425.40	36.17	419.09
Sod1	GGCTTCTGTCGTCTCCTTGCTT	CTGGTTCACCGCTTGCCTTCT	186.25	21.37	199.90	198.85
Uba52	ACCCTGTCCGACTACAACATCCA	TGTACTTCTGGGCAAGCTGACGA	618.42	23.57	556.13	51.39

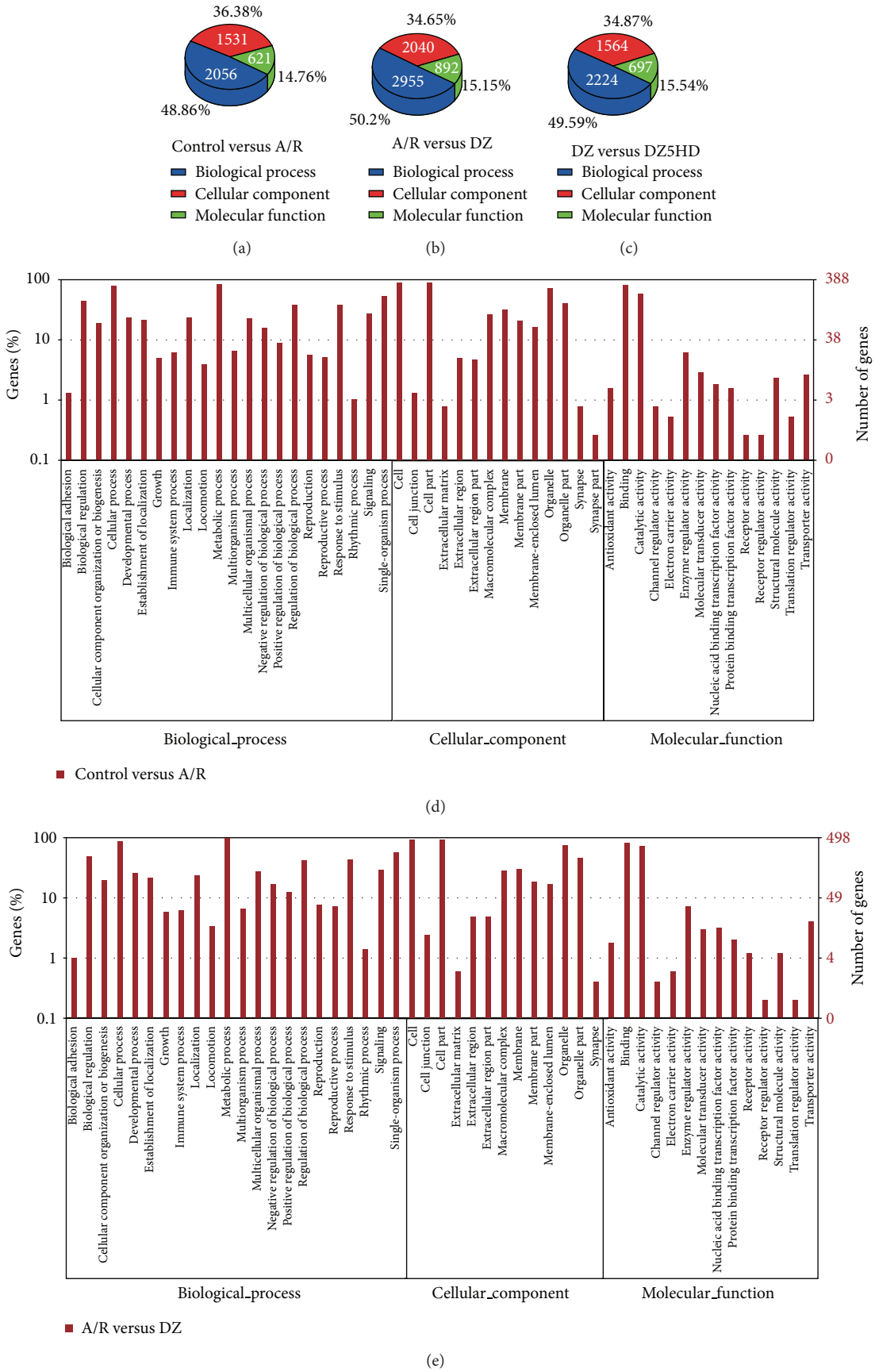

Figure 4: Continued.

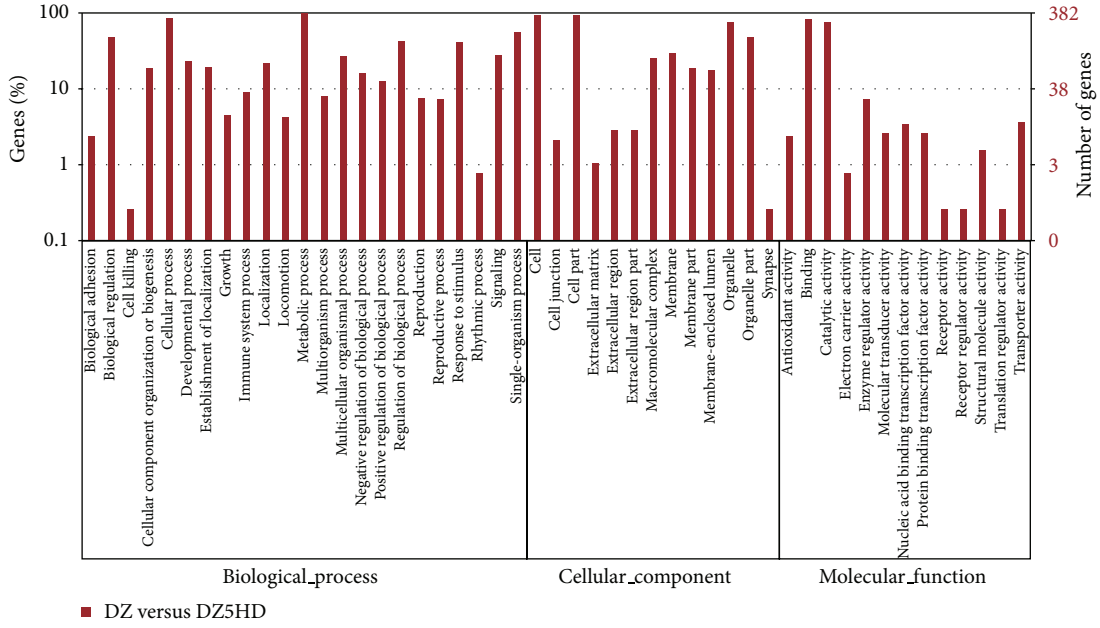

(f)

Figure 4: Ontology and term enrichment of DEGs in Gene Ontology. (a–c): Ontology enrichment for Con versus A/R, A/R versus DZ, and DZ versus DZ5HD. Most of the DEGs from Con versus A/R (2056 DEGs, 48.86%), A/R versus DZ (2955, 50.2%), and DZ versus DZ5HD (2224, 49.59%) participated in the Biological Process ontology. (d–f): Histogram presentation of Gene Ontology functional classification and DEGs' enrichment ((d) Con versus A/R; (e) A/R versus DZ; (f) DZ versus DZ5HD). The results are summarized in three main categories: Biological Process, Cellular Component, and Molecular Function. The y-axis on the right is the number of DEGs in a category. The y-axis on the left is the percentage of a specific category of genes in the main category. For significantly enriched terms (Con versus A/R, A/R versus DZ, and DZ versus DZ5HD), see Supplementary Tables 2–4.

perfusate were capable of enhancing postischemic energy production and increasing contractile function. That study provided evidence that, in heart with limited oxidative capacity, increasing exogenous energy substrate supply and boosting FAO generated more ATP and quickly normalized energy production. From what is mentioned above, mitoK_{ATP} opening may alleviate the energy depletion when adult cardiomyocytes underwent A/R injury by boosting the fatty acid β-oxidation.

6 energy correlated pathways, Peroxisome pathway, PPAR signaling pathway, citrate cycle (TCA cycle) pathway, fatty acid metabolism pathway, and proteasome pathway were DEGs significantly enriched ($P < 0.01$).

TCA cycle and fatty acid metabolism directly generate energy. 7 DEGs from Con versus A/R were enriched in TCA cycle pathway. They were all downregulated after A/R injury. When mitoK_{ATP} was open, all of them were upregulated. It is obvious that A/R suppressed TCA cycle. This could be one of the reasons why A/R decreased ATP content. We could see that DZ saved TCA cycle. 8 DEGs from Con versus A/R and 14 DEGs from A/R versus DZ, including *Acadl*, were enriched in fatty acid metabolism pathway. It seemed that A/R suppressed these two pathways and mitoK_{ATP} reinforced them.

Peroxisome proliferator-activated receptors (PPARs), especially PPAR-α, are sensitive to fatty acids and their derivatives. They are also ligand-activated transcription factors regulating cardiac FAO and energy homeostasis [39, 40]. PPAR-α is expressed highly in the heart and evidence had showed that PPAR-α was involved in the regulation of numerous genes encoding FAO enzymes [41]. Overexpression of PPAR-α and its target metabolic genes promoted FAO as a source of energy under conditions of acute IR [42, 43]. Besides its well-known action on cardiac energy metabolism and lipid homeostasis, emerging evidence indicated that administration of PPAR-α synthetic ligands was myocardial protective in an IR setting, as manifested by improved postischemic recovery of contractile function and reduced infarct size in both *in vivo* and *ex vivo* models [42, 44]. Mice overexpressing PPAR-α in heart displayed increased FAO rates, accumulated triacylglycerides, and decreased glucose metabolism, and they eventually developed cardiomyopathy [45, 46]. Not surprisingly, mice lacking PPAR-α had elevated free fatty acid levels as a consequence of inadequate FAO, rendering them hypoglycemic as a result of their reliance on glucose [47]. In present study, although PPAR-α gene did not change after mitoK_{ATP} opening, 17 DEGs from A/R versus DZ were enriched in peroxisome pathway ($P = 1.3 \times 10^{-7}$) and 16 DEGs significantly enriched in PPAR signaling pathway ($P = 9.9 \times 10^{-7}$). 12 DEGs from DZ versus DZ5HD were enriched in ($P = 1.1 \times 10^{-6}$) peroxisome pathway and 14 enriched in PPAR signaling pathway ($P = 2.4 \times 10^{-5}$). Nevertheless, to test the

Table 5: DEGs highly enriched and energy related pathways.

Pathway name[a]	Pathway ID	Con versus A/R			A/R versus DZ			DZ versus DZ5HD		
		DEGs with pathway annotation (335)	*P* value[b]	*Q* value[c]	DEGs with pathway annotation (467)	*P* value[b]	*Q* value[c]	DEGs with pathway annotation (361)	*P* value[b]	*Q* value[c]
Proteasome	ko03050	14 (4.18%)	$1.605768e-11$	$1.686056e-09$	20 (4.28%)	$2.141436e-16$	$2.323458e-14$	16 (4.43%)	$1.912420e-13$	$2.055852e-11$
Fatty acid metabolism	ko00071	8 (2.39%)	$4.058827e-05$	$6.556567e-04$	14 (3%)	$2.210798e-09$	$6.853474e-08$	9 (2.49%)	$9.205386e-06$	$2.199064e-04$
Peroxisome	ko04146	13 (3.88%)	$2.092966e-06$	$5.494036e-05$	17 (3.64%)	$1.297428e-07$	$2.815419e-06$	12 (3.32%)	$2.463547e-05$	$4.815115e-04$
PPAR signaling pathway	ko03320	14 (4.18%)	$4.72289e-07$	$1.653011e-05$	16 (3.43%)	$9.881599e-07$	$1.446076e-05$	14 (3.88%)	$1.150100e-06$	$4.121192e-05$
TCA cycle	ko00020	7 (2.09%)	$4.474838e-06$	$1.044129e-04$	14 (3%)	$1.954397e-13$	$1.060260e-11$	12 (3.32%)	$4.2606e-12$	$3.053430e-10$

[a] Pathway analysis based on KOBAS server 2.0 [21, 22].

[b] *P* value in hypergeometric test; $P < 0.01$ is considered as DGEs highly enriched.

[c] The *Q* value is similar to the well-known *P*- value, except it is a measure of significance in terms of the false discovery rate rather than the false positive rate [23].

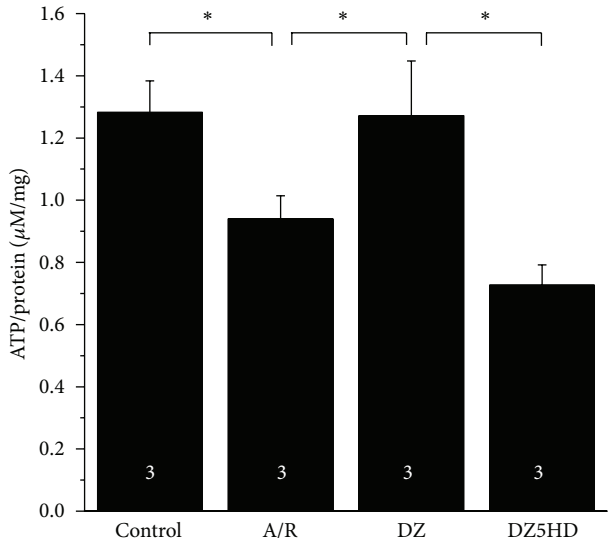

Figure 5: ATP quantitation. At the end of reoxygenation, ATP content was detected by HPLC at a detection wavelength of 254 nm. Protein content was also measured by using the same sample. ATP level of each sample was normalized to protein content of the same sample. Data are mean ± SD. $n = 3$ for each group. $^*P < 0.05$.

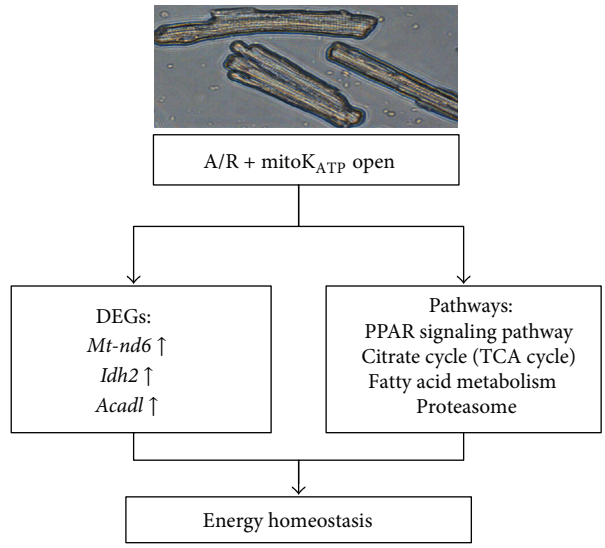

Figure 6: Scheme of the molecular myocardial protective mechanism of mitoK$_{ATP}$ in myocardial A/R setting. MitoK$_{ATP}$ opening-up regulated the expression of *Mt-nd6*, *Idh2,* and *Acadl*. In addition, mitoK$_{ATP}$ opening may recruit DEGs to regulate PPAR signaling pathway, TCA, fatty acid metabolism, and proteasome pathways. Eventually, mitoK$_{ATP}$ opening resulted in an energy homeostasis in the adult rat A/R cardiomyocytes.

relative activity change of PPAR-α after mitoK$_{ATP}$ opening, further studies are needed.

The ubiquitin proteasome system (UPS) degrades targeted abnormal and most normal proteins in cells. Most degradation via the UPS is ATP-dependent. This process involves ubiquitin ligases E1, E2, and E3, which function in concert with chaperones to identify and ubiquitinate appropriate target proteins [48–50]. Then the resulting polyubiquitinated proteins are transferred to the 26S proteasome, where they are degraded into peptides and ubiquitin. Proteasome pathway enriched 14 DEGs from Con versus A/R; 13 DEGs were downregulated in A/R group while 7 DEGs upregulated after mitoK$_{ATP}$ opening. It is obvious that A/R induced the downregulation of UPS and mitoK$_{ATP}$ opening reactivated it. Proteasome that functioned insufficiently had been observed most consistently in MIRI [51, 52]. Such studies supported the hypothesis that IR decreased proteasome activity by reducing ATP levels, as well as oxidative unfolding and damaging proteasome proteins [53]. To test this hypothesis, proteasome gain-of-function or loss-of-function studies in animal models of MIRI were carried out. However, the results showed a paradox: gain-of-function using transgenic mice with increased proteasome activity showed protection from MIRI [54], whereas loss-of-function studies using pharmacological means also revealed protection from MIRI [55–57]. In present study, 13 DEGs were downregulated after A/R (Con versus A/R); this should be a feedback of ATP depletion resulting from A/R. 7 DGEs were upregulated in DZ group (A/R versus DZ); this could be a consequence of ATP recovery after mitoK$_{ATP}$ opening.

Energy was so desperately needed in A/R environment that Metabolic Process was the most enriched GO ontology in Con versus A/R, A/R versus DZ, and DZ versus DZ5HD. In addition, energy metabolism related genes and pathways were significantly interfered with each other (Figure 6). UPS is protein related; TCA cycle pathway controls aerobic metabolism of glucose, PPAR-α, and Acadl effect on β-dehydrogenation of acyl-CoA esters in FAO. To sum up, mitoK$_{ATP}$ regulated the metabolism of 3 main nutriments: glucose, fatty acid, and protein and kept a balance between energy production and consumption at the setting of A/R in adult cardiomyocytes. Strategies to increase energy supply in MIRI may be a good choice. Metabolism correlated genes and pathway nodes may be promising therapeutic targets. At the same time, we must confess that, to assure the effects of specific gene and signaling pathway mentioned above in MIRI, further gain- or/and loss-of-function studies will be needed.

Conflict of Interests

The authors declare that there is no conflict of interests regarding the publication of this paper.

Authors' Contribution

Song Cao and Yun Liu contributed equally to this study.

Acknowledgment

This work was supported by grants from Special Scientific Research Fund for Public Welfare, Ministry of Health of China (Grant no. 200802173).

References

[1] R. Bolli, "Preconditioning: a paradigm shift in the biology of myocardial ischemia," *The American Journal of Physiology—Heart and Circulatory Physiology*, vol. 292, no. 1, pp. H19–H27, 2007.

[2] C. E. Murry, R. B. Jennings, and K. A. Reimer, "Preconditioning with ischemia: a delay of lethal cell injury in ischemic myocardium," *Circulation*, vol. 74, no. 5, pp. 1124–1136, 1986.

[3] C. E. Murry, V. J. Richard, K. A. Reimer, and R. B. Jennings, "Ischemic preconditioning slows energy metabolism and delays ultrastructural damage during a sustained ischemic episode," *Circulation Research*, vol. 66, no. 4, pp. 913–931, 1990.

[4] I. Inoue, H. Nagase, K. Kishi, and T. Higuti, "ATP-sensitive K^+ channel in the mitochondrial inner membrane," *Nature*, vol. 352, no. 6332, pp. 244–247, 1991.

[5] K. D. Garlid, P. Paucek, V. Yarov-Yarovoy et al., "Cardioprotective effect of diazoxide and its interaction with mitochondrial ATP-sensitive K^+ channels: possible mechanism of cardioprotection," *Circulation Research*, vol. 81, no. 6, pp. 1072–1082, 1997.

[6] Y. Liu, T. Sato, B. O'Rourke, and E. Marban, "Mitochondrial ATP-dependent potassium channels: novel effectors of cardioprotection?" *Circulation*, vol. 97, no. 24, pp. 2463–2469, 1998.

[7] K. D. Garlid, P. Paucek, V. Yarov-Yarovoy, X. Sun, and P. A. Schindler, "The mitochondrial K_{ATP} channel as a receptor for potassium channel openers," *The Journal of Biological Chemistry*, vol. 271, no. 15, pp. 8796–8799, 1996.

[8] G. J. Gross, "ATP-sensitive potassium channels and myocardial preconditioning," *Basic Research in Cardiology*, vol. 90, no. 2, pp. 85–88, 1995.

[9] X.-M. Yang, J. B. Proctor, L. Cui, T. Krieg, J. M. Downey, and M. V. Cohen, "Multiple, brief coronary occlusions during early reperfusion protect rabbit hearts by targeting cell signaling pathways," *Journal of the American College of Cardiology*, vol. 44, no. 5, pp. 1103–1110, 2004.

[10] M. Donato, V. D'Annunzio, G. Berg et al., "Ischemic postconditioning reduces infarct size by activation of A1 receptors and K+ATP channels in both normal and hypercholesterolemic rabbits," *Journal of Cardiovascular Pharmacology*, vol. 49, no. 5, pp. 287–292, 2007.

[11] J. Mykytenko, J. G. Reeves, H. Kin et al., "Persistent beneficial effect of postconditioning against infarct size: role of mitochondrial K_{ATP} channels during reperfusion," *Basic Research in Cardiology*, vol. 103, no. 5, pp. 472–484, 2008.

[12] L. Yang and T. Yu, "Prolonged donor heart preservation with pinacidil: the role of mitochondria and the mitochondrial adenosine triphosphate-sensitive potassium channel," *Journal of Thoracic and Cardiovascular Surgery*, vol. 139, no. 4, pp. 1057–1063, 2010.

[13] T. Yu, X.-Y. Fu, X.-K. Liu, and Z.-H. Yu, "Protective effects of pinacidil hyperpolarizing cardioplegia on myocardial ischemia reperfusion injury by mitochondrial KATP channels," *Chinese Medical Journal*, vol. 124, no. 24, pp. 4205–4210, 2011.

[14] T. Yu, Z. Yu, X. Liu, S. Yang, and Y. Ye, "Myocardial protection with pinacidil induced hyperpolarized arrest during cardiopulmonary bypass," *Chinese Medical Journal*, vol. 114, no. 12, pp. 1245–1248, 2001.

[15] A. P. Halestrap, "The regulation of the matrix volume of mammalian mitochondria in vivo and in vitro and its role in the control of mitochondrial metabolism," *Biochimica et Biophysica Acta (BBA)-Bioenergetics*, vol. 973, no. 3, pp. 355–382, 1989.

[16] E. Belisle and A. J. Kowaltowski, "Opening of mitochondrial K^+ channels increases ischemic ATP levels by preventing hydrolysis," *Journal of Bioenergetics and Biomembranes*, vol. 34, no. 4, pp. 285–298, 2002.

[17] P. P. Dzeja, P. Bast, C. Ozcan et al., "Targeting nucleotide-requiring enzymes: implications for diazoxide-induced cardioprotection," *The American Journal of Physiology—Heart and Circulatory Physiology*, vol. 284, no. 4, pp. H1048–H1056, 2003.

[18] E. A. Konorev, S. Vanamala, and B. Kalyanaraman, "Differences in doxorubicin-induced apoptotic signaling in adult and immature cardiomyocytes," *Free Radical Biology and Medicine*, vol. 45, no. 12, pp. 1723–1728, 2008.

[19] E. Riva and D. J. Hearse, "Age-dependent changes in myocardial susceptibility to ischemic injury," *Cardioscience*, vol. 4, no. 2, pp. 85–92, 1993.

[20] I. Ostadalova, B. Ostadal, F. Kolář, J. R. Parratt, and S. Wilson, "Tolerance to ischaemia and ischaemic preconditioning in neonatal rat heart," *Journal of Molecular and Cellular Cardiology*, vol. 30, no. 4, pp. 857–865, 1998.

[21] C. Xie, X. Mao, J. Huang et al., "KOBAS 2.0: a web server for annotation and identification of enriched pathways and diseases," *Nucleic Acids Research*, vol. 39, no. 2, pp. W316–W322, 2011.

[22] J. Wu, X. Mao, T. Cai, J. Luo, and L. Wei, "KOBAS server: a web-based platform for automated annotation and pathway identification," *Nucleic Acids Research*, vol. 34, pp. W720–W724, 2006.

[23] J. D. Storey and R. Tibshirani, "Statistical significance for genomewide studies," *Proceedings of the National Academy of Sciences of the United States of America*, vol. 100, no. 16, pp. 9440–9445, 2003.

[24] M.-J. Son, H. K. Kim, D. T. Thu Huong et al., "Chrysosplenol C increases contraction in rat ventricular myocytes," *Journal of Cardiovascular Pharmacology*, vol. 57, no. 2, pp. 259–262, 2011.

[25] W.-H. Zhang, S.-B. Fu, F.-H. Lu et al., "Involvement of calcium-sensing receptor in ischemia/reperfusion-induced apoptosis in rat cardiomyocytes," *Biochemical and Biophysical Research Communications*, vol. 347, no. 4, pp. 872–881, 2006.

[26] L.-D. Tang, X.-M. Wang, F.-L. Jin, B.-L. Qiu, J.-H. Wu, and S.-X. Ren, "*De novo* sequencing-based transcriptome and digital gene expression analysis reveals insecticide resistance-relevant genes in *Propylaea japonica* (Thunberg) (Coleoptea: Coccinellidae)," *PLoS ONE*, vol. 9, no. 6, p. e100946, 2014.

[27] A. Mortazavi, B. A. Williams, K. McCue, L. Schaeffer, and B. Wold, "Mapping and quantifying mammalian transcriptomes by RNA-Seq," *Nature Methods*, vol. 5, no. 7, pp. 621–628, 2008.

[28] S. Tarazona, F. García-Alcalde, J. Dopazo, A. Ferrer, and A. Conesa, "Differential expression in RNA-seq: a matter of depth," *Genome Research*, vol. 21, no. 12, pp. 2213–2223, 2011.

[29] J. Durban, A. Pérez, L. Sanz et al., "Integrated "omics" profiling indicates that miRNAs are modulators of the ontogenetic venom composition shift in the Central American rattlesnake, *Crotalus simus simus*," *BMC Genomics*, vol. 14, article 234, 2013.

[30] Q. Tu, R. A. Cameron, K. C. Worley, R. A. Gibbs, and E. H. Davidson, "Gene structure in the sea urchin *Strongylocentrotus purpuratus* based on transcriptome analysis," *Genome Research*, vol. 22, no. 10, pp. 2079–2087, 2012.

[31] J. E. Walker, "The NADH: ubiquinone oxidoreductase (complex I) of respiratory chains," *Quarterly Reviews of Biophysics*, vol. 25, no. 3, pp. 253–324, 1992.

[32] G. Ambrosio, J. L. Zweier, and J. T. Flaherty, "The relationship between oxygen radical generation and impairment of myocardial energy metabolism following post-ischemic reperfusion," *Journal of Molecular and Cellular Cardiology*, vol. 23, no. 12, pp. 1359–1374, 1991.

[33] E. J. Lesnefsky, Q. Chen, S. Moghaddas, M. O. Hassan, B. Tandler, and C. L. Hoppel, "Blockade of electron transport during ischemia protects cardiac mitochondria," *Journal of Biological Chemistry*, vol. 279, no. 46, pp. 47961–47967, 2004.

[34] A. Prasad and A. A. Quyyumi, "Renin-angiotensin system and angiotensin receptor blockers in the metabolic syndrome," *Circulation*, vol. 110, no. 11, pp. 1507–1512, 2004.

[35] B. I. Jugdutt and G. Sawicki, "AT1receptor blockade alters metabolic, functional and structural proteins after reperfused myocardial infarction: detection using proteomics," *Molecular and Cellular Biochemistry*, vol. 263, no. 1, pp. 179–188, 2004.

[36] K. Bartlett and S. Eaton, "Mitochondrial β-oxidation," *European Journal of Biochemistry*, vol. 271, no. 3, pp. 462–469, 2004.

[37] H. Bugger and E. D. Abel, "Molecular mechanisms for myocardial mitochondrial dysfunction in the metabolic syndrome," *Clinical Science*, vol. 114, no. 3-4, pp. 195–210, 2008.

[38] M. Ito, J. S. Jaswal, V. H. Lam et al., "High levels of fatty acids increase contractile function of neonatal rabbit hearts during reperfusion following ischemia," *American Journal of Physiology: Heart and Circulatory Physiology*, vol. 298, no. 5, pp. H1426–H1437, 2010.

[39] J. A. Madrazo and D. P. Kelly, "The PPAR trio: regulators of myocardial energy metabolism in health and disease," *Journal of Molecular and Cellular Cardiology*, vol. 44, no. 6, pp. 968–975, 2008.

[40] Q. Yang and Y. Li, "Roles of PPARs on regulating myocardial energy and lipid homeostasis," *Journal of Molecular Medicine*, vol. 85, no. 7, pp. 697–706, 2007.

[41] P. M. Barger and D. P. Kelly, "PPAR signaling in the control of cardiac energy metabolism," *Trends in Cardiovascular Medicine*, vol. 10, no. 6, pp. 238–245, 2000.

[42] T.-L. Yue, W. Bao, B. M. Jucker et al., "Activation of peroxisome proliferator-activated receptor-α protects the heart from ischemia/reperfusion injury," *Circulation*, vol. 108, no. 19, pp. 2393–2399, 2003.

[43] T. Ravingerová, S. Čarnická, M. Nemčeková et al., "PPAR-α activation as a preconditioning-like intervention in rats in vivo confers myocardial protection against acute ischaemia-reperfusion injury: involvement of PI3K-Akt," *Canadian Journal of Physiology and Pharmacology*, vol. 90, no. 8, pp. 1135–1144, 2012.

[44] N. S. Wayman, Y. Hattori, M. C. Mcdonald et al., "Ligands of the peroxisome proliferator-activated receptors (PPAR-γ and PPAR-α) reduce myocardial infarct size," *The FASEB Journal*, vol. 16, no. 9, pp. 1027–1040, 2002.

[45] B. N. Finck, X. Han, M. Courtois et al., "A critical role for PPARα-mediated lipotoxicity in the pathogenesis of diabetic cardiomyopathy: modulation by dietary fat content," *Proceedings of the National Academy of Sciences of the United States of America*, vol. 100, no. 3, pp. 1226–1231, 2003.

[46] B. N. Finck, J. J. Lehman, T. C. Leone et al., "The cardiac phenotype induced by PPARα overexpression mimics that caused by diabetes mellitus," *Journal of Clinical Investigation*, vol. 109, no. 1, pp. 121–130, 2002.

[47] M. Guerre-Millo, C. Rouault, P. Poulain et al., "PPAR-α-null mice are protected from high-fat diet-induced insulin resistance," *Diabetes*, vol. 50, no. 12, pp. 2809–2814, 2001.

[48] F. Kriegenburg, L. Ellgaard, and R. Hartmann-Petersen, "Molecular chaperones in targeting misfolded proteins for ubiquitin-dependent degradation," *FEBS Journal*, vol. 279, no. 4, pp. 532–542, 2012.

[49] X. Wang and J. Robbins, "Heart failure and protein quality control," *Circulation Research*, vol. 99, no. 12, pp. 1315–1328, 2006.

[50] M. S. Willis, W. H. D. Townley-Tilson, E. Y. Kang, J. W. Homeister, and C. Patterson, "Sent to destroy: the ubiquitin proteasome system regulates cell signaling and protein quality control in cardiovascular development and disease," *Circulation Research*, vol. 106, no. 3, pp. 463–478, 2010.

[51] A.-L. Bulteau, K. C. Lundberg, K. M. Humphries et al., "Oxidative modification and inactivation of the proteasome during coronary occlusion/reperfusion," *The Journal of Biological Chemistry*, vol. 276, no. 32, pp. 30057–30063, 2001.

[52] S. R. Powell, K. J. A. Davies, and A. Divald, "Optimal determination of heart tissue 26S-proteasome activity requires maximal stimulating ATP concentrations," *Journal of Molecular and Cellular Cardiology*, vol. 42, no. 1, pp. 265–269, 2007.

[53] X. Wang, J. Li, H. Zheng, H. Su, and S. R. Powell, "Proteasome functional insufficiency in cardiac pathogenesis," *American Journal of Physiology—Heart and Circulatory Physiology*, vol. 301, no. 6, pp. 2207–2219, 2011.

[54] J. Li, K. M. Horak, H. Su, A. Sanbe, J. Robbins, and X. Wang, "Enhancement of proteasomal function protects against cardiac proteinopathy and ischemia/reperfusion injury in mice," *The Journal of Clinical Investigation*, vol. 121, no. 9, pp. 3689–3700, 2011.

[55] B. Campbell, J. Adams, Y. K. Shin, and A. M. Lefer, "Cardioprotective effects of a novel proteasome inhibitor following ischemia and reperfusion in the isolated perfused rat heart," *Journal of Molecular and Cellular Cardiology*, vol. 31, no. 2, pp. 467–476, 1999.

[56] J. Pye, F. Ardeshirpour, A. McCain et al., "Proteasome inhibition ablates activation of NF-κB in myocardial reperfusion and reduces reperfusion injury," *The American Journal of Physiology—Heart and Circulatory Physiology*, vol. 284, no. 3, pp. H919–H926, 2003.

[57] W. E. Stansfield, N. C. Moss, M. S. Willis, R. Tang, and C. H. Selzman, "Proteasome inhibition attenuates infarct size and preserves cardiac function in a murine model of myocardial ischemia-reperfusion injury," *The Annals of Thoracic Surgery*, vol. 84, no. 1, pp. 120–125, 2007.

Hindawi Publishing Corporation
Oxidative Medicine and Cellular Longevity
Volume 2015, Article ID 352723, 12 pages
http://dx.doi.org/10.1155/2015/352723

Review Article

The Ambiguous Relationship of Oxidative Stress, Tau Hyperphosphorylation, and Autophagy Dysfunction in Alzheimer's Disease

Zhenzhen Liu,[1,2] Tao Li,[2] Ping Li,[2] Nannan Wei,[2] Zhiquan Zhao,[2] Huimin Liang,[2] Xinying Ji,[2] Wenwu Chen,[3,4] Mengzhou Xue,[3,4] and Jianshe Wei[1,2]

[1] *Institute of Neuroscience, Henan Polytechnic University, Jiaozuo 454000, China*
[2] *Laboratory of Brain Function and Molecular Neurodegeneration, Institute for Brain Science Research, School of Life Sciences, Henan University, Kaifeng 475004, China*
[3] *Department of Neurology, The First Affiliated Hospital, Henan University, Kaifeng 475000, China*
[4] *Institute of Neurological Disorder, Henan University, Kaifeng 475000, China*

Correspondence should be addressed to Mengzhou Xue; menzhouxue@gmail.com and Jianshe Wei; jswei@henu.edu.cn

Received 7 October 2014; Revised 2 March 2015; Accepted 3 March 2015

Academic Editor: Eugene A. Kiyatkin

Alzheimer's disease (AD) is the most common form of dementia. The pathological hallmarks of AD are amyloid plaques [aggregates of amyloid-beta (Aβ)] and neurofibrillary tangles (aggregates of tau). Growing evidence suggests that tau accumulation is pathologically more relevant to the development of neurodegeneration and cognitive decline in AD patients than Aβ plaques. Oxidative stress is a prominent early event in the pathogenesis of AD and is therefore believed to contribute to tau hyperphosphorylation. Several studies have shown that the autophagic pathway in neurons is important under physiological and pathological conditions. Therefore, this pathway plays a crucial role for the degradation of endogenous soluble tau. However, the relationship between oxidative stress, tau protein hyperphosphorylation, autophagy dysregulation, and neuronal cell death in AD remains unclear. Here, we review the latest progress in AD, with a special emphasis on oxidative stress, tau hyperphosphorylation, and autophagy. We also discuss the relationship of these three factors in AD.

1. Introduction

Alzheimer's disease (AD) is the most common form of dementia in the elderly and a chronic neurodegenerative disease characterized by widespread degeneration of neurons. An estimated 37 million people worldwide currently have AD, which is estimated to increase to 65.7 million by 2030 and 115.4 million by 2050 [1, 2]. AD is a growing health concern in society because patients suffer from progressive functional impairments, emotional distress, loss of independence, and behavioral deficits. It is characterized by the presence of two types of neuropathological hallmarks: senile plaques (SPs) and intracellular neurofibrillary tangles (NFTs). SPs predominantly consist of extracellular amyloid β-peptide (Aβ) deposits. NFTs are formed by intraneuronal aggregation of hyperphosphorylated tau. The amyloid cascade hypothesis theory proposes a dysregulation of amyloid precursor protein processing. This event leads to AD pathogenesis, which involves the aggregation of Aβ (particularly Aβ42), neuritic plaque formation, and consequently the formation of NFTs followed by the disruption of synaptic connections, neuronal death, and cognitive deficits (dementia) [3]. Increasing evidence suggests that Aβ oligomers (AβOs) may be the primary cause of AD because they have a greater correlation with dementia than insoluble Aβ42 [4]. These AβOs bind to a putative receptor and activate the receptor tyrosine kinase EphA4 and Fyn. AβOs binding triggers aberrant activation of NMDARs and abnormal increase in postsynaptic Ca^{2+}. The following events include increased generation of reactive oxygen species (ROS), and membrane lipid peroxidation; mitochondrial fragmentation, Ca^{2+} induced Ca^{2+} release

(CICR), then produces altered surface expression and dysregulation of receptor function, excitotoxicity, dendritic spine retraction, and elimination [4–6].

Aβ also plays a crucial role in inducing neuronal oxidative stress [7, 8]. Aβ-mediated mitochondrial oxidative stress causes hyperphosphorylation of tau in AD brains [8–10]. Mounting evidence clearly links tau to neurodegeneration, indicating that tau hyperphosphorylation may be the necessary point in neural dysfunction and death. However, whether autophagic dysfunction is involved in neuronal death during this event still remains unknown. Recent studies have indicated the importance of defective autophagy in the pathogenesis of aging and neurodegenerative diseases [11–14], especially in AD [15–17]. Autophagy may increase the formation of autophagosome in AD, and autophagic dysfunction may induce the pathogenesis of AD, particularly at the late stage of AD [18–22]. However, the relationship between oxidative stress, tau protein hyperphosphorylation, autophagic dysfunction, and neuronal cells death in AD remains elusive. In this review, we summarize the latest progress in research focused on oxidative stress, tau hyperphosphorylation, and autophagic dysfunction and their relationship with AD.

2. Oxidative Stress in AD

In experimental models and human brain studies of AD, oxidative stress has been shown to play an important role in neurodegeneration [10, 23, 24]. Generally, oxidative stress is caused by the imbalance between reactive oxygen species (ROS) (O_2^-, H_2O_2, HO_2, and ·OH) and the breakdown of chemically reactive species, by reducing agents and antioxidant enzymes, such as manganese superoxide dismutase (SOD_2) [25, 26]. This disequilibrium may result from disease, stressors, or environmental factors. High ROS levels lead to the accumulation of oxidized proteins, lipids, and nucleic acids, thereby directly impairing cellular function if not removed or neutralized [27]. Oxidative damage to cellular components is likely to result in the alteration of membrane properties, such as fluidity, ion transport, enzyme activities, protein cross-linking, and eventually cell death.

Oxidative stress has been reported to be one of the earliest events in AD. Several risk factors for AD may cause or promote oxidative damage, such as advanced age [28, 29] and apolipoprotein E (APOE) $\varepsilon 4$ alleles [30, 31]. Medical risk factors include traumatic brain injury [32], stroke [33], hypertension [34], diabetes mellitus [35], hypercholesterolemia [36], and hyperhomocysteinemia [37]. Environmental and lifestyle-related risk factors include aluminum exposure [38], smoking [39], high calorie intake [40], vitamin D deficiency [41], lack of exercise [42], and lack of intellectual activities [43–45]. Mitochondrial dysfunction is known to be associated with oxidative stress and thus may be an initial trigger for enhanced Aβ production during the aging process [46–48]. Both soluble and fibrillar Aβ may further accelerate oxidative stress, as well as mitochondrial dysfunction [49, 50]. The transgenic (Tg) Thy1-APP751 (SL) mouse model of AD shows increased proteolytic cleavage of APP, increased production of Aβ, and impaired Cu/Zn-SOD activity [51]. Furthermore, oxidative stress is considered as a primary factor of NFT formation in AD [10, 24, 52, 53]. However, the relationship between oxidative stress and tau hyperphosphorylation remains unclear. Okadaic acid is used as a research model to induce tau phosphorylation and neuronal death in AD. Oxidative stress combined with okadaic acid results in tau hyperphosphorylation [54]. Mitochondrial SOD_2 deficiency increases the levels of Ser396 phosphorylated tau in the Tg2576 mouse model of AD [55].

3. Tau Protein in AD

3.1. Tau Protein Physiology and Pathology. Tau protein (known as neuronal microtubule associated protein tau) plays a large role in the outgrowth of neuronal processes and the development of neuronal polarity [56–58]. Tau protein in the central nervous system is predominantly expressed in neurons [59, 60], with its main function to promote microtubule assembly, stabilize microtubules, affect the dynamics of microtubules in neurons [61, 62], and inhibit apoptosis [63], particularly in axons [64, 65]. However, recent reports suggest that excess intracellular tau is released into the extracellular culture medium via membrane vesicles [66]. In the adult human brain, tau consists of six isoforms, and the tau gene contains 16 exons. These isoforms are generated by alternative splicing of exons 2, 3, and 10 of its pre-mRNA [67, 68]. The six tau isoforms differ from each other by the presence or absence of one or two inserts (coded by exon 2 or exons 2 and 3) in the N-terminal part and the presence or absence of the second microtubule-binding repeat (encoded by exon 10) in the C-terminal portion. Depending on the alternative splicing of exon 10, tau isoforms are termed 4R (four microtubule-binding domains, with exon 10) or 3R (three microtubule-binding domains, without exon 10). Adult human brain expresses both 3R-tau and 4R-tau, whereas fetal human brain expresses only 3R-tau [69, 70]. Immunocytochemistry and biochemical analysis indicate that the ratio of 3R- to 4R-tau altered in AD and other neurodegenerative brain disorders [71–73], although in the normal adult human brain the level of 3R-tau is approximately equal to that of 4R-tau [74].

Tau protein normally stabilizes axonal microtubules in the cytoskeleton and plays a vital role in regulating the morphology of neurons. It has more than 30 phosphorylation sites. When tau is abnormally hyperphosphorylated, it destabilizes microtubules by decreasing the binding affinity of tau, affecting its axonal transport and resulting in its aggregation in NFTs [64]. NFTs are composed of paired helical filaments (PHF) of abnormally hyperphosphorylated tau. The pathogenesis of tau-mediated neurodegeneration is unclear but hyperphosphorylation, oligomerization, fibrillization, and propagation of tau pathology have been proposed as the likely pathological processes that induce the loss of function or gain of tau toxicity, which caused neurodegeneration [75]. Tau phosphorylation has been investigated at AD-related sites by using recombinant human tau phosphorylated by DNA damage-activated checkpoint kinase 1 (Chk1) and checkpoint kinase 2 (Chk2) in vitro [76]. This study identified a total of 27 Ser/Thr residues as Chk1 or Chk2 target sites. Among these sites, 13 have been identified

to be phosphorylated in AD brains [77]. The generation of a Tg mouse line overexpressing human tau441 via V337M and R406W tau mutations has been shown to accelerate the phosphorylation of human tau, inducing tau pathology and cognitive deficits [78]. Pseudophosphorylation of tau reduces microtubule interactions, disrupts the microtubule network, and exerts neurotoxicity [79]. Interestingly, doubly pseudophosphorylated tau proteins enhance microtubule assembly activity and are more potent at regulating dynamic instability [80]. However, four singly pseudophosphorylated tau proteins exhibit a loss of function at the same sites (Thr [231], Ser [262], Ser [396], and Ser [404]) [80].

3.2. Tau Protein Kinases and Phosphatase. Tau phosphorylation is mainly determined by a balance between the activation of various tau protein kinases and phosphatases and its disruption results in the abnormal phosphorylation of tau, which is observed in AD. Each tau site is phosphorylated by one or more protein kinases. Tau kinases are grouped into three classes: (1) proline-directed protein kinases (PDPK) containing glycogen synthase kinase-3 (GSK3), dual specificity tyrosine-phosphorylation-regulated kinase 1A/B (Dyrk1A/B), cyclin-dependent protein kinase-5 (CDK5), and mitogen activated protein kinases (MAPK) (e.g., p38, Erk1/2, and JNK1/2/3); (2) non-PDPK, including tau-tubulin kinase 1/2 (e.g., casein kinase $1\alpha/1\delta/1\varepsilon/2$), microtubule affinity regulating kinases, phosphorylase kinase, cAMP-dependent protein kinase A (PKA), PKB/AKT, protein kinase C, protein kinase N, and Ca^{2+}/calmodulin-dependent protein kinase II (CaM kinase II); and (3) tyrosine protein kinases, including Src family kinase (SFK) members (e.g., Src, Lck, Syk, and Fyn) and Abelson family kinase members, ABL1 and ABL2 (ARG).

GSK3 (particularly GSK3β) plays a key role in the pathogenesis of AD, contributing to Aβ production and Aβ-mediated neuronal death by phosphorylating tau in most serine and threonine residues and inducing hyperphosphorylation in paired helical filaments [81]. Inhibition of GSK3 prevents Aβ aggregation and tau hyperphosphorylation [82, 83]. The involvement of CDK5 in tau phosphorylation is shown by the increase in its enzymatic activity and the absence of MT-2 cells neurite retraction in the presence of roscovitine or CDK5 siRNA [84]. Therefore, CDK5 may be a key candidate target for therapeutic gene silencing [85]. p38 MAPK has been identified as one of the kinases involved in the regulation of tau phosphorylation. Thus, under pathological conditions this kinase is likely to play a role in the hyperphosphorylation of tau [86]. CDKs and casein kinase 1 (CK1) are involved in the aggregation of Aβ peptides (forming extracellular plaques) and hyperphosphorylation of tau (forming intracellular NFTs). The expression pattern of CKIδ (an isoform of CK1) plays an important role in tau aggregation in AD [87]. Ser214, Ser262, and Ser409 are major phosphorylation sites of tau that are affected by PKA [88]. In P19 cells stably expressing human tau441, CaM kinase II has been shown to be involved in retinoic acid- (RA-) induced tau phosphorylation-mediated apoptosis [89].

Phosphatases are also usually classified into three classes according to their amino acids sequences, the structure of their catalytic site, and their sensitivity to inhibitors. These groups include (1) phosphoprotein phosphatase (PPP), (2) metal-dependent protein phosphatase, and (3) protein tyrosine phosphatase (PTP). Tau phosphatases belong to the PPP group (protein phosphatase [PP] 1, PP2A, PP2B, and PP5) and PTP group tumor suppressor phosphatase and tensin homolog (PTEN). The activity of PP2A, PP1, PP5, and PP2B accounts for approximately 71%, 11%, 10%, and 7%, respectively, in the normal human brain. However, in the AD brain, the total phosphatase activity (and including overall activity) for tau of PP2A, PP1, and PP5 is significantly decreased by 50%, 20%, and 20%, respectively [90]. PP2A contributes to abnormally hyperphosphorylated tau protein and is the most efficient phosphatase. Moreover, the inhibition of PP2A significantly plays a role in tau hyperphosphorylation [91–93]. It indicated PP2A is downregulated in the Down syndrome (DS) brain and thus may be involved in the abnormal hyperphosphorylation and accumulation of tau [94].

PP2A is regulated by endogenous inhibitor-1 of PP2A (I1PP2A) and inhibitor-2 of PP2A (I2PP2A) in mammalian tissues [95]. In AD brain, I2PP2A is translocated from neuronal nucleus to cytoplasm where it inhibits PP2A activity and promotes abnormal phosphorylation of tau. With inactivation of the nuclear localization signal (NLS) of I2PP2A, ^{179}KRK^{181} $\rightarrow$ ^{179}AAA^{181} along with ^{168}KR^{169} $\rightarrow$ ^{168}AA^{169} mutations in I2PP2A (mNLS-I2PP2A), I2PP2A was translocated from nucleus to the cytoplasm. Cytoplasmic retention of I2PP2A physically interacted with PP2A and inhibited its activity and induced Alzheimer-like abnormal tau protein hyperphosphorylation by the direct interaction of I2PP2A with PP2A and GSK-3β [96]. I2PP2A directly inhibits the activity of PP2A without affecting its expression [97]. GSK-3 activation significantly contributes to tau hyperphosphorylation by inhibiting PP2A via the upregulation of I2PP2A [98]. Okadaic acid is also considered to be a selective and potent inhibitor of serine/threonine phosphatase-1 and PP2A, which induces hyperphosphorylation of tau under in vitro and in vivo conditions [99]. These data indicate that upregulation or downregulation of the phosphorylation system or dephosphorylation system, respectively, of tau protein may be implicated in tau pathologies.

3.3. Tau Protein and Oxidative Stress

3.3.1. Tau Protein Hyperphosphorylation and Oxidative Stress. Oxidative stress is believed to be a prominent early event in the pathogenesis of AD, contributing to tau phosphorylation and the formation of neurofibrillary tangles [48]. However, the relationship and underlying mechanisms between oxidative stress and tau hyperphosphorylation remain elusive. Fatty acid oxidative products provide a direct link between the mechanisms of how oxidative stress induces the formation of NFTs in AD [100]. Data from experiments show that chronic oxidative stress increases the levels of tau phosphorylation at paired helical filaments (PHF-1) epitope (serine 396/404) via the inhibition of glutathione synthesis with buthionine sulfoximine (BSO) in an vitro model of chronic oxidative stress [9]. In primary rat cortical neuronal cultures

stimulated by the combination of the copper chelator, cuprizone, and oxidative stress (Fe^{2+}/H_2O_2), tau phosphorylation is significantly increased by the elevated activity of GSK-3 [101]. Furthermore, treatment of rat hippocampal cells and SHSY5Y human neuroblastoma cells with H_2O_2 at the early stages of oxidative stress exposure results in tau dephosphorylation at the tau1 epitope by CDK5 via PP1 activation [102]. Several studies have suggested that oxidative stress is a causal factor in tau-induced neurodegeneration in *Drosophila* [103–105]. In contrast, a fragment of tau protein has been shown to induce copper reduction, thus contributing to oxidative stress and initiating copper-mediated generation of H_2O_2 [106].

3.3.2. GSK3β, PP2A, and Oxidative Stress. Oxidative stress is likely to play a critical role in tau hyperphosphorylation, which is regulated by tau protein kinase activation and the suppression of phosphatase. Tau hyperphosphorylation may be induced by oxidative stress through the direct interaction with tau protein kinase and phosphatase, particularly GSK-3β and PP2A, respectively, because they are predominant and play an important role. A recent study has indicated that GSK-3β activity is upregulated under oxidative stress [107]. In human embryonic kidney 293/tau cells, H_2O_2 increases GSK-3β activity and tau is hyperphosphorylated at Ser396, Ser404, and Thr231 [107]. Mitochondrial superoxide activates the mitochondrial fraction of GSK-3α/β, resulting in the phosphorylation of the mitochondrial chaperone cyclophilin D [108]. This effect also provides a link between GSK-3β and oxidative stress. Studies have also focused on the link between PP2A and oxidative stress. A recent report shows that rat cortical neurons treated with okadaic acid inhibit PP2A activity, resulting in an abnormal increase in mitochondrial ROS and mitochondrial fission [109]. Other findings reveal that ROS inhibits PP2A and PP5, leading to the activation of JNK and Erk1/2 pathways and subsequently caspase-dependent and caspase-independent apoptosis of neuronal cells [110]. Despite these studies, the relationship of GSK3 and PP2A with oxidative stress remains to be further investigated.

3.3.3. Antioxidants and the Tau Protein. Several epidemiological studies have indicated a link between antioxidant intake and reduced incidence of dementia (particularly AD) and cognitive decline in elderly populations [111–113]. In recent years, antioxidant therapy has received considerable attention as a promising approach for slowing the progression of AD. Research has focused on endogenous antioxidants (e.g., vitamins, coenzyme Q10, and melatonin) and the intake of dietary antioxidants, such as phenolic compounds that are flavonoids or nonflavonoids [114, 115]. This increased interest has thus strengthened the hypothesis that oxidative damage may be responsible for the cognitive and functional decline in AD patients. Melatonin is a free radical scavenger that blocks tau hyperphosphorylation and microtubule disorganization under in vivo and in vitro conditions [116–118]. It also decreases the activity of GSK-3β [119]. Moreover, melatonin may be a potentially useful agent in the prevention and treatment of AD [120]. Other antioxidants, such as vitamins E and C [121, 122], gossypin [123], curcumin [124–127], beta-carotene [128], and *Ginkgo biloba* [129, 130], are also reported to have a protective effect against neurotoxicity. In addition, an association also exists between beta-carotene and tau in AD patients [128]. Demethoxycurcumin has been shown to inhibit the phosphorylation of both tau pS(262) and pS(396) in murine neuroblastoma N2A cells [125]. Curcumin also reduces soluble tau and elevated heat shock proteins involved in tau clearance [126]. These results have therefore led to further investigations of this compound as an antioxidant therapy strategy for AD. Other experiments have shown that the active component of *Ginkgo biloba*, ginkgolide A, inhibits GSK3β and suppressed the phosphorylation level of tau [129].

4. Autophagy in AD

4.1. The Autophagic Pathway. Autophagy is an essential lysosomal degradation pathway that turns over cytoplasmic constituents, including misfolded or aggregated proteins and damaged organelles, to facilitate the maintenance of cellular homeostasis [13, 131–134]. Autophagy is usually activated during nutrient deprivation and stress to enhance cellular survival, and its constitutive activity is recognized to control neuronal survival [14, 132, 135, 136]. Autophagic dysfunction has been reported to contribute to AD [20, 64, 137, 138].

Autophagy includes macroautophagy, chaperone-mediated autophagy, and microautophagy [13, 132, 134]. The most familiar of these types is macroautophagy, which is a process of cellular self-cannibalism in which portions of the cytoplasm are sequestered within double- or multimembraned vesicles (autophagosomes) and then delivered to lysosomes for bulk degradation [139]. Autophagy is induced by two pathways in macroautophagy-mammalian target of rapamycin- (mTOR-) dependent and mTOR-independent signaling pathways [140]. mTOR is an important convergence point in the cell signaling pathway. mTOR kinase activity is modulated in response to various stimuli, such as trophic factors, mitogens, hormones, amino acids, cell energy status, and cellular stress [135, 136]. Rapamycin, as mTOR inhibitor, is a very important tool for autophagy [140, 141]. mTOR complex (mTORC) 1 is involved in autophagy and is the master regulator of cell growth enhancing the cellular biomass by upregulating protein translation [142]. For cells to control cellular homoeostasis during growth, a close signaling interplay occurs between mTORC1 and two other protein kinases, AMP-activated protein kinase (AMPK) [143] and Unc51-like kinase (ULK1) [144]. Autophagy is inhibited by cytosolic p53 via the direct inhibition of AMPK [145]. mTORC1 controls autophagy by directly interacting with the Ulk1-focal adhesion kinase family-interacting protein of 200 kDa (Atg13-FIP200) complex [146]. Several mTOR-independent signals affect the autophagy pathway. When the level of free inositol and myoinositol-1,4,5-trisphosphate IP3 decreases, autophagy is reduced [147]. Furthermore, lower levels of Bcl-2 lead to the release of more Beclin-1, thus forming the Beclin-1-PI3KCIII complex to activate autophagy via the PI3K-AKT-mTOR pathway [148].

4.2. Autophagic Dysfunction in AD Pathology. A growing body of evidence suggests a link between AD and autophagy

[16, 17, 19, 20, 22]. Therefore, the pathological functions of autophagy may be a critical mediator of neurotoxicity [149]. Autophagy develops in AD brains because of the ineffective degradation of autophagosomes, which is controlled by many kinds of autophagy-related genes (Atg), including Atg1–Atg35. Atg8 (mammalian homolog is LC3) is an autophagosomal membrane protein and a marker of autophagosome formation [150]. Beclin-1 (the mammalian ortholog of yeast Atg6) plays a pivotal role in autophagy [151]. In an in vitro study of the pathogenesis of AD, Atg8/LC3 colocalizes with APP and LC3-positive autophagosomes are present [152]. Beclin-1 knockdown increases APP, APP-like proteins, APP-C-terminal fragments, and Aβ [153]. Atg5, Atg12, and LC3 are also associated with plaque, tangle pathologies, and neuronal death in AD [154]. Generally, autophagic vacuoles (AVs) are rare in the normal brain but are increased in brains of AD patients. In the early stages of AD, the expression of lysosome-related component is significantly increased prior to the formation of plaques and NFTs, and autophagy is also induced at this stage; thus its activity is independent of extracellular Aβ deposition and NFT formation [155]. In the late stage of AD, AVs continue to accumulate in large numbers in dystrophic neurites. There are several causes for the dysfunction of autophagy in late-stage AD, including the enhanced processing of APP and Aβ degradation [156] and the toxic effect of high levels of intracellular Aβ on lysosomal function [157]. Inhibition of the AV-lysosome fusion is caused by impaired microtubule-associated retrograde transport, which in turn leads to increased accumulation of AV in dystrophic neurites [134]. Lysosomal enzyme dysfunction may be associated with the accumulation of AVs [158]. Autophagy plays an important role in the degradation of impaired mitochondria in AD [158, 159]. Dysfunction of the autophagy-lysosome system causes insufficient degradation of mitochondria [160]. Conversely, mitochondrial dysfunction may also impair this pathway [161].

4.3. Autophagy and the Tau Protein

4.3.1. Tau Protein Degradation via Autophagy. A variety of forms of tau proteins have been shown to be degraded by the ubiquitin-proteasome system (UPS) and autophagy-lysosome system. UPS may play an important role in the primary clearance of pathological tau. However, the importance of autophagy-mediated tau degradation, particularly at the late stage of NFT formation, is becoming more recognized. The autophagy-lysosomal system has the capacity to engulf protein aggregates and keep tau levels at a low level [162]. Macroautophagy is believed to be an evolutionarily conserved mechanism for intracellular degradation of proteins, such as Aβ and tau. mTOR in negatively regulating autophagy is an important convergence point in cell signaling. Increasing mTOR signaling and PI3K/AKT/mTOR pathway facilitates tau pathology, but reducing this signaling ameliorates tau pathology [11, 20, 163]. Rapamycin has been reported to decrease tau phosphorylation at Ser214 in vitro and reduce tau tangles and insoluble tau in vivo [164, 165]. In a tetracycline-inducible model [tauDeltaC (tauΔC)], tau is abnormally truncated at Asp^{421} and is cleared predominantly by macroautophagy and degraded significantly faster than full-length tau [166]. Autophagy activation suppresses tau aggregation and eliminates cytotoxicity [163]. Moreover, trehalose (an enhancer of autophagy) directly inhibits tau aggregation in primary neurons [167]. Under in vitro conditions, the accumulation of tau species is increased with the autophagic inhibitor, 3-methyladenine, and decreased with trehalose [168]. Overall, these results suggest that tau degradation involves autophagy, and this activity is beneficial for neurons to prevent the accumulation of protein aggregates.

4.3.2. Tau Protein Hyperphosphorylation Leads to Autophagic Dysfunction. The physiological function of tau protein is well known to be associated with microtubule binding and assembly. Autophagosome transport mainly depends on the movement along microtubules in the autophagic pathway. However, the link between tau hyperphosphorylation and autophagic dysfunction is still under debate. Frontotemporal dementia and parkinsonism linked to chromosome 17-(FTDP-17-) mediated tau mutations can disrupt lysosomal function in transgenic mice expressing human tau with four tubulin-binding repeats (increased by FTDP-17 splice donor mutations) and three FTDP-17 missense mutations: G272V, P301L, and R406W [169]. In Tg mice expressing mutant human (P301L) tau, axonal spheroids have been shown to contain tau-immunoreactive filaments and AVs [170]. A recent study has revealed that PP2A upregulation stimulates neuronal autophagy, thus providing a link between PP2A downregulation, autophagy disruption, and protein aggregation [171]. Furthermore, autophagosomes have been shown to be increased in rat neurons treated with okadaic acid [172]. Altogether, tau is known to regulate the stability of microtubules, and tau hyperphosphorylation may result in the destabilization of neuronal microtubules, thus affecting the placement and function of mitochondria and lysosomes. Therefore, tau hyperphosphorylation is likely to play a critical role in the process of autophagic dysfunction.

4.3.3. Autophagic Dysfunction Induces Tau Protein Aggregation and Neurodegeneration. The autophagy-lysosome system is well recognized to play an important role in the clearance of abnormally modified proteins in cells. Several studies have shown that dysfunction of the autophagy-lysosome system contributes to the formation of tau oligomers and insoluble aggregates [22, 173, 174]. Abnormal lysosomal proteases are also found in brains of AD patients [173, 174]. Both phosphorylated tau and GSK3β significantly accumulate in Atg7 conditional knockout brains, although NFTs are absent [20]. The hyperphosphorylation of tau and NFT formation result in the disruption of the neuronal skeleton, thereby contributing to neuronal dysfunction, cell death, and eventually the symptoms of AD. Genetic reduction of mammalian target of rapamycin led to an increase in autophagy induction and ameliorates Alzheimer's disease-like cognitive and pathological deficits [22]. Induction autophagy adaptor protein NDP52 may reduce tau protein phosphorylation in neurons [20]. Therefore, the autophagy-lysosome system plays a crucial role

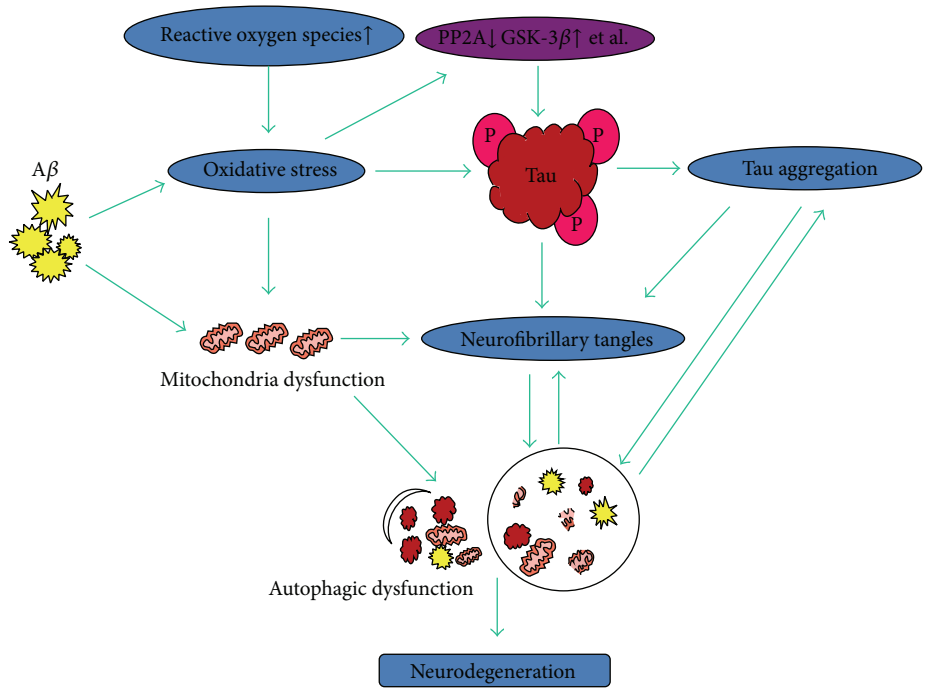

Figure 1: Tau protein NFTs formation and autophagic dysfunction in Alzheimer's disease. Aβ oligomers and ROS production intrigue oxidative stress and mitochondria dysfunction, in which induce tau protein hyperphosphorylation and neurofibrillary tangles formation with protein phosphatase and kinases imbalance. These events converge to autophagic dysfunction and tau protein aggregation to lead to neurodegeneration and cell death in AD.

in the clearance of tau, and its accumulation may be due to autophagic dysfunction in cells.

5. Conclusion

Oxidative stress is reported to be one of the earliest events in AD and can induce tau hyperphosphorylation, which destabilizes microtubules by decreasing the binding affinity of tau, thereby resulting in the formation of NFTs, which are a major pathological hallmark of AD. Aβ and other risk factors play the crucial role in neuronal oxidative stress. Aβ-mediated mitochondrial oxidative stress causes hyperphosphorylation of tau in AD brains, as well as mitochondrial dysfunction. Tau hyperphosphorylation may be the necessary point in neural dysfunction and death. Hyperphosphorylation, oligomerization, fibrillization, and propagation of tau pathology have been proposed as the pathogenesis of tau-mediated neurodegeneration. In addition to oxidative stress, tau protein phosphorylation is also regulated by protein kinase and phosphatase. It indicates the roles of mitochondria and protein phosphatase on oxidative stress and tau protein hyperphosphorylation. Meanwhile it strengthens the hypothesis that oxidative damage is responsible for the cognitive and functional decline in AD patients.

Dysfunctional tau protein is degraded via autophagy-lysosomal pathway. Autophagy is an essential lysosomal degradation process that turns over cytoplasmic constituents, including misfolded or aggregated proteins and damaged organelles, to facilitate the maintenance of cellular homeostasis. Tau hyperphosphorylation is likely to play a critical role in the process of autophagic dysfunction, and dysfunction of the autophagy-lysosome system may also promote the tau aggregation. Altogether, tau is known to regulate the stability of microtubules, and tau hyperphosphorylation may result in the destabilization of neuronal microtubules, thus affecting the function of mitochondria and lysosomes.

These events initiate a series of cascades to induce neurodegeneration and cell death in AD. Aβ oligomers and ROS production intrigue oxidative stress and mitochondria dysfunction, in which they induce tau protein hyperphosphorylation and neurofibrillary tangles formation with protein phosphatase and kinases imbalance. These events converge to autophagic dysfunction and tau protein aggregation to lead to neurodegeneration and cell death in AD (Figure 1). However, the relationships between oxidative stress, tau hyperphosphorylation, and autophagic dysfunction and accurate mechanisms on neurodegeneration, especially mitochondria and protein phosphatase in AD, still require further research.

Conflict of Interests

The authors have no conflict of interests to declare.

Authors' Contribution

Zhenzhen Liu, Tao Li, and Ping Li equally contributed to this study.

Acknowledgments

This work is supported by National Natural Science Foundation of China Grants 81271410 (Jianshe Wei) and 81471174 (Mengzhou Xue). Drs. Wei and Xue are Yellow River Scholars in neurobiology and neurology.

References

[1] T. Cumming and A. Brodtmann, "Dementia and stroke: the present and future epidemic," *International Journal of Stroke*, vol. 5, no. 6, pp. 453–454, 2010.

[2] S. W.-C. Chan, "Family caregiving in dementia: the asian perspective of a global problem," *Dementia and Geriatric Cognitive Disorders*, vol. 30, no. 6, pp. 469–478, 2011.

[3] R. A. Armstrong, "A critical analysis of the 'amyloid cascade hypothesis'," *Folia Neuropathologica*, vol. 52, no. 3, pp. 211–225, 2014.

[4] K. L. Viola and W. L. Klein, "Amyloid β oligomers in Alzheimer's disease pathogenesis, treatment, and diagnosi," *Acta Neuropathologica*, vol. 129, no. 2, pp. 183–206, 2015.

[5] A. C. Paula-Lima, J. Brito-Moreira, and S. T. Ferreira, "Deregulation of excitatory neurotransmission underlying synapse failure in Alzheimer's disease," *Journal of Neurochemistry*, vol. 126, no. 2, pp. 191–202, 2013.

[6] A. K. Y. Fu, K.-W. Hung, H. Huang et al., "Blockade of EphA4 signaling ameliorates hippocampal synaptic dysfunctions in mouse models of Alzheimer's disease," *Proceedings of the National Academy of Sciences of the United States of America*, vol. 111, no. 27, pp. 9959–9964, 2014.

[7] F. G. De Felice, P. T. Velasco, M. P. Lambert et al., "Aβ oligomers induce neuronal oxidative stress through an N-methyl-D-aspartate receptor-dependent mechanism that is blocked by the Alzheimer drug memantine," *The Journal of Biological Chemistry*, vol. 282, no. 15, pp. 11590–11601, 2007.

[8] S. Melov, P. A. Adlard, K. Morten et al., "Mitochondrial oxidative stress causes hyperphosphorylation of tau," *PLoS ONE*, vol. 2, no. 6, Article ID e536, 2007.

[9] B. Su, X. Wang, H. G. Lee et al., "Chronic oxidative stress causes increased tau phosphorylation in M17 neuroblastoma cells," *Neuroscience Letters*, vol. 468, no. 3, pp. 267–271, 2010.

[10] D. Luque-Contreras, K. Carvajal, D. Toral-Rios, D. Franco-Bocanegra, and V. Campos-Peña, "Oxidative stress and metabolic syndrome: cause or consequence of Alzheimer's disease?" *Oxidative Medicine and Cellular Longevity*, vol. 2014, Article ID 497802, 11 pages, 2014.

[11] D. Heras-Sandoval, J. M. Pérez-Rojas, J. Hernández-Damián, and J. Pedraza-Chaverri, "The role of PI3K/AKT/mTOR pathway in the modulation of autophagy and the clearance of protein aggregates in neurodegeneration," *Cellular Signalling*, vol. 26, no. 12, pp. 2694–2701, 2014.

[12] Y. Saitoh, N. Fujikake, Y. Okamoto et al., "p62 plays a protective role in the autophagic degradation of polyglutamine protein oligomers in polyglutamine disease model flies," *Journal of Biological Chemistry*, vol. 290, no. 3, pp. 1442–1453, 2015.

[13] S. Ghavami, S. Shojaei, B. Yeganeh et al., "Autophagy and apoptosis dysfunction in neurodegenerative disorders," *Progress in Neurobiology*, vol. 112, pp. 24–49, 2014.

[14] C.-C. Tan, J.-T. Yu, M.-S. Tan, T. Jiang, X.-C. Zhu, and L. Tan, "Autophagy in aging and neurodegenerative diseases: implications for pathogenesis and therapy," *Neurobiology of Aging*, vol. 35, no. 5, pp. 941–957, 2014.

[15] A. Salminen, K. Kaarniranta, A. Kauppinen et al., "Impaired autophagy and APP processing in Alzheimer's disease: the potential role of Beclin 1 interactome," *Progress in Neurobiology*, vol. 106-107, pp. 33–54, 2013.

[16] D.-S. Yang, P. Stavrides, M. Saito et al., "Defective macroautophagic turnover of brain lipids in the TgCRND8 Alzheimer mouse model: prevention by correcting lysosomal proteolytic deficits," *Brain*, vol. 137, part 12, pp. 3300–3318, 2014.

[17] P. Nilsson, M. Sekiguchi, T. Akagi et al., "Autophagy-related protein 7 deficiency in amyloid $\beta(A\beta)$ precursor protein transgenic mice decreases $A\beta$ in the multivesicular bodies and induces $A\beta$ accumulation in the Golgi," *The American Journal of Pathology*, vol. 185, no. 2, pp. 305–313, 2015.

[18] D. M. Wolfe, J.-H. Lee, A. Kumar, S. Lee, S. J. Orenstein, and R. A. Nixon, "Autophagy failure in Alzheimer's disease and the role of defective lysosomal acidification," *European Journal of Neuroscience*, vol. 37, no. 12, pp. 1949–1961, 2013.

[19] Y. Tian, J. C. Chang, E. Y. Fan, M. Flajolet, and P. Greengard, "Adaptor complex AP2/PICALM, through interaction with LC3, targets Alzheimer's APP-CTF for terminal degradation via autophagy," *Proceedings of the National Academy of Sciences of the United States of America*, vol. 110, no. 42, pp. 17071–17076, 2013.

[20] C. Jo, S. Gundemir, S. Pritchard, Y. N. Jin, I. Rahman, and G. V. W. Johnson, "Nrf2 reduces levels of phosphorylated tau protein by inducing autophagy adaptor protein NDP52," *Nature Communications*, vol. 5, article 3496, 2014.

[21] T. Lu, L. Aron, J. Zullo et al., "REST and stress resistance in ageing and Alzheimer's disease," *Nature*, vol. 507, no. 7493, pp. 448–454, 2014.

[22] A. Caccamo, V. De Pinto, A. Messina, C. Branca, and S. Oddo, "Genetic reduction of mammalian target of rapamycin ameliorates Alzheimer's disease-like cognitive and pathological deficits by restoring hippocampal gene expression signature," *Journal of Neuroscience*, vol. 34, no. 23, pp. 7988–7998, 2014.

[23] E. Martínez, A. Navarro, C. Ordóñez, E. del Valle, and J. Tolivia, "Oxidative stress induces apolipoprotein D overexpression in hippocampus during aging and alzheimer's disease," *Journal of Alzheimer's Disease*, vol. 36, no. 1, pp. 129–144, 2013.

[24] Y. Zhao and B. Zhao, "Oxidative stress and the pathogenesis of alzheimer's disease," *Oxidative Medicine and Cellular Longevity*, vol. 2013, Article ID 316523, 10 pages, 2013.

[25] J. M. Flynn and S. Melovn, "SOD2 in mitochondrial dysfunction and neurodegeneration," *Free Radical Biology and Medicine*, vol. 62, pp. 4–12, 2013.

[26] A. K. Holley, V. Bakthavatchalu, J. M. Velez-Roman, and D. K. St. Clair, "Manganese superoxide dismutase: guardian of the powerhouse," *International Journal of Molecular Sciences*, vol. 12, no. 10, pp. 7114–7162, 2011.

[27] M. P. Mattson and T. Magnus, "Ageing and neuronal vulnerability," *Nature Reviews Neuroscience*, vol. 7, no. 4, pp. 278–294, 2006.

[28] L. Chen, R. Na, and Q. Ran, "Enhanced defense against mitochondrial hydrogen peroxide attenuates age-associated cognition decline," *Neurobiology of Aging*, vol. 35, no. 11, pp. 2552–2561, 2014.

[29] D. Yamazaki, J. Horiuchi, K. Ueno et al., "Glial dysfunction causes age-related memory impairment in *Drosophila*," *Neuron*, vol. 84, no. 4, pp. 753–763, 2014.

[30] H. Tayler, T. Fraser, J. S. Miners, P. G. Kehoe, and S. Love, "Oxidative balance in Alzheimer's disease: relationship to

APOE, braak tangle stage, and the concentrations of soluble and insoluble amyloid-β," *Journal of Alzheimer's Disease*, vol. 22, no. 4, pp. 1363–1373, 2010.

[31] B. H. Han, M. L. Zhou, A. W. Johnson et al., "Contribution of reactive oxygen species to cerebral amyloid angiopathy, vasomotor dysfunction, and microhemorrhage in aged Tg2576 mice," *Proceedings of The National Academy of Sciences of The United States of America*, vol. 112, no. 8, pp. E881–E890, 2015.

[32] P. Nordström, K. Michaëlsson, Y. Gustafson, and A. Nordström, "Traumatic brain injury and young onset dementia: a nationwide cohort study," *Annals of Neurology*, vol. 75, no. 3, pp. 374–381, 2014.

[33] J. Zhou, J. T. Yu, H. F. Wang et al., "Association between stroke and Alzheimer's disease: systematic review and meta-analysis," *Journal of Alzheimers Disease*, vol. 43, no. 2, pp. 479–489, 2015.

[34] D. Cifuentes, M. Poittevin, E. Dere et al., "Hypertension accelerates the progression of Alzheimer-like pathology in a mouse model of the disease," *Hypertension*, vol. 65, no. 1, pp. 218–224, 2015.

[35] M. Barbagallo and L. J. Dominguez, "Type 2 diabetes mellitus and Alzheimer's disease," *The World Journal of Diabetes*, vol. 5, no. 6, pp. 889–893, 2014.

[36] S. H. Park, J. H. Kim, K. H. Choi et al., "Hypercholesterolemia accelerates amyloid β-induced cognitive deficits," *International Journal of Molecular Medicine*, vol. 31, no. 3, pp. 577–582, 2013.

[37] K. Nazef, M. Khelil, H. Chelouti et al., "Hyperhomocysteinemia is a risk factor for Alzheimer's disease in an Algerian population," *Archives of Medical Research*, vol. 45, no. 3, pp. 247–250, 2014.

[38] N. VanDuyn, R. Settivari, J. LeVora, S. Zhou, J. Unrine, and R. Nass, "The metal transporter SMF-3/DMT-1 mediates aluminum-induced dopamine neuron degeneration," *Journal of Neurochemistry*, vol. 124, no. 1, pp. 147–157, 2013.

[39] T. C. Durazzo, N. Mattsson, and M. W. Weiner, "Smoking and increased Alzheimer's disease risk: a review of potential mechanisms," *Alzheimers and Dementia*, vol. 10, no. 3, pp. S122–S145, 2014.

[40] G. M. Pasinetti and J. A. Eberstein, "Metabolic syndrome and the role of dietary lifestyles in Alzheimer's disease," *Journal of Neurochemistry*, vol. 106, no. 4, pp. 1503–1514, 2008.

[41] T. J. Littlejohns, W. E. Henley, I. A. Lang et al., "Vitamin D and the risk of dementia and Alzheimer disease," *Neurology*, vol. 83, no. 10, pp. 920–928, 2014.

[42] O. Ohia-Nwoko, S. Montazari, Y.-S. Lau, and J. L. Eriksen, "Long-term treadmill exercise attenuates tau pathology in P301S tau transgenic mice," *Molecular Neurodegeneration*, vol. 9, article 54, 2014.

[43] A. Nunomura, R. J. Castellani, X. Zhu, P. I. Moreira, G. Perry, and M. A. Smith, "Involvement of oxidative stress in Alzheimer disease," *Journal of Neuropathology & Experimental Neurology*, vol. 65, no. 7, pp. 631–641, 2006.

[44] P. Vemuri, T. G. Lesnick, S. A. Przybelski et al., "Effect of lifestyle activities on alzheimer disease biomarkers and cognition," *Annals of Neurology*, vol. 72, no. 5, pp. 730–738, 2012.

[45] M. Antoniou, G. M. Gunasekera, and P. C. M. Wong, "Foreign language training as cognitive therapy for age-related cognitive decline: a hypothesis for future research," *Neuroscience and Biobehavioral Reviews*, vol. 37, part 2, pp. 2689–2698, 2013.

[46] J. Yao, R. W. Irwin, L. Zhao, J. Nilsen, R. T. Hamilton, and R. D. Brinton, "Mitochondrial bioenergetic deficit precedes Alzheimer's pathology in female mouse model of Alzheimer's disease," *Proceedings of the National Academy of Sciences of the United States of America*, vol. 106, no. 34, pp. 14670–14675, 2009.

[47] V. García-Escudero, P. Martín-Maestro, G. Perry, and J. Avila, "Deconstructing mitochondrial dysfunction in alzheimer disease," *Oxidative Medicine and Cellular Longevity*, vol. 2013, Article ID 162152, 13 pages, 2013.

[48] S. Mondragón-Rodríguez, G. Perry, X. Zhu, P. I. Moreira, M. C. Acevedo-Aquino, and S. Williams, "Phosphorylation of tau protein as the link between oxidative stress, mitochondrial dysfunction, and connectivity failure: implications for Alzheimer's disease," *Oxidative Medicine and Cellular Longevity*, vol. 2013, Article ID 940603, 6 pages, 2013.

[49] J. Yao, H. Du, S. Yan et al., "Inhibition of amyloid-beta (Abeta) peptide-binding alcohol dehydrogenase-Abeta interaction reduces Abeta accumulation and improves mitochondrial function in a mouse model of Alzheimer's disease," *Journal of Neuroscience*, vol. 31, no. 6, pp. 2313–2320, 2011.

[50] A. Pensalfini, M. Zampagni, G. Liguri et al., "Membrane cholesterol enrichment prevents Aβ-induced oxidative stress in Alzheimer's fibroblasts," *Neurobiology of Aging*, vol. 32, no. 2, pp. 210–222, 2011.

[51] K. Schuessel, S. Schäfer, T. A. Bayer et al., "Impaired Cu/Zn-SOD activity contributes to increased oxidative damage in APP transgenic mice," *Neurobiology of Disease*, vol. 18, no. 1, pp. 89–99, 2005.

[52] M. Dumont, C. Stack, C. Elipenahli et al., "Behavioral deficit, oxidative stress, and mitochondrial dysfunction precede tau pathology in P301S transgenic mice," *The FASEB Journal*, vol. 25, no. 11, pp. 4063–4072, 2011.

[53] K. Murakami, N. Murata, Y. Noda et al., "SOD1 (copper/zinc superoxide dismutase) deficiency drives amyloid β protein oligomerization and memory loss in mouse model of Alzheimer disease," *The Journal of Biological Chemistry*, vol. 286, no. 52, pp. 44557–44568, 2011.

[54] D. Poppek, S. Keck, G. Ermak et al., "Phosphorylation inhibits turnover of the tau protein by the proteasome: influence of *RCAN1* and oxidative stress," *Biochemical Journal*, vol. 400, no. 3, pp. 511–520, 2006.

[55] S. Melov, P. A. Adlard, K. Morten et al., "Mitochondrial oxidative stress causes hyperphosphorylation of tau," *PLoS ONE*, vol. 2, no. 6, article e536, 2007.

[56] T. Morita and K. Sobuě, "Specification of neuronal polarity regulated by local translation of CRMP2 and tau via the mTOR-p70S6K pathway," *Journal of Biological Chemistry*, vol. 284, no. 40, pp. 27734–27745, 2009.

[57] L. Li, T. Fothergill, B. I. Hutchins, E. W. Dent, and K. Kalil, "Wnt5a evokes cortical axon outgrowth and repulsive guidance by tau mediated reorganization of dynamic microtubules," *Developmental Neurobiology*, vol. 74, no. 8, pp. 797–817, 2014.

[58] A. Fuster-Matanzo, M. Llorens-Martín, J. Jurado-Arjona, J. Avila, and F. Hernández, "Tau protein and adult hippocampal neurogenesis," *Frontiers in Neuroscience*, vol. 6, article 104, 2012.

[59] J. Avila, J. J. Lucas, M. Pérez, and F. Hernández, "Role of Tau protein in both physiological and pathological conditions," *Physiological Reviews*, vol. 84, no. 2, pp. 361–384, 2004.

[60] D. Gordon, G. J. Kidd, and R. Smith, "Antisense suppression of tau in cultured rat oligodendrocytes inhibits process formation," *Journal of Neuroscience Research*, vol. 86, no. 12, pp. 2591–2601, 2008.

[61] M. Kolarova, F. García-Sierra, A. Bartos, J. Ricny, and D. Ripova, "Structure and pathology of tau protein in Alzheimer disease,"

International Journal of Alzheimer's Disease, vol. 2012, Article ID 731526, 13 pages, 2012.

[62] C. Fauquant, V. Redeker, I. Landrieu et al., "Systematic identification of tubulin-interacting fragments of the microtubule-associated protein Tau leads to a highly efficient promoter of microtubule assembly," *Journal of Biological Chemistry*, vol. 286, no. 38, pp. 33358–33368, 2011.

[63] H.-L. Li, H.-H. Wang, S.-J. Liu et al., "Phosphorylation of tau antagonizes apoptosis by stabilizing beta-catenin, a mechanism involved in Alzheimer's neurodegeneration," *Proceedings of the National Academy of Sciences of the United States of America*, vol. 104, no. 9, pp. 3591–3596, 2007.

[64] T. Rodríguez-Martín, I. Cuchillo-Ibáñez, W. Noble, F. Nyenya, B. H. Anderton, and D. P. Hanger, "Tau phosphorylation affects its axonal transport and degradation," *Neurobiology of Aging*, vol. 34, no. 9, pp. 2146–2157, 2013.

[65] C. Ballatore, K. R. Brunden, D. M. Huryn, J. Q. Trojanowski, V. M.-Y. Lee, and A. B. Smith, "Microtubule stabilizing agents as potential treatment for Alzheimer's disease and related neurodegenerative tauopathies," *Journal of Medicinal Chemistry*, vol. 55, no. 21, pp. 8979–8996, 2012.

[66] D. Simón, E. García-García, F. Royo, J. M. Falcón-Pérez, and J. Avila, "Proteostasis of tau. Tau overexpression results in its secretion via membrane vesicles," *FEBS Letters*, vol. 586, no. 1, pp. 47–54, 2012.

[67] W. Qian and F. Liu, "Regulation of alternative splicing of tau exon 10," *Neuroscience Bulletin*, vol. 30, no. 2, pp. 367–377, 2014.

[68] F. Liu and C.-X. Gong, "Tau exon 10 alternative splicing and tauopathies," *Molecular Neurodegeneration*, vol. 3, no. 1, article 8, 2008.

[69] N. Jovanov-Milošević, D. Petrović, G. Sedmak, M. Vukšić, P. R. Hof, and G. Šimić, "Human fetal tau protein isoform: possibilities for Alzheimer's disease treatment," *The International Journal of Biochemistry & Cell Biology*, vol. 44, no. 8, pp. 1290–1294, 2012.

[70] S. J. Adams, M. A. de Ture, M. McBride, D. W. Dickson, and L. Petrucelli, "Three repeat isoforms of tau inhibit assembly of four repeat tau filaments," *PLoS ONE*, vol. 5, no. 5, Article ID e10810, 2010.

[71] M. Espinoza, R. de Silva, D. W. Dickson, and P. Davies, "Differential incorporation of tau isoforms in Alzheimer's disease," *Journal of Alzheimer's Disease*, vol. 14, no. 1, pp. 1–16, 2008.

[72] M. Fernández-Nogales, J. R. Cabrera, M. Santos-Galindo et al., "Huntington's disease is a four-repeat tauopathy with tau nuclear rods," *Nature Medicine*, vol. 20, no. 8, pp. 881–885, 2014.

[73] D. C. Glatz, D. Rujescu, Y. Tang et al., "The alternative splicing of tau exon 10 and its regulatory proteins CLK2 and TRA2-BETA1 changes in sporadic Alzheimer's disease," *Journal of Neurochemistry*, vol. 96, no. 3, pp. 635–644, 2006.

[74] M. J. Niblock and J. M. Gallo, "Tau alternative splicing in familial and sporadic tauopathies," *Biochemical Society Transactions*, vol. 40, no. 4, pp. 677–680, 2012.

[75] Y. Yoshiyama, V. M. Y. Lee, and J. Q. Trojanowski, "Therapeutic strategies for tau mediated neurodegeneration," *Journal of Neurology, Neurosurgery & Psychiatry*, vol. 84, no. 7, pp. 784–795, 2013.

[76] K. Iijima-Ando, L. Zhao, A. Gatt, C. Shenton, and K. Iijima, "A DNA damage-activated checkpoint kinase phosphorylates tau and enhances tau-induced neurodegeneration," *Human Molecular Genetics*, vol. 19, no. 10, pp. 1930–1938, 2010.

[77] J. Mendoza, M. Sekiya, T. Taniguchi, K. M. Iijima, R. Wang, and K. Ando, "Global analysis of phosphorylation of Tau by the checkpoint kinases Chk1 and Chk2 in vitro," *Journal of Proteome Research*, vol. 12, no. 6, pp. 2654–2665, 2013.

[78] S. Flunkert, M. Hierzer, T. Löffler et al., "Elevated levels of soluble total and hyperphosphorylated tau result in early behavioral deficits and distinct changes in brain pathology in a new tau transgenic mouse model," *American Journal of Neurodegenerative Disease*, vol. 11, no. 4, pp. 194–205, 2013.

[79] C.-X. Gong and K. Iqbal, "Hyperphosphorylation of microtubule-associated protein tau: a promising therapeutic target for Alzheimer disease," *Current Medicinal Chemistry*, vol. 15, no. 23, pp. 2321–2328, 2008.

[80] E. Kiris, D. Ventimiglia, M. E. Sargin et al., "Combinatorial Tau pseudophosphorylation: markedly different regulatory effects on microtubule assembly and dynamic instability than the sum of the individual parts," *The Journal of Biological Chemistry*, vol. 286, no. 16, pp. 14257–14270, 2011.

[81] F. Hernandez, J. J. Lucas, and J. Avila, "GSK3 and tau: two convergence points in Alzheimer's disease," *Journal of Alzheimer's Disease*, vol. 33, no. 1, pp. S141–S144, 2013.

[82] C. Gao, C. Hölscher, Y. Liu, and L. Li, "GSK3: a key target for the development of novel treatments for type 2 diabetes mellitus and Alzheimer disease," *Reviews in the Neurosciences*, vol. 23, no. 1, pp. 1–11, 2011.

[83] J. C. Gandy, M. Melendez-Ferro, G. N. Bijur et al., "Glycogen synthase kinase-3β (GSK3β) expression in a mouse model of Alzheimer's disease: a light and electron microscopy study," *Synapse*, vol. 67, no. 6, pp. 313–327, 2013.

[84] H. Maldonado, E. Ramírez, E. Utreras et al., "Inhibition of cyclin-dependent kinase 5 but not of glycogen synthase kinase 3-β prevents neurite retraction and tau hyperphosphorylation caused by secretable products of human T-cell leukemia virus type I-infected lymphocytes," *Journal of Neuroscience Research*, vol. 89, no. 9, pp. 1489–1498, 2011.

[85] A. López-Tobón, J. F. Castro-Álvarez, D. Piedrahita, R. L. Boudreau, J. C. Gallego-Gómez, and G. P. Cardona-Gómez, "Silencing of CDK5 as potential therapy for Alzheimer's disease," *Reviews in the Neurosciences*, vol. 22, no. 2, pp. 143–152, 2011.

[86] S. A. L. Corrêa and K. L. Eales, "The role of p38 MAPK and its substrates in neuronal plasticity and neurodegenerative disease," *Journal of Signal Transduction*, vol. 2012, Article ID 649079, 12 pages, 2012.

[87] G. Li, H. Yin, and J. Kuret, "Casein kinase 1 delta phosphorylates tau and disrupts its binding to microtubules," *Journal of Biological Chemistry*, vol. 279, no. 16, pp. 15938–15945, 2004.

[88] F. Liu, Z. Liang, J. Shi et al., "PKA modulates GSK-3β- and cdk5-catalyzed phosphorylation of tau in site- and kinase-specific manners," *FEBS Letters*, vol. 580, no. 26, pp. 6269–6274, 2006.

[89] M. Tsukane and T. Yamauchi, "Ca^{2+}/calmodulin-dependent protein kinase II mediates apoptosis of P19 cells expressing human tau during neural differentiation with retinoic acid treatment," *Journal of Enzyme Inhibition and Medicinal Chemistry*, vol. 24, no. 2, pp. 365–371, 2009.

[90] F. Liu, I. Grundke-Iqbal, K. Iqbal, and C.-X. Gong, "Contributions of protein phosphatases PP1, PP2A, PP2B and PP5 to the regulation of tau phosphorylation," *European Journal of Neuroscience*, vol. 22, no. 8, pp. 1942–1950, 2005.

[91] I. Landrieu, C. Smet-Nocca, L. Amniai et al., "Molecular implication of PP2A and Pin1 in the Alzheimer's disease specific

hyperphosphorylation of Tau," *PLoS ONE*, vol. 6, no. 6, Article ID e21521, 2011.

[92] P. Rudrabhatla and H. C. Pant, "Role of protein phosphatase 2A in Alzheimer's disease," *Current Alzheimer Research*, vol. 8, no. 6, pp. 623–632, 2011.

[93] S. S. Park, H.-J. Jung, Y.-J. Kim et al., "Asp664 cleavage of amyloid precursor protein induces tau phosphorylation by decreasing protein phosphatase 2A activity," *Journal of Neurochemistry*, vol. 123, no. 5, pp. 856–865, 2012.

[94] Z. Liang, F. Liu, K. Iqbal, I. Grundke-Iqbal, J. Wegiel, and C. X. Gong, "Decrease of protein phosphatase 2A and its association with accumulation and hyperphosphorylation of tau in Down syndrome," *Journal of Alzheimer's Disease*, vol. 13, no. 3, pp. 295–302, 2008.

[95] L. Martin, X. Latypova, C. M. Wilson, A. Magnaudeix, M.-L. Perrin, and F. Terro, "Tau protein phosphatases in Alzheimer's disease: the leading role of PP2A," *Ageing Research Reviews*, vol. 12, no. 1, pp. 39–49, 2013.

[96] M. Arif, J. Wei, Q. Zhang et al., "Cytoplasmic retention of protein phosphatase 2A-inhibitor 2 (I2PP2A) induces Alzheimer-like abnormal hyperphosphorylation of Tau," *The Journal of Biological Chemistry*, vol. 289, no. 40, pp. 27677–27691, 2014.

[97] L. Arnaud, S. Chen, F. Liu et al., "Mechanism of inhibition of PP2A activity and abnormal hyperphosphorylation of tau by I2(PP2A)/SET," *FEBS Letters*, vol. 585, no. 17, pp. 2653–2659, 2011.

[98] G.-P. Liu, Y. Zhang, X.-Q. Yao et al., "Activation of glycogen synthase kinase-3 inhibits protein phosphatase-2A and the underlying mechanisms," *Neurobiology of Aging*, vol. 29, no. 9, pp. 1348–1358, 2008.

[99] P. K. Kamat, S. Rai, and C. Nath, "Okadaic acid induced neurotoxicity: an emerging tool to study Alzheimer's disease pathology," *NeuroToxicology*, vol. 37, pp. 163–172, 2013.

[100] S. Patil and C. Chan, "Palmitic and stearic fatty acids induce Alzheimer-like hyperphosphorylation of tau in primary rat cortical neurons," *Neuroscience Letters*, vol. 384, no. 3, pp. 288–293, 2005.

[101] M. A. Lovell, S. Xiong, C. Xie, P. Davies, and W. R. Markesbery, "Induction of hyperphosphorylated tau in primary rat cortical neuron cultures mediated by oxidative stress and glycogen synthase kinase-3," *Journal of Alzheimer's Disease*, vol. 6, no. 6, pp. 659–671, 2004.

[102] C. A. Zambrano, J. T. Egaña, M. T. Núñez, R. B. Maccioni, and C. González-Billault, "Oxidative stress promotes τ dephosphorylation in neuronal cells: the roles of cdk5 and PP1," *Free Radical Biology and Medicine*, vol. 36, no. 11, pp. 1393–1402, 2004.

[103] D. Dias-Santagata, T. A. Fulga, A. Duttaroy, and M. B. Feany, "Oxidative stress mediates tau-induced neurodegeneration in *Drosophila*," *The Journal of Clinical Investigation*, vol. 117, no. 1, pp. 236–245, 2007.

[104] B. Frost, M. Hemberg, J. Lewis, and M. B. Feany, "Tau promotes neurodegeneration through global chromatin relaxation," *Nature Neuroscience*, vol. 17, no. 3, pp. 357–366, 2014.

[105] V. Khurana, "Modeling tauopathy in the fruit fly *Drosophila melanogaster*," *Journal of Alzheimer's Disease*, vol. 15, no. 4, pp. 541–553, 2008.

[106] X.-Y. Su, W.-H. Wu, Z.-P. Huang et al., "Hydrogen peroxide can be generated by tau in the presence of Cu(II)," *Biochemical and Biophysical Research Communications*, vol. 358, no. 2, pp. 661–665, 2007.

[107] Y. Feng, Y. Xia, G. Yu et al., "Cleavage of GSK-3β by calpain counteracts the inhibitory effect of Ser9 phosphorylation on GSK-3β activity induced by H_2O_2," *Journal of Neurochemistry*, vol. 126, no. 2, pp. 234–242, 2013.

[108] F. Chiara, A. Gambalunga, M. Sciacovelli et al., "Chemotherapeutic induction of mitochondrial oxidative stress activates GSK-3α/β and Bax, leading to permeability transition pore opening and tumor cell death," *Cell Death and Disease*, vol. 3, no. 12, article e444, 2012.

[109] M.-H. Cho, D.-H. Kim, J.-E. Choi, and E.-J. Chang, "Increased phosphorylation of dynamin-related protein 1 and mitochondrial fission in okadaic acid-treated neurons," *Brain Research*, vol. 1454, pp. 100–110, 2012.

[110] L. Chen, L. Liu, and S. Huang, "Cadmium activates the mitogen-activated protein kinase (MAPK) pathway via induction of reactive oxygen species and inhibition of protein phosphatases 2A and 5," *Free Radical Biology and Medicine*, vol. 45, no. 7, pp. 1035–1044, 2008.

[111] M. A. Beydoun, M. T. Fanelli-Kuczmarski, M. H. Kitner-Triolo et al., "Dietary antioxidant intake and its association with cognitive function in an ethnically diverse sample of US adults," *Psychosomatic Medicine*, vol. 77, no. 1, pp. 68–82, 2015.

[112] S. Gillette-Guyonnet, M. Secher, and B. Vellas, "Nutrition and neurodegeneration: epidemiological evidence and challenges for future research," *British Journal of Clinical Pharmacology*, vol. 75, no. 3, pp. 738–755, 2013.

[113] M. A. Beydoun, H. A. Beydoun, A. A. Gamaldo, A. Teel, A. B. Zonderman, and Y. Wang, "Epidemiologic studies of modifiable factors associated with cognition and dementia: systematic review and meta-analysis," *BMC Public Health*, vol. 14, article 643, 2014.

[114] T. Hamaguchi, K. Ono, A. Murase, and M. Yamada, "Phenolic compounds prevent Alzheimer's pathology through different effects on the amyloid-beta aggregation pathway," *The American Journal of Pathology*, vol. 175, no. 6, pp. 2557–2565, 2009.

[115] J. Teixeira, T. Silva, P. B. Andrade, and F. Borges, "Alzheimer's disease and antioxidant therapy: how long how far?" *Current Medicinal Chemistry*, vol. 20, no. 24, pp. 2939–2952, 2013.

[116] C.-X. Peng, J. Hu, D. Liu et al., "Disease-modified glycogen synthase kinase-3β intervention by melatonin arrests the pathology and memory deficits in an Alzheimer's animal model," *Neurobiology of Aging*, vol. 34, no. 6, pp. 1555–1563, 2013.

[117] G. Benítez-King, L. Ortíz-López, G. Jiménez-Rubio, and G. Ramírez-Rodríguez, "Haloperidol causes cytoskeletal collapse in N1E-115 cells through tau hyperphosphorylation induced by oxidative stress: implications for neurodevelopment," *European Journal of Pharmacology*, vol. 644, no. 1–3, pp. 24–31, 2010.

[118] X.-C. Li, Z.-F. Wang, J.-X. Zhang, Q. Wang, and J.-Z. Wang, "Effect of melatonin on calyculin A-induced tau hyperphosphorylation," *European Journal of Pharmacology*, vol. 510, no. 1-2, pp. 25–30, 2005.

[119] J. B. Hoppe, R. L. Frozza, A. P. Horn et al., "Amyloid-β neurotoxicity in organotypic culture is attenuated by melatonin: involvement of GSK-3β, *tau* and neuroinflammation," *Journal of Pineal Research*, vol. 48, no. 3, pp. 230–238, 2010.

[120] L. Lin, Q.-X. Huang, S.-S. Yang, J. Chu, J.-Z. Wang, and Q. Tian, "Melatonin in Alzheimer's disease," *International Journal of Molecular Sciences*, vol. 14, no. 7, pp. 14575–14593, 2013.

[121] D. R. Galasko, E. Peskind, C. M. Clark et al., "Antioxidants for Alzheimer disease: a randomized clinical trial with cerebrospinal fluid biomarker measures," *Archives of Neurology*, vol. 69, no. 7, pp. 836–841, 2012.

[122] M. Cente, P. Filipcik, S. Mandakova, N. Zilka, G. Krajciova, and M. Novak, "Expression of a truncated human tau protein induces aqueous-phase free radicals in a rat model of tauopathy: implications for targeted antioxidative therapy," *Journal of Alzheimer's Disease*, vol. 17, no. 4, pp. 913–920, 2009.

[123] I. Yoon, H. L. Kwang, and J. Cho, "Gossypin protects primary cultured rat cortical cells from oxidative stress- and β-amyloid-induced toxicity," *Archives of Pharmacal Research*, vol. 27, no. 4, pp. 454–459, 2004.

[124] N. Rajasekar, S. Dwivedi, S. K. Tota et al., "Neuroprotective effect of curcumin on okadaic acid induced memory impairment in mice," *European Journal of Pharmacology*, vol. 715, no. 1–3, pp. 381–394, 2013.

[125] O. B. Villaflores, Y.-J. Chen, C.-P. Chen, J.-M. Yeh, and T.-Y. Wu, "Effects of curcumin and demethoxycurcumin on amyloid-β precursor and tau proteins through the internal ribosome entry sites: a potential therapeutic for Alzheimer's disease," *Taiwanese Journal of Obstetrics & Gynecology*, vol. 51, no. 4, pp. 554–564, 2012.

[126] Q.-L. Ma, X. Zuo, F. Yang et al., "Curcumin suppresses soluble tau dinners and corrects molecular chaperone, synaptic, and behavioral deficits in aged human tau transgenic mice," *Journal of Biological Chemistry*, vol. 288, no. 6, pp. 4056–4065, 2013.

[127] M. Mutsuga, J. K. Chambers, K. Uchida et al., "Binding of curcumin to senile plaques and cerebral amyloid angiopathy in the aged brain of various animals and to neurofibrillary tangles in Alzheimer's brain," *The Journal of Veterinary Medical Science*, vol. 74, no. 1, pp. 51–57, 2012.

[128] H. J. Stuerenburg, S. Ganzer, and T. Müller-Thomsen, "Plasma betacarotene in Alzheimer's disease—association with cerebrospinal fluid beta-amyloid 1-40, (Abeta40), beta-amyloid 1-42 (Abeta42) and total Tau," *Neuroendocrinology Letters*, vol. 26, no. 6, pp. 696–698, 2005.

[129] Y. Chen, C. Wang, M. Hu et al., "Effects of ginkgolide a on okadaic acid-induced tau hyperphosphorylation and the PI3K-Akt signaling pathway in N2a cells," *Planta Medica*, vol. 78, no. 12, pp. 1337–1341, 2012.

[130] F. V. Defeudis, "Bilobalide and neuroprotection," *Pharmacological Research*, vol. 46, no. 6, pp. 565–568, 2002.

[131] R. A. Frake, T. Ricketts, F. M. Menzies, and D. C. Rubinsztein, "Autophagy and neurodegeneration," *The Journal of Clinical Investigation*, vol. 125, no. 1, pp. 65–74, 2015.

[132] M. Damme, T. Suntio, P. Saftig, and E.-L. Eskelinen, "Autophagy in neuronal cells: general principles and physiological and pathological functions," *Acta Neuropathologica*, vol. 129, no. 3, pp. 337–362, 2015.

[133] A. Yamamoto and Z. Yue, "Autophagy and its normal and pathogenic states in the brain," *Annual Review of Neuroscience*, vol. 37, no. 1, pp. 55–78, 2014.

[134] R. A. Nixon, "The role of autophagy in neurodegenerative disease," *Nature Medicine*, vol. 19, no. 8, pp. 983–997, 2013.

[135] A. Efeyan, W. C. Comb, and D. M. Sabatini, "Nutrient-sensing mechanisms and pathways," *Nature*, vol. 517, no. 7534, pp. 302–310, 2015.

[136] J. Bové, M. Martínez-Vicente, and M. Vila, "Fighting neurodegeneration with rapamycin: mechanistic insights," *Nature Reviews Neuroscience*, vol. 12, no. 8, pp. 437–452, 2011.

[137] S. F. Funderburk, B. K. Marcellino, and Z. Yue, "Cell 'self-eating' (autophagy) mechanism in Alzheimer's disease," *Mount Sinai Journal of Medicine*, vol. 77, no. 1, pp. 59–68, 2010.

[138] L. Li, X. Zhang, and W. Le, "Autophagy dysfunction in Alzheimer's disease," *American Journal of Neurodegenerative Disease*, vol. 7, no. 4, pp. 265–271, 2010.

[139] M. Ułamek-Kozioł, W. Furmaga-Jabłońska, S. Januszewski et al., "Neuronal autophagy: self-eating or self-cannibalism in Alzheimer's disease," *Neurochemical Research*, vol. 38, no. 9, pp. 1769–1773, 2013.

[140] J. L. Jewell, R. C. Russell, and K. L. Guan, "Amino acid signalling upstream of mTOR," *Nature Reviews Molecular Cell Biology*, vol. 14, no. 3, pp. 133–139, 2013.

[141] Z. Cai and L. J. Yan, "Rapamycin, autophagy, and Alzheimer's disease," *Journal of Biochemical and Pharmacological Research*, vol. 1, no. 2, pp. 84–90, 2013.

[142] E. A. Dunlop and A. R. Tee, "The kinase triad, AMPK, mTORC1 and ULK1, maintains energy and nutrient homoeostasis," *Biochemical Society Transactions*, vol. 41, no. 4, pp. 939–943, 2013.

[143] Y. Ishizuka, N. Kakiya, L. A. Witters et al., "AMP-activated protein kinase counteracts brain-derived neurotrophic factor-induced mammalian target of rapamycin complex 1 signaling in neurons," *Journal of Neurochemistry*, vol. 127, no. 1, pp. 66–77, 2013.

[144] C. H. Jung, M. Seo, N. M. Otto, and D.-H. Kim, "ULK1 inhibits the kinase activity of mTORC1 and cell proliferation," *Autophagy*, vol. 7, no. 10, pp. 1212–1221, 2011.

[145] M. C. Maiuri, S. A. Malik, E. Morselli et al., "Stimulation of autophagy by the p53 target gene Sestrin2," *Cell Cycle*, vol. 8, no. 10, pp. 1571–1576, 2009.

[146] E. Y. W. Chan, A. Longatti, N. C. McKnight, and S. A. Tooze, "Kinase-inactivated ULK proteins inhibit autophagy via their conserved C-terminal domains using an Atg13-independent mechanism," *Molecular and Cellular Biology*, vol. 29, no. 1, pp. 157–171, 2009.

[147] S. Sarkar, R. A. Floto, Z. Berger et al., "Lithium induces autophagy by inhibiting inositol monophosphatase," *Journal of Cell Biology*, vol. 170, no. 7, pp. 1101–1111, 2005.

[148] J. Zou, F. Yue, X. Jiang, W. Li, J. Yi, and L. Liu, "Mitochondrion-associated protein LRPPRC suppresses the initiation of basal levels of autophagy via enhancing Bcl-2 stability," *Biochemical Journal*, vol. 454, no. 3, pp. 447–457, 2013.

[149] M. Alirezaei, W. B. Kiosses, and H. S. Fox, "Decreased neuronal autophagy in HIV dementia: a mechanism of indirect neurotoxicity," *Autophagy*, vol. 4, no. 7, pp. 963–966, 2008.

[150] T. Shpilka, H. Weidberg, S. Pietrokovski, and Z. Elazar, "Atg8: an autophagy-related ubiquitin-like protein family," *Genome Biology*, vol. 12, no. 7, article 226, 2011.

[151] R. Kang, H. J. Zeh, M. T. Lotze, and D. Tang, "The Beclin 1 network regulates autophagy and apoptosis," *Cell Death and Differentiation*, vol. 18, no. 4, pp. 571–580, 2011.

[152] J. D. Lünemann, J. Schmidt, D. Schmid et al., "β-Amyloid is a substrate of autophagy in sporadic inclusion body myositis," *Annals of Neurology*, vol. 61, no. 5, pp. 476–483, 2007.

[153] P. A. Jaeger, F. Pickford, C.-H. Sun, K. M. Lucin, E. Masliah, and T. Wyss-Coray, "Regulation of amyloid precursor protein processing by the beclin 1 complex," *PLoS ONE*, vol. 5, no. 6, Article ID e11102, 2010.

[154] J. F. Ma, Y. Huang, S. D. Chen, and G. Halliday, "Immunohistochemical evidence for macroautophagy in neurones and endothelial cells in Alzheimer's disease," *Neuropathology and Applied Neurobiology*, vol. 36, no. 4, pp. 312–319, 2010.

[155] W. H. Yu, A. M. Cuervo, A. Kumar et al., "Macroautophagy—a novel Beta-amyloid peptide-generating pathway activated in

Alzheimer's disease," *The Journal of Cell Biology*, vol. 171, no. 1, pp. 87–98, 2005.

[156] J. Perucho, M. J. Casarejos, A. Gomez, R. M. Solano, J. G. de Yébenes, and M. A. Mena, "Trehalose protects from aggravation of amyloid pathology induced by isoflurane anesthesia in APPswe mutant mice," *Current Alzheimer Research*, vol. 9, no. 3, pp. 334–343, 2012.

[157] A. Y. Lai and J. McLaurin, "Inhibition of amyloid-beta peptide aggregation rescues the autophagic deficits in the TgCRND8 mouse model of Alzheimer disease," *Biochimica et Biophysica Acta—Molecular Basis of Disease*, vol. 1822, no. 10, pp. 1629–1637, 2012.

[158] J. Wei, M. Fujita, M. Nakai et al., "Protective role of endogenous gangliosides for lysosomal pathology in a cellular model of synucleinopathies," *The American Journal of Pathology*, vol. 174, no. 5, pp. 1891–1909, 2009.

[159] R. A. Nixon, D.-S. Yang, and J.-H. Lee, "Neurodegenerative lysosomal disorders: a continuum from development to late age," *Autophagy*, vol. 4, no. 5, pp. 590–599, 2008.

[160] S. M. Cardoso, C. F. Pereira, P. I. Moreira, D. M. Arduino, A. R. Esteves, and C. R. Oliveira, "Mitochondrial control of autophagic lysosomal pathway in Alzheimer's disease," *Experimental Neurology*, vol. 223, no. 2, pp. 294–298, 2010.

[161] D. F. F. Silva, A. R. Esteves, D. M. Arduino, C. R. Oliveira, and S. M. Cardoso, "Amyloid-β-induced mitochondrial dysfunction impairs the autophagic lysosomal pathway in a tubulin dependent pathway," *Journal of Alzheimer's Disease*, vol. 26, no. 3, pp. 565–581, 2011.

[162] Y. Wang and E. Mandelkow, "Degradation of tau protein by autophagy and proteasomal pathways," *Biochemical Society Transactions*, vol. 40, no. 4, pp. 644–652, 2012.

[163] A. Caccamo, A. Magrì, D. X. Medina et al., "mTOR regulates tau phosphorylation and degradation: implications for Alzheimer's disease and other tauopathies," *Aging Cell*, vol. 12, no. 3, pp. 370–380, 2013.

[164] Y. Liu, Y. Su, J. Wang et al., "Rapamycin decreases tau phosphorylation at Ser214 through regulation of cAMP-dependent kinase," *Neurochemistry International*, vol. 62, no. 4, pp. 458–467, 2013.

[165] S. Ozcelik, G. Fraser, P. Castets et al., "Rapamycin attenuates the progression of tau pathology in P301S tau transgenic mice," *PLoS ONE*, vol. 8, no. 5, Article ID e62459, 2013.

[166] P. J. Dolan and G. V. W. Johnson, "A caspase cleaved form of tau is preferentially degraded through the autophagy pathway," *The Journal of Biological Chemistry*, vol. 285, no. 29, pp. 21978–21987, 2010.

[167] U. Krüger, Y. Wang, S. Kumar, and E.-M. Mandelkow, "Autophagic degradation of tau in primary neurons and its enhancement by trehalose," *Neurobiology of Aging*, vol. 33, no. 10, pp. 2291–2305, 2012.

[168] S.-I. Kim, W.-K. Lee, S.-S. Kang et al., "Suppression of autophagy and activation of glycogen synthase kinase 3beta facilitate the aggregate formation of tau," *The Korean Journal of Physiology & Pharmacology*, vol. 15, no. 2, pp. 107–114, 2011.

[169] F. Lim, F. Hernández, J. J. Lucas, P. Gómez-Ramos, M. A. Morán, and J. Ávila, "FTDP-17 mutations in tau transgenic mice provoke lysosomal abnormalities and tau filaments in forebrain," *Molecular and Cellular Neuroscience*, vol. 18, no. 6, pp. 702–714, 2001.

[170] W.-L. Lin, J. Lewis, S.-H. Yen, M. Hutton, and D. W. Dickson, "Ultrastructural neuronal pathology in transgenic mice expressing mutant (P301L) human tau," *Journal of Neurocytology*, vol. 32, no. 9, pp. 1091–1105, 2003.

[171] A. Magnaudeix, C. M. Wilson, G. Page et al., "PP2A blockade inhibits autophagy and causes intraneuronal accumulation of ubiquitinated proteins," *Neurobiology of Aging*, vol. 34, no. 3, pp. 770–790, 2013.

[172] S. Y. Yoon, J. E. Choi, H.-S. Kweon et al., "Okadaic acid increases autophagosomes in rat neurons: implications for Alzheimer's disease," *Journal of Neuroscience Research*, vol. 86, no. 14, pp. 3230–3239, 2008.

[173] T. Hamano, T. F. Gendron, E. Causevic et al., "Autophagic-lysosomal perturbation enhances tau aggregation in transfectants with induced wild-type tau expression," *European Journal of Neuroscience*, vol. 27, no. 5, pp. 1119–1130, 2008.

[174] Y. Wang, M. Martinez-Vicente, U. Krüger et al., "Tau fragmentation, aggregation and clearance: the dual role of lysosomal processing," *Human Molecular Genetics*, vol. 18, no. 21, pp. 4153–4170, 2009.

Hindawi Publishing Corporation
Oxidative Medicine and Cellular Longevity
Volume 2015, Article ID 186736, 11 pages
http://dx.doi.org/10.1155/2015/186736

Clinical Study

Dexmedetomidine Analgesia Effects in Patients Undergoing Dental Implant Surgery and Its Impact on Postoperative Inflammatory and Oxidative Stress

Sisi Li,[1] Yang Yang,[1] Cong Yu,[1] Ying Yao,[1] Yujia Wu,[1] Lian Qian,[2] and Chi Wai Cheung[3]

[1]*Department of Anesthesia, Chongqing Key Laboratory for Oral Diseases and Biomedical Sciences, Stomatology Hospital of Chongqing Medical University, No. 426 Songshibeilu, Yubei District, Chongqing 401146, China*
[2]*Duke-NUS Graduate Medical School Singapore, Singapore 169857*
[3]*Department of Anesthesiology, The University of Hong Kong, Hong Kong*

Correspondence should be addressed to Cong Yu; yucongab@sina.com

Received 15 September 2014; Accepted 18 November 2014

Academic Editor: Mengzhou Xue

The aim of the study was to determine whether or not dexmedetomidine- (DEX-) based intravenous infusion in dental implantation can provide better sedation and postoperative analgesia via suppressing postoperative inflammation and oxidative stress. Sixty patients were randomly assigned to receive either DEX (group D) or midazolam (group M). Recorded variables were vital sign (SBP/HR/RPP/SpO_2/RR), visual analogue scale (VAS) pain scores, and observer's assessment of alertness/sedation scale (OAAS) scores. The plasma levels of interleukin-6 (IL-6), tumor necrosis factor alpha (TNF-α), antioxidant superoxide dismutase (SOD), and the lipid peroxidation product malondialdehyde (MDA) were detected at baseline and after 2, 4, and 24 h of drug administration. The VAS pain scores and OAAS scores were significantly lower for patients in group D compared to group M. The plasma levels of TNF-α, IL-6, and MDA were significantly lower in group D patients than those in group M at 2 h and 4 h. In group M, SOD levels decreased as compared to group D at 2 h and 4 h. The plasma levels of TNF-α, IL-6, and MDA were positively correlated with VAS pain scores while SOD negatively correlated with VAS pain scores. Therefore, DEX appears to provide better sedation during office-based artificial tooth implantation. DEX offers better postoperative analgesia via anti-inflammatory and antioxidation pathway.

1. Introduction

Dental implants are considered one of the most common and popular treatment options for edentulous patients in modern dentistry. However, dental implantation remains significantly associated with pain and high levels of anxiety [1, 2]. Implant surgery requires bone preparation, sometimes flap and bone graft treatment. This usually results in tissue ischemia [3] and acute inflammation [4, 5] with concomitant increase in oxidative stress. Mild, even severe pain following implant surgery is extremely to be expected [6]. Implant surgery causes tissue injury, resulting in pain hypersensitivity, as a result of peripheral sensitization (sensitization of primary sensory neurons) [7, 8] and central sensitization (sensitization of spinal cord and brain neurons) [9–11]. More and more dental patients choose general anaesthesia for comfortable and painless surgery. In these cases, the most widely used form is the combination of benzodiazepine with opioid [12, 13]. Our previous study indicated that the DEX/fentanyl regimen appears to be better than the traditional midazolam/fentanyl regimen in terms of intraoperative arousal, patient-surgeon cooperation, postoperative analgesia, and surgeon satisfaction in office-based unilateral impacted tooth extraction [14]. However, the effects and detailed mechanisms of postoperative analgesia effect of DEX in patients undergoing dental implantation surgery have yet to be revealed.

DEX, a selective agonist of α_2-adrenergic receptor, selectively binds to presynaptic α_2 adrenergic receptors norepinephrine release, resulting in a reduction of postsynaptic adrenergic activity [15]. DEX is a potent sedative agent and

also provides analgesia and anxiolytic and sympatholytic effects and has minimal influence on respiratory physiology. Along with its beneficial effects, DEX was reported to exert potential anti-inflammatory and antioxidant effects. Previous studies revealed that DEX significantly decreased the levels of inflammatory cytokines during postpartum bleeding-induced multiple organ dysfunction syndrome in rats [16], in polymicrobial sepsis in mice [17], during cardiac surgery with cardiopulmonary bypass in human [18], and in lung injury in dogs [19] and laparoscopic cholecystectomy in human [20]. DEX also significantly decreased the levels of free radicals on ischemia-reperfusion injury of epigastric island flaps of rats [21] and ischemic rat hippocampus [22]. Our research chose proinflammatory IL-6, TNF-α, SOD, and MDA to reflect inflammatory and oxidation conditions in vivo.

It has been proposed that irrespective of the characteristic of the pain, whether it is sharp, dull, aching, burning, stabbing, numbing, or tingling, all pains arise from inflammation and the inflammatory response [23]. Our study aims to investigate the sedation and analgesia effect of DEX during and after implant surgery compared with midazolam and whether DEX offered better postoperative analgesia by regulating the inflammatory and oxidative stress.

2. Materials and Methods

2.1. Subjects and Study Protocol. Sixty patients enrolled in this project either have previously used DEX, midazolam, paracetamol, and other nonsteroidal anti-inflammatory drugs or had no known allergy to these drugs. All patients provided written informed consent. The patients were of American Society of Anesthesiology (ASA) physical status I or II, between 19 and 60 years old, and with mandibular teeth defect (33, 34, and 35 or 43, 44, and 45). The patients were to have 3 dental implants to be placed and flap and bone graft were to be performed during surgery. Patients were excluded if they had a clinical history or electrocardiographic evidence of heart block, ischemic heart disease, asthma, sleep apnea syndrome, impaired liver or renal function, known psychiatric illness, diabetes, facial pain, psychological problems, smoking history, or chronic use of sedative or analgesic drugs or opioids. Also excluded were those who refused to participate, were pregnant, or presented with preoperative inflammation at the site of surgery.

The 60 patients were randomly divided into two treatment groups using a computer-generated random list. Patients were infused either with midazolam and fentanyl (group M) or with DEX and fentanyl (group D). Each patient had an intravenous cannula inserted. Investigators who were not directly involved in the care of the patient prepared the infusions, while the dental surgeon, anesthetist, and the patients were blinded to the group allocation and drugs given.

Patients in group D received DEX (1.0 μg/kg) and fentanyl (0.001 mg/kg) in 20 mL of normal saline for 10 min and then a continuous infusion of DEX (1.0 μg/kg/h) until the end of the surgery. Patients in group M received midazolam (0.05 mg/kg) and fentanyl (0.001 mg/kg) in 20 mL of normal saline for 10 min, followed by a continuous infusion of midazolam (0.05 mg/kg/h) until the end of the surgery. Ten minutes after the start of the loading dose, local anesthesia was provided with 4% hydrochloric articaine and 1/100000 adrenaline, administered by qualified dental surgeons. Surgeons then performed the standard surgical procedure during which patients were provided with a mouth prop to help keep the mouth open when required. At the end of the operation, patients were kept in the recovery area 4 h after drug administration. Patients were prescribed one analgesic tablet containing 500 mg of paracetamol and then oral amoxicillin capsule 500 mg three times a day and ornidazole capsule 500 mg twice a day until 7 days after surgery.

2.2. Enzyme-Linked Immunosorbent Assay (ELISA). Venous blood samples (3.0 mL each) were drawn at 0, 2, 4, and 24 hours after drug administration for the measurement of plasma cytokines. Plasma samples were immediately separated by centrifugation at 3,000 rpm for 10 min at 4°C and then divided into aliquots and stored at −80°C for subsequent assays by highly sensitive enzyme-linked immunosorbent assays (ELISA) kits to detect the proinflammatory cytokine (IL-6, TNF-α), antioxidant enzyme superoxide dismutase (SOD), and serum levels of lipid peroxidation product (MDA).

The production lot numbers and manufacturer of ELISA kits are SOD Human ELISA Kit (ab119694, abcam, UK); MDA Human ELISA Kit (E90597Hu, biorbyt, UK); TNF-α Human ELISA (BMS223/4CE, eBioscience, USA); Interleukin-6 Human ELISA Kit (501030-96, Cayman, USA).

2.3. Outcome Measures. All indices were recorded before initiating sedation (i.e., baseline) and then at 15 min intervals until 4 h after the start of drug infusion. Systolic blood pressure (SBP), heart rate (HR), rate-pressure product (RPP), breathing rate (RR), and saturation of pulse oxygen (SpO_2) were recorded at 15 min intervals until 4 h after the start of drug infusion. Sedation levels were assessed using observer's assessment of alertness/sedation scale (OAAS). The patients evaluated their level of pain subjectively using a VAS ruler, with zero representing no pain and 10 the worst pain the patient had ever experienced.

2.4. Statistical Analyses. All variables were tested for normal distribution using the Shapiro-Wilk test. The data are expressed as the mean ± standard deviation (SD), median and interquartile range (IQR), or number. The OAAS and VAS scores were analyzed using the Kruskal-Wallis test. SpO_2, HR, RR, and SBP values, age, weight, duration of surgery, number of dental implants, total volume of local anaesthetic used, TNF-α, IL-6, SOD, and MDA concentration were analyzed using the two-sample t-test. Gender was analyzed using the χ^2 test. The correlation between VAS and SOD, VAS and MDA, VAS and TNF-α, TNF-α and MDA, TNF-α and SOD was analyzed using Spearman rank correlation analysis. Statistical analyses were performed using the commercial software SPSS17.0 (SPSS, Institute, Chicago, IL, USA). P values of <0.05 were considered statistically significant.

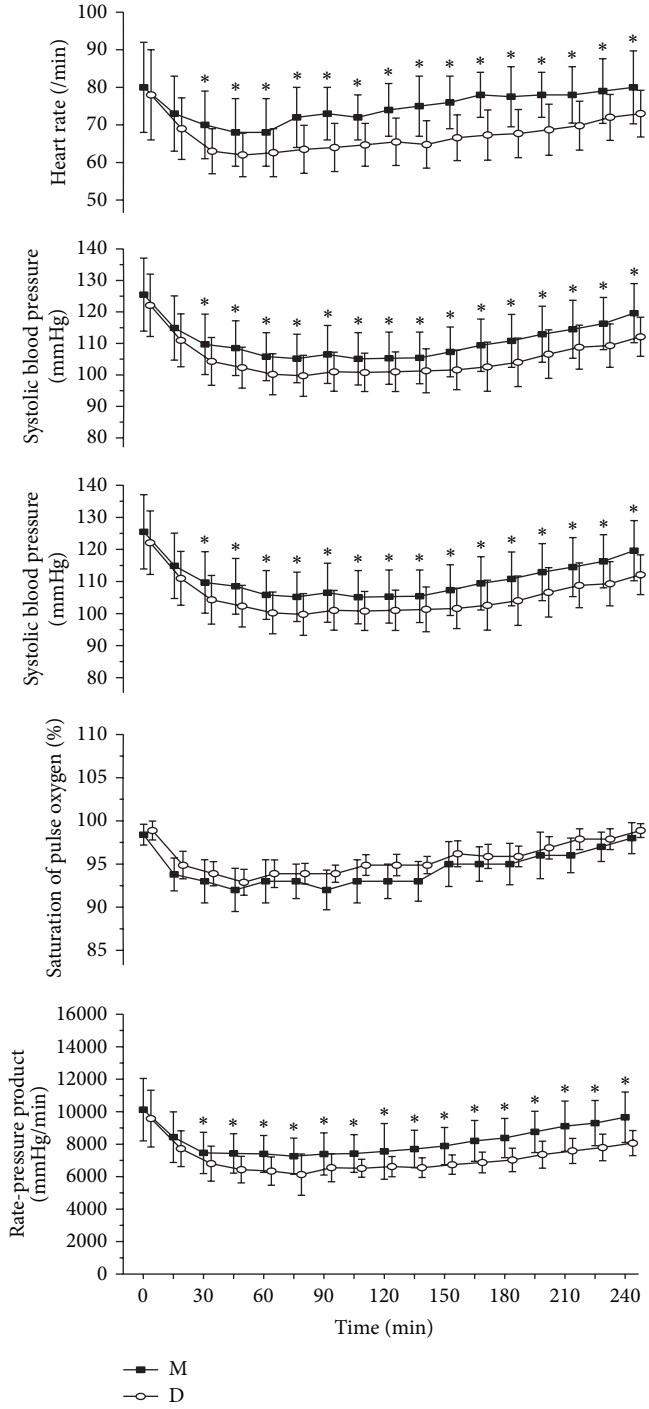

Figure 1: Heart rate, systolic blood pressure values, respiratory rate, saturation of pulse oxygen, and rate-pressure product (mean ± SD) for the two treatment groups (group M and group D) during the course of 240 min. Time 0 min = before drug administration. M: midazolam; D: dexmedetomidine. $^{*}P < 0.05$.

3. Results

Sixty patients were recruited. The patient characteristics and operation data of both groups are shown in Table 1. There was no significant difference in demographic data, surgical characteristics, duration of operation, and total volume of local anaesthetic used between the two study groups. All patients have no preoperative inflammation at the site of surgery. There was also no difference in the overall preoperative pain scores.

3.1. SpO_2, RR, and Haemodynamic Effects. Figure 1 shows the mean SBP, HR, SpO_2, RR, and RPP at different time points in each group. The SBP, HR, and RPP of group D became

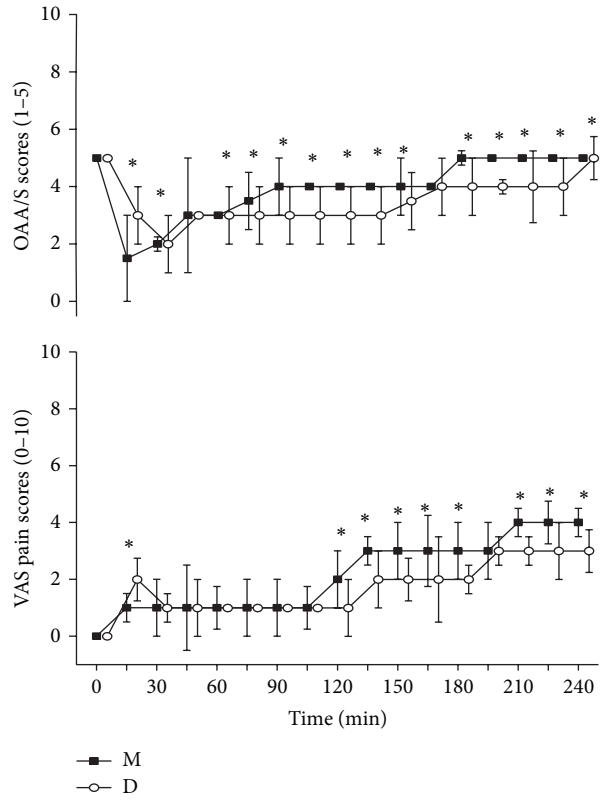

Figure 2: OAAS and VAS pain scores (median ± IQR) for the two treatment groups (group M and group D) during the course of 240 min. Time 0 min = before drug administration. M: midazolam; D: dexmedetomidine. $^{*}P < 0.05$.

Table 1: Clinical characteristics of patients for the two treatment groups, D and M.

Variables	Group D ($n = 30$)	Group M ($n = 30$)	P value
Age (year)	41.61 ± 9.82	43.34 ± 8.43	0.491
Body weight (kg)	61.12 ± 8.63	59.20 ± 7.73	0.384
Males/females	19/11	18/12	0.070
Duration of surgery (min)	60.16 ± 12.21	62.83 ± 10.72	0.372
Number of dental implants	2.53 ± 0.51	2.50 ± 0.51	0.800
Total volume of local anaesthetic used (mL)	1.72 ± 0.38	1.85 ± 0.43	0.232

M: midazolam; D: dexmedetomidine. Data shown are the number or mean ± standard deviation.

significantly lower than those of group M 30–45 min after drug administration and remained so for the rest of the study. There was no difference in SpO_2 or RR between groups D and M.

3.2. Sedative and Analgesic Effects. Figure 2 graphically displays the median ± IQR. OAAS scores and VAS pain scores in both treatment groups were recorded at 15 min intervals until 4h after the start of drug infusion. The sedation level of group D became significantly different from that of group M 60–75 min after drug administration, and the differences remained statistically significant for the rest of the study period. The OAAS scores of group M were lower than that of group D 15–35 min after drug administration. Main reasons are as follows: the onset time of midazolam was 30~60 seconds and it takes 5 minutes to reach peak plasma drug concentration. However the onset time of DEX was 10~15 min and it takes 25~30 minutes to reach peak plasma drug concentration. The VAS pain scores in group D and group M were not statistically different after 30–120 min but became lower than that in group M after 120–240 min after drug administration. The pain is more intense as the local anesthetic wears off. DEX has analgesic effect but midazolam has not. Midazolam has shorter onset time relative to DEX, so the VAS pain score of group M was lower than that of group D 15 min after drug administration.

3.3. Anti-Inflammatory and Antioxidant Effects. As shown in Figure 3, plasma SOD levels were not statistically different either at baseline (0 h) or at 24 h after drug administration in both groups. However, significant reduction of SOD was seen in group M but not in group D at 2, 4 h after drug administration ($P < 0.05$ group D versus group M) (Figure 3(a)), indicating that DEX prevented the reduction in plasma SOD levels. Similarly, plasma MDA level was not statistically different 0, 24 h after drug administration in both groups,

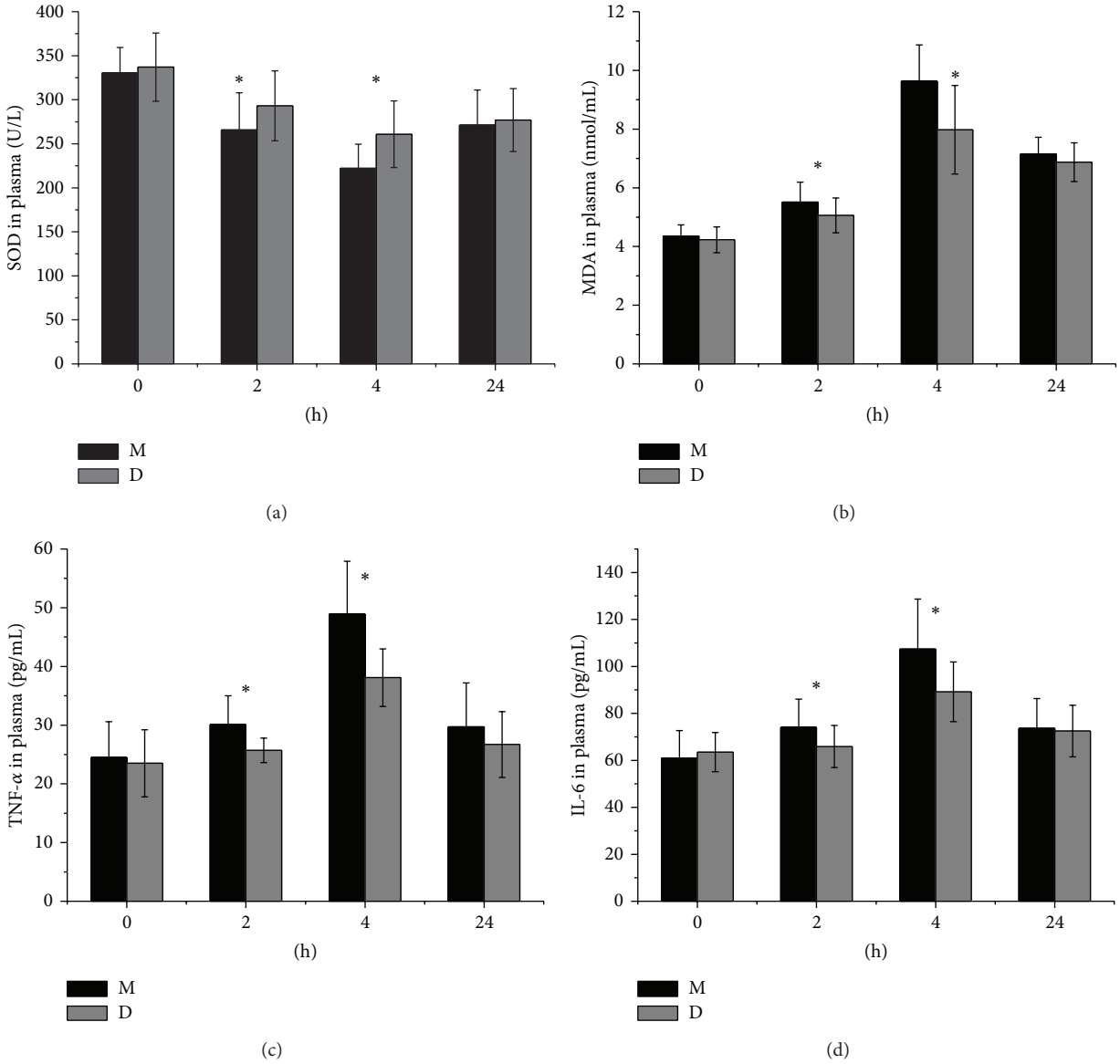

Figure 3: Plasma SOD, MDA, TNF-α, and IL-6 concentrations (mean ± SD) were investigated in each plasma sample for the two treatment groups (group M and group D). Time 0 h = before drug administration. Time 2 h = 2 h after drug administration. Time 4 h = 4 h after drug administration. Time 24 h = 24 h after drug administration. M: midazolam; D: dexmedetomidine. $^*P < 0.05$.

while plasma MDA levels in group D were lower than group M 2, 4 h after drug administration ($P < 0.05$, Figure 3(b)). Plasma levels of IL-6 and TNF-α were lower in group D than those in group M at 2 and 4 h after drug administration ($P < 0.05$, $P < 0.05$, Figures 3(c) and 3(d)). Plasma TNF-α and IL-6 levels were not statistically different 0, 24 h after drug administration in both groups (Figures 3(c) and 3(d)).

3.4. Correlation Analysis. We surmised that DEX offered better postoperative analgesia by regulating the inflammatory and oxidation factors. The correlation analyses between VAS pain scores and plasma concentrations of SOD, MDA, TNF-α, and IL-6 at 2, 4 after drug administration are shown in Table 2. Spearman analysis showed that VAS pain scores and plasma SOD content of the two groups were negatively correlated at 2, 4 h after drug administration. VAS pain scores and plasma MDA content were positively correlated. VAS pain scores were also positively correlated with plasma TNF-α and IL-6 content (Figures 4 and 5). Inflammation may contribute to oxidizing reaction. Our results showed that plasma TNF-α and SOD content of the two groups were negatively correlated, while plasma TNF-α and MDA content of the two groups were positively correlated (Figure 6).

4. Discussion

We have shown in the current study that DEX offered better sedation and postoperative analgesia on implant surgery

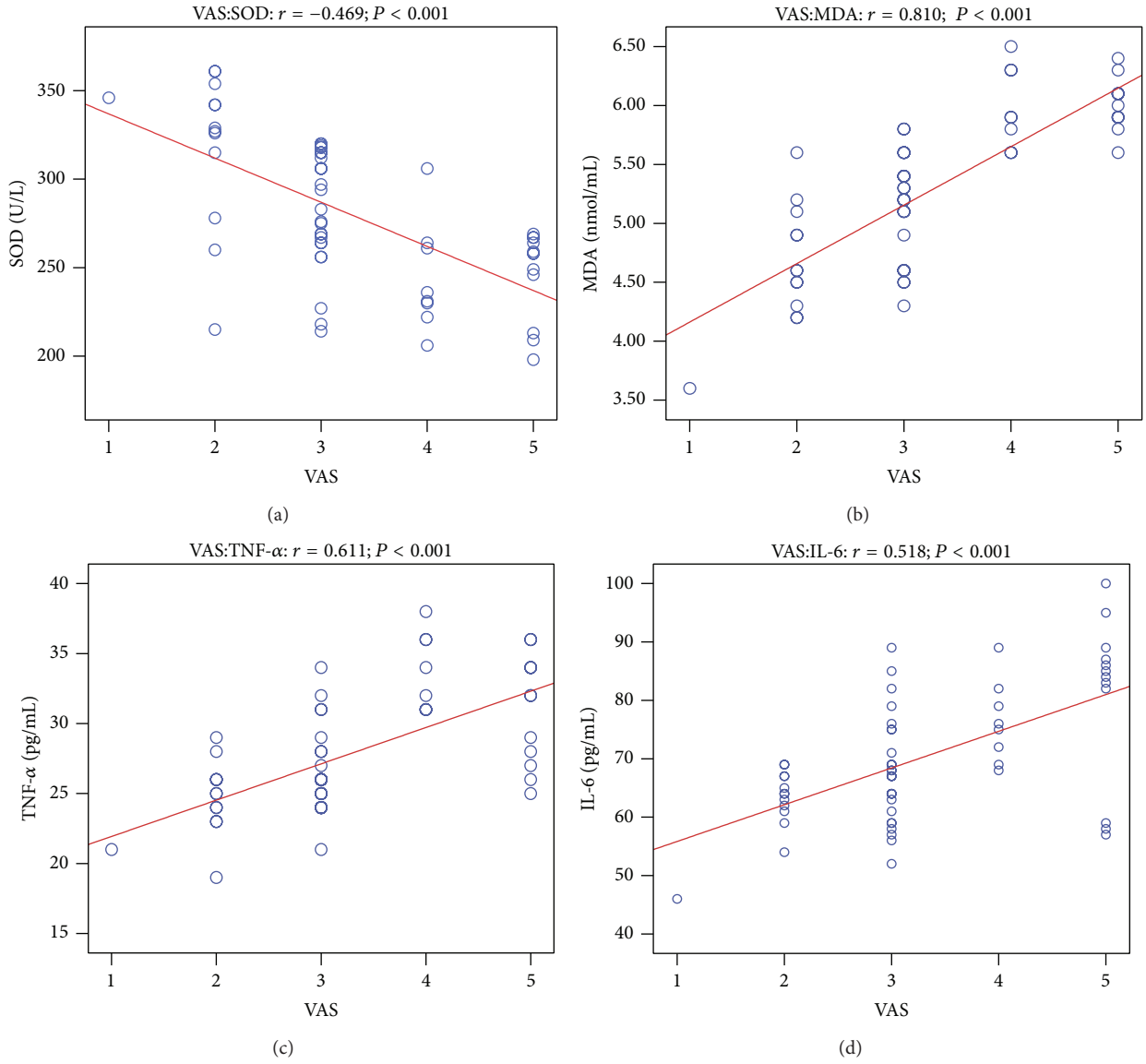

Figure 4: The correlation analysis between VAS pain scores and plasma concentrations of SOD, MDA, TNF-α, and IL-6 at 2 after drug administration. VAS pain scores versus SOD (a); VAS pain scores versus MDA (b); VAS pain scores versus TNF-α (c); VAS pain scores versus IL-6 (d).

compared with midazolam, which was associated with more pronounced reductions of postoperative plasma levels of TNF-α, IL-6, and MDA and an increase in SOD. The positive correlations between VAS and TNF-α, IL-6, and SOD provide evidence to suggest that DEX could offer better postoperative analgesia by suppressing inflammatory and oxidation response during implant surgery.

In addition to treatment for sedation and analgesia, the most significant adverse reactions associated with DEX are hypotension and bradycardia. DEX has been administered to hypertensive patients during surgery [24], suggesting a relaxing effect on peripheral vessels. Previous studies reported that RPP was one of the major determinants of myocardial oxygen consumption and RPP > 20,000 mmHg min^{-1} could precipitate angina pectoris [25]. No patient had an RPP of more than 20,000 mmHg min^{-1} in our study. The effect of DEX on lowering SBP, HR, and RPP could decrease the myocardial oxygen requirement and may be advantageous for patients at risk of coronary artery disease [26]. DEX can be titrated to the desired level of sedation without significant respiratory depression [27]. Midazolam often causes respiratory depression, especially with fentanyl or other opioids [28]. In the present study the SpO_2 and RR did not differ significantly between the groups, despite the fact that the SBP and HR values slightly lower in group D. No incidence of cardiovascular instability that required intervention occurred in any of the patients.

Pain, inflammation, and postoperative trismus are the main symptoms following implant surgery. The pain is more intense from the first three to five hours as the local anesthetic

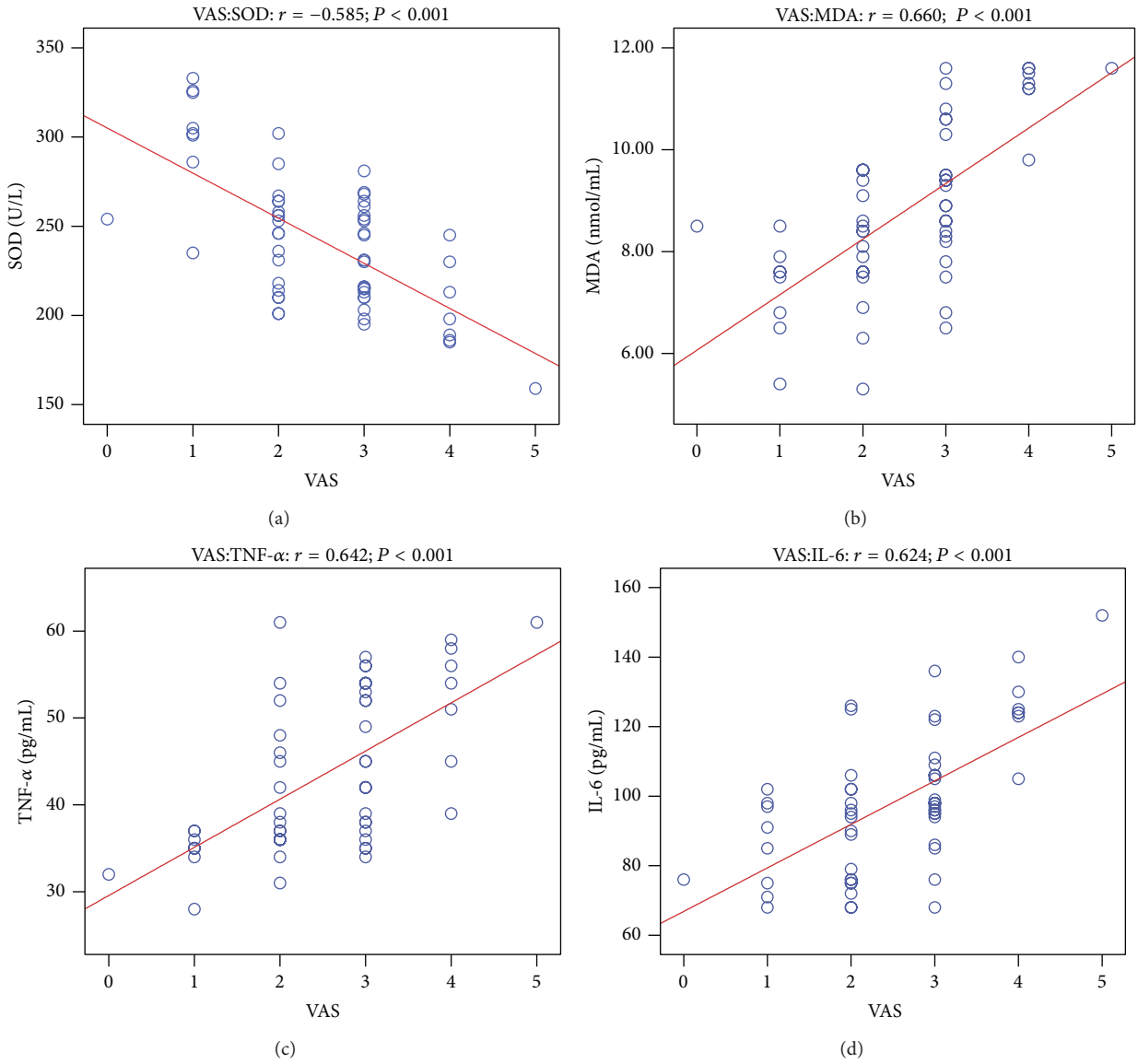

Figure 5: The correlation analysis between VAS pain scores and plasma concentrations of SOD, MDA, TNF-α, and IL-6 at 4 after drug administration. VAS pain scores versus SOD (a); VAS pain scores versus MDA (b); VAS pain scores versus TNF-α (c); VAS pain scores versus IL-6 (d).

wears off [29]. DEX can exert analgesic effects through activation of central α_2-adrenergic receptors in the locus coeruleus [14]. In our study, VAS pain score was below about 4 in both groups during and after implant surgery. VAS pain score in group D was lower than group M during 120 min–240 min. OAAS scores of group D were lower than group M during 60 min–240 min. So, compared with midazolam, DEX offered better sedation and analgesia during and after implant surgery.

It is known that an increase in the level of proinflammatory cytokines, including TNF-α and IL-6, is an early feature of acute injury. Recent studies found that DEX has an anti-inflammatory effect by reducing the levels of inflammatory cytokines. A body of animal and clinical trials [30, 31] have shown that DEX decreases cytokine (TNF-α, IL-6) secretion after endotoxin injection and that DEX reduced the mortality rate in endotoxemia-induced shock rat models in a dose-dependent manner. In addition, several studies [32–34] have demonstrated that DEX could exert a potential protective effect by suppressing inflammatory responses on ventilator, lipopolysaccharide, or α-naphthylthiourea-induced acute lung injury. Compared to group M, our results showed that DEX exhibited potent activity in inhibiting TNF-α and IL-6 in dental surgery, particularly 4 h after drug administration. Although studies have shown the regulatory effects of DEX on inflammatory reactions, the exact mechanisms responsible for these actions are not well understood.

TNF-α is a major proinflammatory cytokine produced not only in the immune system but also in the peripheral and central nervous system, especially under the pathological

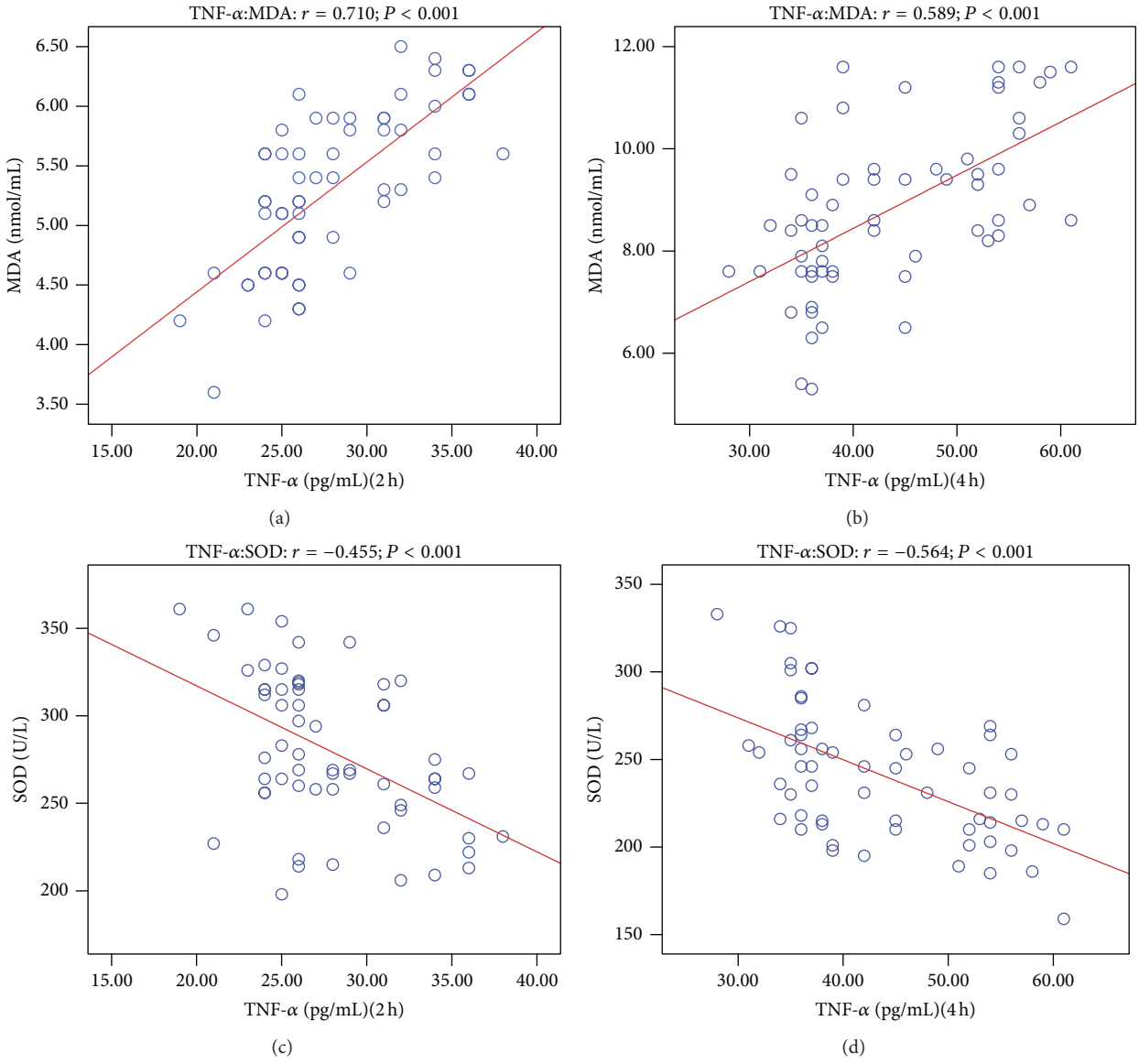

Figure 6: The correlation analysis between plasma concentrations of MDA and TNF-α after 2 h of drug administration (a); the correlation analysis between plasma concentrations of MDA and TNF-α after 4 h of drug administration (b); the correlation analysis between plasma concentrations of SOD and TNF-α after 2 h of drug administration (c); the correlation analysis between plasma concentrations of SOD and TNF-α after 4 h of drug administration (d).

conditions [35]. TNF-α is also known for its substantial role in periodontitis [36]. Increasing evidence suggests a critical role of TNF-α in the pathogenesis of pain including neuropathic pain [37, 38] and acute and persistent inflammatory pain [9, 39]. IL-6 induces muscle and joint hyperalgesia [40] and mediates the development of injury-induced hyperalgesia [41]. Following surgery, IL-6 levels are associated with postoperative pain [42]. In samples of patients with pain, levels of IL-6 have been shown to correlate with higher pain severity [43, 44]. Collectively, these findings support that proinflammatory cytokines are likely to play a facilitatory role in the development and maintenance of persistent pain syndromes. Our results showed VAS pain scores and plasma TNF-α, IL-6 content were positively correlated at 2, 4 h after drug administration. This suggests that postoperative pain may be caused by acute inflammation and that reducing inflammation cytokine release should have played an important role in DEX mediated reduction of postoperative pain in patients undergoing implant surgery.

SOD has strong antioxidant and physical activity and serves as a major free radical scavenger of body [45]. MDA, the end product of lipid peroxidation [46], was assessed in combination with SOD to evaluate the effects of DEX on oxidative stress during and after dental implant surgery in the current study. Some studies [22, 47, 48] have shown that DEX can attenuate the increase of MDA level and enhance SOD activities. In our study, the plasma MDA was higher in group M as compared to group D, while SOD activities

Table 2: The correlation analysis between VAS pain scores and plasma concentrations of SOD, MDA, TNF-α, and IL-6 at 2, 4 after drug administration.

Source	Dependent variable	Spearman correlation	Sig. (2-tailed)
VAS pain scores	SOD	-0.649^{**} (2 h)	<0.001
		-0.585^{**} (4 h)	<0.001
	MDA	0.810^{**} (2 h)	<0.001
		0.660^{**} (4 h)	<0.001
	TNF-α	0.611^{**} (2 h)	<0.001
		0.642^{**} (4 h)	<0.001
	IL-6	0.518^{**} (2 h)	<0.001
		0.624^{**} (4 h)	<0.001

**Correlation is significant at the 0.01 level (2-tailed).

were significantly lower in group M as compared to group D. These results pointed to possible antioxidant effects of DEX in the dental implant region. A few studies reported that various reactive oxygen species (ROS) scavengers and antioxidants reduce hyperalgesic behaviours in rat models of persistent pain [45]. Superoxide anion (O_2^-) is critical for sensitization of spinal neurons and persistent pain [49, 50]. Antioxidant enzyme SOD is concerned with the removal of superoxide anion. One study shows that saliva and serum antioxidants and serum MDA levels were elevated in patients with complex regional pain syndrome-type I [50]. Our results showed VAS pain scores and plasma SOD content of the two groups were negatively correlated. VAS pain scores and plasma MDA content were positively correlated. This suggests that postoperative pain may be caused in part by acute oxidative stress reaction. Thus, reduction of postoperative oxidative stress should also play an important role in DEX mediated attenuation of pain.

An exaggerated inflammatory response to tissue injury, ischemia, and reperfusion injuries can all result in excessive production of free radicals [51]. Free radicals, in turn, can increase vascular permeability, release neuropeptides (i.e., substance P), enhance inflammation, and cause further tissue damage [52, 53]. TNF-α increased the levels of superoxide anion and MDA and then induced oxidative stress and cell toxicity [54, 55]. A small dose of hydrogen peroxide enhances toxicity of TNF-α in inducing human vascular endothelial cell apoptosis [56]. Our result showed that plasma TNF-α and MDA, SOD content were correlated closely. While correlation relationship does not necessarily indicate a causal relationship, the findings of our current study provide mechanistic clues for future in-depth study to elucidate the mechanism of dexmedetomidine in clinical settings.

5. Conclusions

Our study demonstrates that DEX appears to provide better sedation, postoperative analgesia than traditional medicine midazolam during office-based artificial tooth implantation. Further, our findings provide evidence to suggest that reduction of postoperative inflammatory and oxidative stress plays important role in DEX postoperative analgesic effects, although detailed mechanism needs further study.

Conflict of Interests

The authors declare that there is no conflict of interests regarding the publication of this paper.

Acknowledgments

The Medical Ethics Committee of the Stomatology Hospital of Chongqing Medical University approved this study. This study was supported by the Research Project of Health Bureau of Chongqing (2013-1-031, Chongqing, China) and the Chongqing Science & Technology Commission (cstc2014yykfB10010, Chongqing, China). This study was conducted from February 2013 to March 2014. The authors thank surgeons from Implant Department of the Stomatology Hospital of Chongqing Medical University, China, and the peers of previously published papers on this topic.

References

[1] S. C. Pani, B. AlGarni, L. M. AlZain, and N. S. AlQahtani, "Assessment of the impact of stress and anxiety on pain perception in patients undergoing surgery for placement of their first dental implant," *Oral Health and Dental Management*, vol. 13, no. 2, pp. 464–468, 2014.

[2] M. Morino, C. Masaki, Y. Seo et al., "Non-randomized controlled prospective study on perioperative levels of stress and dysautonomia during dental implant surgery," *Journal of Prosthodontic Research*, vol. 58, no. 3, pp. 177–183, 2014.

[3] R. Gvetadze, E. K. Krechina, S. V. Abramian, A. A. Ivanov, and A. P. Nubarian, "Study of blood circulation microdynamics in gingival mucosa after dental implantation with the use of custom-made healing abutments," *Stomatologiia*, vol. 92, no. 3, pp. 109–111, 2013.

[4] Z. Vlahovic, A. Markovic, M. Golubovic, M. Scepanovic, M. Kalanovic, and A. Djinic, "Histopathological comparative analysis of peri-implant soft tissue response after dental implant placement with flap and flapless surgical technique. Experimental study in pigs," *Clinical Oral Implants Research*, 2014.

[5] A. Figueiredo, P. Coimbra, A. Cabrita, F. Guerra, and M. Figueiredo, "Comparison of a xenogeneic and an alloplastic material used in dental implants in terms of physico-chemical characteristics and in vivo inflammatory response," *Materials Science and Engineering C*, vol. 33, no. 6, pp. 3506–3513, 2013.

[6] Y. K. Kim, H. S. Kim, Y. J. Yi, and P. Y. Yun, "Evaluation of subjective satisfaction of dental implant patients," *Journal of the Korean Association of Oral and Maxillofacial Surgeons*, vol. 40, no. 3, pp. 130–134, 2014.

[7] A. I. Basbaum, D. M. Bautista, G. Scherrer, and D. Julius, "Cellular and molecular mechanisms of pain," *Cell*, vol. 139, no. 2, pp. 267–284, 2009.

[8] T. Hucho and J. D. Levine, "Signaling pathways in sensitization: toward a nociceptor cell biology," *Neuron*, vol. 55, no. 3, pp. 365–376, 2007.

[9] Z. Z. Xu, L. Zhang, T. Liu et al., "Resolvins RvE1 and RvD1 attenuate inflammatory pain via central and peripheral actions," *Nature Medicine*, vol. 16, no. 5, pp. 592–597, 2010.

[10] P. W. Mantyh and S. P. Hunt, "Setting the tone: superficial dorsal horn projection neurons regulate pain sensitivity," *Trends in Neurosciences*, vol. 27, no. 10, pp. 582–584, 2004.

[11] R.-R. Ji, T. Kohno, K. A. Moore, and C. J. Woolf, "Central sensitization and LTP: do pain and memory share similar mechanisms?" *Trends in Neurosciences*, vol. 26, no. 12, pp. 696–705, 2003.

[12] Ö. Göktay, T. Satilmiş, H. Garip, O. Gönül, and K. Göker, "A comparison of the effects of midazolam/fentanyl and midazolam/tramadol for conscious intravenous sedation during third molar extraction," *Journal of Oral and Maxillofacial Surgery*, vol. 69, no. 6, pp. 1594–1599, 2011.

[13] P. Zeyneloglu, A. Pirat, S. Candan, S. Kuyumcu, I. Tekin, and G. Arslan, "Dexmedetomidine causes prolonged recovery when compared with midazolam/fentanyl combination in outpatient shock wave lithotripsy," *European Journal of Anaesthesiology*, vol. 25, no. 12, pp. 961–967, 2008.

[14] C. Correa-Sales, B. C. Rabin, and M. Maze, "A hypnotic response to dexmedetomidine, an $\alpha 2$ agonist, is mediated in the locus coeruleus in rats," *Anesthesiology*, vol. 76, no. 6, pp. 948–952, 1992.

[15] C. Yu, S. Li, F. Deng, Y. Yao, and L. Qian, "Comparison of dexmedetomidine/fentanyl with midazolam/fentanyl combination for sedation and analgesia during tooth extraction," *International Journal of Oral and Maxillofacial Surgery*, vol. 43, no. 9, pp. 1148–1153, 2014.

[16] L. Xianbao, Z. Hong, Z. Xu, Z. Chunfang, and C. Dunjin, "Dexmedetomidine reduced cytokine release during postpartum bleeding-induced multiple organ dysfunction syndrome in rats," *Mediators of inflammation*, vol. 2013, Article ID 627831, 7 pages, 2013.

[17] L. Xu, H. Bao, Y. Si, and X. Wang, "Effects of dexmedetomidine on early and late cytokines during polymicrobial sepsis in mice," *Inflammation Research*, vol. 62, no. 5, pp. 507–514, 2013.

[18] M. Ueki, T. Kawasaki, K. Habe, K. Hamada, C. Kawasaki, and T. Sata, "The effects of dexmedetomidine on inflammatory mediators after cardiopulmonary bypass," *Anaesthesia*, vol. 69, no. 7, pp. 693–700, 2014.

[19] C. Chen, Z. Zhang, K. Chen, F. Zhang, M. Peng, and Y. Wang, "Dexmedetomidine regulates inflammatory molecules contributing to ventilator-induced lung injury in dogs," *Journal of Surgical Research*, vol. 187, no. 1, pp. 211–218, 2014.

[20] S.-H. Kang, Y.-S. Kim, T.-H. Hong et al., "Effects of dexmedetomidine on inflammatory responses in patients undergoing laparoscopic cholecystectomy," *Acta Anaesthesiologica Scandinavica*, vol. 57, no. 4, pp. 480–487, 2013.

[21] H. Y. Uysal, S. S. Cuzdan, O. Kayíran et al., "Preventive effect of dexmedetomidine in ischemia-reperfusion injury," *Journal of Craniofacial Surgery*, vol. 23, no. 5, pp. 1287–1291, 2012.

[22] O. Eser, H. Fidan, O. Sahin et al., "The influence of dexmedetomidine on ischemic rat hippocampus," *Brain Research*, vol. 1218, pp. 250–256, 2008.

[23] S. Omoigui, "The biochemical origin of pain—proposing a new law of pain: the origin of all pain is inflammation and the inflammatory response. Part 1 of 3—a unifying law of pain," *Medical Hypotheses*, vol. 69, no. 1, pp. 70–82, 2007.

[24] A. Koroglu, H. Teksan, O. Sagir, A. Yucel, H. I. Toprak, and O. M. Ersoy, "A comparison of the sedative, hemodynamic, and respiratory effects of dexmedetomidine and propofol in children undergoing magnetic resonance imaging," *Anesthesia and Analgesia*, vol. 103, no. 1, pp. 63–67, 2006.

[25] B. F. Robinson, "Relation of heart rate and systolic blood pressure to the onset of pain in angina pectoris," *Circulation*, vol. 35, no. 6, pp. 1073–1083, 1967.

[26] J. D. Tobias, "Dexmedetomidine: applications in pediatric critical care and pediatric anesthesiology," *Pediatric Critical Care Medicine*, vol. 8, no. 2, pp. 115–131, 2007.

[27] Y.-W. Hsu, L. I. Cortinez, K. M. Robertson et al., "Dexmedetomidine pharmacodynamics: part I: crossover comparison of the respiratory effects of dexmedetomidine and remifentanil in healthy volunteers," *Anesthesiology*, vol. 101, no. 5, pp. 1066–1076, 2004.

[28] P. L. Bailey, N. L. Pace, M. A. Ashburn, J. W. B. Moll, K. A. East, and T. H. Stanley, "Frequent hypoxemia and apnea after sedation with midazolam and fentanyl," *Anesthesiology*, vol. 73, no. 5, pp. 826–830, 1990.

[29] S. E. Fisher, J. W. Frame, P. G. Rout, and D. J. McEntegart, "Factors affecting the onset and severity of pain following the surgical removal of unilateral impacted mandibular third molar teeth," *British Dental Journal*, vol. 164, no. 11, pp. 351–354, 1988.

[30] M. Tasdogan, D. Memis, N. Sut, and M. Yuksel, "Results of a pilot study on the effects of propofol and dexmedetomidine on inflammatory responses and intraabdominal pressure in severe sepsis," *Journal of Clinical Anesthesia*, vol. 21, no. 6, pp. 394–400, 2009.

[31] T. Taniguchi, A. Kurita, K. Kobayashi, K. Yamamoto, and H. Inaba, "Dose- and time-related effects of dexmedetomidine on mortality and inflammatory responses to endotoxin-induced shock in rats," *Journal of Anesthesia*, vol. 22, no. 3, pp. 221–228, 2008.

[32] Q.-Q. Shi, H. Wang, and H. Fang, "Dose-response and mechanism of protective functions of selective alpha-2 agonist dexmedetomidine on acute lung injury in rats," *Saudi Medical Journal*, vol. 33, no. 4, pp. 375–381, 2012.

[33] V. Hanci, G. Yurdakan, S. Yurtlu, I. Ö. Turan, and E. Y. Sipahi, "Protective effect of dexmedetomidine in a rat model of α-naphthylthiourea-induced acute lung injury," *Journal of Surgical Research*, vol. 178, no. 1, pp. 424–430, 2012.

[34] C.-L. Yang, C.-H. Chen, P.-S. Tsai, T.-Y. Wang, and C.-J. Huang, "Protective effects of dexmedetomidine-ketamine combination against ventilator-induced lung injury in endotoxemia rats," *Journal of Surgical Research*, vol. 167, no. 2, pp. e273–e281, 2011.

[35] M. Schäfers, C. Geis, C. I. Svensson, Z. D. Luo, and C. Sommer, "Selective increase of tumour necrosis factor-alpha in injured and spared myelinated primary afferents after chronic constrictive injury of rat sciatic nerve," *European Journal of Neuroscience*, vol. 17, no. 4, pp. 791–804, 2003.

[36] B. F. Boyce, P. Li, Z. Yao et al., "TNFα and pathologic bone resorption," *Keio Journal of Medicine*, vol. 54, no. 3, pp. 127–131, 2005.

[37] C. Sommer and M. Kress, "Recent findings on how proinflammatory cytokines cause pain: peripheral mechanisms in inflammatory and neuropathic hyperalgesia," *Neuroscience Letters*, vol. 361, no. 1–3, pp. 184–187, 2004.

[38] M. Schafers, C. I. Svensson, C. Sommer, and L. S. Sorkin, "Tumor necrosis factor-α induces mechanical allodynia after spinal nerve ligation by activation of p38 MAPK in primary sensory neurons," *Journal of Neuroscience*, vol. 23, no. 7, pp. 2517–2521, 2003.

[39] L. Zhang, T. Berta, Z.-Z. Xu, T. Liu, J. Y. Park, and R.-R. Ji, "TNF-alpha contributes to spinal cord synaptic plasticity and inflammatory pain: distinct role of TNF receptor subtypes 1 and 2," *Pain*, vol. 152, no. 2, pp. 419–427, 2011.

[40] O. A. Dina, P. G. Green, and J. D. Levine, "Role of interleukin-6 in chronic muscle hyperalgesic priming," *Neuroscience*, vol. 152, no. 2, pp. 521–525, 2008.

[41] G. J. Summer, E. A. Romero-Sandoval, O. Bogen, O. A. Dina, S. G. Khasar, and J. D. Levine, "Proinflammatory cytokines mediating burn-injury pain," *Pain*, vol. 135, no. 1-2, pp. 98–107, 2008.

[42] B. Lisowska, P. Małdyk, E. Kontny, C. Michalak, L. Jung, and R. Ćwiek, "Postoperative evaluation of plasma interleukin-6 concentration in patients after total hip arthroplasty," *Ortopedia Traumatologia Rehabilitacja*, vol. 8, no. 5, pp. 547–554, 2006.

[43] A. Koch, K. Zacharowski, O. Boehm et al., "Nitric oxide and pro-inflammatory cytokines correlate with pain intensity in chronic pain patients," *Inflammation Research*, vol. 56, no. 1, pp. 32–37, 2007.

[44] A. L. Davies, K. C. Hayes, and G. A. Dekaban, "Clinical correlates of elevated serum concentrations of cytokines and autoantibodies in patients with spinal cord injury," *Archives of Physical Medicine and Rehabilitation*, vol. 88, no. 11, pp. 1384–1393, 2007.

[45] H. K. Kim, J. H. Kim, X. Gao et al., "Analgesic effect of vitamin E is mediated by reducing central sensitization in neuropathic pain," *Pain*, vol. 122, no. 1-2, pp. 53–62, 2006.

[46] M. Uchiyama and M. Mihara, "Determination of malonaldehyde precursor in tissues by thiobarbituric acid test," *Analytical Biochemistry*, vol. 86, no. 1, pp. 271–278, 1978.

[47] X. Dong, Q. Xing, Y. Li, X. Han, and L. Sun, "Dexmedetomidine protects against ischemia-reperfusion injury in rat skeletal muscle," *Journal of Surgical Research*, vol. 186, no. 1, pp. 240–245, 2014.

[48] M. Cosar, O. Eser, H. Fidan et al., "The neuroprotective effect of dexmedetomidine in the hippocampus of rabbits after subarachnoid hemorrhage," *Surgical Neurology*, vol. 71, no. 1, pp. 54–59, 2009.

[49] E. S. Park, X. Gao, J. M. Chung, and K. Chung, "Levels of mitochondrial reactive oxygen species increase in rat neuropathic spinal dorsal horn neurons," *Neuroscience Letters*, vol. 391, no. 3, pp. 108–111, 2006.

[50] E. Eisenberg, S. Shtahl, R. Geller et al., "Serum and salivary oxidative analysis in Complex Regional Pain Syndrome," *Pain*, vol. 138, no. 1, pp. 226–232, 2008.

[51] T. J. Coderre, D. N. Xanthos, L. Francis, and G. J. Bennett, "Chronic post-ischemia pain (CPIP): a novel animal model of complex regional pain syndrome-Type I (CRPS-I; reflex sympathetic dystrophy) produced by prolonged hindpaw ischemia and reperfusion in the rat," *Pain*, vol. 112, no. 1-2, pp. 94–105, 2004.

[52] N. Yonehara and M. Yoshimura, "Effect of nitric oxide on substance P release from the peripheral endings of primary afferent neurons," *Neuroscience Letters*, vol. 271, no. 3, pp. 199–201, 1999.

[53] L. van der Laan, P. J. C. Kapitein, W. J. G. Oyen, A. A. J. Verhofstad, T. Hendriks, and R. J. A. Goris, "A novel animal model to evaluate oxygen derived free radical damage in soft tissue," *Free Radical Research*, vol. 26, no. 4, pp. 363–372, 1997.

[54] S. Lei, W. Su, H. Liu et al., "Nitroglycerine-induced nitrate tolerance compromises propofol protection of the endothelial cells against TNF-α: the role of PKC- β2 and nadph oxidase," *Oxidative Medicine and Cellular Longevity*, vol. 2013, Article ID 678484, 9 pages, 2013.

[55] J. Han, D. Wang, B. Yu et al., "Cardioprotection against ischemia/reperfusion by licochalcone B in isolated rat hearts," *Oxidative Medicine and Cellular Longevity*, vol. 2014, Article ID 134862, 11 pages, 2014.

[56] T. Luo and Z. Xia, "A small dose of hydrogen peroxide enhances tumor necrosis factor-alpha toxicity in inducing human vascular endothelial cell apoptosis: reversal with propofol," *Anesthesia & Analgesia*, vol. 103, no. 1, pp. 110–116, 2006.

Hindawi Publishing Corporation
Oxidative Medicine and Cellular Longevity
Volume 2014, Article ID 134862, 11 pages
http://dx.doi.org/10.1155/2014/134862

Research Article

Cardioprotection against Ischemia/Reperfusion by Licochalcone B in Isolated Rat Hearts

Jichun Han,[1] Dong Wang,[2] Bacui Yu,[1] Yanming Wang,[1] Huanhuan Ren,[1] Bo Zhang,[1] Yonghua Wang,[1] and Qiusheng Zheng[1,3]

[1] *Key Laboratory of Xinjiang Endemic Phytomedicine Resources, Pharmacy School, Shihezi University, Ministry of Education, Shihezi 832002, China*
[2] *Qianfoshan Hospital of Shandong Province, Jinan 250014, China*
[3] *Binzhou Medical University, Yantai 264003, China*

Correspondence should be addressed to Yonghua Wang; dcpwyh@163.com and Qiusheng Zheng; zqsyt@sohu.com

Received 6 July 2014; Revised 4 August 2014; Accepted 4 August 2014; Published 21 August 2014

Academic Editor: Zhengyuan Xia

The generation of reactive oxygen species (ROS) is a major cause of heart injury induced by ischemia-reperfusion. The left ventricular developed pressure (LVDP) and the maximum up/down rate of left ventricular pressure ($\pm dp/dt_{max}$) were documented by a physiological recorder. Myocardial infarct size was estimated macroscopically using 2,3,5-triphenyltetrazolium chloride staining. Coronary effluent was analyzed for lactate dehydrogenase (LDH) and creatine kinase (CK) release to assess the degree of cardiac injury. The levels of C-reactive protein (CRP), interleukin-8 (IL-8), tumor necrosis factor-α (TNF-α), and interleukin-6 (IL-6) were analyzed to determine the inflammation status of the myocardial tissue. Cardiomyocyte apoptosis analysis was performed using the In Situ Cell Death Detection Kit, POD. Accordingly, licochalcone B pretreatment improved the heart rate (HR), increased LVDP, and decreased CK and LDH levels in coronary flow. SOD level and GSH/GSSG ratio increased, whereas the levels of MDA, TNF-α, and CRP and activities of IL-8 and IL-6 decreased in licochalcone B-treated groups. The infarct size and cell apoptosis in hearts from licochalcone B-treated group were lower than those in hearts from the I/R control group. Therefore, the cardioprotective effects of licochalcone B may be attributed to its antioxidant, antiapoptotic, and anti-inflammatory activities.

1. Introduction

Ischemic heart disease is a leading cause of death worldwide and is the most common consequence of coronary artery disease. Reperfusion of an occluded human coronary can effectively reduce overall mortality; the restoration of blood flow through the previously ischemic myocardium can elevate reperfusion injury symptoms, including cardiomyocyte dysfunction and cell death [1]. Previous studies showed that the myocardial response to ischemia-reperfusion can be manipulated to delay injury. Thus, studies on the mechanisms of cardioprotection were conducted. Various interventions that target the preischemic period and/or reperfusion have been investigated for their efficacy in preventing myocardial injury after ischemic insult. Among the most effective experimental strategies are interventions such as ischemic preconditioning and its pharmacological mimicking [2].

Myocardial ischemia-reperfusion injuries in pathological disorders include reperfusion arrhythmias, transient mechanical dysfunction, myocardial stunning, and cell death [3]. Oxidative stress caused by reactive oxygen species (ROS) has a considerable role in ischemia/reperfusion (I/R) injury, which impairs cardiac function [4]. Ischemia/reperfusion leads to an imbalance between antioxidants and the accumulation of toxic free radicals, which increase the susceptibility of tissues to oxidative damage via lipid peroxidation, protein oxidation, and DNA oxidation [5]. The cardioprotective effects of various antioxidants have been studied in vivo and in vitro using hearts [6]. Several studies revealed that the addition of antioxidants or scavengers, such as superoxide dismutase (SOD) and catalase, could reduce infarct size [7–10].

Flavonoids have unique antioxidant properties and other pharmacological activities that may be relevant to protecting

the heart from ischemia-reperfusion injury. These flavonoids may prevent production of oxidants (e.g., by inhibition of xanthine oxidase and chelation of transition metals), may inhibit oxidants from attacking cellular targets (e.g., by electron donation and scavenging activities), may block propagation of oxidative reactions (e.g., by chain-breaking antioxidant activity), and may reinforce cellular antioxidant capacity (e.g., by minimizing the effects of oxidants on antioxidants and by inducing expression of endogenous antioxidants). Flavonoids also possess anti-inflammatory and antiplatelet aggregation effects by inhibiting relevant enzymes and signaling pathways. Such activities ultimately lower oxidant production and enhance the reestablishment of blood in the ischemic zone. Finally, flavonoids exhibit vasodilatory effects through a variety of mechanisms, one of which may be the interaction with ion channels. These multifaceted activities of flavonoids corroborate their use as potential therapeutic intervention tools to ameliorate ischemia-reperfusion injury [11].

Licochalcone B, which belongs to the retrochalcone family, is isolated from the roots of Chinese licorice. Studies on the biological activities of licochalcone B are in the initial stage. Licochalcone B showed high antioxidant and free radical-scavenging activities [12, 13]. Experimental studies suggested that licochalcone B has several other useful pharmacological properties, such as anti-inflammatory activities [14], leukotriene inhibition action [15], and preventive activity against glucose-mediated protein damage [16]. We aimed to evaluate the cardioprotective effects of licochalcone B and mechanisms underlying such effects.

2. Materials and Methods

2.1. Animals. Adult male SD rats, weighing 250 g to 300 g, were obtained from Xinjiang Medicine University Medical Laboratory Animal Center (SDXK 2011-004) and housed in a room at 22°C to 25°C, 50% to 60% relative humidity, and a 12 h light/12 h dark cycle. All experimental procedures were approved by the Institutional Animal Care and Use Committee of National Institute Pharmaceutical Education and Research.

2.2. Test Compounds, Chemicals, and Reagents. Licochalcone B (purity ≥ 98%) was purchased from Shanghai Li Chen Biotechnology Co., Ltd. (Shanghai, China). 1,1,3,3-Tetramethoxypropane was obtained from Fluka Chemical Co. (Ronkonkoma, NY). 2,3,5-Triphenyltetrazolium chloride (TTC), oxidized glutathione, and reduced glutathione were purchased from Sigma Chemical Co. (St. Louis, MO). Other chemicals and reagents were of analytical grade.

2.3. Drug Administration and Surgical Procedure. The rats were randomly divided into seven groups as follows: control (Sham), I/R, and licochalcone B (0.5, 1, 3, and 5 μg/mL). Hearts in the control group were perfused during the 90 min stabilization period. Hearts from the IR group were subjected to 20 min of zero-flow global ischemia and 45 min of reperfusion after stabilization. Hearts in licochalcone B treatment group were stabilized for 30 min and treated with Krebs-Henseleit (K-H) buffer solution containing licochalcone B (0.5, 1, 3, and 5 μg/mL). Global ischemia and reperfusion were established for 45 min.

2.4. IR. Rats were anesthetized with chloral hydrate (350 mg/kg). The hearts were excised quickly and immediately immersed in ice-cold K-H buffer (pH 7.4) containing 118 mM NaCl, 1.2 mM KH_2PO_4, 4.7 mM KCl, 1.7 mM $CaCl_2$, 1.2 mM $MgSO_4$, 20 mM sodium acetate, and 10 mM glucose. The buffer was maintained at a temperature of 37°C and infused continuously with oxygen. The excised hearts were cannulated through the aorta by a Langendorff apparatus and were perfused in retrograde with K-H buffer containing 95% O_2 and 5% CO_2 throughout the experiment. Perfusion pressure was maintained at 75 mmHg. A water-filled latex balloon coupled to a pressure transducer (Statham) was inserted into the left ventricular cavity via the left auricle for pressure recording. Ventricular end-diastolic pressure (VEDP) was adjusted between 5 and 12 mmHg. The hearts were stabilized for 30 min, after which global ischemia and reperfusion were established for 15 and 45 min, respectively. The hearts from the control group were perfused and subjected to a 90 min stabilization procedure. During the experiment, left ventricular developed pressure (LVDP), LVEDP, heart rate (HR), and rate of developed pressure during contraction and relaxation ($\pm dp/dt_{\max}$) were monitored continuously using a 4S AD Instruments biology polygraph. The heart effluents were collected at 1 min intervals at selected times to determine coronary flow.

2.5. Measurement of Cellular Injury. Lactate dehydrogenase (LDH) and creatine kinase (CK) release is measured to evaluate the presence of necrotic cell death [15]. At the end of the experiment, levels of LDH and CK in the perfusate were determined spectrophotometrically via cytotoxicity detection LDH and CK kits (Nanjing Jiancheng Biological Product, Nanjing, China).

2.6. Evaluation of Myocardial Infarct Size. The artery was occluded for 20 min and reperfused for 45 min before the end of the experiment. These durations of ischemia and reperfusion have been successfully used in the same experimental model. To evaluate tissue death, the hearts were removed and washed in phosphate buffered saline, frozen and stored at −20°C for 30 min, and sliced into 1 mm sections perpendicularly along the long axis from apex to base. The slices were incubated in 1% TTC in pH 7.4 buffer at 37°C for 10 min to 15 min, fixed in 10% formaldehyde solution, and photographed with a digital camera to distinguish the red-stained viable and the white-unstained necrotic tissues. Areas stained in red and white were measured using an Image-Pro Plus 7.0 (Media Cybernetics, Wyoming, USA). The infarction size percentage was calculated by the following equation:

$$\%\text{Infarct volume} = \frac{\text{Infarct volume}}{\text{Total volume of slice}} \times 100. \quad (1)$$

Table 1: Effect of licochalcone B on cardiac function in rats subjected to I/R (values are means with their standard deviation, $n = 8$).

Physical index	Reperfusion (%)		
	15 min	30 min	45 min
LVDP			
Control	96.31 ± 3.27	94.45 ± 4.12	93.67 ± 4.92
I/R	40.50 ± 4.59$^{\#\#}$	47.18 ± 4.08$^{\#\#}$	48.76 ± 5.88$^{\#\#}$
0.5 μg/mL licochalcone B	79.76 ± 2.06**	78.28 ± 3.79**	74.13 ± 5.39**
1 μg/mL licochalcone B	85.39 ± 2.73**	82.23 ± 2.83**	81.49 ± 3.41**
3 μg/mL licochalcone B	63.88 ± 5.54*	57.46 ± 3.99*	55.16 ± 2.53*
5 μg/mL licochalcone B	58.54 ± 3.97	52.96 ± 3.82	51.10 ± 4.28
$+dp/dt_{max}$			
Control	117.68 ± 2.59	116.79 ± 3.63	113.03 ± 3.71
I/R	42.26 ± 3.27$^{\#\#}$	52.83 ± 3.41$^{\#\#}$	52.62 ± 3.92$^{\#\#}$
0.5 μg/mL licochalcone B	68.48 ± 4.84*	75.29 ± 7.46*	74.59 ± 4.40*
1 μg/mL licochalcone B	95.11 ± 3.50**	95.76 ± 1.84**	92.27 ± 2.94**
3 μg/mL licochalcone B	61.05 ± 4.83*	60.36 ± 4.50*	57.68 ± 3.66*
5 μg/mL licochalcone B	55.90 ± 3.60*	55.09 ± 2.10*	54.22 ± 3.97*
$-dp/dt_{max}$			
Control	102.69 ± 3.72	99.30 ± 4.93	97.35 ± 5.01
I/R	49.22 ± 5.88$^{\#\#}$	56.47 ± 3.28$^{\#\#}$	56.05 ± 4.49$^{\#\#}$
0.5 μg/mL licochalcone B	72.96 ± 5.38*	74.12 ± 2.42*	66.78 ± 5.68*
1 μg/mL licochalcone B	85.60 ± 2.40**	83.62 ± 5.14**	84.76 ± 7.00**
3 μg/mL licochalcone B	54.59 ± 6.85*	53.50 ± 5.25*	50.12 ± 5.55*
5 μg/mL licochalcone B	49.80 ± 4.91	48.27 ± 2.96	47.90 ± 4.25
CF			
Control	107.34 ± 3.16	107.09 ± 3.53	104.18 ± 5.97
I/R	90.57 ± 8.78$^{\#}$	100.72 ± 7.65$^{\#}$	99.92 ± 10.00$^{\#}$
0.5 μg/mL licochalcone B	98.83 ± 1.78	98.72 ± 4.89	99.99 ± 3.45
1 μg/mL licochalcone B	95.52 ± 6.18	97.95 ± 5.91	98.22 ± 7.16
3 μg/mL licochalcone B	85.84 ± 3.91*	90.73 ± 8.34*	92.49 ± 7.77*
5 μg/mL licochalcone B	89.78 ± 5.44*	90.07 ± 7.32*	91.88 ± 3.67*
HR			
Control	118.13 ± 8.05	118.96 ± 3.81	122.56 ± 3.91
I/R	86.49 ± 10.97$^{\#\#}$	78.49 ± 8.81$^{\#\#}$	69.00 ± 3.50$^{\#\#}$
0.5 μg/mL licochalcone B	94.99 ± 8.90	93.01 ± 11.05*	86.99 ± 1.34*
1 μg/mL licochalcone B	105.46 ± 8.29*	100.55 ± 9.07**	97.07 ± 4.36**
3 μg/mL licochalcone B	97.86 ± 8.53	89.68 ± 6.47	86.47 ± 5.02
5 μg/mL licochalcone B	87.00 ± 9.40	80.49 ± 8.98	74.13 ± 3.57

Left ventricular developed pressure (LVDP); maximum rise velocity ($+dp/dt_{max}$); maximum down velocity ($-dp/dt_{max}$); coronary flow (CF); heart rate (HR).
$^{\#\#}P < 0.01$ and $^{\#}P < 0.05$ compared with control group; $^{*}P < 0.05$ and $^{**}P < 0.01$ compared with the I/R group.

2.7. Assay of Oxidative Stress. At the end of the perfusion treatments, the hearts were harvested and maintained at −70°C for subsequent analysis. The frozen ventricles were crushed to a powder using liquid nitrogen-chilled tissue pulverizer. For tissue analyses, the weighed amount of the frozen tissues was homogenized in appropriate buffer using microcentrifuge tube homogenizer.

The SOD, malondiadehyde (MDA), and glutathione/glutathione disulfide (GSG/GSSH) concentrations were analyzed spectrophotometrically according to the instruction of the assay kits (Nanjing Jiancheng Bioengineering Institute, Nanjing, China).

2.8. Inflammation Assay. TNF-α, CRP, IL-8, and IL-6 were analyzed spectrophotometrically according to the instruction of the Rat Tumor Necrosis Factor Alpha ELISA Kit, Rat C-reactive protein ELISA Kit, Rat Interleukin 8 ELISA Kit, and Rat Interleukin 6 ELISA Kit (Tsz Biosciences, Greater Boston, USA).

Table 2: Effect of licochalcone B on levels of CK and LDH in coronary flow of I/R injury (values are means with their standard deviation, $n = 8$).

Physical index	Before ischemia	Reperfusion	
	20 min	20 min	45 min
LDH (U/L)			
Control	18.3 ± 4.67	17.1 ± 3.84	16.70 ± 7.17
I/R	17.6 ± 6.37	64.0 ± 4.67$^{\#\#}$	58.5 ± 8.43$^{\#\#}$
0.5 μg/mL licochalcone B	17.79 ± 5.14	37.53 ± 6.61**	29.17 ± 5.61**
1 μg/mL licochalcone B	17.6 ± 5.64	22.5 ± 6.49**	27.5 ± 7.26**
3 μg/mL licochalcone B	17.60 ± 7.70	55.38 ± 2.75*	50.99 ± 3.42*
5 μg/mL licochalcone B	19.35 ± 7.91	60.51 ± 8.54	53.34 ± 5.50
CK (U/L)			
Control	28.19 ± 9.07	25.22 ± 5.89	26.02 ± 9.01
I/R	23.36 ± 7.55	366.98 ± 15.24$^{\#\#}$	126.36 ± 14.13$^{\#\#}$
0.5 μg/mL licochalcone B	23.91 ± 3.95	276.47 ± 14.09**	93.54 ± 17.35**
1 μg/mL licochalcone B	19.03 ± 11.12	243.63 ± 16.35**	72.00 ± 17.24**
3 μg/mL licochalcone B	25.77 ± 9.73	310.97 ± 18.10	98.97 ± 14.89**
5 μg/mL licochalcone B	27.49 ± 5.88	325.17 ± 18.33	106.27 ± 18.77

$^{\#\#}P < 0.01$ compared with the control group; $^{*}P < 0.05$ and $^{**}P < 0.01$ compared with I/R group.

2.9. General Histology. The rat's heart was fixed in 10% formaldehyde and preserved at normal temperature. The heart was observed under an optical microscope after HE coloration. A small piece (2 mm × 1 mm × 1 mm) of subendocardial myocardium from the root of left ventricular papillary muscle was obtained and fixed in 0.1 mmol/L phosphate buffer (pH 7.2), which included 3% glutaraldehyde and 1.5% paraformaldehyde at 4°C. The piece was cut into small pieces of 1 mm^3 and subsequently fixed in the abovementioned solution for 4 h. Moreover, the piece was fixed in 1% osmic acid again at 4°C for 1.5 h after being rinsed with phosphate buffer. Afterwards, the tissue was dehydrated by alcohol followed by dimethylbenzene and embedded in epoxy resin 618. The tissue was located by semithin sectioning and sliced into ultrathin sections (60 nm). The sections were dyed with uranium acetate and lead citrate and observed under an optical microscope.

2.10. Terminal Deoxynucleotidyl Transfer-Mediated dUTP Nick End-Labeling (TUNEL) Staining. We conducted TUNEL by using an In Situ Cell Death Detection Kit, POD (Roche, Germany), according to the manufacturer's instructions. After deparaffinization and rehydration, the sections were treated with protease K at 10 mmol/L concentration for 15 min. The slides were immersed in TUNEL reaction mixture for 60 min at 37°C in a humidified atmosphere in the dark. Converter-POD was used to incubate the slides for 30 min to show blue nuclear staining. The slides were analyzed by optical microscopy. The TUNEL index (%) was the ratio of the number of TUNEL-positive cells divided by the total number of cells and was used to evaluate the apoptosis index of the heart TUNEL-stained tissues. For each sample, eight randomly selected areas of TUNEL-stained slices were counted, and the average value was calculated.

2.11. Statistical Analysis. Data were presentedas means ± SD from at least three independent experiments and evaluated by analysis of variance (ANOVA) and followed by Student's t-test. The values of $P < 0.05$ were considered statistically significant. The analyses were performed using the Statistical Program for Social Sciences Software (IBM SPASS, International Business Machines Corporation, Armonk City, New York, USA).

3. Results

3.1. Licochalcone B Enhanced the Recovery of I/R-Altered Cardiac Function. We evaluated cardiac function by monitoring hemodynamic parameters, which are important indices of cardiac function. The doses of licochalcone B used in the experiments were determined during the preliminary experiments. Licochalcone B concentration of 0.5, 1, 3, or 5 μg/mL was selected. The hemodynamic parameters were continuously monitored using a computer-based data acquisition system (PC PowerLab with Chart 5 software, 4S AD Instruments). The effects of licochalcone B treatment on LVDP, $\pm dp/dt_{max}$, CF, and HR during I/R in the control, I/R, and licochalcone B-treated hearts are shown in Table 1. Compared with the unprotected I/R hearts, licochalcone B significantly improved functional recovery during early reperfusion, and 1 μg/mL of licochalcone B group significantly improved LVEDP, $\pm dp/dt_{max}$, and HR ($^{*}P < 0.05$).

3.2. Licochalcone B Attenuated I/R-Induced Enzyme Release in Rat's Heart. To evaluate the degree of myocardial injury, we measured the release of LDH and CK. This method has been used in previous studies to evaluate the presence of necrotic cell death. Prior to ischemia, LDH and CK levels in the effluents from the control, I/R, and licochalcone B-treated groups were fundamentally similar. After 20 min of ischemia

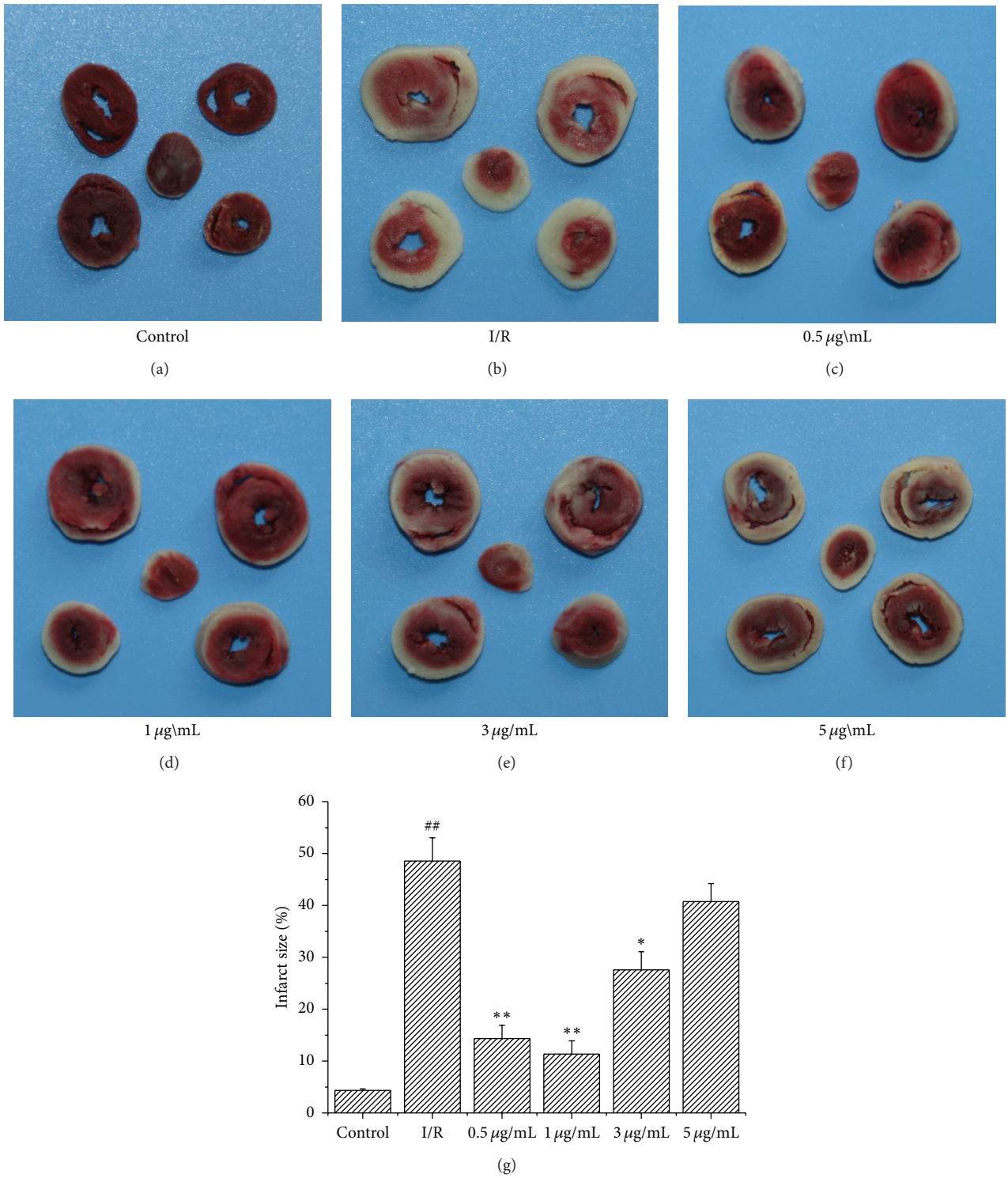

Figure 1: Effect of licochalcone B on the reduction of I/R-induced infarct size. $^{\#\#}P < 0.01$ compared with control group; $^{*}P < 0.05$ and $^{**}P < 0.01$ compared with the I/R group.

followed by 20 and 45 min of reperfusion, the leakage of CK and LDH notably increased in the I/R group compared with the control (Table 2). Pretreatment with licochalcone B at 0.5 and 1 μg/mL significantly reduced the I/R-induced increase in LDH and CK release in rat's heart ($^{**}P < 0.01$).

3.3. Licochalcone B Reduced I/R-Induced Infarct Size. Myocardial infarct size can be an indicator of myocardial injury. I/R group hearts subjected to global myocardial ischemia for 20 min followed by 45 min of reperfusion showed a significant increase of risk area infarct (48.55% ± 4.47%).

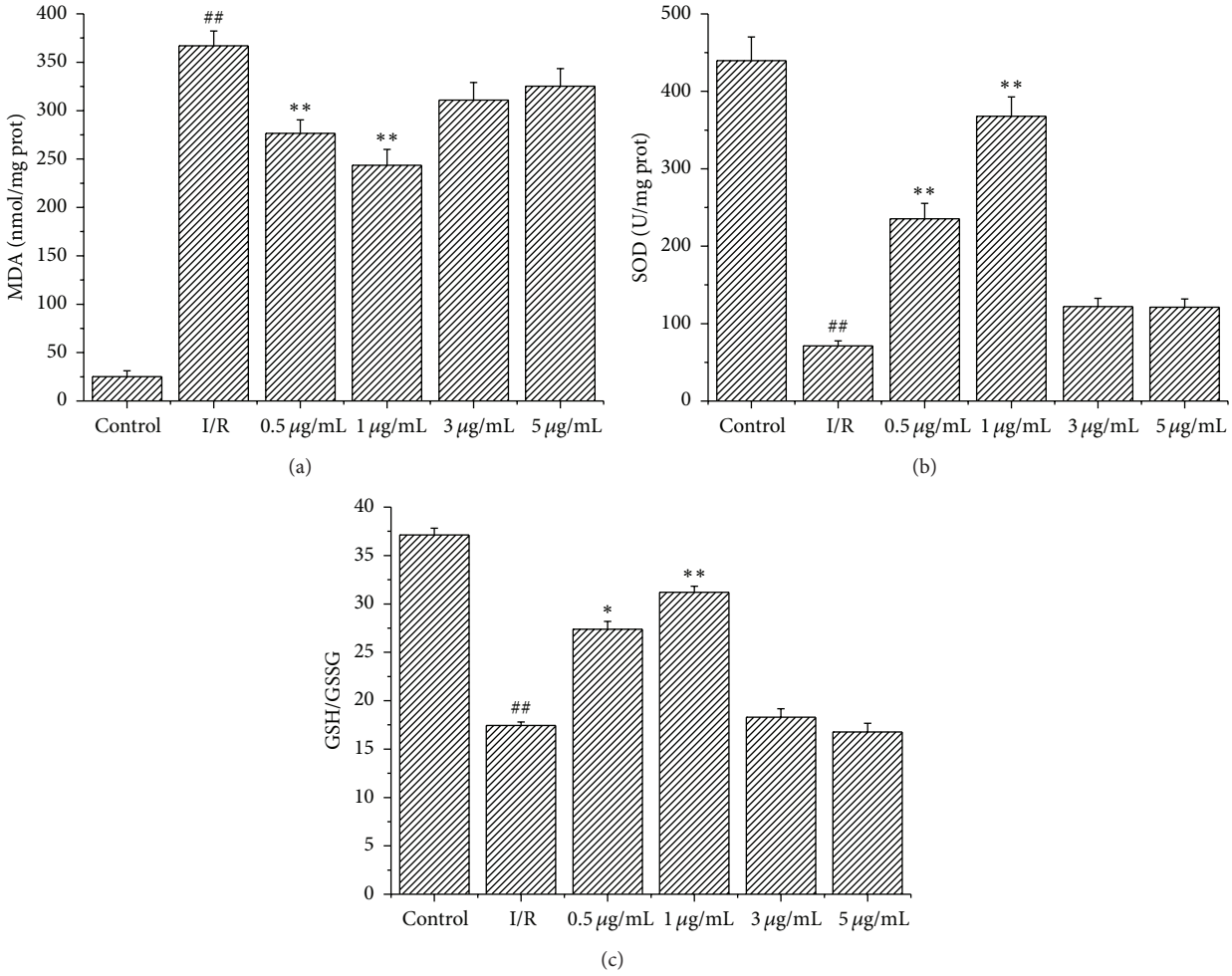

Figure 2: Effect of licochalcone B on cardiac contents of MDA, SOD, and GSH/GSSG in rats subjected to I/R (values are means with their standard deviation, $n = 8$). $^{\#\#}P < 0.01$ compared with control group; $^{*}P < 0.05$ and $^{**}P < 0.01$ compared with the I/R group.

By contrast, licochalcone B preconditioning reduced the percentage of the I/R-induced myocardial infarct size (Figure 1). Licochalcone B preconditioning at 0.5 and 1 μg/mL reduced the I/R-induced percentage of myocardial infarct size (14.34± 2.56% and 11.36 ± 2.53%, resp.).

3.4. Licochalcone B Alleviated Oxidative Stress Induced by I/R. ROS generation is a major factor in I/R injury. SOD, MDA, and the ratio of GSH/GSSG are indicators of oxidation. The SOD activity, MDA level, and ratio of GSH/GSSG were determined in myocardial tissue to identify the possible mechanisms underlying the cardioprotective effects of licochalcone B. MDA level significantly decreased (Figure 2(a)), whereas SOD activity (Figure 2(b)) and GSH/GSSG ratio (Figure 2(c)) significantly increased in the group pretreated with 1 μg/mL licochalcone B compared with the I/R group. The 5 μg/mL licochalcone B pretreatment group showed no significant difference compared with the I/R group.

3.5. Licochalcone B Reduced Myocardial Structure Injury Induced by I/R. The changes in the morphological structure of myocardial tissue were elevated by HE coloration. The optical microscopy of rat myocardial structure is shown in Figure 3. The myocardial structures of the control group (Figure 3(a)) were as follows: muscle fibers were neatly arranged; interstitial substance contained no edema; muscle membrane was not damaged; and muscle fibers showed no fracture, degeneration, and necrosis. By contrast, the myocardial structures of I/R group (Figure 3(b)) were as follows: muscle fibers were irregularly arranged; interstitial substance exhibited edema; muscle membrane was damaged; and muscle fibers showed fracture, degeneration, and necrosis. Compared with the I/R group, the group pretreated with licochalcone B at 0.5 (Figure 3(c)) and 1 μg/mL (Figure 3(d)) showed significantly reduced I/R-induced myocardial structure injury. However, the groups pretreated with licochalcone B at 3 (Figure 4(e)) and 5 μg/mL (Figure 4(f)) indicated no significant difference compared with the I/R group.

3.6. Licochalcone B Reduced Cardiomyocyte Apoptosis Induced by I/R. The results of ischemic reperfusion myocardium in cardiomyocyte apoptosis were evident in the section. We

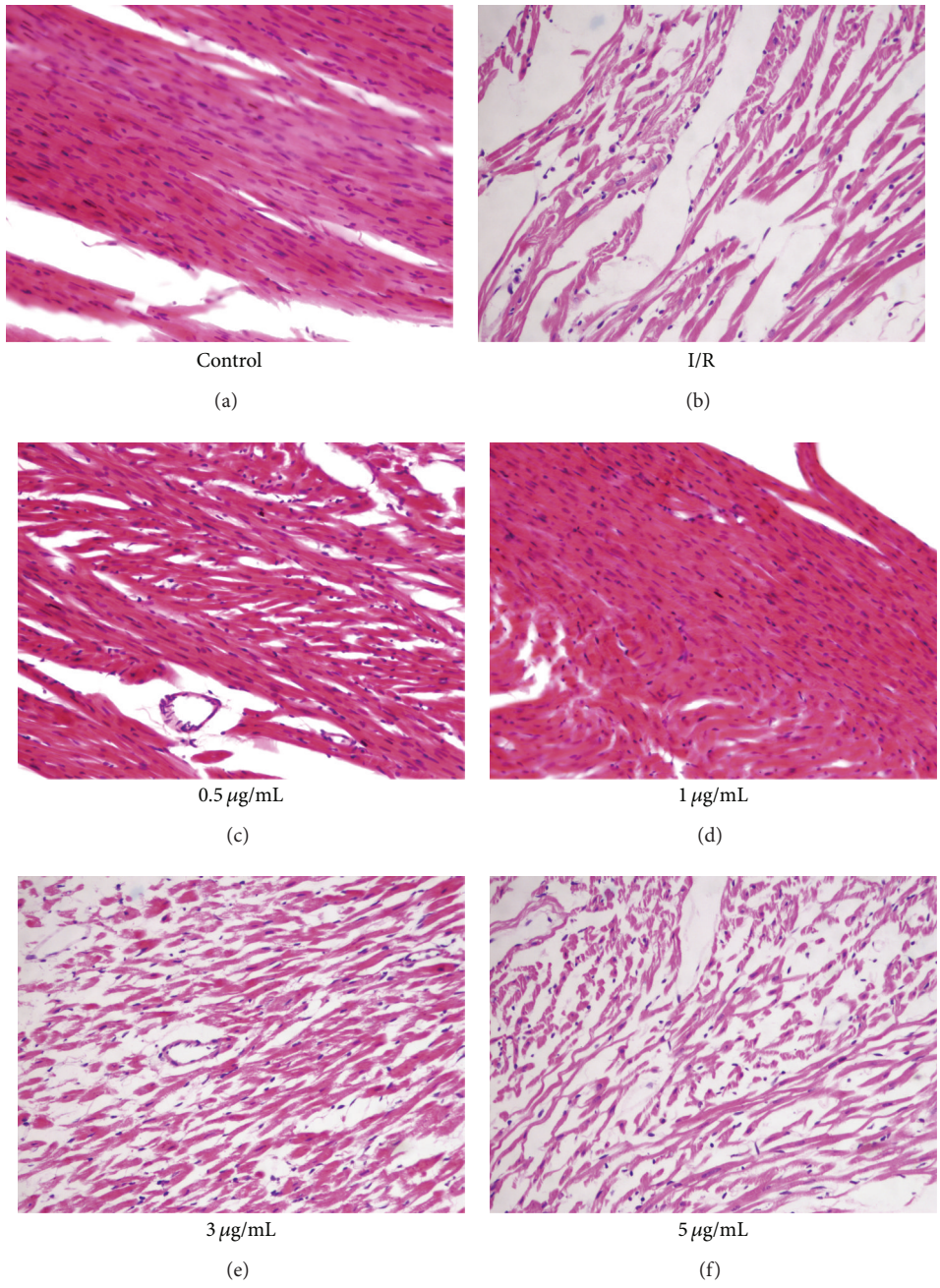

Figure 3: Effects of licochalcone B on cell morphology and hematoxylin and eosin (HE) staining (×200).

performed TUNEL staining to observe cardiomyocyte apoptosis. Under optical microscopy, TUNEL staining showed the absence of apoptosis in the control group (Figure 4(a)). The number of apoptotic cells increased dramatically in the I/R group (Figure 4(b)), whereas the groups pretreated with licochalcone B at 0.5 (Figure 4(c)) and 1 μg/mL (Figure 4(d)) showed an obviously reduced number of apoptotic cells. The groups pretreated with licochalcone B at 3 (Figure 4(e)) and 5 μg/mL (Figure 4(f)) showed no significant difference compared with the I/R group. The apoptosis percentage is shown in Figure 4(g).

3.7. Licochalcone B Reduced Inflammation Induced by I/R. Inflammation is an important mechanism underlying myocardial I/R injury. The presence of inflammatory cytokines (IL-6, CRP, IL-8, and TNF-α) associated with I/R was determined in myocardial tissue to identify the possible mechanisms underlying the cardioprotective activity of licochalcone B. The levels of IL-6 and CRP and the activities of IL-8 and TNF-α were determined. The content of IL-6 in the group pretreated with 1 μg/mL licochalcone B (45.36 ± 2.53 pg/mL) was significantly lower ($P < 0.01$) than that in the I/R group (68.55 ± 4.47 pg/mL) (Figure 5(a)). The activity

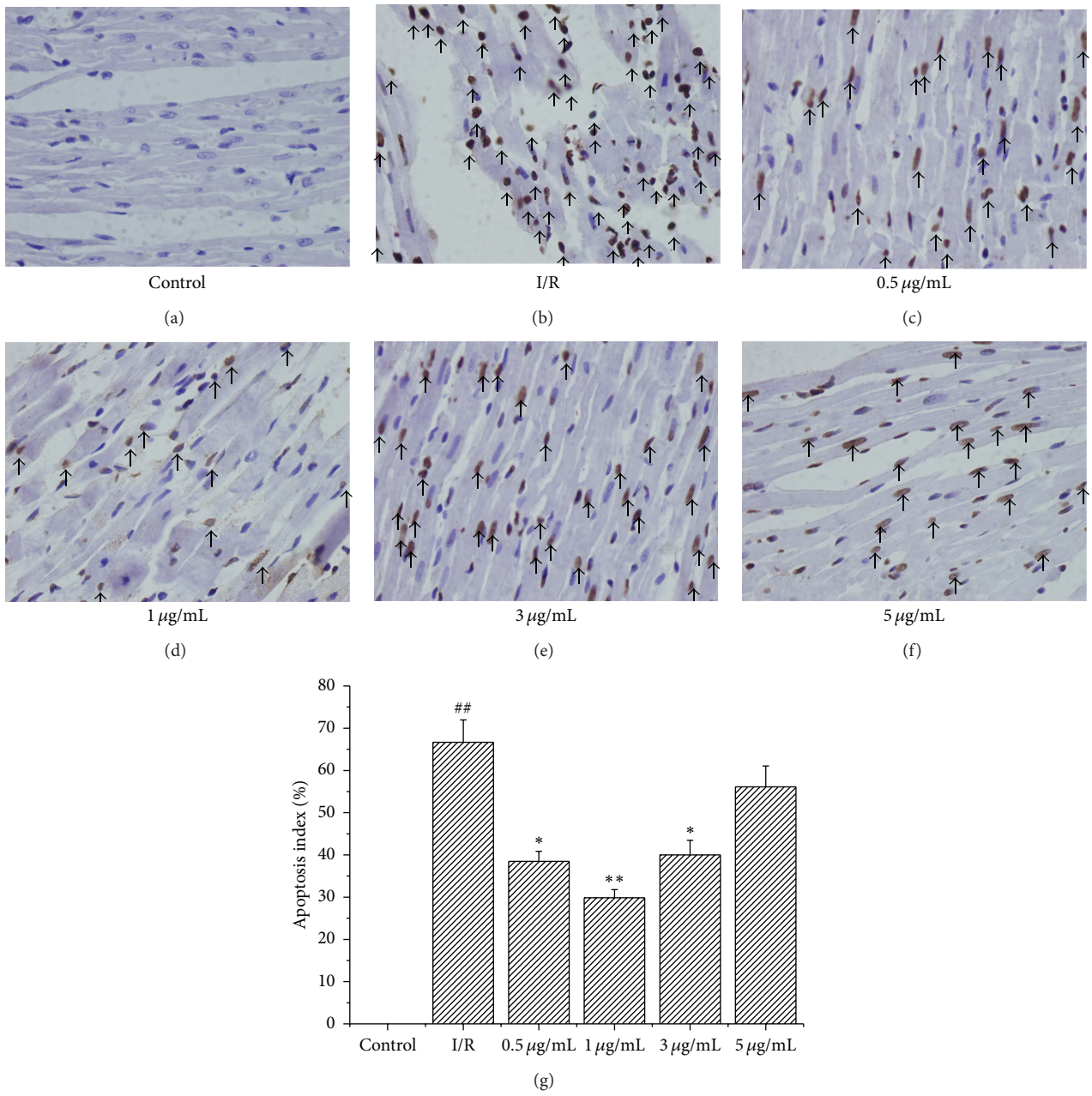

Figure 4: Effects of licochalcone B suppression on cardiomyocyte apoptosis (×400). Arrows indicate the apoptosis cardiomyocyte nucleus. $^{\#\#}P < 0.01$ compared with control group; $^{*}P < 0.05$ and $^{**}P < 0.01$ compared with the I/R group.

of TNF-α decreased from 300.24 ± 21.58 pg/mL in the I/R group to 132.97 ± 10.45 pg/mL in the group pretreated with 1 μg/mL licochalcone B ($P < 0.01$) (Figure 5(b)). Compared with I/R group (461.12 μg/L ± 28.10 μg/L), CRP level decreased significantly in the group treated with 1 μg/mL licochalcone B (199.47 pg/mL ± 15.08 pg/mL) ($P < 0.01$) (Figure 5(c)). The activity of IL-8 decreased from 124.61 ± 19.82 ng/L in the I/R group to 62.04 ± 6.49 ng/L in the group treated with 1 μg/mL licochalcone B ($P < 0.01$) (Figure 5(d)).

The levels of IL-6 and IL-8 activities and CRP level and TNF-α activity in the group treated with 0.5 μg/mL licochalcone B decreased significantly compared with the I/R group ($P < 0.05$). No significant difference was indicated between the group treated with high doses of licochalcone B (3 and 5 μg/mL) and the I/R group.

4. Discussion

We observed the following: (1) the middle-dose licochalcone B (0.5 and 1 μg/mL) pretreatment reduced I/R injury; (2) middle-dose licochalcone B suppressed the I/R-induced increase in MDA level and decrease in SOD activity and GSH/GSSG ratio; (3) middle-dose licochalcone B reduced

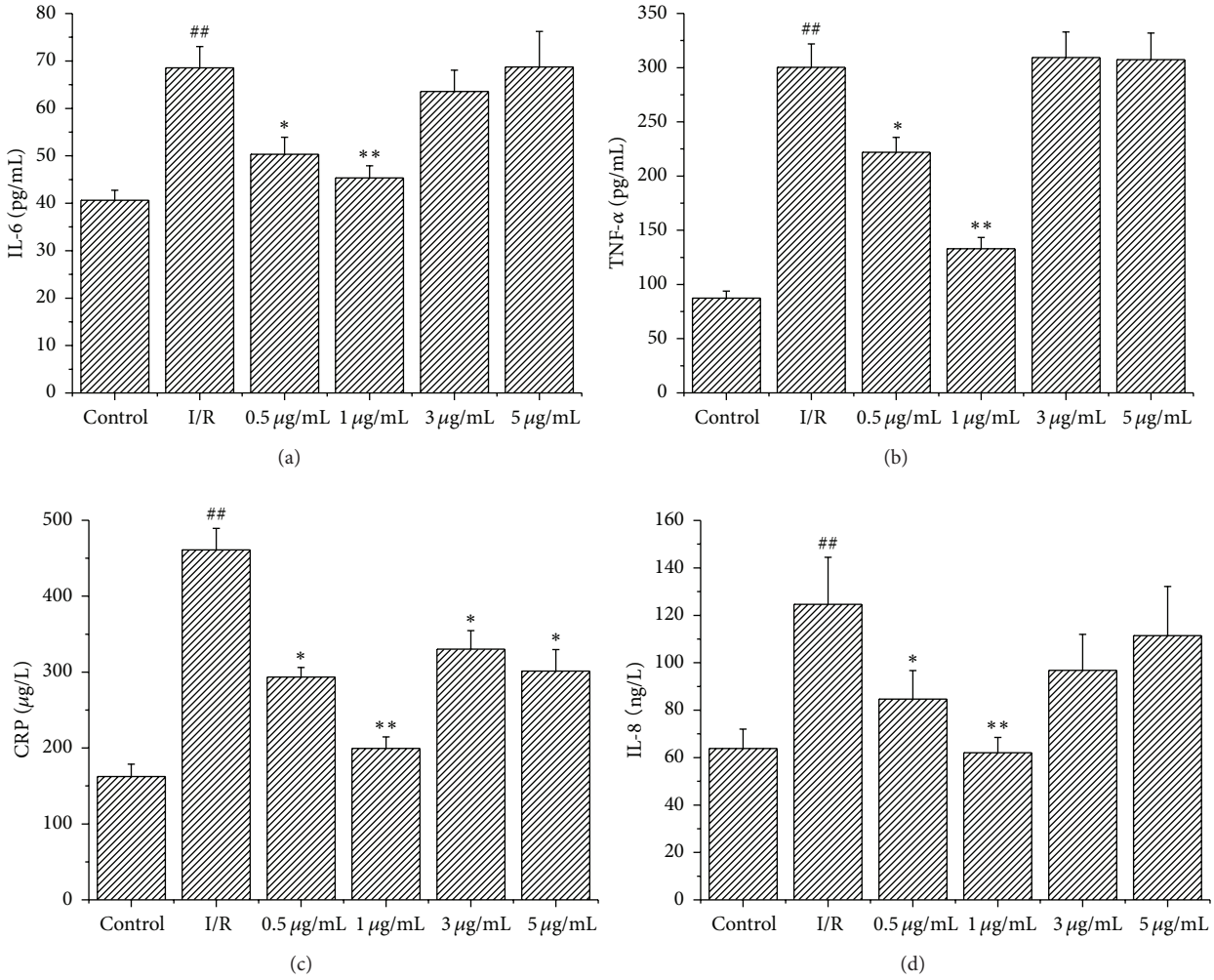

Figure 5: Effect of licochalcone B on cardiac composition of IL-6 and TNF-α in rats subjected to I/R (values are means with their standard deviation, $n = 8$). $^{\#\#}P < 0.01$ compared with control group; $^{*}P < 0.05$ and $^{**}P < 0.01$ compared with the I/R group.

cardiomyocyte apoptosis induced by I/R; and (4) high-dose licochalcone B (3 and 5 μg/mL) indicated no cardioprotective effects. Thus, the cardioprotective effects of licochalcone B may be attributed to its antioxidant, antiapoptotic, and anti-inflammatory activities.

Studies have suggested that ROS generation is among the major factors in I/R injury [17, 18]. Under normal conditions, ROS concentration can be reduced by antioxidant systems, including antioxidant enzymes, such as SOD, and antioxidant molecules, such as GSH [19]. However, when the amount of ROS is beyond the capacity of the abovementioned enzymes and cannot be diminished in reperfusion, oxidative stress occurs. Several studies demonstrate that ROS produced in the reperfused myocardium causes oxidative stress mediated injury under antioxidant protection [11, 20]. Therefore, reducing oxidative stress is an advantageous strategy to alleviate I/R injury. Flavonoids have long been acknowledged for their unique antioxidant properties [21]. Licochalcone B is widely recognized as a major active chemical component isolated from licorice and possesses versatile biological activation, such as antioxidant and anti-inflammatory mechanisms [22]. The present results show that licochalcone B protected the tissues against myocardial I/R-induced injury. Licochalcone B treatment attenuated MDA production and enhanced SOD activity and GSH/GSSG ratio. Therefore, one of the mechanisms of the cardioprotection of licochalcone B was associated with its antioxidant effects. Licochalcone B pretreatment resulted in the attenuation of IL-6 activity and TNF-α production, thereby indicating that one of the mechanisms of the cardioprotection of licochalcone B was associated with its anti-inflammatory effects.

Reperfusion of the ischemic myocardium results in cardiomyocyte apoptosis and heart dysfunction [23, 24]. We observed significant myocardial dysfunction, including changes in hemodynamic parameters (LVDP, $\pm dp/dt_{\max}$, CF, and HR), release of enzymes (CK and LDH), and induced myocardial infarct after reperfusion of the ischemic myocardium. We also observed significant cardiomyocyte apoptosis. These phenomena are in agreement with results of numerous reports indicating that reperfusion is a key initiator

of myocardial dysfunction and cardiomyocyte apoptosis associated with I/R injury. Licochalcone B significantly improved the recovery of I/R-altered hemodynamic parameters (LVDP, $\pm dp/dt_{max}$, CF, and HR), decreased I/R-induced enzyme release (CK and LDH) and cardiomyocyte apoptosis rate, and attenuated infarct size.

Inflammation is involved in I/R injury. CRP, IL-8, IL-6, and TNF-α are proinflammatory cytokines that function in the inflammatory system [25–29]. To investigate the relationship between anti-inflammatory and the cardioprotective effects of licochalcone B, an experiment was performed to examine whether licochalcone B affected the changes in CRP, IL-8, IL-6, and TNF-α induced by I/R. I/R increased CRP, IL-8, IL-6, and TNF-α production, whereas licochalcone B treatment reduced the concentrations of these cytokines. Therefore, the suppressed infiltration of inflammatory cytokines by licochalcone B treatment may contribute to the cardioprotective effects of this flavonoid after reperfusion. Overall, licochalcone B can potentially inhibit myocardial I/R injury via anti-inflammatory activities.

Licochalcone B exhibited significant cardioprotective effects during I/R injury. These effects included the decrease in infarct volume, thereby preventing cell apoptosis. Licochalcone B decreased LDH and CK release and functioned as an anti-inflammatory agent. Licochalcone B increased the capacity of antioxygen free radical. Thus, we hypothesize that licochalcone B deserves additional experimental and clinical research in the cardiovascular milieu.

Conflict of Interests

The authors declare that they have no financial conflict of interests.

Authors' Contribution

Jichun Han and Dong Wang contributed equally to the work.

Acknowledgments

This study was supported by the Science and Technology Project of Shihezi City, Natural Science Foundation of Shandong Province (no. ZR2011HL013) to Dong Wang, the Xinjiang Production and Construction Corps Fund for Distinguished Young Scientists (2011CD006), and the International Cooperation Project 2012BC001 to Qiusheng Zheng.

References

[1] C. Pantos, A. Bescond-Jacquet, S. Tzeis et al., "Trimetazidine protects isolated rat hearts against ischemia-reperfusion injury in an experimental timing-dependent manner," *Basic Research in Cardiology*, vol. 100, no. 2, pp. 154–160, 2005.

[2] E. Murphy and C. Steenbergen, "Mechanisms underlying acute protection from cardiac ischemia-reperfusion injury," *Physiological Reviews*, vol. 88, no. 2, pp. 581–609, 2008.

[3] L. M. Buja and P. Weerasinghe, "Unresolved issues in myocardial reperfusion injury," *Cardiovascular Pathology*, vol. 19, no. 1, pp. 29–35, 2010.

[4] H. Inafuku, Y. Kuniyoshi, S. Yamashiro et al., "Determination of oxidative stress and cardiac dysfunction after ischemia/reperfusion injury in isolated rat hearts," *Annals of Thoracic and Cardiovascular Surgery*, vol. 19, no. 3, pp. 186–194, 2013.

[5] P. H. Chan, "Reactive oxygen radicals in signaling and damage in the ischemic brain," *Journal of Cerebral Blood Flow & Metabolism*, vol. 21, no. 1, pp. 12–14, 2001.

[6] R. Bolli, "Causative role of oxyradicals in myocardial stunning: a proven hypothesis. A brief review of the evidence demonstrating a major role of reactive oxygen species in several forms of postischemic dysfunction," *Basic Research in Cardiology*, vol. 93, no. 3, pp. 156–162, 1998.

[7] G. Ambrosio, L. C. Becker, G. M. Hutchins, H. F. Weisman, and M. L. Weisfeldt, "Reduction in experimental infarct size by recombinant human superoxide dismutase: insights into the pathophysiology of reperfusion injury," *Circulation*, vol. 74, no. 6, pp. 1424–1433, 1986.

[8] L. G. Chi, Y. Tamura, P. T. Hoff et al., "Effect of superoxide dismutase on myocardial infarct size in the canine heart after 6 hours of regional ischemia and reperfusion: a demonstration on myocardial salvage," *Circulation Research*, vol. 64, no. 4, pp. 665–675, 1989.

[9] S. Kilgore, G. S. Friedrichs, C. R. Johnson et al., "Protect-ive effects of the SOD-mimetic SC-52608 against ischmia/reperfusion damage in the rabbit isolated heart," *Journal of Molecular and Cellular Cardiology*, vol. 26, no. 8, pp. 995–1006, 1994.

[10] U. Näslund, S. Häggmark, G. Johansson, S. L. Marklund, S. Reiz, and A. Öberg, "Superoxide dismutase and catalase reduce infarct size in a porcine myocardial occlusion-reperfusion model," *Journal of Molecular and Cellular Cardiology*, vol. 18, no. 10, pp. 1077–1084, 1986.

[11] M. Akhlaghi and B. Bandy, "Mechanisms of flavonoid protection against myocardial ischemia-reperfusion injury," *Journal of Molecular and Cellular Cardiology*, vol. 46, no. 3, pp. 309–317, 2009.

[12] J. Furusawa, M. Funakoshi-Tago, T. Mashino et al., "Glycyrrhiza inflata-derived chalcones, Licochalcone A, Licochalcone B and Licochalcone D, inhibit phosphorylation of NF-κB p65 in LPS signaling pathway," *International Immunopharmacology*, vol. 9, no. 4, pp. 499–507, 2009.

[13] Y. Kimura, H. Okuda, T. Okuda, and S. Arichi, "Effects of chalcones isolated from licorice roots on leukotriene biosynthesis in human polymorphonuclear neutrophils," *Phytotherapy Research*, vol. 2, no. 3, pp. 140–145, 1988.

[14] T. Nakagawa, T. Yokozawa, Y. A. Kim, K. S. Kang, and T. Tanaka, "Activity of Wen-Pi-Tang, and purified constituents of Rhei Rhizoma and glycyrrhizae radix against glucose-mediated protein damage," *The American Journal of Chinese Medicine*, vol. 33, no. 5, pp. 817–829, 2005.

[15] L. Shan, J. Li, M. Wei et al., "Disruption of Rac1 signaling reduces ischemia-reperfusion injury in the diabetic heart by inhibiting calpain," *Free Radical Biology and Medicine*, vol. 49, no. 11, pp. 1804–1814, 2010.

[16] Q. Pan, X. Qin, S. Ma et al., "Myocardial protective effect of extracellular superoxide dismutase gene modified bone marrow mesenchymalstromal cells on infarcted mice hearts," *Theranostics*, vol. 4, no. 5, pp. 475–486, 2014.

[17] X. Zhu and L. Zuo, "Characterization of oxygen radical formation mechanism at early cardiac ischemia," *Cell Death & Disease*, vol. 5, no. 4, article e787, 2013.

[18] J. Jiang, X. Yuan, T. Wang et al., "Antioxidative and cardioprotective effects of total flavonoids extracted from Dracocephalum moldavica L. againstacute ischemia/reperfusion-induced myocardial injury in isolated rat heart," *Cardiovascular Toxicology*, vol. 14, no. 1, pp. 74–82, 2014.

[19] A. Toth, R. Halmosi, K. Kovacs et al., "Akt activation induced by an antioxidant compound during ischemia-reperfusion," *Free Radical Biology and Medicine*, vol. 35, no. 9, pp. 1051–1063, 2003.

[20] M. Khan, S. Varadharaj, L. P. Ganesan et al., "C-phycocyanin protects against ischemia-reperfusion injury of heart through involvement of p38 MAPK and ERK signaling," *American Journal of Physiology-Heart and Circulatory Physiology*, vol. 290, no. 5, pp. H2136–H2145, 2006.

[21] Y. Fu, J. Chen, Y. Li, Y. Zheng, and P. Li, "Antioxidant and anti-inflammatory activities of six flavonoids separated from licorice," *Food Chemistry*, vol. 141, no. 2, pp. 1063–1071, 2013.

[22] M. Shen, R. X. Wu, L. Zhao et al., "Resveratrol attenuates ischemia/reperfusion injury in neonatal cardiomyocytes and its underlying mechanism," *PLoS ONE*, vol. 7, no. 12, Article ID e51223, 2012.

[23] M. Khan, S. Varadharaj, L. P. Ganesan et al., "C-phycocyanin protects against ischemia-reperfusion injury of heart through involvement of p38 MAPK and ERK signaling," *American Journal of Physiology: Heart and Circulatory Physiology*, vol. 290, no. 5, pp. H2136–H2145, 2006.

[24] Y. Oh, M. Ahn, S. Lee, H. Koh, S. H. Kim, and B. Park, "Inhibition of Janus activated kinase-3 protects against myocardial ischemia and reperfusion injury in mice," *Experimental and Molecular Medicine*, vol. 45, no. 5, article e23, 2013.

[25] P. Markowski, O. Boehm, L. Goelz et al., "Pre-conditioning with synthetic CpG-oligonucleotides attenuates myocardial ischemia/reperfusion injury via IL-10 up-regulation," *Basic Research in Cardiology*, vol. 108, no. 5, pp. 1–16, 2013.

[26] S. Bonney, D. Kominsky, K. Brodsky, H. Eltzschig, L. Walker, and T. Eckle, "Cardiac Per2 functions as novel link between fatty acid metabolism and myocardial inflammation during ischemiaand reperfusion injury of the heart," *PLoS ONE*, vol. 8, no. 8, Article ID e71493, 2013.

[27] H. Li, Y. Bian, N. Zhang et al., "Intermedin protects against myocardial ischemia-reperfusion injury in diabetic rats," *Cardiovascular Diabetology*, vol. 12, no. 1, article 91, 2013.

[28] B. H. Heijnen, I. H. Straatsburg, N. D. Padilla, G. J. van Mierlo, C. E. Hack, and T. M. van Gulik, "Inhibition of classical complement activation attenuates liver ischaemia and reperfusion injury in a rat model," *Clinical and Experimental Immunology*, vol. 143, no. 1, pp. 15–23, 2006.

[29] K. Watanabe, C. Iwahara, H. Nakayama et al., "Sevoflurane suppresses tumour necrosis factor-a-induced inflammatory responses in small airway epithelial cells after anoxia/reoxygenation," *British Journal of Anaesthesia*, vol. 110, no. 4, pp. 637–645, 2013.